

UNCLASSIFIED

AD 273 515

*Reproduced
by the*

**ARMED SERVICES TECHNICAL INFORMATION AGENCY
ARLINGTON HALL STATION
ARLINGTON 12, VIRGINIA**



UNCLASSIFIED

NOTICE: When government or other drawings, specifications or other data are used for any purpose other than in connection with a definitely related government procurement operation, the U. S. Government thereby incurs no responsibility, nor any obligation whatsoever; and the fact that the Government may have formulated, furnished, or in any way supplied the said drawings, specifications, or other data is not to be regarded by implication or otherwise as in any manner licensing the holder or any other person or corporation, or conveying any rights or permission to manufacture, use or sell any patented invention that may in any way be related thereto.

273 515

BULLETIN No. 30

**SHOCK, VIBRATION
AND
ASSOCIATED ENVIRONMENTS
PART III**

FEBRUARY 1962

**OFFICE OF
THE SECRETARY OF DEFENSE**

Research and Engineering



ASTIA

DEFENSE DOCUMENTS

1962

1962

Washington, D. C.

BULLETIN No. 30

**SHOCK, VIBRATION
AND
ASSOCIATED ENVIRONMENTS**

PART III

FEBRUARY 1962

**OFFICE OF
THE SECRETARY OF DEFENSE**

Research and Engineering

The 30th Symposium on Shock, Vibration, and Associated Environments was held at the Statler-Hilton Hotel, Detroit, Michigan on October 10-12, 1961. The Department of the Army was host.

Washington. D. C.

**INTERSERVICE TECHNICAL GROUP FOR SHOCK,
VIBRATION, AND ASSOCIATED ENVIRONMENTS**

ARMY MEMBERS

Mr. David Askin
Frankford Arsenal
Philadelphia, Pennsylvania

Dr. W. B. Brierly
Quartermaster Research and
Engineering Command
Natick,

Dr. Joseph S. diRende
Scientific Director
U.S. Army Transportation
Research Command
Fort Eustis, Virginia

Mr. Joseph Kaufman
Office of the Chief of Ordnance
U.S. Army
Pentagon Annex No. 2
Washington 25, D. C.

Mr. Frederick J. Lindner
Packaging Development Branch
U.S. Army Engineer Research and
Development Laboratories
Fort Belvoir, Virginia

Mr. Joseph J. Oliveri
Engineering Science Department
U.S. Army Signal Research and
Development Laboratories
Fort Monmouth, New Jersey

NAVY MEMBERS

Mr. J. M. Crowley
Code 439
Office of Naval Research
Washington 25, D. C.

Mr. E. R. Mullen
U.S. Naval Air Development Center
Johnsville, Pennsylvania

Mr. R. H. Oliver
Code 423
Bureau of Ships
Washington 25, D. C.

Mr. Harry Rich
David Taylor Model Basin
Washington 7, D. C.

Mr. Theodore Soo-Hoo
Office of the Chief of Naval Operations
Pentagon
Washington 25, D. C.

Mr. George Stathopoulos
U.S. Naval Ordnance Laboratory
White Oak
Silver Spring, Maryland

AIR FORCE MEMBERS

Mr. E. A. Catenaro
Rome Air Development Center
Attn: RCSSM
Griffiss Air Force Base, New York

Mr. C. Golueke
Wright Air Development Division
Attn: WWFEVD
Wright-Patterson Air Force Base
Ohio

Mr. D. C. Kennard
Wright Air Development Division
Attn: WWFEV
Wright-Patterson Air Force Base
Ohio

Mr. H. A. McGrath
Wright Air Development Division
Attn: WWRMD
Wright-Patterson Air Force Base
Ohio

Mr. Howard W. Wolko
Air Force Office of Scientific Research
Tempo D Building
Washington 25, D. C.

Dr. George A. Young
Air Force Special Weapons Center
Kirtland Air Force Base
New Mexico

**DEFENSE ATOMIC SUPPORT
AGENCY MEMBER**

Mr. John Lewis
Defense Atomic Support Agency
Pentagon
Washington 25, D. C.

**NATIONAL AERONAUTICS AND
SPACE ADMINISTRATION MEMBER**

Mr. John C. New
Code 320
National Aeronautics and Space
Administration
Goddard Space Flight Center
Greenbelt, Maryland

**OFFICE OF DIRECTOR OF DEFENSE
RESEARCH AND ENGINEERING MEMBER**

Mr. G. B. Wareham
Equipment and Supplies Division
Washington 25, D. C.

CONTENTS

Foreword	v
Section 1	
<u>Measurement and Definition of Transportation Environments</u>	
What Should be Known to Evaluate Rail Shipping Damage.....	1
R. M. Mains, General Electric Company, Schenectady, New York	
Measurement of the Cross-Country Terrain Environment	8
H. P. Simon and C. D. Roach, U.S. Army Transportation Research Command Fort Eustis, Virginia	
Rail Transport Dynamic Environment	16
R. W. Hager, R. L. Partington, and R. J. Leistikow, The Boeing Company Seattle, Washington	
Definition and Measurement of Shipping Vibration Environments	27
H. R. Welton, L. L. LeBrun, R. Carmichael, and W. Harger, Northrop Corporation Hawthorne, California	
Shock and Vibration of Standard Military Vehicles in Over-the-Road Application.....	36
R. Kennedy, U.S. Army Transportation Research Command, Fort Eustis, Virginia	
Vibration Loads on a Wheeled Vehicle	45
S. J. Grabowski, U.S. Army Ordnance Arsenal, Detroit, Michigan	
Section 2	
<u>Isolation of Packaged Items</u>	
Trends in the Isolation of Packaged Items.....	57
R. K. Stern, Forest Products Laboratory, Madison, Wisconsin	
An Approach to the Solution of Shock and Vibration Isolation Problems as Applied to Package Cushioning Materials.....	66
C. D. Henny and F. R. Leslie, The Boeing Company, Seattle, Washington	
Design and Evaluation of Packages Containing Cushioned Items, Using Peak Acceleration Versus Static Stress Data.....	76
T. J. Grabowski, Research and Development Center, Armstrong Cork Company Lancaster, Pennsylvania	
Recent British Developments in Package Cushioning, Dynamic Testing and Instrumentation.....	87
S. C. Schuler, Royal Radar Establishment, Malvern, England	
Low-Temperature Static-Dynamic Urethane Foam Cushioning Studies.....	100
W. B. Tolley, Tucson Engineering Laboratory, Hughes Aircraft Company, Tucson, Arizona	
Section 3	
<u>Simulation of Transportation Environments</u>	
A Proposal to Establish Valid Ground Transportation Tests	111
A. E. Surosky, General Testing Laboratories, Moonachie, New Jersey	
Theoretical and Practical Bases for Specifying a Transportation Vibration Test	122
G. S. Mustin and E. D. Hoyt, Reed Research, Inc., Washington, D. C.	
Some Shock Spectra Comparisons Between the ATMX 600 Series Railroad Cars and a Railroad Switching Shock Test Facility	138
R. H. Rector, Sandia Corporation, Albuquerque, New Mexico	

Rough Handling Tests of Reusable Containers	165
F. Yee, Detroit Arsenal, Detroit, Michigan	
Simulation of Rail Car Coupling Environment	173
W. H. Brown and R. L. Dyrdahl, The Boeing Company, Seattle, Washington	

Section 4
Design of Containers and Transporters

Design and Engineering Evaluation Testing of the Terrier Missile Shipping Container	185
R. L. Munson, General Dynamics, Pomona, California	
Shock Response of a Nonlinear Missile Suspension System.	194
E. Y. W. Tsui and P. Stern, Lockheed Missiles and Space Division, Sunnyvale, California	
Lightweight Shock Isolation System for a Mobile Nuclear Power Plant	211
J. W. Blakley, Research and Development Division, Aerojet-General Nucleonics San Ramon, California	
Shock and Vibration of APCHE Trailer.	222
S. A. Lever, Radio Corporation of America, Van Nuys, California	
Missile Transporter Vibration Analysis	243
R. R. Simun and R. S. Peterson, Douglas Aircraft Company, Santa Monica, California	
Container Design for Nike Zeus Missile	250
J. R. Erkenbrack, Douglas Aircraft Company, Inc., Santa Monica, California	
Design Criteria for Underwater Ordnance Missile Containers	257
R. J. Sefing, Minneapolis-Honeywell Regulator Company, Duarte, California	

Section 5
Aerial Delivery of Supplies and Equipment

Cushioning for Aerial Delivery	261
J. Neils Thompson and E. A. Ripperger, Structural Mechanics Research Laboratory The University of Texas, Austin, Texas	
Design of Cushioning Systems for Air Drop.	276
M. P. Gionfriddo, QM Research and Engineering Center, Natick, Massachusetts	
Problems of Efficiency, Definition, and Measurement of Shock Associated with Parachuted Loads	290
G. W. H. Stevens, Royal Aircraft Establishment, Farnborough, England	
The Response of Yielding Structures to Shock Loading	302
E. A. Ripperger and W. T. Fowler, Structural Mechanics Research Laboratory The University of Texas, Austin, Texas	
Aerial Delivery of a Heavy Unit Load by Parachute Extraction	317
2nd Lt. D. C. Turk, USAF, Hq. 6511th Test Group (Parachute), El Centro, California	
The Telemetering Clevis	327
Capt. W. Gourlay, Jr., USAF, 6511th Test Group (Parachute), El Centro, California	
A Simple Efficient, One-Shot Energy Absorber	331
C. K. Kroell, General Motors Research Laboratory, Warren, Michigan	

Section 6
Panel Session I

Engineering Approach to the Protection of a Fragile Item	339
--	-----

FOREWORD

The theme of "Transportation and Packaging Environments" was chosen for half of the 30th Symposium on Shock, Vibration, and Associated Environments because there appeared to be a very serious need for an opportunity to discuss problems in this area. It has been several years since these symposia have dealt with this very important field except in a very limited way.

Nearly all of the papers dealing with the transportation theme are contained in this volume. The reader will surely find many of them both thought provoking and helpful, but it should not end here. Since this Activity is dedicated to provide a medium for exchange of technical information in the environmental field, we are anxious to receive suggestions on specific areas where information is lacking and to be notified of new developments that might be of assistance to others. In short, the subjects treated at these symposia are largely selected on the basis of the demands of the participants. Send your suggestions and comments to Code 4021, U.S. Naval Research Laboratory, Washington 25, D. C.



February 1962

Section 1

MEASUREMENT AND DEFINITION OF TRANSPORTATION ENVIRONMENTS

WHAT SHOULD BE KNOWN TO EVALUATE RAIL SHIPPING DAMAGE

R. M. Mains
General Electric Company
Schenectady, New York

The parameters to be considered in evaluating rail shipping damage are discussed. Equations relating track input force to lading response are developed. The difficulties of evaluating potential damage, making necessary measurements, and analyzing the data are assessed.

SUMMARY

In trying to evaluate the likely damage to be sustained by a very heavy item during shipment on a railroad, the question arose of what should be known in order to evaluate this damage properly. It seemed that the lading, the car, and the track constituted the essential system to consider, with the irregularities of the track providing the excitation.

The equations for relating a track input force to lading response are developed, first for single-degree-of-freedom elements, and then for multidegree-of-freedom elements. These equations show what must be measured or calculated in order that measurements made on one lading and car combination can be carried over to a different lading. The impedance functions from the track to the car-lading interface and from the car-lading interface to the monitor points on the lading are required. Once these are known (either by measurement or calculation), it is then possible to calculate the track input force for a measured lading response. Similarly, the lading response to a given track force input can be calculated.

Once the lading response has been calculated, it must then be evaluated for potential damage. The point is made that until more adequate data are available on damage processes, it does little good to get too sophisticated about track input and car impedance functions.

The conclusion is drawn that it is not surprising that complete data including car impedance functions and track input are not available at present since the problem is complex and costly. Furthermore, it is hard to justify such work, since it is not possible at present to predict potential damage from rail shipment except in a few oversimplified cases. It is recommended that an effort be commenced to plug these gaps in our information so that we may be more rational about the next rail shipment.

GENERAL BACKGROUND

Recently a problem arose in which a very heavy and very expensive item was to be shipped by rail from the factory to the site of

use. The question posed by this problem was: Just what information must we have in order to evaluate the potential damage to the lading in its travels? To make the problem more interesting, the complex metal structure comprising the lading was much heavier than the special drop-bed flat car that was to carry it.

Let us first consider what would be a logical sequence leading to a damage evaluation. Assume that the vehicle (a special drop-bed flat car) and the road (the available railroad trackage between the shipping terminals) are known and definite, and the lading is defined by a complete set of manufacturing drawings. We need first to establish the probable driving forces exerted on the flat car by reason of its motion over the roadbed. Then we need to determine how these driving forces are modified in passing through the flat car to the sensitive parts of the lading. If we can predict the response of these sensitive parts in this way, then an estimate of damage potential may be possible.

To estimate damage potential from predicted responses, the damage mechanism (e.g., fatigue, abrasion, brittle fracture) must be known and the manner in which damage accumulates must be known or assumed. For purposes of this discussion, fatigue will be taken as the damage mechanism and the linear damage accumulation rule attributed to Palmgren [1] and Miner [2] will be assumed.

SIMPLE THEORY

Consider the series impedance picture of Fig. 1, in which the forces at A, B, and C are related as follows, for any particular frequency:

$$\left. \begin{aligned} f_a &= z_{aa} v_a + z_{ab} v_b \\ f_b &= z_{ba} v_a + z_{bb} v_b = z'_{bb} v_b + z_{bc} v_c \\ f_c &= z_{cb} v_b + z_{cc} v_c \end{aligned} \right\} \quad (1)$$

in which

f_n = force

z_{nn} = direct impedance

z_{nm} = cross impedance

v_n = velocity.

Now, by the reciprocity theorem,

$$z_{nm} = z_{mn}. \quad (2)$$

Thus, if the z 's are the unknowns, we have 5 independent z 's and three equations relating them. To determine z by measurement then requires that we apply a driving force to at least two points separately, and measure the resulting forces and velocities in order to have enough equations. (This is similar to the open-circuit and short-circuit measurements to determine electrical impedances.)

If the A-B element in Fig. 1 is something small enough to handle conveniently, we can first terminate B in some structure and drive on A, while we measure f_a , v_a , f_b , and v_b . Then by reversing the element and driving on B while A is terminated in some structure, and measuring the same quantities again, we have enough relationships to solve for the z 's. The measurements must be made over the frequency range of interest, and both amplitude and phase of each quantity are needed. Alternatively, the in-phase and out-of-phase components of the various quantities can be measured. (This latter is the preferable procedure in the presence of noisy signals, since phase meters are often poor for noisy signals. A wide-frequency range multiplier and an operational amplifier can be used to multiply the driving signal by the responding function to get the in-phase components, and the integral of the driving signal by the responding function to get the out-of-phase components. A two-phase oscillator or alternator can also be used, one phase for driving and multiplying, and the other for multiplying only.)

APPLICATION TO RAILWAY CAR

The simple theory is all very neat, and is available in Ref. 3. When we try to apply it to the railway car and lading problem, however, the simplicity disappears and some troublesome practical difficulties arise. For example, consider Fig. 2 where the A terminals represent the 12 wheels of the car, the B terminals represent the eight attachment points of the lading to the car, and the C terminals represent the several possibly sensitive elements in the lading.

Equation (1) still applies, but it is now a matrix equation:

$$\begin{bmatrix} F_a \\ F_b \\ F_c \end{bmatrix} = \begin{bmatrix} z_{aa} & z_{ab} \\ z_{ba} & z_{bb} \\ z_{cb} & z_{cc} \end{bmatrix} \begin{bmatrix} V_a \\ V_b \\ V_c \end{bmatrix} \quad (3)$$

$$\begin{bmatrix} F_a \\ F_b \\ F_c \end{bmatrix} = \begin{bmatrix} z'_{bb} & z_{bc} \\ z_{cb} & z_{cc} \end{bmatrix} \begin{bmatrix} V_b \\ V_c \end{bmatrix} \quad (4)$$

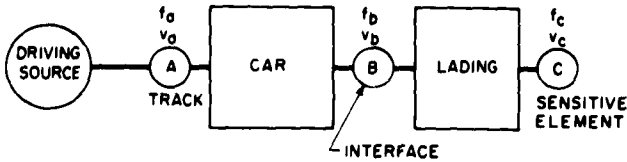


Fig. 1 - Simple impedance picture (two bodies)

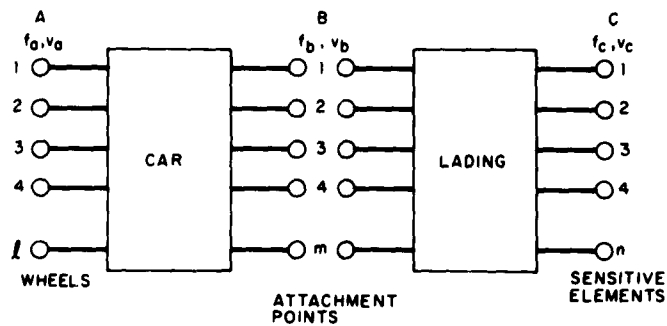


Fig. 2 - Multipoint impedance picture (two bodies)

in which

F_a = the force vector at A, ($\ell \times 1$) dimension

z_{aa} = the direct impedance matrix for A, ($\ell \times \ell$) dimension

z_{ab} = the cross impedance matrix, A to B, ($\ell \times m$) dimension

z_{ba} = the cross impedance matrix, B to A, ($m \times \ell$) dimension

z_{bb} = the direct impedance matrix for B, ($m \times m$) dimension

v_a = the velocity vector at A, ($\ell \times 1$) dimension

v_b = the velocity vector at B, ($m \times 1$) dimension,

and similarly for B-C.

Now, by the reciprocity theorem,

$$z_{ab}^T \cdot z_{ba} = z_{ab} \text{ transposed} \quad (5)$$

and

$$z_{bc}^T \cdot z_{cb} = z_{bc} \text{ transposed.} \quad (6)$$

Thus, Eqs. (3) and (4) become

$$\begin{bmatrix} F_a \\ F_b \\ F_c \end{bmatrix} = \begin{bmatrix} z_{aa} & z_{ab} \\ z_{ab}^T & z_{bb} \end{bmatrix} \quad (7)$$

$$\begin{bmatrix} F_b \\ F_c \end{bmatrix} = \begin{bmatrix} z_{bb}' & z_{bc} \\ z_{bc}^T & z_{cc} \end{bmatrix} \quad (8)$$

Now, the full z matrix in Eq. (7) is symmetric, so there are

$$\frac{\ell}{2}(\ell+1) + (\ell \times m) + \frac{m}{2}(m+1) = \frac{1}{2}[(\ell+m)^2 + \ell+m] \quad (9)$$

independent terms and only

$$(\ell+m) \quad (10)$$

independent relationships. If we measured all the f 's and v 's while we drove on each point in turn, we would have

$$\ell(\ell+m) + m(\ell+m) = (\ell+m)^2 \quad (11)$$

equations, or enough to solve for the z 's without taking advantage of symmetry. Now driving

on the B points is straightforward for the railway car, but driving the A points (wheels) while maintaining enough preload on each A point to overcome slack or nonlinearity is hardly feasible. The only practical recourse is, then, to take advantage of symmetry and drive only on the B points (but measuring f and v at the A points, of course). For this to work, the number of B points must equal or exceed the number of A points, and this can be made to be the case if we wish. There is nothing to prevent us from measuring a B-A point which we later treat as a dummy point by letting it attach to a zero impedance B-C point.

To recapitulate, we can make $m \geq l$ arbitrarily, then drive on each B point in turn while we measure the f 's and v 's at all other B and A points. We can then form a matrix of the measured values of f by ordering the columns, and adjust it to symmetry (since measurement errors will produce assymetry). We can do the same for the measured v 's and write

$$F_{ij} = z_{ij} v_{ij} \quad (12)$$

Since each of these matrices has the dimensions $(l + m)$ by $(l + m)$ and is symmetric, we can use

$$[z_{ij} v_{ij}]^T = v_{ij} z_{ij}, \quad (13)$$

so that $F_{ij}^T = [z_{ij} v_{ij}]^T = v_{ij} z_{ij}$.

whence $v_{ij}^{-1} F_{ij}^T = v_{ij}^{-1} v_{ij} z_{ij}$

or $z_{ij} = v_{ij}^{-1} F_{ij}^T$. (14)

which provides the impedances we want. So mathematically the problem is solvable, but the total number of measurements required is huge.

APPLICATION TO THE LADING

The measurement and calculation problem for the B-C element in Fig. 2 is identical with that for the A-B element. If we make $m \geq n$ and find a way to support the lading on the B points while we drive on each B point in turn, then the measured values can be put into Eq. (14) and the z 's can be found. If the lading is not available for measurement, then the manufacturing drawings can be used to calculate the necessary impedances as follows:

1. Determine the points at which masses should be lumped in order to define the response for possibly sensitive elements.

2. Calculate the flexibility, K^{-1} , and mass matrix, M , for these lumped masses.

3. Decide how to handle damping and construct a damping matrix. One way is to form the product,

$$M \times K, \quad (15)$$

in which

M = mass matrix

K = stiffness matrix (inverse of flexibility),

but calculate only those terms from the diagonal to the right. Then assume some reasonable value of the critical damping ratio, ζ , and calculate

$$2\zeta \sqrt{k_{ij} m_{ij}} \quad (16)$$

for each term of Eq. (15). Then complete the damping matrix, C , by making it symmetric.

4. Now solve the equation

$$\begin{bmatrix} -\omega^2 M + K + \omega C \\ -\omega C - \omega^2 M + K \end{bmatrix} \begin{bmatrix} a \\ b \end{bmatrix} = \begin{bmatrix} f_1 \\ f_2 \end{bmatrix} \quad (17)$$

for the values of a and b for a range of values of ω (the frequency) and for each individual element of $f_1 = 1$ in turn while all the other f_1 's and f_2 's are zero. Then

$$\left. \begin{array}{l} a_{ij}\omega = \text{in-phase mobility at } i \text{ for a driving force at } j. \\ b_{ij}\omega = \text{out-of-phase mobility at } i \text{ for a driving force at } j. \end{array} \right\} \quad (18)$$

Note that a similar operation could be performed to calculate mobilities for the railway car. Also note that it is a good idea to solve $M\ddot{x} + Kx = 0$ for normal frequencies before step 4 so that the range of ω 's can include the resonance frequencies.

To get impedance matrices from the calculated mobilities, we can make use of the fact that impedance is the reciprocal of mobility, or

$$\begin{bmatrix} a\omega & ib\omega \\ ib\omega & a\omega \end{bmatrix} \begin{bmatrix} z_{RE} & iz_{IM} \\ iz_{IM} & z_{RE} \end{bmatrix} = \begin{bmatrix} 1 & 0 \\ 0 & 1 \end{bmatrix}, \quad (19)$$

whence

$$\begin{aligned} z_{RE} &= +\frac{1}{\omega} [a^2 + b^2]^{-1} a \\ z_{IM} &= -\frac{1}{\omega} [a^2 + b^2]^{-1} b \end{aligned} \quad (20)$$

DETERMINATION OF THE LOAD (OR DRIVING FUNCTION)

To measure the effective driving force involved in the motion of the railway car along the track is not feasible directly. It is necessary instead to measure responses of the car-lading system and deduce effective driving force from the measured responses and the measured (or calculated) impedance functions. It is desirable to attach a dummy load of approximately the correct weight to the car, with the attachment points and weight distribution similar to the final shipment. Then measurement of velocities of selected points on the dummy lading leads to the deduction of effective driving forces as shown below.

For Fig. 2 and Eqs. (3) and (4), we can eliminate F_b between the two equations for F_b and get

$$[V_b] = [z'_{bb} - z_{bb}]^{-1} [z_{ab}^T v_a - z_{bc} v_c]. \quad (21)$$

This value substituted in the equations for F_a and F_c gives:

$$\begin{bmatrix} F_a \\ 0 \end{bmatrix} = \begin{bmatrix} \beta_{aa} & \beta_{ac} \\ \beta_{ca} & \beta_{cc} \end{bmatrix} \begin{bmatrix} V_a \\ V_c \end{bmatrix}. \quad (22)$$

If we select points to measure on the lading where $F_c = 0$, and if

$$\left. \begin{aligned} \beta_{aa} &= z_{aa} + z_{ab} [z'_{bb} - z_{bb}]^{-1} z_{ab}^T \\ \beta_{ac} &= -z_{ab} [z'_{bb} - z_{bb}]^{-1} z_{bc} \\ \beta_{ca} &= z_{bc}^T [z'_{bb} - z_{bb}]^{-1} z_{ab} \\ \beta_{cc} &= z_{cc} - z_{bc}^T [z'_{bb} - z_{bb}]^{-1} z_{bc} \end{aligned} \right\}, \quad (23)$$

we can now eliminate V_a between Eqs. (22) and get

$$F_a = [\beta_{ac} - \beta_{aa} \beta_{ca}^{-1} \beta_{cc}] V_c \quad (24)$$

$$F_a = Z V_c. \quad (24a)$$

(Note that this is an equation of complex frequency functions, not of time functions.)

Now at this point there is a choice to be made: we can either deal with Eq. (24a) as a complex equation, using the complex values of the frequency transform of measured velocities for v_c and the complex Z 's either measured or calculated; or we can square Eq. (24a) and deal with the mean square of measured velocities and the square of the absolute value of the Z 's. The former procedure would require a statistical treatment of the deduced F_a 's, while the latter procedure treats the measured velocities statistically before they are used. The latter procedure is recommended, and it summarizes thus:

1. Sample the measured velocities either at fixed time intervals or at random times during the trip, to get $v(t)$.

2. Perform the Fourier integral transform for each sample to get

$$\left. \begin{aligned} V_{RE} &= \int_0^T v(t) \cos \omega t dt \\ V_{IM} &= \int_0^T v(t) (-\sin \omega t) dt \\ \text{and} \quad V^2 &= V_{RE}^2 + V_{IM}^2 \end{aligned} \right\} \quad (25)$$

3. Find the average V^2 for each frequency of interest and for all the samples, this gives the mean square velocity, \bar{V}_c^2 . It is also desirable to determine the distribution of amplitudes at each frequency for later use.

4. We form the $|Z|^2$ matrix by squaring each z_{RE} element and adding to it the square of its corresponding z_{IM} element.

5. Then

$$\bar{F}_a^2 = |Z|^2 \times \bar{V}_c^2. \quad (26)$$

PREDICTION OF THE RESPONSE OF THE ACTUAL SHIPMENT

To predict the response of the actual shipment, we substitute its calculated impedances for the B-C part of Fig. 2, calculate the A-C impedances as in Eq. (23) and get Z as in Eq. (24). The mean square velocity response is then

$$V_c^2 = |Z^{-1}|^2 \times F_a^2 . \quad (27)$$

EVALUATION OF DAMAGE POTENTIAL

With the mean square velocity responses known, and their amplitude distributions presumed similar to those for the dummy shipment, we can now proceed with damage evaluation studies. We can calculate accelerations, displacements, forces, stresses, and the like. If we either assume or have experimental data on damage accumulation, we can evaluate damage by whatever criterion we wish [4]. Unfortunately damage accumulation rules and damage criteria are by no means well established, so that the true significance of the

answers obtained is debatable. One might well ask why so much trouble and expense would be undertaken for a questionable answer, and a reply would be difficult to make.

CONCLUSION

It has been shown what is needed to predict transportation responses for a given shipment. One such prediction requires huge amounts of calculation and measurement, so it is easy to see why studies like this have not been made very often in the past. In this case, the project was dropped because of its cost and the uncertainty of the results. Some simpler and cheaper way must be found to provide better transportation data than is presently available.

REFERENCES

- [1] A. Palmgren, "The Endurance of Ball-Bearings," Z.V.D.I., Vol. 68, 1924, p. 339.
- [2] M. A. Miner, "Cumulative Damage in Fatigue," Journ. Appl. Mech., v. 12, Trans. ASME, Vol. 67, 1947, p. 159.
- [3] Mechanical Impedance Methods, ASME Publication, Dec. 2, 1958.
- [4] Random Vibration, edited by S. H. Crandall, Wiley and Sons, 1958, Chapter 12.

DISCUSSION

Mr. Rice (Goodyear Aircraft): I'm on an AIA Committee Subpanel in which we're trying to get some kind of uniformity into what the various companies use for criteria for shipping, and this very problem that Dr. Mains has outlined is one of the big problems that we have to face. Where do you start? I admire his courage for starting some place because this has been, I believe, our biggest problem. We have always been afraid to start, so I am in favor of supporting him in any way we can. I thought, as a suggestion, that we should get some kind of national program, Mr. Pusey might sponsor it, in which many companies shipping these big items could instrument cars and then get a statistical distribution instead of getting this short time interval Dr Mains speaks of. We must get many kinds of railroads and many kinds of locations, many kinds of cars which vary from car to car depending on how much they have deteriorated, and we must get an east, west, north, south statistical distribution that we all pour into some common funnel, some contract in which we all accumulate these impedances. Then we start to take a look. Do most railroads look the same? Do most railroad cars in

spite of their age come up with the same kind of distribution? Do these enormously heavy loads such as we ship, we have these big antennas that weight 10 to 20 thousand pounds, do their responses differ completely from items of 5 and 6 thousand pounds? But Dr. Mains put his finger on the real problem; one little piece of information might be completely misleading, and unless you get a tremendous program going you can never whip this problem. So I would like to see what he advocates started but with many people participating and thus generating a statistical distribution.

Dr. Mains: I would like to add just a word to that. The Association of American Railroads has been making measurements for a good many years. I don't know the present state of their data; however, I know one particular railroad that we were dealing with in this specific case which alleges to have what they call "track profiles." What amounts to the track input, that they have measured in terms of the wheel hub velocities as the car goes down the track. Now if these wheel hub velocities are in good usable form, we have something that can be

used for an input. Next we need the car impedance transfer functions, and we're in business. Incidentally, you have to add a cipher to your weight numbers to get up to the weight class I was talking about. It's 2, 3, or 4 hundred thousand pounds. This was a 250-ton flat car, and it didn't have a lot of spare capacity.

J. Burgess (United Technology Corp.) I would like to point out that the rail joints are apt

to be a major source of excitation and that the track profiles are apt to hide that information.

Dr. Mains: The railroad company we were dealing with contended that the rail joints were the principal factor and that their profile emphasized this. How they did this they didn't say specifically. We had to drop the project because of cost too soon to get the real details.

* * *

MEASUREMENT OF THE CROSS-COUNTRY TERRAIN ENVIRONMENT

Herman P. Simon and Charles D. Roach
U. S. Army Transportation Research Command
Fort Eustis, Virginia

This paper deals with the theory, measurement, and presentation of shock and vibration data on cross-country terrains. A theory is postulated for interpreting terrain profiles in statistical terms to obtain a more realistic description of roughness. An instrument for obtaining more reliable data for rough terrains is described and the methods of presenting resultant data are discussed.

INTRODUCTION

The word "mobility" as now used by the military has many definitions, but for the vehicle and package designer it defines a difficult area and environment with which to cope. This is the terrain *in situ*—not only roads, trails, or paths, but the ground as nature has conditioned it by erosion, vegetation, climate, etc. The ability to traverse cross-country terrain involves many considerations, one of the most important of which is rough ground performance, which is indicated by vehicle speed, human tolerance to vibration (low frequency, high amplitude), and limiting forces on cargo and equipment.

To provide adequate design criteria, methods must be developed and analyses must be made to predict performance. It is not the purpose of this paper to present a lengthy review of analytical studies of vehicle, human, and cargo dynamics. Several such reviews currently exist: Bekker, Bogdanoff and Kozin, Roach, Sattinger on vehicles [1-6]; Horneck, Boettcher, and Simons on humans [7]; and many others. These analyses in one form or another are dependent on the assumption of forces imposed on vehicle(s) traveling cross country. The validity of these assumptions and the use of the methodology developed can be proved only by an extensive collection of accurate information on the geometric characteristics of the terrain over which vehicles must operate.

This paper deals with the measurement of terrain profiles for the purpose of providing power spectral density distributions for use in related dynamic analysis. The need for this type of information is evidenced by the numerous reports lamenting the fact that so little

work has been done in characterizing ground roughness statistically.

THE PROBLEM - TO DEFINE ROUGHNESS

Roughness as applied to vehicle design has been a matter of opinion rather than one of definition. While specifications exist and are hopefully evoked regarding design and construction of highways, these usually resolve into measurements of divergence from a given chord length, or essentially a measure of permissible curvature.

What is needed now for the military designer is a definition of off-road roughness. The definition should include all typical terrain traverses over which a vehicle might be called upon to travel. Perhaps at this time we need to "define" the definition. We hold as a postulate—yet to be proved by extensive traverses and their analysis—that similar earth surfaces, when subjected to similar forces of nature, will erode, corrode, and otherwise be convoluted in a similar manner. Thus, for example, all areas having a clay soil of like consistency, covered by similar herbal growth and having the same wind and rain, will, perforce, erode in a like manner; and so for all other geological formations. This premise does not seem unreasonable as we mentally characterize terrain into a rather limited number of types.

It seems reasonable, then, that we may find a "double handful" of terrain roughness configurations that typify, say, 95 percent of all terrains extant.

In looking at "roughness," we find that we must further define or perhaps delimit those discontinuities that we wish to consider. It must be recognized that roughness is a relative term—relative always to the vehicle cargo or instrument under consideration. Certainly what is "rough" for a roller bearing race is quite adequately smooth for, say, a motor truck; and for the purposes of designing a vehicle suspension, we would wish to exclude traversing hills and mountains and even gentle slopes.

What we will consider as roughness in the analysis, then, must be defined—it has no absolute meaning. If we relate the terrain roughness to the typical vehicle of today, we are considering the tires, tracks, and spring and damper systems with which we are familiar. Certainly, we would wish for a more distinct characterization. The root-mean square (rms) measurement of roughness used in many surface analyses seems to be a fair index of roughness in the sense that the divergences from the mean plane are characterized by this number. The rms is defined as the square root of the squared divergences of the terrain from the mean divergences thus:



$$\text{rms} = \left[\frac{\sum_{y=0}^{y=y_n} (y_n - y_m)^2}{n} \right]^{1/2}$$

It is also important to know not only the height of the bumps, which in an average way is indexed by the rms, but also by the frequency of occurrence. The number of bumps per mile allows the vehicle designer to determine the number of stress reversals that might be expected in the time that the vehicle is traversing this particular terrain. The number of reversals of the terrain can be estimated statistically or measured and averaged for a particular terrain. Of course, the actual number of stress reversals is the result of the vehicle's response to the terrain, and this must be computed.

While the root-mean-square is of value as an index, the vehicle responds to terrain, not to indices; therefore, after characterization and description, we must then reconstitute a terrain profile that is truly (statistically) representative.

Now, let us examine a terrain, the Belgian Block Course A, Section I (a typical test course), at Aberdeen Proving Ground, Maryland. A rod-and-level traverse was run on this course. Elevations were read every foot for 307 feet. The course is substantially level, varying from an elevation of 0.67 feet to 1.22 feet over the entire course. Figure 1 gives the distributions of elevations as measured and the normal distribution curve having the same distribution. It will be noticed that the curve is hardly Gaussian, and the probability of this set of points chosen from the infinite set of points within the population could have been described from a normal Gaussian distribution,

$$y = \frac{N}{\sigma \sqrt{2\pi}} e^{-\frac{x^2}{2\sigma^2}} \quad (2)$$

less than 0.4 percent of the time based on x^2 (not a highly reliable estimate).

Examination of terrain strictly by elevation distribution does not seem to be appropriate. As we suspect, if ever a terrain had some

random characteristics, it would be the Belgian Block Course. We would suspect that, because of the block size or the methods of laying it, certain periodic functions would occur. The classical analysis that would result in a continuous aperiodic system would be the Fourier integral equation,

$$y(t) = \int_0^\infty a_p \omega \cos \omega t d\omega + \int_0^\infty b_p (\omega) \sin \omega t d\omega, \quad (3)$$

where a_p and b_p are defined as

$$a_p(\omega) = \frac{1}{\pi} \int_{-\infty}^{\infty} y_p(t) \cos \omega t dt$$

$$b_p(\omega) = \frac{1}{\pi} \int_{-\infty}^{\infty} y_p(t) \sin \omega t dt .$$

By dividing the profile record into regions and analyzing each region, a continuous profile may be described exactly. The difficulty in evaluating a_p and b_p from the profile record is

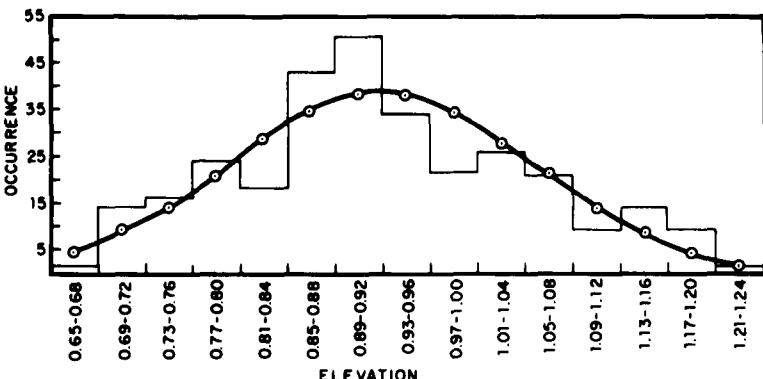


Fig. 1 - Distribution of elevation measured
(Belgian Block A course)

not precise, and the extension of this analysis beyond the limits of the time interval is impossible, as the value $y(t)$ is identically zero beyond these limits.

If we consider the terrain profile in statistical terms and represent the profile as an aperiodic system having a continuous energy spectrum, it is possible to describe the terrain in a realistic manner. Work by Pierson [8], Tukey [9], and St. Denis [10] with respect to ocean waves, noise, and sampling theory suggest a method by which this problem might be solved.

While the profile may not be strictly Gaussian, the points can be taken from the power spectral record by Gaussian selection; such selection would allow statistical tractability.

PHYSICAL MEASUREMENT OF TERRAIN

It appears that in the analysis of the terrain profile, we are faced with two problems. The first problem concerns the possibility that the several profiles can be typified. This really is the crux of the whole idea. This can be done only by the analysis and categorization of a rather large sample of terrain profiles properly correlated with both geological and meteorological information.

The collection of this profile data becomes a mammoth task, unless some reasonable approach is taken to the delineation of topographical areas. In the past, the military has utilized the terms "desert," "subartic," "tropic," "temperate," etc. Though these terms are too generalized, they can be used if a specific

number of reoccurring land forms typify an area. If this approach is satisfactory, then the problem of gathering data becomes more reasonable. We can obtain specific sampling of reoccurring land forms by tying the microgeometry to any system that tends to classify the macrogeometry. The Waterways Experiment Station of the Corps of Engineers is currently engaged in such a classification [11].

Many devices have been built for recording pavement roughness [12]. These can be classified as follows:

1. Devices that plot a profile from level notes, or devices which utilize a similar reference plane.
2. Devices that measure deviations with a straight edge laid on the surface; the reference plane corresponds to the two highest spots within the length of the straight edge.
3. A mobile beam with a single wheel at either end and a center recording wheel free to move vertically.
4. Devices that record vertical oscillations of a wheel with reference to a suspended weight or mass (the U. S. Bureau of Public Roads built such a device using the front axle of an automobile).
5. Devices in which the reference plane represents the mean of a number of points of contact with the road surface.
6. Devices that measure the slopes of the profile by measuring the angle generated by two wheels some distance apart with reference to a vertical plane (slope integration method).

All the devices use a continuously changing plane of reference, and some require a transposition of data into a usable form. It appears that a profile-measuring system should be accurate, reliable, and mobile and should have a data output that can be fed directly to a computer.

Investigation of various systems that have been tried indicated that a new system developed by Wright Air Development Division for measuring airport runway roughness could be modified to provide the system required.

The system consists of two parts: the collimator, which projects a highly collimated light beam toward a profilometer, and a profilometer that is equipped with a photoelectric sensor. As the profilometer moves, the sensor is held centered on the light beam by a servosystem. A direct drive introduces the profile variations between the surface and sensor position generating a usable output.

The system will be capable of measuring elevations at 6-inch intervals at speeds up to 5 miles per hour. The collimator includes a high-intensity light source (Fig. 2) and a collimating lens system which is capable of projecting a well-defined beam of light for approximately 2500 feet under reasonable atmospheric conditions. This light source establishes a reference plane.

The profilometer (Fig. 3) consists of a wheel cam follower, which follows the terrain profile, and a photoelectric sensor (Fig. 4), which is kept vertically centered on the light source by action of the servosystem. The distance between the wheel and the sensor is thus a direct measure of the elevation of the profile with respect to the horizontal reference beam. At 6-inch intervals, a switch, driven by the profile wheel follower, causes data to be read out of the encoder into the digitizer and onto a paper tape. This punched tape can then be used directly on existing data-processing equipment. Tests on runways have indicated that profile measurements made by the system were within ± 0.2 inch of those made by rod and transit.

It will be recognized that the determination of an adequate sample of terrain is a task in itself. All terrain is, to an extent, oriented in its features. For example, a plowed field is certainly rougher when the traverse crosses the furrows than when it runs along, or parallel to, the furrows. In like manner, the fact that surface water erodes in patterns roughly parallel to its flow vector shows that care must be taken to have our results truly descriptive.

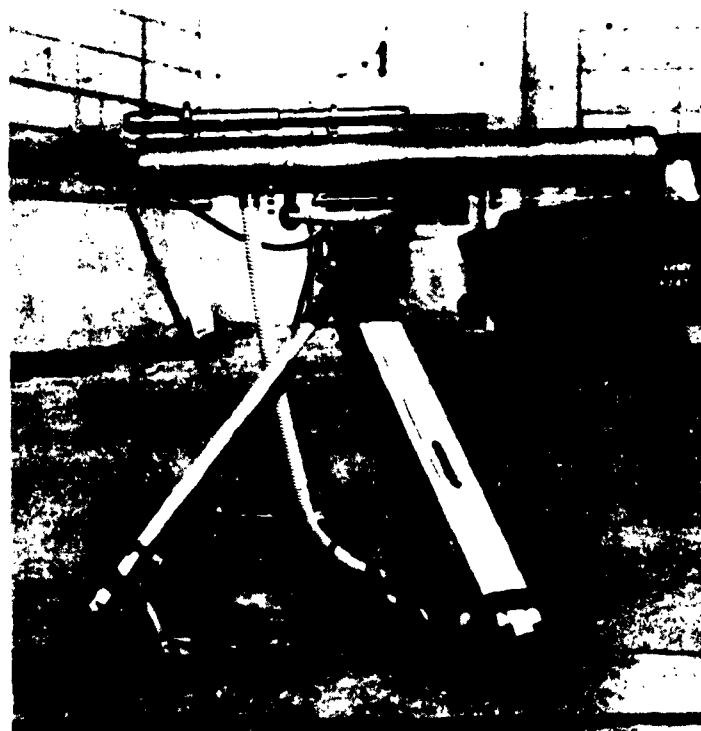


Fig. 2 - Collimated light source

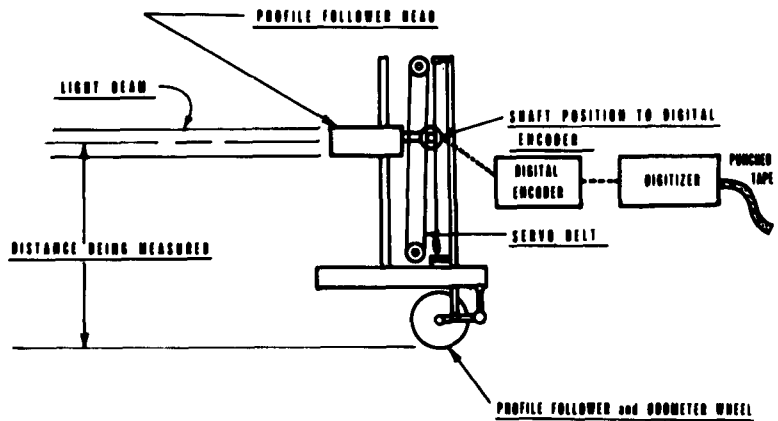


Fig. 3. Schematic of profilometer

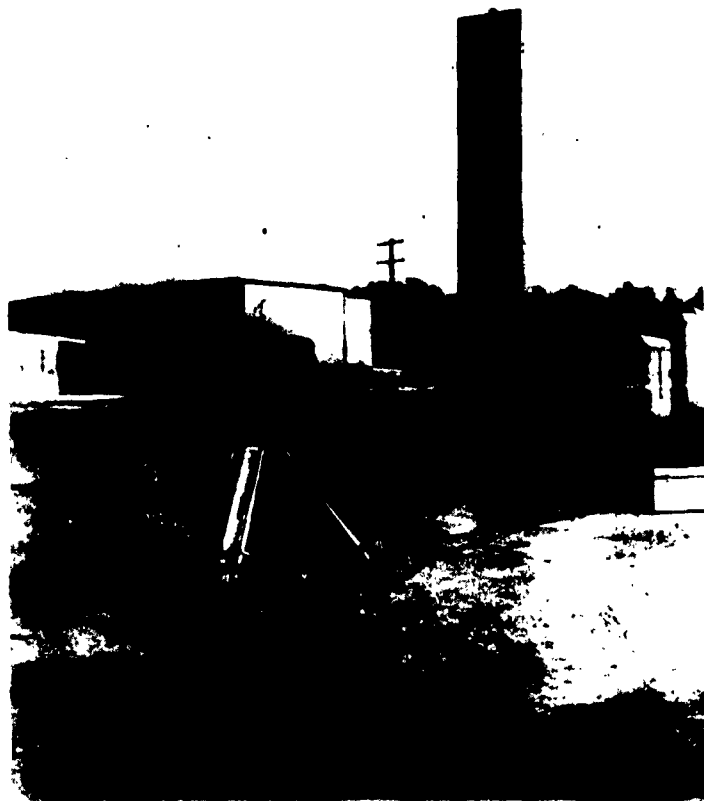


Fig. 4. Optical sensing head mounted on polecat vehicle

of all characteristics and not biased by the direction of the traverse. To eliminate this possibility and to give equal weight to each terrain convolution, the traverse should be circular or fan-shaped so that the results would constitute an orthogonal-like set.

In order that the grade of the gross traverse might be removed—and after all, we are considering roughness as distinguished from grade—we must average out the grade or, in effect, match the plane of reference so that it will be parallel to the general grade of the traverse.

Ordinates of the profile, then, to be analyzed will be taken from this reoriented base plane, the points of which now ignore the "hill" and represent the "bumps."

DETERMINATION OF POWER SPECTRA

The statisticians have given us another powerful tool in both typifying and analyzing terrain. Press and Tukey [9] point out the value of power spectra in analyzing gust loads on aircraft. The problem of bump loading of vehicles is a direct analogy. In our case, moreover, it offers an opportunity to correlate the essential features of the individual type of terrain. It is proposed that a "best-fit" curve of the power spectra of the individual terrain profile types be developed. From this "best-fit" curve, we then can reconstitute a terrain profile by existing methods discussed by St. Denis [10]. These will be discussed later in this paper.

The following has been taken largely from Tukey's analysis and adapted to our problem only by nomenclature and definition. First, the recorded profile is divided into Δt intervals, with care being taken to choose small enough intervals to insure that appreciable power does not exist at frequencies above the highest resolved, or Nyquist frequency,

$$\omega_{ny} = \frac{\pi}{\Delta t} \quad (4)$$

Dividing the profile record into $x_1, x_2, x_3, \dots, x_n$, the values of the ordinates are used to produce the lagged products,

$$R_p = \frac{1}{n-p} \sum_{q=1}^{n-p} x_q x_{q+p} \quad (p = 0, 1, \dots, m). \quad (5)$$

The values of p indicate the number of lagged intervals. Since this equation must recognize

that the mean value of the x 's is not zero, the modified equation, as follows, should be used:

$$R_p = \frac{\sum_{q=1}^{n-p} x_q x_{q+p}}{n-p} - \frac{\sum_{q=1}^{n-p} x_q}{(n-p)} \sum_{q=1}^{n-p} x_{q+p} \quad (6)$$

Then take the Fourier cosine transform of the form,

$$L_h = \frac{2\Delta t}{\pi} \sum_{p=0}^m \epsilon_p \cos \frac{np\pi}{m} R_p, \quad (7)$$

where

$$\epsilon_p = \begin{cases} 1 & \text{if } 0 < p < m \\ 1/2 & \text{if } p = 0 \text{ or } m \end{cases},$$

having the dimension of power per radian per second.

Pierson [9] points out the fallacy of reducing Δt in order to get more data points. Where, in Pierson's example, N has about 750 points, $m = 30$ and there are 50 degrees of freedom. If Δt is halved, in order to obtain the same resolution the m must be equal to 60 and the degrees of freedom must remain approximately the same, that is, 50. Therefore, it appears that no great benefits are obtained by the inclusion of a multiplicity of points taken from the same data time sequence by interpolating the sequence beyond a reasonable point, this reasonable point being determined by experience and the Nyquist frequency. In general, m will lie between 10 and 60.

A question is here raised (and not answered) as to the efficacy of whitening the raw data prior to developing the power spectral density. A number of aeronautical engineers concerned with this problem are of the opinion that such averaging techniques tend to mask the severe convolutions that will exist. In general, it was felt that 3 to 5 points of data taken per cycle ($\omega/3$) would be adequate to describe the actual power spectra.

Smoothing of the results of the cosine transform may be accomplished by the von Hann method; that is,

$$\begin{aligned} \Phi_o &= \frac{1}{2} L_o + \frac{1}{2} L_1 \\ \Phi_h &= \frac{1}{2} L_{h-1} + \frac{1}{2} L_h + \frac{1}{2} L_{h+1} \quad 1 \leq h \leq m-1 \\ \Phi_m &= \frac{1}{2} L_{m-1} + \frac{1}{2} L_m \end{aligned} \quad (8)$$

where

$$\Phi_h = \Phi \left(\omega = \frac{h\pi}{m\Delta t} \right).$$

Then

$$\omega = \frac{\pi h}{m\Delta t} \quad (9)$$

and

$$(\Phi \omega_h)^2 = \frac{\Phi n \Delta t m}{\pi}. \quad (10)$$

The curve of Fig. 5 gives an indication of the form of Φ_h versus h or the power spectra.

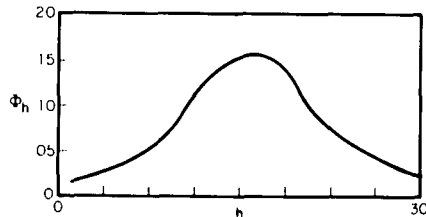


Fig. 5. Power spectra of Belgian Block A Course

After getting a "best-fit" curve of these spectra for individual terrain types, we can analyze vehicles by comparison of the frequency response characteristics with the reconstituted continuously generated profile.

"TYPICAL" PROFILE

By considering the terrain profile in statistical terms and representing it as an aperiodic

system having a given continuous energy spectrum, it is possible to reconstitute the profile for use in analysis. This must be a continuous function. Use of the Lebesque integral is suggested by St. Denis [10], where

$$y(t) = \int_0^\infty \cos [\omega t + \epsilon(\omega)] \cdot \sqrt{[y_m(\omega)]^2} d\omega, \quad (11)$$

which is not strictly integrable. Instead, a partial sum is proposed, which, in the limit, approaches the Lebesque integral.

$$y(t) = \sum_{n=0}^q \cos [\omega_{2n+1} t + \epsilon(\omega_{2n+1})] \cdot \sqrt{\Phi(\omega_{2n+1})^2 (\omega_{2n+2} - \omega_{2n})}. \quad (12)$$

$$\sqrt{\Phi(\omega_{2n+1})^2 (\omega_{2n+2} - \omega_{2n})}.$$

$\epsilon(\omega)$ is chosen at random in accordance with the equation

$$P[0 < \epsilon(\omega) < 2\pi a] = a \quad (13)$$

with $0 \leq a \leq 1$.

$[\Phi \omega_{2n+1}]^2$ is chosen from the power spectral curve for each $2n$ interval.

Such an analysis may give to the designer the type of loading or forcing functions that so long have been a tool of the aircraft designer. In this regard, it is to be noted that Bogdanoff and Kozin [1-3] have developed the linear response operators for a number of simple vehicles. The previously derived profile functions can be applied directly to computations on analogue-type computers, and it is from this use that the maximum value can be anticipated. By such analysis procedures, the design of vehicle and packaging may be simplified and reliability enhanced, and the degree of testing may be reduced.

REFERENCES

- [1] M. G. Bekker, Theory of Land Locomotion, The University of Michigan Press, Ann Arbor, Michigan, 1956.
- [2] J. L. Bogdanoff, and F. Kozin, "Behavior of a Linear One-Degree of Freedom Vehicle Moving With Constant Velocity on a Stationary Gaussian Random Track," Report 48, Land Locomotion Research Laboratory, Detroit Arsenal, Center Line, Michigan, February 1959.
- [3] J. L. Bogdanoff, and F. Kozin, "On the Behavior of a Linear Two-Degree of Freedom Vehicle Moving With Constant Velocity on a Stationary Random Track," Report 56, Land Locomotion Research Laboratory, Detroit Arsenal, Center Line, Michigan, November 1959.
- [4] J. L. Bogdanoff, and F. Kozin, "On the Statistical Analysis of the Motion of Some Simple Vehicles Moving on a Random

- Track," Report 65, November 1959, and Report 66, April 1960, Detroit Arsenal, Center Line, Michigan.
- [5] Charles D. Roach, "Equations for Calculating the Resonance Frequencies of Four-Wheel Vehicles Without Spring Suspension," RTM 29, U. S. Army Transportation Research Command, Fort Eustis, Virginia, July 1959.
- [6] F. J. Sattinger, "Methods of Evaluating the Effects of Terrain Geometry on Vehicle Mobility," Proceedings of the Interservice Vehicle Mobility Symposium, conducted by the Office of Ordnance Research, U. S. Army, 18-20 April 1955.
- [7] R. J. Hornick, C. A. Boettcher, and A. K. Simons, "The Effect of Low Frequency, High Amplitude, Whole Body, Longitudinal and Transverse Vibration Upon Human Performance," Final Report, Bostrom Research Laboratories, Milwaukee, Wisconsin, July 1961.
- [8] W. J. Pierson, Jr., and W. Marks, "The Power Spectrum Analysis of Ocean Wave Records," Transactions, American Geophysical Union, Volume 33, Number 6, December 1952.
- [9] H. Press, and J. W. Tukey, Power Spectral Methods of Analysis and Application in Airplane Dynamics, Bell Telephone System Monograph 2606.
- [10] M. St. Denis, and W. J. Pierson, Jr., "On the Motion of Ships in Confused Seas," Transactions, The Society of Naval Architects and Marine Engineers, Volume 61, 1953.
- [11] A Technique for Preparing Desert Terrain Analogs, Handbook, Waterways Experiment Station Technical Report No. 3-506, May 1959.
- [12] F. N. Hveem, "Devices for Recording and Evaluating Pavement Roughness," Bulletin 264, Highway Research Board, Washington, D. C., 1960.

BIBLIOGRAPHY

1. D. F. Turner, and R. S. Brown, "Automatic Runway Profile Measuring Instrumentation," WADC Technical Report, Wright Air Development Division, Wright-Patterson Air Force Base, Ohio, May 1960.*
2. W. F. Lovitt, and H. F. Holtzclaw, Statistics, Prentice-Hall, Inc., New York, 1931.
3. H. U. Sverdrup, and W. H. Munk, "Wind, Sea and Swell: Theory of Relations for Forecasting," Hydrographic Office Publication 601, 1947.
4. A. E. Waugh, Laboratory Manual and Problems for Elements of Statistical Method, McGraw-Hill Book Company, Inc., New York, 1944.
5. N. Weiner, Nonlinear Problems in Random Theory, John Wiley and Sons, Inc., New York, 1958.

*Working papers not available for distribution.

* * *

RAIL TRANSPORT DYNAMIC ENVIRONMENT

R. W. Hager, R. L. Partington, and R. J. Leistikow
The Boeing Company, Seattle, Washington

A series of tests to determine and verify environment for use in the design of the Mobile Minuteman missile cars are described. Factors to be considered in conducting the tests, instrumentation, recording and data reduction techniques as well as detailed results are presented. The acceptability of the environment for different applications will be established.

INTRODUCTION

The dynamic environment encountered during rail transportation is of a complex nature but consists primarily of two general types: (1) the relatively high-level longitudinal shocks occurring during humping or coupling and (2) the vertical and lateral excitation encountered during rail travel.

The environment encountered during coupling or humping is a transient occurrence dependent upon the speed of impact, the configuration of cars impacted, and the undercarriage design of the car being studied. Establishment of this environment is based on defining a rational limiting or designing impact speed and car configuration and the selection of an under-frame design.

The environment encountered during rail travel, however, is more complex and will be the subject of this paper. Although it is relatively simple to state the environment in general or subjective terms, the determination of the actual levels and characteristics presents many problems both from the data acquisition and data interpretation standpoints. To be useful the data must show the level, frequency content, and general characteristics of the dynamic environment. In short, give a description of the actual time history which can be interpreted and applied in the analysis of a new design.

If the package to be transported is relatively small, the response will not significantly change the rail car environment, and data from the floor of the type of rail car to be used is valid for the package design. Suitable data of this type is available. However, if the package is large or the whole car is being designed to

protect the package, as in the case of the Mobile Minuteman System, then the input environment must be more general. The data required in this case is a definition of the rail roughness, independent of the particular rail car design yet inclusive of the response of the rail, tie, and soil to the car travel. Data of this type has not been available.

During 1960 the Boeing Company conducted a series of tests to determine dynamic environment of this type for use in design analysis of the Mobile Minuteman Cars.

DATA ACQUISITION

The first consideration was to select the type of data and the location at which it was to be acquired. The measurement of the rail contour, similar to that successfully used in measuring road roughness for wheeled vehicles, could not be used because the rail contour changes significantly under the high axle loads. The rail car floor was not suitable either, as the resulting environment would be dictated by the suspension system characteristics of the rail car. Therefore as the required measurement is the absolute vertical and lateral motion of the contact point between rail car and rail, the most suitable location for obtaining this data is the rail car axle. This location represents an optimum from practical instrumentation aspects and since the axle incorporates the effects of a rolling wheel the data requires the least interpretation for use in analyses. Absolute displacement of the axle is a parameter which could in theory be measured but requires the establishment of a reference plane which is not practical. Axle acceleration was selected as it represents the most practical

method from instrumentation considerations as well as being easily interpreted in analyses.

The second consideration was the selection of a data recording method. To obtain any reasonable sample of the environment, a considerable amount of data must be recorded. Because of the complex nature of the environment the recorded data would require some analysis and reduction. In order to meet these two requirements magnetic tape was selected as the recording method. An Ampex Model 300 Tape Recorder was selected because it was easily transportable and rugged enough to withstand environment levels which might be encountered during the test.

The rail cars used for the tests were selected primarily on their availability and their conformity in size, weight, and suspension characteristics to the Mobile Minuteman rail cars. As will be discussed later the selection of the car type is relatively unimportant to the axle dynamic environment.

TESTS

Four separate rail car tests were conducted. Two tests were conducted using baggage cars to determine the range of environment, and to obtain initial environmental data with which to conduct missile car design analyses. Acceleration environment data was then obtained during two evaluation and qualification tests of the preprototype missile car, to verify the initial data and to obtain additional information. The total distance covered during the tests was approximately 4500 miles and data was recorded for approximately 1600 miles of travel. These tests are described in more detail as follows.

Test No. 1

The purpose of Test No. 1, conducted in the Seattle area, was to define the limits of the environment. The plan called for testing a heavy car at various speeds on both good and poor track. For this test, a six-axle Great Northern Railroad baggage car was selected. The car was ballasted to a total loaded weight of 200,000 pounds. The suspension system had a 6-1/2-inch static deflection when loaded.

The first portion of this test was run with 7 Statham Model A-5-A 50g accelerometers located as shown in Fig. 1. CEC Model 113B carrier amplifiers and the Ampex Model 300 tape recorder were used. The system had a linear output to 300 cps. The amplifiers were shock mounted on a pallet and the tape recorder

TEST NO. 1 SEATTLE, WN.

LOCATION	RANGE	RESP.	DIRECTION
1	*	*	VERTICAL
2			LATERAL
3			VERTICAL
4			VERTICAL
5			LATERAL
6			LATERAL
7			VERTICAL

* 50 G 0-300 CPS ACCELEROMETERS
WERE USED FOR FIRST RUNS

12 G 0-100 CPS ACCELEROMETERS
WERE USED FOR OTHER RUNS

TEST NO. 2 BERWICK, PA.

LOCATION	RANGE	RESP.	DIRECTION
1	50	0 - 500	
2	50	0 - 500	
3	20	0 - 500	
4	20	0 - 500	
5	20	0 - 500	
6	20	0 - 500	
7	20	0 - 500	
8	20	0 - 500	

Fig. 1 - Location and particulars of accelerometers for Tests 1 and 2

was shock mounted within a steel frame attached to the car floor. The instrumented car was attached as part of a high-speed Great Northern passenger train. Data was recorded continuously at speeds up to 60 mph over main line track. Approximately 150 miles of travel were recorded.

The second portion of the test was run with 7 Miller 402-C accelerometers with 0 to 12g rating and flat response from 0 to 100 cps. Miller CD-2 amplifiers and the Ampex 300 tape recorder were used. For this portion of the test, the instrumented car was first attached to a slow-speed freight train. Data was recorded continuously over 180 miles of main line and branch line track. The branch line track was generally in poor condition and maximum speed was limited to 40 mph. The instrumented car was then attached to both high-speed passenger

and freight trains. Speeds up to 70 mph were encountered and data was recorded continuously over approximately 300 miles of main line track in top condition.

By referring to the test log of conditions encountered, the data tapes containing the highest level environment were determined. These data tapes were then played back on an oscilloscope and specific areas selected for analysis. A difficulty arose in this test which caused erroneous data and resulted in voiding data below approximately 10 cps. The motor-generator set supplying power to the recording equipment was found to vary slightly in frequency, which caused fluctuations in the magnetic tape speed. When the tape was played back, this fluctuation appeared as low-frequency data. In subsequent tests this problem was alleviated by using the motor-generator to drive a constant frequency power source which in turn supplied power to the tape recorder.

Test No. 2

The purpose of Test No. 2 was to obtain data on the acceleration environment during the evaluation test of preprototype command car rolling stock. This test was conducted by American Car and Foundry Division of ACF Industries. An Atlantic Coast Line Baggage Car was used for the test because of its similarity to the proposed command car in size, weight, and running gear. The total loaded weight was 173,000 pounds and the loaded suspension deflection was 8.5 inches.

For this test, two Statham 50g and 6 Statham 20g model A-5-A accelerometers were located as shown in Fig. 1. CEC 113-B carrier amplifiers and the Ampex model 300 recorder were used giving linear outputs to 300 cps. The shock mounted pallet board was eliminated and the "bungee" cord support for the tape recorder was made stiffer to decrease the low-frequency motion environment. All recording equipment was mounted in a separate instrumentation car.

One test was made by recording data continuously while running over mainline and branchline tracks at speeds up to 60 mph. A second run was made recording only specific predetermined conditions such as switches, bridges, crossings, and different types of curves at various speeds. The test track and areas for recording were selected by ACF test engineers to give the most severe conditions. This same portion of track is used by ACF to check out their rolling stock. Data were taken for a total of 150 miles of track.

Areas for detailed data analysis were again selected from the test log and by viewing the data on the oscilloscope. Analysis of shorted input channels on the wave form analyzer showed that the low-frequency problem of the preceding test had been alleviated but the fluctuations were still too great to give good data below approximately 10 cps. This problem was subsequently traced to a mechanical oscillation in the recorder tape drive system induced by the environment in the instrument car.

Test No. 3

During an evaluation test of the preprototype missile car at Berwick, Pennsylvania, acceleration data were obtained both on the axles and on the car floor to verify the proposed design. The preprototype missile car, built by American Car and Foundry Division of ACF Industries, accurately represented the proposed missile car in weight, c.g. location, and suspension system. The gross weight of the car and missile was 315,000 pounds and the total static deflection of the suspension was 10.15 inches.

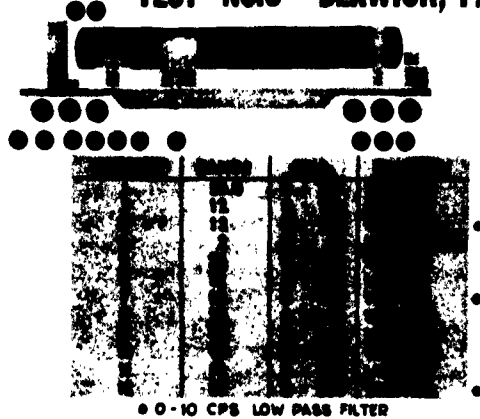
A total of 12 accelerometers ranging from 2g to 25g, with locations as shown in Fig. 2, were used to insure that both high and low level data would be obtained. Car axles were instrumented with Statham A-5A 25g accelerometers to record peak values and with Miller 402-C 12g accelerometers with 10 cps low pass filters to record low level data.

For this test the low frequency recording problem was substantially decreased by minor modifications to the drive motor mounting and by adding foam rubber around the recorder, in addition to the "bungee" cord, to decrease the effect of the environment. A special test train was used and the recording equipment was mounted in a separate car. Sections of track were selected and recorded to give the maximum environment as in the preceding test. The total data taken represented about 150 miles of track. All data was reviewed by condensing it on slow speed oscillograms and by selecting portions of data showing high accelerations for analysis.

Test No. 4

Acceleration data were obtained on the preprototype missile car during the Strategic Air Command train test to obtain environment over different rail networks and to substantiate previous data.

TEST NO.3 BERWICK, PA.



TEST NO.4 S.A.C. TRAIN

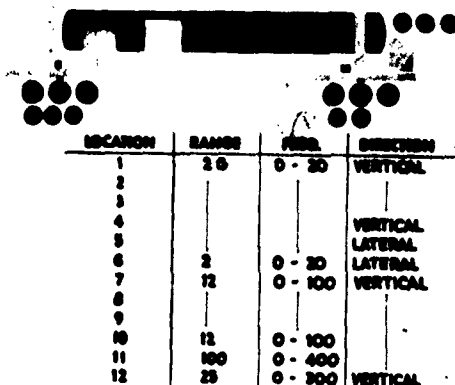


Fig. 2 - Location and particulars of accelerometers for Tests 3 and 4

The preprototype car was instrumented with 12 accelerometers placed on the car floor, spring plank, and axle. Statham 2g, 25g, and 100g and Miller 402-C 12g accelerometers were located as shown in Fig. 2. A CEC 113B amplifier and the Ampex 300 recorder were used. Recording equipment was mounted in a separate instrumentation car and the recorder was shock mounted with foam rubber and "bungee" cord as in the preceding test.

The preprototype car and instrumentation cars were part of the Minuteman Strategic Air Command train which traveled approximately 3300 miles through Nevada, California, Oregon, Washington, and Idaho. The trip represented typical running conditions for the proposed train and data were taken intermittently throughout the test to sample all types of track at various speeds. Data were recorded for about 700 miles of track at speeds up to 70 mph.

Areas for detailed reduction were selected by condensing all the magnetic tapes onto slow speed oscilloscopes and then selecting areas of high acceleration.

DATA REDUCTION

The axle vertical acceleration data measured showed the environment to consist of relatively low level continuous vibration with high transient levels resulting from the wheel passing over a track discontinuity such as a switch, cross-over, or rail joint. The levels were highest for a major discontinuity such as a switch. A somewhat lower level occurred each time the wheel passed over a rail joint. Figure 3 shows the vertical acceleration data as measured for the front truck axle and the rear truck axle on the same side for a switch at a speed of 60 mph during Railroad Test No. 3. This figure shows the similarity of environment at the front and rear axles and the time difference between the front axle crossing a switch and the rear axle crossing the same switch. A comparison of accelerations at the right and left ends of the same axle showed that both ends felt accelerations of nearly equal magnitude as the car passed over a switch, although the accelerations were not necessarily of the same frequency or in phase.

As the most significant portion of the axle environment data is transient in nature, data reduction methods which average the environment over a period of time will not obtain data suitable for design analyses. The method selected for reduction of the data consisted of replaying the selected sections of the tape recorded acceleration data through 7 bandpass filters with center frequencies of 4, 6, 8, 10, 20, 30, and 40 cps and recording the filtered data on an oscilloscope. The bandpass filters were

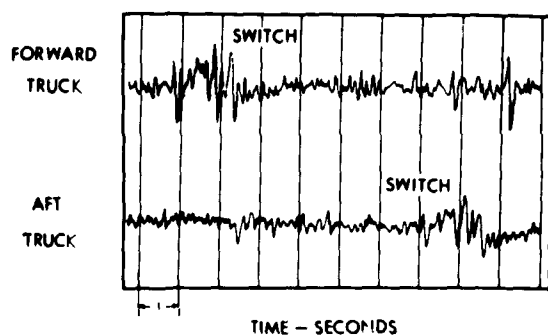


Fig. 3 - Comparison of axle vertical acceleration at fore and aft trucks

formed by combining a low pass and a high pass filter such that the ratio of output to input was reduced by 6 db at the center frequency and was reduced 24 db at one octave on either side. The filters were designed to minimize the distortion of the signal due to filter ringing. This was demonstrated on several records when the magnitude of a single-frequency component could be determined from the trace of more than one bandpass filter.

In order to locate the major resonances on the magnetic tape, the tapes were edited visually on an oscilloscope or were replayed through the bandpass filters and recorded at a low speed on an oscillograph. By these methods, a total of 15 switches or other events were selected from the Test No. 3 data and 12 events selected from the Test No. 4 data.

The results of playing a section of data from Test No. 3 through the filters is shown in Fig. 4. As the original recorded data had a 10-cps cutoff frequency filter to prevent overdriving the accelerometers and tape with high frequencies, each bandpass has a different calibration. As can be seen from the record, there are several relatively constant sinusoidal components at each major occurrence with durations of 4 to 6 cycles. The method of reduction used was to average the 4 to 6 cycles of maximum amplitude for each significant frequency.

Figure 5 shows the vertical axle acceleration spectrum for the single occurrence shown in Fig. 4. It should be noted that the spectrum is not a continuous curve, but is composed of discrete frequency components. An harmonic

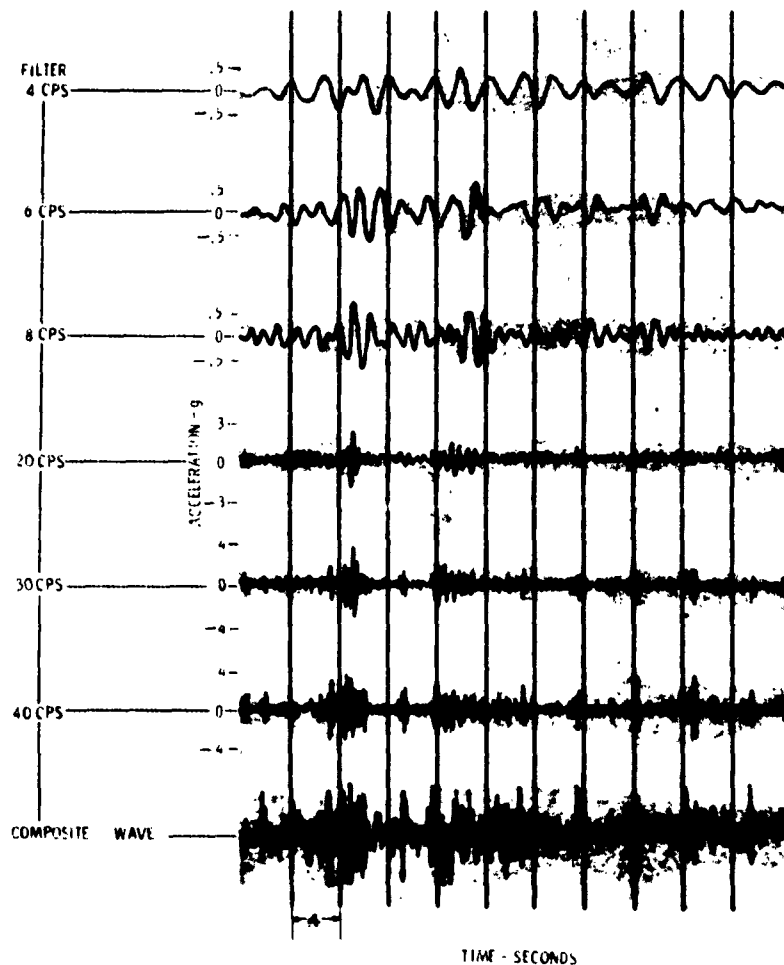


Fig. 4 - Filtered axle vertical acceleration

analysis was made by a Davies Analyzer of 1.5 seconds of data which contained the 6 highest peaks of the 4-cps oscillation. Figure 6 shows the comparison between the electronic harmonic analysis (Davies) and the averaging of 4 to 6 oscillations obtained from the oscillograph record shown in Fig. 4. It is apparent that the Davies analysis averages the accelerations over the time length of the record being analyzed, and is therefore not suitable for obtaining maximum environment levels.

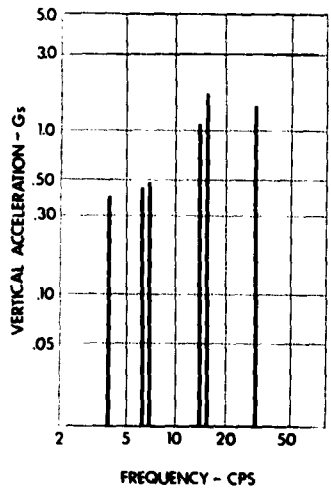


Fig. 5 - Axle vertical acceleration spectrum for a single occurrence - 4 to 6 cycle average

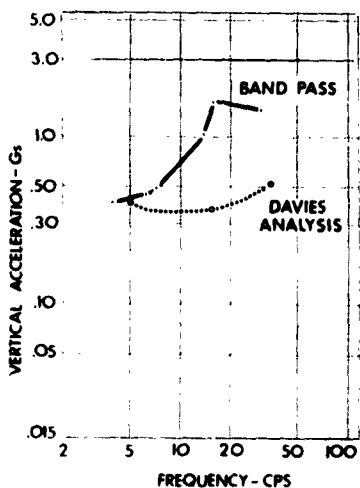


Fig. 6 - Comparison of data reduction methods. Bandpass filters versus Davies analysis

SUMMARY OF DATA AND DISCUSSION

From the 27 major occurrences selected a series of spectra similar to that shown in Fig. 5 were obtained. The resulting spectra indicated that there were no predominate frequency common to all occurrences and, furthermore, an event which produced a maximum at one frequency would not, necessarily, produce maximum accelerations at other frequencies. Therefore, if an envelope were drawn through the peaks of the spectra, the envelope could be used to determine the maximum possible acceleration for any frequency component. The axle vertical acceleration envelope is shown in Fig. 7 and the axle lateral acceleration envelope is shown in Fig. 8.

The frequency range of the axle acceleration envelopes is that normally associated with a car and package structure. Due to instrumentation acceleration range limitations, the components below 4 cps could not be determined. These lower frequency components would be necessary if the car trucks were to be designed. For most applications, however, only the structure above the trucks will be under design and lower frequencies near the suspension frequency will be avoided.

Although the majority of the data analyzed was obtained on Test Nos. 3 and 4, axle acceleration from the other tests showed that the frequency components, acceleration levels and time history remained substantially the same even though the test site and test car were different. For instance the rail car axle acceleration envelopes were derived from data measured on rail cars having wheel loads of different magnitudes, 16,700 to 26,200 pounds per wheel, but this had no significant effect on the environment. Therefore, the axle environment curves are applicable to other rail cars having wheel loads within or near the tested range.

The longitudinal accelerations as measured at the axle cannot be extrapolated to the car floor as there is a more significant input through the coupler during rail travel. Undercarriage design and location in the train are so significant that no specific environment can be established. For the Minuteman short train configuration the levels are so low (approximately 0.10g for the preprototype missile car) that humping or coupling is the only significant longitudinal environment.

The lateral and vertical acceleration data measured on the preprototype missile car floor were reduced in the same manner as the axle

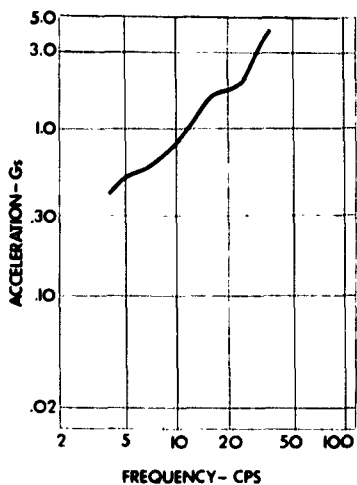


Fig. 7 - Axle vertical acceleration envelope

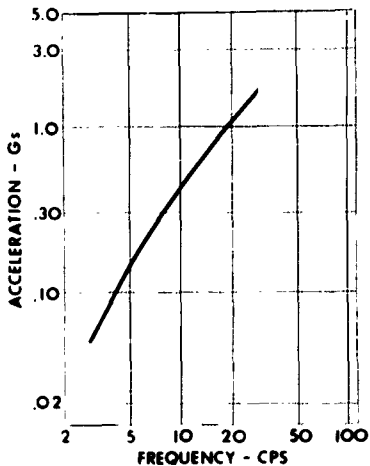


Fig. 8 - Axle lateral acceleration envelope

accelerations. The envelopes of maximum accelerations are shown in Fig. 9. These envelopes show the high degree of isolation which can be obtained with the type of suspension used on the Mobile Minuteman missile cars.*

*The truck suspension system for the missile car consists of a combination air and coil spring system in the vertical direction and a pendulum system with snubbers in the lateral direction. Damping is provided for both directions of motion. In the longitudinal direction isolation is provided by a sliding center sill and hydraulic cushioning unit.

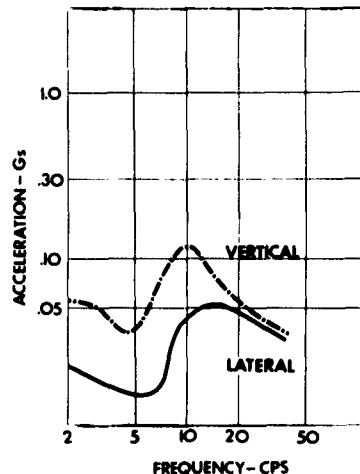


Fig. 9 - Missile car floor acceleration envelopes

ANALYTICAL APPLICATION

The purpose in obtaining the environment was to develop data with which to design the Mobile Minuteman missile cars. Preliminary data from the baggage cars were used to establish the design. The environment was verified by the data from the preprototype missile car.

The method employed in the analysis was to apply a unit sinusoidal input at all frequencies to a direct analog simulation of the complete car and missile including the rail car trucks. From the analog the structural loads, accelerations, and displacements for a unit input at each critical frequency were obtained. As the analysis was linear, these responses were multiplied by the axle environment levels for each frequency. The resulting loads are somewhat conservative, as the axle environment levels are an average of the maximum 4 to 6 cycles of acceleration rather than a continuous sinusoid as was used as input in the analysis. For a system with 6 percent of critical damping, which is reasonable for built-up structures, the response to 4 to 6 cycles is 80 percent to 90 percent of the maximum response to a continuous sinusoid. This would mean that an analysis using continuous sinusoids equal to the axle environment levels will have responses 10 percent to 25 percent greater than with a 4 to 6 cycles input. Variations were made in the dynamic parameters of suspension spring rate, damping, structural bending stiffness, etc., to arrive at an optimum design which did

not exceed missile capabilities. The environment envelope was applied to all axles at both ends of the car either in phase or out of phase. This also represents some conservatism because of the correlation between front and rear and one side of the car to the other side.

As the environment envelope represents maximum levels at each frequency, the response at each significant frequency of the car-missile system represents the maximum which will occur regardless of time. The environment as shown by Fig. 5 for a single transient occurrence is a composite of a limited number of discrete frequency sinusoids. The levels at any instant of time although possibly a maximum for one of the frequencies are less than the maximum environment at the other discrete frequencies. In addition, although one resonant response frequency of the package may coincide with a discrete frequency in the environment, the probability of more than one frequency coinciding is very small. For these reasons, and as the environment is highly transient, use of the maximum single-frequency response without addition of the responses at all frequencies is considered to be conservative.

To check the order of the conservatism associated with the simplified approach adopted, the actual measured data for one reel of tape from Test No. 4 was used as the input to the analog simulation. The maximum structural loads in the missile using this approach were approximately 90 percent of the single-frequency levels obtained from the simplified sinusoidal analysis approach. The technique of using the actual environment as an input is more complicated as it requires recording of the analog responses on tape or oscillograph and individual inspection of records to obtain the peaks. Only a limited number of channels can be checked. For design studies with a large number of variables and possible critical points to monitor, the sinusoidal approach is more appropriate.

Based on the similarity of results for a wide range of axle loads, the acceleration envelopes are considered valid for any loaded rail car. Two other rail transport designs have been established using these data. One system is a missile transporter in a piggyback

configuration and the other is a missile shipping container which is transported on a special purpose rail car. The direct analog was used for both of these studies.

For analyses in the lateral directions, the simulation of the rail car truck suspension is more complex. The system generally consists of a pendulum suspension with lateral excursions limited by bumpers which results in a nonlinear system. To be realistic, the analysis must include both lateral translation and roll motions. For the Minuteman Missile car lateral analysis, input data from the preprototype missile car floor was used. This data was for the car floor directly over the trucks and included both lateral and roll environment.

CONCLUSIONS AND RECOMMENDATIONS

The purpose of this paper was to present rail transport dynamic environment in a form suitable for general use in design analysis of large packages or complete cars. Axle environment is the most suitable data for analyses of this type as the input must be independent of the particular rail car or package design.

The maximum axle environment occurs when crossing a major rail discontinuity and consists of a limited number of discrete frequency sinusoidal components with high level durations for 4 to 6 cycles. The vertical and lateral axle acceleration envelopes represent an average of the highest 4 to 6 cycles at each frequency for all the data recorded, and are valid for any loaded rail car.

A conservative simplified analysis method using a sinusoidal input of magnitude equal to the axle acceleration envelope levels has been established and used for analysis of three rail car transport designs.

As the accelerations were recorded on magnetic tape, the actual data is still available in a form which can be analyzed for other applications. One area for which the data can be used is the determination of long-term environment for evaluation of fatigue under rail transport.

DISCUSSION

Mr. O'Hearn (Martin Co.): It seems to me that you lay yourself open to the possibility of being unconservative when you apply these single sinusoids to your simulated system. They're picked from the level on your envelope whereas if you looked at your input as a complex wave, you could have more than one sinusoid being applied simultaneously. This comes from the way you reduced your data.

Mr. Hager: Your statement is well taken, but I think that we have investigated this area quite thoroughly. There are two reasons why we feel that this system is conservative. First of all there are a limited number of frequencies to which your package can respond. Although the frequency, let's say, in a package may coincide with one of the discrete frequencies in the input spectrum, the probabilities of more than one coinciding are very small. In addition, as we pointed out, although the environment is a maximum at one frequency, it is less than this at all the other frequencies. Again I would like to point out that we felt the same way you did at first that we would have to add some of these components. In order to check this we took the actual inputs and put them into the wheels, these are the actual measured data, and got out of our analysis the actual time history of bending moment in the missile. We compared this level against the level with the sinusoidal input and we found that we were within about 90 percent of it. We realized that the sinusoidal input approach as simplified, is open to some discussion. However, we feel that the use of this approach is much better because you can gather a lot more data and make a lot more parametric studies. And we feel that it is not that unconservative.

Mr. O'Hearn. Yes, I recognize that and I think it is an easy way of performing the analysis, but you should watch for this trend. I would also like to ask, would it have been possible to make more runs on your simulated system using actual data?

Mr. Hager: The problem with using actual data in this simulation is that the output first must be recorded on tape, in order to get it, and then it must be played out on an oscillogram and checks made for the highest loadings. In the particular design we are talking about many parametric studies were required. There were a lot of data points which had to be monitored, actually on the order of 35 to 40 critical points,

both for acceleration, displacement, force and bending moment. You cannot do this very easily. It is very time consuming to use the actual data.

Mr. Padgett (General Dynamics/Pomona): I was wondering if there is any correlation between severity and velocity?

Mr. Hager: This was one of the parameters that we investigated. There is no correlation between the velocity and the acceleration data on the axle. All you can do is talk about it in general terms, the faster you are going the higher it will be. It is primarily dictated by the discontinuity that you are crossing.

Mr. Howard (General Dynamics/Pomona): Did I understand you to say that the suspension system under static load deflected 8 inches in one of your tests? Is that a total of 8 inches?

Mr. Hager: It was 8-1/2 inches and this would be the total equivalent static deformation of the system. Actually there are stops on it so it can't always go up all the way. But the equivalent static deflection of the system is 8-1/2 inches. On our preprototype missile car this deflection is actually well over 10 inches, a very soft ride system.

Mr. Noonan (David Taylor Model Basin): I was a little bit surprised when I got the impression we were skipping over the longitudinal input rather lightly. It was always my understanding that, as you did mention, the humping operation was severe. Also if your car happens to be toward the tail end of a 200-car freight train, probably one of the larger inputs would be the longitudinal input and for this reason there have been a number of car designs which include floating platforms to attenuate this.

Mr. Hager: That is correct. As I pointed out, I wasn't planning on covering the whole environment today. I think that the coupling and humping is a separate problem which has to be investigated and discussed and hopefully there will be a presentation on it at this meeting. In the case of the long train configuration it is true that if you are at the end of a very long train, say 200 cars, you have a very severe environment, associated with this in the longitudinal direction. For the short train configuration, which we tested and worked with in this particular application, the longitudinal accelerations are very low. Also, we were using cushion underframe cars all the way through in our design. So this also affects it.

Dr. Morrow (Aerospace Corp): As I understand it before you drew your envelope and while you were still interested in complex spectra you picked a sample length and performed a Fourier analysis of this sample. How did you decide on the sample length?

Mr. Hager: The sample length was taken by reviewing all the data in condensed form, either by oscilloscope or by oscillogram. From this we picked the major occurrences. This data was then fed through the filters and the results from the filters played out on an oscillograph. We then took the predominant frequency components that showed up and these in general were say of 4 to 6 cycles duration. Then we averaged these acceleration-wise. Does this answer your question?

Dr. Morrow: Not quite. That is if you are getting a Fourier spectrum for something which is essentially a shock type phenomenon, I'd expect you'd have to pick some sample to use as a basis for this-some duration.

Mr. Hager: Well, again we were looking for the peak values of acceleration. For our particular work we are looking for the maximum responses that we can obtain due to rail travel. For this we selected 4 to 6 cycle lengths for our input data.

Dr. Morrow: Four to Six?

Mr. Hager: Yes.

Dr. Morrow: Well the g values you get will depend on the duration you pick.

Mr. Hager: That's correct. If we picked a very long duration you would find that the acceleration levels would be very low, based on an rms. This would tend to mislead you somewhat in the design analysis that you were conducting unless you were worried about such things as fatigue. In our case we were worried about peak loadings, and we feel that the 4 to 6 cycles will produce about, say, 80 to 90 percent of the maximum response that a continuous sinusoid will produce. We felt that this was very adequate for our use.

Dr. Morrow: You could put this on a more absolute basis by using a Fourier spectrum of a continuous variety or a shock spectrum?

Mr. Hager: Yes, that's correct.

Mr. Ferguson (Association of Am. RR Res. Center): Did I understand you to indicate that four cycles per second was your minimum response on this equipment?

Mr. Hager: No. There, of course, are responses, particularly of the rail car and truck suspension which are much lower, down below 1 cps. The limitation of our data at this time was purely due to the accelerometers. Getting adequate, correct data below 4 cps was very difficult, except for the car floor where we had a little different range of accelerometers and were able to go down to about 3. We did not cover the acceleration that would be associated with the predominate response in the suspension system.

Mr. Ferguson: One of the important dynamic actions we have found in ordinary railroad equipment is the roll mode. Some of the equipment like the new trailer cars, that go down to about 1/2 a cycle a second, can hit resonance caused by rail joints at rather low speeds, and we think maybe get harmonics at higher speeds and we sometimes get severe oscillation. I think probably your equipment has damping that might prevent that, but we have made studies on the roll mode and found it one of the most important things with ordinary equipment.

Mr. Gieck (Firestone): Can you tell us in general the kind of isolation hardware that you used to achieve these results in the three modes which you had checked out?

Mr. Hager: You mean longitudinal, vertical, and lateral? Well, actually I should have an ACF man up here to help me discuss this but in general the vertical suspension consists of a combination of air bag and coil suspension. In the lateral mode-also there are dampers associated with these trucks. The lateral mode has a bumper system in it, unfortunately I am not as well versed in this design as I should be. In the longitudinal direction we are using a sliding center sill approach on the rail car with a hydraulic cushioning unit.

Mr. Feder (Bell Laboratories): Was there any work done here on mechanical coupling to the lading itself or was this just done on the car?

Mr. Hager: You mean the suspension of our package, being the missile in this case, to the car?

Mr. Feder: Yes, that's right.

Mr. Hager: Yes, this was done on a computer. The suspension points, the stiffness of the so-called strong back which supports the missile, the internal suspension points between missile and container were all analyzed in parametric variations on this particular analysis in order to keep our missile loads down below the allowables. I might point out that this is a very heavy fragile missile, and when it is being transported in the horizontal attitude it just does not have the strength that you have to

have for ground handling, so you have to protect it.

Mr. Feder: Well what would be the order of mechanical coupling in this case? What sort of g's were you running into as far as the lading itself was concerned?

Mr. Hager: Well, we have some design goals, and then we also have some numbers that we're hitting. I would like to defer this point because this is the subject of discussion at the present time.

* * *

DEFINITION AND MEASUREMENT OF SHIPPING VIBRATION ENVIRONMENTS

Harper R. Welton, L. L. LeBrun, R. Carmichael,
and W. Harger
Northrop Corporation, Norair Division
Hawthorne, California

A current research program for the evaluation of portable shock and vibration indicators is described. The status of vibration requirements in packaging specifications and current AIA Committee action with respect to establishing packaging vibration design and test standards are discussed.

INTRODUCTION

Packaging Engineering has grown tremendously in stature since World War II and in many respects it has become a recognized profession. During this evolutionary period, we have seen this profession emerge from the shipping function to a fairly full-flown engineering activity. However, concepts for packaging vibration design and test have yet to mature.

The vibration problems encountered in packaging and shipping are, on occasion, of such a magnitude as to make them as significant as many of the worst vibration problems experienced in the design and operation of an entire weapon system. Understanding and solving such vibration problems demands the background of dynamic specialists.

The purpose of this paper is to outline the status of current packaging specifications and

weapon system programs concerning vibration requirements, to discuss a test program for evaluating current equipment for measuring vibration environments during actual shipments, and to propose a series of levels of vibration design and test standards compatible with specific operational logistic patterns.

STATUS OF EXISTING SPECIFICATIONS

It can be said that majority of our military equipment is packaged without firm vibration requirements for container design or test. Our standard packaging specifications (Table 1) do not include vibration requirements. These are the specifications under which most of our military packaging is accomplished, all without vibration requirements.

TABLE 1
Standard Packaging Specification Which Do Not
Include Vibration Requirements

Designation	Title or Subject
MIL-P-9024B	Packaging, Air Weapons Systems, Specification and General Design Requirements for
MIL-P-116D	Preservation, Methods of
JAN-P-100	Packaging and Packing for Overseas Shipment, General Specification

(Table Continues)

TABLE 1 (Cont)
Standard Packaging Specification Which Do Not
Include Vibration Requirements

Destination	Title or Subject
MIL-P-7936A	Parts and Equipment, Preparation for Delivery
AFLCM 71-2	Packaging and Materials Handling, Preservation Packaging, Methods, and Instructions for Coding (This specification includes the latest in packaging of the Air Force, but does not include any vibration requirement)
MIL-E-17555E	Electronic and Electrical Equipment and Associated Repair Parts, Preparation for Delivery of (like- wise no vibration requirement)

There are, of course, a number of packaging specifications (Table 2) which do include various requirements. Fig. 1 compares the existing vibration requirements of these specifications with a recent proposed revision to

MIL-P-7936. However, it is interesting to note that none of these specifications reflect a concept which we will propose later in this paper, that of a series of vibration requirements, compatible with various specific logistic patterns.

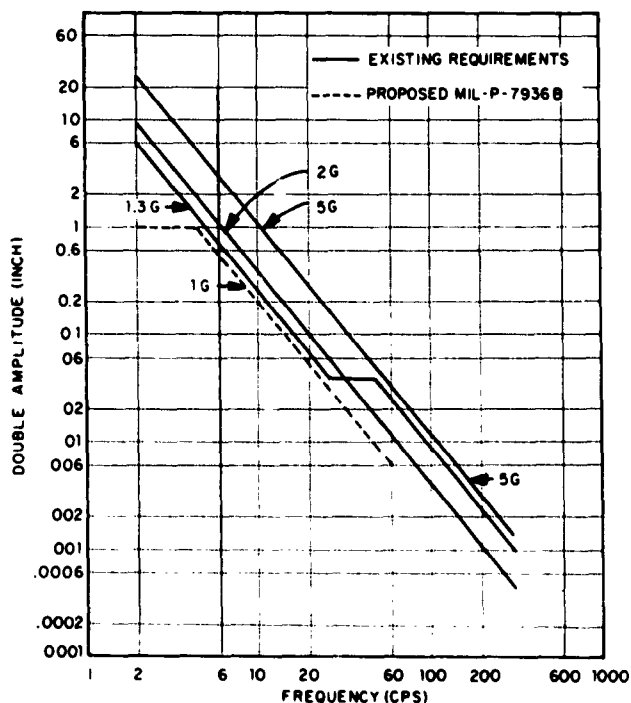


Fig. 1 - A comparison of existing vibration requirements (for the specifications of Table 2) with a recent proposed revision of MIL-P-7926

TABLE 2
Standard Packaging Specification Which Do
Include Vibration Requirements

Designation	Title or Subject
MIL-E-4970A	Environmental Testing, Ground Support Equipment, General Specification for
MIL-C-5584B	Containers, Shipping, Aircraft Engine, Metal, Reusable
MIL-W-21927	Weapons; Handling and Preparation for Delivery of
General Electric Specification NCS 1702A	Environmental Specification for WS 107A-1 and -2, AF/A37E-4 (SC-1), Re-Entry Vehicle Ground Support Equipment, and Transportation Handling, and Storage of Spare Parts for the Re-Entry Vehicle and GSE
Northrop Corp. Spec. NAI-57-202A	SM-62A Packaging Test Criteria
Douglas Performance Specification DS-2146	Packaging, Weapon System, WS-138A (GAM-87)
SUBAMA	"Rule of Thumb" Standard for Air Force Ballistic Missile Program

STATUS OF CURRENT PROGRAMS

Depending on one outlook, the status regarding vibration design and test requirements for packaging of many of our current aircraft, missile, and space programs may come as a surprise. Results of a cursory review of current

programs in general reflects a minimizing of vibration consideration. Identification of specific systems will be avoided to minimize controversy, however, the tone of the existing situation of packaging programs may be summarized as follows:

Supersonic Trainer Aircraft Present Strategic Aircraft Newer R and D Advanced Aircraft Electronics	Little use of transportation vibration requirements Little use of transportation vibration requirements No transportation vibration requirement, although consideration is being given to establishing a Bulletin 115 philosophy. However, Bulletin 115 does not present actual requirements, but does present general data to acquaint the designer with environmental conditions A minimizing of transportation vibration requirements
---	---

Ballistic Missile Guidance	Usually no packaging vibration requirement exists at present time, although requirements are being written into programs in some cases
Ballistic Missile Propulsion Units	Usually no requirement, especially with liquid engines
Overall Ballistic Missile Program	Usually no vibration requirement, although various agencies lean towards various design goals. Some testing has been accomplished.

While various specific programs may deviate from the norm, the above reflects the typical cross section of these programs. It would appear, then, that a majority of our major programs minimize packaging vibration requirements, especially in spares packaging.

PORABLE SHOCK AND VIBRATION INDICATORS

Extensive test data have been accumulated through measurements taken on the transporting vehicle and containers during shipment to determine experimentally the actual shipping environment. Much work remains to be done to factually establish these environments. Generally, precise measuring equipment is bulky and costly. Also, instrumentation which is not visible to operating personnel may yield more typical results. A portable device is needed, small enough to be hidden in the container and sufficiently inexpensive to permit extensive use. It should indicate or record data over a broad-frequency range.

There are a sizeable number of portable shock and vibration recorders on the market, and Northrop Corporation, Norair Division is currently conducting a test to evaluate performance of a cross section of the existing shelf item units. This work is being done under contract to BuWeps and is expected to be completed in early 1962.

The various available types of portable shock and vibration recorders are being evaluated and compared, and design factors limiting performance determined. A performance specification has been written and the preliminary design of an extended performance recorder is under development. The test program includes three basic areas: vibration, shock, and constant acceleration. Under vibration, the frequency response and natural frequency of each recorder will be determined

under dynamic laboratory conditions. Linearity is to be determined by the application of several acceleration amplitudes at various frequencies. The shock portion of the evaluation most accurately simulates the damaging spectrum of the actual shipment environment. A drop table is used for this test and the shock impulse shapes (sinusoidal, square, or triangular) are varied by inserting various cushioning materials at the base of the drop.

For the constant acceleration test, all graph recorders will be subjected to five increments of constant "g" levels in a centrifuge to determine static linearity. One-shot indicators are wired with an electric open circuit that will close with triggering of the unit. It is then possible to correlate the time of release with the acceleration levels being experienced.

The results of this study will be available in several months.

PROPOSED VIBRATION STANDARD

Table 1 shows that many of our current packaging specifications do not include vibration requirements. Also, there are no vibration requirements for a majority of the containers used in our current defense weapons systems. Undoubtedly an overwhelming percentage of all the damage encountered during shipping is caused by transient shocks, and not by vibration in a continuous sense. However, this is not a valid reason to ignore the vibration problem. There should be an engineering approach, both in the design and test of the container that will insure a high probability that no damage due to vibration will occur. Caution must be exercised in establishing packaging vibration standards to insure not only that they are adequate, but also that excessive requirements are not made mandatory. The Aerospace Industries Association Preservation and Packaging Committee is studying the area of packaging vibration requirements. However, no conclusions have as yet been developed by the

AIA-PPC, and the proposal made here is that of the writers' only.

At the Symposium presentation of this paper a film was shown of a packaged piece of equipment being subjected to the requirements of MIL-E-4970. The vibration tables shown were a special Hawk missile shaker, and the large 75,000-force-pound electrohydraulic shaker developed at Northrop-Norair. Below 20 cps the input was ± 1.3 g for the worst conditions shown. This film showed the effect of an unrealistic test criteria. It should be noted that this low-frequency requirement does not exist in the A revision of MIL-E-4970. There is no doubt that the 1.3 g and higher were accurately measured on the bed of a truck or railroad car during a normal transportation run. There is extreme doubt, however, that this condition was continuous. It was probably measured as the truck hit a chuck hole, or rolled off a curb, or crossed some railroad tracks, or during some other transient event. To subject a container to 30 or 60 minutes of this amplitude at the natural frequency of the container isolation system is unrealistic for shipments made within the continental limits of the United States over normal transportation routes.

There are those who say that the environment simulated in the film can happen and that we must design for it. It would usually be more economical to design containers for a more reasonable level and lose the equipment that is shipped on the flat-wheeled railroad car, or on the truck driven over washboard road at the speed required to produce this environment.

This brings up the question of the value of the resonance test, which is probably the least understood and most misused vibration test yet devised. The continuous vibration environment which the resonance test simulates originates in conditions such as the following:

Truck - Washboard road

Rail - Side sway, regular track imperfections, wheel imperfections

Air - Resonant response of supporting floor, response of fuselage in vertical and lateral bending modes (primarily in response to gusts and manuevers).

It is contended that for transportation within the continental limits of the United States over

regular commercial routes, the above conditions do not warrant a resonance test when certain conditions to be defined later are fulfilled.

The resonance vibration test does, however, provide an economical method of demonstrating the fatigue resistance of the package isolation system, if used with proper judgement. The main troubles are that the amplitudes are too high, and in some cases, excessive heat is generated causing unwarranted deterioration of the properties of the isolation mounts.

Before we become involved in the proposed vibration test criteria, let us discuss the fragility level concept. The concept of a given number of g's sometimes erroneously used in describing the shock resistance of equipment has absolutely no significance in describing a safe vibration level. Frequency, amplitude, time, probability, and the nature of the vibration, must be defined in describing the fragility level in regard to vibration. This, incidentally, has never been accomplished even for the simplest of equipment.

The fragility level concept can, however, have some significance in lessening the risk involved in reducing the vibration test criteria. The frequencies inducing the highest stresses during a vibration test at a constant acceleration are the resonant frequencies. The most severe resonant frequencies are dwelt at for reasonably long lengths of time during the qualification tests of the equipment. The stresses induced by these resonant dwells may be above the endurance limit, but they must be well below the yield stress or the equipment will fail. If it is known that the package isolation system major resonant frequency is approximately one octave below the lowest natural frequency of the equipment, then the equipment will respond to the amplified response of the package isolation system as a rigid body and the stresses induced will be well below those induced during the equipment qualification test. This is of course dependent on the level of the acceleration input of the equipment qualification test and the response accelerations of the package isolation system. There are many applications of this principle which can be applied analytically by the dynamicist and thus eliminate the intuitive and possibly dangerous approach of the packaging engineer — just ignoring the vibration aspect.

This approach has been applied in MIL-T-4807A, "Tests, Vibration and Shock, GSE," and is implied in the A revision of MIL-E-4970A, "Environmental Testing, GSE," in which a requirement is that the lowest natural frequency

of the equipment is to be above 20 cps and the fundamental natural frequency of the package isolation system must be below 20 cps.

When one proposes a general test criteria, especially for the uncontrolled environment encountered during shipping, one is immediately faced with the exceptions and the special cases. These will always exist and thus the test criteria becomes merely a guide and should never be employed without first determining its applicability.

There can be no common vibration test that will adequately simulate the vibration environments of different modes of transportation, of truck, rail, air, or ship. Indeed, there can be no common test criteria that will adequately simulate the vibration environment encountered when shipping by truck from Chicago to Los Angeles and that encountered between Chicago and Nome, Alaska. Further, there must be different test criteria for the single shipment container and the container that will be used many times with many modes of transportation and destinations. Thus, the test criteria must account for the mode of transportation, the conditions encountered in transit, and the service life of the container.

One problem with which we are confronted is the huge quantity of test data available on transportation vibration. Validity of much of the data may be in question, and for similar conditions, a wide range of transportation environments can be read from the available data. Therefore, great discretion must be exercised in selecting our vibration standards.

Our proposal is best presented in the form of a revision to the proposed "B" version of MIL-P-007936 (Wep), "Parts and Equipment, Preparation for Delivery." Firstly, we recommend that the vibration standard be not included under the rough handling tests, but separately identified as paragraph 4.5.4, Vibration Design and Test Standards. Secondly, we recommend that the section under Vibration be deleted and replaced by the following, to be compatible with specified logistic patterns.

4.5.4.1 Procedure I - This vibration test is intended for items to be shipped on normal primary transportation routes within the continental limits of the United States. This test requirement may be waived for single shipment containers by the procuring agency if the packaged item can be shown to possess no resonant frequencies below

20 cps and the container isolation system fundamental resonant frequency is below 15 cps. The vibration tests shall be conducted along three mutually perpendicular axes with the container rigidly attached to the shaker table.

4.5.4.1.1 Low-Frequency Cycling - The low-frequency cycling test shall consist of continuous cycling between the frequencies one-half and 1-1/2 times the container isolation system fundamental natural frequency for a duration of 30 minutes. The cyclic rate may be linear or logarithmic and the time for each cycle (from low to high and return) shall be two minutes. The input amplitude shall be as shown by Curve A of Fig. 2. If more than one resonant mode of approximately equal or greater severity than the fundamental should exist, the upper limit of the low-frequency cycling test shall be extended to include the effect of the higher resonant mode.

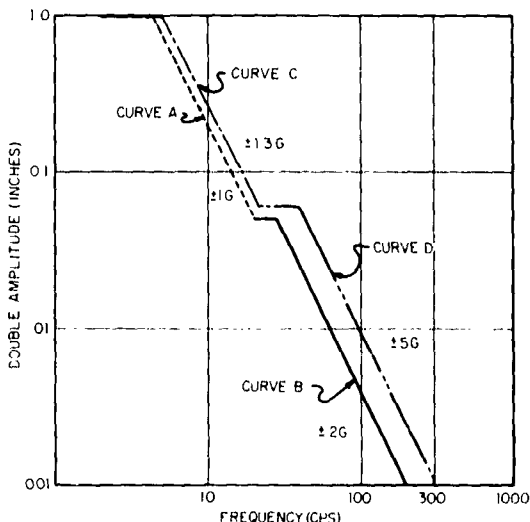


Fig. 2 - Proposed vibration standard

4.5.4.1.2 High-Frequency Cycling - The high-frequency cycling test shall consist of cycling between 20 and 300 cps at the amplitude shown by curve D of Fig. 2 for a duration of 30 minutes along each axis. The rate of frequency cycling shall be logarithmic and such that 15 minutes are required

to cycle from 20 to 300 and back to 20 cps. When there is no provision for logarithmic cycling, a linear rate of frequency change may be used. If the container is reusable and must preserve its pressure-tight integrity, the most severe resonant frequency of the container along each axis shall be vibrated for a period of 15 minutes at the amplitude shown by curve B of Fig. 2.

4.5.4.2

Procedure II - This vibration test procedure is intended for items to be shipped overseas or over routes that do not compare favorably with the normal primary transportation routes within the continental limits of the United States. This test requirement may be waived for single shipment containers by the procuring agency if the packaged item can be shown to possess no resonant frequencies below 20 cps and the container isolation system fundamental resonant frequency is below 15 cps. The vibration tests shall be conducted along three mutually perpendicular axes with the container rigidly attached to the shaker table. A simulation of the packaged item may be employed provided that weight distribution, moments of inertia, lowest natural frequencies, and the structure involved in the failure mode corresponding with these natural frequencies, are simulated.

4.5.4.2.1

Low-Frequency Cycling - The low-frequency cycling test is intended for single shipment containers when the possibility of an equipment resonance below 20 cps exists. The low-frequency cycling test shall consist of continuous cycling between the frequencies one-half and 1-1/2 times the container isolation system fundamental natural frequency for a duration of 30 minutes for each axis. The cyclic rate may be linear or logarithmic and the time for one cycle (from low to high and return) shall be two minutes. The input amplitude shall be as shown by curve C of Fig. 2. If more than one resonant mode of approximately equal or greater severity than the fundamental should exist, the upper limit of the low-frequency cycling

test shall be extended to include the effect of the higher resonant mode.

4.5.4.2.2

Low-Frequency Resonance - The low-frequency resonance test is intended for reusable containers. The container shall be vibrated along each axis for a period of 30 minutes at the fundamental resonant frequency of the container isolation system with the input as shown by Curve C of Fig. 2. The fundamental resonant frequency is defined as the frequency producing the maximum response at the input as shown by curve C of Fig. 2.

4.5.4.2.3

High-Frequency Cycling - The high-frequency cycling test shall consist of cycling between 20 and 300 cps at the amplitude shown by curve D of Fig. 2 for a duration of 30 minutes along each axis. The rate of frequency cycling shall be logarithmic and such that 15 minutes are required to cycle from 20 to 300 and back to 20 cps. When there is no provision for logarithmic cycling, a linear rate of frequency changes may be used. If the container is reusable and must preserve its pressure-tight integrity, the most severe resonant frequency of the container along each axis shall be vibrated for a period of 15 minutes at the amplitude shown by curve D of Fig. 2.

4.5.4.3

Procedure III - This vibration test procedure is intended for items having a special and closely controlled logistic pattern, differing from the above. At the discretion of the Procuring Agency, a special vibration standard may be negotiated.

4.5.4.4

Combined Temperature and Vibration - When there is reasonable cause to suspect that extreme high and low temperature will have an effect on the dynamic properties of the container isolation system to the degree that the protection afforded the packaged item is significantly jeopardized, the procuring agency may, at their discretion, cause the tests of paragraphs 4.5.4.1 and 4.5.4.2 to be conducted at high and low temperatures

specified by the procuring agency as well as at room temperature. Division of test times for each temperature condition shall be at the discretion of the Procuring Agency.

- 4.5.4.5 Cause for Rejection - At the conclusion of the tests, the container shall show no evidence of damage that would jeopardize the protection afforded to the packaged item. The integrity of sealed barriers shall be proven intact in accordance with the quick leak and

vacuum retention tests of Specification MIL-P-116. During the vibration tests, hard bottoming of the isolation system or insufficient sway space shall be cause for rejection.

In conclusion, it is our recommendation that MIL-P-7936 be revised to include the proposed vibration design and test standards, placing these requirements in consonance with their respective operational logistic patterns. This will permit us to maintain system reliability at minimum cost.

DISCUSSION

Mr. Coler, (IBM Corp.): I noticed, particularly in this last presentation and in much of the other data that I have seen both here and other places, that there is a certain amount of emphasis placed on normal means of transportation within the continental U.S. I don't know what can be answered here within the grounds of the classification but are there any safety factors or is it considered, since most of our equipment is military, that in any hostilities, the continental U.S. will not be normal but will approximate a battleground condition? Trucks may be forced to drive over roads that are at least in part rubble filled. Because of direct enemy action or sabotage they may be forced to use detours or routes that could be a long way from normal. The urgency of delivering equipment may preclude normal routes, may require higher than normal speeds, flying under conditions that normally would not be attempted in peacetime, all of which will usually result in more severe landing conditions. Is this being considered in some of these specs?

Mr. Pusey, (Centralizing Activity, Chairman): Well, I might make a brief comment on that. I think Mr. Simon in his presentation this morning, although it might not have been completely evident, was attempting to take into consideration some of these rather adverse, cross-country or rough-extremely rough-roads, muddy conditions, etc. This is certainly being considered in light of the military philosophy concerning mobility — not the kind that Bob Mains was talking about — the kind, moving across rather uncrossable terrain. Yes, it is being considered. How much of it we can talk about here I am not quite sure.

Mr. Simon (TRECON): It is really nice to disagree with the chairman. I don't think it's

being considered enough. Frankly, there are no specifications that I know, that actually depict this particular environment. As somebody here has stated there has to be a central agency for gathering this data. Essentially, what the specifications consist of, in the vehicle field, is a description of the terrain in rather generalized terms. Sixty-percent gradability, a certain type of terrain, or perhaps some stylized courses that we may have available. But I don't know actually of specific criteria that have been established that the designer can go to. This is a tremendous lack.

Mr. Coler: Let me rephrase the question a little bit. What I am really asking, for military equipment in particular, is this—is a spec which calls for normal transportation routes on which we are measuring all our data in peacetime, even a reasonable specification for military equipment to start with? I grant that there are some economic factors but the real point is that we can lose every bit of military equipment we ship in peacetime without disaster, but if we lose any appreciable percent of it under wartime conditions, we are in trouble. What I am really asking, is there a great deal of sense in a specification that is based completely on peacetime transportation conditions within the U.S., which conditions so far in our previous conflicts we have been able to maintain, but which it is very doubtful that we can do in the next one? Or should we really be approaching a spec that is much closer to a battleground specification?

Mr. Simon: All I can say is going to be personal opinion. I agree with you. We should actually be getting a spec which will portray the battlefield condition and I don't think anything like that has been done. But, whether or not an attempt is being made, there are attempts being made to try to describe this condition and this idea of within the continental U.S. or overseas

shipment. I think your point is very well taken. We should not be considering it this way at all. Of course we do not know what the continental U.S. is going to be like and I would say from my point of view the type of specification which would be adequate would be that which would describe other than normal conditions.

Mr. Welton: Well, one point might be that much of the equipment that is shipped now is shipped under an R&D situation. A lot of the shipping that is actually accomplished is to support our development programs. I do not believe this is a thing we need consider to support our test programs. However, usually in supporting a shipment the packaging engineer is fairly well aware of the end use of this particular shipment and when we come up to an emergency situation why then I believe we would have to increase these levels. In our own proposal we would then, the packaging engineer for Z1 shipments, would then jump to the more stringent level for overseas shipment and uncontrolled situations which is what we had thought we had included.

G. Mustin (Reed Research): As the proposal of MIL-P-7936 does stem from some work that I did and on which I will be speaking later I will not comment directly on Harper's proposal now. I will let my own paper explain the background. I do want to emphasize at this time, however, that the proposed MIL-P-7936, if I understand it correctly, is aimed at specialty containers primarily and I wanted to emphasize that my belief, based on a number of years experience in packaging and package testing, is that you cannot ignore a vibration test of some sort, ever. Specifically I think that just a simple jumble test, if you want to call it that, on a package vibration tester—a

low frequency tester—is an essential prerequisite to any other form of testing you do. Even if you regard this only as a conditioning prior to other forms of performance testing, it must be done if you are going to be able to evaluate the shipping performance of your container in advance.

Mr. Rice (Goodyear Aircraft): I think sooner or later we are going to have to come to the conclusion, in view of these remarks and others, that we are going to have to have more than one specification for more than one condition. In the statistical language, we are going to have to design for the three-sigma case as well as the one-sigma case. In other words there are a lot of things that we ship around here some of which, as Harper said, we can afford to lose from an economic standpoint. There are other things that we cannot possibly afford to lose. I have shipped items on which I could put a value of \$20,000,000, because if that one item were destroyed before it got to its ultimate base, the whole project would stop. I'd classify that as a 3 sigma. I will spend any amount of money within reason and I will design for earthquakes, tornadoes, atom bombs, anything that comes along because I have to get it there in working condition. Sooner or later we are going to have to design our specifications in three categories — one for normal use, one for this wartime condition, and one for the unusual case. It's up to the procuring agency to say, I deem this to be a situation where you must guarantee that it gets there, and this can be done. But to saddle Harper or anyone else with the task of covering this wide range is such an impossible thing that we could never get off first base. Sooner or later I would like to see specifications written to embrace more than just a standard range of applicability.

* * *

SHOCK AND VIBRATION OF STANDARD MILITARY VEHICLES IN OVER-THE-ROAD APPLICATION

Robert Kennedy
U.S. Army Transportation Research Command
Fort Eustis, Virginia

This paper describes a basic approach to the evaluation of standard military vehicles in over-the-road applications designed to determine the shock and vibration effects caused by different road conditions and by vehicle suspension components, particularly the tires. Results which have been obtained to date are indicated.

INTRODUCTION

Transportation of cargo and the consequent shock and vibration effects on the cargo present a field in which the approach must be refined and specific when the handling of sensitive materials is considered. Most previous work in this field resulted either from a requirement to solve a problem concerning damage that is of a specific type or from a need to include all possible types of cargo in order to show the versatility of a particular product to be sold.

The relationship between safety and shock and vibration in the transporting of sensitive materials is such that the results would be disastrous if the shock and vibration were exaggerated or if the effects of the shock and vibration were minimized. If the degree of shock and vibration input were estimated below the actual amount of g's and if serious damage to the cargo resulted, the negative results would be quite obvious. On the other hand, if the degree of shock and vibration were overestimated, the mobility of the items would be seriously impeded and again an unsafe condition would exist.

It is imperative that the shock and vibration input to the cargo by various modes of transport under all conditions be accurately determined. Our objective is to insure not only that a sensitive cargo has a safe trip but that it has as broad a range of transportability

as possible. With most commercial shipments, a trial and error procedure of checking damage claims against various shipping routes and modes of travel is sufficient to determine safeguards for the future against damage caused by shock and vibration. Obviously, this method cannot be used in such determinations for our present weapons.

The over-all program is a continuing study covering shock and vibration effects on cargos transported by many types of vehicles and by all modes of transportation. The problem of transporting sensitive materials occurs in five general areas of transportation; namely, highway, rail, air, amphibious, and sea. This paper is limited to a discussion of a small portion of the highway phase only. A standard military truck was selected as the first vehicle to be studied since this vehicle is one of the most commonly used transportation media.

The test of a standard military vehicle is also designed to determine the shock and vibration effects caused by different road conditions and by vehicle suspension components, particularly the tires. It is the intent of this paper to show the basic approach to the evaluation and to indicate the results that have been analyzed to date.

EVALUATION

An M-52 truck tractor operating in combination with an M-127 semitrailer (Fig. 1) was



Fig. 1 - M-52-M-127 tractor-semitrailer combination

selected for initial shock and vibration studies. This combination is a general-purpose vehicle. The truck tractor is classed as an M-52, 5-ton, 6x6, 167-inch wheel-base tractor; the semi-trailer is classed as an M-127, 12-ton, 4-wheel, dual-axle trailer with a cross-country payload of 24,000 pounds and a smooth-highway payload of 36,000 pounds. The combination was tested over a range of roadways, the test-run courses consisting of a typical highway, a secondary road, a low-type road, a paved road with a rail crossing, and a corduroy-type road, any or all of which could be encountered during cross-country road movements.

All tests have been completed, but, to date, only the results of the tests on the corduroy-type road have been analyzed. Data on the other type road conditions are currently being compiled and analyzed. Figure 2 shows the corduroy road over which the shock and vibration tests were conducted. The road consists of logs 12 to 24 inches in diameter, placed crosswise on a firm sand base. The course is approximately 14 feet wide and 400 feet long. This type road generates perhaps the most severe low-frequency vibration for the vehicle and the load. It is certainly the most severe of all of the test conditions in the program.

The principal instrumentation was comprised of 5 accelerometer transducers, all mounted in a vertical direction and located on the trailer as shown in Fig. 3. All accelerometers were of the Statham unbonded strain-gage type and had a natural frequency of 350

cps and a flat range of up to 200 cps. Data from the transducers were recorded on a Consolidated Engineering Corporation 18-channel recorder in conjunction with a direct-current balancing bridge. The galvanometers limited the frequency response with a natural frequency of 100 cps and a flat range of up to 60 cps.

Four accelerometers were located on the main suspension members of the bed and one was located on the axle, as shown in Fig. 3. The accelerometer on the axle was used to aid in the comparison of the tires and also to correlate the shock imparted to the road. Accelerometers were placed at various locations on the truck bed to pick up any differences attributed to location.

The recording instruments and power supply were housed in a separate 3/4-ton truck. This proved to be a cumbersome arrangement and presented a problem; the test vehicle and the vehicle carrying the recording instruments had to operate approximately parallel to each other during a test run in order to maintain electrical contact between the power and the transducers. Telemetering equipment is now available and will be used in future vehicle tests.

Tests on the corduroy road were run with the following vehicle variables: standard military tire (11:00 x 20); military sand tire (14:75 x 20); recommended tire pressure and one-half recommended tire pressure; speeds of



Fig. 2 - Corduroy road

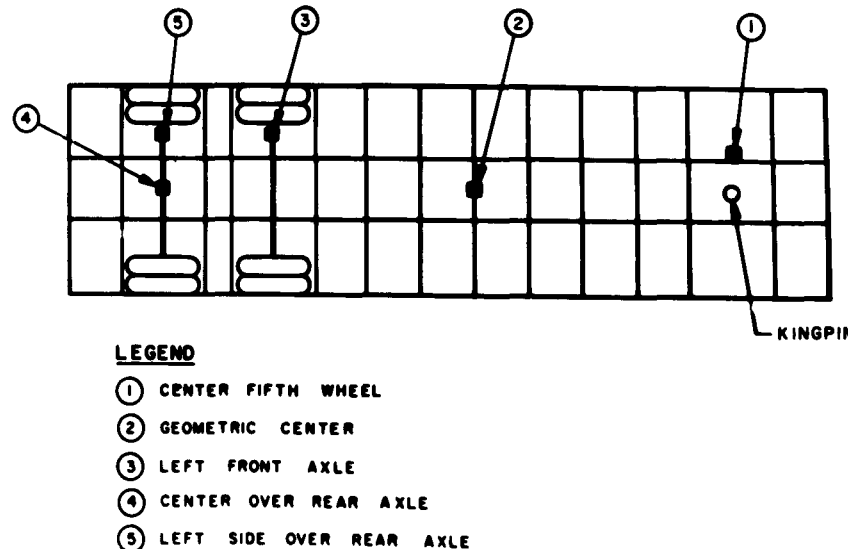


Fig. 3 - Instrumentation sketch M-127 semitrailer

4 and 6 miles per hour; load condition, empty, and load condition, 24,000 pounds.

The peak accelerations were measured for a specific frequency over a given time interval of the trace. These accelerations were then recorded on IBM tape for use with an IBM 1620 computer. The 1620 computer was then used to compute various statistical expressions as

the mean and standard deviation. The net result is that the computer program produced a smooth curve fitted and determined by good statistical practice. Actually, the original data produced good curves and probably were sufficient for our purposes. A check of a few runs shows that the statistical expressions altered the original data curves very little.

RESULTS

Four accelerometers were located on the flatbed to record differences and out-of-phase relationships throughout the trailer bed. After a check had been made of a few individual accelerometers by means of the computer, it was readily noted that the accelerometer in each location gave substantially the same statistical results. For the results that were considered, all accelerometer readings were combined to increase the number of occurrences over a given time interval in order to improve the statistical results.

Resultant data from the corduroy road test are plotted in the form of frequency distribution curves as shown in Figs. 4 and 5. The percent occurrence scale was reversed from a standard-frequency distribution curve to read

from 100 to 0. The curves then showed the percent of occurrences that are above a given g level. In Fig. 4, for example, run one shows 9 percent of occurrences to be above 8 g's and 23 percent to be above 6 g's.

Run 1 in Fig. 4 shows the frequency of the vibration to be 5.4 cps or 5.4 (60) (60) cycles per hour. Cycles per hour divided by miles per hour will give cycles per mile, or $5.4 (60) (60)/6 = 3240$ cycles per mile. The occurrences were measured in half cycles, or peaks, and 9 percent of these peaks exceeded 8 g's; therefore there were $3240 (2) (0.09) = 583$, 8-g accelerations per mile.

The ultimate goal is to be able to predict the number of all accelerations per mile for all conditions. This type of data, if it is tied in with fatigue data on sensitive or other types

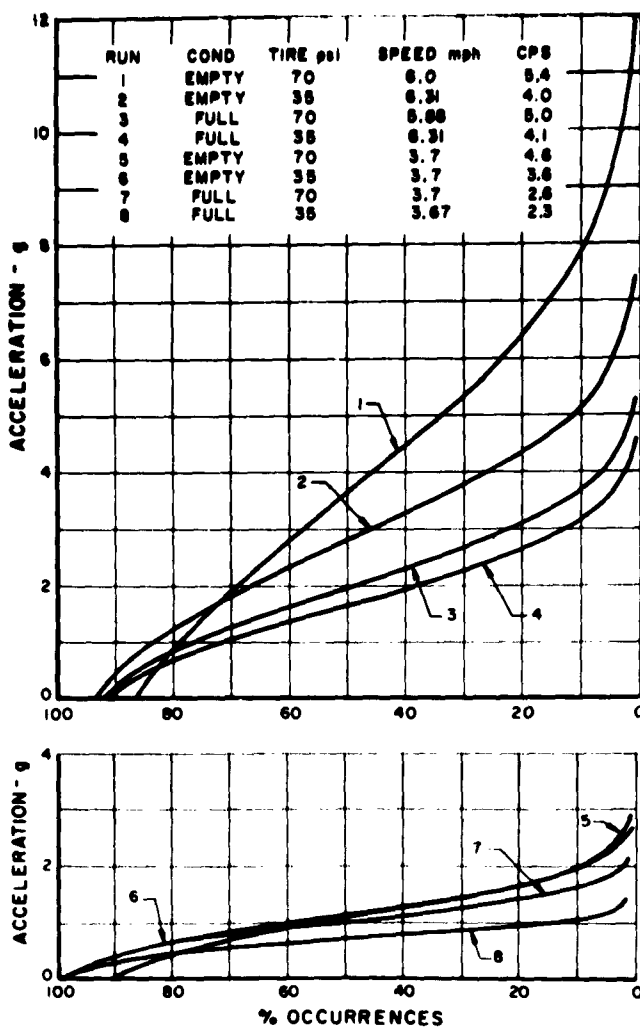


Fig. 4 - Vehicle accelerations for standard tires over corduroy road

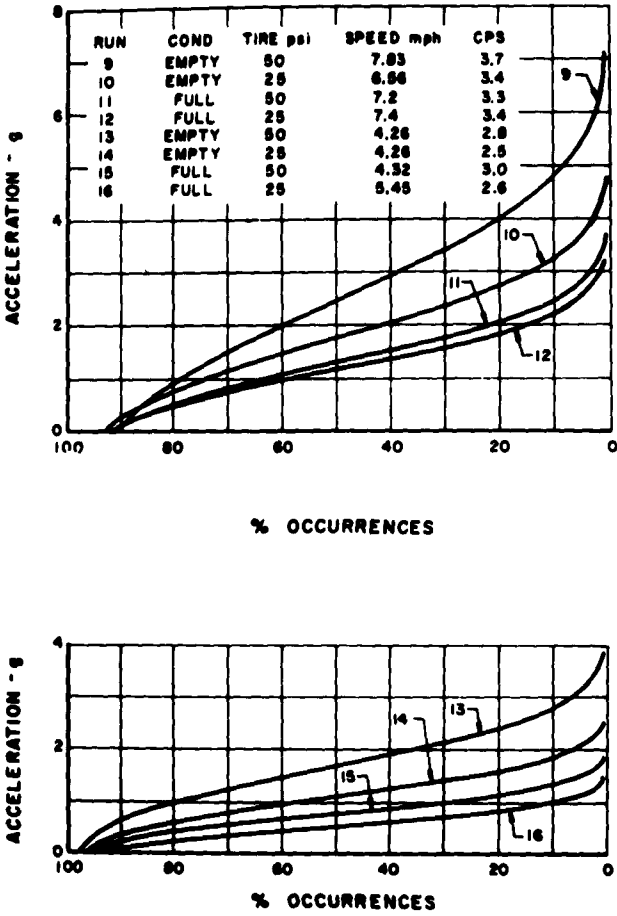


Fig. 5 - Vehicle accelerations for desert tires over corduroy road

of cargo, should furnish the basis for specifying or designing transportation routes for cargos. A general approach of this nature on other modes, such as rail and air, should furnish a basis for mixing routes or should furnish a combination of modes to make up a route knowing the magnitude and frequency of the shock to the cargo.

The tests, even for the corduroy road portion, were run for more load and speed conditions than are shown here. It might be argued that any slight change in any of the variables will drastically alter the results so that an infinite number of frequency distribution curves will be required to depict the road movement of a sensitive cargo. At present, the sensitivity of the variables (road condition, tire pressure, type of tire, mass of cargo, etc.) is being studied, and it appears that not too many groupings will be necessary if the

combinations are used in conjunction with a reasonable safety factor. As new developments cause large changes in the variables, the new data can be added to the existing data and new results obtained in a matter of days. If the digital computer, semiautomatic data reduction, and standard test courses are used, a rapid-test process results, which is extremely important for military considerations of shock and vibration.

The number of transportation variables is automatically reduced because, when the tests show certain conditions produce high accelerations, these conditions would subsequently not be recommended for transport. Figure 6 shows the distribution curve for high tire pressure, high speed, and for a full and an empty load. It should be noted that 6 miles per hour is the maximum speed for this course and that any further increase is considered too risky for

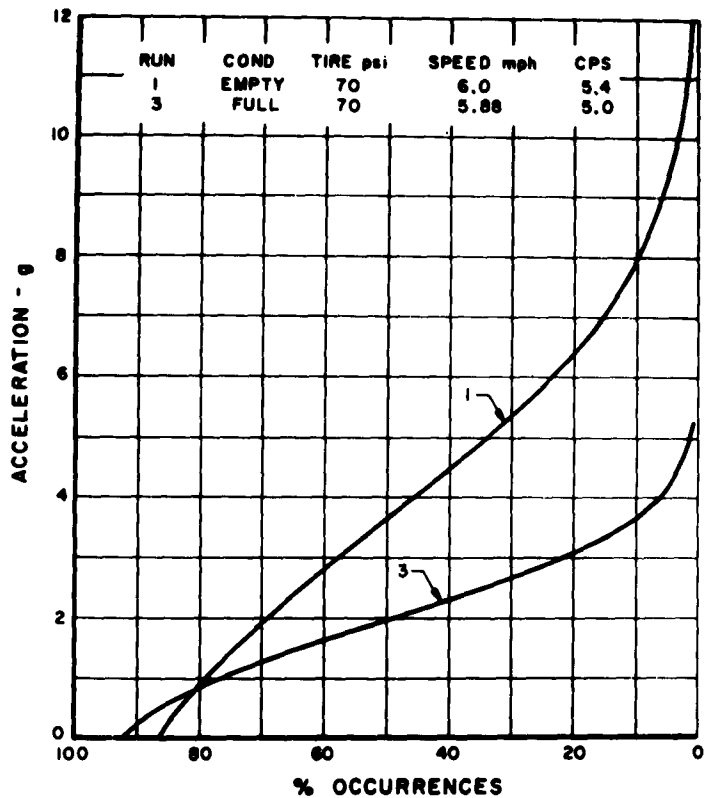


Fig. 6 - Comparison of full 24,000 pound load and empty load

the driver. It is apparent that an extremely light cargo is subjected to almost double the acceleration level of a heavy cargo. This was apparent, in general, before the test was run; however, the exact number of accelerations per mile can now be determined, and this will pinpoint the importance of density to a specific cargo.

Figure 7 shows the results of the tests that were conducted when all the variables, except speed, were the same. An increase in speed from 3.7 miles per hour to 5.8 miles per hour again shows an increase in acceleration severity by a factor of almost 2. Here again speed must be weighed against military considerations and against the specifications of the cargo in order to determine the optimum requirements for transport.

Results of change in tire pressure, with the other conditions held substantially fixed, are shown in Fig. 8. The change in tire pressure did not produce a change as severe as that effected by other variables. Reduction in

tire pressure is usually made because of mobility considerations; moreover, some bonus is received in the reduction of accelerations.

Figure 9 shows the reduced accelerations that were attained by the use of desert tires. It must be noted that the recommended pressure for desert tires is 50 psi and that the recommended pressure for standard tires is 70 psi. The reduced shocks seem to be attributed in part to differences in tire pressure. The curves show the number of accelerations for each tire at its recommended tire pressure.

It is realized that much more evaluation and analysis are necessary to determine fully the behavior of a cargo throughout a given movement. As part of this program, more test work has been performed on paved roads with the same test vehicle described herein. A visual examination of the oscillograph traces indicates that the most severe vibrations for these tests were encountered on a paved highway at a railroad crossing. It is further

realized that more testing should be performed in the higher frequency range.

The initial tests and results have been encouraging, and it is planned to continue the effort this year in additional load and road vibration studies and tests. Increased emphasis on analysis of vibrations in all planes (roll and pitch vibrations as well as vertical) will be

included in the plans. Also, tests are planned to extend the number of road and off-road conditions in order to develop a broader range of road effects. Efforts will be expanded to measure more locations and more mechanical data on a vehicle. In addition, more extensive use will be made of travel transducers and strain gages for vibration measurements.

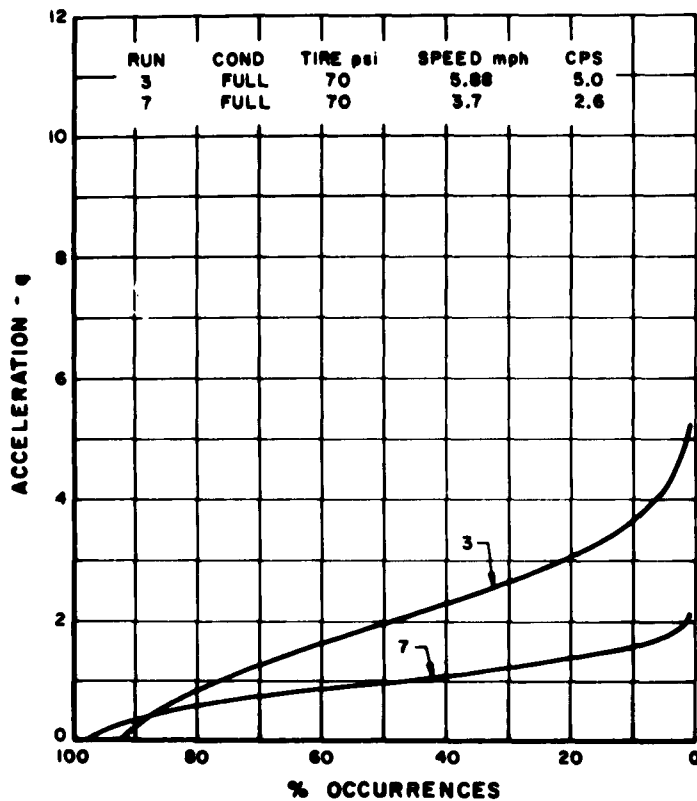


Fig. 7 - Comparison of 3.7-mph and 5.8-mph test runs

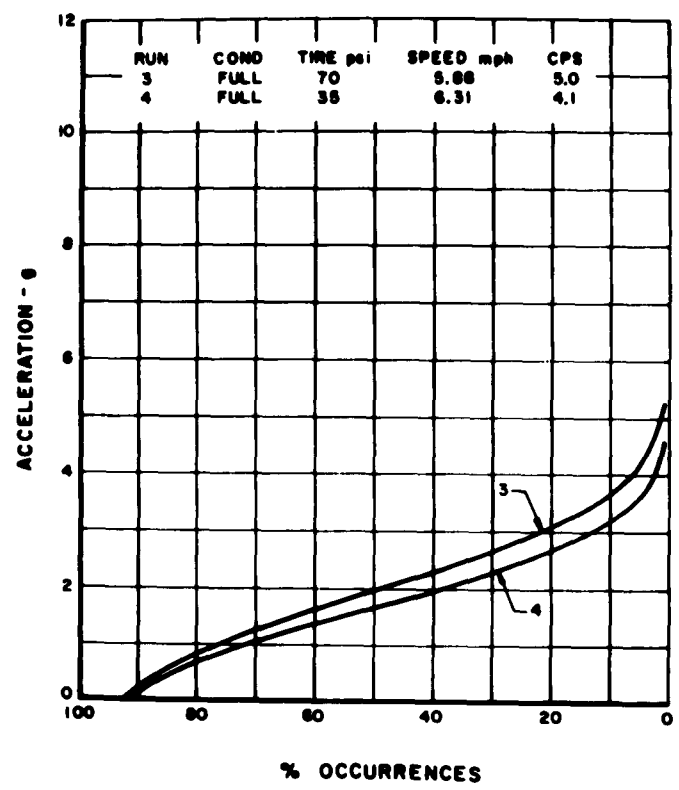


Fig. 8 - Comparison of 70-psi and 35-psi tire pressures

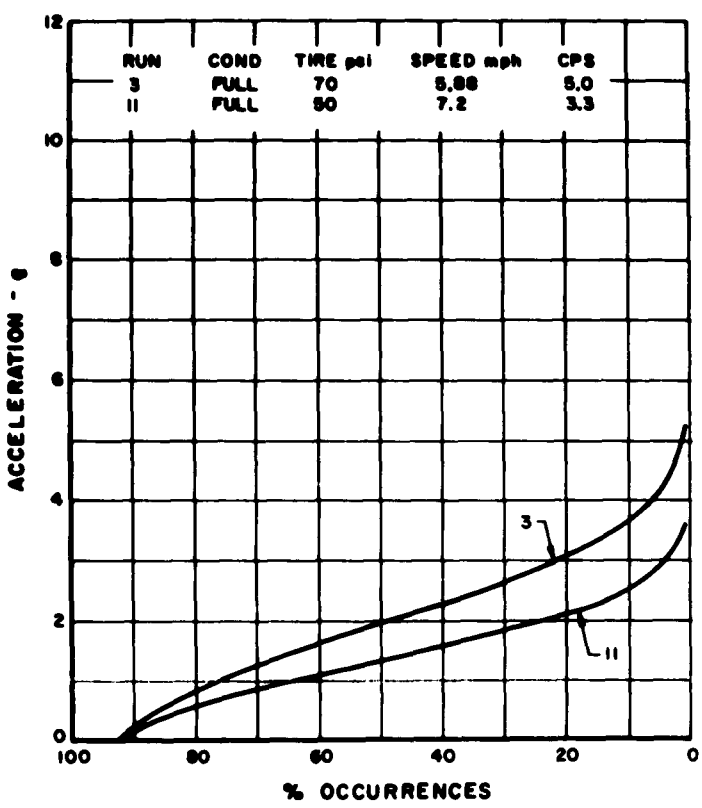


Fig. 9 - Comparison of standard tires and desert tires

* * *

VIBRATION LOADS ON A WHEELED VEHICLE

Simon J. Grabowski
U.S. Army Ordnance Arsenal
Detroit, Michigan

This paper presents the results of a vibration study on a 2-1/2-ton cargo carrier truck, M35.

INTRODUCTION

Components and systems can be designed better when designers are provided with realistic environmental data. Present specifications include vibration requirements based on sources long since forgotten or simply on seat-of-the-pants reasoning. Vibration forces generated during vehicle operation are transmitted to vehicle components and eventually to the cargo. Vibration studies, therefore, must be complementary. That is, they should be conducted on vehicle components as well as containers and cargo.

Extensive study programs designed to determine shock and vibration characteristics on both wheeled and tracked vehicles have been conducted by Detroit Arsenal Laboratories. An important purpose of tests of this nature has been to establish experimental data upon which realistic and modern requirements may be based.

This paper presents some results of a vibration study on a 2-1/2-ton, cargo carrier truck, M35. Figure 1 shows the cargo truck with an attached trailer. The trailer was pulled for certain phases of the vibration study.

TEST PROCEDURE

Tests were conducted on a dry, hard, black top surface at Detroit Arsenal. The vehicle was loaded to a gross vehicle weight of 22,650 pounds. The vehicle was driven with the transfer case in both low and high range, at various road speeds, and with

transmission in first, second, third, fourth, and fifth gears. Vibration was measured by crystal, linear accelerometers. A block diagram of accelerometer instrumentation is shown in Fig. 2.

Crystal accelerometers were used to sense accelerations. Signals were amplified through three stages, and finally recorded with an Ampex tape recorder. The oscilloscope was used to monitor the signal and for trouble-shooting.

Accelerometers were mounted on blocks and the blocks were secured to components on the vehicle. Where difficulty in mounting the blocks was encountered, plates were provided to facilitate block installation. Figure 3 is a top view of accelerometers mounted on the Cylinder Head.

Three accelerometers were mounted on each block so that vibrations in three mutually perpendicular axes could be recorded simultaneously. For the vibration study, the following components on the M35 were instrumented:

- (1) Cylinder head, top
- (2) Engine mount, rear
- (3) Engine front, mounting support
- (4) Transmission control housing
- (5) Rear-rear axle housing
- (6) Frame, crossmember, near center of vehicle
- (7) Bed, forward in cargo body
- (8) Instrument panel

Data recording instrumentation was carried in cargo compartment of the M35.



Fig. 1 - M35 cargo truck -- side view of the test equipment

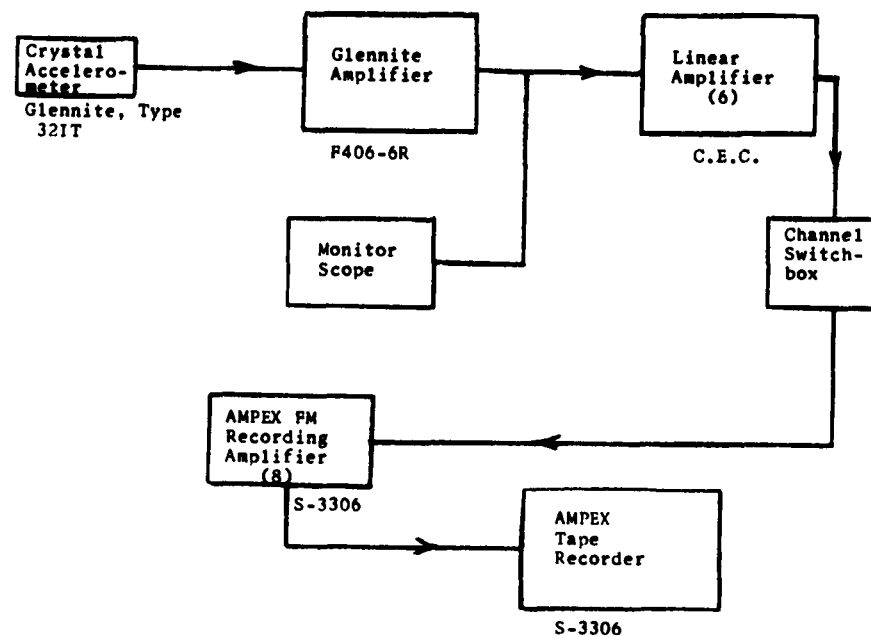


Fig. 2 - Block diagram of accelerometer instrumentation

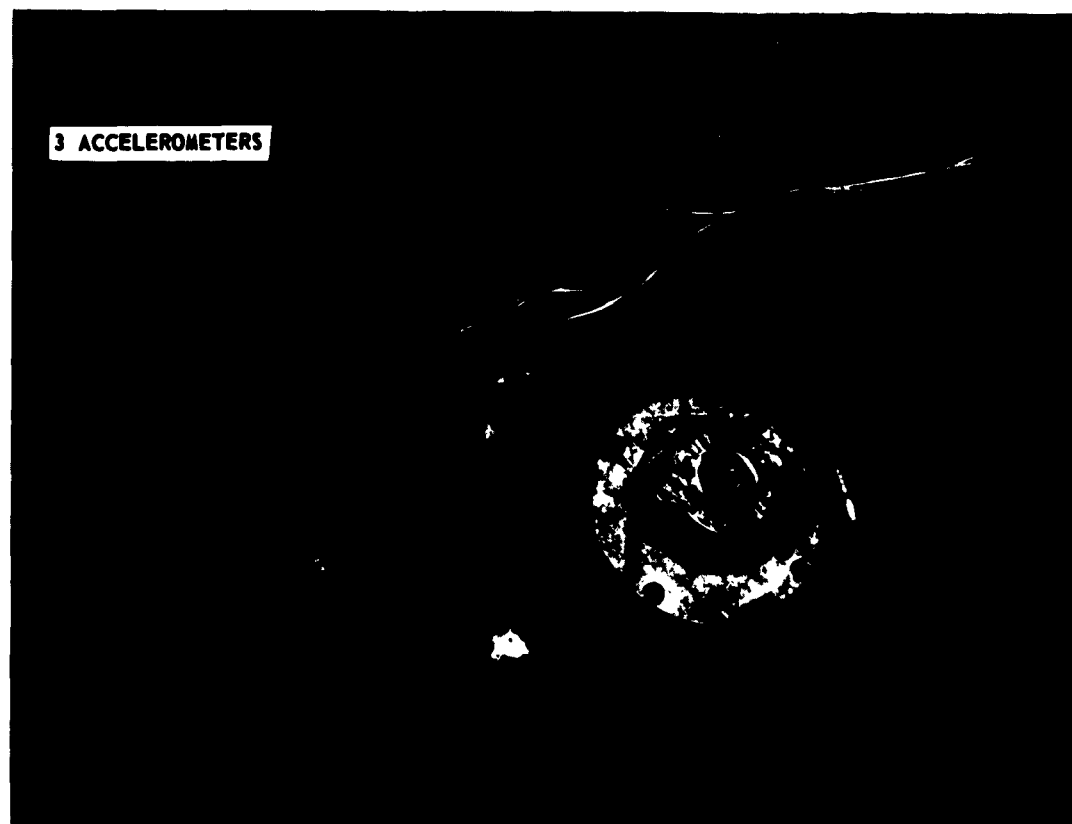


Fig. 3 - Accelerometers mounted on cylinder head

In this paper accelerations recorded at the transmission control housing, rear-rear axle housing, frame crossmember, and bed cargo body are discussed. Also presented are recordings taken under seven conditions of vehicle operation.

RESULTS AND DISCUSSION

The method of data analysis with a typical oscillogram is discussed first. Then, data taken from traces on oscillograms are presented in tabular form.

Data Analysis System

Signals recorded on tape were analyzed as shown in the instrumentation block diagram (Fig. 4). The signals from the tape were amplified, passed through the frequency analyzer filter system, and then were recorded with an oscillograph. The low-frequency bandpass filter was used for scanning at different times. A dual scope was used for viewing signals before and after passage through the frequency analyzer system. Figure 5 shows a typical 4 A level recorder oscillogram of accelerations on rear-rear axle housing in the vertical direction.

Vibrations are rms g values. Results were obtained while the M35 was driven on dry, black top surface, transfer case in low, transmission in fifth gear, at 30 mph.

A short description of each component that was instrumented will serve to supplement the tables.

Transmission

The transmission of the M35, shown in Fig. 6, is of the manually shifted, selective gear type with five speeds forward and one reverse. It is mounted on and supported by the flywheel housing and includes part of the clutch. The clutch release bearing and throw-out shaft mechanism is in the clutch housing and is attached to and considered part of the transmission. The clutch was always in the engaged position during data collection. A block for accelerometers was mounted on a plate and secured to the transmission control housing.

Accelerations at various frequencies, recorded in three perpendicular directions on the transmission control housing, are shown in Table 1.

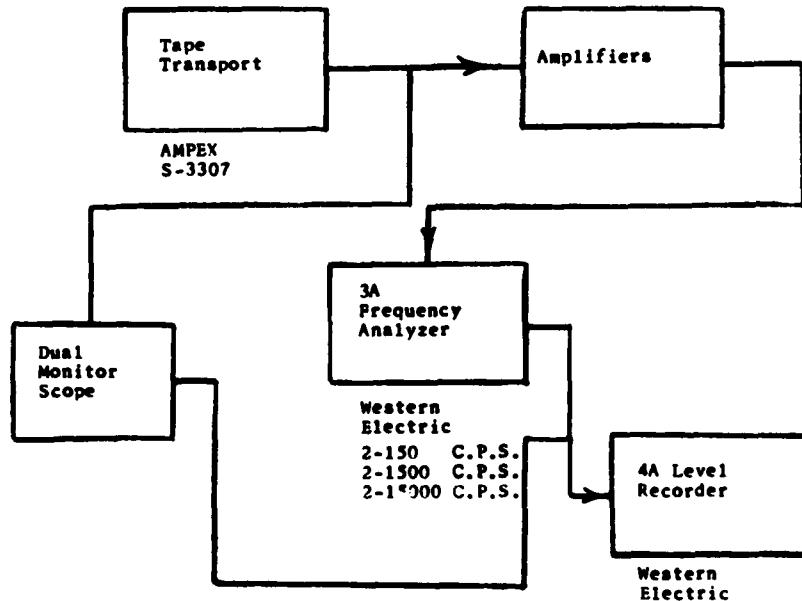


Fig. 4 - Block diagram of data analysis instrumentation

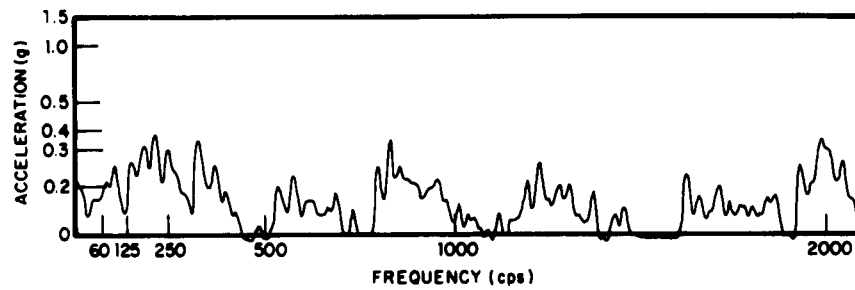


Fig. 5 - Typical oscillogram of acceleration of vibration on rear-rear axle housing

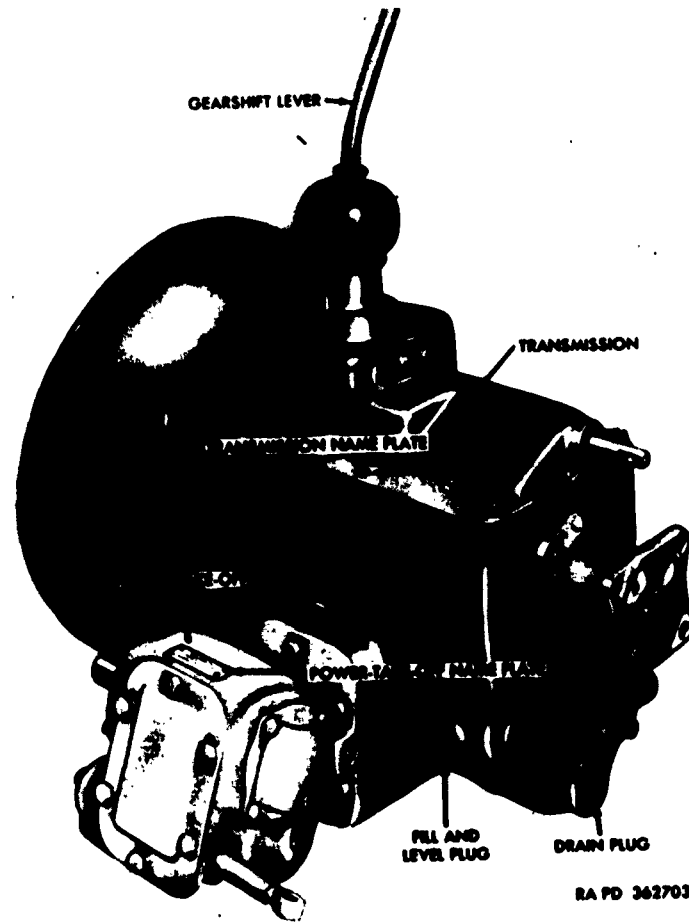


Fig. 6 - Transmission utilized in the M35

TABLE 1
**Accelerations at Various Frequencies in Three Mutual
 Directions on Transmission Control Housing**

Direction of Accelerometer Sensitivity	Acceleration (g) at Different Frequencies					Vehicle Operation Conditions			
	60 cps	125 cps	250 cps	500 cps	1000 cps	2000 cps	Transfer Case	Transmission Gear	Vehicle Speed mph
Vertical	a	.4	1.0	.7	1.2	.4	Low	Second	7
Vertical	.4	.4	.7	.8	.8	.5	Low	Fourth	20
Vertical	a	.3	.3	.5	.3	a	Low	Fifth	25
Vertical	.3	.4	.6	.6	.6	.4	Low	Fifth	30
Vertical	.2	.8	a	.3	.2	.2	High	Second	10
Vertical	.3	.4	a	.3	.6	.5	High	Third	20
Vertical	.3	.2	a	.2	.2	a	High	Fifth	35
Lateral	a	1.0	.9	.9	.6	.4	Low	Second	7
Lateral	.5	1.4	1.0	.9	1.5	.7	Low	Fourth	20
Lateral	.3	.4	.6	.9	.7	.4	Low	Fifth	25
Lateral	.3	.5	1.1	1.0	.9	.5	Low	Fifth	30
Lateral	.3	.6	.2	.6	.3	.3	High	Second	10
Lateral	.3	.7	.3	.8	.8	.5	High	Third	20
Lateral	.2	.4	.3	.4	.3	a	High	Fifth	35
Longitudinal	.2	.6	.4	.7	.5	.3	Low	Second	7
Longitudinal	.2	.6	.9	.5	.6	.4	Low	Fourth	20
Longitudinal	.2	.3	.4	.3	.3	.2	Low	Fifth	25
Longitudinal	.3	.3	.5	.3	.6	.5	Low	Fifth	30
Longitudinal	1.0	.5	.3	.3	a	a	High	Second	10
Longitudinal	.2	.4	a	.3	.3	.2	High	Third	20
Longitudinal	a	.3	.2	a	a	a	High	Fifth	35

NOTES: a - value on trace less than 0.2 g.

Use of the transfer case in low or high during vehicle operation did not significantly affect vibrations on the transmission control housing. But up to 25 mph and operating at road speeds near limits for transmission gear speeds, higher accelerations were recorded than at speeds below the limits. The highest acceleration shown in Table 1 is 1.4 g at 125 cps in the lateral direction.

If for any reason it is desirable to reduce any of the accelerations shown in Table 1, the following would be helpful:

Stricter quality control on components utilized in gear system;

Redesign of shock isolators for engine installation;

Redesign of various components in gear system.

Rear Axle

The rear-rear axle assembly of the M35 is shown in Fig. 7. Both rear axles are bevel drive, top mounted, double reduction, single-speed type. Forward-rear and rear-rear axles are mounted in tandem with torque rods on each side interconnecting the axles.

Power is transmitted from the transfer case by a propeller shaft to the forward-rear-axle differential and from the forward-rear-axle

to the rear-rear-axle differential by another propeller shaft. Driving force is transmitted from axles to chassis frame by six torque rods, four attached to the lower brackets and two attached to the upper brackets. Three torque rods are attached to each axle and take all driving and braking loads.

The axle shafts are full floating-type with flanges forged at the outer ends. These shafts transmit driving power from the differentials to the wheels. Stresses caused by turning, skidding, and wobbling of the wheels are taken entirely by the axle housing through the wheel bearings.

Accelerations at various frequencies recorded in three perpendicular directions on the rear-rear-axle housing are shown in Table 2.

Accelerations at frequencies above 1250 cps were not significant until road speeds above 20 mph were encountered. As can be seen from Table 2, most of the accelerations above 0.2 g occurred in the vertical and lateral directions. At the axle housing, vibrations are caused by the driving forces of the vehicle and by the type of terrain traversed. Because most stresses are transmitted from wheels to axle housing through wheel bearings, the vertical direction was one of the major axes for vibration transmittal. To decrease vibrations on this component of the vehicle, the choice of types of wheel bearing assemblies and of lubricant should be reconsidered.

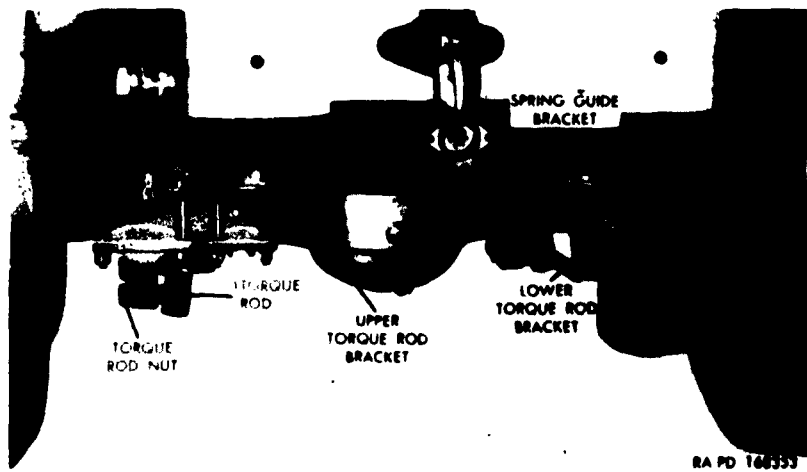


Fig. 7 - Housing for the rear-rear axles

TABLE 2
Accelerations at Various Frequencies in Three Mutual Directions on Rear-Rear Axle Housing

Direction of Accelerometer Sensitivity	Acceleration (g) at Different Frequencies						Vehicle Operation Conditions		
	60 cps	125 cps	250 cps	500 cps	1000 cps	2000 cps	Transfer Case	Transmission Gear	Vehicle Speed mph
Vertical	.3	a	a	a	a	a	Low	Second	7
Vertical	a	.3	a	a	a	a	Low	Fourth	20
Vertical	.3	a	.7	a	a	a	Low	Fifth	25
Vertical	a	a	.3	a	a	.3	Low	Fifth	30
Vertical	.3	a	a	a	a	a	High	Second	10
Vertical	.5	a	a	a	a	a	High	Third	20
Vertical	.3	a	.4	a	a	.3	High	Fifth	30
Lateral	.5	a	a	a	a	a	Low	Second	7
Lateral	.4	.3	.4	.3	.3	.3	Low	Fifth	25
Lateral	.5	.5	.3	.4	.3	.4	Low	Fifth	30
Lateral	.4	a	a	a	a	a	High	Third	20
Lateral	.5	.2	.5	.3	.3	a	High	Fifth	30
Longitudinal	a	.3	a	a	a	a	Low	Fifth	30
Longitudinal	.2	a	.3	a	a	a	High	Fifth	30

NOTES: a - value less than 0.2 g.

Frame, Crossmember

Frame side members are pressed-steel channels to which gussets, brackets reinforcements, crossmembers, and other various brackets and supports are riveted (Fig. 8).

Accelerations at various frequencies recorded on the frame crossmember are shown in Table 3.

At this location the major axes for vibration transmittal were longitudinal and vertical. The highest acceleration was 1.5 g at 60 cps in the vertical direction.

In the lateral direction, transfer case in low, vibration loads were not significant until vehicle was operated at road speed limits for transmission gears.

Cargo Body

The M35 truck is provided with a 12-foot flat bed, steel cargo body, mounted on auxiliary sills which raise the body floor above the tires (Fig. 9). Accelerations on the cargo bed are shown in Table 4.

At this location vibrations were transmitted significantly in the three axes. As can be seen from the table, most of the accelerations were at frequencies of 60 cps and 125 cps. Operation of the vehicle with transfer case in low range or high range did not influence the vibrations significantly.

The cargo bed is of much concern in transportation. Vibrations on the cargo bed are affected by the action of suspension system, type of material used for the cargo bed, and terrain to be traversed. Therefore, to decrease loads on the cargo bed these areas should be considered for a thorough evaluation.

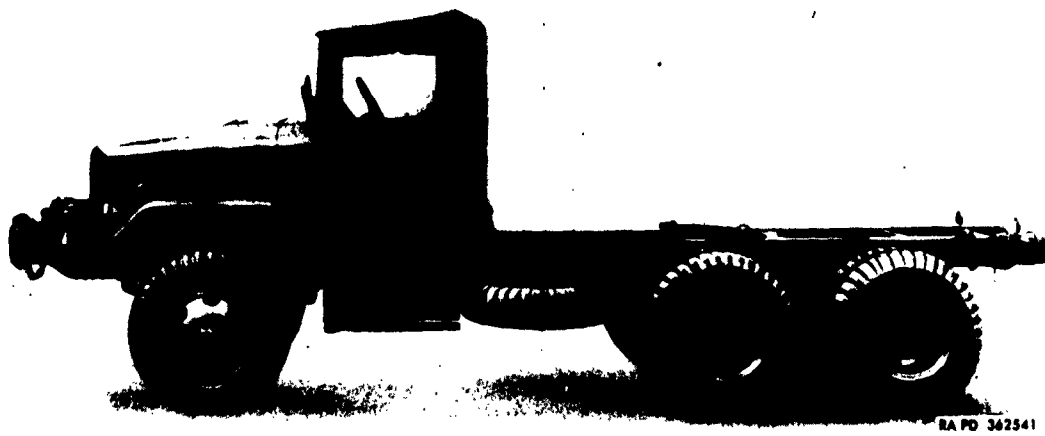


Fig. 8 - Chassis of the M35 cargo truck

TABLE 3
Accelerations at Various Frequencies in Three Mutual
Directions on Frame, Crossmember

Direction of Accelerometer Sensitivity	Acceleration (g) at Different Frequencies						Vehicle Operation Conditions		
	60 cps	125 cps	250 cps	500 cps	1000 cps	2000 cps	Transfer Case	Transmission Gear	Vehicle Speed mph
Vertical	a	a	.3	a	a	a	Low	Second	7
Vertical	a	a	.3	.3	a	a	Low	Fourth	20
Vertical	a	a	.5	a	a	a	Low	Fifth	30
Vertical	1.5	.4	a	.3	.5	a	High	Second	10
Vertical	.2	a	.3	a	a	a	High	Fifth	35
Lateral	a	a	.2	a	a	a	Low	Second	7
Lateral	a	a	.2	a	a	a	Low	Fourth	20
Lateral	.3	a	a	a	a	a	High	Second	10
Lateral	a	.2	a	a	a	a	High	Third	20
Lateral	.2	a	a	a	a	a	High	Fifth	35
Longitudinal	a	a	.3	a	.3	a	Low	Second	7
Longitudinal	a	a	.3	a	a	a	Low	Fourth	20
Longitudinal	a	a	.3	a	.3	a	Low	Fifth	25
Longitudinal	a	a	.6	a	.6	a	Low	Fifth	30
Longitudinal	a	a	.5	.3	a	a	High	Third	20
Longitudinal	.3	a	.6	a	.3	a	High	Fifth	35

NOTES: a - values on trace were below 0.2 g.

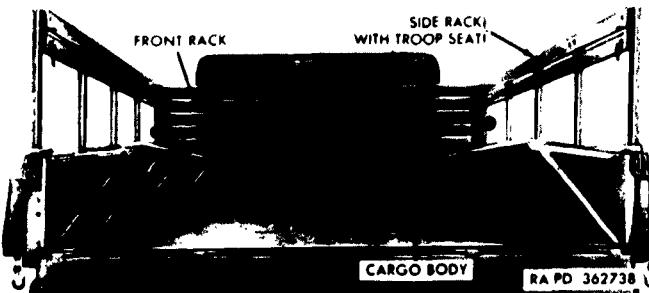


Fig. 9 - Cargo body of the M35

TABLE 4
Accelerations at Various Frequencies in Three Mutual Directions on Cargo Body

Direction of Accelerometer Sensitivity	Acceleration (g) at Different Frequencies						Vehicle Operation Conditions		
	60 cps	125 cps	250 cps	500 cps	1000 cps	2000 cps	Transfer Case	Transmission Gear	Vehicle Speed mph
Vertical	.3	.3	a	a	a	a	Low	Fifth	25
Vertical	a	a	.3	.5	a	a	Low	Fifth	30
Vertical	.3	.3	a	a	a	a	High	Second	10
Vertical	a	a	a	a	.6	a	High	Fifth	30
Lateral	.3	.3	a	a	a	a	Low	Second	7
Lateral	.3	.3	a	a	a	a	Low	Fourth	20
Lateral	.3	.3	a	a	a	a	Low	Fifth	25
Lateral	.3	.3	a	a	a	a	Low	Fifth	30
Lateral	.3	.3	a	a	a	a	High	Second	10
Lateral	.3	.3	a	a	a	a	High	Third	20
Lateral	.3	.4	a	a	a	a	High	Fifth	30
Longitudinal	a	.3	a	a	a	a	Low	Second	7
Longitudinal	.2	.3	a	a	a	a	Low	Fourth	20
Longitudinal	.3	.3	a	a	a	a	Low	Fifth	25
Longitudinal	a	.3	a	a	a	a	Low	Fifth	30
Longitudinal	a	.3	a	a	a	a	High	Second	10
Longitudinal	a	.3	a	a	a	a	High	Third	20
Longitudinal	.2	.3	a	a	.5	a	High	Fifth	30

NOTES: a - values on trace were below 0.2 g.

CONCLUSION

Comparison of the values presented in Tables 1 through 4 shows that results were most pronounced at the transmission control housing.

Use of the instrumentation described in this paper resulted in functional data, that is, values of accelerations at specific frequencies were readily established. Data from this and similar vibration programs at Detroit Arsenal are used in numerous applications, for example: Revision of specifications, input

values for vibration tables in testing vehicular components, and input values for vibration studies in the laboratory on full-sized and scaled-down models of vehicles.

As additional vibration studies will be conducted at the Arsenal, data reliability will be furthered. Likewise, some of the mechanics (block plans, factorial experiments) from the science of statistics will be utilized to further study the data reliability. Vibration frequencies will be given in various modes, the modes to be determined theoretically and then experimentally.

BIBLIOGRAPHY

1. Technical Manual 9-8022, Department Of The Army
2. Technical Manual 9-8000, Department Of The Army
3. "Twenty-Fifth Shock and Vibration Bulletin, Part II," December 1957, Office Of The Secretary of Defense Research and Engineering
4. N. O. Myklestad, "Fundamentals of Vibration Analysis," McGraw-Hill Book Company, Inc., New York, N.Y., 1956
5. Ken N. Tong, "Theory of Mechanical Vibration," John Wiley & Sons, Inc., Copyright 1960

* * *

Section 2

ISOLATION OF PACKAGED ITEMS

TRENDS IN THE ISOLATION OF PACKAGED ITEMS

R. K. Stern
Forest Products Laboratory,* Forest Service,
U.S. Department of Agriculture

This paper presents a resumé of current cushioning practices, recent progress by American Society for Testing Materials and Forest Products Laboratory, and recommendations for future work in the field of cushioning.

SURVEY OF CUSHIONING PRACTICES

In cooperation with the Packaging Research and Development Branch, Brookley Air Force Base, Alabama, the Forest Products Laboratory recently conducted a survey of current cushioning practices. Two important questions were to be answered; "How are items currently being protected from shock and vibration during shipment?" and "How good are present package cushioning application and design methods?"

The objective of the project was to learn what type of data and information would be most needed in a guide for the correct use of package cushioning materials by the Air Force and its contractors. Detailed questionnaires were sent to Air Force procurement management districts, to certain Air Force packaging specialists, and to 33 different companies or major divisions of corporations that manufacture aircraft and missile hardware for the Air Force. Replies from these companies would probably be more indicative of scientific cushioning application practices than

replies from manufacturers that supply miscellaneous material to the Air Force.

Additionally, all general packaging specifications were reviewed (excluding specific commodity specifications) to determine which specifications contain requirements that establish cushioning design requirements.

A summary of some of the more pertinent findings of these surveys follows:

1. The principal specifications that establish cushioning design levels by specifying particular rough-handling tests, in their order of importance, are MIL-P-7936, MIL-P-116, and JAN-P-100.

2. Air Force procurement management districts exercise little direct control over cushioning selection procedures in the procurement of material from prime contractors. Instead, responsibility for this function is usually left to the discretion of the Air Force packaging specialist or packaging personnel employed by the contractor.

*Maintained at Madison, Wis., in cooperation with the University of Wisconsin.

3. Of the 33 companies queried, 22 guessed fragility values; 17 claimed to calculate fragility values occasionally, and 14 conduct shock and vibration tests intermittently to determine fragility values.

4. The estimates expressed by different companies regarding fragility ratings for their products varied widely, but the range of 10 to 60 g included the majority of estimates.

5. The most frequently used cushioning application method (rated first by 21 companies) involves complete encapsulation of the item with cushioning material within the outer container. Corner pads and shock mounts were rated equally as being next in importance. Shear pads were rated next highest in importance, and steel spring suspension systems were rated lowest.

6. According to the weighted summary shown in Fig. 1, the order of importance of cushioning materials based upon amount used

is: First, cellulose wadding (including longitudinally compressed wadding); second, rubberized hair; third, urethane foam (including polyester and polyether base material); and fourth, corrugated fiberboard pads.

7. The favorite cushioning design method (used by 24 companies) involved the use of "peak acceleration-static stress curves." "Optimum cushion factors" or "cushion factor-stress" curves were used by 16 companies at least part time.

8. The chief sources of cushioning design information listed by packaging engineers employed by industry are manufacturers or vendors of cushioning materials and tests conducted by the companies themselves or by the parent organizations. Nine companies conduct dynamic compression tests of cushioning materials, but the resultant data generally is not published for use by other companies. Apparently, cushioning design articles published by trade journals, or listed in ASTIA bulletins,

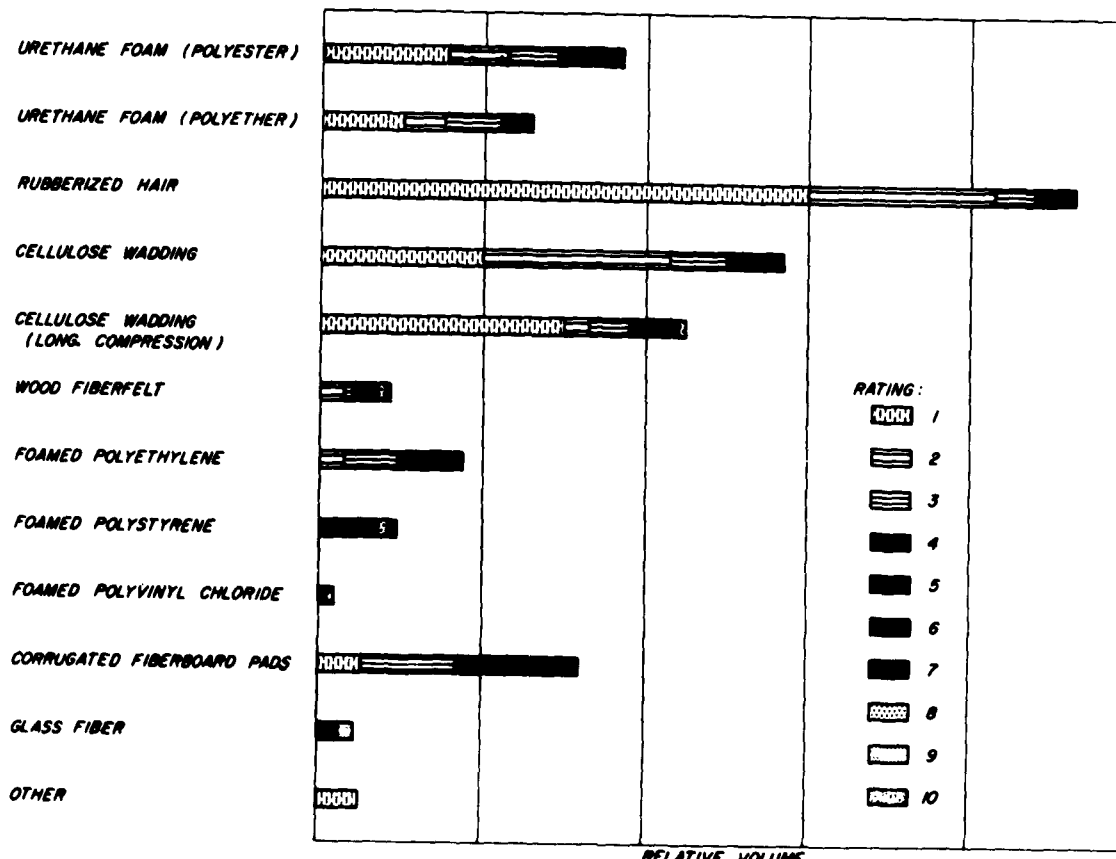


Fig. 1 - Relative volumes of different kinds of cushioning materials used by 33 different companies to cushion fragile equipment

Department of Commerce publications, or similar documents are seldom utilized directly by most packaging engineers. Furthermore, only a few manufacturers of cushioning materials can furnish information about the dynamic compression and creep characteristics of their products. Therefore, a general lack of reliable cushioning design information prevails.

9. Although the packaging engineers queried expressed an awareness of the importance of avoiding excessive creep, they indicated no general agreement on what constitutes a maximum tolerable creep rate. This is also generally true for vibration transmissibility characteristics of cushioning materials.

CURRENT TRENDS

Perhaps the most important current trend in the field of cushioning is the increasing awareness by packaging personnel of the desirability of an analytical approach to cushioning problems in preference to guessing. Three formidable obstacles have hampered widespread use of such methods. These are:

First, the problem of obtaining fragility ratings for delicate equipment by packaging personnel is as acute as ever. Most packaging specialists agree with Hessler's conclusion [1] that the only practicable general procedure for determining the fragility of miscellaneous complex, fragile items involves testing the material to the point where malfunction or damage occurs. Despite this agreement, the survey has indicated that only slightly more than 40 percent of the manufacturers of complex, high-value items actually test items — even on an intermittent basis — in order to determine fragility ratings. Furthermore, most companies who do test items merely use test conditions of sufficient severity to ensure conformance with operational performance requirements (such as those prescribed by MIL-E-5272, MIL-E-4970, and MIL-S-4456) and not acceleration values corresponding with damage or malfunction of items. Therefore, by such testing these companies do not determine actual fragility values. Nevertheless, these or guessed values are frequently the only values available to packaging engineers for use in packaging design.

Second, a great deal of uncertainty still exists about shipping environmental conditions, as indicated by the attention at this symposium.

Third, despite the volume of research that has been conducted on the subject of package

cushioning design, the newcomer to this field usually has considerable difficulty in deciding upon a practicable, universally applicable cushioning design method and even more difficulty in obtaining accurate usable design data for the various kinds of cushioning materials.

Some of the principal causes are:

Research workers themselves still disagree on what constitute the most advantageous design methods, forms of performance data, and testing methods and equipment.

The published literature is voluminous but nebulous. Frequently, important literature is unavailable to the average person because he is not entitled to distribution services (from agencies such as ASTIA, PATRA, Government agencies, etc.), and because private companies often prohibit circulation of reports for proprietary or economic reasons.

Manufacturers of cushioning materials advertise product data in different forms that favor their products but confuse the neophyte.

An important trend indicated in the survey summary is the shift by packaging engineers from the use of "cushion factor" [2] and its variation, "cushion factor-stress" curves [3], as a basic cushion design method to the use of "peak acceleration-static stress" curves. The deficiencies of the cushion factor theory were described in 1957 by Kerstner [4], who suggested the use of peak acceleration-static stress curves as a basic cushioning design method.

The survey indicates that considerable work remains to be done in the determination of creep rates for various materials, development of a practicable testing procedure, and in the determination of what creep rates are tolerable.

Another cushioning characteristic which has been receiving an increasing amount of attention is the vibration transmissibility of materials. This subject will be treated in considerable detail at this symposium.

Use of static test data for design problems involving dynamic loading conditions has continued to decline. The steady rise in importance of cellular elastomers in packaging and their obvious damping characteristics undoubtedly accelerated the realization that small to large differences in cushioning test data can be obtained, depending upon the loading rate.

ASTM COMMITTEE D-10

The development of sufficiently accurate dynamic compression testing systems and testing procedures have largely been solved, especially through the efforts of ASTM Committee D-10 (on Packaging), Subcommittee VI. The development of ASTM D 1596-59T, a standard dynamic compression testing procedure for measuring the shock isolation capability of cushioning materials, was the work of many leaders in the field of cushioning research. Their work involved extensive literature review, analysis of design methods for which the resultant data could be used, theoretical investigations of frequency response limitations and calibration techniques for recording systems, study of shock wave propagation in cushioning materials and shock-excited vibrations in components of testing systems, design and construction of basically different testing systems, and roundrobin testing of similar materials.

Among other things, Subcommittee VI is now working to the development of standard testing procedures for vibration transmissibility and creep characteristics of cushioning materials.

FOREST PRODUCTS LABORATORY ACTIVITY

In the field of cushioning research the Forest Products Laboratory is currently investigating the cushioning ability of corrugated fiberboard, preparing a cushioning design manual for the Department of Defense, and developing a cushioning selection guide. The initial version of this cushioning selection guide will be based upon the shock isolation capability of various cushioning materials expressed in terms of peak acceleration-static stress curves, creep rates, and initial cost of material. Later revisions will probably incorporate vibration transmissibility data as it becomes available. All dynamic compression test data has been derived according to D 1596-59T.

The threat that the behavior effects of outer containers might seriously distort the accuracy of the data for cushioning materials required investigation. Accordingly, rigid cubical and cylindrical dummy items having provisions for mounting three mutually perpendicular accelerometers near their centers of gravity and with loading capability between 1.95 and 149 pounds were constructed. Also, corner pads of various sizes of rubberized hair (MIL-C-7769, type IV, 3.9 p.c.f.) and

urethane foam (polyester type, 3.9 p.c.f.) were prepared. Rubberized hair and urethane foam were selected because they represented extremes in cushioning materials with variable damping characteristics. A rather extensive series of cornerwise drop tests was then made with the dummy items and corner pads inside paper-overlaid veneer containers (PPP-B-601A, style A), corrugated fiberboard containers (RSC domestic B-flute, 226 p.s.i. Mullen strength), and steel drums (MIL-C-6054). Cornerwise drop tests were made rather than flat drop tests because this type of test is one of the common rough-handling tests specified by Specifications MIL-P-7936, MIL-P-116, and JAN-P-100. The strain gage accelerometers were attached to each dummy item and their output was fed into a dual- and single-beam cathode ray oscilloscope. The test setup is shown in Fig. 2. The complete acceleration-time records were added vectorially and the peak instantaneous acceleration values for the first impact on the samples were averaged and plotted against loading head weight per unit area as peak acceleration-static stress curves. A comparison between the curves for the performance of both kinds of cushions according to ASTM D 1596-59T versus that for the same materials inside the different kinds of containers is shown in Figs. 3 and 4. The relative effects of containers upon data for both materials were similar. The curve for the combined performance of the corrugated fiberboard containers and rubberized hair pads (Fig. 3) was located at consistently lower values of peak acceleration than the curve for rubberized hair alone. As shown in Fig. 4 this was also true for the performance of urethane foam in corrugated fiberboard through a stress range up to about 0.3 psi. The steep upward swing of the curve in this stress range reflects "bottoming" of the corner of the item through the pad. However, this condition does not cause great concern because the practical usable upper limit in static stress for polyester-type urethane foam is about 0.3 psi. Static loading beyond this value produces excessive creep unless auxiliary support is employed.

For both materials the effect of the steel drum was to cause higher peak acceleration values below the range of 0.07 - 0.1 psi and lower values in the static stress range above the referenced range. To a lesser extent this was also true for the effects of the cleated-plywood container.

The deviation of data for transmitted peak acceleration values caused by container effects appears to be related to the stiffness of



Fig. 2 - Test setup for drop testing packages containing dummy items

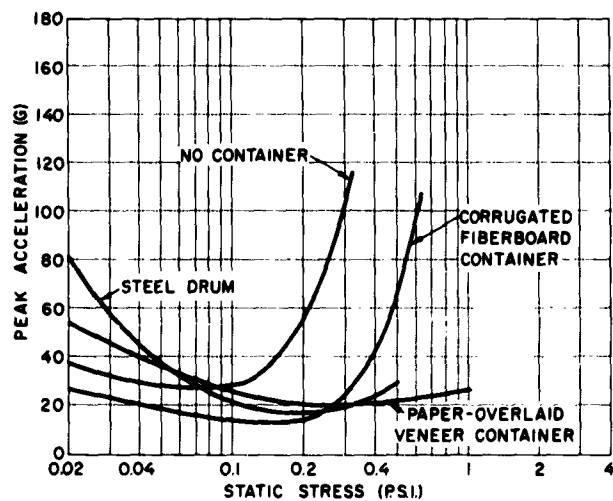


Fig. 3 - The effects of various kinds of containers upon compressive test data for rubberized hair

the container — the stiffer the container, the more divergence from data derived by ASTM D 1596-59T will be experienced, especially at very low values of static stress.

Although more work on this relationship is needed, the test series provides a partial

indication that cushioning test data derived according to ASTM D 1596-59T is reasonably accurate (within the stress range below the limit established by excessive creep) for design for free-fall cornerwise drops of complete packages, except where stiff containers, such as steel drums, are to be used with very light items.

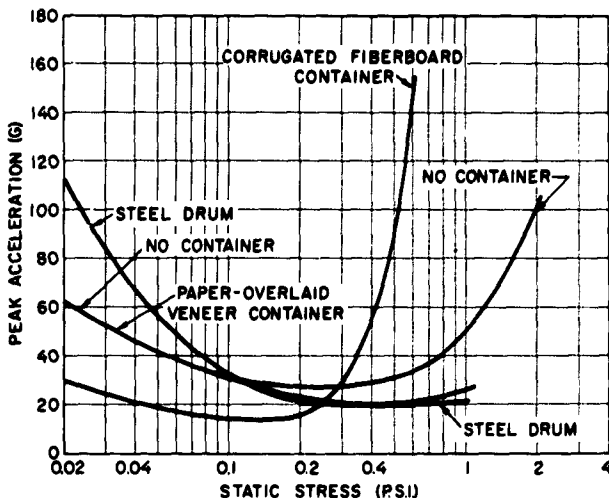


Fig. 4 - The effects of various kinds of containers upon compressive test data for urethane foam

SPECIFICATION MIL-C-26861

A prerequisite for the success of the cushioning selection guide being developed by FPL is that the performance of cushioning materials must somehow be stabilized. This can probably be best accomplished by acceptance of Specification MIL-C-26861, "Cushioning Material, Resilient Type, General." The present version of the specification, MIL-C-26861A, is now being coordinated; it represents the combined efforts of a large number of persons and organizations over a period of 7 years. Comments received by the coordinating activity, MOAMA (MONSSF), Brookley Air Force Base Alabama, indicate widespread agreement among private industries, industry advisory organizations, producers, and military installations with the general format of the specification, its classification scheme, and its objectives. However, minor changes and improvements still are needed.

The principal objective of this specification is to provide a single document to classify cushioning materials according to their shock absorption capabilities. In order to qualify for this specification, cushioning materials must be subjected to a standard dynamic compression test (a refinement of ASTM D 1596-59T) by the use of a qualified testing system and the data plotted as a "peak acceleration-loading range (static stress)" curve. This curve is then superimposed upon a grid, based upon categories of peak acceleration and static stress, and the material is classified

according to grade and class by the way the curve intersects the categories.

To qualify within a particular grade and class, the curve must occur completely below the boundary for the grade and through the entire stress range represented by the class. For example, the hypothetical curve shown in Fig. 5 would qualify under class 1, grades C and D; class 2, grades C and D; class 3, grades B, C, and D; class 4, grades B, C, and D; and class 5, grade D. A manufacturer need only have his material qualified once providing he does not alter the manufacturing process or basic material. If the material meets the other specification requirements, it is then listed on a qualified products list.

Qualification testing is based upon dynamic compression tests with an impact velocity corresponding to a drop height of 24 inches. This parameter was selected as a compromise between the high and low extremes of drop height that are required by Specifications MIL-P-7936, MIL-P-116, and JAN-P-100. Obviously, the shock isolation data produced directly by qualification testing will not produce data that is usable directly for cushioning design problems that involve substantially different drop heights. However, material performance will at least be standardized, and data already derived at FPL indicates that performance of materials at different impact velocities will follow a regular pattern. Once material performance has been stabilized, it will become feasible to evaluate the relationship between performance according to specification quality testing and

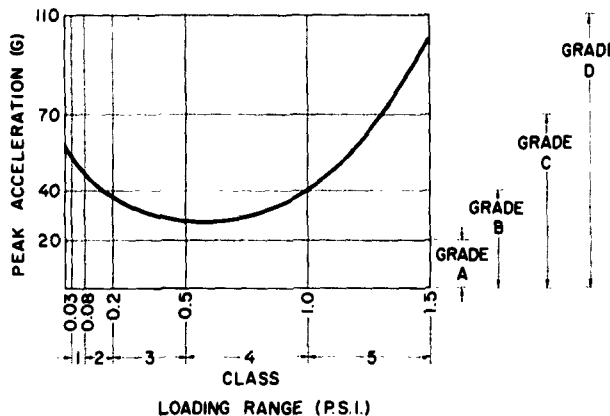


Fig. 5 - The classification scheme for cushioning materials according to their shock absorption characteristics in Specification MIL-C-26861

performance at different impact velocities for different materials. This information can then be made available to users.

Similarly, dynamic compression testing is required only at $73^{\circ} \pm 2^{\circ}\text{F}$. The forthcoming specification will omit a requirement for dynamic compression testing at high and low temperatures, except when deemed necessary by the procuring agency, and thereby reduce manufacturers' qualification expense. However, the cost of qualification, though nominal, will effect standardization by deterring frequent alteration of material.

LOOKING AHEAD

Undoubtedly, the most difficult task facing packaging engineers is the ascertainment of fragility values of items. Nevertheless, it is imperative that a reasonably simple, yet accurate and meaningful, fragility evaluation procedure be determined.

Once general agreement can be obtained on these matters, an earnest effort by the packaging profession will be needed to educate management personnel on the necessity of authorizing fragility testing whenever economically feasible. A supporting argument might be that often only minor expense will be required to repair or recalibrate items used for fragility testing, instead of the large expense of total destruction of material — a common conception regarding fragility testing.

Statistical determination of shock and vibration levels associated with shipment is

another important need. Actual evaluation of these hazards and incorporation of the resultant information into specifications has been stymied principally by a lack of a suitable measuring and recording instrument. However, a promising device which has been under development by the Corps of Engineers, ERDL, Fort Belvoir, Va., for several years, might fill this need.

Additionally, statistical information is needed to reflect the relative importance of cushioning performance at such temperature extremes as 160° and -65°F in shipment of military materiel. This information is needed particularly by specification writers in order to enable them to include or exclude specific provisions. That this problem exists is made obvious by the fact that both urethane foam and rubberized hair, two of the most commonly used cushioning materials for military packaging, perform poorly at -65°F .

As discussed previously, the stabilization and standardization of the performance of cushioning materials is another prerequisite for accurate cushioning design.

Determination of standard testing procedures and maximum tolerable limits for creep and vibration transmissibility of cushioning materials are needed refinements to existing cushioning design technology. Perhaps, the key to the solution of the problem of where to set maximum tolerable creep limits for materials lies in the determination of the correlation between different degrees of looseness of an item in a package and the severity of vibration experienced by the item during transportation vibration.

Finally, greater emphasis in design of new, superior cushioning materials and in the application of existing materials should be placed upon the use of the "buckled column" principle, as described by Reinert [5], Pearsons and Ungar [6], and others. Utilization of this principle by loading rubberized hair on edge is

commonplace abroad, but is seldom employed in the United States.

Considerable potential also exists in the possibility of development of improved cushioning materials, as indicated by Burgess [7] and by Ungar and Hatch [8] by the synthesis of materials having more favorable damping characteristics.

REFERENCES

- [1] Hessler, R. D., "Fragility Study, Part I," Boeing Airplane Co., Renton, Wash., July 1960.
- [2] Janssen, R. R., "Selecting Package Cushioning Materials to Provide Minimum Container Cubage," North American Aviation Corp., Los Angeles, California, October 1952.
- [3] Jones, R. E. and James, W. L., "Simplified Methods of Selecting and Designing Package Cushioning Materials," U. S. Forest Products Laboratory Report No. 2031, April 1955.
- [4] Kerstner, O. S., "General Principles of Package Design," Northrop Aircraft, Inc., Hawthorne, California, February 1957.
- [5] Reinert, G., "Which Shock-Absorbing System Will Do The Job?" Product Engineering, May 1961.
- [6] Pearsons, K. S. and Ungar, E. E., "Development of Packaging Material With Constant Restoring Force," Bolt, Beranek, and Newman, Inc., July 1960.
- [7] Burgess, J. C., "Distributed Resilient Media for Shock and Vibration Isolation," Stanford Research Institute, October 1960.
- [8] Ungar, E. E. and Hatch, D. K., "Your Selection Guide to High Damping Materials," Product Engineering, April 1961.

DISCUSSION

Mr. Mustin (Reed Research): You made a statement about poor performance of rubberized hair and polyurethane foams at low temperatures. I was wondering if you would care to define low temperature for us because I think this should be done.

Mr. Stern: What I am referring to there is a temperature, approximately -65°F, which appears very frequently in procurement documents. My reason is that elastomeric substances like polyurethane foam and even rubberized hairs with their binders tend to stiffen very markedly and in some instances become very brittle so that they can hardly render a reasonable performance at such temperatures.

Mr. Jones (Nopco, Chairman): I think it is interesting to note, in that respect, that in the proposed revision of MIL-C-26861 they

have changed the low-temperature requirements to -30° F.

Mr. Holmes (Westinghouse): What are the trends or what schemes are there for eliminating creep where heavy static loads are anticipated? With polyurethane foams, for instance?

Mr. Stern: I don't know of a great deal that is being done. I am sure most of you are familiar with Jim Hardig's proprietary device which involves the use of a rubber tube inside a urethane foam pad. It is intended, to some extent, to help in this direction. I think individual innovators have gone to die-cut pads in some instances but basically we are still troubled with the primary problem of the fact that materials will creep. We might compensate for it somehow by attempting to have a degree of precompression of the material, but

I think most people will agree that you can accept a certain amount of looseness in the pack produced, of course, by creep and the initial deflection of the material, but that there is

some point at which we get excessive looseness and get into real trouble through out-of-phase collisions with the container during rail shipment and that sort of thing.

* * *

AN APPROACH TO THE SOLUTION OF SHOCK AND VIBRATION ISOLATION PROBLEMS AS APPLIED TO PACKAGE CUSHIONING MATERIALS

Carl Henny and Frank Leslie
The Boeing Company,
Seattle, Washington

This paper describes methods of testing and evaluating vibration isolation characteristics of cushioning materials. The problems of vibration on packaged items will be discussed. The work the Boeing Company is doing to solve the problems of vibration isolation when cushioning materials are used is included.

INTRODUCTION

When packages are handled and transported, they are subjected to a mechanical environment. This environment has the capability of damaging the items contained within the package. Damage is caused by shock and vibration when the fragility level of the packaged item is lower than the forces resulting from the induced environment.

Unlike an airplane, a weapon system is not flown to its destination as a unit, but, instead, is packaged and shipped. These shipments include a whole missile, ground support electronic equipment, and all necessary spare parts.

Needless to say, if any missile component arrives in a damaged condition, the operational status of a missile weapon system can be seriously impaired. To achieve the greatest reliability, the mechanical environment to which a packaged part is subjected must be defined. Thus, an isolation system must be designed into the package to reduce the damage potential of the environment. The purpose of this paper is to discuss problems and possible solutions encountered in the selection of proper isolator materials.

DEFINITION OF A MECHANICAL ENVIRONMENT

Packaging specifications usually define the anticipated mechanical environment in terms of the rough handling to which a package may be subjected. More sophisticated specifications used by The Boeing Company define this anticipated environment in terms of shock and vibration spectra. These spectra are described as an input and response of a given g magnitude and frequency range. The shock spectrum is used in qualifying packages with drop tests where drop height is a function of part weight. The vibration spectrum is shown in Fig. 1. Here, acceleration in g is plotted versus frequency. A definition of the input is:

5 - 10 cps	0.4-inch D.A.
10 - 22 cps	± 2 g
22 - 35 cps	0.08-inch D.A.
35 - 300 cps	± 5 g.

The allowed response curve is:

5 - 16 cps	0.4-inch D.A.
16 - 50 cps	± 5 g
50 - 300 cps	± 2.2 g.

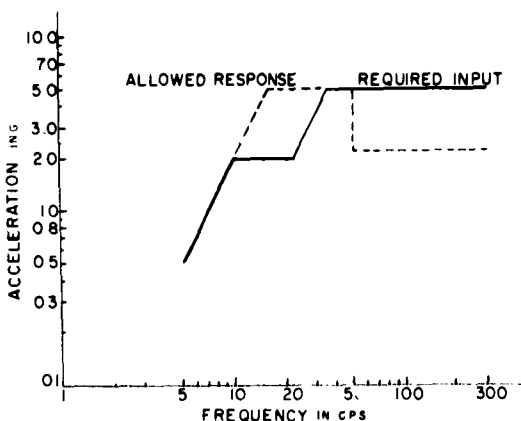


Fig. 1 - Vibration spectrum -- required input and allowed response

ISOLATOR MATERIALS

Materials which lend themselves for use as economical isolators include the various types of plastic foams and latex bound fibers. These materials are available in a wide range of properties, forms, and prices. Normally the performance characteristics of these materials are described in terms of their chemical resistant properties. Further data may include a stress-strain curve. This information indicates only generally how the material will perform in a mechanical environment. In order to describe the performance of a material, extensive shock and vibration testing is required.

SHOCK TESTING

The Boeing Company has designed and fabricated a cushion tester capable of performing to the requirements stated in MIL-C-26861 and ASTM D 1596-59T. This cushion tester is shown in Fig. 2.

Briefly, these specifications for shock testing of cushioning materials require that a weight impact a cushion specimen at a known impact velocity. The impact thus eliminates a cushioned item being dropped from a specified drop height.

The cushion tester consists of a vertically mounted guided platen, an impact anvil, a lift mechanism, and controls. Weights varying from 8 to 100 pounds can be attached to the platen, and the drop height can be adjusted from 6 to 48 inches. A maximum specimen

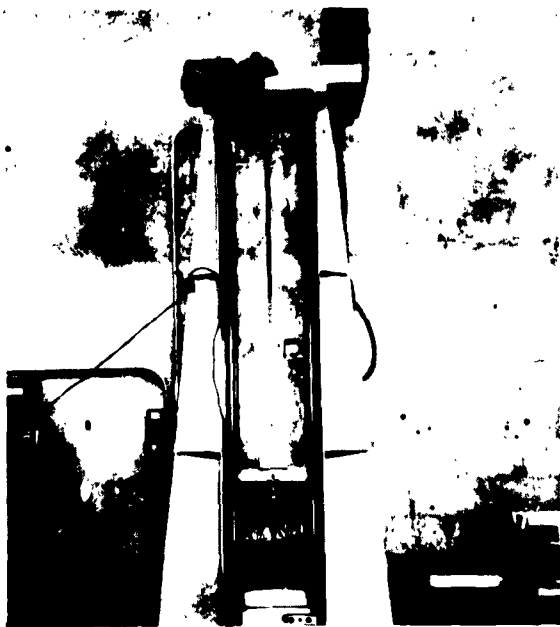


Fig. 2 - Cushion tester

size of 10 inches by 10 inches by 7.5 inches thick can be used for testing.

In addition to an accelerometer, the drop head is instrumented to record the impact velocity. Thus, a calibration for impact velocity versus drop height is established. A recording oscilloscope and amplifier system is used in conjunction with strain gauge accelerometers for data gathering. This system is shown pictorially in Fig. 3 and schematically in Fig. 4.

The impact velocity is measured by recording the time elapsed during the final increment of travel prior to impact on the drop head. It has been found that the impacting head has an acceleration of 366 inches per second per second. The acceleration is independent of drop height and drop weight. This value can be used to compute the drop height necessary for a particular impact velocity. Thus, guided drops equivalent to free fall drops can be made. A sample recording of a peak acceleration-time curve and a velocity calibration curve for a typical material is shown in Fig. 5.

The shock performance characteristics of a cushioning material are measured at certain

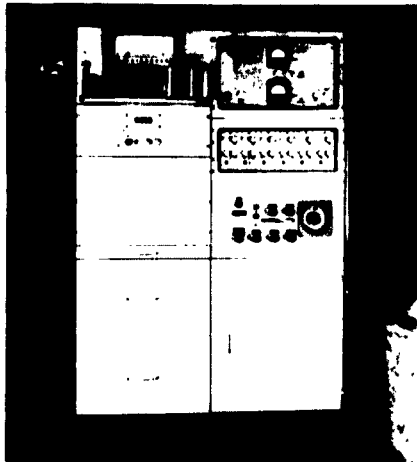


Fig. 3 - Data recording console

heights and bearing stresses. A plot of peak acceleration versus bearing stress is drawn for combinations of material type, cushion thickness, and drop height. A package designer, by knowing the part dimensions and weight, can obtain the bearing stress for a cushion. The drop height to which the part must be tested can be determined from appropriate packaging specifications. By knowing the fragility level of a part and considering

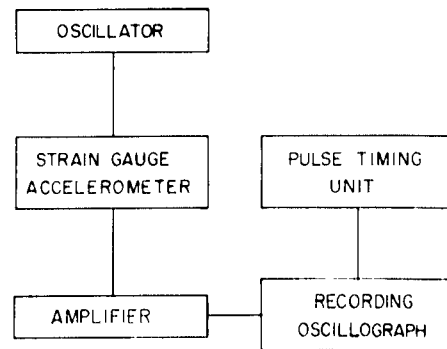


Fig. 4 - Block diagram
of instrumentation

the acceleration versus bearing stress curves, the proper material and cushion thickness can be selected. Thus, adequate shock protection is afforded for the packaged part. Typical curves for a polyurethane foam when impacted by weights dropped from 16 and 22 inches are shown in Fig. 6.

VIBRATION TESTING REQUIREMENTS

Because of their nonlinear spring rates and damping characteristics, cushioning materials are difficult to analyze. For this reason, testing was selected as a more practical approach for the determination of isolation characteristics. Material testing, as opposed to testing each equipment item in its packages, will yield better long range results.

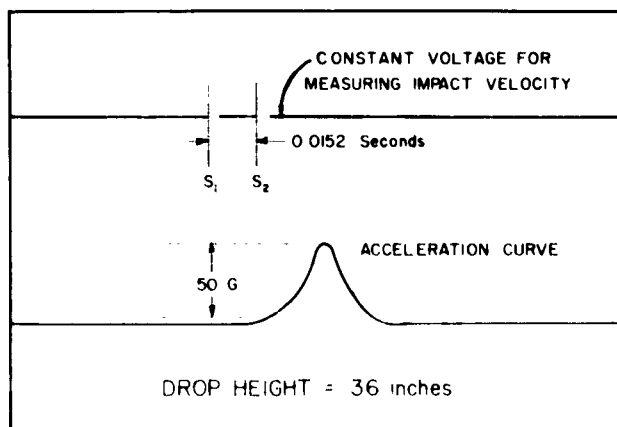


Fig. 5 - Sample recording of a typical cushioning material shock response curve and a velocity calibration curve

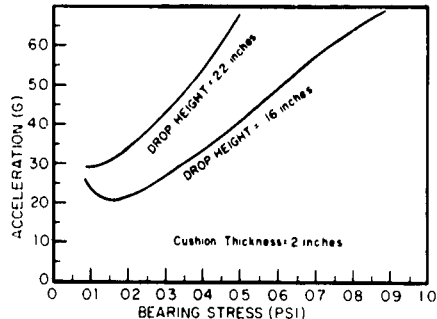


Fig. 6 - Acceleration versus bearing stress curves for a typical polyurethane foam

The Company has two methods of using cushioning materials which require two different vibration fixtures. One method uses cushion pads in a conventional manner with the part surrounded by cushions used as compression pads. An example is shown in Fig. 7. The second method uses a pallet which supports the packaged item and is commonly referred to as a "sandwich" pallet pack. This "sandwich" consists of a sheet of foam material bonded between two rigid surfaces. The foam is free to act in tension and compression. An example is shown in Fig. 8. The actual testing was dependent on a fixture design which would simulate a cushioned item in a package. The design of the fixture had to allow for testing either



Fig. 7 - Typical package with cushion pads

two cushions in compression or one cushion in tension and compression.

VIBRATION TEST

Based upon the test requirements listed in Table 1, the test fixture for testing cushions in compression was designed. This fixture is shown in Fig. 9. The weight of the test fixture was held to a minimum by fabricating it from one-inch magnesium plates. The rigidity was

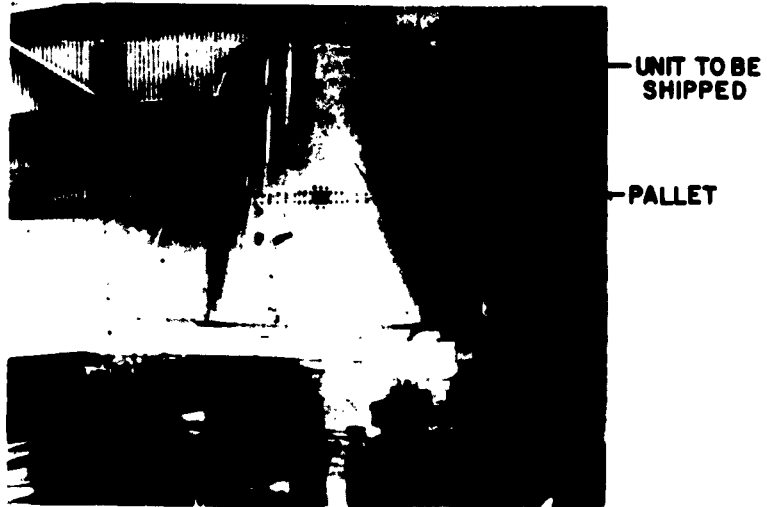


Fig. 8 - A "sandwich" pallet pack with packaged item mounted for a vibration test

TABLE 1
Vibration Test Procedure

Sample Number	Bearing Stress in psi	Frequency Range in cps	Vibration Input in "g"
1, 2, 5	0.11	5-300	1.0, 2.5, 5.0
1, 2, 4, 5	0.23	5-300	1.0, 2.5, 5.0
1, 3, 4, 5	0.30	5-300	1.0, 2.5, 5.0
1, 3, 5	0.50	5-300	1.0, 2.5, 5.0

acquired by stiffeners welded in place. The test fixture was designed to hold two cushions with the bearing load placed between them. Both cushions were held in place by the top plate, which was attached to the frame. The plate did not add appreciable load to either cushion.

The frame of the test fixture for a pallet is the same as the frame of the test fixture for cushions in compression. A box which is part of the bearing load is attached to the pallet to

prevent extraneous motion. The first resonance of either fixture, with a maximum bearing load, is above 350 cycles per second and exceeds the test frequency range.

By decreasing the area of the pallet pack, the same weights will yield higher bearing loads. Since the total weight is constant, additional force is not required from the vibrator.

The vibrators, which were designed and fabricated by The Boeing Company, provided the input for the test. The vibrators are shown in Figs. 9 and 10. The larger vibrator is rated at 7500 force pounds and is driven by a 30-kva amplifier. The smaller unit is a 750-force pound vibrator driven by a 10-kw amplifier. The maximum double amplitude available from the larger vibrator is 0.50 inch at low frequencies without objectionable waveform distortion. The smaller vibrator has a double amplitude of 1.0 inch. The maximum acceleration obtainable at the lower frequencies is limited by the effective double amplitude and is defined by the formula:

$$g = \frac{(D.A.) (F)^2}{19.558}$$



Fig. 9 - Magnesium cushion test fixture with specimen mounted on large vibrator

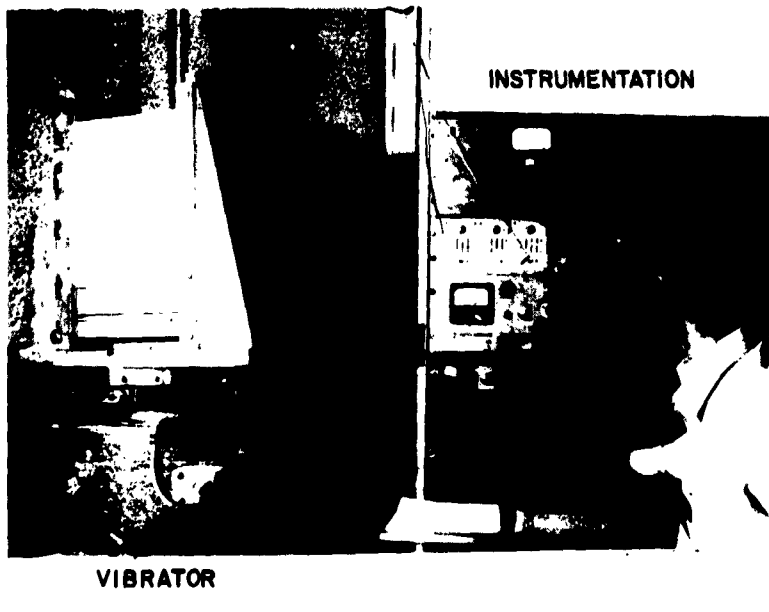


Fig. 10 - Pallet pack fixture mounted on 750-pound vibrator and instrumentation

This formula is derived as follows:

$$S = D \sin (\omega t)$$

$$A = \frac{d^2S}{dt^2} = D \omega^2 \sin (\omega t)$$

$$\text{Let } \sin (\omega t) = i$$

$$\text{Then } A = S(2\pi F)^2 \text{ and } S = \frac{D \cdot A}{2}$$

$$\therefore 386 \text{ g} = \frac{D \cdot A}{2} (2\pi F)^2$$

$$g = \frac{D \cdot A \cdot (F)^2}{19.36}$$

where

D = Peak Amplitude	D.A. = Double Amplitude
S = Vector Amplitude	F = Frequency in cps
A = Acceleration	$\omega = 2\pi F$
G = Acceleration in gravity units of in/sec ² or $\frac{A}{386}$	t = Time

A block diagram of the instrumentation for monitoring and recording the input and response of the cushion or the pallet, is shown in Fig. 11. The sine wave output of the oscillator is fed through the amplifier. The vibration input required is maintained by monitoring the input accelerometer. This method obtains response acceleration from a specific input at discreet frequencies. Thus, a smooth curve can not be drawn from the data.

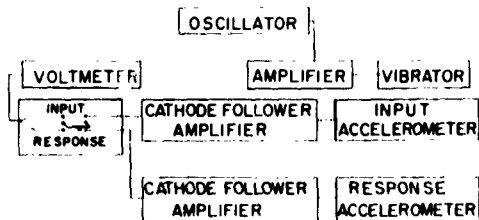


Fig. 11 - Block diagram of instrumentation for hand plotting

The instrumentation for continuously recording the input and response data is shown in Fig. 12. The input and response signals are fed through a logarithmic converter, and a continuous curve is directly plotted on log-log paper. A direct current voltage which is proportional to the logarithm of the frequency is obtained from a potentiometer-voltage divider network. This network is part of the automatic frequency scanning device on the oscillator. Figure 13 is a reproduction of one of the response curves recorded with this instrumentation. The accelerometers used were piezoelectric transducers. The cathode-follower amplifiers have gain and attenuation allowing a wide range of output in millivolts per g.

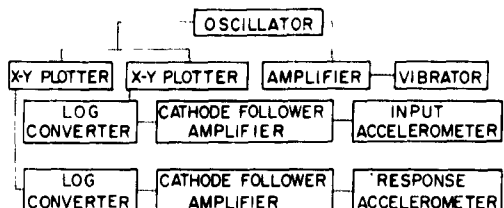


Fig. 12 - Block diagram of instrumentation for automatic plotting

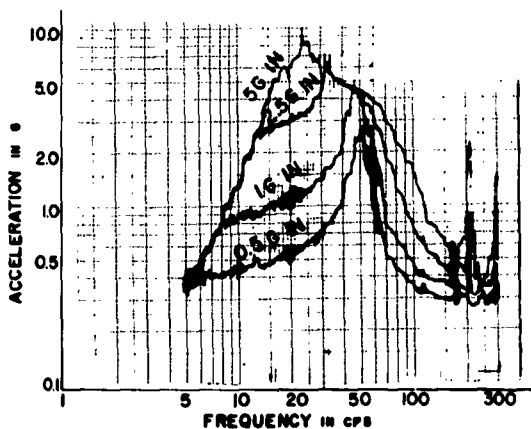


Fig. 13 - X-Y plot of response from automatic plotter

The time required to set up the test, obtain the data, and reduce the data to graphical form, is approximately eight hours per curve employing the hand plotting method. Five samples of a particular material are generally tested (Table 1). An average time of one hour is required to set up, test, and record the response of one sample with one bearing stress at all three vibration levels.

VIBRATION TEST RESULTS

An example of vibration test results is shown in Fig. 14. The transmissibility versus the forcing frequency is plotted for a 2-inch thick sample of polyurethane foam at a bearing stress of 0.23 pound per square inch. Plots of response to four different g inputs of 0.5, 1.0, 2.5, and 5.0 are shown. As can be seen in this figure, an increase of dynamic load decreases the natural frequency and peak transmissibility. In addition, a plot of the response of a 2-inch thick cushion at bearing stresses of

0.11, 0.23, 0.3, and 0.5 pound per square inch and subjected to a g input of 2.5 is shown in Fig. 15. As shown in Fig. 14, an increase in load decreases the natural frequency and peak transmissibility.

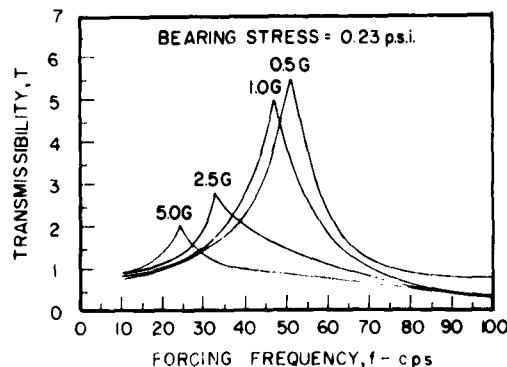


Fig. 14 - Transmissibility versus forcing frequency curves for a 2-inch cushion thickness and a bearing stress of 0.23 psi

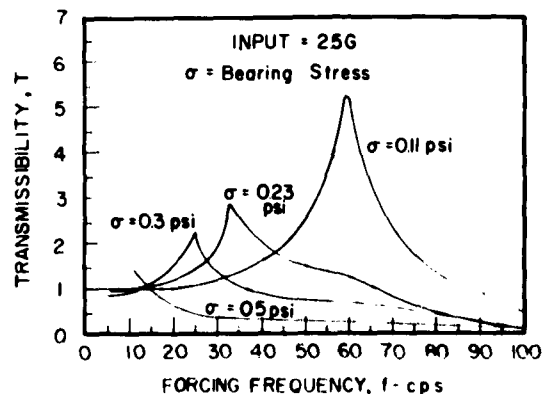


Fig. 15 - Transmissibility versus forcing frequency curves for a 2-inch cushion thickness and an input of 2.5 g

The response of a cushioning material to the vibration input illustrated in Fig. 1 is shown in Fig. 16. In this test, a 2-inch thick cushion with a bearing stress of 0.81 pound per square inch was vibrated. Note that the natural frequency is below 5 cycles per second, which was the lowest frequency tested. In addition, the test was repeated with the same cushion at -65 degrees Fahrenheit. The response of this material indicates a natural frequency between 23 and 26 cycles per second.

This is shown in Fig. 17. Hand plotting does not describe the response in sufficient detail to show the exact natural frequency.

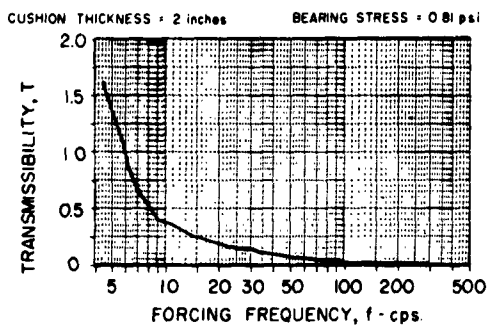


Fig. 16 - Response of a cushioning material to the simulated vibration transportation environment of Fig. 1

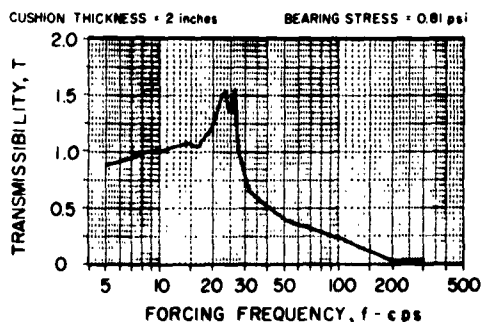


Fig. 17 - Response of a cushioning material to the simulated vibration transportation environment of Fig. 1 at a temperature of -65°F

DISCUSSION OF TEST RESULTS

To use these results effectively, a package designer must compromise between the shock data and vibration response data. Normally this compromise will consist of cushion loading values near the minimum indicated on the acceleration-bearing stress curves. However this value must be sufficiently high to provide effective vibration isolation.

In the instance cited, the bearing stress to obtain optimum shock and vibration isolation characteristics is between 0.23 and 0.30 pound per square inch. Relating this bearing stress to the stress-strain curve in Fig. 18, it is

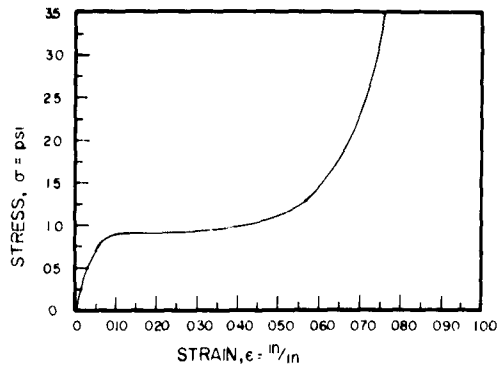


Fig. 18 - Stress versus strain curve for a polyester polyurethane foam

found that this loading yields an initial strain of approximately 3 percent. However, a strain value of 3 percent should not be construed to be a general rule regarding optimum loading of all polyurethane foams.

The testing of the cushion material is not an end in itself, but is essential to supply data to the packaging engineer. Following design, fabrication, and satisfactory completion of shock testing, the package is ready for dynamic vibration analysis. For the packaging to meet the required specification the maximum acceleration measured on the item being tested must be within the allowed response curve of Fig. 1.

Some packages to be shipped are quite large. Figure 8 shows a shipping container mounted on four 750 force pound vibrators. The input to the package is measured at the head of each vibrator and is recorded on tape. The response of the packaged item is also recorded on the tape. Voice and frequency information are also recorded. After the test has been completed, the taped data is transferred directly to an X-Y plotter.

SUMMARY

A simulation of the shock and vibration environment present during packaging and transporting of missile items has been described. In general, the spectra which represent these environments are specified by the government or by the contracting agency. In addition, the methods by which The Boeing Company determines shock and vibration isolation characteristics of cushioning materials have been presented.

Finally, a discussion of shock and vibration performance characteristics of cushioning materials has been presented. This discussion was intended to provide the package designer with data for reliable packaging of missile components. Shock performance can be determined by following the requirements stated in MIL-C-26861. Vibration isolation can be determined by applying the Proposed Standard Method of Test to Determine the Vibration Transmission Characteristics of Package

Cushioning Materials. This method has been recently submitted to ASTM Committee D-10 for acceptance as a tentative method.

ACKNOWLEDGMENT

The authors wish to express their thanks to Vernon Knight for his assistance in reducing much of the vibration data of cushioning materials presented in this paper.

DISCUSSION

Mr. Munson (General Dynamics): One of your slides shows a transmissibility of 2.5 to be within acceptable limits in certain frequency ranges. Are we to understand that this is the maximum that you advocate?

Mr. Leslie: No, this isn't the maximum. This was merely information for the package designer that he could have. Not that he would use it the way it was used. It would be up to the designer to determine whether he wanted to use this equipment, this particular specimen, at that particular stress level or not.

Mr. Munson: I see, then this curve as shown on the slide is simply a "for instance" curve and not what you suggest as a criteria.

Mr. Leslie: No. This was not a criteria curve. Our criteria curve was our input and response curve (Fig. 1). This the package designer must have; his package must respond within this allowed response curve.

Mr. Lawrence (Douglas Aircraft): You made several references to the vibration spectrum input. I would be interested to know where this came from and also if you used the same one regardless of the logistic pattern for which the part that you were designing a container is intended.

Mr. Henny: Well, the vibration spectrum, the input, is what we have specified as being in existence in shipping environments. This covers the whole range of vibration, that is, frequency and g level, and this is the range that we anticipate getting in handling and packaging situations. The allowed response curve is the curve that the designers for the components are designing to on Minuteman components. So we have the level which the components can take and we know the level of the

environment. We just put them together and we have our allowed response curve.

Mr. Preis (Hazeltine Corp.): I'd like to know from Mr. Leslie if you had ever done any testing on silicone rubber as compared to this foam type of material, and if you have, what transmissibilities you got? I've heard of this temperature problem several times and it plagued us, and I wondered if you had any other results.

Mr. Leslie: No, we haven't tested any silicone rubber materials yet, so I am afraid I can't help you. I'm sorry.

Mr. Opalinski (Woodland Container): I was wondering if Boeing had used many molded urethane pads, where they were actually molded to the item, and in the molding did you actually have to make the molded part slightly undersize, or just the size?

Mr. Henny: Right now we are in the development stage of using molded or foam-in-place urethane foam. In these cases we make up a simulated part, that is dimension wise, and we place this in the container and pour in a predetermined amount of the urethane foam and we let it foam up. This bonds directly to the inside of the outer container and by using appropriate parting agents we get the simulated part out again. The molded foam conforms quite closely to the outer dimensions of the part being packaged. We have done some vibration and shock testing on this material, but nothing very extensive at this time. In a lot of instances the materials that we can get for foam-in-place are stiffer than we buy in sheet stock and this is what we are looking for - stiff urethane foams. For these cases they do work out quite well.

Mr. Lawrence: You made passing reference at one point to a urethane sandwich operating in tension under certain circumstances. What experience, if any, have you had with your sandwiches operating in tension. Do you test them in tension and, if so, do you test them long enough for fatigue of the cushion to present itself?

Mr. Leslie: In the pallet pack the urethane foams are free to act in compression or tension. Since the weight is sitting on top of it, the part goes up and down, so when we hit the top of the sine wave input we actually get the cushion in tension. At the lower end we get the cushion in compression. We have tested the parts. We have cycled from 5 to 300 cycles and back to 5 in about 30 minutes twice. This is our longevity test. Some of the foams take it and some of them do not. I would have to wait until I got back to Boeing to tell you which ones have worked better than others. But the part in tension, we have not noticed as much failure as I expected. After all, large pallets are not subjected to turning upside down.

Mr. Gertel (Allied Research): What did you do about the difference between the low-temperature performance and the conventional performance? Do you accept the low temperature increased stiffness and does this cause any problems with your acceptable transmissibility curves or fragility curves?

Mr. Henny: To date we haven't done much testing at -65°F for shock absorbing characteristics. We have done some on vibration testing of materials. It is interesting to note that in a couple of instances with the vibration spectrum to which we were testing, the material at room temperature did not pass, but at -65°F it came close enough so that we could say it did pass. It was very, very close. It just missed a corner of the curve. Right now exactly what performance requirements are to be met at -65°F are not really clearly specified to us, and with this in mind we are just ignoring testing it at -65°F at this time. We haven't gone very extensively into it.

* * *

DESIGN AND EVALUATION OF PACKAGES CONTAINING CUSHIONED ITEMS, USING PEAK ACCELERATION VERSUS STATIC STRESS DATA

T. J. Grabowski
Research and Development Center
Armstrong Cork Company
Lancaster, Pennsylvania

A series of investigations to correlate data obtained by the ASTM Dynamic Test Procedure for Cushioning Materials, with actual performance data in a package, is described and the results of these investigations are presented.

INTRODUCTION

The problem of providing suitable cushioning during shipment of highly complex equipment and components, particularly in the military and electronic fields, has been simplified somewhat during the past two years by a new approach to the methods for determining package cushioning requirements. The new approach uses peak acceleration versus static stress data. In effect, this so-called "dynamic test procedure" determines to a large degree the actual drop conditions.

In an attempt to bring a new and realistic approach to the problem of designing package cushioning, the American Society for Testing Materials issued less than two years ago a new procedure, D1596-59T, entitled "Dynamic Properties of Package Cushioning Materials." About the same time, Military Specification MIL-C-26861 (U.S. Air Force) was issued. This specification listed a USAF Bulletin No. 139 which included the use of almost the same procedure as that issued by ASTM.

The basis for these standard procedures was the employment of a rigorously defined drop test, in which varied weights were dropped from varied drop heights onto cushioning material specimens of a given area with varied thicknesses, the specimens being mounted on a solid base. This approach was intended to simulate actual drop tests of a package.

Various methods to determine proper cushion thicknesses have been tried in the past but most of them used what could be called "static" stress strain data obtained from a relatively slow-moving compression machine. Compression tests were on a relatively thin sample, and usually data were obtained on one thickness only. Although these data and their use may be sufficient for certain types of cushioning materials, it has been demonstrated conclusively that such information is totally unacceptable for many cushioning materials, notably the foamed plastics. With the increasing use of foamed plastics, particularly the resilient form, for cushioning purposes, it was necessary to develop a more reliable method of determining thickness and size.

The dynamic test procedure results in a mass of empirical data which can be put into very usable form to provide a simple means of determining cushioning requirements. For every series of drop tests performed under a single set of conditions, an average maximum acceleration or peak g is determined from the recording instruments. When a sufficient number of tests are conducted in which suitable conditions are varied, a plot of peak g versus static stress can be obtained. Thus, at a single given drop height, the testing of a number of thicknesses of a standard area cushion provides a suitable form from which cushion design can be easily obtained. Figure 1 is an example of such a plot.

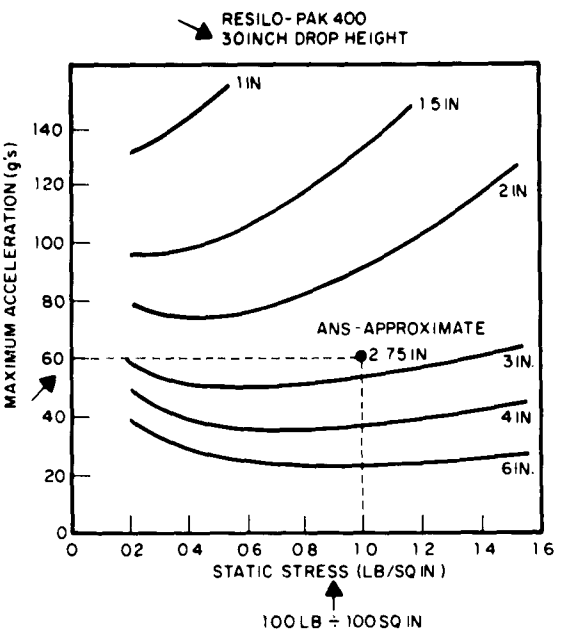


Fig. 1 - Tests of Resilo-Pak 400 for a single drop height and various thicknesses

CUSHIONING MATERIAL DATA AND THEIR USE

For the purposes of the investigations here presented, a single material, resilient foamed polystyrene, manufactured by the Armstrong Cork Company, known as Resilo-Pak 400, has been exhaustively tested according to D1596-59T. Note in Fig. 1 the very smooth plots of peak acceleration versus static stress for each thickness. Although these curves are for but one drop height, 30 inches, similar data were also obtained at 12, 18, 24, and 36 inches. The same series of tests was repeated for two other grades of this material, Resilo-Pak 200 and 300. With such empirical data, it has been possible to determine cushion requirements for practically any problem involving protective cushioning. In a few cases, where conditions were outside those tested in the series, suitable extrapolations were made.

To illustrate the manner in which this plot is used, let's refer to the example shown in Fig. 1. If an item weighing 100 pounds is supported on a cushion 10 x 10 inches (or an area of 100 square inches), a static stress of 1 lb/sq in. is imposed. Assuming a handling hazard equivalent to a 30-inch drop height, and knowing that the fragility of the item to be packaged is

60, it is a simple matter to project lines from 1 lb/sq in. static loading and the 60 g's to intersect between the curve of 2 inches of thickness and the curve of 3 inches of thickness, resulting in an interpolated value of 2-3/4 inches as the requirement for this condition.

If, however, the material is to be used at its most efficient static loading for the given condition, the static loading is moved to a lower pressure psi, which means simply increasing the size of the cushion in area. As a result, even less thickness could be used. For example, at 0.5 psi, a fragility of 60 would require about 2.5 inches of cushion thickness. This obvious reduction in thickness means less cubage of the package, but this may have to be balanced off by the additional cost of material based on the increased area. In a similar fashion, the cushion size could be reduced without too much sacrifice of protection provided.

Much more could be said on the use of such data, but the example given at least demonstrates the basic principle of operation of such plots.

CONFIRMATORY TESTS

Although this represents a milestone in the science of package cushioning, there remained some uncertainty because it was felt that a rigorously controlled standard procedure was used. What about the performance of the actual cushion in a practical package? Would there tend to be wide differences in performance which might invalidate what appear to be beautiful data based on a standardized test method?

To answer these questions the Armstrong Cork Company Research and Development Center conducted a rather wide series of tests, using the test equipment shown in Fig. 2. The drop test apparatus consisted of a drop head or platen which was practically frictionless because of the use of spherical bearings. Weights could be added to this dropping platen to vary the static loading. The drop head was impacted on the cushion sample which was mounted on a solid base, and the entire equipment was anchored in an 8-inch thick concrete basement floor on-grade consisting of crushed rock on a substrate of solid rock. The accelerometer used was a barium titanate piezoceramic transducer manufactured by Columbia Research Laboratories, commonly known as a crystal accelerometer. It was mounted in the center of the head. The accelerometer was connected with properly shielded cable to a cathode follower and from

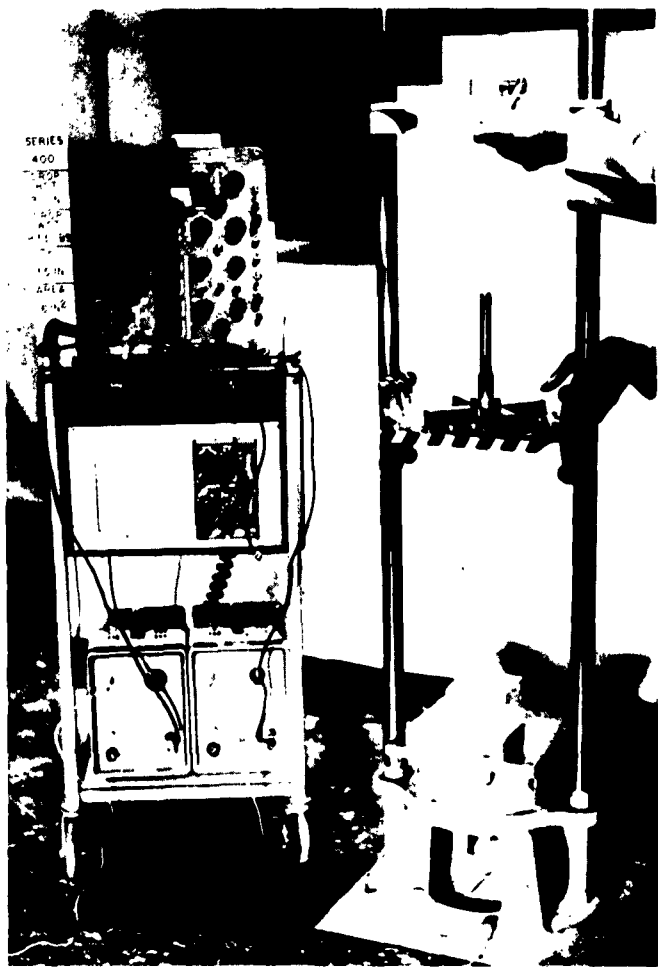


Fig. 2 - ASTM D-1596 drop test

there to a Hughes Aircraft Company Memo-scope, Type 104E, an oscilloscope on which the tracing can be retained almost indefinitely. We have found that no filters are required with this setup, and the nature of the tracings obtained justifies this opinion. Impacting velocity has been checked for every set of runs using a suitable wiper-switch circuit and electronic counter. The equipment used for the package drop test was a standard LAB piece of equipment as shown in the other photographs.

Three series of tests were made, the first series using a corrugated container (Fig. 2, 3, 4), the second a wooden crate (Fig. 2, 5, 6) and the third a steel drum (Fig. 2, 7, 8). In these tests, the operator first

tested the cushioning material, the result of which can be seen on the oscilloscope traces. The same cushion was then installed in the container. A dummy weight, equal to that dropped in the preceding test, was then placed in the container. We used a cushion pad system which we call the "satellite pack", a package using the cushioning as center pads for each face (Figs. 9 and 10). The package was placed at the same drop height as in the drop tester and the arm was released. The close-ups of the oscilloscope show the relationship between the two tracings. The peak g was, of course, calculated from the maximum peak of the curve recorded.

Similar results were obtained with all three packages. In the case of the steel drum, it will be noted that the tracing was more distorted than

Fig. 3 - Corrugated package drop test, same cushion, same conditions

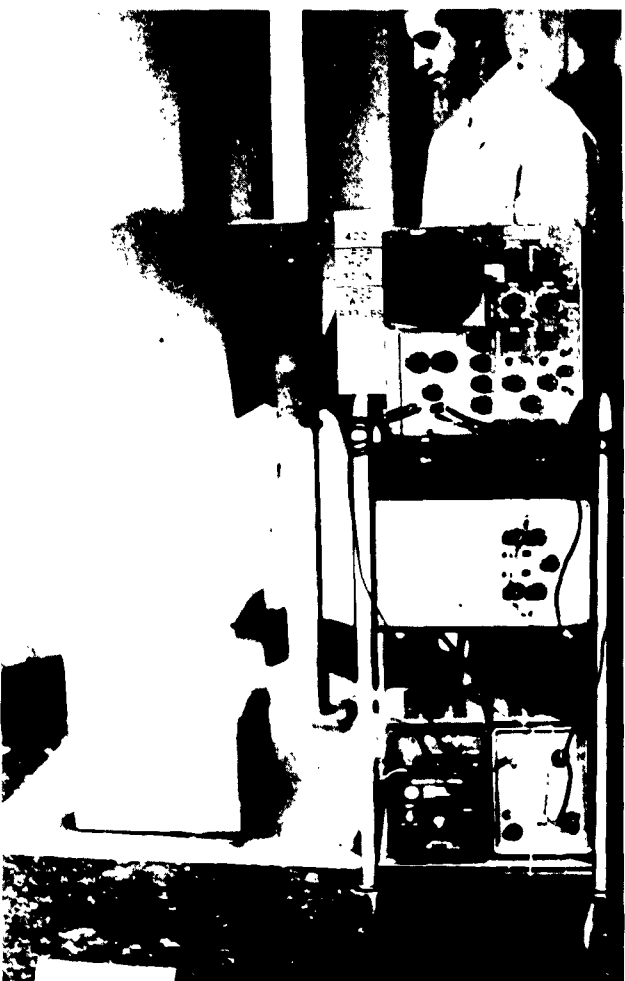


Fig. 4 - Close-up of superimposed tracing of the shock-package on left, D-1596 test on right

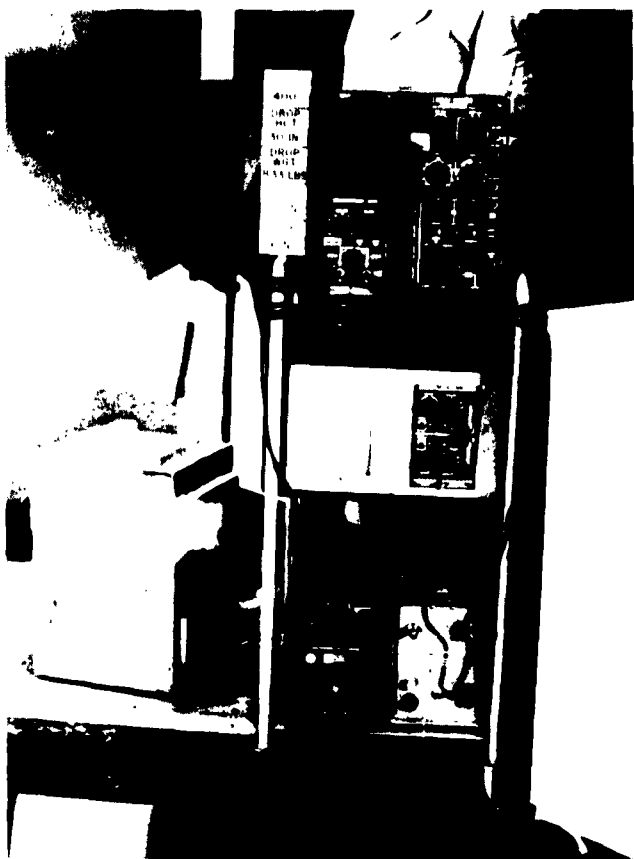


Fig. 5 - Wooden crate drop test,
same cushion, same condition



Fig. 6 - Close-up of superimposed tracing on
the shock package on left, D-1596 test on right

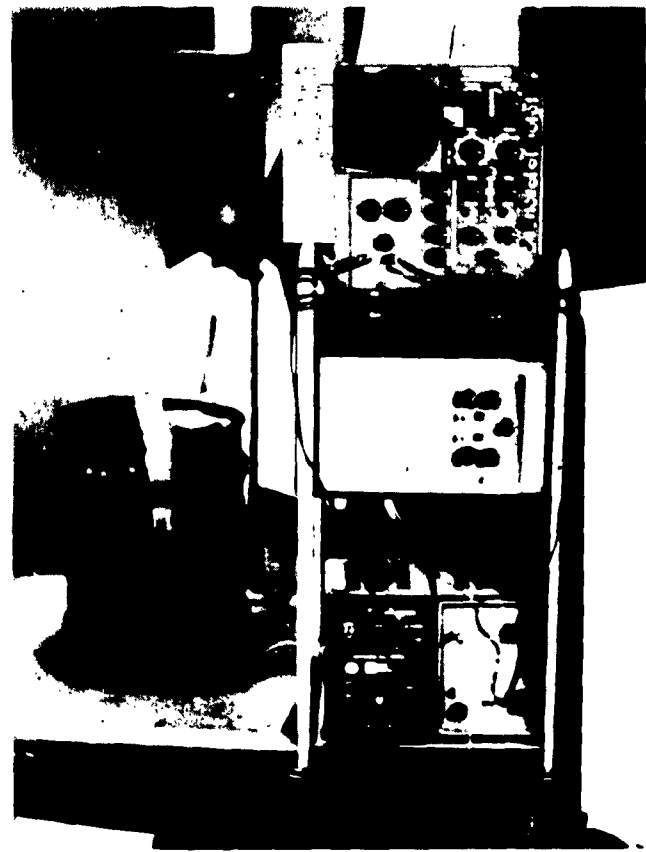


Fig. 7 - Steel drum, same cushion,
same condition

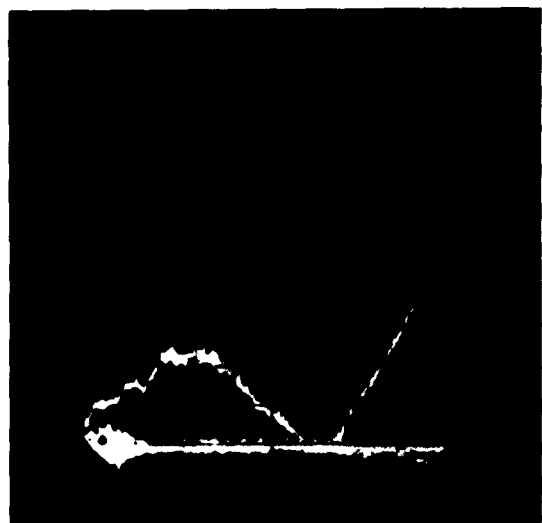


Fig. 8 - Close-up of superimposed tracing of the
shock-package on left, D-1596 drop test on right



Fig. 9 - Wooden crate and corrugated board container - assembled container view. Package is approximately 23 x 25 x 30 inches.

that observed with the corrugated board box and the wooden crate, and we believe this was due to the chime of the steel drum, the flat bottom upon which the cushion was mounted behaving as a diaphragm. Each accelerometer has its own calibration factor, so that when calculation is made on the basis of the settings on the oscilloscope, only a few g's difference occurs, even though it appears that the difference is greater.

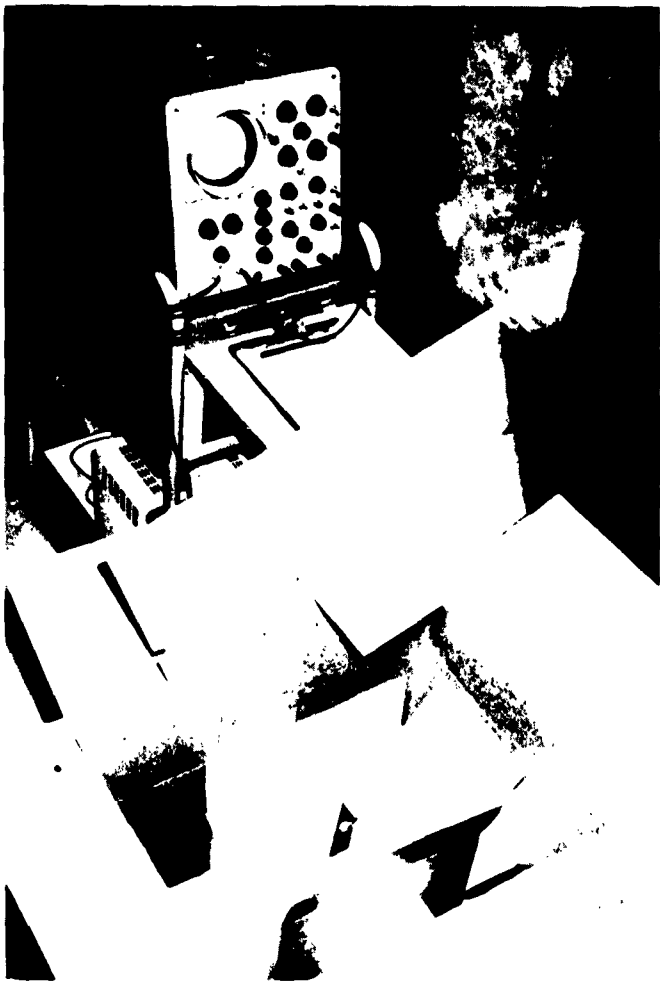
RESULTS

It has been established that in practically every case involving flat drops, the

container or package result is slightly less than that which would have been obtained from the standard test. This attests to the relative conservatism of the standard drop test, which is an added safety feature to those who employ the data for design as illustrated earlier.

Table 1 shows a series of results comparing the package drop test with that of the standard test. It will be noted that except for some data at the bottom involving a steel drum, results of the container drop test are generally lower than those for the standard test. This may be expected because of the contribution of the container or package or both to the protection provided.

Fig. 10 - Interior package assembly - a wooden dummy item, showing accelerometer mounting, is placed within a corrugated container. Cushioning pads of foamed polystyrene, 6 x 6 x 6 inches, mounted on corrugated board inserts, isolate the inner package from an outer corrugated container. This outer corrugated container is then enclosed in the wooden crate, according to military packaging requirements for overseas shipment.



One factor which must be strongly emphasized is the nature of the design of the packages shown. With a material like resilient foamed polystyrene, this cushion placement technique is comparable to the nature of the testing of the cushioning material by the ASTM procedure. Knowledgeable people in this field have indicated a lack of correlation of results in containers compared to dynamic cushioning properties based on D-1596. This lack of correlation may be due to the use of cushioning material in the package in a manner different from that by which the dynamic properties were obtained.

The ASTM procedure prescribes the loading or impacting of the entire surface area of the pad or cushion in an unconfined condition. Many cushioning materials are used in packages under confinement; furthermore, the item being cushioned does not compress the entire cushioning pad, rather it may indent into the larger

surface area or be supported by corner mounts. We have not evaluated resilient foamed polystyrene in this way. It is felt that the design which was used is entirely satisfactory and practical. As a matter of fact, this method is preferred and is recommended so as to use the material efficiently and in accordance with the design data.

It is to be noted that dynamic cushioning properties are but one of three basic factors needed for engineered design of cushioning. Similar information on vibration characteristics is desirable, but this is a far more complex problem. The third factor, creep, is also involved insofar as the properties of the material contribute to the design of the cushioning. We are looking rather critically at the former aspect, and are working actively in ASTM on the latter aspect. It is further recognized that many other factors, such as

TABLE 1
Comparison of Cushioning Performance in a Package With Cushioning Performance
According to ASTM D-1596-59T

	Static Stress (lb/sq in.)	Thickness (in.)	D-1596 g's (Avg)*	Package g's (Avg)*
I. CORRUGATED BOARD CONTAINERS				
(a) 48-inch Drop Height	0.76	4	56	45
(b) 30-inch Drop Height	0.19	1-3/4	90	72
	0.19	2-3/4	66	61
	0.19	5-1/4	40	36
	0.18	1-1/2	108	84
	0.18	2-1/2	70	61
	0.18	5	42	41
II. WOOD CRATE + CORRUGATED BOARD CONTAINER (30-inch Drop Height Only)				
(a) At Room Temperature	0.64	4-3/4	32	29
	0.64	5	30	27
	0.64	5	30	24
	0.64	5-1/2	28	25
	0.64	5-3/4	27	23
	0.64	7-1/8	21	21
	0.64	7-7/8	20	22
(b) At +150°F	0.64	5-1/2	28	23
(c) At -40°F	0.64	4-3/4	32	30
	0.64	5-1/8	30	26
	0.64	7-1/8	22	21
	0.64	7-1/4	22	21
III. SMALL STEEL CYLINDRICAL CONTAINER (30-inch Drop Height Only)				
	0.72	3	49	47
	0.52	3	50	55
	0.72	4	36	33
	0.52	4	38	45
	0.72	5	31	29
	0.52	5	33	41
	0.72	6	26	24
	0.52	6	29	31

* Rounded to the nearest whole g

location of center of gravity, protrusions, uneven surfaces, restriction of movement, limitations on outer container size, conditions of temperature and humidity, and so on, enter into the final design of a cushioned package. Finally considerations of economics and cubage may well be overriding factors. In connection with the previous additional factors mentioned, I would like to point out that protection provided by the cushioning material should be essentially the same at -65°F, or at +160°F, the extremes quoted in military specifications, as they are at room

temperature. We have found that the resilient foamed polystyrene fulfills this requirement.

The results we have obtained have given us a good deal of confidence regarding the usefulness of dynamic cushioning properties in package cushioning design. It is our experience that many of the other practical problems involved in the package as mentioned earlier will still stimulate the ingenuity of the individual designer for his individual package. But the correlation observed represents to us a notable step in the right direction in the science of package cushioning.

DISCUSSION

Mr. Weiner (Picatinny Arsenal): In Table 1 you show a correlation in peak g's at low temperatures and it was not clear to me whether both the package and the test specimen in your drop test procedure were both tested at low temperatures or was the drop test procedure on your standard ASTM test done at room temperature and the package done at low temperature?

Mr. Grabowski: We did it both ways. We have checked the material through the same series of tests for a limited number of thicknesses and drop heights at -80°F and we found relatively good agreement. But in this case I was comparing the room temperature value with the value observed in the package after it was subjected to -40°F overnight and tested quickly. We tried to do it within 30 seconds after removal from the cold temperature room. We think we did it fast enough.

Mr. Stern (Forest Products Lab.): I would like to make two comments here. First, in regard to this matter of the approach that is suggested here, namely that we test solely the performance of the cushioning material and then check out the container effect, this brings up a point that has not so far been covered here. There are essentially two schools of thought in the cushion testing field. One which advocates testing the materials alone, as in the case of the ASTM procedure, and the other which favors the incorporation of container effects directly in the construction of the apparatus. Personally, I advocate the separation of the effects for two reasons. One is that in the ASTM procedure it is rather clear cut that we want to test the materials only, without a particular bias that might be associated with a particular testing system; and the other thing is that it is very cumbersome to run these complete container drop

tests as compared to the streamlined version, let's say, according to the ASTM procedure. Personally, I find it encouraging that we can get this sort of correlation. The other comment I would like to make is in regard to your statement that you have observed an increase in values particularly with the drum as you get down to lower stress values. I think it might be a noteworthy point to make that your material is a very stiff material in comparison to other commonly used cushioning materials. It has been our experience, I'll admit limited, but nevertheless our experience to some extent that as you get to softer materials, to lower loading ranges, that this effect becomes pronounced. I touched on that briefly. While we need a lot more work on this point I do think that this tendency will increase as we go to lighter loading ranges with softer materials.

Voice: I notice in your plot of peak g versus static stress that, especially at the low g levels, the curves were very linear with a very limited slope. Is this true of materials in general or only of this particular material? At the lower g levels your sample thickness is essentially a standard for any degree of dynamic cushioning that you would like to obtain. I wonder if these slopes vary with other materials so that you can actually vary your thickness?

Mr. Grabowski: Yes, they definitely do vary, as Bob pointed out. For softer materials they will rise, they will rise substantially and significantly. What you said seems to be true of a stiffer cushioning material—I think that is the answer. Maybe somebody else has a better opinion on the subject.

Mr. Cipponeri (Sperry Utah): I don't know whether you tried taking the sheet pads and cutting a square piece out of the center. I

believe that you will get better value readings by using that method. Have you tried that yet?

Mr. Grabowski: This is a technique that can be used and it may work out. However, I don't have any specific data to comment upon at this time.

Mr. Wishart (Naval Construction Res. Est., Scotland): I would like to ask the speaker if he has come across any, what we call, shape factor effect? You can have a pad 10 x 10 inches, 100 square inches, or you can have a pad 33 x 3 inches. Is there a difference in the performance of these two pads?

Mr. Grabowski: I wish I could answer your question knowledgeably. All I can say is that the range of testing that our equipment permits is from about 12 x 12 inches down to, say, 3 x 3 inches. We haven't noticed for this range of area, or sample size, much difference but I would not speculate on very large areas compared to the ones which are tested according to ASTM D-1596. I might point out that that procedure does suggest or recommend a certain size sample which, I think, is about 8 x 8. I would not care to speculate on very large pads compared to, say, very little ones. For the range of 12 x 12 inches down to about 3 x 3 inches, we observed very little difference, at least for our material. I don't know that this applies—it may—across the board for other materials.

Mr. Jones (Nopco Chairman): I would like to comment myself on that question. Generally, materials that can be called pneumatic will exhibit this type of effect. If the material has a fairly small cell such as a foam material, and if the stiffness of material is, say, reasonably low so that the air escaping contributes an

appreciable or significant portion of the dynamic force, why then if you change the peripheral area or the shape of the specimen, or the thickness of the specimen, you can get different dynamic properties because anything you do that will change the ease with which the air escapes from the cushion will change its property. Now on so-called nonpneumatic materials, and there are plenty of those, either because they are much stiffer or because they have a very open structure, such as the curled hair, you would probably not get very much of this effect. I presume you are not talking about a 1 inch x 1 inch x 4 feet or something like that—any reasonable configuration.

Mr. Grabowski: I hope you weren't referring to a very tall, very thin column, because I think this would get you into trouble.

Mr. Schell (Aeronautical Sys. Div., WPAFB): I have a comment to make on that last question. I think that one of the things that contributes here is the fact that each cell at the edge is unsupported, whereas each cell in the center of the pad is supported on all sides. I think that Ripperger and Thompson have covered this in the honeycombs in which they find that the energy absorption characteristics of these honeycombs varies as the perimeter to area ratio. The end cells of the honeycomb are supported on one side only while the center cells are supported on all sides.

Mr. Wishart: May I just come back on that? The effect or the factor which the last speaker mentioned is in fact the shape factor which we use in Britain. It is the area of the loaded surface over the free area. I presume that's what he really meant.

* * *

RECENT BRITISH DEVELOPMENTS IN PACKAGE CUSHIONING, DYNAMIC TESTING AND INSTRUMENTATION

S. C. Schuler
Royal Radar Establishment, Malvern, England.

The paper gives a review of United Kingdom practice for equipment fragility assessment, some notes of the design of an equipment for dynamic evaluation of cushioning materials using an analogue computer and a brief survey of developments in the field of cushioning materials and devices.

INTRODUCTION

The design of a satisfactory cushioned package involves the consideration of several factors which include:

- (i) The shock and vibration conditions to which a packaged equipment will be subjected in transit and handling;
- (ii) The fragility characteristics of the equipment to be packaged, embracing the maximum permissible acceleration, deflections and resonant frequencies of the various assemblies and components of the equipment; and
- (iii) The shock absorption, vibration isolation, load supporting properties and stability of cushioning materials.

In this paper a brief account is given of current trends and recent developments in British Package cushioning materials, the approach to equipment fragility assessment and some details of dynamic testers for evaluating cushioning materials.

EQUIPMENT FRAGILITY ASSESSMENT

Military devices, particularly electronic assemblies, are complex structures and the assessment of equipment fragility can be a complicated process. In the United Kingdom various machines of the guided drop tester type are used for fragility assessment. A representative machine is the Royal Radar Establishment drop tester, [1] which uses a

pneumatic ram for retardation of the equipment under test. The machine consists of a robust frame and a guided test cradle, mounted on the underside of which is a pneumatic ram which will provide a peak deceleration in the range 5 to 90 g with duration times of 10-15 milliseconds, variation in drop heights from 1 foot to 4 feet 6 inches and table loads up to 100 pounds. Figure 1 shows the pneumatic ram with a cathode ray tube on the cradle ready for testing.

Typical acceleration waveforms are shown in Fig. 2, and it will be seen that these are similar to those experienced with many bulk cushioning materials—but not the more efficient materials which have a hyperbolic or anomalous load/deflection characteristic. Other guided drop test machines use a variety of retardation methods including sand, pads of bulk cushioning materials and the penetration of a spike into a lead block.

There will of course be a considerable variation in both impact pulse time and shape with the various means of retardation. Under shock conditions a component or sub-unit mounted on an equipment may receive a greater shock than that imparted to the chassis. The extent of the amplification is dependent upon the relationship between the natural frequency of the mounted component and the impact pulse time and shape characteristics. Situations can arise where a component within an equipment fails at, say, 50 g during fragility assessment with a certain impact pulse time and shape, and at 30 g when packaged using a cushioning system with an entirely different impact pulse time and shape.

Because of the various assumptions which have to be made, it is unlikely that fragility

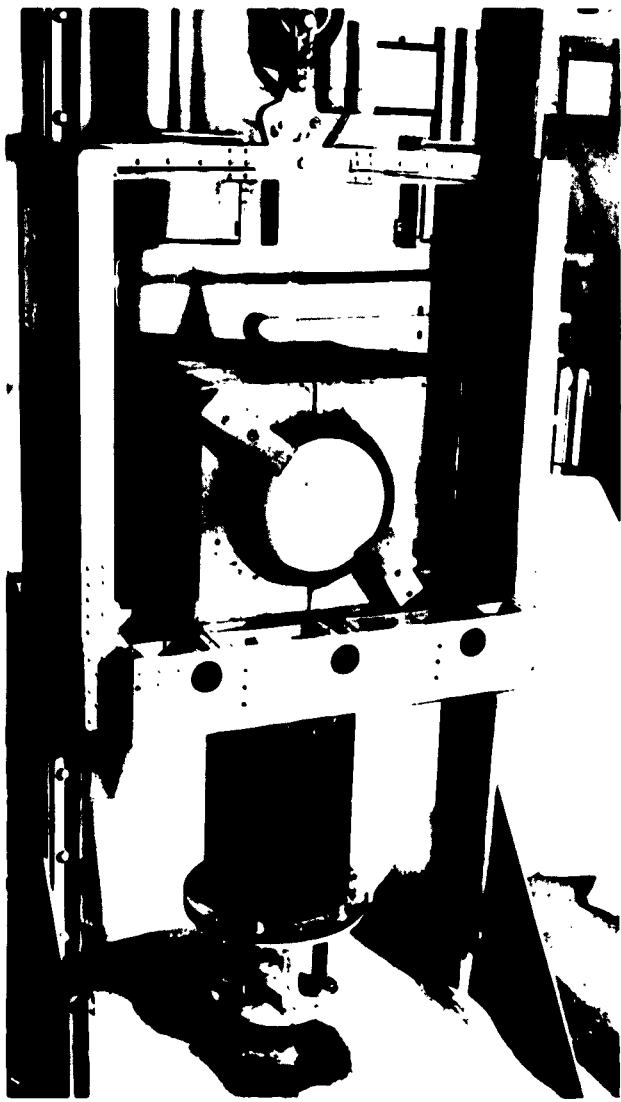


Fig. 1 - Pneumatic ram

assessment can give more than a close approximation. However, we consider that this is an area where further investigation is worth while, and some of the problems are currently being investigated by E. P. S. (R&D) Ltd. in conjunction with R. R. E.

Figure 3 shows amplification factor plotted against time ratio. The rise time of the applied pulse divided by the natural period of the sub-unit amplification factor is the time ratio and the amplification factor is defined as the ratio of g experienced by the sub-unit to the g applied to the unit. These curves were obtained using a lead block decelerator giving

a near square waveform pulse, and cushioning systems giving approximately triangular pulse shape. It will be noted that rise time has been used in defining the time ratio; this is because it was found that the near square waveform pulse obtained in the lead block decelerator did, in fact, have a finite rise time, and it was this that governed the amplification factor and not the pulse duration. This actually is true only if the pulse duration is greater than half the natural period of the sub-unit, which is the case in practice with the pulse duration obtained and with the range of natural frequencies of equipment normally encountered.

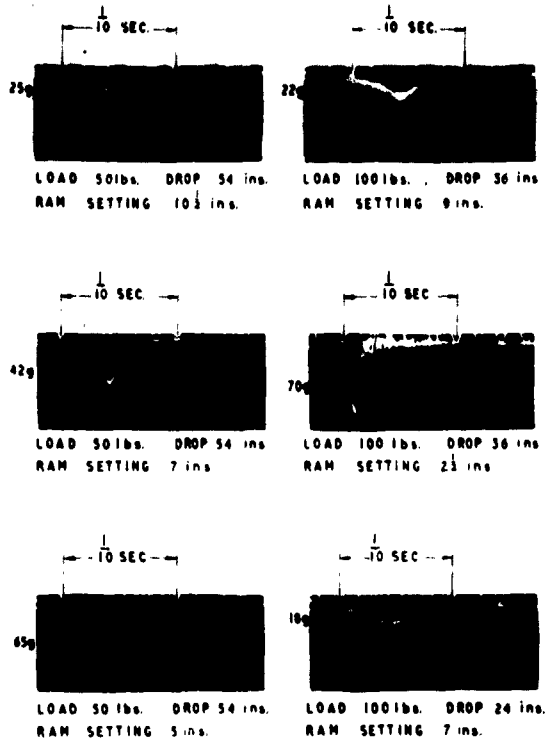


Fig. 2 - Acceleration waveforms

With triangular and sinusoidal pulses, the rise time is, of course, directly proportional to the pulse duration.

With the lead block decelerator machine used to define the amplification curves, the rise time varied between 2.5 and 6 milliseconds. With these figures, the limiting values of the time ratio that will be met may be calculated. They are 0.2 and 0.72, which means amplification factors between 1.6 and 1.9.

An investigation into the results of a considerable number of instrumented package drop tests has shown that the rise time of the impact pulse varies between 7.5 and 25 milliseconds. Taking the frequency range of equipments as between 80 and 120 cycles per second, this gives the limiting values for common cushioning materials as 0.6 to 3, which means amplification factors between 1.05 and 1.4. These values, for the lead block decelerator and cushioning materials producing approximately triangular pulse shapes are shown in the amplification factor curves (areas A and B in Fig. 3). This shows the maximum and minimum amplification factors of 1.6 and 1.9 for the lead block decelerator, and the maximum and minimum amplification factors of 1.05 and 1.4, which may be experienced with common cushioning materials. This means that, using

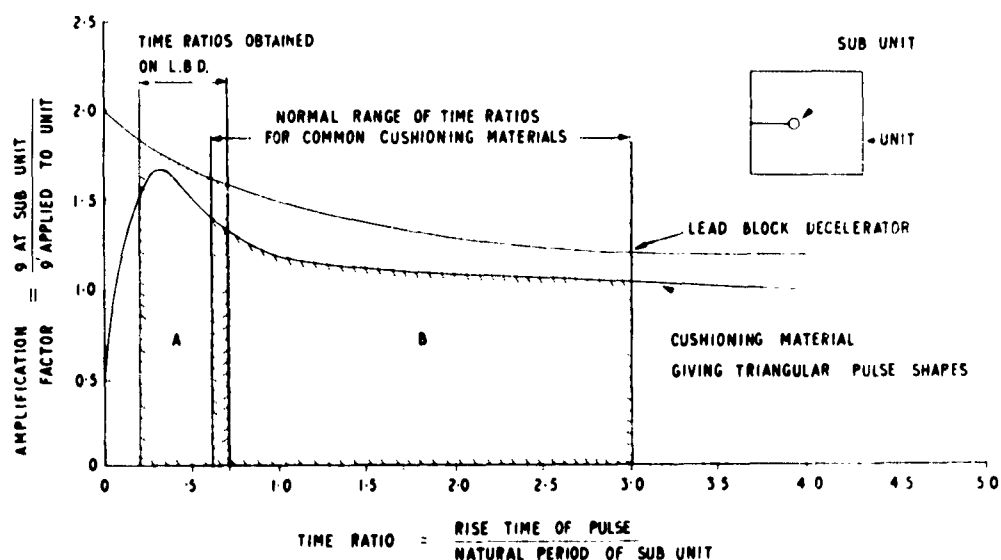


Figure 3

the lead block decelerator as a method of fragility assessment, a "built-in" safety factor, would be obtained which varied between approximately 1.2 and 1.8.

By careful design of the lead block decelerator, the boundaries shown for the area A could be extended to cover lower amplification factors. This would enable us to make a choice of safety factor, depending upon the importance of the item to be packaged.

DYNAMIC TESTERS FOR EVALUATING CUSHIONING MATERIALS

During recent years much progress has been made in the UK on methods of evaluating the properties of cushioning materials under dynamic conditions. Several machines of the guided vertical drop tester type have been constructed and one is briefly discussed. Guided drop testers have the advantage of being relatively easy to construct, and ease of operation enables tests to be made on materials of approximately 12 inches square with a wide range of stiffness. The main disadvantages of the

guided drop tester and pendulum type machines are: Inadequate control over the shape of the force pulse; influence of mechanical resonance of the striker plate; force is only measured indirectly via an accelerometer; the machines are bulky and testing under various climatic conditions would involve very large chambers. These aspects have been considered in an alternative method, developed at the University of Southampton, which uses an electrodynamic force generator.

Guided Vertical Drop Testing Machine

Figure 4 is a general view of the machine which we have at R.R.E. The guide tracks are 8 feet tall steel angle, accurately machined, and the working faces are hard chromium plated.

The carriage weighs 20 pounds and is approximately 12 inches x 12 inches (working area) x 10 inches deep. It consists of an upper and lower light alloy plate, cemented to resin-coated plywood support plates and interlocked vertical plywood panels. A piezoceramic

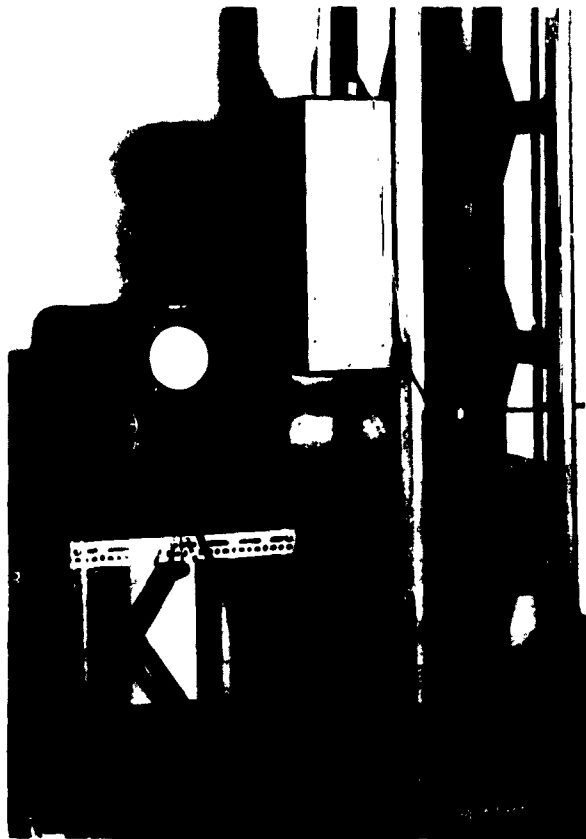


Fig. 4 - R. R. E. dynamic cushion tester

transducer is mounted to the upper plate, and fasteners for rigidly mounting steel loading plates are also provided. Light alloy wheel locating fittings are secured between the corners of the upper and lower alloy plates, and can be accurately adjusted horizontally, so that the wheels may be retracted for removal of the drop carriage from the framework and subsequently replaced and set to run true on the tracks. The wheels are of hard rubber-faced alloy, having a 90°V surface to engage the tracks. They are self-aligning and the steel shafts run in nylon bushes to minimize track noise. A rigidly mounted earthed aluminium-clad plywood plate forms one plate of the capacitance pick-up used in the cushion deflecting measuring system.

Associated with the machine is the electronics unit comprising:

(i) A time and trigger unit using a thyratron-controlled relay to initiate the sweep circuits of an external CR oscilloscope. (A biased switch simultaneously operates this unit and the bomb release holding the drop carriage. Delay is adjusted according to the drop height required.)

(ii) A carriage position indicator giving a display of the deflection of the carriage on the cushion under test. (17 kc/s oscillator is used to feed a capacitive potential divider consisting of a fixed 200 picofarad capacitor and the variable capacitor formed by the carriage plate and an insulated brass plate fitted at the rear of the machine. Output across the variable capacitor is detected and the rectified signal fed to the C.R.O. The range of measurement is about 12 inches from the base with a resolution of 1/20th inch.)

(iii) A twin beam long persistence cathode ray oscilloscope. (This permits simultaneous display of deceleration and deflection pulses during dynamic compression of the cushion—or both outputs may be applied to one beam, and a hysteresis-type compression/deflection curve displayed.)

In order to reduce the weight of the carriage, for tests on light density foam materials, and to overcome carriage resonance difficulties when testing materials with a very short rise time, a new cradle is being designed for this machine. Aluminium honeycomb is being used as the mass, with a metal plate bonded to it at the top and bottom. One accelerometer is mounted on the lower plate.

The general arrangement at the carriage is shown in Fig. 5. Also incorporated is a cantilever beam, to which another accelerometer is mounted. This beam is intended to represent an element of a packaged equipment. For experimental purposes its natural frequency can be adjusted by using beams of different sections and lengths. The ratio between the shock recorded by the beam accelerometer and that recorded by the base mounted accelerometer is a measure of the shock amplification experienced on this beam.

During evaluation tests on materials, checks will be made with the beam unit to ensure that high-cushioning efficiency is not being attained at the cost of high levels of shock amplification.

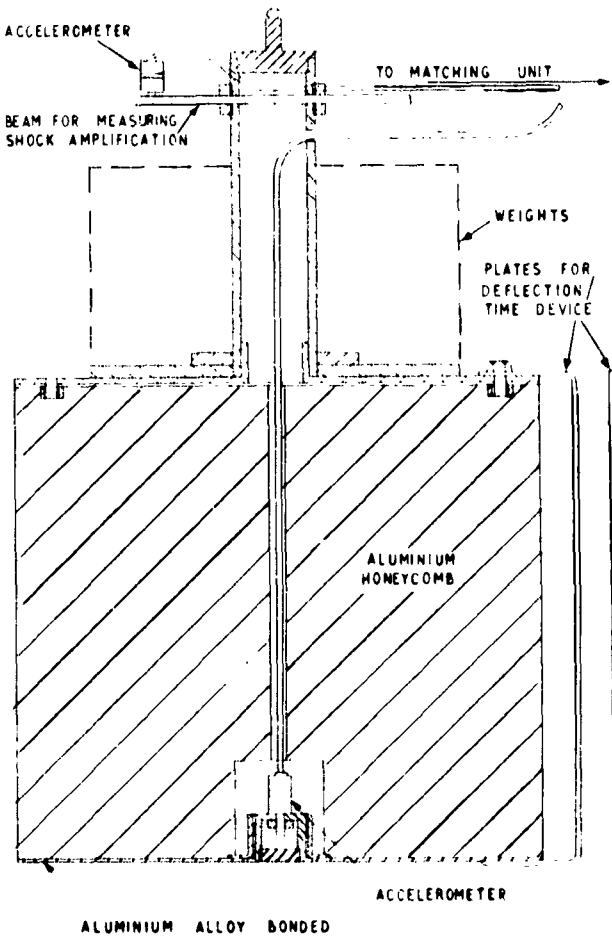


Fig. 5 - Design for a lightweight drop test cradle

Dynamic Compression Measurements of Cushioning Materials Utilizing an Electrodynamic Force Generator

Analogue Computer Analysis-Theoretical analysis of the design of a cushioned package is readily carried out on an electronic analogue computer, but to introduce a realistic stiffness term it is necessary to know the dynamic performance under conditions similar to that of the actual impact.

An interesting system which has been developed by Vanning and Guttridge of the University of Southampton [2] uses an electrodynamic force generator with force and displacement transducers to incorporate a sample of cushioning material into the analogue system, thus solving the cushioning problem under dynamic conditions. At the same time, waveforms of force-time and force-displacement are produced, showing the nature of the non-linear stiffness and the extent of energy dissipation.

Figure 6 (b) shows a block schematic diagram in which four analogue units A-D are interconnected to simulate the simple system of

Fig. 6 (a) using the static stiffness characteristic of the cushion. To incorporate the real stiffness element, unit D is replaced by a dynamic unit shown in Fig. 7. The requirement for this is that at any instant within the compression cycle when the displacement is x_1 , it compresses a sample of the cushioning material to that displacement and produces an output proportional to the force used, i.e., the $V_F(x)$ is now obtained via the actual cushion instead of using a static curve.

Cushion Material Measurements-A simplified system can be used for rapid evaluation of cushioning materials. For compression tests one face of the cushion sample is in contact with a moving pressure-plate driven by the electrodynamic unit, which is similar to a moving-coil vibration generator except that the coil slides freely to give a movement of several inches, displacement being monitored by a variable capacitance pick-up system. The other face of the cushion is held against a force transducer, which records the total force transmitted through the cushion, so that oscillographic records of force-time, displacement-time and force-displacement are simultaneously available, all with a response extending from dc to about 10 kc/s.

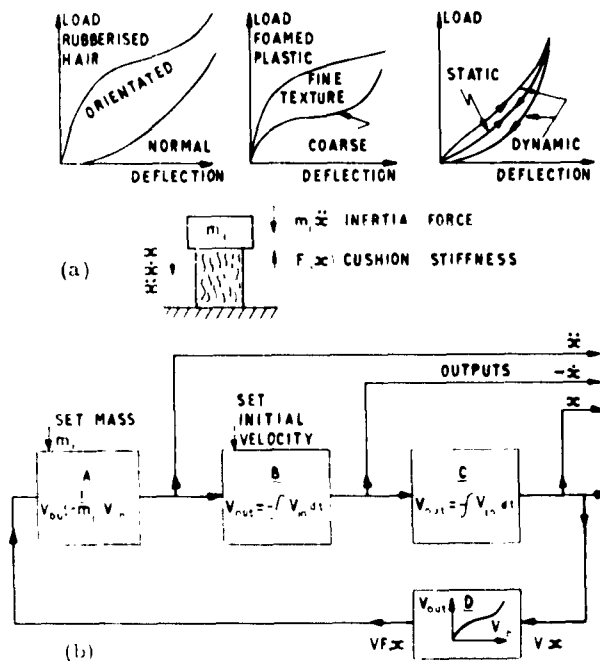


Fig. 6 - (a) Load-deflection curves, (b) analogue computer for static cushion law

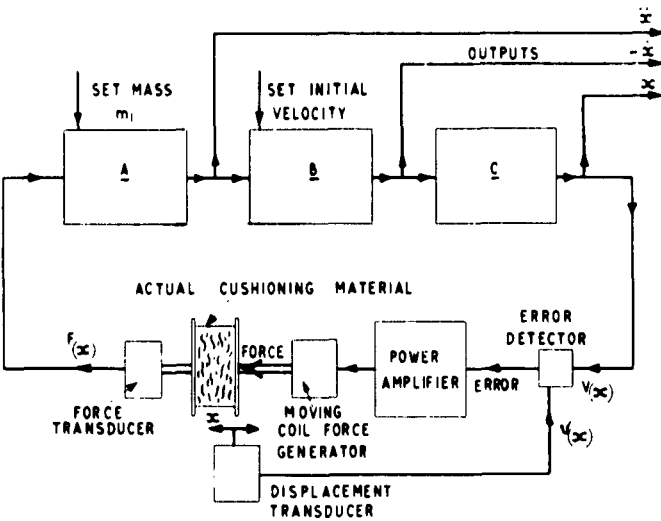


Fig. 7 - Analogue computer with dynamic stiffness element

Slow movement of the pressure-plate by hand gives a static, or slow compression characteristic. For dynamic operation, the coil is driven by a single current pulse of controlled amplitude and waveform, which provides the total force to accelerate the moving mass of the coil and pressure-plate and to compress the cushion. With the present equipment, at pulse lengths above 50 milliseconds the speed of response is such that the compression force follows the current pulse, giving complete control of waveform, but below 50 milliseconds the inertia and frictional forces cause the compression pulse to degenerate into something approaching a half-sine form when the current pulse is rectangular. The peak force is also limited to 25 pounds, so that most results have been taken on samples of polyurethane foam materials up to 20 square inches in area, with compressions of 60 percent on 1-1/2 inches thickness.

Considerable development potential exists, both to increase the peak force to 150 pounds and travel to 6 inches, and to increase the speed of response to give full control of waveform down to 5-millisecond pulse length. Alternative arrangements for holding samples allow measurements to be made in shear and in tension, and the compact nature of the unit is admirably suited to environmental testing in climatic chambers, where the size of the chamber need be only a little larger than the material sample.

Figure 8 shows the mechanical arrangement of the moving coil force generator, a Goodmans Model 390A, with the coil and magnet system

modified to give a travel of 2 inches. The pressure plate is of resin bonded plywood construction and the total moving mass is 7 ounces.

The force transmitted through the cushion is measured by a variable-capacitance pick-up having a high natural frequency. The pick-up is used in conjunction with a frequency modulated system where change of pick-up capacitance alters the frequency of a Franklin oscillator. The displacement transducer is also a variable capacitance pick-up.

Some typical results for samples of various cushioning materials are shown in Fig. 9 (a) through 9 (d), and these demonstrate the

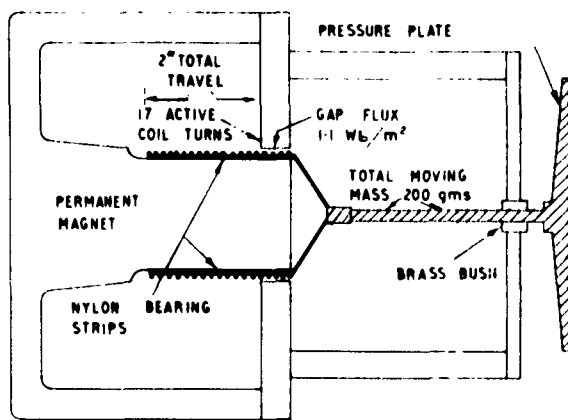


Fig. 8 - Cross section of moving coil force generator

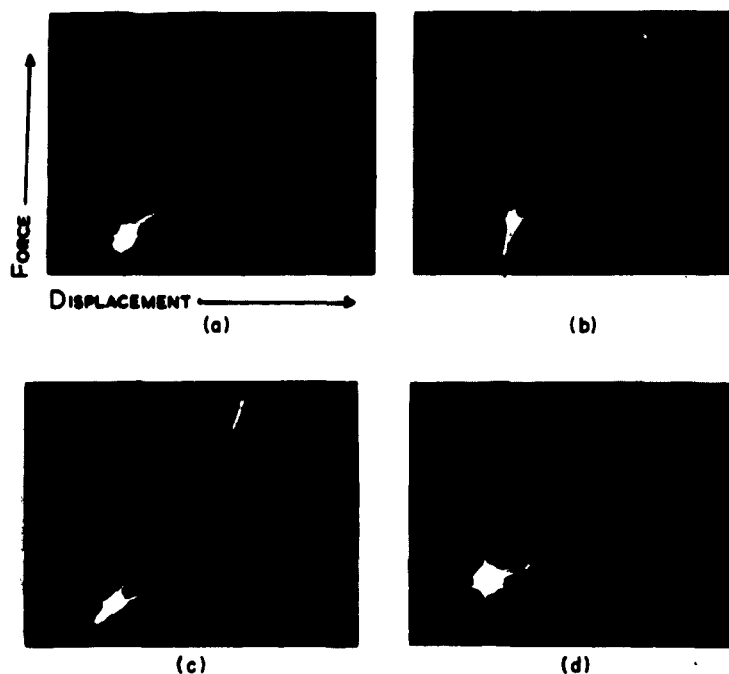


Fig. 9 - Dynamic tests using electrodynamic force generator: (a) polyether foam 1.8 lb/cu ft opencell 4 x 4 x 1.5 inches in compression, 20-millisecond pulse, 60-percent compression; (b) material as (a) but bonded to plywood; (c) as in (b) but tested in shear (tangential) shear movement 0.5 inches; (d) rubberised hair 4 lb/cu ft, 2-1/2 x 2-1/2 x 1-1/2-inch compression.

possibilities that exist in this method of measuring the dynamic performance of cushion samples. Figure 9 (a) is with polyurethane foam (polyether), 1.8 lb/cu ft, open cell 4 x 4 x 1.5 inches in compression, unbonded, between two plywood faces; 20-millisecond pulse; 60 percent compression. Figure 9 (b) is from a 4 x 4 x 1.5-inch sample of the same material, in compression, but bonded to plywood so that it can also be measured in tension. Note that closing the outer cells seems to have removed some of the desirable "knee" characteristic. Figure 9 (c)—a 3 x 6 x 1-1/2-inch sample of same material in shear, faces kept parallel at 1-1/2-inch separation; characteristic becomes almost tangential; maximum shear movement is 0.5 inch. Figure 9 (d) is with 2-1/2 x 2-1/2 x 1-1/2-inch rubberised hair, 4 lb/cu ft, in compression; normal tangential stiffness.

CUSHIONING MATERIALS AND DEVICES

In the United Kingdom there are some 50 companies manufacturing various types of packaging cushioning materials and devices.

Materials such as foamed polystyrene and polyurethane are finding increased applications but rubberised hair, in moulded and sheet form, is the more widely used cushioning material. Some investigations which we made into the use of resin bonded synthetic fibres indicated that these have several advantages, but the basic price per pound of the materials is too expensive for economic use, and research work has been discontinued. Some new techniques which have recently been developed are summarised below.

Corrugated Solid Rubber Cushions

This is a promising new form of cushioning pad under active development at the laboratories of the Rubber and Plastics Research Association of Great Britain [3].

The familiar types of deformation of rubber materials, such as compression and shear, do not always suffice to give stress-strain relations of the required form. Experiments are being made with rubber pad designs in which a "buckling strut" is introduced.

The form of the cushion is shown in Fig. 10, together with a stress-strain curve, which shows the following characteristics: (a) At low strains, the stress is initially proportional to the strain; (b) At about 0.15 strain, there is an inflection in the curve and the stress-strain becomes parallel to the strain axis; (c) At high strains, the stress increases rapidly with strain.

The reason for this behaviour is that at low strains the arched structure acts in compression, but when a limiting stress is reached the arch collapses, and there is a large increase in strain with little change in stress. This continues until the completely collapsed arch structure is subjected to a compressive stress and there is then a rapid increase of stress with further straining.

The shape of the stress-strain curve allows for a substantial increase in energy absorption over many conventional materials.

The results of dynamic tests on experimental samples, while confirming the good energy absorption properties, did show a high degree of shock excitation in the frequency range 80 - 120 cps. The pads are now being redesigned with thinner walls to give a lower initial stiffness. This will have the incidental advantage of increasing the deflection available up to bottoming point.

Recent Developments in Rubberised Hair

Rubberised hair in mouldings and sheet form has been widely used in the UK for package cushioning. This material has been improved during the past few years, particularly in respect of dimensional stability, uniformity and dynamic performance.

More use is now made of structural configuration in rubberised hair, and it is possible to change the shape of the load compression curve by this means to suit particular applications.

Figure 11 shows some typical examples of the form of constructions developed by the Hairlok Company. They are described below.

Orientated Rubberised Hair (O. R. H.) Corner Blocks—These are made in a range of sizes, and the mitred faces, together with the adhesive of the wall sides, effectively prevent "brushing" of the material. The blocks are self-locating, provide good cargo stability and are particularly suitable for heavy loading at the higher g levels.

Rubberised Hair Moulded Modules—These are moulded, hollow blocks 3 x 3 x 1 or 2 inches thick, connected together by a thin moulded flash. They are normally supplied in slabs of 36 modules. They can be folded sharply or curved to fit the contours of the cargo and they

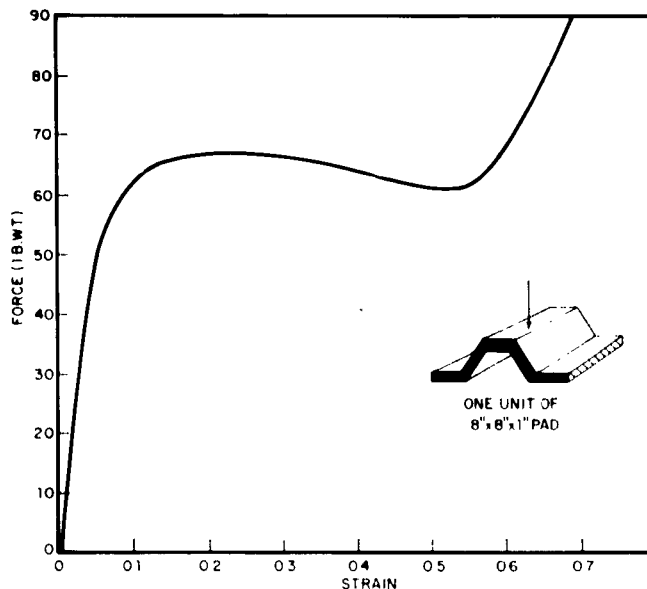


Figure 10

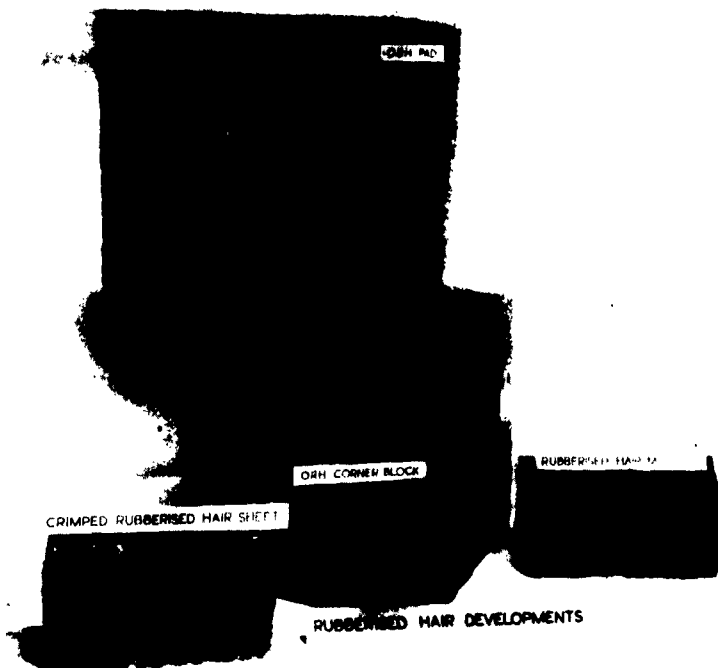


Fig. 11—Rubberised hair developments

enable manufacturers to make efficient packs to a known performance with an "off the shelf" material.

Crimped Rubberised Hair Sheet—This new process gives a crimped structure as a result of needling during the manufacture of the sheet material. The material is made in densities of 4 and 6 pounds per cu ft, and is available in 6 x 3-feet sheets in thicknesses of 1, 1-1/2 and 2 inches. The energy absorption performance is superior to normal rubberised hair sheet; half the weight of material is required for equivalent performance. Crimped rubberised hair sheet is not as efficient as O. R. H. but it removes the additional costs inherent in fabricating O. R. H. pads.

Torsion Bar Cushioning Unit

Figure 12 shows a general view of an experimental torsion bar unit. Ten round steel torsion bars (1/8-inch dia wire) are located in a flat metal housing which forms the base of the unit. One end of each bar is clamped in the housing and the other ends are suitably bent to form a radius arm. The free end of each arm is held at 45° to the vertical by a wire-retainer which is anchored to the base plate. The torsion bars are arranged in two sets of five with

the arms crossing in order to keep the length of the plate as short as possible. When a load is applied, the plate moves down and the arms deflect so that at maximum compression the arms are horizontal. The unit is 3-1/4 inches tall and has a working deflection of up to 2-1/2 inches. It applies a constant retarding force of approximately 160 pounds.

Suspension Mounts Using Coiled Springs of the Hairpin Type

This type of suspension unit has been designed to accept compression and shear loads and consists of a number of wound hairpin type springs situated radially and attached to circular mounting plates at each end. Figure 12 shows a typical pedestal configuration; a range of performance curves can be achieved by varying the gauge of wire, diameter of coils and angle of arms. This spring unit was designed and manufactured by Wilmot Mansour & Co. Ltd., and a variant of this basic design suitable for cylindrical pads is seen in Fig. 13, which shows a container for a missile fore body. The welded aluminium container is approximately 5 feet long with a 3-foot diameter and uses two spring suspension systems mounted on telescopic runners to secure and cushion the equipment. The cargo is 250 pounds, the container weight

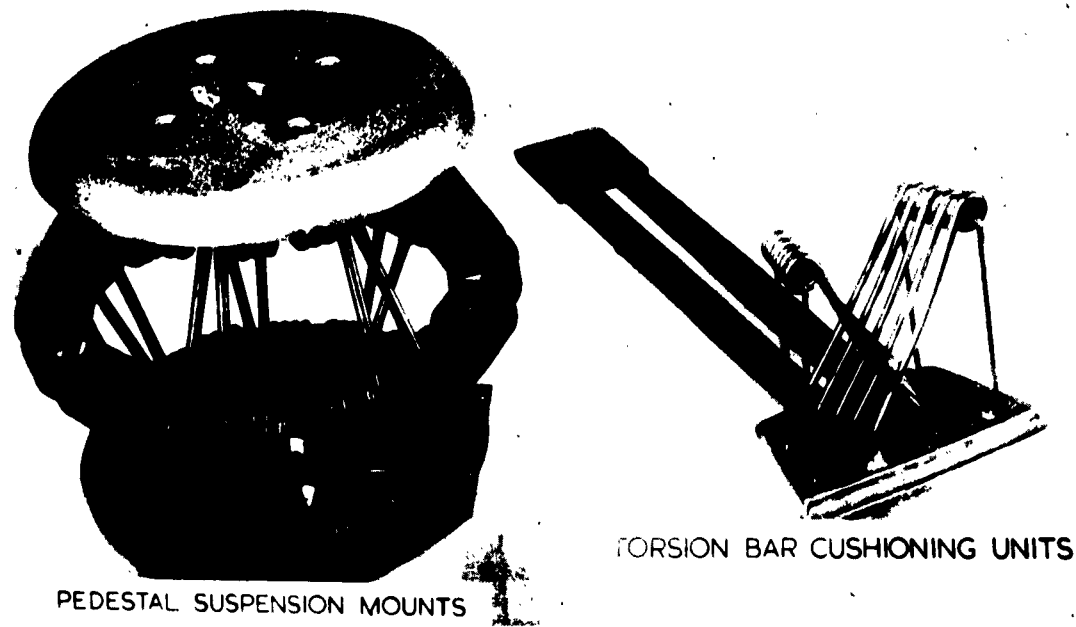


Figure 12

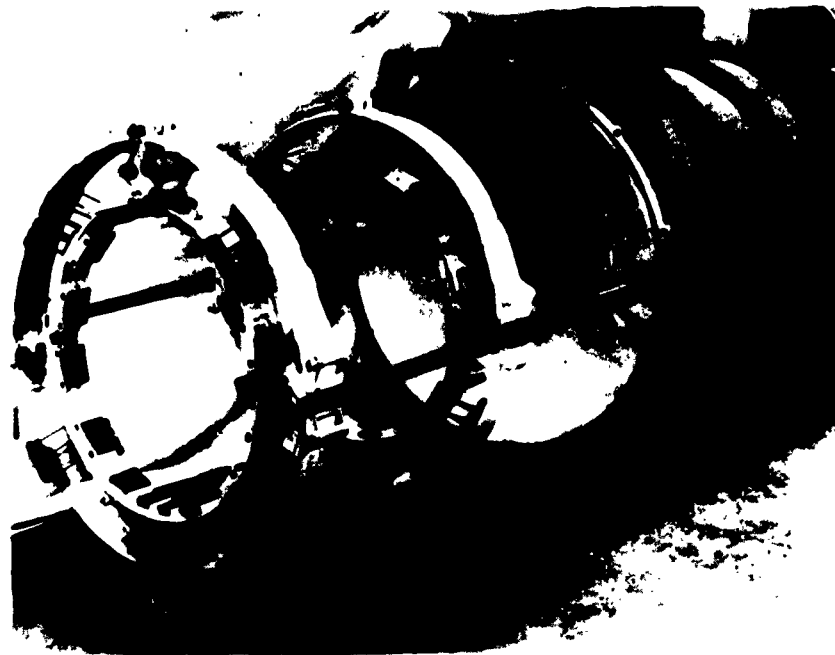


Fig. 13 - Container for missile forebody

being 445 pounds. The domed lid spinning is welded to a cast aluminium alloy ring and, when closed, fits against a similar ring welded to the container body which carries a semi-recessed "O" sealing ring. The lid is secured with 12 hexagon recess headed screws captive to the lid. A retractable wheel, fitted to the base of the forward suspension band, operates automatically when withdrawing the suspension system to counteract stresses on the telescopic runners. The suspension system reduces the shock at the cargo to 15 g under drop tests and simulated shunting (coupling) tests.

Lightweight Containers with Foamed Plastic Cushioning

For the packaging of large thermionic valves and electronic subassemblies, a packaging technique has been evolved using an outer skin of high impact thermoplastic material (such as Acrylonitrile Butadiene Styrene) which is vacuum formed to the shape required. The cushioning is provided by a semi-rigid polyurethane material which is foamed directly on to

the skin and which is formed to take up the shape of the cargo.

The technique has several advantages over the normal made up pads for small assemblies, such as a carton with fitted wooden inserts; these advantages include lightweight construction, simpler final packaging of units reusability and ease of production.

Figure 14 shows a typical pack for a printed circuit computer board. In this design the cargo is sealed in a polythene bag and the two halves of the pack are finally taped together. Hinges or mechanical closures could be provided where necessary.

CONCLUSIONS

Equipment fragility determination is a difficult problem, but recent work suggests that the lead block decelerator has many advantages. The transit and handling environmental levels currently used in the UK for testing packages are somewhat empirical and more research is needed to obtain data on these conditions.

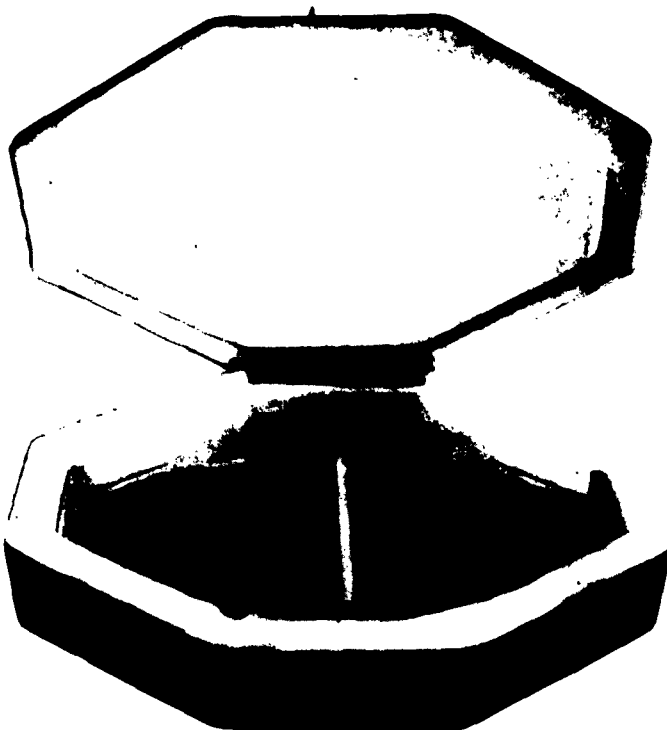


Fig. 14—Foamed plastic pack for computer subassembly

There is a considerable development potential in the use of electrodynamic force generators for the evaluation of cushioning materials. This technique is also being investigated as a method for the calibration of accelerometers and for equipment fragility analysis.

Some useful improvements have been made to the well tried rubberised hair material by the introduction of new structural configurations. Rubber pads in corrugated form, foamed plastics and honeycomb materials are other promising developments.

REFERENCES

- [1] S. C. Schuler, "The Packaging of Electronic Equipment," J.I.E.E., Vol. 4, No. 38, February 1958.
- [2] B. H. Venning and J. Gutteridge, "Dynamic Compression Measurements of Cushioning Materials Utilizing an Analogue Computer," British J. of Appl. Phys. (In print).
- [3] A. R. Payne, "Design of Shock Absorption Mat of Solid Rubber," Research Report No. 102, Rubber and Plastics Research Assoc. of Great Britain.

* * *

LOW TEMPERATURE STATIC-DYNAMIC URETHANE FOAM CUSHIONING STUDIES

W. B. Tolley
Tucson Engineering Laboratory
Hughes Aircraft Company
Tucson, Arizona

Data are presented which show a correlation from +78°F to -85°F between the easily performed static load deflection (compression) test and a dynamic drop test for urethane foam used in the Falcon shipping container. These data allow prediction of the temperature limitation of dynamic cushioning from static test data. Information obtained from a general survey of materials available for cushioning at low temperature (-65°F) will be discussed briefly.

INTRODUCTION

The Hughes Aircraft Company requires cushioning material in various design configurations for transportation cushioning of the Falcon series of supersonic missiles. A wealth of information is presently available on cushioning materials, the theory of packaging design, and dynamic testing methods. However, the bulk of such information is applicable to materials tested at room ambient conditions, +70°F to +80°F. It is known that most of the elastic materials used in cushioning become harder as temperature is lowered and many become rock-hard at -65°F. Since military packaging systems often require cushioning from -65°F to +160°F, it is evident that the foamed rubbers and plastics have a basic temperature limitation and may not be suitable for low temperature use.

Evaluation of materials for low-temperature missile cushioning is costly and time consuming if done by drop testing of experimental containers. It was therefore desirable to obtain information on the degradation of a material's cushioning capacity at these reduced temperatures from a simple, easily performed test. Polyurethane foam was chosen as a typical test material for such a study, since the low-temperature limitation had not been determined.

OBJECTIVES

The general purposes of this test program were to study by static and dynamic testing the effect of low temperature on the load-bearing capacity and damping capacity of polyurethane foam, and if possible, to correlate these data so that predictions of dynamic drop-test performance could be made from data obtained by the easily performed static load-deflection (compression) test. If a correlation between the static and dynamic tests could be obtained, it appeared desirable to survey the suppliers of cushioning materials, obtain samples of interest and test them at low temperature by the static compression test. Information gained on low-temperature damping capacity of different classes of materials would be valuable in future design programs where low-temperature cushioning was required. Specifically, the program was resolved into the following areas of study:

1. To evaluate the effect of moisture absorbed by the pads in a high (40-70 percent) relative humidity laboratory environment. This moisture is trapped in the form of ice particles during low-temperature testing.
2. To evaluate quantitatively the changes in load-bearing capacity of the urethane foam by the static load-deflection test as temperature is lowered.

3. To study quantitatively the effect of reduced temperatures on the cushioning capacity of the urethane foam by a dynamic drop test designed to simulate container drop test conditions.

4. To evaluate the dynamic drop-test data and the static compression test data to determine if a correlation exists between the two tests.

5. To determine if materials are available for low-temperature cushioning and to evaluate their dynamic cushioning properties at -65°F.

GENERAL DISCUSSION

The material used for the low-temperature comparison of static and dynamic testing was a polyurethane foam. This material was selected to determine its low-temperature limitations for future design programs and also because it is representative of the organic foamed materials available. Testing techniques evolved should then be applicable to other systems, urethanes, vinyls, olefines, neoprenes, etc. The urethane foam studied has a density of 4.1 ± 0.4 pounds per cubic foot, an ultimate strength of 30 ± 3.0 psi with approximately 210-percent elongation.

The testing of the foams for load bearing and cushioning capacity was accomplished under static and dynamic conditions. In the static tests the foams were compressed at a constant rate - 2 inches per minute. From this test a load-versus-deflection curve was obtained. Typical load-deflection curves are presented in Figs. 1, 2 and 3. The load-deflection curve shows a yield point, an ultimate load for a given deflection and a hysteresis effect that is a measure of the energy absorbed by the foam material during compression. This mode of testing has been termed static because the compression is relatively slow allowing the foam to nearly reach equilibrium condition of load for a given deflection during the progress of the test. Therefore, the flow curve is considered to be the equilibrium load condition on the foam for the imposed deflection. Actually, the rate of compression of the foam changes the load-deflection curve obtained. Rapid compression raises the curve slightly. However, within the compression rates of 0.2 to 4.0 inches per minute, the flow curve can be considered as constant and the test is therefore defined as static. The yield point is defined as the maximum load obtained prior to elastic

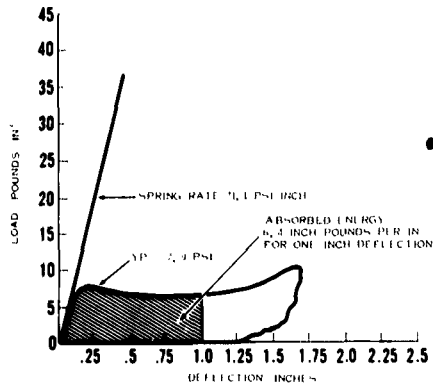


Fig. 1 - Urethane foam static compression curve -20°F

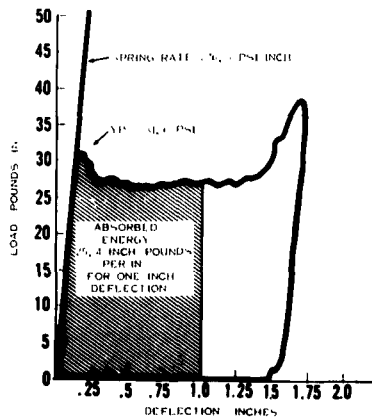


Fig. 2 - Urethane foam static compression curve -50°F

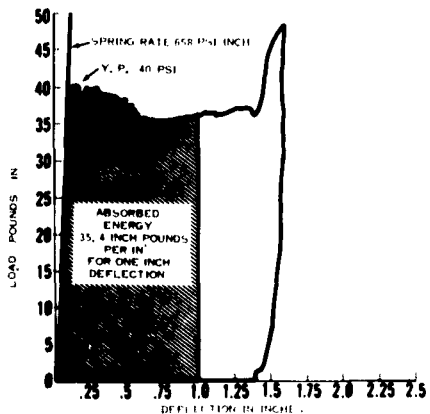


Fig. 3 - Urethane foam static compression curve -80°F

breakdown of the foam, resulting in a rapid deflection for a slight increase in load. This is not a true yield point, since the system is in a state of elastic yielding at all times. A yield point in metal systems is defined as the point in the flow curve at which the linear portion representing elastic yielding is replaced by a nonlinear portion representing plastic yielding, as measured by the offset method. However, the term yield point has been applied to this value in an elastic system for lack of a better name and because it resembles a true yield point obtained in a low-carbon steel system.

The dynamic test consisted of drop impact loading of the foamed urethane plastic. A drop-test jig was fabricated to simulate the missile loading in the container. The data available from this test were the peak g level to which the foam specimen was subjected, and the peak g level transmitted through the foam to the dummy missile surface.

STATIC TESTS

Static Test Procedure

The static test procedure consisted of placing the urethane foam in a compression machine and compressing at a constant rate of 2 inches per minute until the load reached a 1000 pounds or the deflection had reached about 1.75 inches. The test pad thickness was three inches, and the surface area was maintained at twenty square inches. This was the largest pad size on which compression curves could be run at extremely low temperatures without exceeding the 1000-pound load limit of the compression machine.

Since a cold chamber that could be incorporated in the compression machine was not available, a method of insulating the pads during the compression test was devised. In initial runs, the pads were insulated while in the compression test machine by a plywood box that encased the sample on three sides. A wood block was used as the compression head to insulate the fourth surface. The plywood box and wood compression head, with the foam sample in place, were brought to the test temperature as a unit. This assembly was then placed in the compression machine and the load-deflection curve run. The total elapsed time from removal of the sample from the cold chamber to completion of the run was less than one minute. Temperature

measured within the foam pad matrix, less than half an inch from the compression face, did not vary during the test. In later runs the cumbersome wooden box was replaced with two 3/4-inch plywood panels that insulated the foam from the steel compression faces of the load-deflection machine. The plywood pieces were brought to temperature with the foam and inserted in the test machine as a unit. No difference could be detected using this method and that employing the totally enclosed box. This technique was used for all subsequent low-temperature compression tests.

Effect of Moisture on the Flow Curve

At the start of this program, consideration was given to the possible effect of moisture from laboratory air (40-70-percent relative humidity) on the flow curve of the urethane foam during the low-temperature compression tests. The slight amounts of moisture present would be frozen at these temperatures and it seemed reasonable to assume that these fine layers of ice in the urethane foam matrix could significantly affect the load-versus-deflection curve.

Compression tests were run to check this hypothesis. Samples of the foam material were equilibrated in an atmosphere of dry nitrogen (dew point -60°F) or dry argon (dew point -130°F). The dried pads were then placed in a dehumidified cold chamber held at the desired test temperature. Compression curves were run on pads containing moist air and on the dried pads at the temperatures of -65°F, -50°F and -35°F. The flow curves obtained with the moisture laden foams were found to be identical to the dried foam curves. It was concluded that the moisture in the pad had a negligible effect on the flow curve of the foams measured at temperatures below zero. Henceforth, all runs were made using foams equilibrated in the laboratory air.

Effect of Low Temperature on the Flow Curve

Quantitative data on the low-temperature compression properties of the urethane foam and of other packaging materials presently in use were not available. Information on the urethane foam was of interest for future design programs which might require low-temperature cushioning.

A series of load-deflection (compression) tests was performed on 4.5 x 4.5 x 3-inch

samples at ten temperatures from +75°F to -110°F. The results represent tests on the same urethane pad. However, initial tests were performed on different samples of the same foam material and showed that consistent results were obtained from sample to sample. The compression test was run at the rate of two inches per minute and was continued until the flow curve began to rise sharply to 1000-pound load (50 psi on the 20 in.² pads) or about 1.75 inches of deflection in the pad. The time lapse during a run was always less than one minute. Typical load-deflection curves for three of the ten test temperatures are shown in Figs. 1, 2 and 3.

Normally (temperatures down to about -5°F) the complete compression cycle produces a hysteresis loop. The closed loop then represents the energy absorbed by the foam specimen during the static cycle and should be an indication of the ability of the foam to function as a dynamic cushioning material. However, when the foams are tested at temperatures below -5°F they fail to recover when the stress is removed. The set that is frozen into the pad is recovered as the material warms. An increased area in the hysteresis loop would normally indicate greater energy absorbing and damping ability of the foam, a desirable condition for cushioning materials. In this case, the increase in the apparent hysteresis loop is actually meaningless as the cycle has not been completed. Since the foam is becoming harder as temperature is lowered, it is losing its cushioning ability.

Analysis of Static Test Data

The spring rate in psi per inch of deflection was obtained from the initial linear portion of the load-deflection curve, Figs. 1, 2 and 3. The spring rate becomes more difficult to measure accurately at low temperatures since the slopes become so steep that small errors are greatly magnified. However, the slope of the linear portion of the load-deflection curve was found to increase as temperature was lowered. This function was plotted against temperature as shown in Fig. 4. At -10°F the curve begins to rise rapidly with decreasing temperature, indicating a hardening or increase in resistance to deformation of the foam pads.

A second function obtained from the load-deflection curve (Figs. 1, 2 and 3) was yield point. The value in psi was again plotted against temperature. The yield point is easily

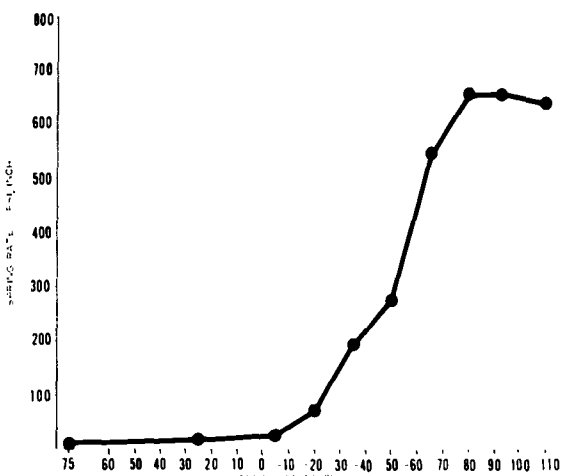


Fig. 4 - Urethane foam spring rate versus temperature

and accurately measured and when plotted versus temperature produces a curve (Fig. 5) that is strikingly similar to that previously obtained from spring rate versus temperature. Again it is evident that at -10°F the yield point begins to increase almost exponentially.

A third measure of the increase in hardness of the pads as temperature is reduced was also obtained from an analysis of the load-deflection curves. The energy under the stress-strain curves is a measure of the energy absorbed during compression of the

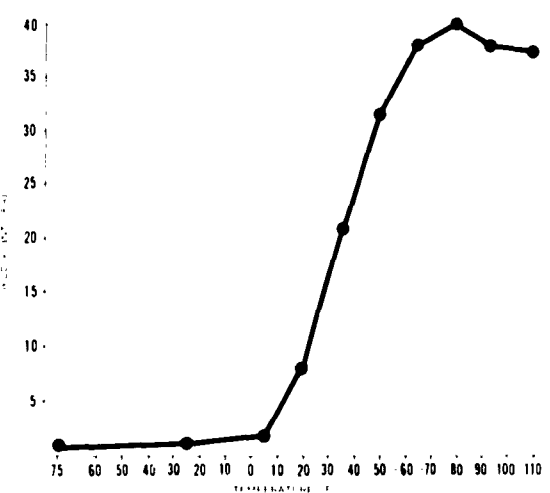


Fig. 5 - Urethane foam yield point versus temperature

foam. The flow curves were integrated to 1-inch deflection. This gives an energy value in inch-pound to deflect the foam one inch. The energy value obtained for a 1-inch deflection of the 20-inch² foam sample has been reduced to unity. The units are seen to be straight-forward (energy as inch-pound per square inch of foam surface per inch of compression of the pad or inch-pound/inch²/in deflection). Fig. 6 shows a plot of absorbed energy versus temperature. Again a rapid increase in total energy absorbed during a compression cycle is obtained as temperature is lowered below -10°F.

The three functions, spring rate, yield point, absorbed energy, plotted against temperature yield similar curves. At -10°F, all three functions rise with decreasing temperature until at -55°F to -65°F they flatten out and tend to remain constant with decreasing temperature. This type of data provides information on the effect of temperature on the hardness or load carrying capacity of the urethane foam. Such an analysis should be applicable to any of the flexible plastic foams (vinyls, olefines) or to the rubber materials (silicones, neoprenes, bunas). It would be expected that at -10°F the cushioning ability or damping capacity of the urethane would begin to rapidly degrade. Dynamic drop tests were performed to verify this assumption.

DYNAMIC TESTS

Dynamic Test Equipment

The equipment used in the dynamic drop testing of the urethane foam is standard with the exception of the drop-test jig fabricated at Hughes Aircraft Company. The following units are used to make up the drop test station:

1. Shock equipment: (a) Barry 150-400 VD Medium Impact Shock Machine, Serial No. 242, 12 blocks, 0.0065-second pulse duration, (b) drop-test fixture fabricated at Hughes Aircraft Company.

2. Measuring equipment: (a) Model 2213 Endevco Accelerometers, (b) Endevco Accelerometer Amplifier, Model 2614, (c) LC filter matched to amplifier to filter frequencies above 300 cycles, fabricated at Hughes Aircraft Company.

3. Indicating equipment: Tektronix Type 545, Oscilloscope with dual trace preamplifier, Serial No. 15357.

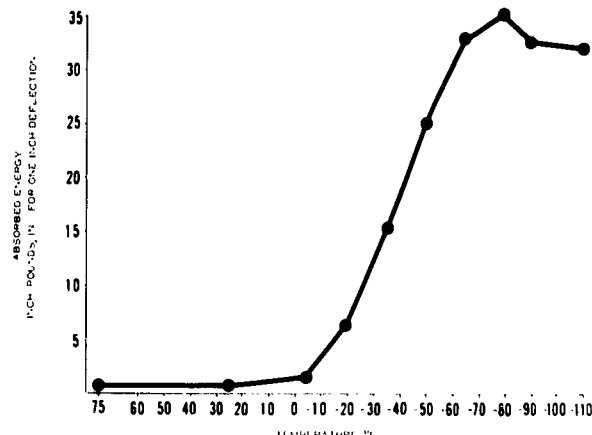


Fig. 6 - Urethane foam absorbed energy versus temperature

4. Recording equipment: Land Polaroid Oscilloscope Camera.

5. Conditioning equipment: Revco Sub-Zero Chamber.

The drop-test fixture (Fig. 7), simulates the loading to which the missile is subjected in the closed container. The fixture is designed to hold a 6 x 10 x 3-inch thick pad of foam. The dead weight (simulated missile load) can be varied within limits. The pads can be compressed by tightening down the frame bolts to any degree of precompression to simulate the precompression produced in

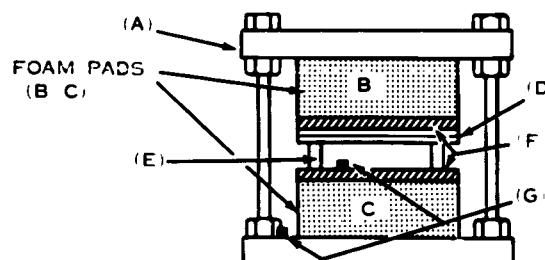


Fig. 7 - Drop test jig: (A) adjustable in height to apply precompression to the pads; (B) simulates the top pad in the container; (C) simulates the bottom pad on which the missile rests; assembly consists of variable weights (D), spacers (E), compression plates (F), simulates the missile load; (D) allow the missile load on the bottom pad to be varied from about 0.1 to 2.0 psi; (E) provide space for accelerometer installation; (G) one mounted on frame base to measure input acceleration from the drop, the second mounted on the cushioned section to measure the acceleration response.

the pads on closing the container lid. The accelerometers were positioned to measure the peak shock applied to the fixture and the peak response of the cushioned missile preload section.

Effect of Low Temperature on Cushioning Capacity

The foam pads were positioned in the test fixture with a 0.5-psi missile load and a 15-percent precompression. This approximates the missile dead weight on the bottom pad and the additional precompression obtained when the container lid is closed. The test fixture with pads in place was equilibrated at the desired temperature, removed from the cold chamber and mechanically fastened down to the drop tower. Three drops were made from heights of 8, 12 and 16 inches at eight temperatures from +75°F to -85°F. The total lapsed time from removal of the test fixture from the cold box to completion of the three drops at a given temperature was less than three minutes. The temperature of the pads and the fixture remained constant during the drops due to the large heat capacity of the heavy metal frame of the test fixture.

The initial 8-inch drop height was chosen empirically. A shock value between 20-30 g was desired for the -65°F drop, since Hughes specifications frequently limit the shock load to the 30 g figure in the temperature range of +160°F to -65°F. It was found that the 8-inch drop height gave an average value of 24 g on the cushioned accelerometer. Therefore, the 8-inch height was chosen as the standard and was always run immediately after removal of the fixture from the cold chamber. The g values at the other heights may reflect slight errors of softening of the pads due to energy input from the previous drop and softening due to slight warm-up of the fixture. A photo was taken of the acceleration traces on an oscilloscope. It was found necessary to incorporate an LC filter to eliminate the high-frequency noise that was masking the trace of the cushioned accelerometer. This noise was attributed to high-frequency transients which arose from secondary vibrations in the floating missile section of the drop test fixture. The LC filter eliminated all frequencies above 1000 cps with about one half attenuation at 600 cps. All frequencies below 300 cps were passed.

The data obtained from the drop test include peak g value of the drop measured on the frame of the test fixture, the peak g value on the cushioned missile preload section and

the amount of excursion of the floating missile section. The most interesting presentation of the data is shown in Figs. 8, 9 and 10. Here the peak g value on the cushioned accelerometer is plotted against temperature for each drop height. The curves are strikingly similar to the static test functions of spring rate, yield point and absorbed energy versus temperature. In the static tests the functions all begin to rise sharply as temperature drops below -10°F while the loss of damping or cushioning capacity is shown to occur at this same temperature as indicated by the increasing

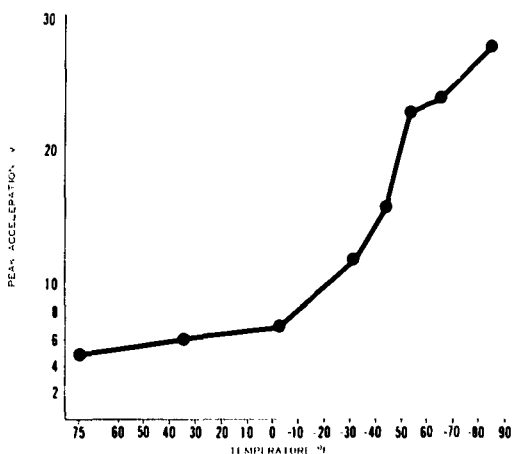


Fig. 8 - Peak acceleration versus temperature 8-inch drop

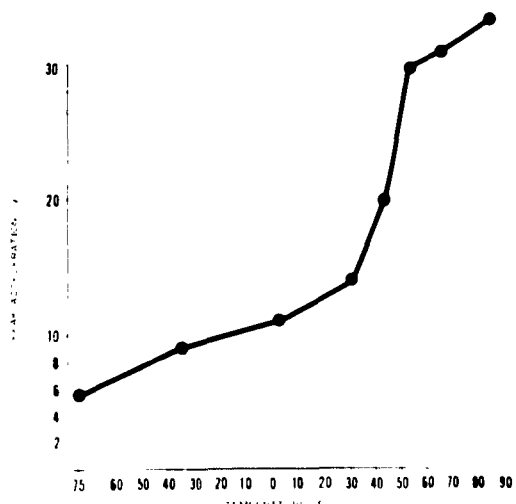


Fig. 9 - Peak acceleration versus temperature 12-inch drop

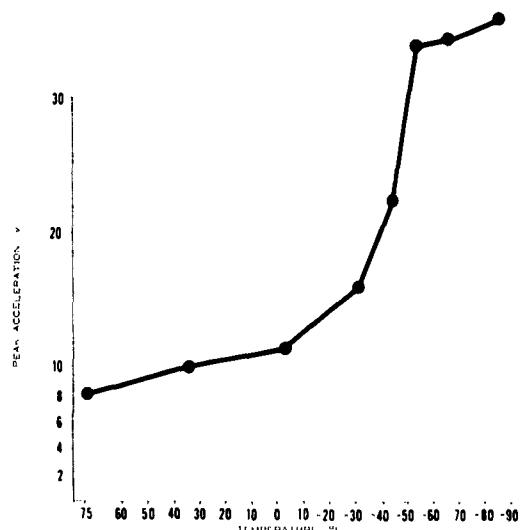


Fig. 10 - Peak acceleration versus temperature 16-inch drop

peak g value of the cushioned accelerometer. Both the static and dynamic functions increase as the temperature is lowered to values of -55°F to -65°F . The dynamic and static functions then remain constant to -85°F and -110°F respectively. It is expected that further reductions in temperature would not cause any of the static or dynamic functions to increase.

Figure 11 indicates the effect of increased drop height on the peak shock of the cushioned missile section. It is seen that as the

temperature is lowered the curve for each series of drops moves to higher values of shock.

Most of the foamed organic materials could be expected to show a limiting temperature below which they would rapidly lose their cushioning properties. This limiting temperature range can be evaluated from the easily performed static test. The static test should be applicable to any materials, organic or inorganic, in the form of foams, cellular structures, mats or batting. This static test therefore provides a rapid and inexpensive method for evaluating materials for low-temperature cushioning. Promising materials could then be dynamically tested in a fixture or fabricated to form and tested in final packaging assemblies.

EVALUATION OF OTHER MATERIALS

Test Methods

Samples of the more promising materials obtained as a result of a survey of manufacturers were tested at -65°F and $+75^{\circ}\text{F}$. by the static compression test. These tests provided a comparison of the low temperature and room ambient load-deflection curves for each sample and permitted the evaluation of the merit of the material for low-temperature cushioning.

Materials Tested

Seventeen different materials were evaluated by the static techniques. Only two classes

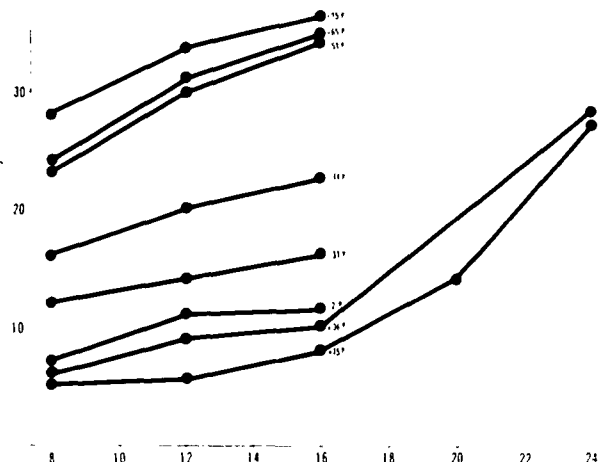


Fig. 11 - Peak acceleration versus drop height

proved to have superior low-temperature properties. All others became hard showing a large increase in yield point at the -65°F test temperature. Some of the materials tested at -65°F may have reasonably good cushioning ability at some intermediate temperature (-10°F to -40°F). However, investigations were not carried to the point of testing at other temperatures. The materials and classes tested that show degraded low-temperature cushioning are listed below. Individual samples within a class were from different manufacturers and could be expected to show a variation in low-temperature properties.

<u>Material Class</u>	<u>Materials Sampled</u>
Polyethylene	1
Polyvinyl Chloride	2
Polyurethane	8
Acrilinitrile Rubber	1
Neoprene Rubber	1

Three samples of silicone foams were tested. The -65°F load-deflection curve for each of these three materials was found to be identical to the +75°F curve. This indicates that the low-temperature dynamic cushioning is identical to the cushioning ability at +75°F. The three materials tested were of a rather high density and would not be expected to provide exceptional cushioning at +75°F. However, the fact that the load-deflection curves are identical at +75°F and -65°F is significant. This class of materials should have application as a low-temperature cushioning material. Silicone foams could be developed, if they are not already on the market, that would have a wide range of load bearing properties, resiliency and strength. However, the silicones as a class have some definite disadvantages that would temper a decision for their use.

The silicones are, in general, relatively expensive; they often have poor tensile and tear strength; they may take a large permanent set on aging under load; and hydraulic fluids will attack many of them at varied rates causing a general deterioration over a period of time.

Drop-test requirements (e.g., MIL-P-9024) often require a given drop height at ambient temperature and some lesser height, often one third the ambient drop at the low- and high-temperature limits. In an application having a requirement of this kind, a silicone sponge sandwiched between two urethane

foam pieces might provide a cushioning package that would combine the desirable properties of the two materials. The less costly and tougher urethane would protect the silicone surfaces and, with the silicone, would damp or cushion the room temperature drop. At low temperature the urethanes tend to become hard and nonfunctional as cushions. Since the drop height would be some fraction of the room ambient drop, a lesser amount of foam would be required for cushioning. Therefore, the costly silicone foam could be kept to a minimum, and in addition, would be protected by a tough, hydraulic fluid and solvent-resistant urethane material.

A fiberglass flexible pad material was tested and also proved to have identical load-deflection curves at +75°F and -65°F. This material is fabricated from layup of a network of fiberglass bats which limits the cushioning properties to one plane. The fiberglass pad could be supplied in varied shapes, thicknesses, densities and load capacities if demand warranted. The material appeared to have the following limitations: the tensile strength of the pad in the direction normal to the layup of the glass fibers is poor; the service life of the pad may be short; the fiberglass would be expected to crack and fracture during repeated compression cycles, causing a loss of load bearing ability or strength.

A situation where low-temperature cushioning is desired, but where repeated cushioning service over long periods of time is not required, would appear to be an area for which the fiberglass cushioning might be adapted.

It is seen that most organic materials have a limiting temperature below which they lose their resiliency. In the silicones, this temperature is well below -65°F thus permitting their use as low-temperature cushioning. Only two classes, silicones and fiberglass, were found to offer promise for very low-temperature pad cushioning. The use of the static compression test to evaluate new materials for dynamic cushioning should prove of value in that costly dynamic studies need to be performed only on those materials that show promise in easily performed static tests.

CONCLUSIONS

The major conclusions reached during the study follow:

1. Moisture from humid air in the laboratory had no noticeable effect on the low-temperature load bearing properties of the urethane foams.

2. The urethane foam tested loses some cushioning properties at low temperatures. Degradation of performance during static tests began at -10° F.

3. Degradation of performance during dynamic cushioning tests also began at -10° F.

4. The easily performed static compression tests can be used to predict low-temperature dynamic performance.

5. Most organic foam materials have a low-temperature limit below which their cushioning ability degrades rapidly. This low-temperature limit may vary widely in different material classes.

6. The silicone foams and the fiber-glass batting tested have excellent low-temperature cushioning possibilities.

BIBLIOGRAPHY

"Foam Plastics," Walter Brenner, Materials and Methods Manual, No. 127, Materials and Methods, June 1956.

"Fundamentals of Guided Missile Packaging, Shock and Vibration Design Factors," RD 219/3, Office of the Assistant Secretary of Defense Research and Development. July 1956, ASTIA No. ATI 210000.

"The Theory and Operation of a Dynamic Tester for Evaluating Package Cushioning Material," Materials Laboratory, Wright Air Development Center, September 1956, ASTIA No. AD 97327.

"Cushioning for Air Drop, Part VII, Characteristics of Foamed Plastics Under Dynamic Loading," The University of Texas, Structural Mechanics Research Laboratory for Quartermaster Research and Development Command, March 28, 1957, ASTIA No. AD 215412.

"Optimum Cushioning Properties of Packaging Cushioning Materials," North American Aviation, Inc., Materials Research, May 15, 1957, ASTIA No. AD 143980.

"Investigation of Shock Waves Developed During Dynamic Tests of Cushioning Materials," Forest Products Laboratory, Wright Air Development Center, August 1957, ASTIA No. AD 131019.

"Polyurethanes," B. A. Dombrow, Reinhold Plastics Application Series, Reinhold Publishing Corporation, 1957.

"The Development of a Non-Adhering Chemically Foamed-In-Place Polyurethane Cushioning Material for Packaging Purposes," Materials Laboratory, Wright Air Development Center, January 1958, ASTIA No. AD 142282.

"Properties of Flexible Urethane Foams," Research Department, Mobay Chemical Co., Chemical and Engineering Data Series, Vol. 3, No. 1, April 1958, Page 153.

"The Theory and Operation of a Dynamic Tester for Evaluating Package Cushioning Material," Materials Laboratory, Wright Air Development Center, May 1958, ASTIA No. AD 151195.

"The Cushion Factor-Stress Curve and its Value for Classifying and Selecting Package Cushioning Materials," Forest Products Laboratory, Wright Air Development Center, November 1958, ASTIA No. 205071.

"Cushioning Materials Study Program," by General Electric Co., Light Military Electronic Equipment Department, 1958, ASTIA No. AD 211161.

"Investigation of Design Criteria for Cushioning Materials," Materials Laboratory, Wright Air Development Center, March 1959, ASTIA No. AD 210227.

"Materials, Techniques, and Economics of Foamed-in-Place Polyurethane Cushioning for Packaging," Materials Laboratory, Wright Air Development Center, April 1959, ASTIA No. 211913.

"The Urethanes Grow Up - Part 2," Thiokol Chemical Corp., Reprint from Modern Plastics, April 1959.

"The Effects of Simulated Space Environments on Cushioning Materials," Bolt Beranek and Newman Inc., for Materials Laboratory, Wright Air Development Center, September 1959, WADC Technical Report 58-667.

"Silicones," R. N. Meals and F. M. Lewis, Reinhold Plastics Application Series, Reinhold Publishing Corporation, 1959.

"Low Temperature Properties of HMS-16-1172-1 Urethane Foam," W. B. Tolley, Hughes Aircraft Company Technical Report, Reference Number 4271.6/9, October 24, 1960.

"Search for and Evaluation of Materials for EGSC-3A Container Pads," W. B. Tolley, Hughes Aircraft Company Technical Report, Reference Number 4171.6/21, February 17, 1961.

* * *

Section 3

SIMULATION OF TRANSPORTATION ENVIRONMENTS

A PROPOSAL TO ESTABLISH VALID GROUND TRANSPORTATION TESTS

Alan E. Surosky
General Testing Laboratories
Moonachie, New Jersey

The need for defining test procedures which will assure equipment adequacy with regard to ground transportation shock and vibration is discussed. The current state of instrumentation and test techniques is outlined. Problem areas are illustrated by case histories and suggestions are offered for future programs.

INTRODUCTION

After performing "transportation" tests in accordance with various specifications for a number of years, our Laboratory developed an euphoria concerning its ability to evaluate material for transportation adequacy. Consequently, we had no misgivings when we were asked by Highway Trailer Company to evaluate their Flexi-Drum, a collapsible plastic bulk container (Fig. 1).

Since the drum was to be used indefinitely in all types of transportation service, it was proposed to prepare a test program which would define both the adequacy and the longevity of the test item. The initial program was developed by abstracting various military and commercial specifications and by applying accepted "rules of thumb" with regard to the equivalence of test time and transportation mileage.

Examination of both the proposed tests and the test package by our technical review committee created some intuitive doubt concerning the validity of the program. For this reason, it was decided to make a survey of existing test

methods with particular regard to their scientific validity. The results of the survey indicate some significant gaps in available information as well as the need for some dramatic measures in test development.

GROUND TRANSPORTATION ENVIRONMENT

Ground transportation is unique among transportation environments in that its deleterious effects cannot be related, except on a statistical basis, to the times and distances involved. In any specific instance local ground transportation can be more destructive than trans-continental shipment.

National Safe Transit Committee data indicate that the most severe shock in transit generally occurs in handling. Figure 2 represents shipping shock of an air-cargo package shipped Cleveland to New York to Cleveland. The shock zones are as indicated by a Savage Impact Register. The significance of these "shock zones" is questionable and will be discussed later, but it is probable that these

values have some direct mathematical relationship to the destructive potential of the shock. The results of a series of such N.S.T.C. tests are summarized in Fig. 3.



Fig. 1 - Highway trailer company "flexidrum container"

If we accept the idea that handling can be more destructive than extended transit periods, and if we realize that an item of equipment in a surface vehicle can survive several thousand miles of road transport and then be damaged by a single road defect, the requirement for a statistical approach to transportation testing becomes obvious.

INSTRUMENTATION

Ground transportation shock and vibration can, of course, be measured by the same sophisticated accelerometers and read-out instrumentation employed for airborne equipment. The cost and complexity of these instruments, as well as the difficulty of reduction of the erratic source data dictate the use of simpler devices. The most popular instrument currently used for this work is the mechanical accelerometer in any of a number of configurations.

Typical of these devices is the Three-Way Accelerometer manufactured by the Impact Register Company and shown in Fig. 4. This accelerometer will record triaxial acceleration versus time on a relatively slow time base. Thus, the number, chronology, and peak value of shocks along three major axes can be determined. The shock duration cannot be determined.

Another g-reading instrument with a time base is the Impactograph (Fig. 5). This unit is similar in operation to the Impact Register but, due to difference in instrument response, does not always give comparable results.

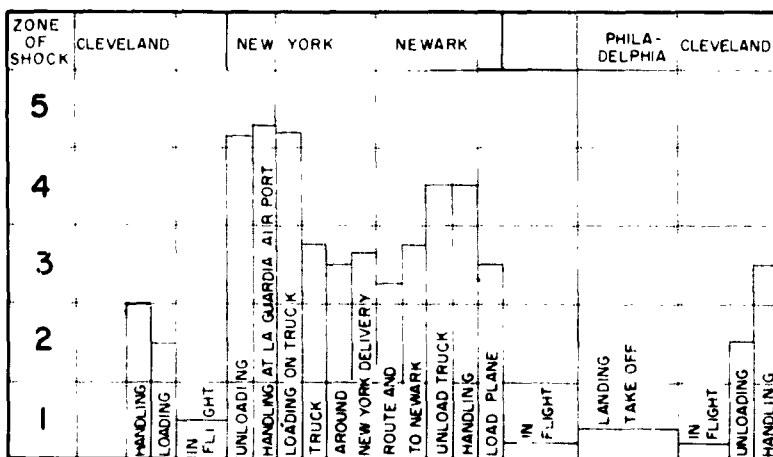


Fig. 2 - Shocks as received by a packaged product shipped as air cargo from Cleveland to New York to Cleveland, including truck transportation from La Guardia airport to Newark airport (N.S.T.C.)

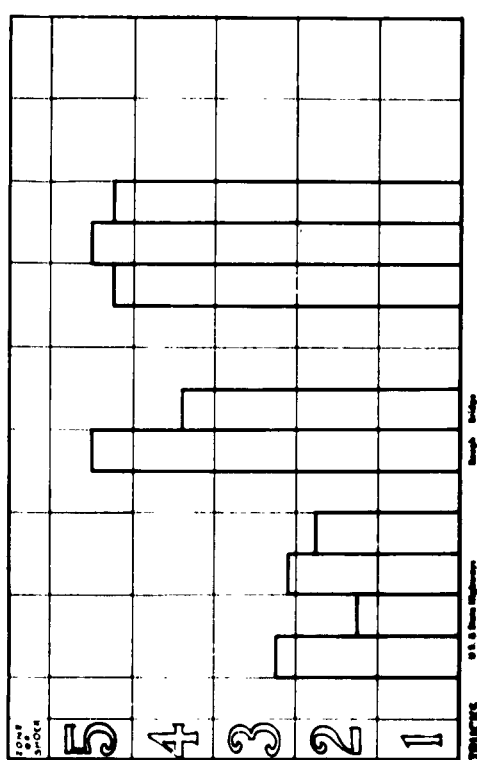
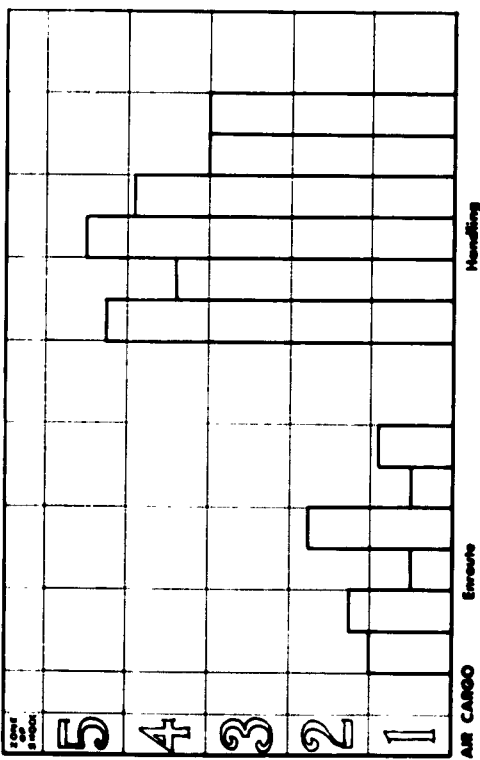
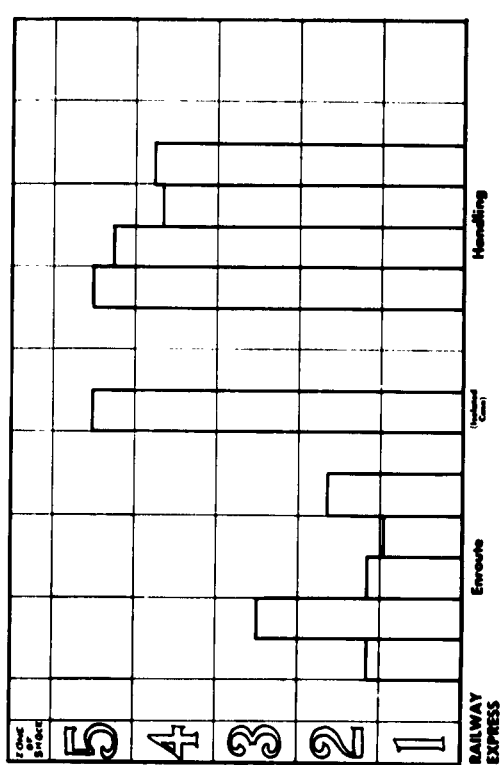
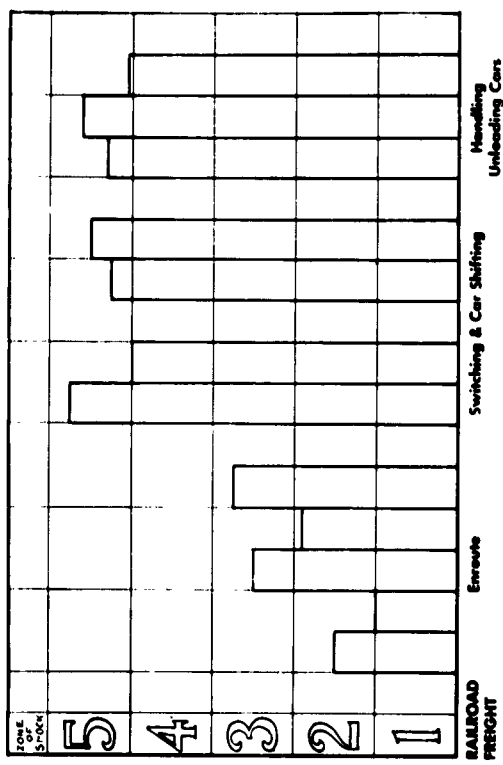


Fig. 3 - Summary of averages for all test shipments, for all modes of transportation (N. S. T. C.)

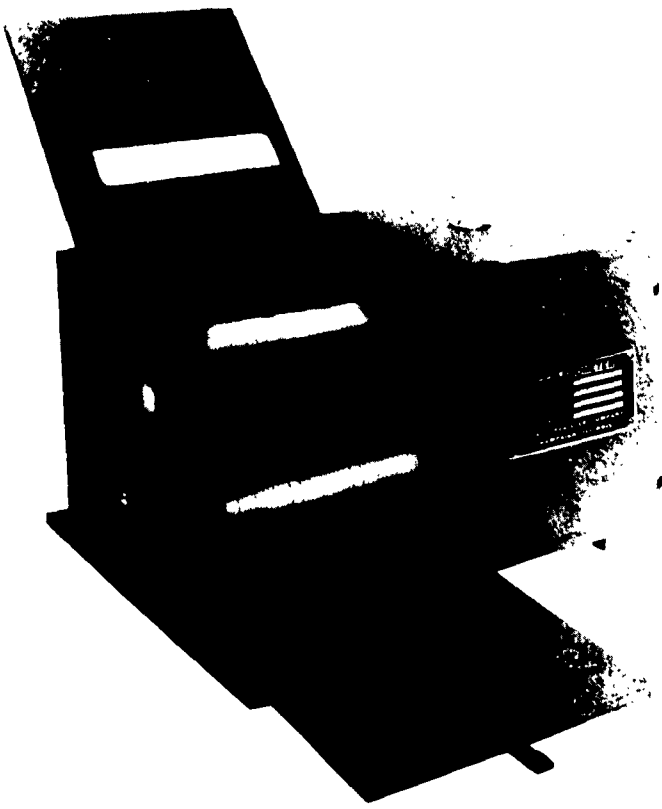


Fig. 4 - Model RM-three way accelerometer; length: 9 x 5/8 inches; width: 6 x 1/2 inches; height: 5 x 3/4 inches; weight: 12 pounds. The Impact Register Company

Pace Engineering Company manufactures an inertia-type maximum-indicating-shock recorder (Fig. 6), the results of which are translatable into g's under the same limitations as the previously described instruments.

Inertia Switch Company has developed a device, (Fig. 7) which provides essentially the same information as the previously discussed instruments but which also automatically reduces the information to a statistically usable form. This instrument consists essentially of a series of shock-sensitive mechanical switches which can be preset to different g levels thus providing a count of the number of shocks above each level.

The primary difficulty in correlating information reported by these instruments with actual transit damage is that the N.S.T.C. and the American Association of Railroads adopted as a

standard the Savage Impact Register which records shock level in "zones" rather than g's. For all of these inertia-type instruments a correlation between zones and g's can be obtained only for certain discrete pulse durations inasmuch as the inherent response of the instruments is a factor in the readings they produce.

The Savage instrument was originally designed for freight car use and the zones from 1 to 5 indicated progressively poorer handling of the cars. The initial intent of the zone designation was that it would be proportional to the speed of the car immediately before impact. Since the actual shock was a function not only of the speed but also of the relative weights and couplings of the respective cars, the "zones" became an arbitrary standard. The "zone" bears some relationship to shock energy rather than g level. For example, a fifth zone shock

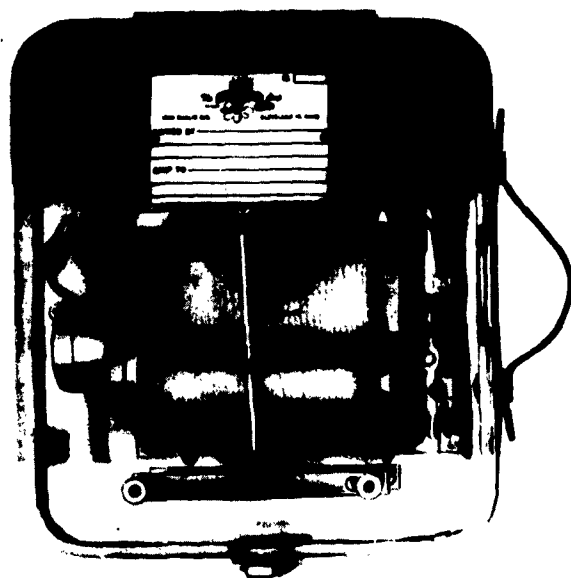


Fig. 5 - Impactograph

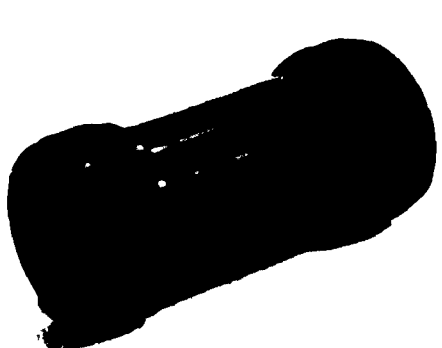


Fig. 6 - Pace engineering shock recorder

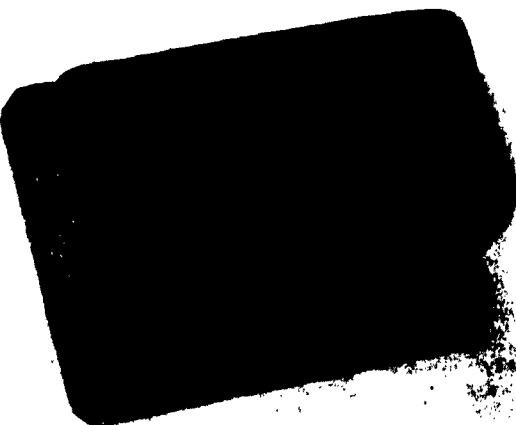


Fig. 7 - Inertia switch impact recorder

on a freight car will be registered where the peak g value is somewhat less than 10. A fifth zone shock on a Conbur Test Ramp will be obtained when peak g values are in excess of 50.

Some attempts have been made to design instruments which will respond to shocks of the duration believed to be most commonly destructive. There is a general impression that the most common destructive shock duration is of the order of 10 milliseconds but we have been unable to obtain experimental information to verify this.

SHOCK DAMAGE POTENTIAL

There is some question as to what factors determine the damage potential of shock. A watch dropped several inches to a table top may experience short duration shocks in excess of 100 g's without damage. On the other hand, a 10 g shock with a duration in excess of 75 milliseconds is sufficient to severely damage a freight car. There is no doubt that peak g level is a



Fig. 8 - Pallet load prior to shock (Lakehurst Naval Air Station photograph)



Fig. 9 - Pallet load after 100 ms 8 g shock (Lakehurst Naval Air Station photograph)

contributory but not controlling factor in shock destruction.

We recently had occasion to perform an 8-g, 100-millisecond shock on a pallet carrying a 10,000-pound load. The setup prior to test is shown in Fig. 8. The tiedown gear is standard webbing theoretically capable of withstanding the shock loads. Figure 9 shows the results of the approximately rectangular shock pulse. The failure mode in the webbing is shown in Fig. 10.

Certainly in this case the relatively long shock duration was instrumental in causing

damage. However, this same tiedown gear has been used to restrain an 80,000-pound load with the pallet in a vertical position equivalent to the top of a very long duration 8-g rectangular shock pulse. It is thus apparent that the rate of rise of the shock pulse determines, to some extent, the damage potential of the shock.

It is probable that shock damage to a rigid structure can be correlated with shock energy. Transportation shock in general, is applied to loosely mounted packages. Thus, the intensity of shock damage potential can be amplified or attenuated by the location and mounting of the



Fig. 10 - Failure mode pallet shock test (Lakehurst Naval Air Station photograph)

package in the vehicle. One of the primary gaps in our knowledge of the nature of transportation damage is the type of shock causing the actual damage, whether the low-intensity, long-duration primary or the high-intensity, short-duration secondary shock.

FIELD TEST FACILITIES

It would appear, superficially, that a field test facility should afford the best means of assessing the ability of a package to withstand the transportation environment. The field course in practice leaves something to be desired as a general purpose test facility.

The Munson Test Course at Aberdeen Proving Grounds (Fig. 11), is representative of a first-class field installation combining a number of test surfaces. The washboard surfaces are effectively recurring concrete sine waves with double amplitudes of two and six inches and wavelengths of two and six feet, respectively. The spaced bump surface is a series of rounded bumps three inches high and three feet long at thirty-foot intervals, and at varying angles to the direction of travel. The Belgian Block course is a cobblestone road providing a bumpy surface so graded that a vehicle travelling over them is also subjected to pitching and rolling.

Test speeds over these surfaces are usually determined by driver capability,

vehicle safety, or most severe shock and vibration conditions, whichever factor is controlling. Typically, speeds vary from 5 to 25 mph for the various surfaces. Maximum vehicular bed accelerations of 4-g peak are typical while impact accelerations on loosely stowed cargo can run much higher.

It is the writer's opinion that the results of a series of tests over the Munson Course are interesting and significant on a qualitative basis. There is certainly some question, however, concerning the relationship between a test of this type and the actual transportation environment. There is also the problem of reproducibility not only between various facilities but even at the same facility.

Tests run on a thirty-inch mobile searchlight at the Engineer Proving Grounds at Fort Belvoir illustrate this problem. Duplicate tests were run over a buried log course at six-month intervals. The original tests, run in October, showed the wheels of the trailer to leave the ground by no more than several inches. Tests run the following March, ostensibly identical, showed over two feet of daylight between the wheels and the ground. It is probable that the logs were elevated somewhat during the winter by frost heaving. It is also probable, however, that there were slight but significant differences in ground condition, tire pressure, lubrication, vehicular springing, and speed.

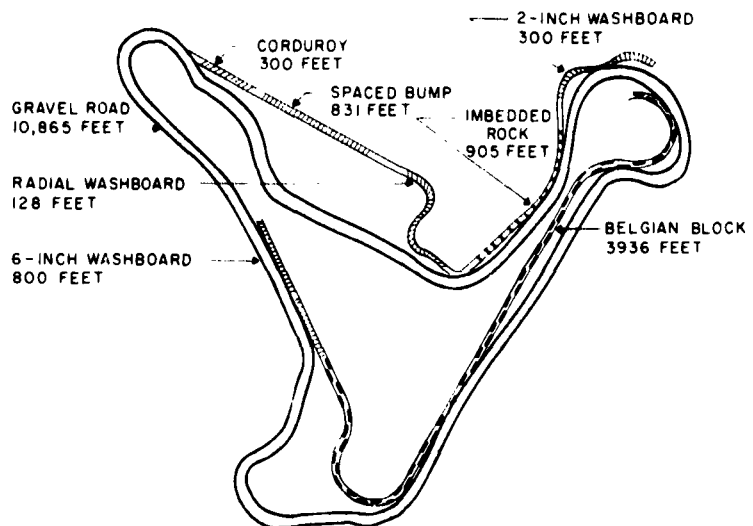


Fig. 11 - Munson test course, Aberdeen Proving Ground, Maryland

These "difficult to control" variables create some doubt as to the reproducibility of field-type transportation tests.

A further problem is the lack of standardization in field test facilities. It appears that most test sites have been constructed according to the ingenuity and whim of the designer. Savanna Ordnance Depot for example, constructed a test course of railroad ties projecting six inches above the roadway on alternate sides on ten-foot centers and then on eight-foot centers. This course was run at speeds to produce the most violent vertical and rolling motion in testing rocket motor packaging. The results were interesting but certainly did not lend themselves to duplication at other test sites.

The field test course cannot be replaced as a means of evaluating the mobility and handling characteristics of wheeled or track-laying equipment. Its value in general transportation testing is severely limited by high initial cost, difficulty of control of test conditions, and a lack of standardization of facilities.

LABORATORY TEST FACILITIES

Ground transportation shock and vibration test equipment in the laboratory has become standardized along lines defined by the National Safe Transit Committee. The application of this

equipment varies considerably according to specification requirements.

The standard low-frequency vibration exciter with a range of 5 to 55 cps at low displacements is occasionally used for so-called "transportation vibration" testing. While this test can be quite severe for certain package designs, it neither simulates the service environment nor produces the failure modes generally experienced during transportation.

The most practical laboratory tests are accomplished employing a transportation simulator combined with either the Conbur impact ramp or a free drop apparatus.

The transportation simulator, manufactured by L.A.B. Corporation or by Gaynes Engineering Company, in various capacities to 10,000 pounds is typically shown in Fig. 12. The table is driven by two shafts at speeds from 150 to 300 rpm and at a fixed displacement of one inch. The maximum speed corresponds to a vertical acceleration of 1.25 g's which causes an unrestrained package on the table to separate from the table and undergo a bounce shock on each cycle.

The table can be operated in any of several modes. Synchronous in-phase operation of the shafts produces circular motion in a vertical plane and is the most commonly used test method. Synchronous out-of-phase operation is

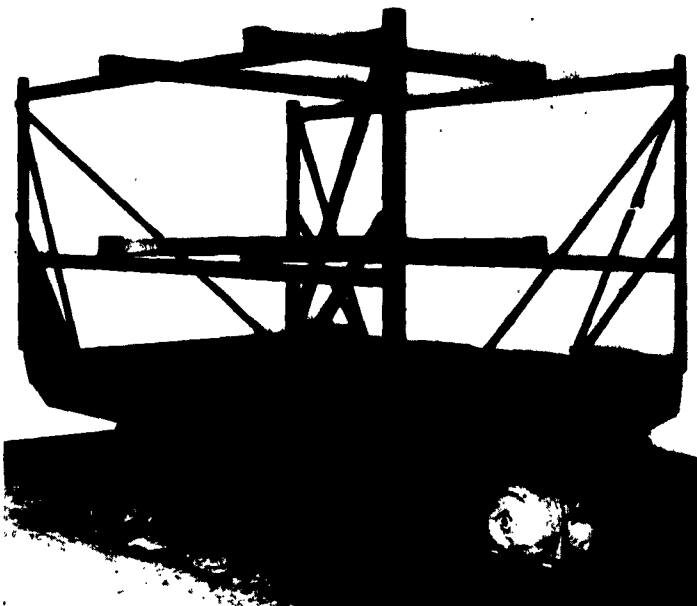


Fig. 12 - L.A.B. corporation 6000-pound vibration transportation simulator

accomplished with the eccentrics 30 degrees out of phase resulting in elliptical motion in a vertical plane. This mode reduces top swing of high-c.g. loads. A third mode, less frequently used, is nonsynchronous operation. In this case the two shafts operate at different speeds providing a constantly changing phase relationship. The motion produced most closely simulates the bounce and sway motion of actual transportation but is difficult to evaluate due to its irregular nature. In rare cases with small-base, high-c.g. loads, a pure vertical motion can be generated reducing toppling effects to a minimum.

It is a rule-of-thumb that one hour of test time is equivalent to 1000 miles of shipping distance. This is based on the fact that 270-rpm operation of the simulator produces 16,200 shocks hourly of 1-g intensity. This corresponds to the worst case of 16,800 shocks below 1-g in a 1000-mile high-speed trip reported by the Association of American Railroads in a 1940 survey. Inasmuch as it has previously been shown that handling and switching shocks can be considerably more severe than that imposed by extended transport, the value of this approximation is questionable.

The Conbur Impact Tester consists of a 10-degree ramp of an appropriate length to provide

a 20-inch vertical rise for 2000-pound machine and an 18-inch rise for larger machines. The load, supported on a dolly, is allowed to roll down the ramp and strike a composite steel and wood barrier ballasted to at least eight times the package weight. The purpose of this test is to simulate poor handling and humping of box cars.

An alternate to the Conbur Test for packages either weighing less than 100 pounds or not adaptable to the Conbur Ramp is the drop test. This consists of dropping a package on an edge or corner a specified distance to a specified surface. This is accomplished for smaller packages by the use of a special drop test device and for larger packages by means of quick release hooks.

TEST PROCEDURE

The transportation test equipment and instrumentation available in the laboratory is sufficient to carry out a series of valid tests to determine equipment adequacy with regard to transportation environment. The problem, hitherto unanswered, is to determine and specify what tests are reasonable and proper.

The N.S.T.C. tests have been developed specifically for packaged products. Since a reasonable degree of overpackaging is not unduly expensive for commercial equipment, the test levels have been set arbitrarily high. Consequently, any package meeting N.S.T.C. requirements can be expected to perform satisfactorily in service. The same degree of overtesting for military material, frequently transported unpackaged, can establish uneconomically high design requirements.

The Federal Government adopted the N.S.T.C. procedures literally in Specification PPP-P-600. Several military specifications have adopted the procedures with changes which do not appear justified on the basis of existing knowledge of the transportation environment. Some examples of differences in test requirements are cited below.

PPP-P-600 calls for synchronous operation of the transportation simulator at a speed such that the package clears the table by approximately 1/16-inch. Signal Corps technical requirement SCL 6836A for nickel-cadmium batteries specifies a fixed machine speed of 285 rpm.

MIL-T-4807A(USAF), the specification for shock and vibration testing of ground electronic equipment calls for operation at any speed below 285 rpm such that the average maximum acceleration at a top corner of the package is 10 g's. Inasmuch as various packages can exhibit tremendously different isolation characteristics this requirement is nebulous at best. Additionally, this specification calls for two hours of synchronous and two hours of nonsynchronous operation. This test level is arbitrary but may not be unreasonably severe for some packages. On the other hand, the writer has seen portable instruments battered to destruction in this test through treatment more severe than they should reasonably be required to stand.

There are a number of other permutations of the transportation vibration test as well as for transportation shock. Certainly some standardization based on scientific investigation is in order.

TEST DEVELOPMENT

The missing link in the chain of information required to define adequate and valid test procedures is the quantitative relationship between laboratory-induced failure and that

experienced in the transportation environment. The following series of tasks is suggested as a direct approach to the solution of the problem.

First, it is suggested that equipment be categorized with regard to the nature of failure most often encountered or anticipated. Precision equipment subject to noncatastrophic failure such as frequency drift or loss of tolerance might be one category. Equipment subject primarily to catastrophic failure due to shock or vibration fatigue might comprise another. Large equipment difficult to handle and subject to structural failure due primarily to mishandling could comprise a third. It is possible that five or six categories would be sufficient to classify all materiel.

Second, a set of standard test packages should be designed representative of each of the previously chosen categories. These packages should be so fabricated that transportation damage would be measurable and progressive in proportion to the severity of the transportation environment. A typical package might, for example, contain a series of wires of different gages and under varying tensions so chosen that some would break under the most gentle handling while others would withstand any stress level except that induced by collision. Alternately or additionally, the package might contain glass tubes or rods. Another standard package might contain electronic circuitry subject to change in performance as a function of the stress level of the transportation environment.

Third, these standard packages should be shipped repeatedly by all appropriate means until a statistical basis is developed to establish probability of damage levels for the various package types and transportation modes. The standard packages should then be used to calibrate laboratory transportation test equipment to determine drop heights, machine speeds and test durations corresponding to the actual service failure levels.

Fourth, equipment should be grouped according to its required reliability in the transportation environment with regard to both economic and tactical considerations. The equipment category together with the reliability grouping could then be used to select appropriate test levels in accordance with the findings of the previous task.

The standard packages might be employed to fill one additional information void. A series of tests to determine the damage potential of

shock pulses as a function of wave shape and pulse duration would permit standardization of response of transportation instrumentation at an appropriate value. This in turn would permit a more meaningful analysis of damage data collected during the past several decades.

The program proposed here is one of a number of possible approaches to developing

sound generalized ground transportation shock and vibration procedures. Whatever the approach, any program aimed at correlating service and simulated service test data for ground transportation shock and vibration will fill a need felt both by the purchaser and the supplier of military equipments.

BIBLIOGRAPHY

1. Aberdeen Proving Ground Report No. DPS-214, "Road Shock and Vibration Test."
2. Savanna Ordnance Depot Progress Report 2-61, "Road and Rail Impact Tests."
3. E.R.D.L., Fort Belvoir, private communication.
4. "Transportation Shock and Vibration Tests Railroad and Military Truck," P.H. Adams, R.A. Buck and R.G. McKay, Shock & Vibration Bulletin No. 21, p. 127, November 1953.
5. Fimage, D.A., "Transportation Shock and Vibration Studies," Final Report No. 5105, Engineering and Industrial Experimental Station, University of Florida.

DISCUSSION

Mr. Keller (White Sands Missile Range): I am interested in how you applied this 8-g, 100-millisecond shock. With what did you apply it? In which direction and at what point was it applied and how did you measure it?

Dr. Surosky: The 8-g, 100 millisecond shock was applied using the steam catapult test facility at Lakehurst Naval Air Station. It is a standard military test for a 7 x 9-foot airborne pallet. This pallet was speeded up to about 20 mph on the car and then braked in about a foot and a half to a dead stop. The instrumentation showed that we got a pretty good 8-g, 100-millisecond shock — a square wave. The test was run both longitudinally and along the short axis of the pallet. So, actually we had a pallet with a 10,000-pound load and a 4 foot high c.g. What we did was to stop the pallet in a foot and a half and the load tried to keep on going. It did.

Mr. Schell (Aeronautical Systems Division): In the panel session last night and in your paper today, it seems that the damage potential of a shock has been expressed as the g-level and the duration. Dr. Ripperger gave a paper the other

day in which he showed that the pulse shape is pretty important in the characterization of the damage potential of a shock. Other investigators have suggested that the third derivative of the motion, sometimes called jerk, is perhaps a better criterion for fragility than just a plain, simple g. Actually, I think the pulse shape and the third derivative are nearly the same criteria. Would you care to make any comments as to why you would not want to get into anything more complicated than the frequency or the time duration and the acceleration?

Dr. Surosky: My immediate answer is, I agree. I think that here, maybe, we're taking the approach that I have tried to avoid. That is trying to analyze the destructive potential of a shock in terms of what we think it should be. I missed the panel session last night, unfortunately, and I wouldn't agree or disagree with anyone on just what it is that does cause shock destruction. What I would like to offer is that up to now no one has carried out a program which purely and simply shows for a fact what the damaging characteristics of a shock are. That is one of the things we suggested should be done.

THEORETICAL AND PRACTICAL BASES FOR SPECIFYING A TRANSPORTATION VIBRATION TEST

G. S. Mustin and E. D. Hoyt*
Reed Research Inc.,
Washington, D. C.

A description is given of the derivation of an expression of equivalence for a sinusoidal vibration test to a random environment. A standard vibration test for shipping containers is proposed consistent with the theory.

INTRODUCTION

Practically everyone seems to have his pet transportation vibration test. Figure 1 illustrates some of the more popular test methods applicable to shipping containers. It does not include the tests found in MIL-STD-167, MIL-T-18404, MIL-E-5400, MIL-T-945, MIL-STD-353, and similar equipment specifications.

This paper is the result of a commission from the Packaging Branch, Bureau of Naval Weapons, to seek out a logical basis for a standard vibration test to be used on missile containers.[†]

The basic approach we followed was:

(a) To find an expression of the response of an elastically supported item to random vibration. (The sinusoidal environment can be considered a special case of the random).

(b) To use the response expression so found, to develop an expression of equivalence to the response obtained in a sinusoidal test, to permit, if possible, using the less costly method.

(c) To extract any lessons possible from the theoretical results, emphasizing practical

ability to comply with any specification requirement which might be drawn.

This paper is a resumé of the limited but promising results achieved.

RESPONSE OF A SUSPENDED ITEM TO RANDOM MOTION

Let the item be suspended on a linear spring with damping ratio ζ . Assume, further, that the load does not bottom the spring nor strike the container walls during vibration. Then, using the concept of normal modes and the methods outlined in the literature [1], it is possible to write a generalized function for the mean square relative motion response (σ_1^2):

$$\sigma_1^2 = \frac{1}{2\pi} \int_0^\infty \left| \frac{H}{\omega_1^2} \right|^2 S_1 d\omega. \quad (1)$$

Where

ω_1 = natural frequency

S_1 = input acceleration spectral density

H = complex magnification factor defined below.

The magnification factor, H , is defined by

$$H = \frac{1}{1 + \frac{\omega^2}{\omega_1^2} + 2 \zeta \frac{\omega}{\omega_1} \sqrt{1 - \zeta^2}}. \quad (2)$$

*Current address: Robert Taggart, Inc.

[†]For those interested in the complete logic and all derivations, see Reed Research Report RR 1175-36, 25 February 1960.

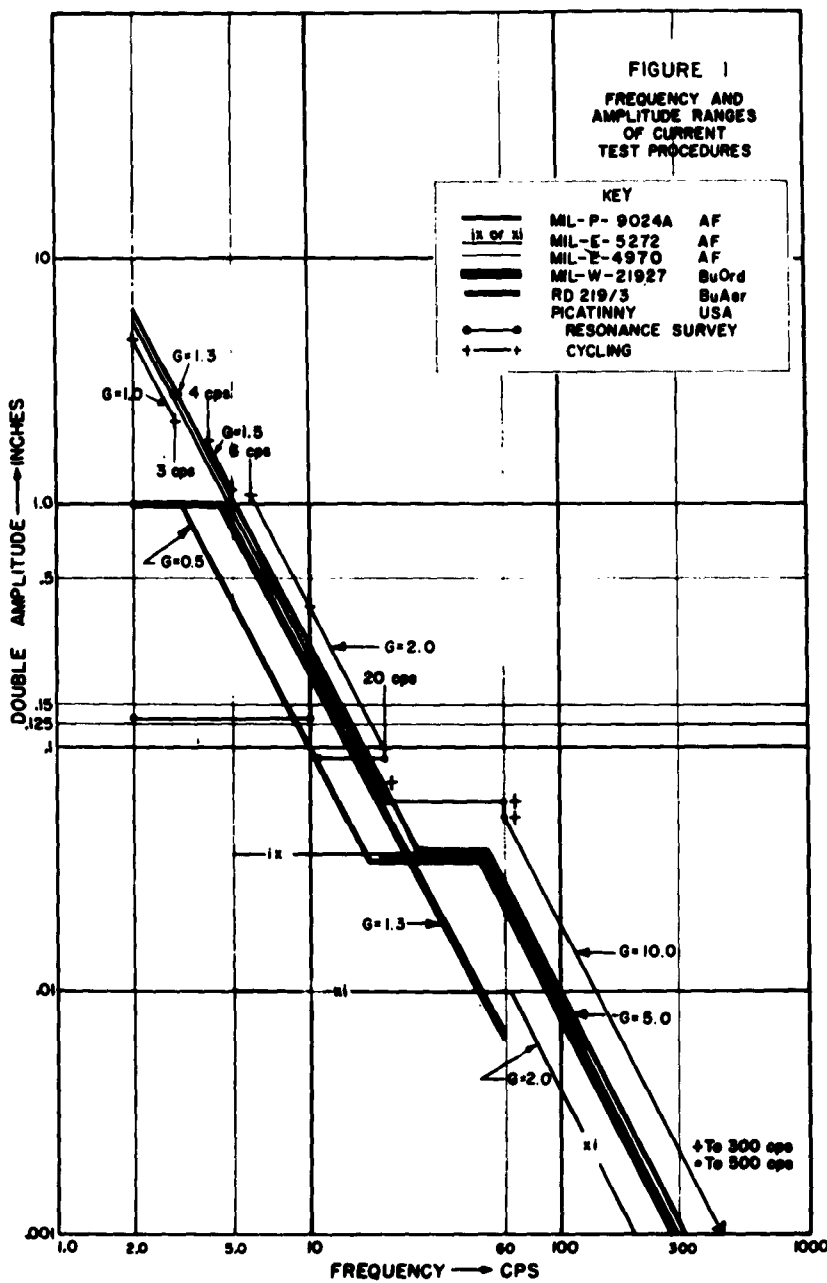


Fig. 1 - Frequency and amplitude ranges
of current test procedures

Note that the motion may be complex, requiring vector notation to describe the components.

If the input acceleration spectral density is not reasonably flat near the natural

frequency, as is to be expected where, say, rail car spring natural frequency is a predominant forcing frequency, then S_1 is a variable during integration of Eq. (1). A suitable normalizing function is

$$S_1 = \frac{B^2 \omega^2 / \omega_1^2}{[1 - \omega^2 / \omega_1^2] + B^2 \omega^2 / \omega_1^2} \quad (3)$$

Where

B = bandwidth of S_2

S_2 = acceleration spectral density at ω_1 .

Substituting Eqs. (2) and (3) into Eq. (1) and performing the indicated straightforward, albeit tedious, integration, we have

$$\sigma_1^2 = \frac{S_2}{8\omega_1^3 \zeta \left[1 + \frac{2\zeta}{B} \right]} \quad (4)$$

Should S_1 be reasonably flat in the region of ω_1 , than

$$\sigma_1^2 \approx \frac{S_1}{8\omega_1^3 \zeta} \quad (5)$$

EQUIVALENT STEADY STATE MOTIONS

If, in test, a sinusoidal motion is applied, the mean square response (σ_2^2) to this motion is

$$\sigma_2^2 = \frac{1}{8\zeta^2} X_2^2 \quad (6)$$

Where X_2 = the input amplitude in test.

Equivalence could then be written by equating σ_1 and σ_2 , and solving for X_2^2 . Thus

$$X_2^2 = \frac{\zeta S_2}{\omega_1^3 \left[1 + \frac{2\zeta}{B} \right]} \quad (7)$$

In this test motion, the power dissipated and heat generated in the package would substantially equal that in service, but distribution of amplitudes would differ. If the service amplitude is a Rayleigh distribution, then X (which is $\sqrt{2}$ times the rms value of service amplitudes) would be exceeded 40 percent of the time; twice X would be exceeded 1 percent of the time.

Since it may be these excess amplitudes that cause damage or mount failure, Eq. (7) was rejected as not being a proper statement of equivalence.

We concentrated, therefore, on developing an expression for producing the same effect in

test on the mounting system as does the service environment. This step converts the test to a measurement of mount reliability. Without mount reliability, all other measures of mounting performance are useless.

Failure in a vibratory environment is closely related to fatigue. Using Miner's [2] or Palmgren's [3] linear cumulative fatigue hypotheses* permits us to express life expenditure with time (E_1) as

$$E_1 = \int \frac{dn}{N} \quad (8)$$

Where

N = number of cycles to failure at an amplitude x_1 .

The number of occurrences per unit time for which the peak value (x_1) is between x_1 and $x_1 + \Delta x_1$ is [6]:

$$dn = \frac{\omega_1 t_1}{2\pi} \frac{x_1}{\sigma_1^2} e^{-\frac{x_1^2}{2\sigma_1^2}} dx_1 \quad (9)$$

Where t_1 = time in service.

Miles [7] has suggested that fatigue S-N curves can be quite validly plotted as a log-log relationship. Thus

$$\log x_1 = \log a - b \log N$$

from which

$$\frac{1}{N} = \left[\frac{x_1}{a} \right]^{1/b} \quad (10)$$

Where a = constant

b = slope of the S-N curve.

Substituting Eqs. (9) and (10) into Eq. (8) and letting the endurance limit motion (x_3) be characterized by $x_3 = 2\sigma_1^2 K$, we have

$$E_1 = \frac{\omega_1 t_1}{2\pi a}^{1/b} \int_x^{\infty} x_1^{\frac{b+1}{b}} e^{-\frac{x_1^2}{2\sigma_1^2}} dx_1 \quad (11)$$

*The Corten-Dolan [4] nonlinear hypothesis does not necessarily negate what follows. See, for example, the same fatigue life using either hypothesis found by Mains [5].

Introducing the notation $\rho^2 = (x_1^2)/(2\sigma_1^2)$, and its corollaries, Eq. (11) becomes

$$E_1 = \frac{\omega_1 t_1}{\pi} \left[\frac{2\sigma_1}{a} \right]^{1/b} \int_k^\infty \rho^{\frac{b+1}{b}} e^{-\rho^2} d\rho. \quad (12)$$

The integral is an incomplete Gamma function in ρ^2 . The solution to Eq. (12), therefore, is

$$E_1 = \frac{\omega_1 t_1}{2\pi} \left[\frac{2\sigma_1}{a} \right]^{1/b} \Gamma(1 + 1/2b) \left[1 - \frac{\gamma\left(\frac{1}{1+2b}, K\right)}{\Gamma(1+1/b)} \right]. \quad (13)$$

The life expenditure function (E_2) in a sinusoidal vibration test of a suspension exhibiting a log-log S-N curve may be written as

$$E_2 = \frac{\omega_1 t_2}{2\pi} \left[\frac{x_2}{a} \right]^{1/b} \quad (14)$$

Where

t_2 = test time

x_2 = response amplitude in sinusoidal test.

Equating E_1 and E_2 and solving for the ratio of test times

$$\frac{t_2}{t_1} = 2 \left[\frac{\sigma_1^2}{X_2^2} \right]^{1/2b} \Gamma(1 + 1/2b) \left[1 - \frac{\gamma\left(\frac{1}{1+2b}, K\right)}{\Gamma(1+1/b)} \right] \quad (15)$$

Miles [7] has also suggested that, in most practical situations, the endurance limit is ill-defined or even nonexistent. Under such circumstances, the incomplete Gamma function contribution may be safely ignored and Eq. (15) reduced to

$$\frac{t_2}{t_1} = \left[\frac{2\sigma_1^2}{X_2^2} \right]^{1/2b} \Gamma(1 + 1/2b). \quad (16)$$

These functions are defined only by the values of σ_1^2 from Eq. (4) or (5), X_2^2 , the slope of the S-N curve and the value of the endurance limit if it exists. Suitable values for the complete and incomplete Gamma functions with $n = 1/2b$ can be taken from the literature [8, 9]. Equation (16) is plotted as Fig. 2.

It is interesting to compare the effects of varying sinusoidal test amplitudes on test times. For a specific design (assuming that the service environment being simulated is unchanged), σ_1 , b , and K are constants. Thus we may write

$$\frac{t_2'}{t_2''} = \left[\frac{X_2''}{X_2'} \right]^{1/b} = \left[\frac{X_t''}{X_t'} \right]^{1/b}. \quad (17)$$

Where

t_2' = a sinusoidal test time

t_2'' = another sinusoidal test time

X_2' = response amplitude at t_2'

X_2'' = response amplitude at t_2''

X_t' = input test amplitude at t_2'

X_t'' = input test amplitude at t_2'' .

This equation holds only when the peak values of the response motions are less than the one-time-failure stress motion and more than the endurance-limit motion.

Thus, we have shown that suspension fatigue in service can be quantitatively duplicated by a laboratory sinusoidal test motion, provided we have information concerning S_2 , B , and t_1 from the environment and b , $S \omega_1$, and k from the mounting system characteristics.

We have shown also that the time of test can be varied provided that there be concomitant variation of test amplitudes within limits. It follows, therefore, as is graphed in Fig. 2, that suspension fatigue is evaluated most rapidly with the maximum response amplitude, i.e., at the lowest "resonant" frequency. It also follows that vibration at this frequency is sufficient to evaluate suspension reliability.

Thus, even in the absence of quantitative data concerning the environment, it is possible to simplify some of the confusion of Fig. 1, with reasonable confidence in the test significance.

PROPOSAL FOR A STANDARD VIBRATION TEST

To specify a sinusoidal resonance test, it is necessary to prescribe:

- The test input amplitudes considered acceptable
- The frequency range in which resonance will be sought
- In the absence of field data, the time of the test.

We will take up these problems in turn.

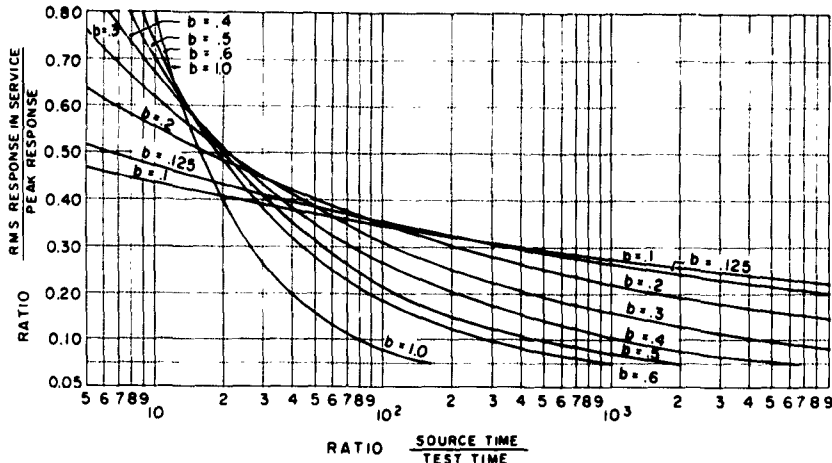


Fig. 2 - Effect of varying amplitudes on test time

Test Amplitudes

Because of the interrelation between test amplitude and time, we consider amplitude to be a target optimum.

We have defined target optimum as the largest amplitude that can be practically achieved by shaker devices generally available. We cannot justify construction of extremely expensive contraptions unless and until they are clearly needed on the basis of quantitative evidence.

Figures 3 through 8 present the results of a survey of vibrator capacities for several gross weights. While we fully realize that you can always use a heavy-duty machine for a light load, with some exceptions two things are clear from the figure. One, it is not generally feasible to achieve total excursions greater than one inch. Two, there is considerable difficulty in guaranteeing ability to produce any input acceleration amplitudes in excess of 1g for heavy weights.

The major exceptions are noted in Fig. 8. To the best of our knowledge, there is one facility on the West Coast and one on the East Coast now capable of high g and very low-frequency testing.

We feel quite strongly that this is insufficient capacity to support the volume of testing actually required. We have, therefore, recommended that the government's target requirements for amplitude be:

- 1 inch total excursion to 4.5 cps
- 1 g acceleration above 4.5 cps.

Frequency Range

Such data as are available indicate that input frequency range varies from around 2 cps to more than 10,000 cps. It is not, however, necessary to search for lowest suspension resonance throughout this range. Most specialty containers, such as for missiles, engines, transmissions and the like must also pass a reasonably severe drop test while holding accelerations to modest values. Figure 9 shows the results of such a design requirement on natural frequency of linear systems. From this curve, it is reasonable to conclude that input frequencies in test very rarely need to exceed 60 cps. As a practical matter, further, it should be noted that amplitude of 0.003 inch at 60 cps has an equivalent acceleration of 1.3 g. Such amplitudes would probably be damped out in almost any simple structure, such as a layer of corrugated fibreboard. Many test engineers feel that high-frequency testing evaluates the testing fixture more than it does the container suspension.

The combination of frequencies and amplitudes recommended is shown in Fig. 10.

Test Time

The theoretical derivation discloses no basis for recommending test time in the absence of valid field data. Many commercial containers have, however, been tested under the procedures of the National Safe Transit Committee in a condition approaching resonance at 1-inch double amplitude. Test time was one hour. It is unreasonable to expect military containers to do less.

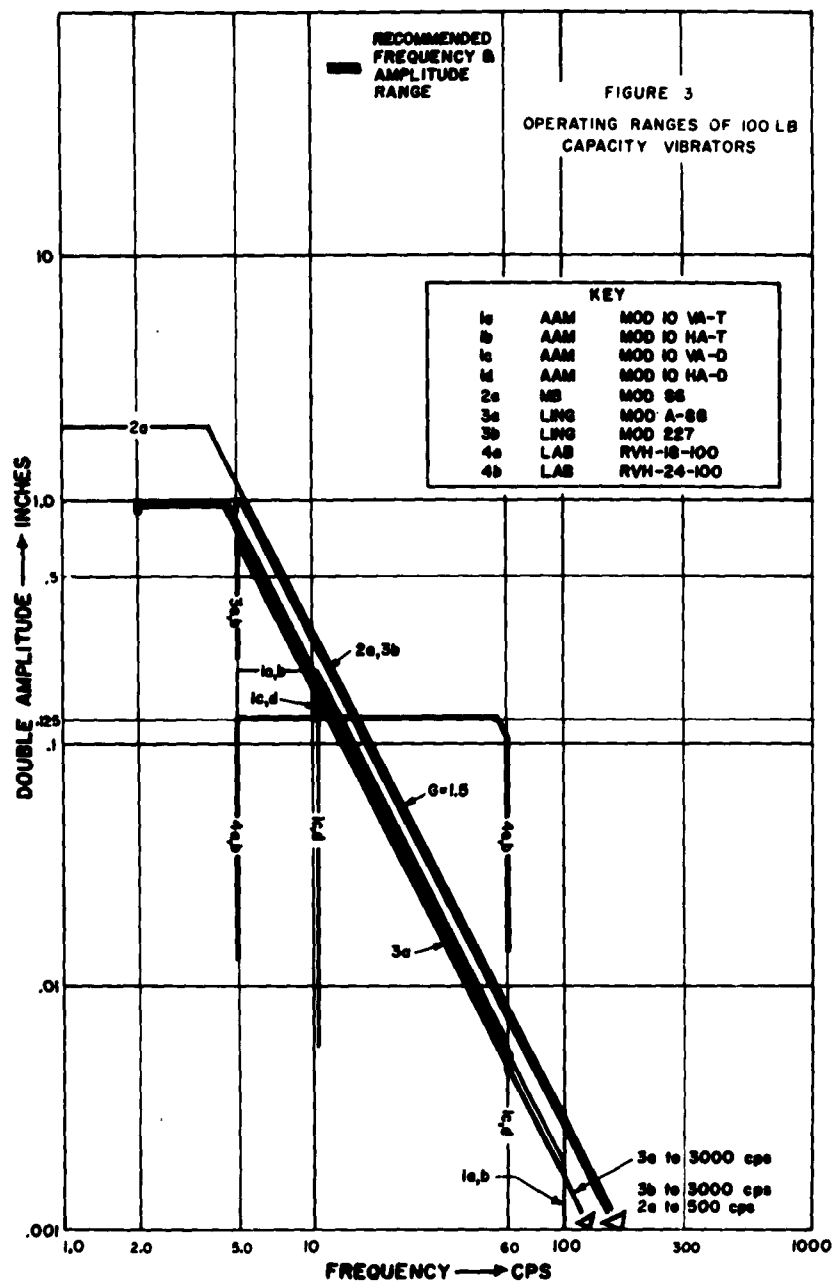


Fig. 3 - Operating ranges of 100-pound capacity vibrators

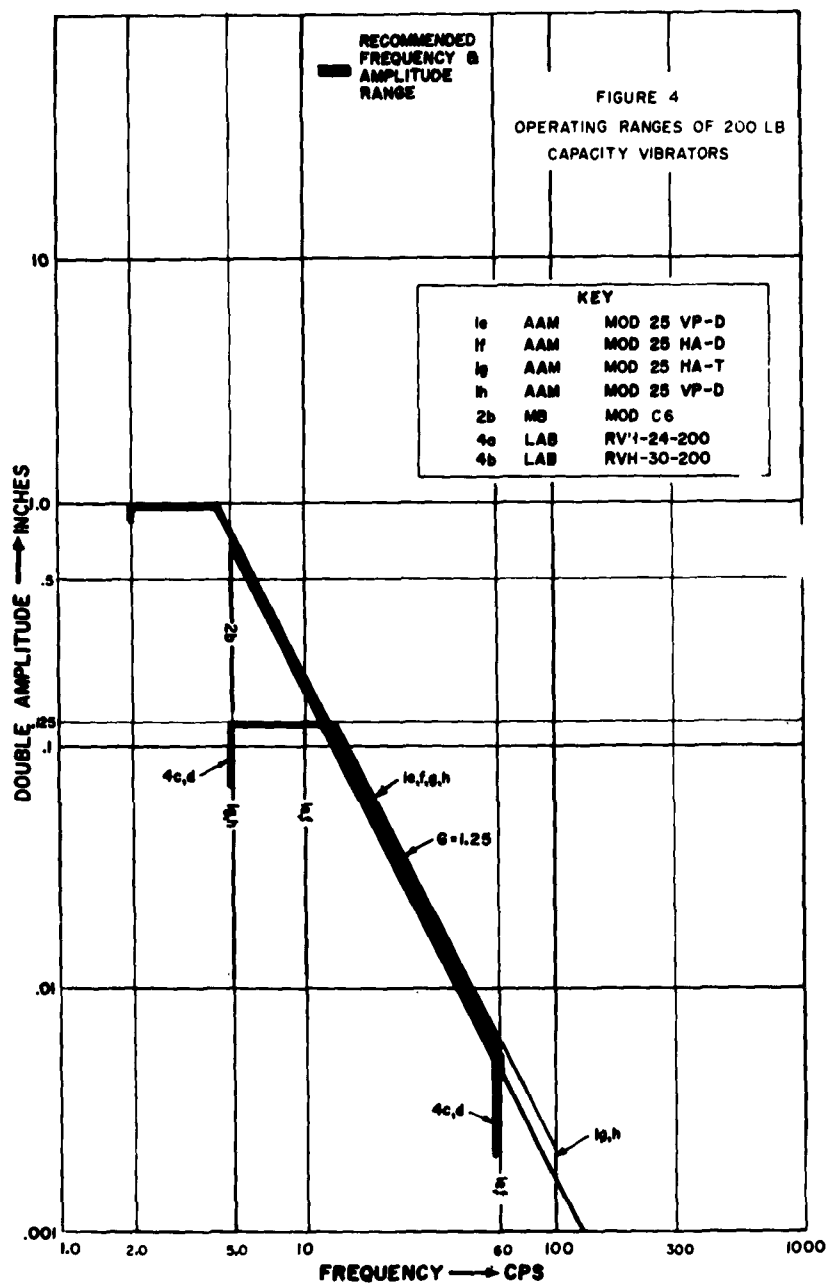


Fig. 4 - Operating ranges of 200-pound capacity vibrators

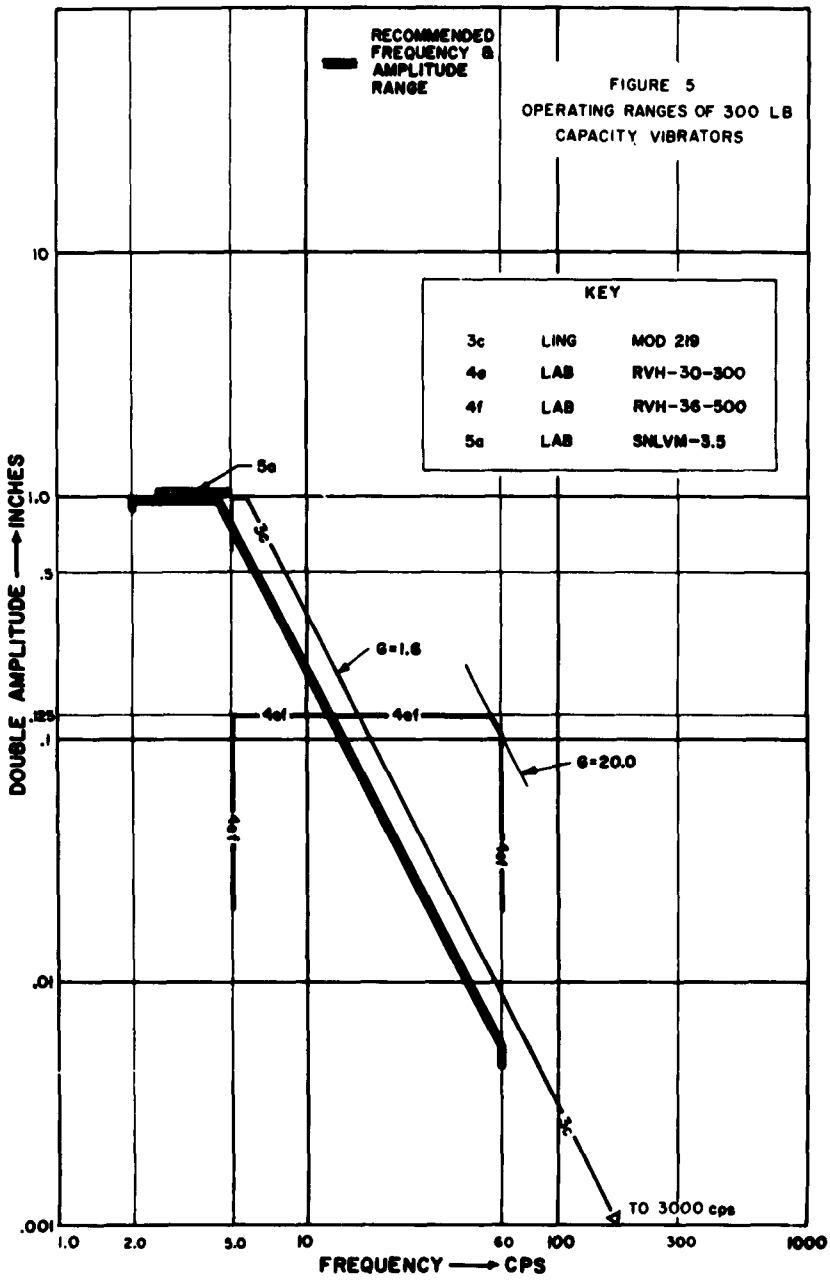


Fig. 5 - Operating ranges of 300-pound capacity vibrators

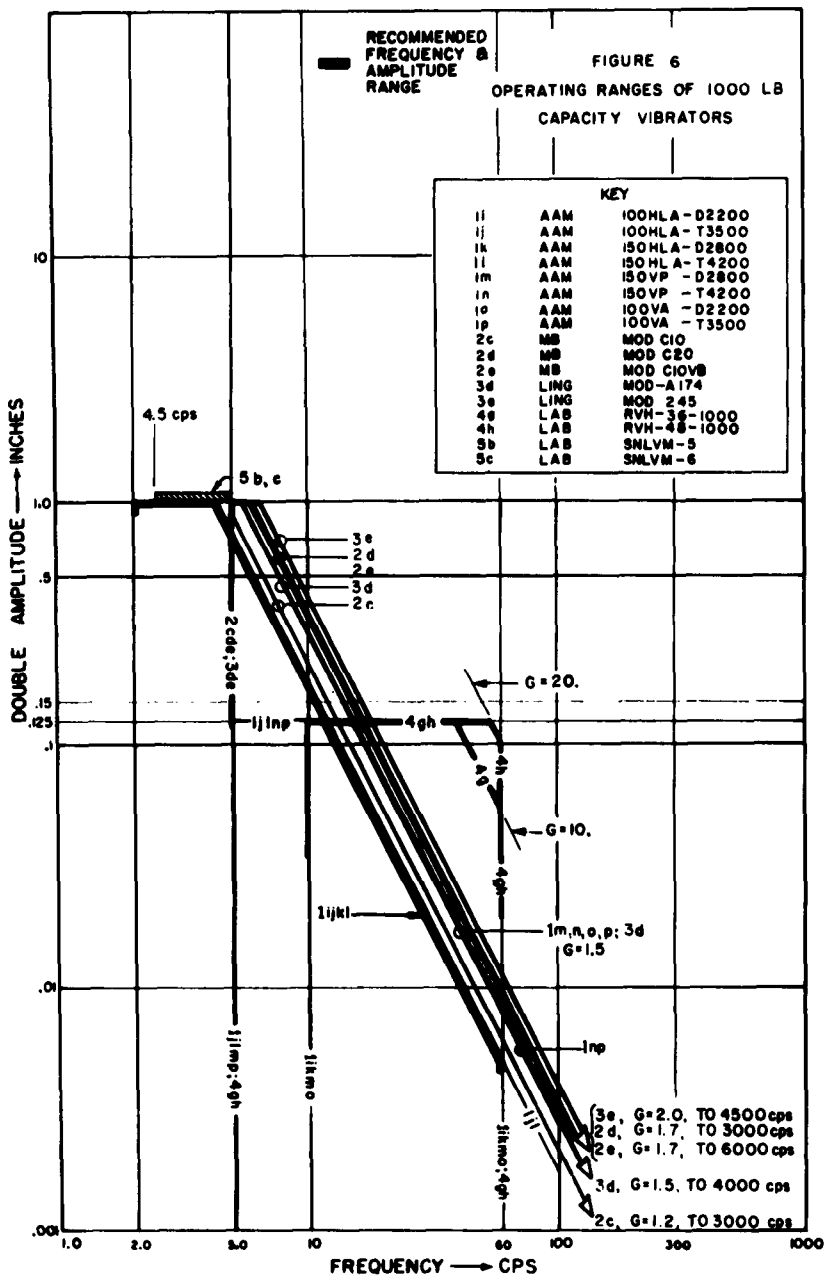


Fig. 6 - Operating ranges of 1000-pound capacity vibrators

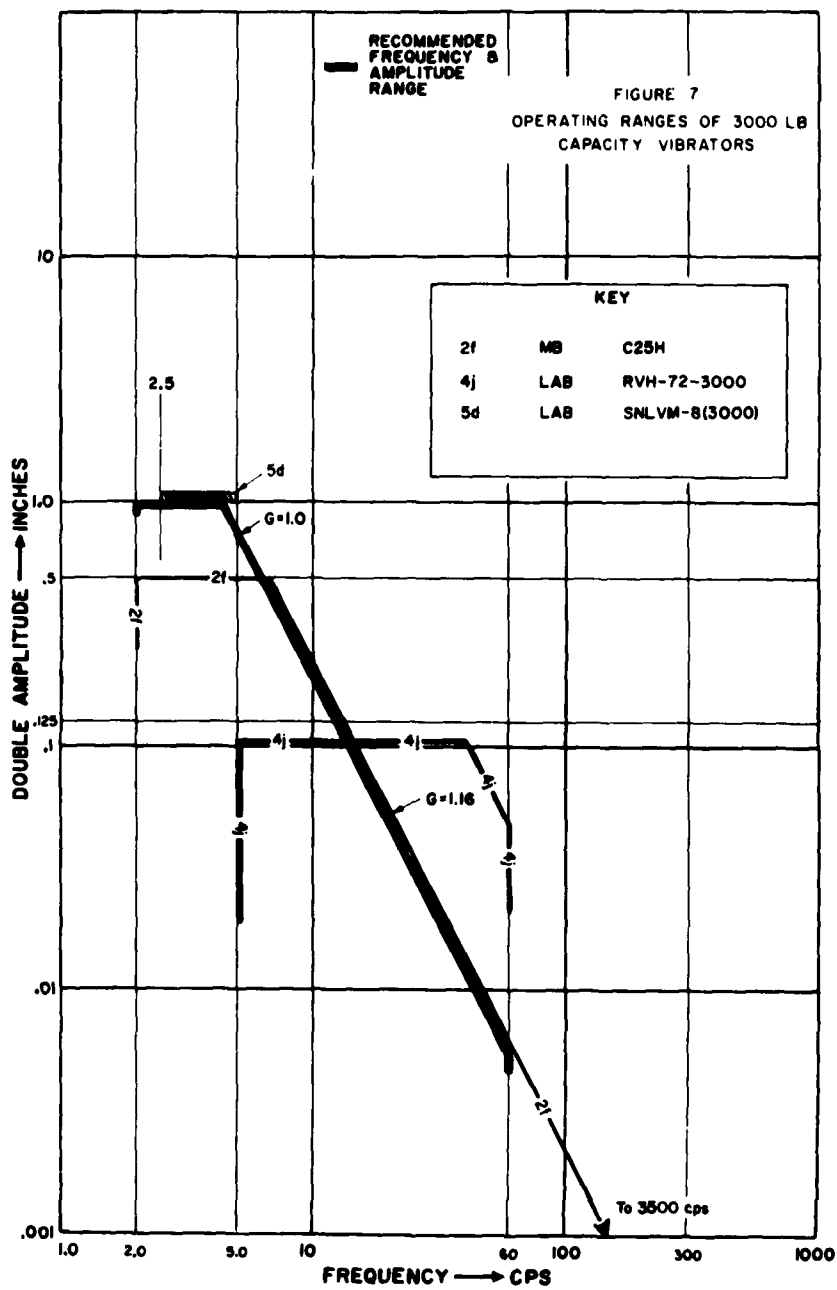


Fig. 7 - Operating ranges of 3000-pound capacity vibrators

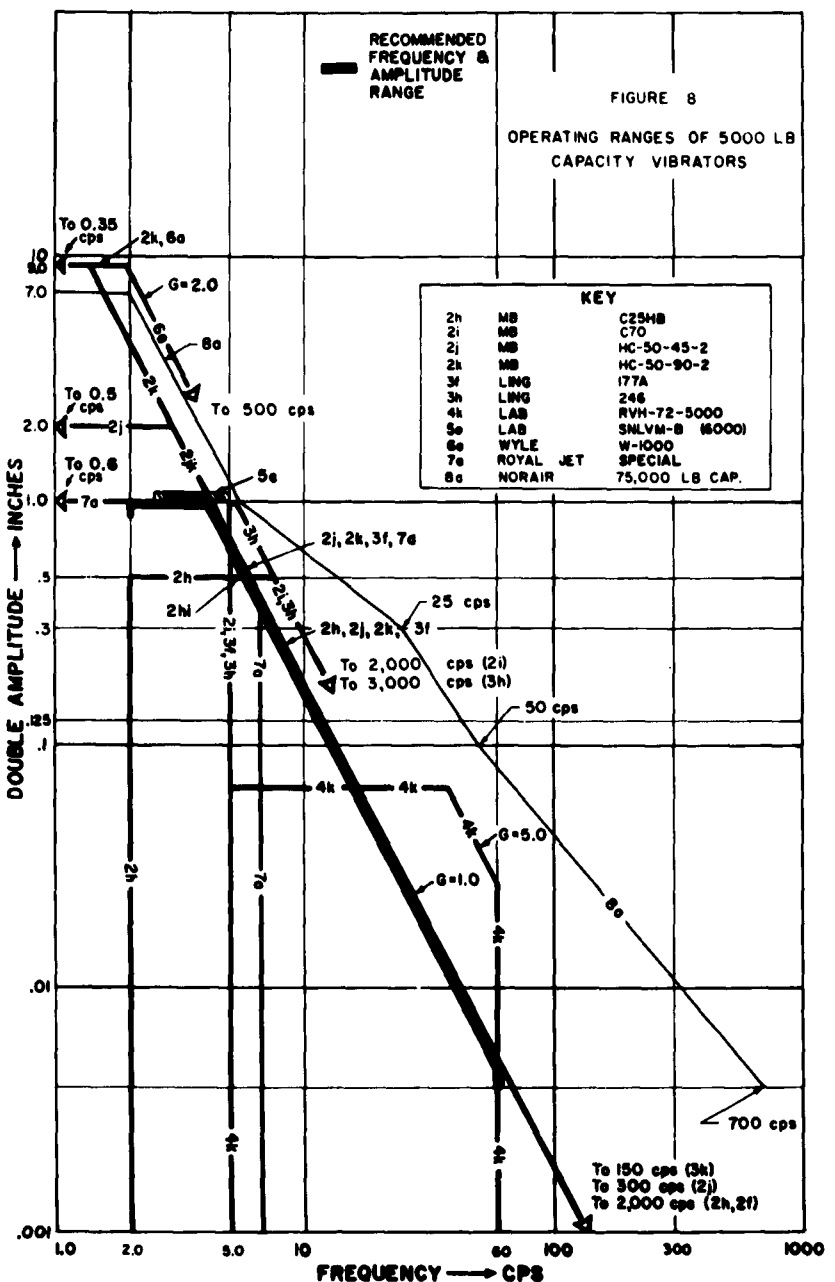


Fig. 8 - Operating ranges of 5000-pound capacity vibrators

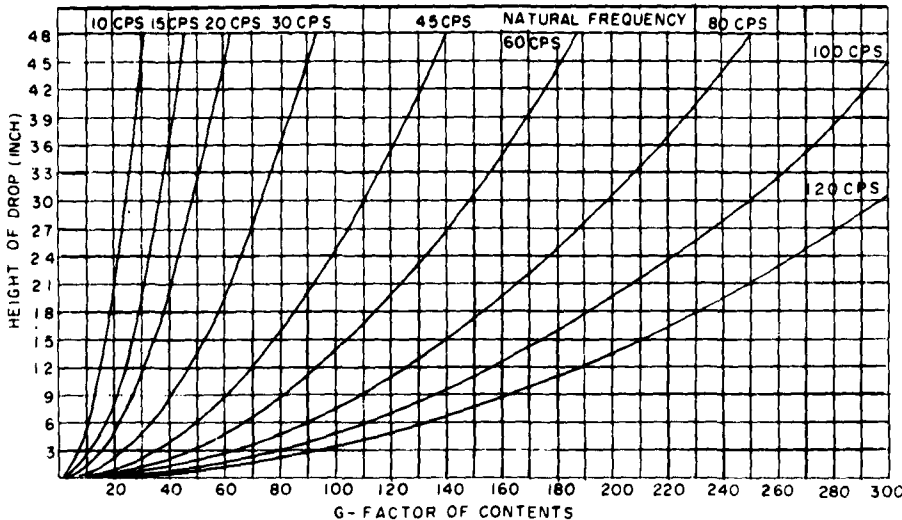


Fig. 9 - Relation of G-factor, height of drop and translational uncoupled natural frequency

Accordingly, we have recommended that the standard time at the standard amplitude be 1 hour. Equation (17) shows that allowing test time variation with amplitude variation is desirable. Figure 11 shows that this practice is mandatory if testing of odd sizes is to proceed.

One means of permitting variation in time and amplitude is to state that total work must remain constant. Since work for a given sine wave cycle is conveniently measured by the mean square amplitude, we find that total work is the same when the ratio of test times is inversely proportional to the mean square amplitudes, or

$$\frac{t'_2}{t'_1} = \left[\frac{\sigma''_2}{\sigma''_1} \right]^2 = \left[\frac{x''_2}{x''_1} \right]^2 = \left[\frac{x_t''_2}{x_t''_1} \right]^2 \quad (18)$$

Equation (18) is plotted in Fig. 12. This curve is a part of our recommendations. Technically speaking, it permits use of high capacity machines, if available, and on the other hand, permits consistent solution of problems engendered by the situations cartooned in Fig. 11.

Equation (18) is obviously, directly parallel to Eq. (17) though setting $b = 0.5$.

DISCUSSION

We concede that there are deficiencies in the approach taken and the solutions advocated herein. To moderate criticism a trifle, we will now discuss some of the more obvious difficulties.

Theory Lacks Experimental Verification

Agreed. We hunted high and low for data to plug into our equations as a test of their practical value. Perhaps as a result of not hunting in the right places, but only perhaps, we did not find any. We already have made, and now make again, strong recommendations for collecting data in usable form. It is quite possible that our theory will be disproved. We will abandon our theory as soon as a replacement founded upon data is available.

A Vibration Isolator is Supposed to Protect the Item

Yet, it is. But against what? There are a host of environmental specifications the item designer is supposed to meet. When a "shotgun-type" container specification is used, we are saying, in effect, that the shipping container still must correct all item design deficiencies. We have rejected this attitude in favor of promoting a test intended to evaluate the one criterion common to all containers, suspension reliability.

We see no logical objection to expanding the vibration test syllabus in specific cases to see what happens at specific frequencies, provided this be done after the reliability of the suspension is established and, further, provided the container designer has some fair warning that particular frequencies would be harmful.

FIGURE 10

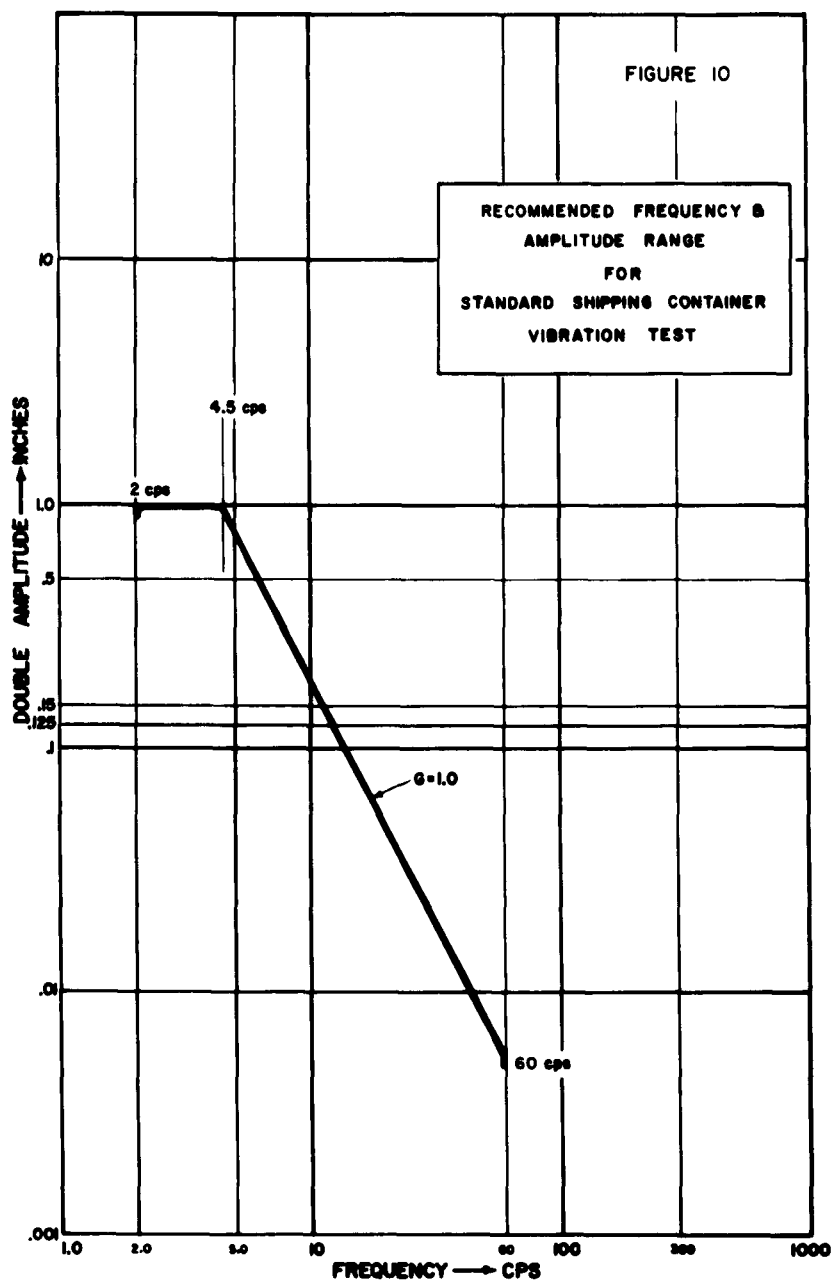
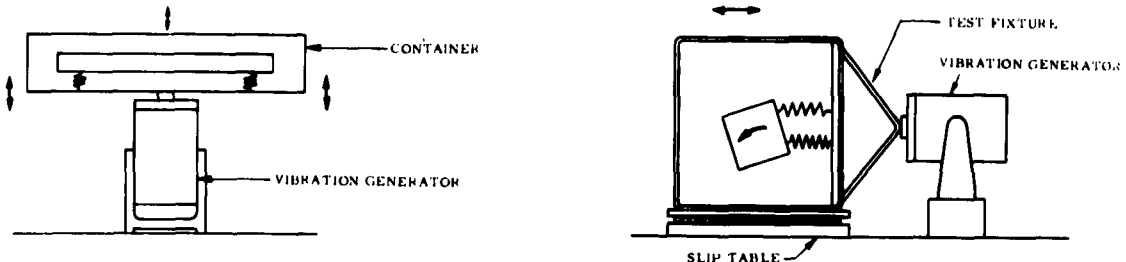
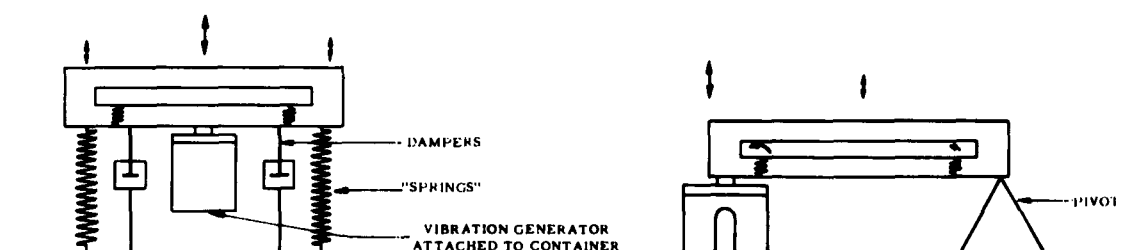


Fig. 10 - Recommended frequency and amplitude range for standard shipping container vibration test



A. BAD OVERHANG. END MOTION GREATER THAN CENTER. VERY SEVERE ON CONTAINER. IF CONTAINER MOTION AT ITEM MOUNT LOCATIONS SAME AS STIPULATED, COULD BE ROUGHLY EQUIVALENT TO SPECIFICATION.

B. CONTAINER TOO HEAVY. TEST ON SIDE. CONTAINER MOTION CAN BE HELD TO REQUIRED VALUES IF FIXTURE IS PROPERLY DESIGNED (SOMETIMES EXPENSIVE). MAJOR DISADVANTAGE IS PRODUCTION OF UNDESIRED ROTATIONAL MODE IN MOUNT SYSTEM.



CONTAINER TOO HEAVY OR TOO LONG. RESONANT BEAM TEST. CONTAINER IS USED AS BEAM OR SOMETIMES BEAM IS UNDERNEATH. RESONANT FREQUENCY MUST BE FOUND FIRST AND THEN SPRINGS AND DAMPERS MUST BE DESIGNED TO PRODUCE REQUIRED MOTION. MOTION AT GENERATOR IS GREATER THAN AT ENDS BECAUSE OF BEAM DEFLECTIONS.

D. MODIFIED RESONANT BEAM. DOUBLES CAPACITY OF ANY MACHINE. MOTION AT CENTER ONLY 1/2 MOTION AT MOVING END. THE MOUNT INPUT MOTIONS ARE PROPORTIONAL TO SPACING. AS A MINIMUM, SWAP ENDS HALFWAY THROUGH TESTS. TO BE ROUGHLY EQUIVALENT, MOUNT LOCATION MOTION SHOULD BE EQUAL TO SPECIFIED VALUES. NOTE. SOME ROTATIONAL COUPLING INEVITABLE.

Fig. 11 - Some variations on brute force vibration testing

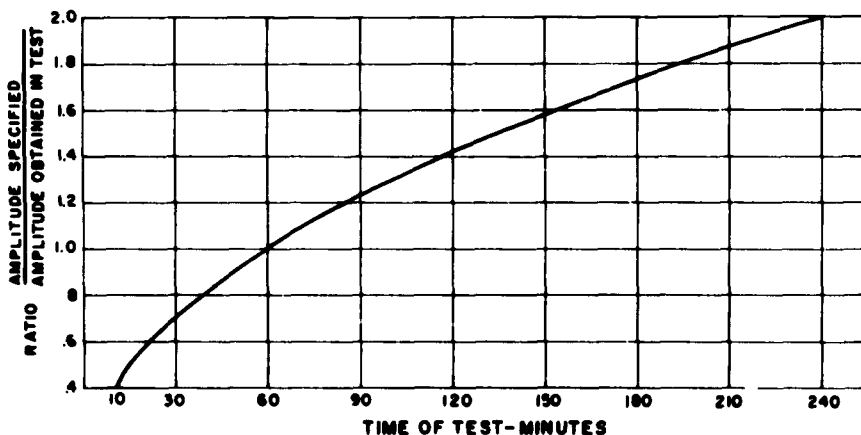


Fig. 12 - Suggested time of test at amplitudes differing from those given in Fig. 10

Low-Frequency, High-Amplitude Vibrations Do Occur in Service

We agree that they do. We do not agree, however, that we must test at these high amplitudes until a statistical measure of these occurrences is established that demonstrates necessity. With reasonable control of system damping, item accelerations and excursions in the environment will always be less than those encountered in drop test. Hence, the test at high amplitudes evaluates system fatigue characteristics. Our theory indicates that it is possible to perform this latter function at lower test amplitudes.

Four-Hour Testing at Low Amplitudes May Not Be Above the Endurance Limit and, is, Therefore, Meaningless

Quite so. We have recommended separately that work be initiated to establish the existence

of endurance limits in container suspensions and to find out what values these limits might have. In the meantime, however, we submit that controlled deviation is better than uncontrolled. Careful reading of several of the applicable specifications will indicate that, in spite of the fancy charts, completely uncontrolled deviation in amplitude is explicitly authorized and without a compensating time increase.

In the final analysis, we have developed a theoretical statement of equivalence between random shipping environment and a sinusoidal laboratory test. We have then proposed a practical test consistent with this statement. We have then proposed a practical test consistent with this statement. We submit our offering as an improvement over Fig. 1 and seek cooperation in finding experimental evidence leading to even greater improvement.

REFERENCES

- [1] Crandall, S. H., et al, "Notes for the M.I.T. Special Summer Program on Random Vibration," Technology Press, Cambridge, Massachusetts, 1958.
- [2] Miner, M. A., J. Appl. Mech., 12, A159, 1945.
- [3] Palmgren, A., Z. Verein Deuts. Ing., 68, 339, 1924.
- [4] Corten, H. A., and Dolan, T. J., Intl. Conf. on Fatigue of Metals, Session 3, Paper 2, IME and ASME, Sept. 1956.
- [5] Mains, R. M., S and V Bull No. 25, Part II, p. 236, Dec. 1957.
- [6] Crandall, et al, op. cit., p. 4-12.
- [7] Miles, J. W., J. Aero. Sci., 21, 758, 1954.
- [8] Pearson, K., "Tables of the Incomplete Gamma Function" H. M. Stationery Office, London, 1922, (Reissue 1934, Biometrika Office, University College, London).
- [9] Jahnke, E. and Emde, F. "Tables of Functions with Formulae and Curves," 4th ed., pp. 12-17, Dover Publications, New York, New York.

DISCUSSION

Comment by Mr. Mustin: I think it appropriate to comment briefly on my reaction to Mr. Welton's paper. In the main, I don't find any really basic inconsistency between his proposal and mine, except that he is talking in terms of a 30-minute test time in lieu of an hour on his lower curve and on his more severe curve he is asking us to test at 1.3 g's. At the risk of being

thought slightly facetious, I would say he's got the contraption that can do this. Also, he seems, at least from reading his written paper, to be having two rather arbitrarily derived test syllabi. He may be correct; I do not know. I'm only offering one arbitrary solution rather than two.

Mr. O'Hara (NRL): I have two short questions. Those equations you had, were they for linear packaging materials and systems? Also, in the limited amount of data that you did have, did you take into account structural interaction impedance effects?

Mr. Mustin: Yes, very definitely we did assume linearity and the work should be extended to a nonlinear system. To be quite honest about it, I found the mathematics hairy enough on linear systems and quit while I was ahead. As to your second question, we did not consider that. I'm not sure I even know how to handle it. We worked primarily on relative motion response starting out from the random vibration discussions in Crandall's excellent symposium up at M.I.T.

Mr. O'Hearne (Martin Co.): It strikes me that the peak input spectrum at the resonant frequency of the package which you had labeled as general is really a rather special case. The relatively flat spectrum is more general, at least in the absence of any specific knowledge on the nature of your input spectra. This certainly has implications on when you go to use cumulative damage hypotheses because of the difference in the distribution of the peaks in your output.

Mr. Mustin: In effect, what I'm being accused of is assuming that the acceleration spectral density curve would be peaked in the neighborhood of the natural frequency of the suspension system. The charge really is that this is a special case and that it's at least equally likely that the curve would have a valley in this neighborhood, or that it is equally likely perhaps that it could be flat. I can only plead guilty to this charge. If you can come up

with a better expression of rms response than the one we came up with then the rest of the derivation of equivalence still holds. If you will recall, I had sigma one in that second set of equations as a value having been determined in some fashion from the data. The effect of it is, of course, that if the curve has a valley in this neighborhood, then your test acceleration factor is very much larger.

Mr. Goodill: I find myself somewhat in disagreement with the vibration test that you outlined. The reason for this is I think that it will unnecessarily handicap the package engineer. It will result in a much more complicated and a much more expensive suspension system than those presently used. Past history has shown that the suspension systems that are presently used, unless they are extremely soft, are very adequate to protect the equipment in the container and that there is no difficulty of the suspension system failing due to vibration.

Mr. Mustin: The same comment, I think, was made to me informally by Rip Seely, in effect saying that he didn't believe that we need to be worried about a fatigue function in suspension systems. I replied that I had had two unfortunate experiences with shipping mount failures, one occurring many years ago, when I was in the Bureau of Aeronautics, on an aircraft engine container. To my knowledge nobody has repeated that particular mistake in the aircraft engine container program. The other one was far more intimately concerned with me in that I butchered the design of a mounting system and had these failures occur. Gentlemen, the cat that has once sat on a hot stove is not going to sit on a cold one.

SOME SHOCK SPECTRA COMPARISONS BETWEEN THE ATMX 600 SERIES RAILROAD CARS AND A RAILROAD SWITCHING SHOCK TEST FACILITY

R. H. Rector
Sandia Corporation
Albuquerque, New Mexico

Railcar accelerations were measured during switching operations when impacted into three stationary gravel-loaded stopper cars with their brakes on at varying impact speeds. The shock spectra of these measurements are compared to the spectra of the Sandia Test Ramp Facility. A discussion is given on how this information can be applied by designers and test engineers.

INTRODUCTION

Several years ago, Sandia Corporation designed a test facility to simulate shock sustained by Sandia designed equipment during railroad switching operations [1]. This test facility was designed by using for environmental criteria the shock data obtained from actual railroad switching of a standard freight car under various controlled conditions. Since that time, ATMX 600 Series cars have been designed and are now in use by the railroad. The ATMX car uses a Miner RF-333 draft gear which imposes a different shock condition (thus different structural response) from the standard freight car. Therefore, additional shock data are required if railroad switching operations in this type of car are to be simulated.

The object of this study is to obtain shock data which will enable the ramp test facility to simulate more easily and more closely the actual railroad switching operations encountered by ATMX cars. Acceleration signatures and shock spectra of the dynamic response of ATMX 600 Series railroad cars during controlled switching operations were determined for one specific condition (explained in the procedure). This study is based on the comparison of shock spectra of the ATMX car with shock spectra of the Sandia Corporation Engineering Test Ramp Facility. Shock spectra are given here in the longitudinal direction only, since this is the direction of primary interest. Also, an investigation of shock spectra in the ver-

tical and lateral directions revealed negligible values for the natural frequencies of interest (12.5 cps and under).

TEST PROCEDURE

ATMX Car #613 Test

The entire series of switching shock tests was run by impacting an instrumented ATMX car into three stationary gravel-loaded gondola cars with their brakes set. The total weight of the gravel-loaded cars was approximately 480,000 pounds. The weight of the ATMX car was approximately 128,000 pounds which included an 8000-pound weight bolted to the floor. The natural frequency of this system was between 1 and 2 cps. The test setup is shown in Fig. 1. Impact tests were made in the following manner. The instrumented ATMX car was accelerated by a small engine to the desired velocity which was read on a speedometer in the engine cab. At a predetermined location (29 feet from the impact point), brakes were applied to the engine, and the ATMX car was allowed to roll into the stationary gravel-loaded cars. The impact velocity was measured 6 feet from impact by the time required for the front wheel of the ATMX car to make the contacts of two microswitches which were 1 foot apart. The time was read immediately on a Beckman/Berkeley counter-timer. Tests were made with impact velocities varying from 3.7 mph to 12.0 mph. The ATMX car was instrumented on the

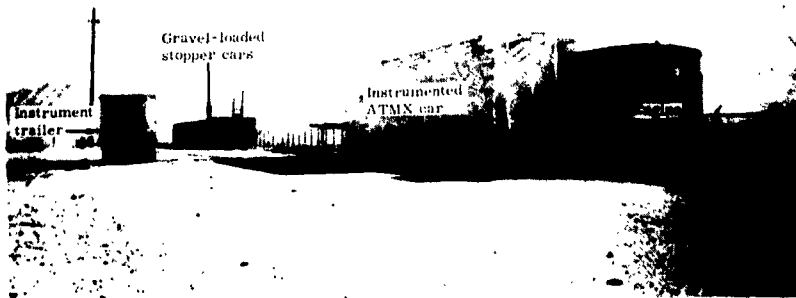


Fig. 1 - ATMX Car setup

center of the car floor with a Statham Model A8A accelerometer. Other test equipment consisted of a Miller carrier amplifier system and a CEC oscillograph recorder with 1000-cps galvanometers.

Engineering Ramp Facility Test

Test ramp acceleration signatures were obtained by impacting the empty ramp cart into short lead cylinders mounted on a fixed bumper.

The lead cylinders were 6 inches in diameter and 4-1/4 or 4-1/2 inches long. The last 1/4 or 1/2 inch of length of the cylinder was cone shaped to help achieve a desired pulse. The ramp cart was raised up the inclined ramp (Fig. 2) to a predetermined height necessary to achieve the desired impact velocity. The cart was set in motion by a quick release and allowed to roll into the bumper material which was mounted on the fixed bumper. The impact velocity for this facility was measured in the

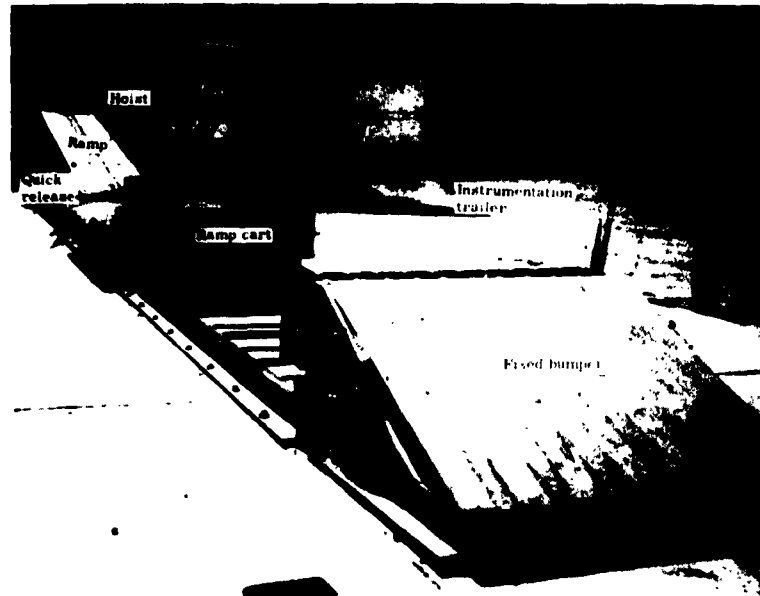


Fig. 2 - Ramp test facility

same manner as explained for the ATMX car test. Tests were made at impact velocities varying from 4.7 mph to 11 mph. The ramp cart was instrumented with a Statham Model A5A accelerometer. Accelerations were read on the same type system as mentioned for that part of the study made on the ATMX car.

DATA ANALYSIS AND REDUCTION PROCEDURE

Shock spectra give the equivalent static accelerations sustained by linear, single degree-of-freedom systems with discrete natural frequencies and specified damping, as a result of being subjected to dynamic forces. The major postulation is that those systems must be considered as single degree-of-freedom systems in order that the shock spectra of the test facility may be compared with those of the ATMX car for simulation of the car's environment. The equation of motion for the mass of a simple system with specified viscous damping acted upon by a dynamic force was used to obtain equivalent static acceleration from the test data. This equation is:

$$-\frac{m\ddot{x}(y - x)}{dt^2} = \frac{cdy}{dt} + ky$$

$$Z = y - x \quad (1)$$

where

y = movement of the mass with respect to base

ky = force exerted on the spring

c = viscous damping coefficient

$\frac{cdy}{dt}$ = force caused by damping

x = movement of base

$y - x = Z$ = movement of mass in space

$$\frac{m\ddot{x}(y - x)}{dt^2} = \text{force or reaction on mass.}$$

Rearranging terms of Eq. 1 gives:

$$\frac{d^2y}{dt^2} + \frac{c}{m} \frac{dy}{dt} + \frac{k}{m} y = \frac{d^2x}{dt^2} \quad (2)$$

d^2x/dt^2 is the acceleration of the base as a result of the applied load. Assume that this acceleration causes a maximum relative displacement, y_{max} , of the mass. A static load or static acceleration (static load/mass acted upon) exists which, when applied gradually to the mass with the base fixed, will cause the same relative displacement of the mass as the dynamic load. This static acceleration $(k/m)y$ is then equal to A_{st} , since under static conditions $d^2y/dt^2 = 0$ and $dy/dt = 0$, and is known as an equivalent static acceleration.

When a transient acceleration d^2x/dt^2 is applied to the base, a maximum value of $(k/m)y$ will exist. This represents the maximum dynamic response of the mass to the applied acceleration and is the equivalent static acceleration sustained by the mass.

Since this system is a linear, single degree-of-freedom system, vibrations will be excited in simple harmonic motion with a resonant frequency of vibration, w_n , with the amplitude of vibration limited by a damping coefficient, α . If the damping factor, α , is small then the following relationship holds: $w \approx w_n = \sqrt{k/m}$, $\alpha = c/c_c < 0.1$. The critical damping coefficient $c_c = 2w_n m$, and w_n = natural frequency. Substituting in Eq. 2:

$$\frac{d^2y}{dt^2} + 2\alpha w_n \frac{dy}{dt} + w_n^2 y = \frac{d^2x}{dt^2} = F(t). \quad (3)$$

$w_n^2 y = (k/m) y$ and is the term to be solved for in Eq. 3 in order to determine the equivalent static acceleration (or maximum dynamic response) for a given linear single degree-of-freedom to the transient $F(t)$.

$w_n^2 y$ is solved by developing an equation (using Laplace transforms) which can be solved in the IBM 704 computer. Equation 3,

$$\frac{d^2y}{dt^2} + 2\alpha w_n \frac{dy}{dt} + w_n^2 y = F(t)$$

represents forcing a system whose unit impulse response is

$$\frac{e^{-\alpha w_n t}}{w_n \sqrt{1 - \alpha^2}} \sin w_n \sqrt{1 - \alpha^2} t$$

with the function $F(t)$. By performing a convolution involving $F(t)$ and the impulse response, the following equation is developed:

$$w_n^2 y(t) = \frac{w_n}{\sqrt{1 - \alpha^2}} \int_0^t e^{-\alpha w_n (t-\tau)} \sin w_n \sqrt{1 - \alpha^2} (t - \tau) F(\tau) d\tau.$$

This approach is discussed in many texts including Transformation Calculus and Electrical Transients by Goldman.

By factoring and separating terms:

$$\begin{aligned} w_n^2 y(t) &= \frac{w_n}{\sqrt{1 - \alpha^2}} e^{-\alpha w_n t} \left[\sin w_n \sqrt{1 - \alpha^2} t \int_0^t e^{\alpha w_n \tau} \right. \\ &\quad \cos w_n \sqrt{1 - \alpha^2} \tau F(\tau) d\tau \\ &\quad \left. - \cos w_n \sqrt{1 - \alpha^2} t \int_0^t e^{\alpha w_n \tau} \right. \\ &\quad \left. \sin w_n \sqrt{1 - \alpha^2} \tau F(\tau) d\tau \right]. \end{aligned} \quad (4)$$

In solving for $w_n^2 y$ in Eq. 4, $F(t)$ is known and is the transient acceleration applied to the base of the test item mounted on the ATMX car floor or the ramp cart. It is the dynamic response of the ATMX car floor or the ramp cart to the impact conditions. These responses were teletread from the oscillograph records obtained, and digitized for the IBM 704 computer. The shock acceleration signatures recorded in the longitudinal direction for the ATMX car at an impact velocity of 9.8 mph and for the ramp cart at an impact velocity of 4.7 mph are shown in Figs. 3 and 4, respectively. Along with this input, the computer program supplied assigned values of w_n , α , and t . Equation 4 was solved for $w_n^2 y$ with small frequency intervals with 0-percent damping, 0.5-percent damping, and 5-percent damping. The computer hunts for and tabulates the maximum values of $w_n^2 y$. The resulting maximum values were then plotted as shock spectra.

To determine the accuracy of the IBM program used, a rectangular pulse and a half sine pulse of given values were supplied to the computer. The resulting values of equivalent static

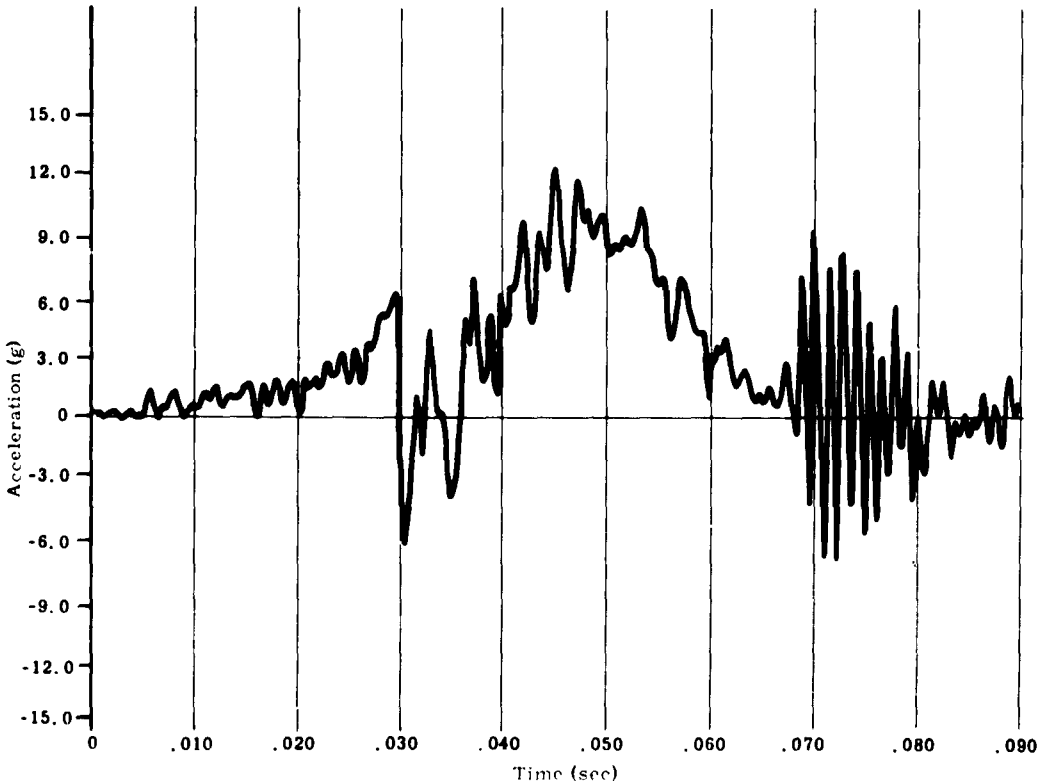


Fig. 3 - Shock signature for ATMX Car at impact velocity of 9.8 mph

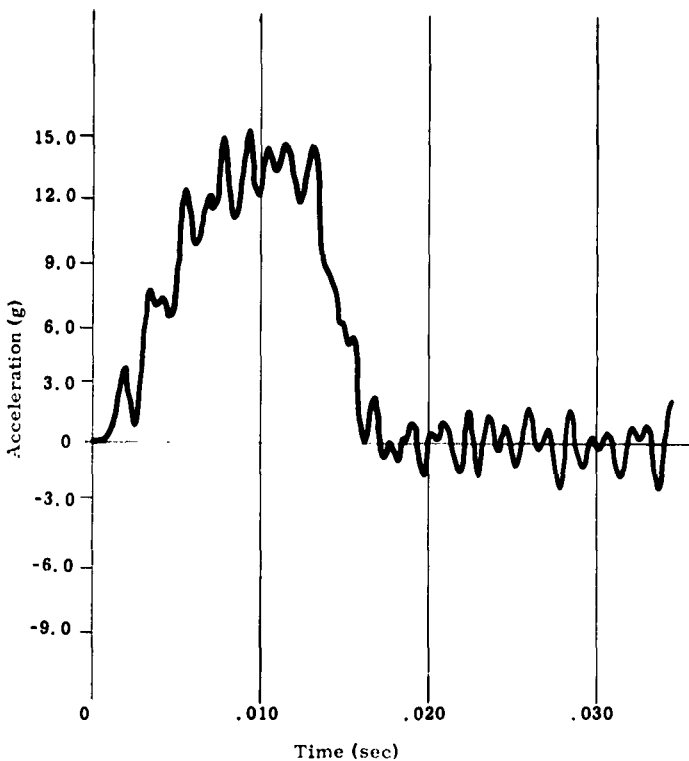


Fig. 4 - Shock signature for ramp at impact velocity of 4.7 mph

acceleration were within 1 percent of the calculated values for the frequencies of interest. It is believed that the computer results are accurate to within 4 percent for systems with natural frequencies up to 150 cps. It should be mentioned that use of this equation and program requires an acceleration input to the computer of sufficient duration to insure excitation of the low-frequency systems. In other words, should the shock pulse be short, the input should not be cut off at the end of the pulse but an input of zero should be added to the computer to insure an ample response time for the system being excited. If the pulse were too short, and the input to the computer were stopped at the end of the pulse, the resulting value of equivalent static acceleration would be smaller.

RESULTS

The longitudinal shock signature for the ATMX Car floor at an impact velocity of 9.8 mph is shown in Fig. 3. The initial portion of the pulse indicates some movement (buckling) of the cars under impact, and compression of

draft gear) prior to the major shock pulse of 40 ms duration. The logarithmic decaying portion of the dynamic response of the ATMX Car floor appears at the end of the shock pulse for each impact test. Then follows a period of some 180 ms of pulse duration of low amplitude which indicates movement of the entire mass of gravel-loaded stopper cars under impact. The amplitude for this last portion reached a maximum of 1.5-2 g. It is interesting to note that the 40 ms impulse portion of this complex waveform contains a velocity change of 5.9 mph. Movement of the entire mass of gravel-loaded stopper cars under impact spreads the velocity change of 9.8 mph over 230 ms. One cannot, therefore, describe test conditions by use of ATMX Car impact velocities alone.

The longitudinal shock signature for the ramp cart at an impact velocity of 4.7 mph (Fig. 4) shows virtually all of the velocity change under the initial pulse. Because structurally yielding impact blocks were selected for ramp tests, negligible rebound occurred and impact velocities are within 2 percent of the actual velocity changes appearing under the

shock pulses which vary from 15 to 20 ms duration.

Since it is not possible to compare accurately impact velocities between the ATMX Car and the ramp test facility for environmental test simulation, shock spectra of the motions of the ATMX Car and the ramp cart are used. Shock spectra provide an excellent method for comparing shock conditions between the ATMX Car and the ramp test facility. Shock spectra are not new and curves of the shock spectra of many types of shock machines and natural environments have been published. A shock spectrum is widely known as the maximum responses of many simple systems to a shock motion in terms of the natural frequencies of these systems. Shock spectra, the graphical representation of equivalent static acceleration

(static load) versus frequency, simply indicate the damage potential of shock motions, and are extremely useful to this extent.

It is understood that the ramp cart response may vary (as may the dynamic response of the ATMX Car floor) as the mass and natural frequency of the test weight varies. The question of the validity of using these shock spectra is based on the simplifying assumption that the mechanical impedance of the test specimen is many times smaller than the structural impedance of the railroad car or the test facility. To partially substantiate this assumption with relation to the ramp cart (at least with a test weight of 1000 pounds or less), reference to the shock spectra of a 7.0 mph impact velocity test with 1000 pounds on the cart (Fig. 5) and a 6.8 mph impact velocity test on

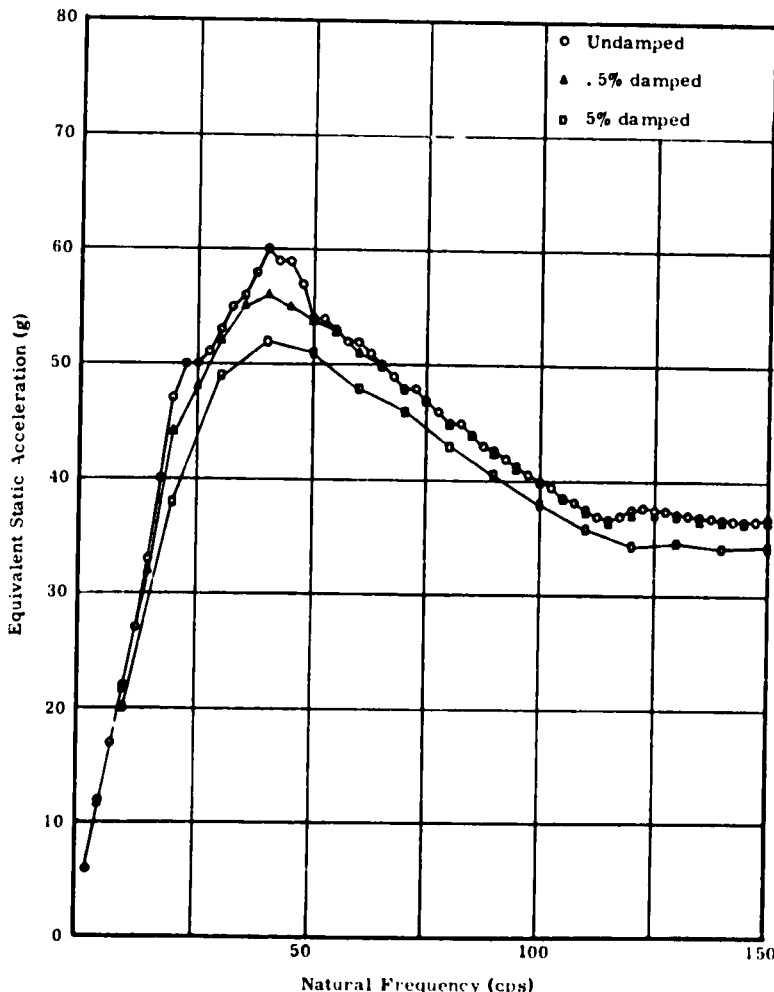


Fig. 5 - Shock spectrum for systems with 0-percent, 0.5-percent, and 5-percent damping, 7 mph impact velocity (ramp test facility)

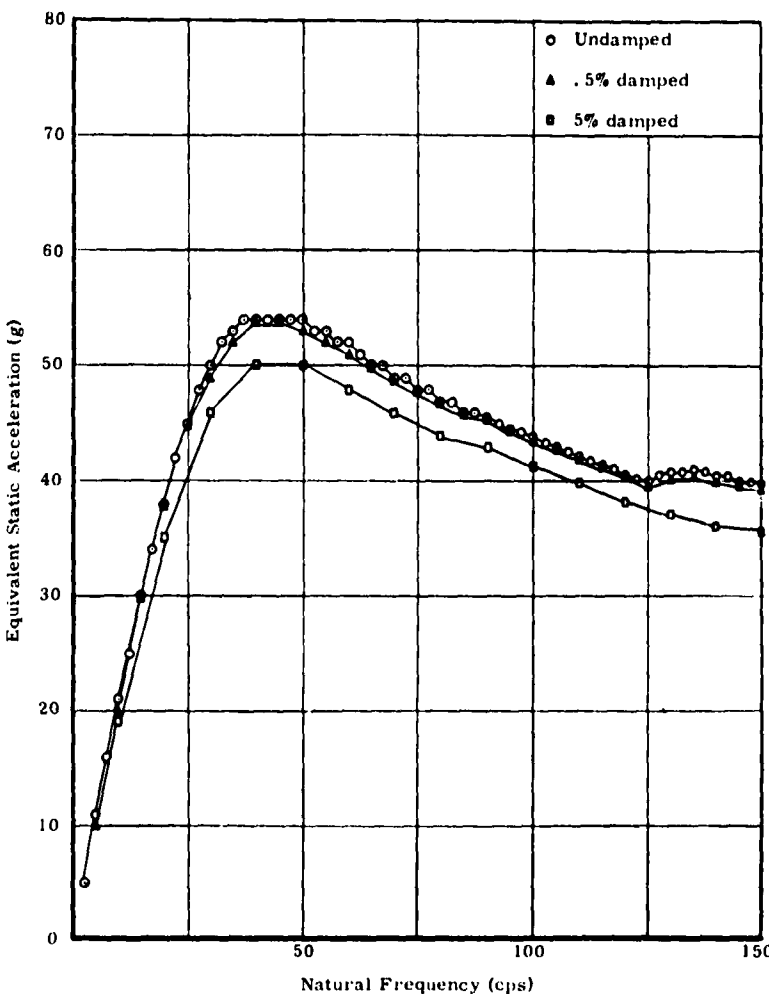


Fig. 6 - Shock spectrum for systems with 0-percent, 0.5-percent, and 5-percent damping, 6.8 mph impact velocity (ramp test facility)

the empty cart (Fig. 6) shows very favorable comparisons for systems with natural frequencies of 12.5 cps and under. The values compare within 4 percent with the higher values for the 7 mph impact. The fact that the 7 mph impact velocity is 3 percent higher than the 6.8 mph impact should account for most of the difference. For the ATMX Car floor, the shock signatures (Fig. 3) indicate a natural frequency of the floor of approximately 700-800 cps in the longitudinal direction. The logarithmic decaying portion of the response of the ATMX Car floor to switching shock (see Fig. 3) appears at the end of the main shock pulse for every test. Since the test specimens involved in this study possess low frequencies and low masses (1000 pounds), they should only negligibly affect the dynamic response of the ATMX Car floor in the

longitudinal direction. Consequently, the shock spectra of the car should also be negligibly affected. Preliminary studies of the vertical and lateral shock spectra show negligible values for systems with natural frequencies of 12.5 cps and under. These values, although negligible, also compare favorably with the ramp cart comparison test mentioned above. For systems with higher natural frequencies, the vertical shock spectra should be investigated and considered.

COMPARISONS

To simulate environmental conditions, the test engineer merely has to refer to the shock spectra of the test facility as well as those of

the railroad car and then subject the test specimen to the equivalent static acceleration expected under actual environment for a system of that natural frequency. For example, the shock spectra for the ATMX Car on a 7.5 cps system (Fig. 7) yield a value of 11 g equivalent static acceleration at an impact velocity of 9.2 mph. Reference to the shock spectra for the ramp cart (Fig. 8) shows that an impact velocity of 4.7 mph will impose the same shock damage potential on a 7.5 cps system. A 12.5 cps system which is designed to withstand an impact velocity of 9.2 mph in an ATMX Car should also be exposed to approximately 4.7 mph on the test facility for adequate testing. A 7 mph impact velocity on the ramp facility would subject a test item of 2.5 cps natural

frequency to the same shock that it would experience under an 11 mph impact velocity in an ATMX Car.

Longitudinal shock spectra for the ATMX Car floor under other impact velocities for systems with 0-percent, 0.5-percent, and 5-percent damping are shown in Figs. 9 through 17. Comparisons can be made between the longitudinal shock spectra for the ramp test facility under other impact velocities and systems with 0-percent, 0.5-percent, and 5-percent damping as shown in Figs. 18 through 25. It will be noticed that systems with natural frequencies of 12.5 cps and under will at least be adequately tested for an 11 mph impact condition on the ATMX Car by an input obtained from

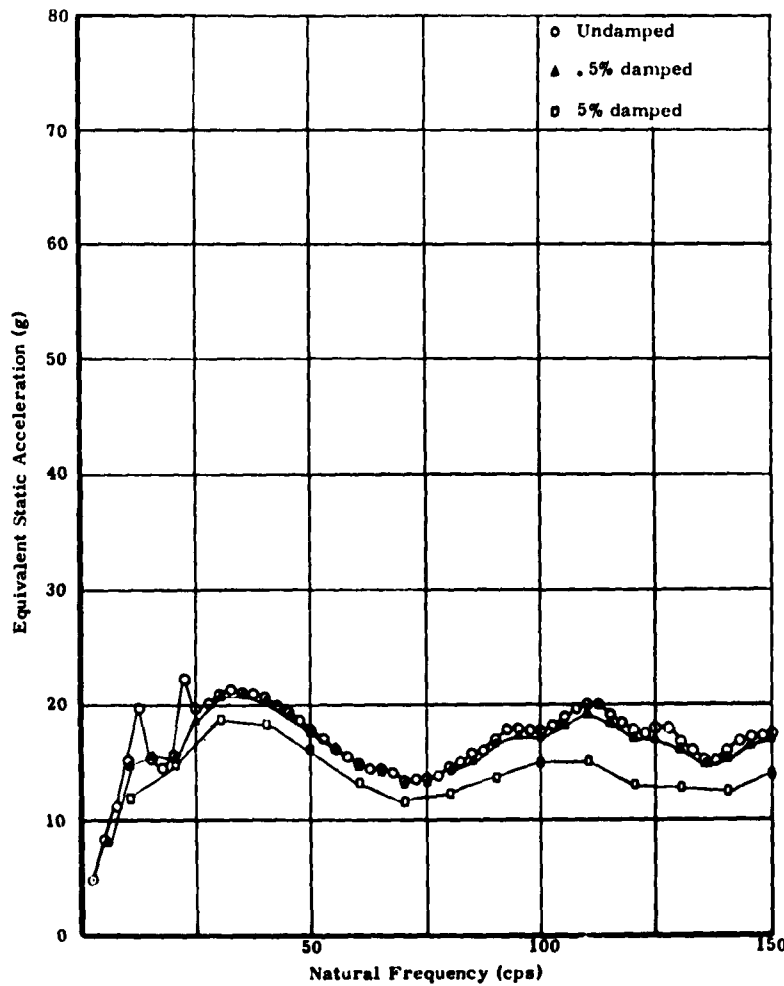


Fig. 7 - Shock spectrum for systems with 0-percent, 0.5-percent, and 5-percent damping, 9.2 mph impact velocity (ATMX Car)

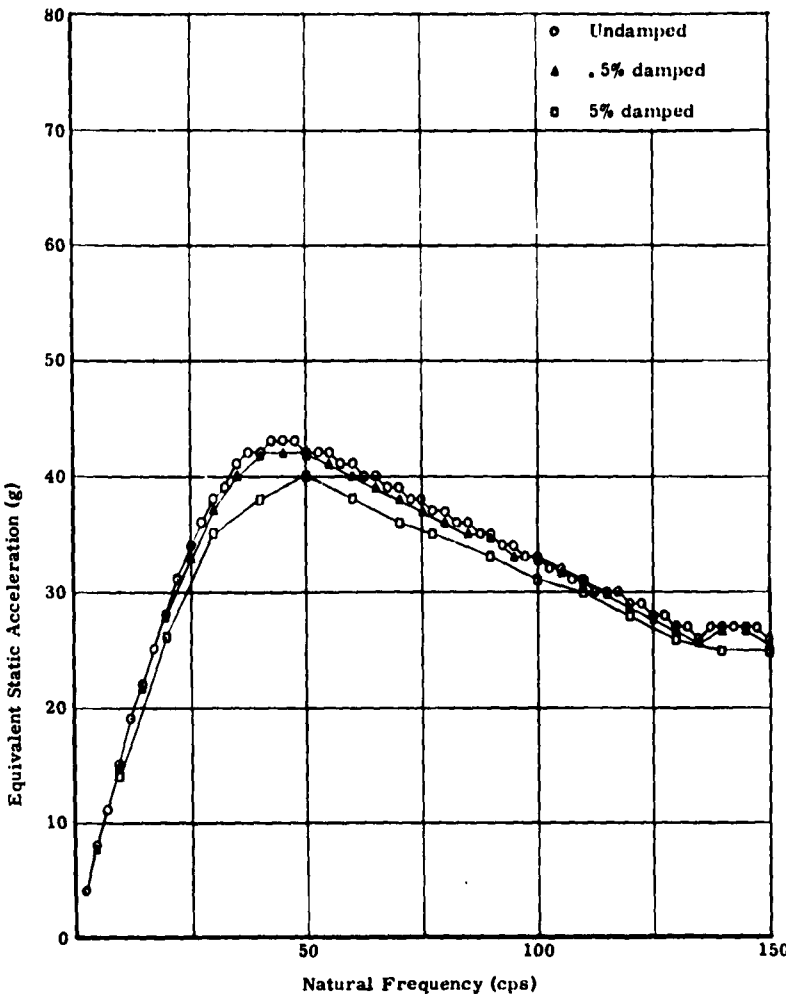


Fig. 8 - Shock spectrum for systems with 0-percent, 0.5-percent, and 5-percent damping, 4.7 mph impact velocity (ramp test facility)

a 7.0 mph impact velocity or less on the ramp test facility. Actual impact velocity is dependent upon the natural frequency of the system being tested.

Although this paper is entirely concerned with the test simulation of railroad switching environment, shock spectra are directly applicable to several techniques for dynamic design [2]. In order to use the shock spectra in design, however, it is necessary to assume that the structure is elastic and linear to the point of failure. Theoretically, then, a designer of Sandia Corporation transportation containers which are to be subjected to the environment of the ATMX Car switching shock loads need only refer to the shock spectra, select the specific

natural frequency of the design, and determine the expected damage potential. Conversely, the shock spectra will furnish the designer with an optimum natural frequency for design of the equipment against this environment.

CONCLUSIONS AND DISCUSSION

The shock spectra given should produce good results in the simulation of this particular environment for systems with natural frequencies of 12.5 cps and lower. It should be remembered that the conditions under which the ATMX Car shock signatures were obtained were controlled and identical for each impact velocity. The mass remained constant, brakes

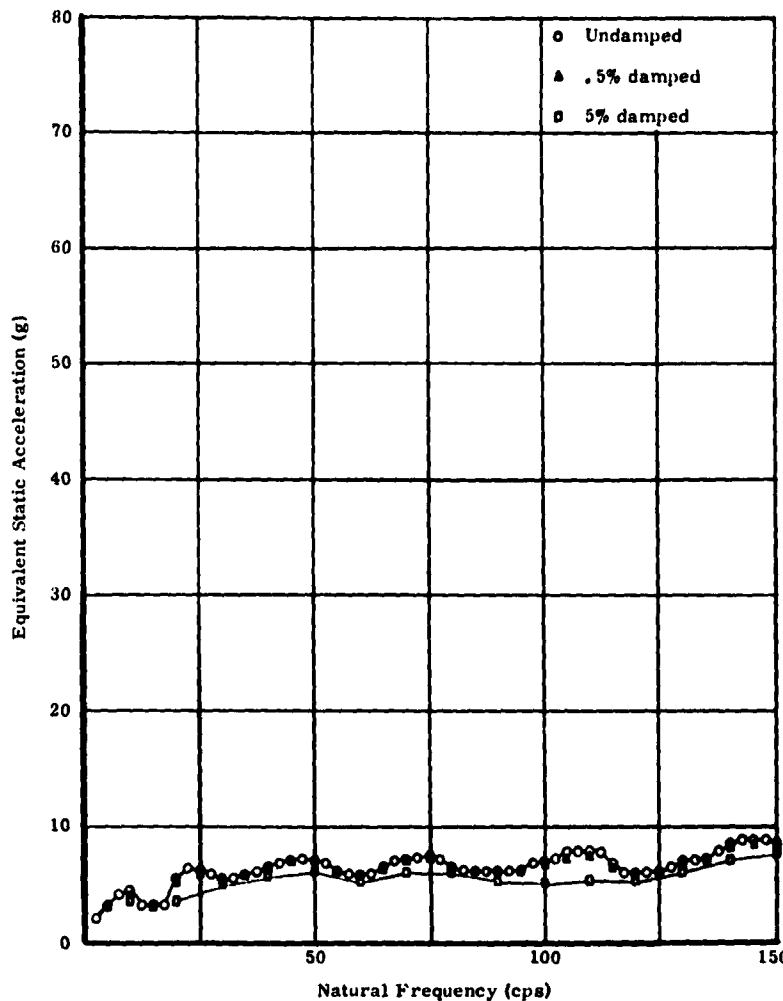


Fig. 9 - Shock spectrum for systems with 0-percent, 0.5-percent, and 5-percent damping, 3.7 mph impact velocity (ATMX Car)

were set each time on the stopper cars, and all slack was removed from each of the couplers on the stopper cars. Although the stopper cars used employed different draft gear from the ATMX cars, it was believed that the overall condition was representative of that which the ATMX Car would experience under actual conditions. Although the shock spectra may be interpolated between impact velocities for tests of specific frequencies, the shock spectra should be computed for closer frequency intervals than are shown here, so that a greater number of systems with different natural frequencies may be accurately tested. The shock spectra should not be interpolated between frequencies, since peaks and valleys may occur which are not evident in the graphs. The points between discrete frequencies are connected only

to simplify the reading of the spectra and do not indicate values between measured points.

Further impact tests are being performed in the ATMX Car with instrumentation at other locations and with different weights mounted in the car. Stopper cars with a mass totaling 780,000 pounds are being used for these tests. These tests are being conducted to ascertain that the worst condition of shock load to which Sandia designed equipment could be exposed has been considered. Shock spectra have not as yet been computed for those tests. Further tests will also be made on the ramp test facility. Shock spectra are needed for ramp impact velocities under 4.7 mph, so that tests may be accurately simulated for equipment which needs to withstand velocity impacts of 6 mph or less

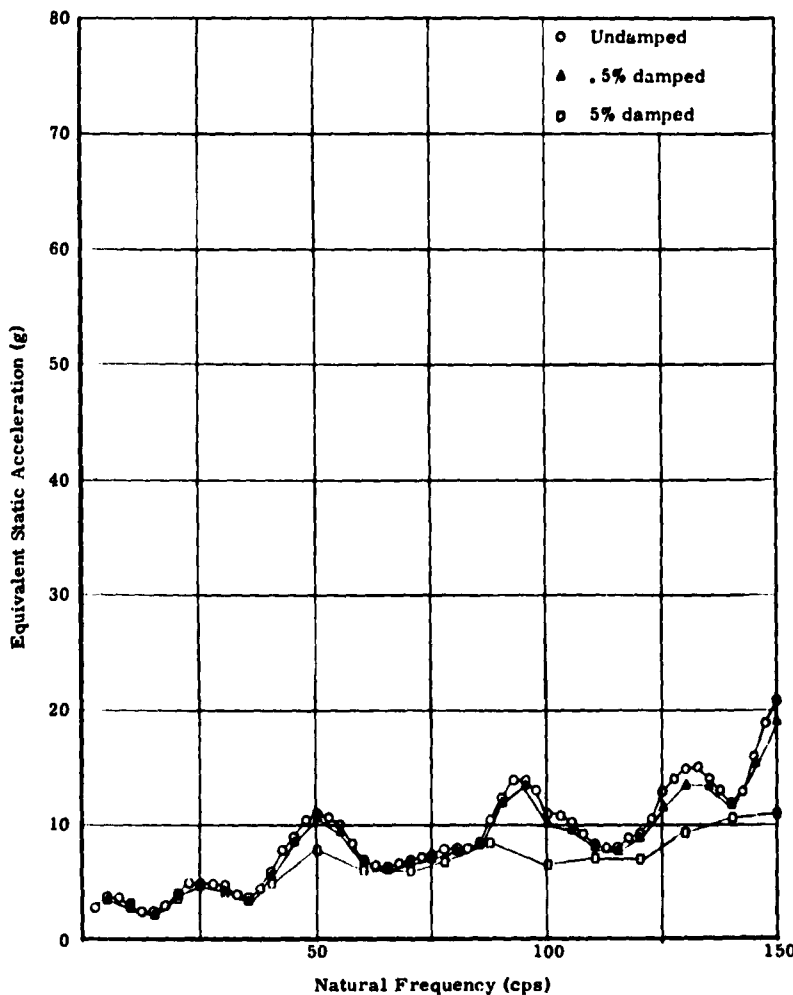


Fig. 10 - Shock spectrum for systems with 0-percent, 0.5-percent, and 5-percent damping, 4.6 mph impact velocity (ATMX Car)

in the ATMX Car. Ideally, sufficient shock spectra should be available to enable the test engineer to refer to a complete family of curves for simulation of a wide variety of environmental conditions.

The possibility of measuring the mechanical impedance of the ATMX Car floor under these conditions is being considered. Equipment with varying natural frequencies and greater mass might then be more accurately tested without the ever-present danger of over-

testing or undertesting. Future work is necessary and will be conducted.

In summary then the object of this study has been fulfilled, to a limited degree, in that comparison of the shock spectra obtained should enable the test engineer to simulate more closely and more easily the actual railroad switching operations encountered by ATMX cars. As a side product, engineers designing simple systems could also refer to the shock spectra to determine the damage potential to their system if they know its natural frequency.

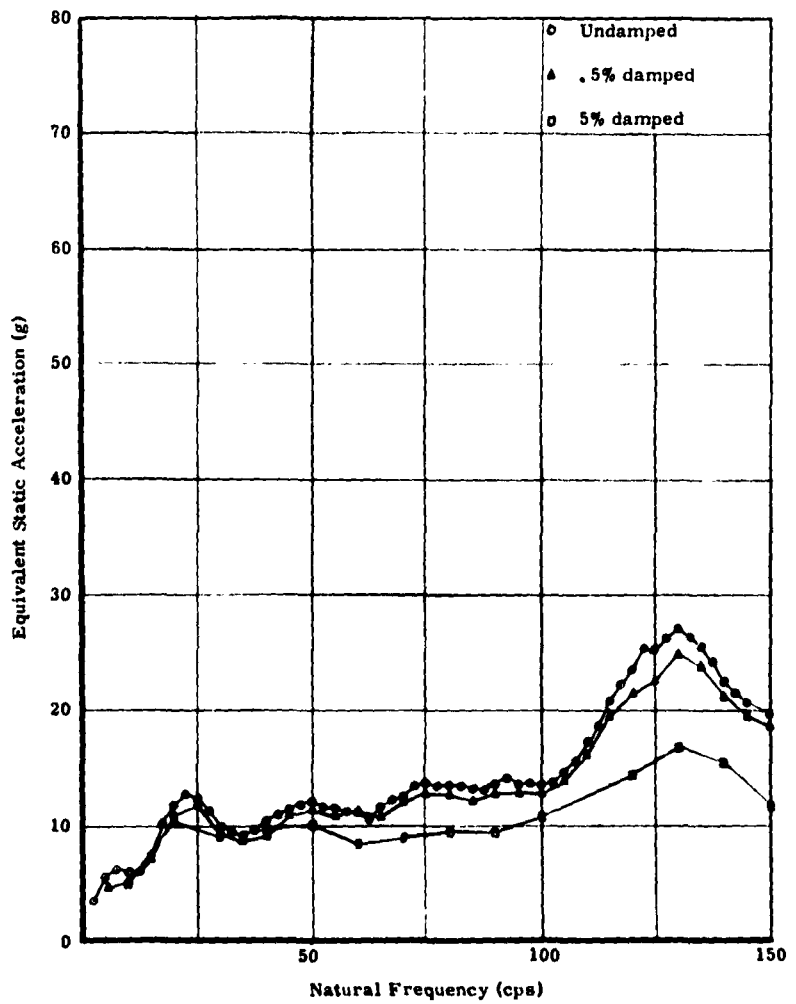


Fig. 11 - Shock spectrum for systems with 0-percent, 0.5-percent, and 5-percent damping, 6.2 mph impact velocity (ATMX Car)

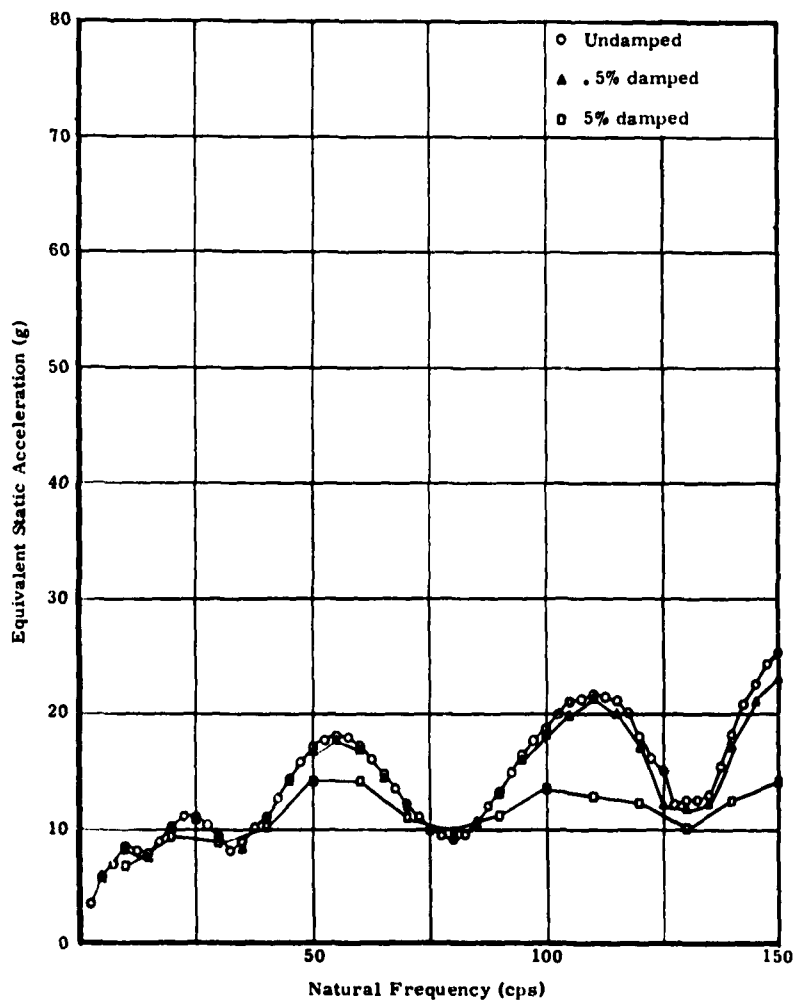


Fig. 12 - Shock spectrum for systems with 0-percent, 0.5-percent, and 5-percent damping, 6.8 mph impact velocity (ATMX Car)

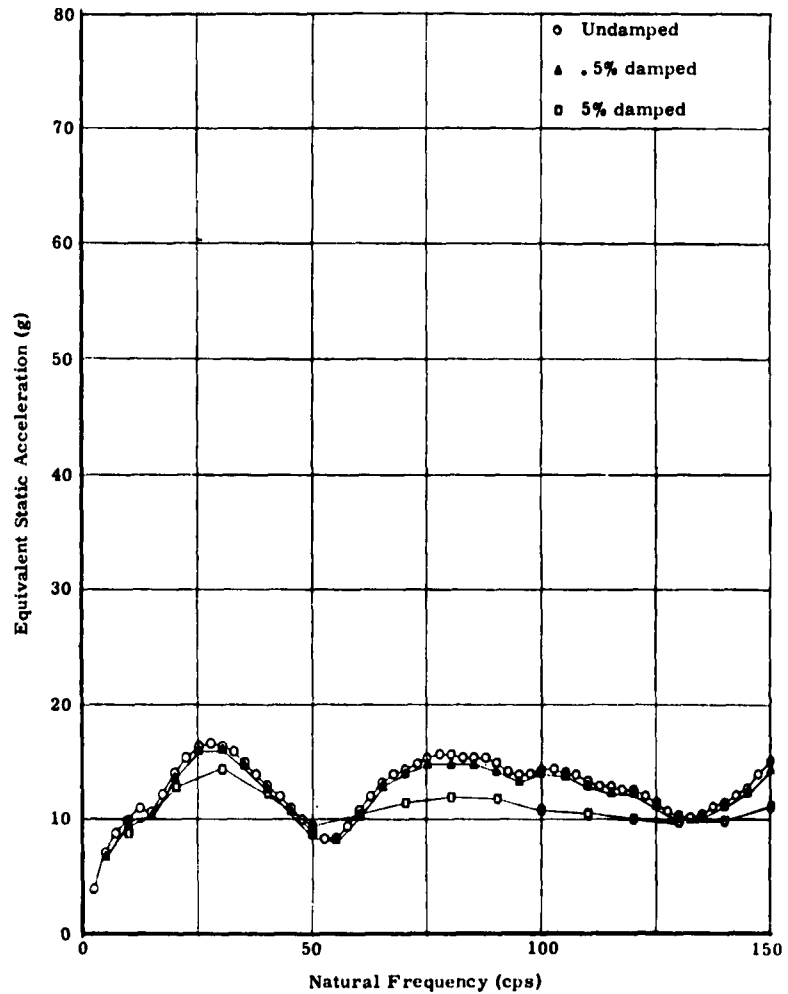


Fig. 13 - Shock spectrum for systems with 0-percent, 0.5-percent, and 5-percent damping, 7.2 mph impact velocity (ATMX Car)

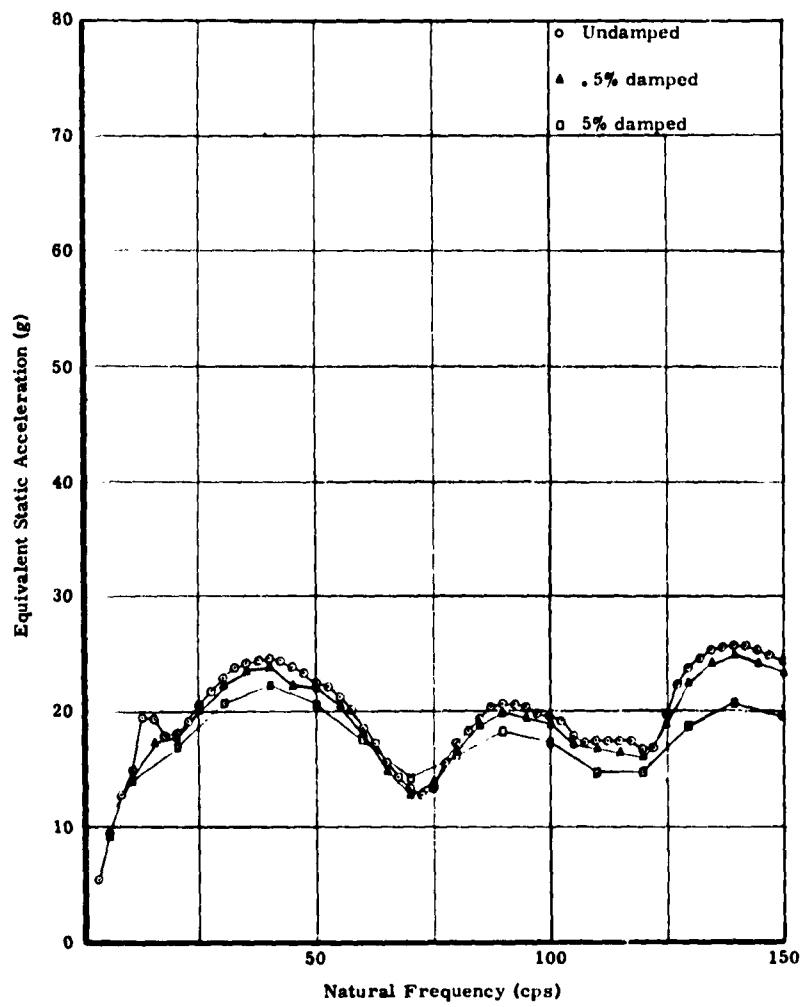


Fig. 14 - Shock spectrum for systems with 0-percent, 0.5-percent, and 5-percent damping, 9.8 mph impact velocity (ATMX Car)

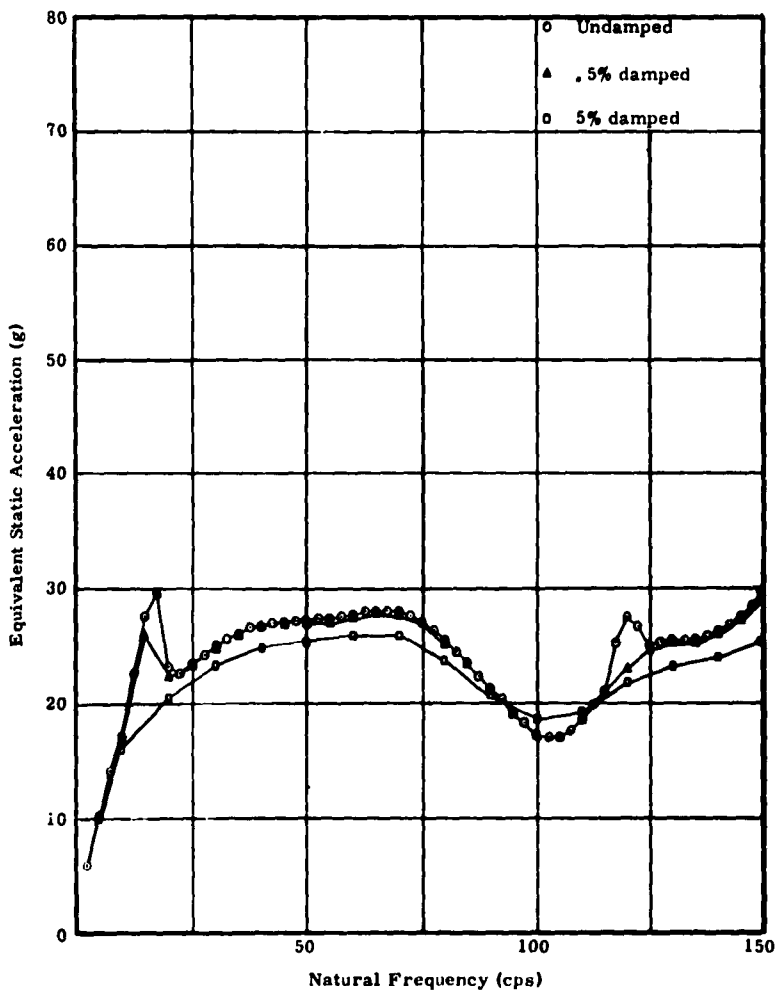


Fig. 15 - Shock spectrum for systems with 0-percent, 0.5-percent, and 5-percent damping, 11.0 mph impact velocity (ATMX Car)

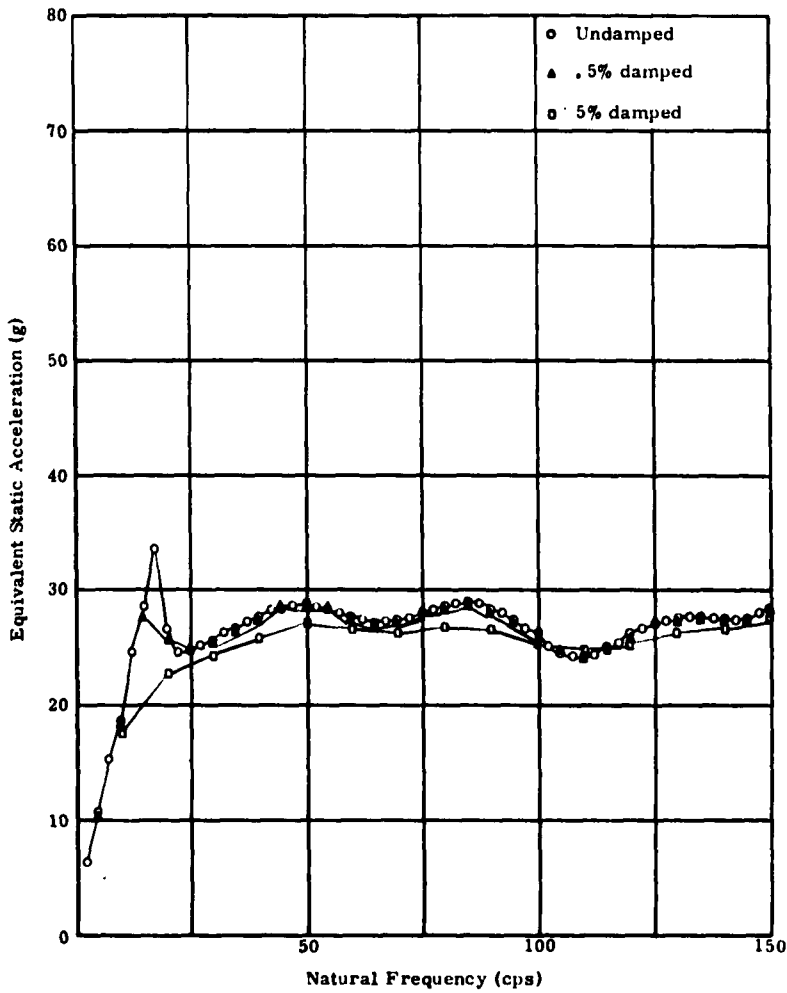


Fig. 16 - Shock spectrum for systems with 0-percent, 0.5-percent and 5-percent damping, 11.8 mph impact velocity (ATMX Car)

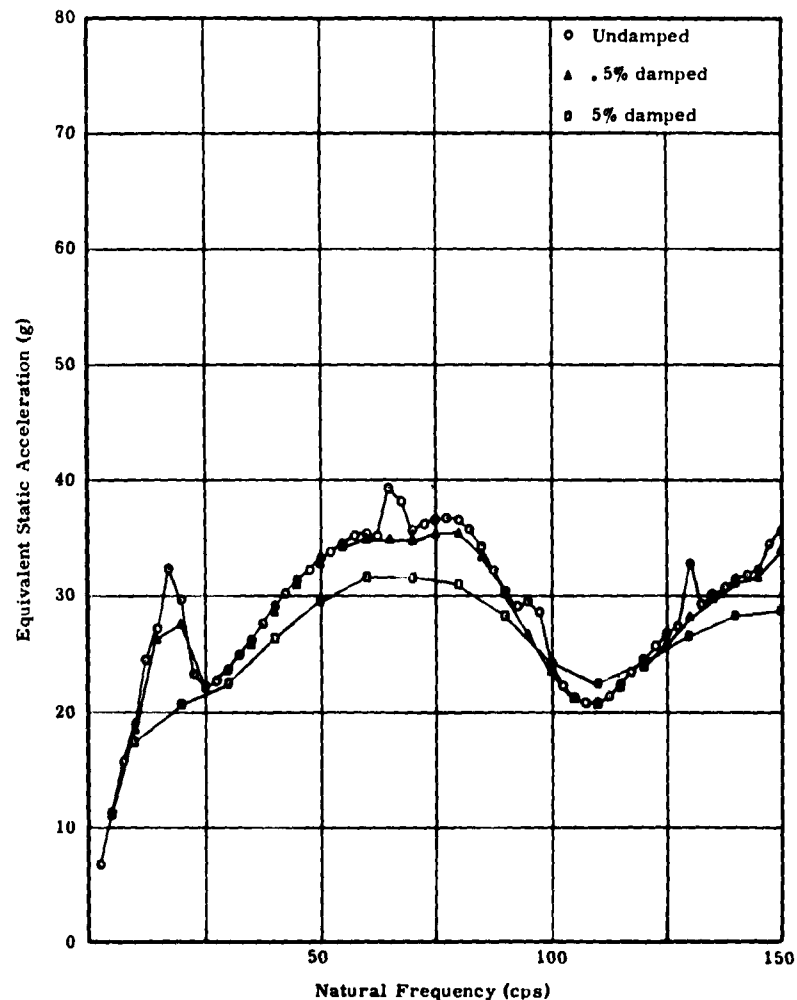


Fig. 17 - Shock spectrum for systems with 0-percent, 0.5-percent, and 5-percent damping, 12.0 mph impact velocity (ATMX Car)

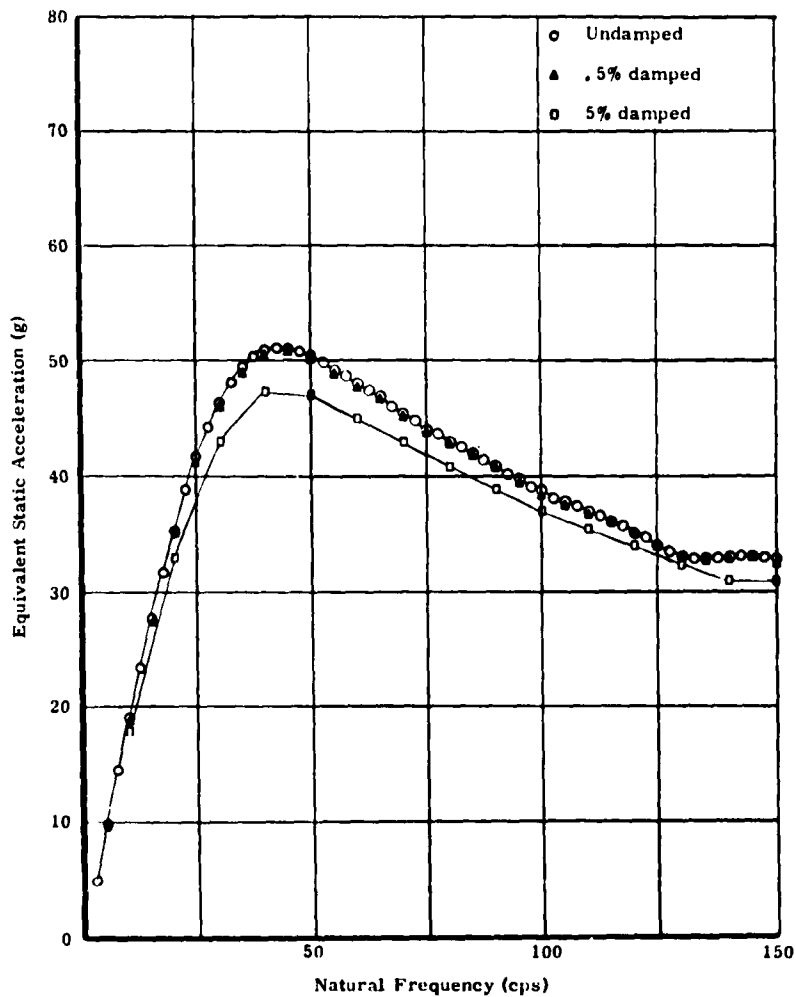


Fig. 18 - Shock spectrum for systems with 0-percent, 0.5-percent, and 5-percent damping, 6.1 mph impact velocity (ramp test facility)

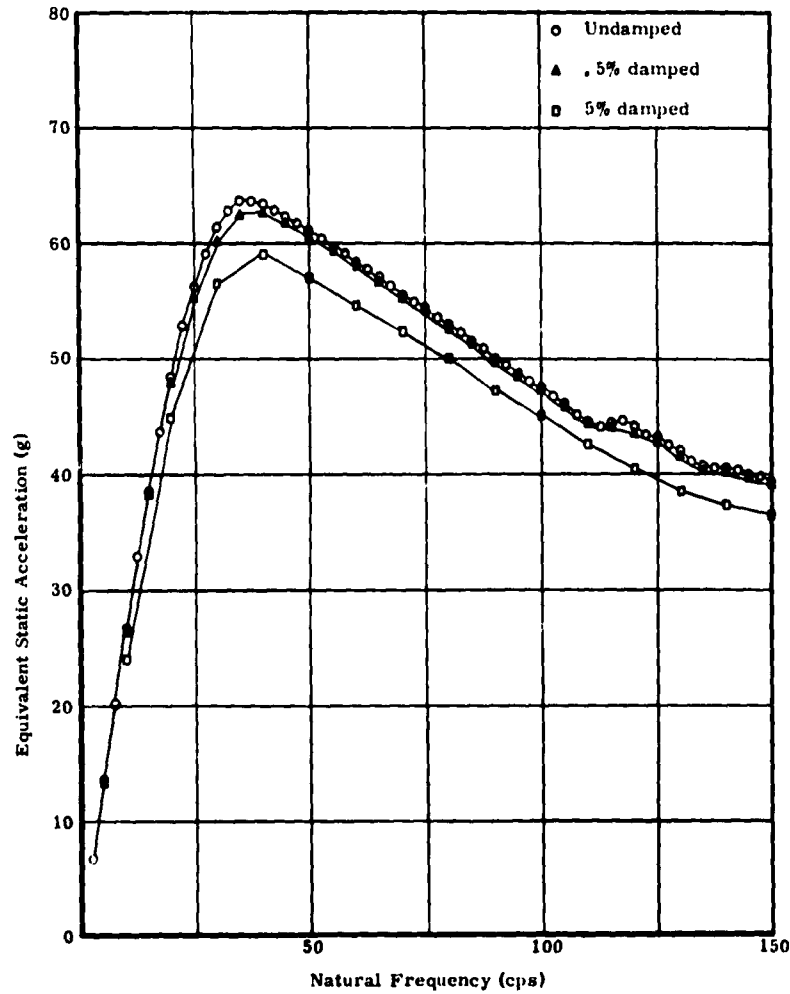


Fig. 19 - Shock spectrum for systems with 0-percent, 0.5-percent, and 5-percent damping, 8.9 mph impact velocity (ramp test facility)

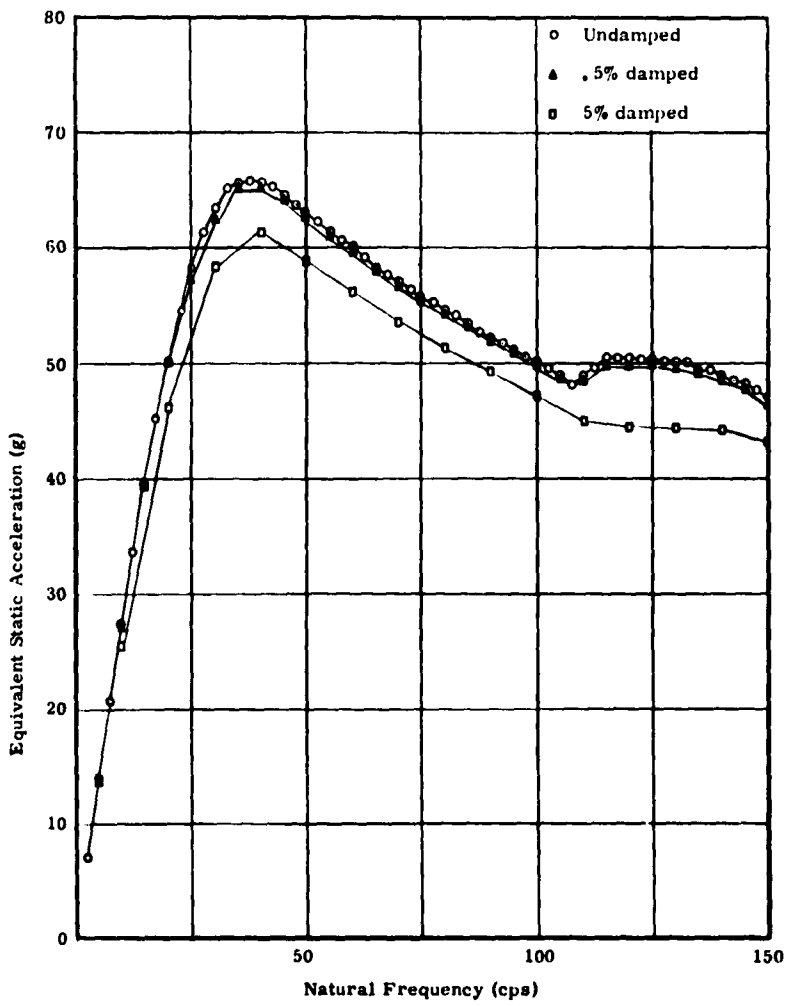


Fig. 20 - Shock spectrum for systems with 0-percent, 0.5-percent, and 5-percent damping, 9.3 mph impact velocity (ramp test facility)

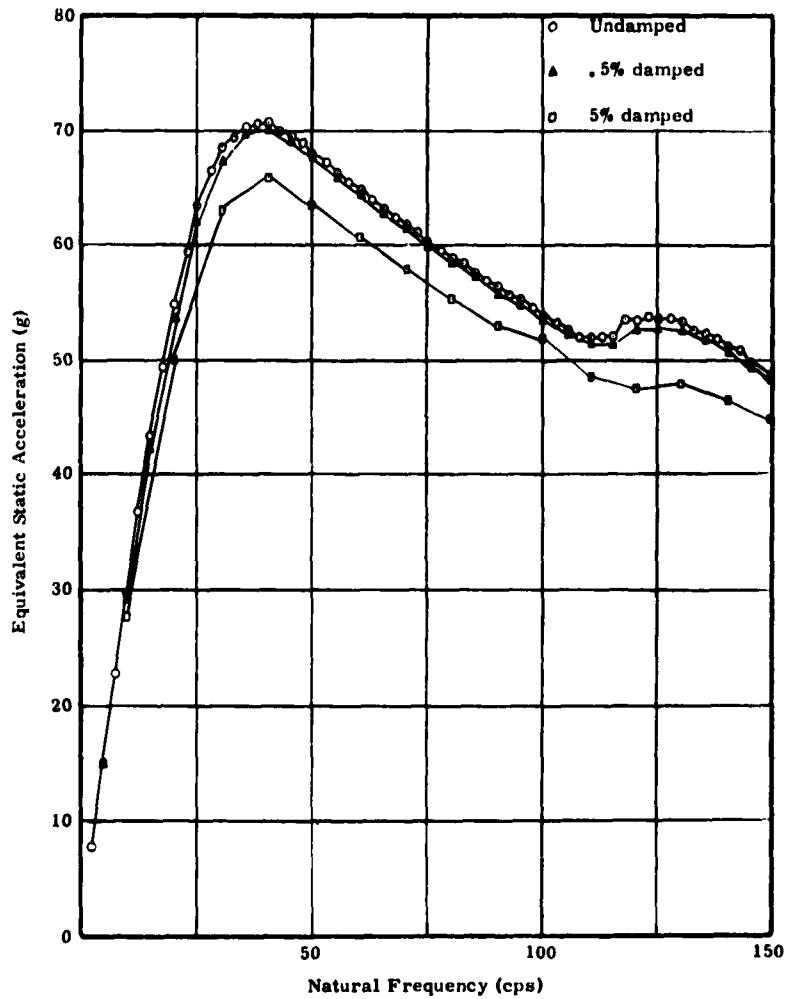


Fig. 21 - Shock spectrum for systems with 0-percent, 0.5-percent, and 5-percent damping, 9.9 mph impact velocity (test ramp facility)

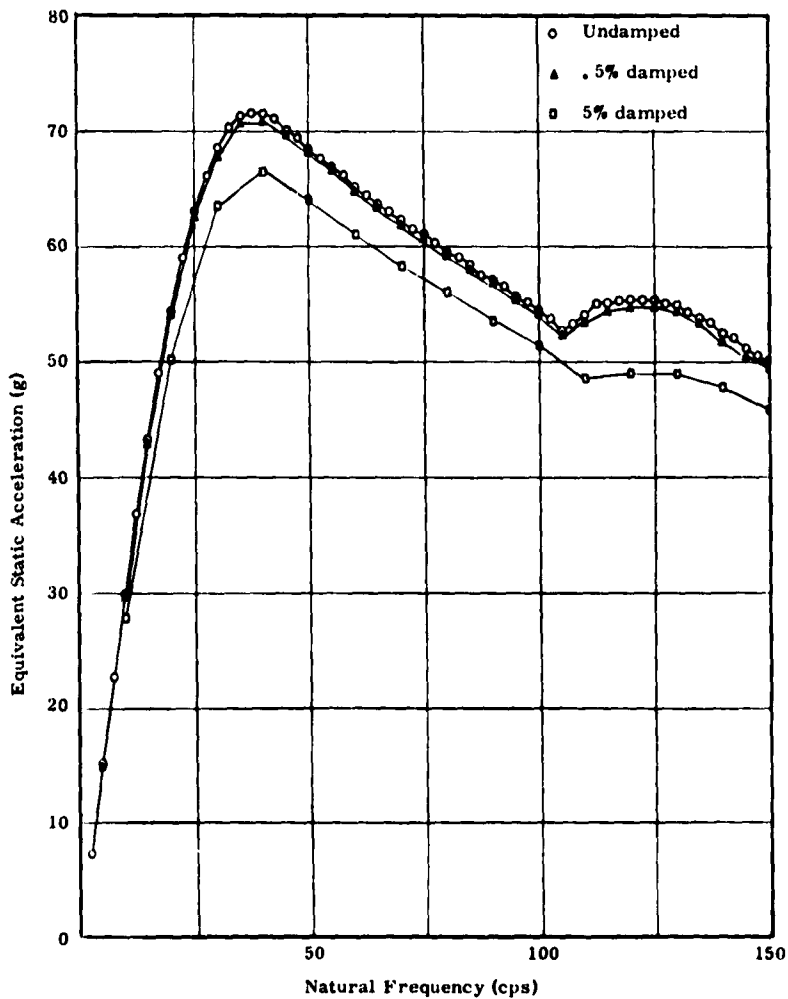


Fig. 22 - Shock spectrum for systems with 0-percent, 0.5-percent, and 5-percent damping, 10.1 mph impact velocity (ramp test facility)

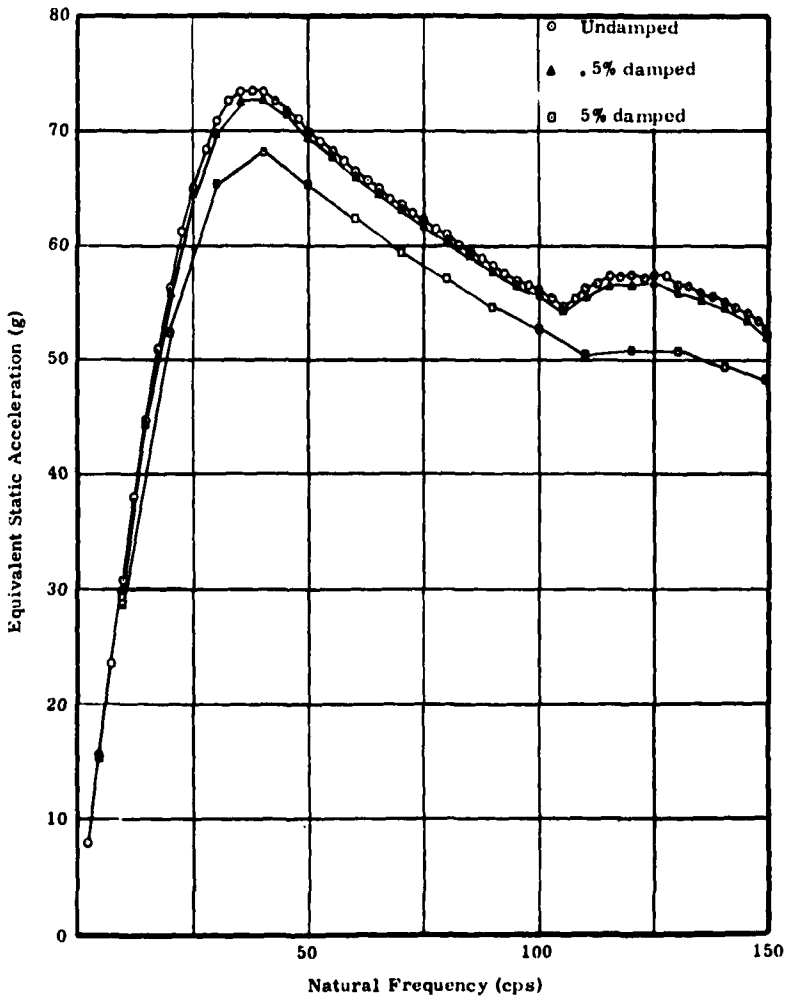


Fig. 23 - Shock spectrum for systems with 0-percent, 0.5-percent, and 5-percent damping, 10.5 mph impact velocity (ramp test facility)

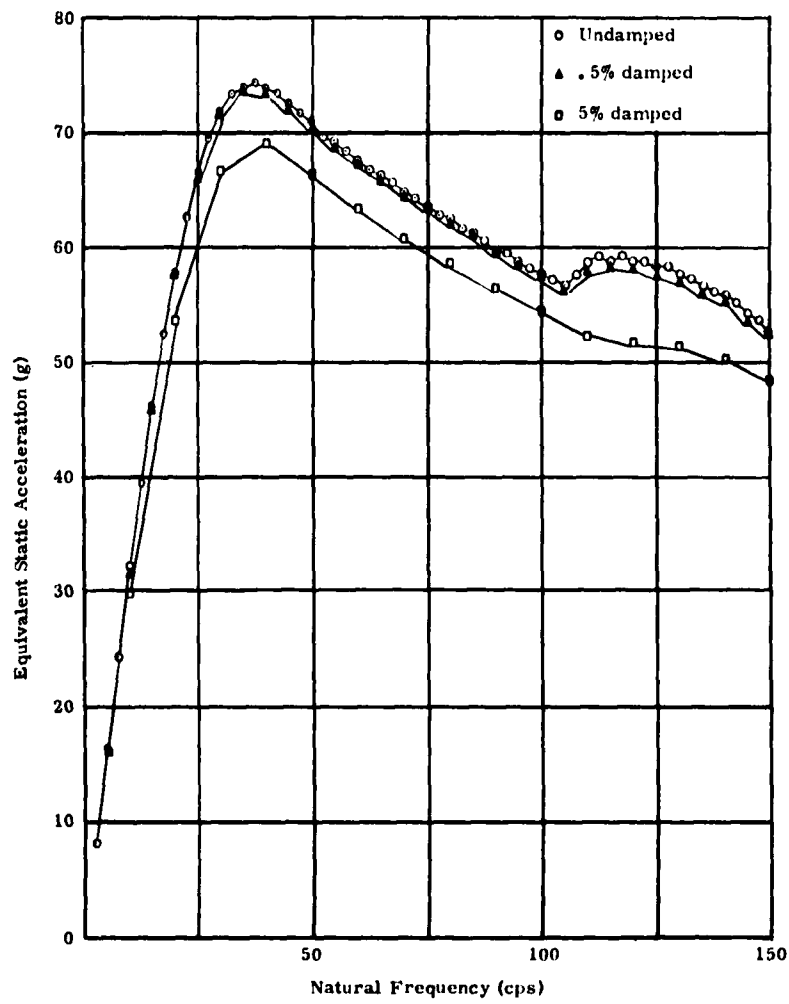


Fig. 24 - Shock spectrum for systems with 0-percent, 0.5-percent, and 5-percent damping, 10.6 mph impact velocity (ramp test facility)

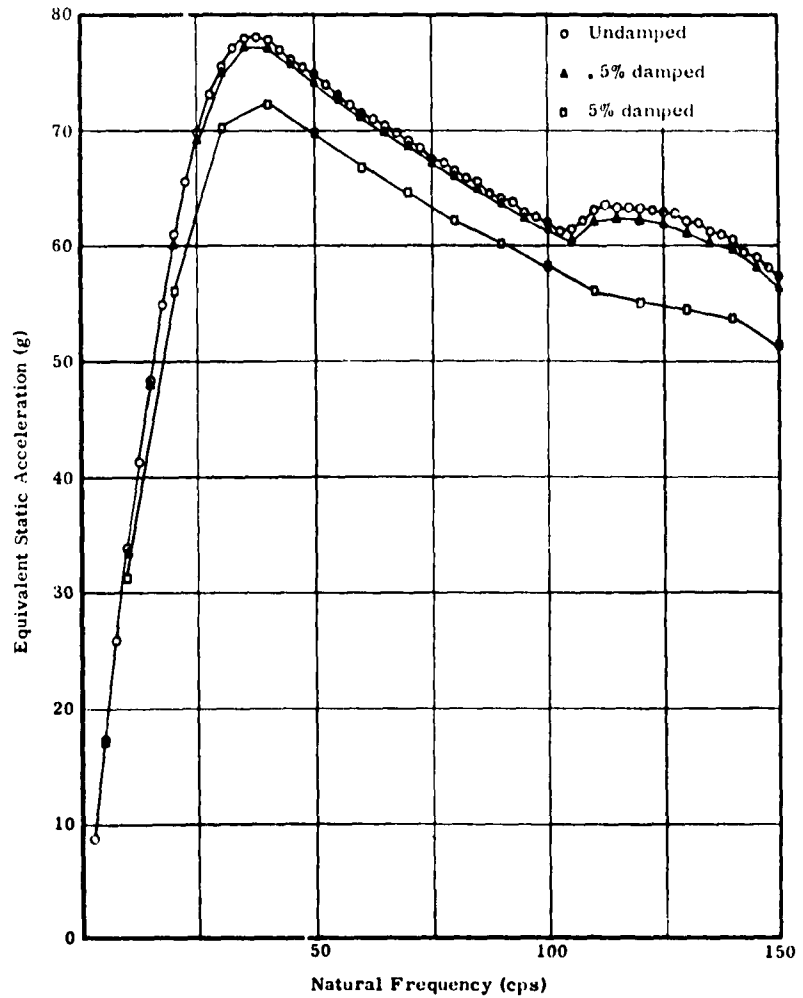


Fig. 25 - Shock spectrum for systems with 0-percent, 0.5-percent, and 5-percent damping, 11.1 mph impact velocity (ramp test facility)

REFERENCES

- [1] "Shock Tester for Shipping Containers," W. H. Cross and Max McWhirter, ASTM Special Technical Pub. No. 176, pp. 141-148, 1955.
- [2] "The Equivalent Static Acceleration of Shock Motions," J. P. Walsh and R. E. Blake, Proc. Soc. Exp. Stress Analysis, Vol. 6, No. 2, pp. 150-158, 1949.

DISCUSSION

Mr. Jones (MSFC, NASA): My first comment concerns the first car concept in impacting, where we can load up 50 freight cars in a row. There is going to be a limited number in the front end which actually cause the acceleration effect and if the first car is heavy enough, it's the first car. The second car, maybe, only contributes 10 percent. Of course, this only determines that initial pulse where, you say, maybe 40 percent of the velocity is represented. Secondly, there is an equivalent static acceleration which you say is a function of the frequency. I don't believe it can exceed 12 g's because of limitations of tie downs. In other words you'll bust your load loose from the freight car before you exceed about 12 g's in most heavy item concepts. Thirdly, I take exception to the simulator because, in the actual freight car impact, it is something like the billiard ball with a little bit of a spring in front of it. We are accelerating the mass of that first car, so that a simulator should consist of a very heavy mass and an exceedingly strong spring so that when you hit the spring you accelerate the mass.

Mr. Rector: Maybe you should have presented these one at a time. Taking the last one, I was not concerned with the pulse that would have resulted from the impact of the mass, but rather with the shock spectrum in this pulse. In the past we have been testing by putting in a shock pulse which would more than adequately test any item. This is a slight deviation from that method, in that I'm trying to duplicate the

shock spectrum of the condition on the ramp. In this case I don't think the shock pulse is of too much importance as long as, of course, the natural frequency of the system being tested is excited. Now, you say the equivalent static acceleration cannot exceed 12 g.

Mr. Jones: Somewhere in that neighborhood. I'm merely saying that when we tie an object onto a freight car, we rarely tie it with tie lines that are hard enough so that you can get these 12 g plus pulses through. You can get pulses through and they cause greater than 12 g accelerations on the test load, but this is resonance in the test load due to the pulse. Simply stated, I'm saying we can't very well get better than 12 g's through most tie downs.

Mr. Rector: These are not, if I interpret your question correctly, equivalent static accelerations but rather dynamic accelerations that you are referring to. This is true. I have noticed also that the dynamic accelerations on the shock pulses have not exceeded 12 g's, or maybe 14—but then this is perhaps, error in the reading instruments. In answer to your first question about the number of cars impacted into determining the initial pulse, this is true, but I have been led to believe that there may not be any more than a dozen ATMX cars to make up a train.

Mr. Jones: The weight of the first car is the important thing.

* * *

ROUGH HANDLING TESTS OF REUSABLE CONTAINERS

Fulton Yee
Detroit Arsenal
Detroit, Michigan

A discussion is given of test methods employed by Detroit Arsenal, along with analysis of results of rough handling tests of reusable containers. Instrumentation selection and placement is discussed. Tests were illustrated by high-speed movies.

INTRODUCTION

Loss and damage in shipment of contents in containers are often caused by rough handling or environmental factors. Damage may be mechanical or nonmechanical in nature. A few of the major causes are improper sealing, rough handling and inadequate tie-down fittings.

Improper sealing may cause water soaking that will result in surface marring, corrosion or introduction of fungus. In addition, if the container is not sealed properly the contents may be infested with pests or contaminated by dust and sand.

Rough handling may cause shock damage or even breakage of the item and container by exceeding the ultimate strength of the material or by fatigue.

Inadequate tie-down fittings may result in scratching, marring or jarring of external surfaces coming in contact with container wall support structure or adjacent items.

Rough handling tests conducted in the laboratory have been designed to simulate hazards encountered in the field during handling of packages by men and equipment. The following sketch (Fig. 1) shows a typical handling-environment story from the time the product leaves the assembly line until it is ready for use at its destination. The story includes hand truck; the drop in the truck; a rough ride; loading on carrier; humping; unloading, and so to the user.

Because of the variables involved in storage, handling and shipping, direct relationships

between these factors are difficult to establish. However, laboratory testing serves to provide a procedure for determining container qualities and resistances to impact.

The object of this paper is to present test methods and analysis of results of rough-handling tests of reusable containers conducted by Laboratories of the Detroit Arsenal.

ROUGH HANDLING TESTS OF REUSABLE CONTAINERS

Instrumentation

In shock-testing a package, the severity or magnitude of the shock is determined by using accelerometers and associated electronic recording equipment.

The accelerometers employed in these tests were of the unbonded strain gage type having the following characteristics:

Range	±25 g's
Natural Frequency	375 cps
Damping	0.6 to 0.7
Response	approximately flat from 0-100 cps
Accuracy	±1 percent.

The carrier amplifier used was a complete amplification system included in a single

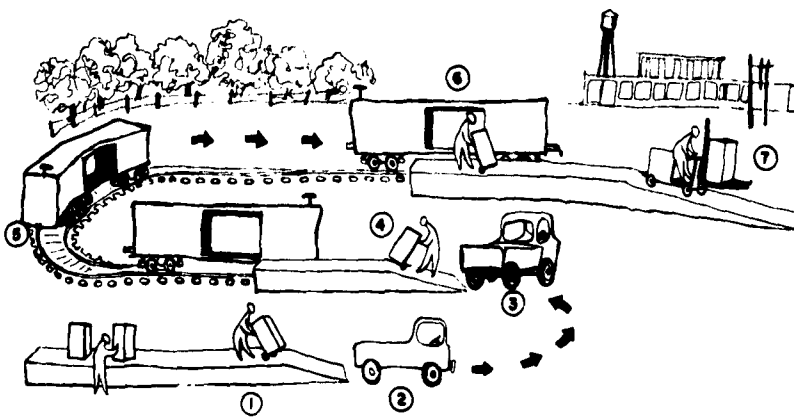


Fig. 1 - Typical container handling sequence from manufacturer to user

cabinet: a 3-kilocycle carrier oscillator, four carrier amplifiers, a regulated power supply and control for balancing setting sensitivity, metering output and calibration. A direct recording oscillograph with paper speed of 25 inches per second was used.

The wiring was completely shielded, and the system was grounded to eliminate the pick-up of stray voltage. The instrumentation block diagram (Fig. 2) shows the hook-up between accelerometers and recording equipment.

It must be remembered that shock recorded by an accelerometer will be the shock at the point it is located. It is therefore

necessary to establish the location most likely to receive the greatest impact load.

Theoretically, the sensing device (accelerometer) should be mounted at the center of gravity of the package. However, in actual practice, it is not easy to achieve this without considerable disassembly or destruction of the package. Shock or impact may be induced to the package from any direction during dropping. Therefore, it is necessary to use three accelerometers to record the shock in three specific directions. These are referred to as the vertical, longitudinal and lateral axes. An illustration of how three accelerometers were mounted on a transmission in a container is shown in Fig. 3.

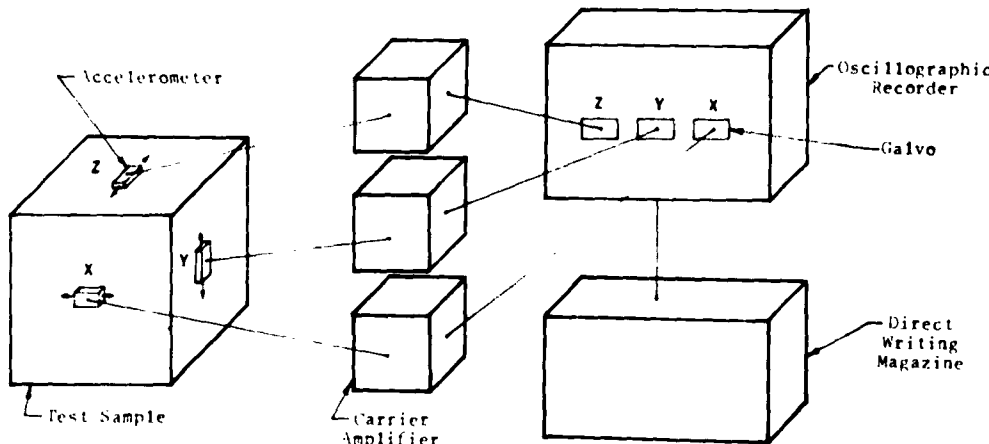


Fig. 2 - Instrumentation diagram



Fig. 3 - Accelerometers mounted on transmission

Test Methods Employed

Air Leakage—The container was assembled and closed in the normal way, except that the relief valve was blocked off. The container was filled to 15 psi air pressure (gage) and placed in water (Fig. 4). Container was submerged so that all surface area was brought underwater and observation of air bubble formation could be made at the precise point of leakage. An alternate method was employed using a saturated water-soap solution applied with a brush over all seams and closures. Leakage was indicated by soap bubbles increasing in size or being blown away by escaping air.

Edgewise Drop—The loaded container was supported at one end of its base on a wood sill approximately 5 inches in height, placed at right angles to the skids. The opposite end of the container was raised (Fig. 5) and allowed to drop freely from a height of 12, 24 and 36 inches, successively, to a metal surface. This test was applied to each end of the container.

Cornerwise Drop—The loaded container was supported at one corner of its base on a block 5 inches high. A block 12 inches in height was placed under the other corner of

the same end of the container. The opposite end of the container was raised (Fig. 6) and allowed to fall freely from a height of 12, 24 and 36 inches, successively, to a metal surface. This test was applied to one diagonally-opposite corner of each end of the container.

Tip-Over—The container, erect on its base on a hard, level floor, was slowly tipped to the side (Fig. 7) until it fell freely and solely by its own weight to the floor. After righting the container, the test was repeated to the opposite side.

Flatwise Drop—The container was raised so that its base was parallel to the floor (Fig. 8) and allowed to fall freely once each from a height of 6 and 12 inches to a metal surface.

Pendulum Impact—An impact test was applied to each end of the container. The container was suspended as a pendulum at the end of four or more cables. The cables were sufficient in length to preclude any interference or binding. A flat, vertical, stationary metal barrier with a 2-inch maximum thickness of wood between the barrier and container was provided for the container to strike against. The suspended container was hoisted vertically to a height which allowed the lowest point of the container (while swinging through the arc

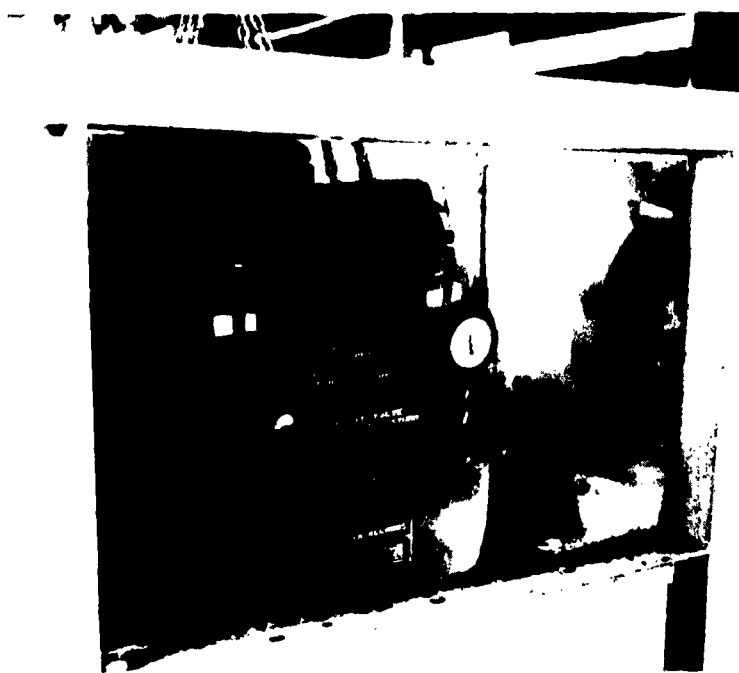


Fig. 4 - Air leakage test



Fig. 5 - Edgewise drop test



Fig. 6 - Cornerwise drop test

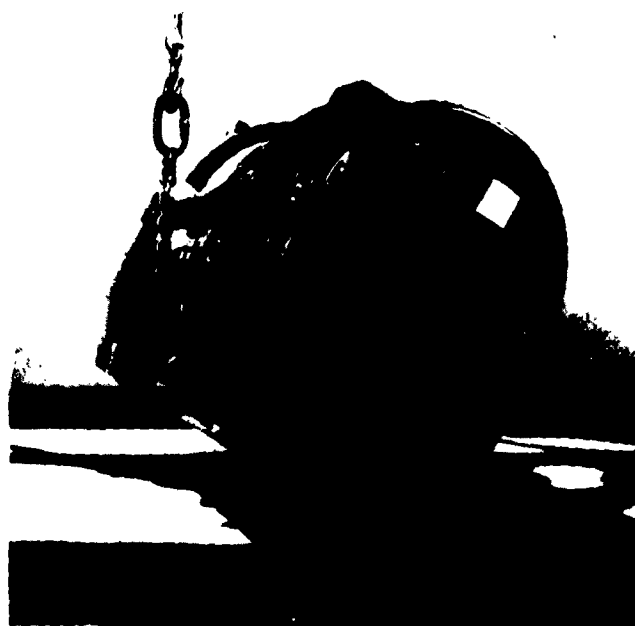


Fig. 7 - Tip-over test

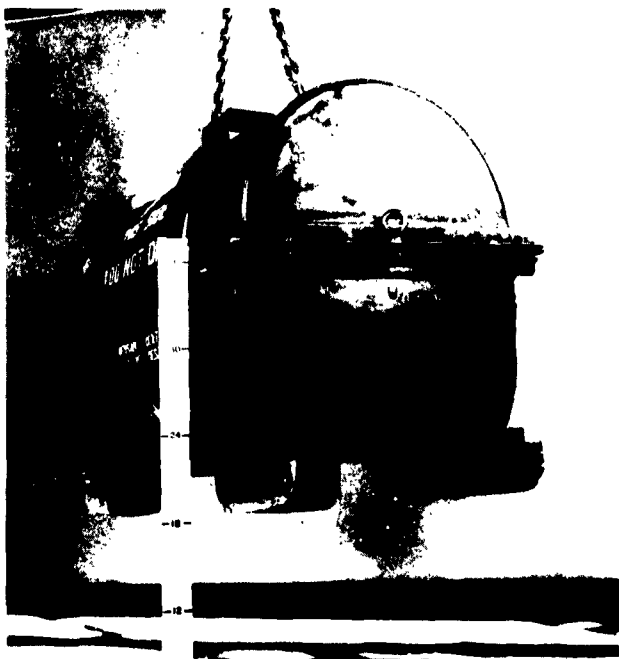


Fig. 8 - Flat wise drop test

of the pendulum) to clear the floor. The suspended container was pulled back with a straight, even pull until a height of 18 inches plus floor clearance measurement was reached. This measurement was taken from the measuring reference point on the container (center of balance) to the floor. Then the container was released in a manner to allow a smooth, even travel to the barrier.

Air Leakage—The air leakage test was repeated.

Test Results

After completion of the tests, the container was opened for visual inspection to determine whether there had been interference between the container and suspension system or between the container and contents during the tests.

Impacts are known in the study of mechanics as vector quantities. Therefore, they must be computed as such. A typical trace obtained from a drop test is presented in Fig. 9. Note that the deflection or trace of each accelerometer is called the component of the impact in the direction of, and with relation to, the

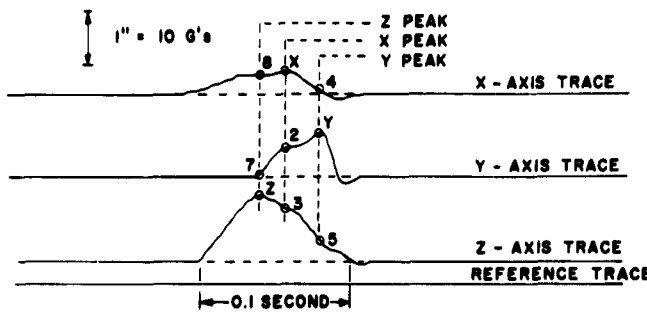
axis of the accelerometer. Determination of the impact (*g* value) that the package received on the drop was done by measuring the peak value on the X axis and corresponding value on the Y_2 and the Z_3 axis.

The resultant impact value was obtained mathematically by taking the square root of the sum of the squares of the three components.

The resultant impact value for corresponding Y- and Z-axis peak was determined by a similar method. Maximum *g* readings will not always appear in phase or close together. It is, therefore, necessary, if the peak values are not grouped close together, to check intermediate points for the maximum reading of impact load.

Table 1 presents representative peak shock values taken from each test. Significant relationship comparisons were proved for each axis.

In conclusion, test methods and values given serve as a guide in establishing drop-height requirements for various size containers. These methods and techniques are used by the laboratories of the Detroit Arsenal to assist in developing standards as well as evaluating container performance.



METHOD OF DETERMINING RESULTANT AT X PEAK:

CALIBRATION - G's / IN ↓ HEIGHT OF TRACE, INCHES ↓

$$X \text{ PEAK} = 10 (0.4) = 4$$

$$Y_2 = 10 (0.6) = 6$$

$$Z_3 = 10 (0.95) = 9.5$$

$$\text{RESULTANT} = \sqrt{x^2 + y^2 + z^2}$$

$$= \sqrt{4^2 + 6^2 + 9.5^2}$$

$$= 11.9 \text{ G's}$$

Fig. 9 - Calculation for determining resultant value

TABLE 1
Typical Test Results

Test	Engine Acceleration (in g Maximum)		
	Vertical	Longitudinal	Lateral
● <u>Edgewise drop</u> inches height 36	9.8	6.2	3.4
● <u>Cornerwise drop</u> inches height 36	8.4	6.4	4.2
● <u>Tip-Over</u> From bottom of left side	4.6	2.0	9.2
● <u>Flatwise drop</u> inches height 12	10.4	2.8	4.2
● <u>Pendulum impact</u> inches height 18	4.2	7.8	4.8

DISCUSSION

Mr. Sandler (Autonetics): I wonder if the input acceleration was monitored by the use of a low-pass filter?

Mr. Yee: We didn't use a filter system in our recording equipment.

Mr. Keller (White Sands Missile Range): I have both a comment and a question. Several years ago we at White Sands had the requirements to perform almost identical tests to these except we had the additional requirement of maintaining 5 psig throughout all our testing. We found out that by testing with this saturated soap and water solution we could not find the majority of the leaks. We finally had to go to a halogen leak detector and Freon 12, because we missed about 85 percent of these leaks by using water as a test. We had to drill holes into the side of the container to get our instrumentation cabling in there and we had to plug them back up again. My question is did you finally conclude from this test that the container was sufficient to withstand the tests you had given it?

Mr. Yee: I have tested quite a few containers and in answer to your first comment I more or less agree with you about using the bubble method in order locate leakage in the container. I only suggested that as an alternate method. Of course, if you had a facility, a water tank that is big enough to accommodate your package by all means that is by far the best method.

Mr. Keller: I can't agree with that. We actually couldn't find a pressure gage, sensitive enough to measure this low pressure change. We finally had to build an 8-foot open end manometer with which we could actually measure and resolve pressure changes of 0.07 psi.

Mr. Yee: We use a 15 psig pressure.

Dr. D. Rinde (TRECOM) Chairman: It's a question, perhaps of using greater pressure or more sensitive techniques.

Mr. Eustace (Martin Co): What is your opinion of the use of three accelerometers for

the end rotation test, corner drop test and the like, where we have considerable pitching and motions beyond the three classical translation modes. In other words, if you have three accelerometers located at the center of gravity of a system for other than a classical example how do you propose to get the maximum accelerations and therefore compute your maximum response? My point is that in our tests we have considered five as an absolute minimum for a survey as extensive as you claim you are conducting. In other words, one vertical on each end, one lateral on each end and a longitudinal in order to obtain what you might term the worse condition. Now, c.g. mountings may completely cancel out or not record any motion other than the pure translation.

Mr. Yee: I agree with you. The number of accelerometers you use mounted on your package, they will give you the best advantage. As a matter of fact, the three accelerometers, I would say that would be the minimum. You could actually locate the impact imposed on the package and anywhere in the package as you desire and you could use as many as you desire but I would say three would be the minimum.

Mr. Eustace: Providing you had a minimum of three may I ask would you still want them at the c.g. as opposed to say the end of the container which will see the worst pitching response in unusual end rotation or corner-wise tests?

Dr. Rendi: I believe Mr. Yee did make that point that they should be in as close to the c.g. as possible.

Mr. Breen (Aeroflex Labs.): I may have missed the point but as a matter of interest was the fragility factor for the engine established and how did the engine itself fare? Did it sustain damage in these tests?

Mr. Yee: We tested a number of engines and transmissions. After the impact test we installed the transmission in a truck, performed a load test and found it functioned satisfactorily.

SIMULATION OF RAIL CAR COUPLING ENVIRONMENT

W. H. Brown and R. L. Dyrdahl
The Boeing Company
Seattle, Washington

This paper uses the experience of the Mobile Minuteman System to present an example of simulation in both analysis and test in establishing the proper test procedure and configuration. The dependence of test on analysis is shown by an example and the increased value of tests developed from analysis is illustrated.

INTRODUCTION

A discussion of valuable cargo shipment with a railway official disclosed a reluctance to ship more than a single extremely valuable car per train with present equipment and operations. For Mobile Minuteman the rail transport equipment and operation must remove the risk to trains made of extremely valuable cars. Standard practice in the rail industry urges the use of long established test procedures for operational simulation. These procedures have proven adequate for many systems since their introduction but are not suited to trains with extremely valuable cars. Efficient system development for equipment of greater size, complexity and reliability requires both analysis and test, with simulated cargo and simulated environment, which are thorough enough to investigate all areas of concern to the system operation.

The Mobile Minuteman tactical cars, consisting of missile cars, a power car and a command car, are designed to transport, protect, erect and fire a Minuteman Missile. The weapons system requirements for continuous operation, high reliability, rapid erection and accurate firing demand a high degree of tactical car protection from excessive loads and accelerations. In addition missile performance cannot be compromised by designing for ground handling, hence the missile car design must reflect the effect of low allowable missile loads. The equipments to perform these functions result in rail car weights 1.5 to 2.0 times the weight of normal freight cars. Though several types of rail cars are required for the Mobile

Minuteman this discussion will be limited to the missile car. The major components of the missile car are shown in Fig. 1. The missile is supported in a protective erectorable structure called a strongback. This strongback is supported vertically at three points, and longitudinally at the trunnion on the floor of a car externally resembling a railway baggage car. The car body is mounted on "soft ride trucks" of 10 inches equivalent static displacement. The longitudinal impact is transmitted through both a rubber draft gear and a cushioning unit connected by a "sliding center sill" column.

TEST METHODS AND SIMULATION

The original proposals for rail car impact testing consisted of two railroad "industry practice" methods; first, the AAR "Recommended Procedure for Conducting Field Impact Tests of Loaded Freight Cars" and second, a "ramp test" with extensive instrumentation. The AAR test, as shown by Fig. 2, consists of impacting a test car into a string of five empty cars, stretched to maximum length, on level track with the brakes set. The ramp test, shown in Fig. 3, used a stationary test car with brakes set, on a level track impacted by a loaded car (210,000-pound maximum) brought to velocity by a ramp.

Examination of these test configurations and procedures for use in the Mobile Minuteman impact tests raised questions of whether the test mass was large enough to simulate operations with the heavy missile car and whether the simulation of multiple cars would produce

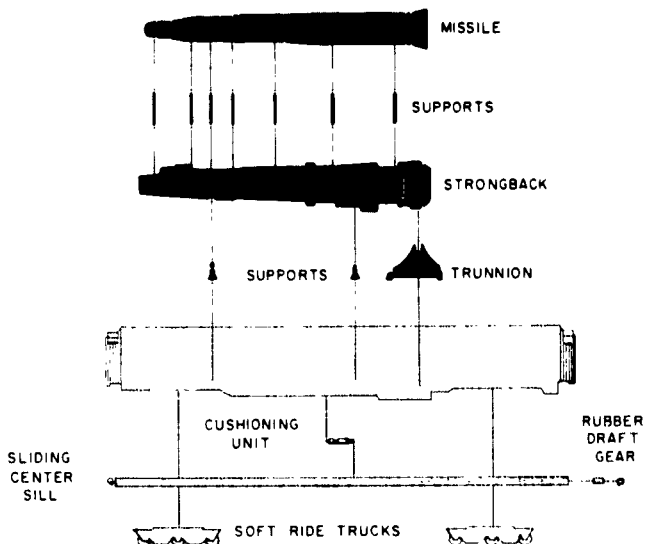


Fig. 1 - Missile car components

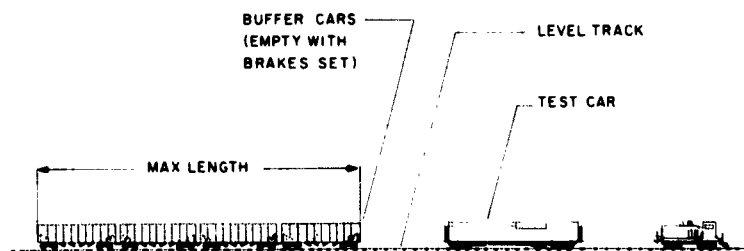


Fig. 2 - Recommended field impact test of loaded freight cars

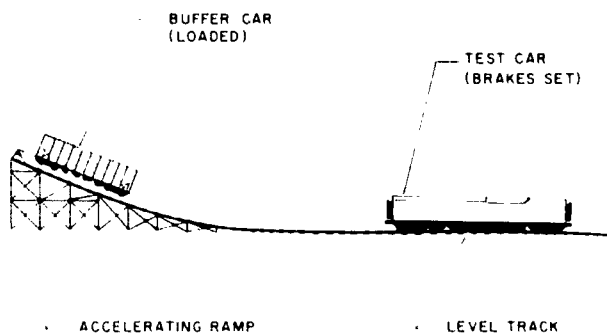


Fig. 3 - Recommended laboratory test

a missile response that could be considered representative of Mobile Minuteman system operation. The evaluation of these effects by testing was not feasible for reasons of cost and time, so dynamic analyses were conducted

prior to testing to select the critical test configuration. In addition to determining test procedure, the analyses allowed study of the proposed "sliding center sill" cushioning unit characteristics.

The dynamic analysis necessitated methods that were capable of investigating the required number of degrees of freedom, variation of boundary conditions and the use of nonlinear components. The analysis used idealized model simulation and dynamic environment simulation which were adequate to express system response under operating conditions. The selection of the idealized model and environment simulations require knowledge of both the rail transport system and the available simulation systems. Knowledge of the rail transport system is required to facilitate construction of idealized models and to choose reliable input containing all major interactions between the railroad system and the missile system. Knowledge of the available simulation systems is required to choose the best methods and models to accomplish the analysis as inexpensively as possible within the time schedule of the design.

For the Minuteman system simulations, mathematical, electrical and physical analogies were used. The work was accomplished in four phases. The first and third phases utilized the PACE differential analyzer (Appendix A) to solve the equations of motion of an idealized structure. The second phase used the CEA (Computer Engineering Associates) direct structural analog (Appendix B) to build an idealized car structural model with analogous electrical quantities to study one car loads and motions. The fourth phase used the available full scale car components and simulated missile system weights in a test program to substantiate the analytical methods and prove the acceptability of car components.

Dynamic Analysis, First Phase

In the first phase simulation on the PACE differential analyzer, a two mass idealized missile car was used as shown in Fig. 4. The car mass was connected to the sliding center sill mass by a spring and damper simulating the characteristics of the longitudinal cushioning unit. External forces were applied to the sliding sill beam through a spring and damper simulating the characteristics of the coupler. The equations of motion for this idealized system were written and entered into the PACE differential analyzer by simulation of equation components. In order to expedite preliminary answers and establish analysis technique the circuitry was simplified for the first phase only by not using the wheel friction force, coupler slack and bottoming capability of the cushioning unit.

This analysis consisted of longitudinal motion only, i.e., no vertical or pitch freedom was included. The car was brought to a constant velocity and the coupler impacted into a rigid stop (an infinite mass). Pulse shapes for various cushioning unit parameters were established for use in second phase simulation.

Dynamic Analysis, Second Phase

The second phase of the simulation was conducted on the CEA direct analog to determine missile loads and accelerations plus the effects of vertical and pitch degrees of freedom. The idealized model for use in the CEA analog, shown in Fig. 5, actually consisted of two models; one for vertical and pitch motion and the other for longitudinal motion with interconnections to permit cross excitation. Each model used an array of mass segments connected by springs and hinges to simulate stiffness. The pitch vertical motion system simulated translational and rotational inertias of each segment while the springs and hinges transmitted moment, vertical forces, rotation and vertical motion between segments. The longitudinal system contained segments to simulate the translational inertia while springs transmitted longitudinal motion and forces. The electrical simulation of the idealized structure was accomplished by direct substitution of electrical components for mass, stiffness and geometrical parameters. Excitation of the system could be accomplished at any point by application of currents or voltages proportional to motion or force but the primary excitation point for this study was the cushioning unit connection to the car floor. Output also could be read at any point in the circuit as current or voltage with a meter or oscilloscope. For transient phenomena, such as coupling impact, the input was a pulse with the response output defined by an oscilloscope trace, and photographed.

A series of longitudinal pulse studies simulating various impact velocities were conducted on the direct analog (CEA). Pulse shapes determined in the PACE analysis were used for input in the CEA analog. In addition to obtaining missile loads and accelerations for the various impact velocities, the results showed primarily rigid body longitudinal response of the car, strongback and missile with only negligible excitation of vertical and pitch motions. These results were significant because they proved that the two rigid bodies with only longitudinal motion freedom as assumed for the PACE analog analysis were sufficient.

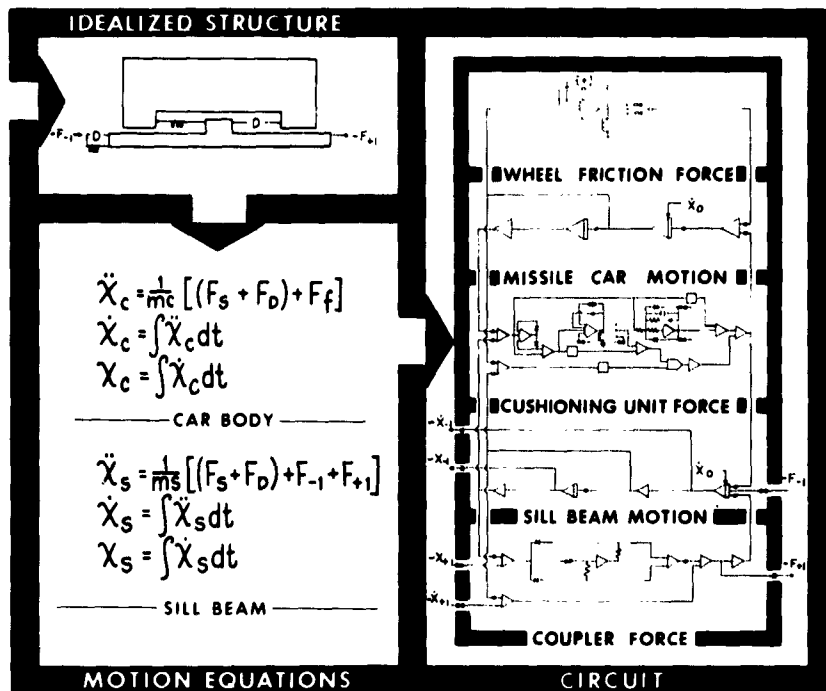


Fig. 4 - Differential analog simulation

Dynamic Analysis, Third Phase

The third phase of the simulation was conducted on the PACE analog after the basic method had been verified by the complex CEA analysis. The basic components of the idealized model and analogous circuit were shown in Fig. 4. The analog circuitry was expanded beyond that used in the first phase to include additional buffer cars, a braking force, coupler slack components and bottoming capability of the cushioning unit. The series of cars could be arranged in any order and impacts could be studied to determine car response. Boundary conditions were imposed on each car and as the coupling occurred the energy transfer of the cars could be recorded.

A series of car arrangements, as expected, produced a wide variation of test car response as illustrated by Fig. 6. Also, as expected, the case of the test car impacting a solid wall produced the maximum response. This condition was studied only as an extreme upper limit to be used for comparison with conditions to be expected in service. Configurations consisting of loaded cars striking a parked test car, and a

test car striking loaded parked cars, were studied. The broad band shown in the middle of Fig. 6 is formed by these studies. The upper band edge represents three tactical cars impacting a parked test car while the lower edge represents a test car impacting three parked cars.

The lower curve of Fig. 6 shows the results of the study of the proposed ramp test with a 210,000-pound impact car. These results show that the ramp test is a much less severe test than the above conditions. The study of the ramp test was extended using successively heavier impact car weights to find an acceptable test configuration. It was found that the required impact car weight had to be 2 to 3 times the weight of the test car to achieve a test car response in the hardest operational impact area. Large single cars were not available for this test and the ramp size did not permit multiple cars. Therefore, the ramp test was unsatisfactory.

Maximum coupling acceleration versus weight ratios of buffer cars to test car, for various velocities, is shown in Fig. 7. The importance

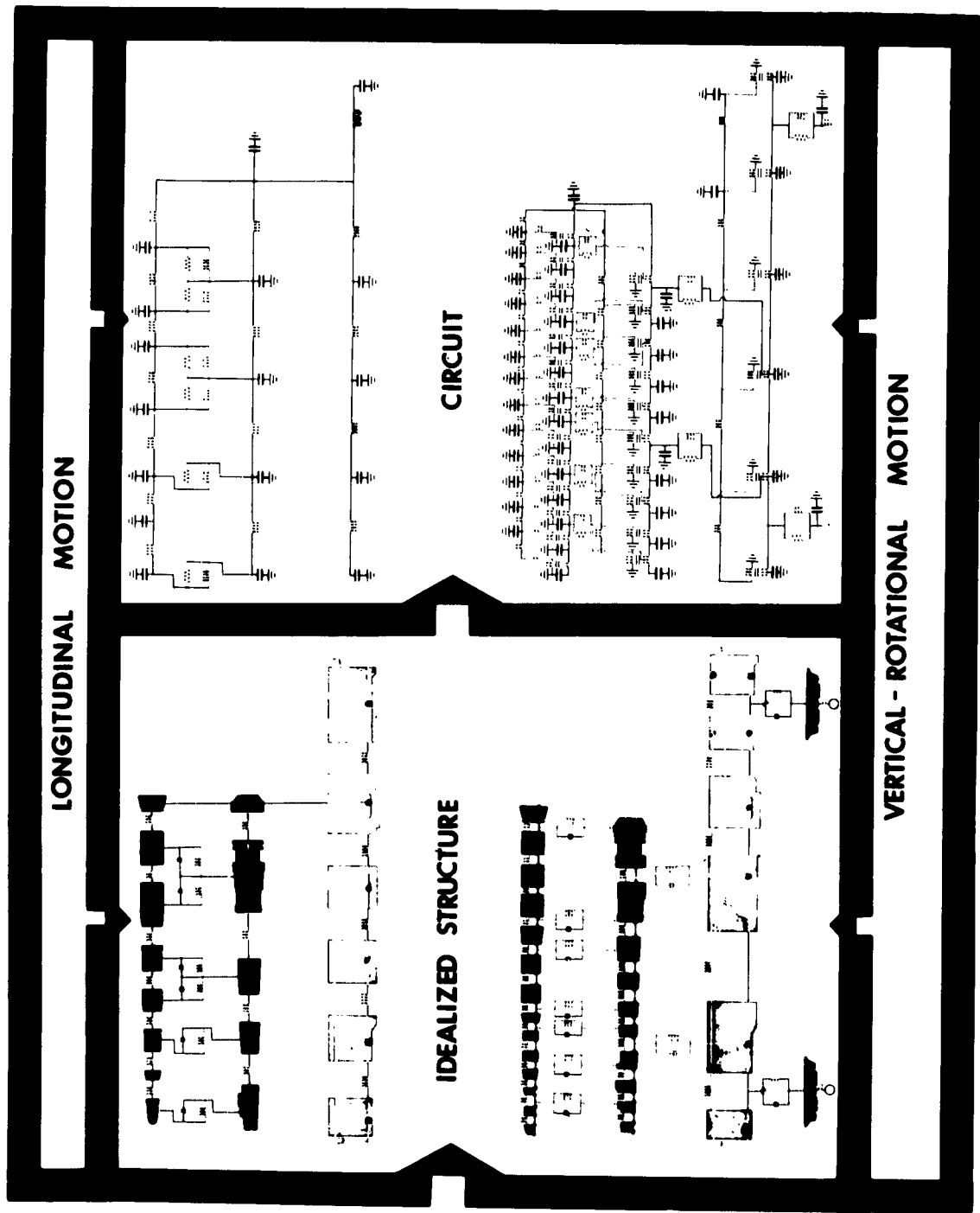


Fig. 5 - Direct electrical analog simulation

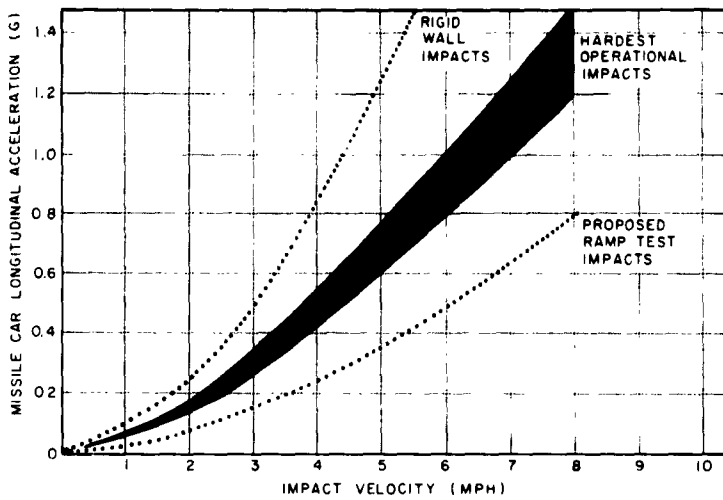


Fig. 6 - Analog impact study comparison

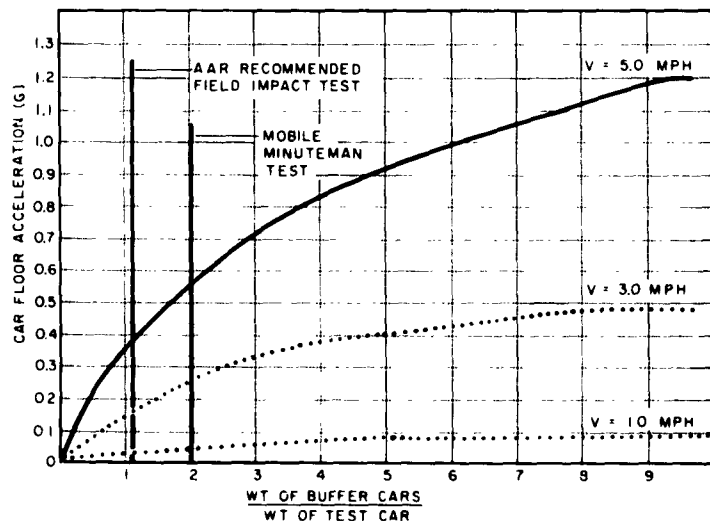


Fig. 7 - Coupling weight ratio comparison

of train size during coupling operation is illustrated by this plot as well as the necessity of considering operational procedures. The size of the Minuteman trains made a choice of weight ratios of 2.0 acceptable for test simulation. It is evident that longer trains with high-

impact velocities should use a larger weight ratio for test. Since the weight of buffer cars for the AAR test is constant, the ratio for different weight test cars vary and the recommended value shown applies only to the missile car. The lower weight ratio of the AAR test

coupled with the attenuating effects of coupler slack resulted in classifying this test as unsatisfactory for Mobile Minuteman.

Full Scale Tests

The fourth phase of the simulation consisted of a full scale test with simulated cargo and simulated dynamic environment. The procedure and configuration of the "flat switching test", shown in Fig. 8, was established from the previous three simulation phases. The 315,000-pound test car was to be impacted into a string of buffer cars consisting of a 210,000-pound car with rubber draft gear backed with three gondolas loaded to 169,000 pounds with brakes set and no slack between buffer cars.

Since the preparations for the ramp test, with a 210,000-pound impact car, had been completed at the same time as the analysis, and since the test would provide needed design confirmation, the noncritical "ramp test" was completed prior to the critical "flat switching" test. Comparisons, shown in Fig. 9, between ramp and flat switching tests showed the predicted increase in car floor acceleration and sliding sill travel.

Comparison of actual and predicted cushioning unit force versus stroke is shown in Fig. 10. The high degree of correlation between analytical and actual cushioning units established confidence in the analytical simulation. The shape of this curve and the area

beneath it are both of importance dynamically as they relate to the energy exciting the car dynamic motion. The product of acceleration and sill travel from the previous comparison is also a rough indicator of energy. Since the product for flat switching is consistently greater than the ramp test this product is indicative of a more severe test. The shape of the curve in Fig. 10 and the nominal increase in acceleration and sill travel shown in Fig. 9 verify that the cushioning unit is efficient over a range of impulses. Further confidence in the analysis is established by peak car floor accelerations shown in Fig. 11. Comparison of test points with the analysis curve show the analytical predictions to be approximately 10-percent high for a wide range of impact velocities. Both predicted and test accelerations are comparable with the stringent requirements put on the missile car by the missile.

CONCLUSION

The analysis permitted evaluation of the effects of test car weight and weight of buffer cars, coupler slack, and brake settings. As a result the Mobile Minuteman development was expedited and confidence in realistic design was established.

The results of the study show the necessity of reviewing standard coupling test procedures when considering a new rail car design and show the value of analytical simulation in establishing the proper test configuration.

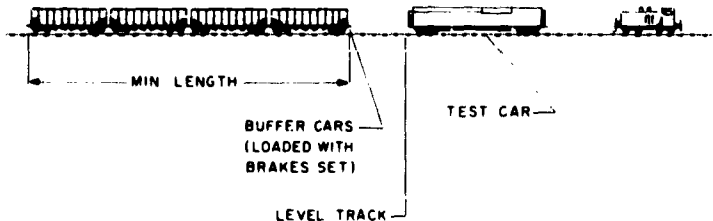


Fig. 8 - Flat switching test

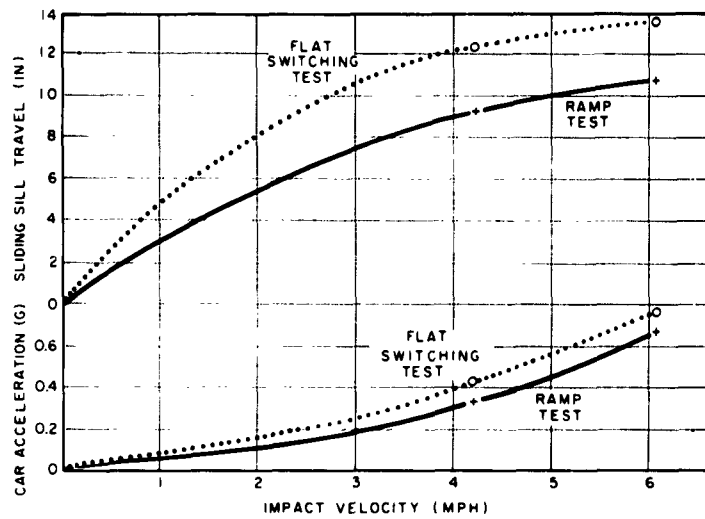


Fig. 9 - Ramp and flat switching test comparison

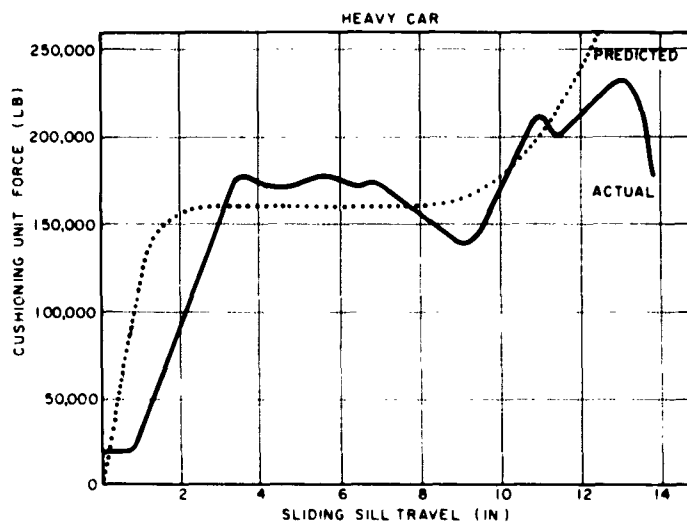


Fig. 10 - Analog experimental data comparison

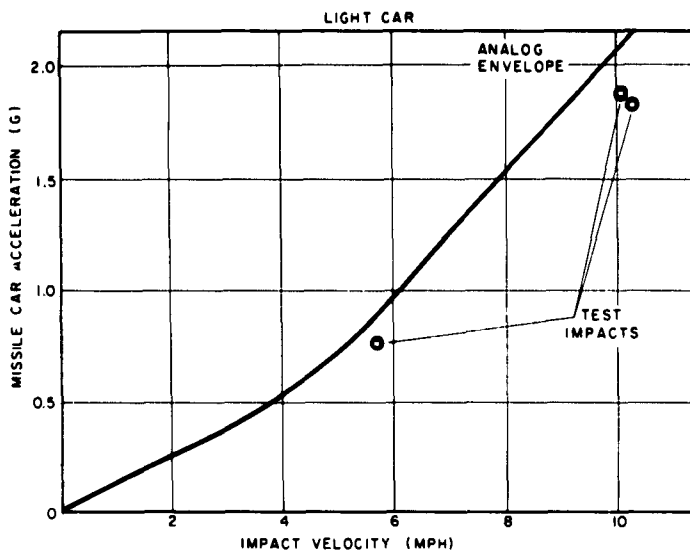


Fig. 11 - Analog experimental data comparison

APPENDIX A Differential Analog Simulation

A differential analog contains circuitry analogous to mathematical equations. To use the differential analog in simulation requires that a physical system be visualized as an ideal model whose actions can be described by mathematical equations which may be simulated in

the analog. Voltage measurements of the circuit are proportional to the mathematical term simulated. Table A1 identifies the components used in the Minuteman example while Table A2 identifies the mathematical analogies of portions of the example circuit.

TABLE A1
Components and Symbols used in Analog Simulation

Symbol	Name	Symbol	Name
	Summing amplifier		Capacitor
	Integrating amplifier		Ground
	Multiplier		Inductor
	Potentiometer		2-Pole switch
	Function generator		Diode
	High-gain amplifier		Zener diode
			Resistor

TABLE A2
Mathematical and Electrical Analogies

Circuit Component	Function	Equation Component
	$C(t)$	$= - (A(t) + B(t))$
	$C(t)$	$= - \int (A(t) + B(t)) dt$
	$C(t)$	$= A(t) \times B(t)$
	$B(t)$	$= k A(t) \quad 0 \leq k \leq 1.0$
	$B(t)$	$= f(t)$
	$B(t)$ $B(t)$	$= C(t) \quad A(t) < 0$ $= D(t) \quad A(t) > 0$
	$B(t)$	$= A(t) $
	$B(t)$ $B(t)$	$= Ck_1 \quad A(t) < 0$ $= Ck_2 \quad A(t) > 0$
	$B(t)$ $B(t)$	$= \pm A(t) \mp \frac{a}{2} \quad A(t) < \frac{a}{2}$ $= 0 \quad A(t) > \frac{a}{2}$

APPENDIX B
Direct Electrical Analog Simulation

A direct electrical analog contains electrical components analogous to structural values of spring rates, damping, mass and rigid beam lengths. To use the direct electrical analog in simulation requires that the physical system be idealized in a mental model and model components converted to circuit components. The electrical mode analogy used in the Minuteman example inherently contains the physical-electrical analogy expressed mathematically as follows.

$$C \frac{de}{dt} + \frac{1}{R} e + \frac{1}{L} \int e dt = I(t)$$

$$m \ddot{x} + c \dot{x} + kx = F(t).$$

From this mathematical expression it is evident that force, acceleration and displacement may be obtained by measuring current in the appropriate portions of the circuit and applying proper scale factors while velocity may be derived by measuring the appropriate voltage and applying the proper scale factor. Either voltage or current inputs or outputs may be used dependant on the analogous quantity desired. Table B1 shows the analogous structural-electrical model components.

TABLE B1
Direct Electrical Analog Simulation

Electrical		Structural	
Symbol	Name	Symbol	Name
	Resistor (R)		Damper (c)
	Inductor (L)		Spring (k)
	Capacitor, ground (C)		Mass (m)
	Transformer		Rigid beam segment
	Node		Joint

* * *

Section 4

DESIGN OF CONTAINERS AND TRANSPORTERS

DESIGN AND ENGINEERING EVALUATION TESTING OF THE TERRIER MISSILE SHIPPING CONTAINER

R. L. Munson
General Dynamics, Pomona
A Division of General Dynamics Corporation

A complete story of the development of the Terrier shipping container is given, including establishment of design criteria, design of container and shock isolation system, and the test and evaluation program.

INTRODUCTION

The design of guided missile containers is an important and increasingly complex aspect of the missile engineering field. The technology of missile containers advances not only through research and creative design but also, and perhaps equally, by the exchange of ideas and information throughout the industry. It is hoped that this paper describing the design and evaluation of the Terrier shipping container will contribute to this exchange.

THE CONTAINER DESIGN PROBLEM

Missile Configuration

The Terrier logistic system requires that the same basic container be suitable for shipment and storage of the following missile and missile component configurations:

- The Terrier BT-3 Missile is approximately 13-1/2 inches in diameter and 168 inches long (Fig. 1 (a)). There are handling attachments clamped on at two locations along its length which are used in conjunction with the missile strikdown equipment aboard combat ships. The control surfaces at the aft end of the missile fold over for compactness. They are erected just before launch. Four dorsal

fins extend along the mid portion of the missile. They are located radially in line with the tail control surfaces.

- Bipack: The forward and aft guidance sections are joined by means of a connector ring to form a unit called the guidance and control group or "bipack," (Fig. 1(b)). The bipack and four dorsal fins form the General Dynamics unit for shipment to the assembly depot. The bipack is approximately 13-1/2 inches in diameter and 55-1/2 inches long. Two bipacks are shipped in each container.

- The Sustainer Rocket Motor (Fig. 1(c)) is 13-1/2 inches in diameter and 54 inches long. Two rockets are shipped in each missile container.

Missile Severe Environment Capabilities

The Terrier Missile and its components can withstand the following severe environments:

- Shock: Up to 30 g in vertical and lateral directions and 10 g in longitudinal directions.

- Vibration: The missile can withstand steady state vibrations (period of 1 hour) in the range of 2 to 25 cycles per second at peak inputs up to 4 g and vibrations in the range of

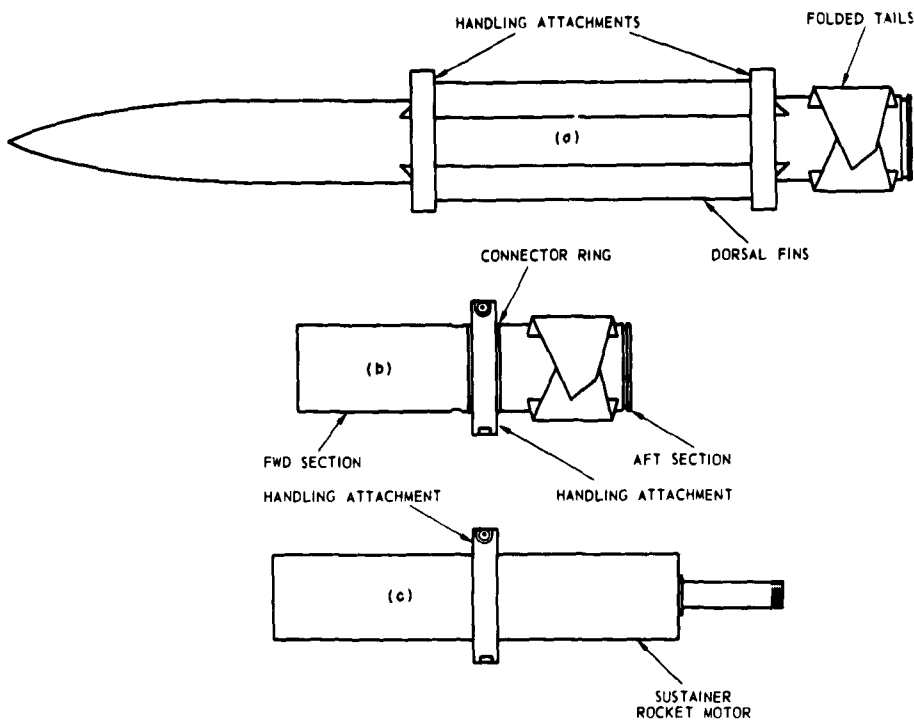


Fig. 1 - Terrier Missile and missile component configuration; (a) the missile, (b) the Bipack, and (c) the sustainer

25 to 300 cycles per second at peak inputs up to 1/2 g.

- **Humidity:** Up to 40 percent R.H. for long storage periods. (Up to 5 years with 6-month maintenance periods.)

- **Temperature:** -65°F to +160°F.

Container Requirements

The container must be capable of protecting the missile from environmental conditions which exceed those which the missile can safely withstand. In order to assure the ability of the container to do this (without a gross amount of over protection and resultant cost), the severity and frequency of occurrences of all of these conditions must be predicted as accurately as possible. Under a separate BuWeps contract General Dynamics, Pomona conducted an extensive survey in this field. As a result of this survey, it was possible to forecast many of the hazards in the Terrier transit and storage system. It has been possible to estimate the approximate height of accidental drops and

to determine the critical vibration frequencies and amplitudes of boxcars, trucks, airplanes, and ships. The amount of moisture that may be taken into a nonpressurized missile container due to breathing through pressure release valves under tropical conditions has been determined and maximum humping velocities during railroad shipment have been estimated. For practicality these environmental conditions have been essentially duplicated by laboratory tests such as drop tests, vibration tests, leakage tests, etc.

In addition to providing protection, the container must satisfy the missile system logistic requirements and limitations. Width is limited to 27-inch maximum for ease in boxcar loading and height must not exceed 38 inches for storage aboard ammunition ships where there is limited head room for stacking. Weight must be held to a minimum consistent with structural requirements. The lid must be light enough to be lifted by two men. The container must be compatible with all of the lifting and moving devices in common use in the logistic system.

The Design Approach

The design approach consists mainly of decisions. These decisions are concerned with the choice of materials, the shape, the shock isolation system, and the method of closure.

Some of the materials considered in the design approach phase of the Mk 199 container were plywood, plywood faced with steel, plywood faced with aluminum, aluminum honeycomb, aluminum sheet, and steel sheet. The material affects the weight of the container and the method of fabrication. Furthermore, in the selection of the material for the container its availability must be considered. Are stock sizes that are compatible with manufacturing practices readily available? Would the material be critical in times of war?

Some of the container configurations considered were round end opening, rectangular clam shell, rectangular top opening, and round clam shell.

Three complete shock isolation systems were studied and analyzed before a selection was made. One of these was a completely external shock mounting system. The container would be placed into a shell and the shock mounts would connect the shell to an external frame so that the frame could be removable for storage and added for shipment.

There were no obvious choices in any of these areas of design decision. Extensive research and investigation was required in each area. Materials and processes specialists were consulted. Conferences were held with Factory and Tooling representatives. Dynamics design specialists analyzed the dynamic characteristics of several shock mount systems, and the Stress and Weights engineers studied many structural configurations. In each area of decision, the processes of evaluation, elimination, and compromise were conducted and often repeated until decisions were reached. There were parallel design efforts in some areas where decisions could not be made at the beginning of the container design program.

Having reached decisions in all of the aforementioned major or basic design areas, the proposal drawings were prepared and reviewed by the cognizant group of the Navy BuWeps. Their comments, suggestions, and objections were noted and their preliminary design approval was given.

THE CONTAINER DESIGN

Polyurethane foam was selected for cushioning the missile against shock and vibration. For those not familiar with this material, it is a cellular expanded plastic foam which resembles sponge rubber in appearance and behavior. Had this material been used alone, the missile would have been supported throughout its length. There were, however, objections to this method of cushioning. The effective spring constant of the foam increases as the impact velocity of the cushioned item is increased. Or, to explain further, if one applies a relatively slow, steady pressure on a block of polyurethane foam there is little resistance; but, if one strikes the foam suddenly and forcefully, he will feel a considerable amount of resistance. This in effect means that dynamically, the foam material is a hard spring. The obvious correction for this was to decrease the area of the foam under the missile and, thereby decrease the magnitude of the dynamic resistance. This was done. Instead of full-length support, the missile was supported on individual blocks of polyurethane foam, each measuring 10x10x8 inches thick. But there was another problem. The static load carrying ability of polyurethane foam is low. Hence, the static weight of the missile caused an excessive amount of initial deflection, so that there remained little or no deflection distance to absorb handling shocks. Apparently solving one problem created another. If the amount of bearing area was made large enough to keep the initial or static deflection low, then the cushion became extremely hard; that is, it developed too high a spring constant under dynamic or drop load conditions, and the missile would have been subjected to excessive "g" loads. To effectively use polyurethane foam cushioning, which offers excellent dampening and dynamic characteristics, it is necessary to support the static load or weight of the missile by some different means which will allow the missile to deflect under drop loads. There was also the problem of restraining the missile against fore and aft motion in the container. It was decided that the two problems could be solved at once. Figure 2 shows how it was done. The handling attachments were excellent support points. They are clamped around relatively "hard" spots along the missile structure, and their square shape makes them easy to hold. By sliding them into channels, and restraining the channels against fore and aft motion, the missile was itself restrained fore and aft. The next step was to restrain the

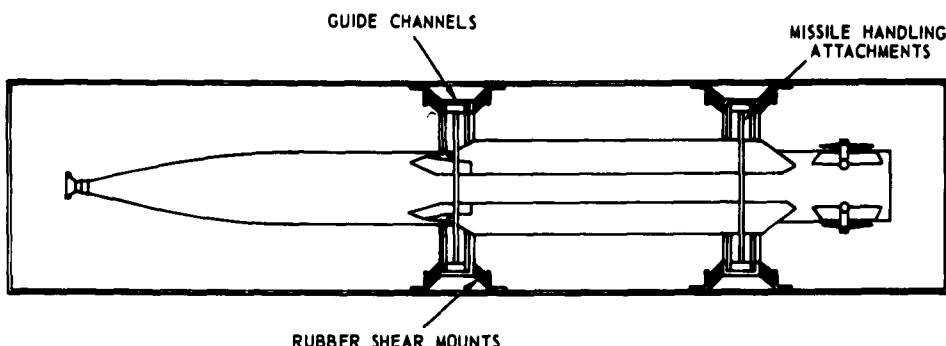


Fig. 2 - Missile on rubber shear mounts

channels against fore and aft motion and yet permit vertical and lateral deflection. The rubber shear mount or "Lord" mount was the answer. When used as shown, the mounts supported the missile statically. They deflected vertically and laterally in shear but not in compression. Shear mounts having a spring rate of approximately 450 pounds per inch at ambient temperature were designed. Eight of these mounts were used, four at each handling attachment guide channel.

The first step in constructing the container or "structure" was the basic shell, the means of enclosing the missile. The container is nonpressurized, but it must still be sealed within certain leakage limits. If the assembly is enclosed in a trough shaped aluminum sheet and the top is closed off with a lid and a lid joint seal, then the missile will be effectively enclosed. Figure 3 shows a pictorial view of this shell without the lid and it can be seen that it resembles a deep trough. The shell is composed of three skin sections and two deep drawn ends.

The method of joining the skins is of considerable interest: Doublers are employed at the skin joints and the skins are riveted to the doublers. Sealing the joint is accomplished by the use of an epoxy-impregnated tape between the doubler and skins which, after a heat cure, forms not only a tight seal but a structural bond which approaches the metal itself in shear strength. This bonding process is used extensively in the construction of the Convair B-58 Hustler and the 880 and 600 jet transports.

At this point in the design, the missile was shock mounted and fully enclosed in an aluminum shell. The shell had little strength or

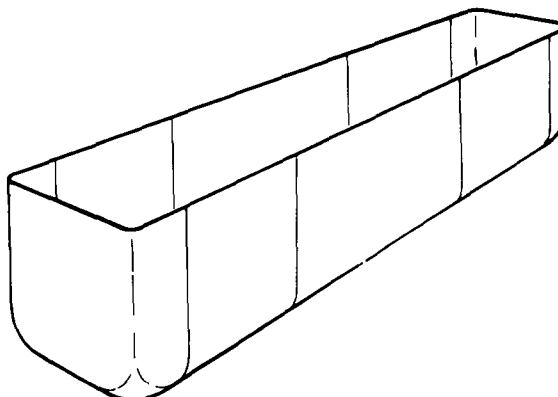


Fig. 3 - Container shell structure without lid

rigidity, however, so the design had to be elaborated so that the container was capable of withstanding the rough handling tests in the engineering evaluation program and, subsequently, the environmental conditions in the transit and storage system. To provide a fully adequate structure and yet keep overall weight at a minimum there had to be, as nearly as possible, complete utilization of all materials in the container. The top extrusions, with their relatively large cross-sectional areas, were adequate as stiffeners for the rim around the top of the container (Fig. 4), and the channels were strong enough to prevent the sides of the open container from bowing in the area of the center of the container span. The skin could be made to work in tension to add beam strength to the container, so all of the material in the container could be put to work structurally.

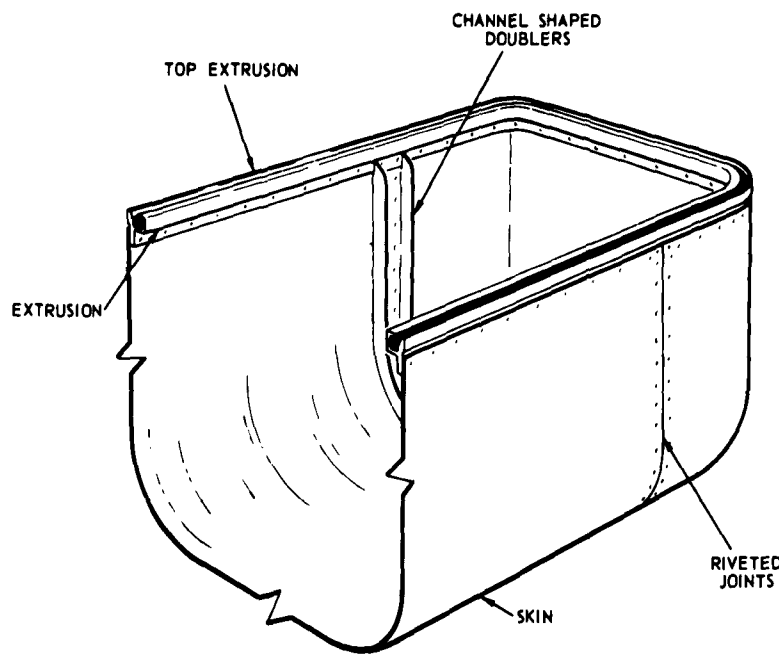


Fig. 4 - Container basic shell structure

Figure 5 is a side view in outline of the container, as it would appear at the instant of impact during a rotational flat drop. Consider the container as a beam supported at each end. The points at which the weight of the missile are being carried are located somewhat near the center of the span of this beam, particularly the forward handling attachment which is near the missile c.g. Obviously, there must be a structural member added to the skin to provide beam

strength. Looking now at Fig. 6, it can be seen that by adding heavy gauge stringers along the entire length of the missile and joining them to the skin as shown, there will be box sections formed which are excellent beam members. By cross-connecting the stringers at the bottom of the containers and the extrusion at the top, the whole container becomes a structural beam of box section with the container skin working as a shear web. This cross-connecting is

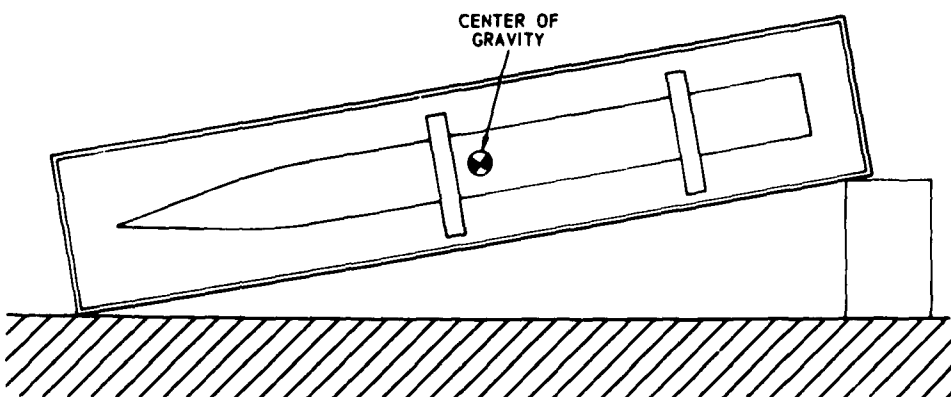


Fig. 5 - Container shown as simple beam

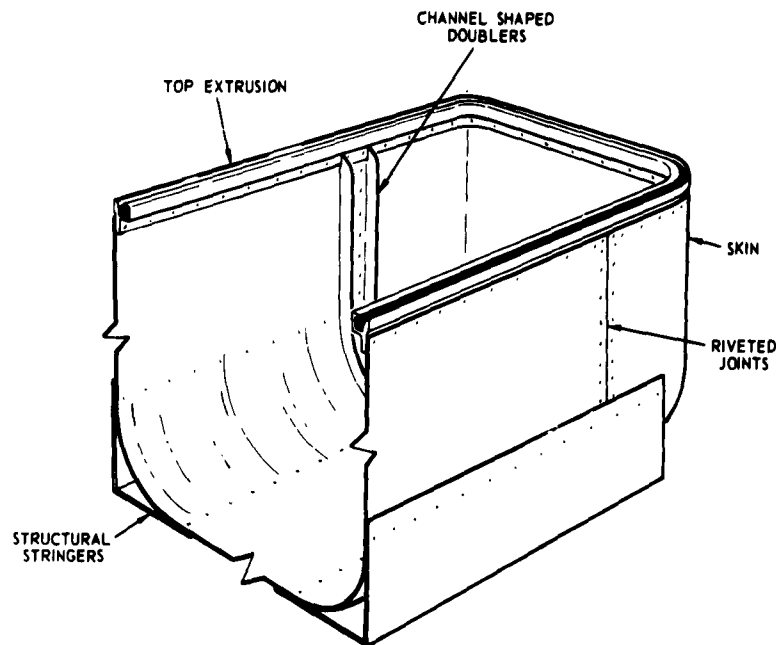


Fig. 6 - Basic shell structure with structural stringers

accomplished partly by the channels or doublers already mentioned, and by the steel angles by which the handling attachment guides are mounted through the shear mounts on the container structure.

The container without support from the lid is structurally capable of withstanding all of the anticipated rough handling shock and vibration loads. Any structural contribution made by the lid is an added strength margin. It has been mentioned in the system requirements that the lid must be light in weight so that it can be lifted easily by two men. As described earlier, the cross-section of the lid extrusion had already been determined. It was now necessary to provide a panel to span the area of the lid. A single thickness of aluminum sheet could do the job, but the lid would be flimsy and would require several cross members to prevent buckling or "oil canning." An aluminum-faced honeycomb panel provided the answer. This panel provided almost complete rigidity so that no cross-members were required, and it resulted in a lid weight of 120 pounds, considerably less than the 150 pounds allowed. The aluminum facing was bonded to the lid extrusion (Fig. 7). Figure 8 shows the complete Mk 199, Mod 0 container with Terrier missile.



Fig. 7 - Bonded lid construction

THE ENGINEERING EVALUATION TESTS

The engineering evaluation tests were designed to simulate as nearly as possible the environmental extremes that were anticipated in the storage, transit and handling of the missile in the logistic system.

Rotational End Drop Tests

All drop tests were conducted at ambient and at high (+165°F) and low (-65°F) temperatures. The loaded container was supported at one end of its base by two blocks — one block approximately 5 inches high under one corner and the other approximately 11 inches high under the other corner. The opposite end of

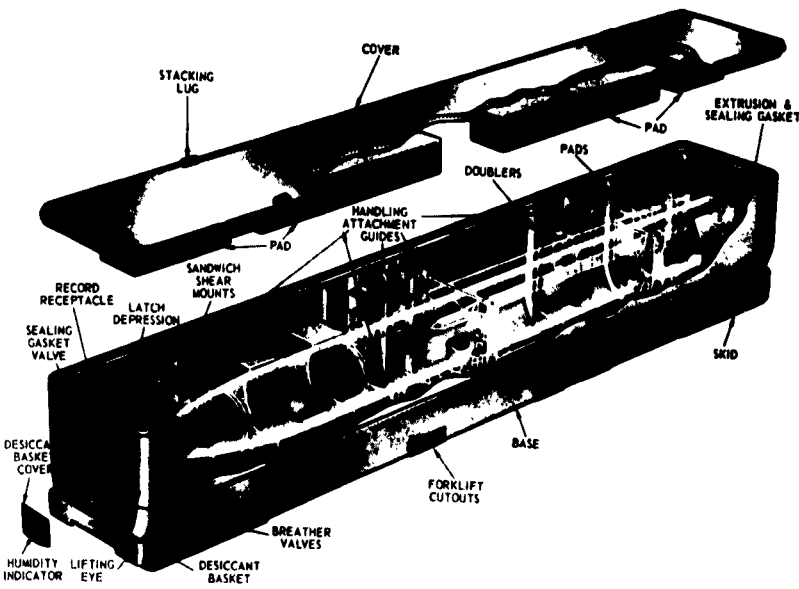


Fig. 8 - Missile container with Terrier Missile

the container was raised so that the lower corner (the one diagonally opposite the 11-inch block) was raised 18 inches off the concrete floor (Fig. 9).

The container was then allowed to drop to the floor. This procedure was repeated for each end of the sides and bottom for a total of six drops.

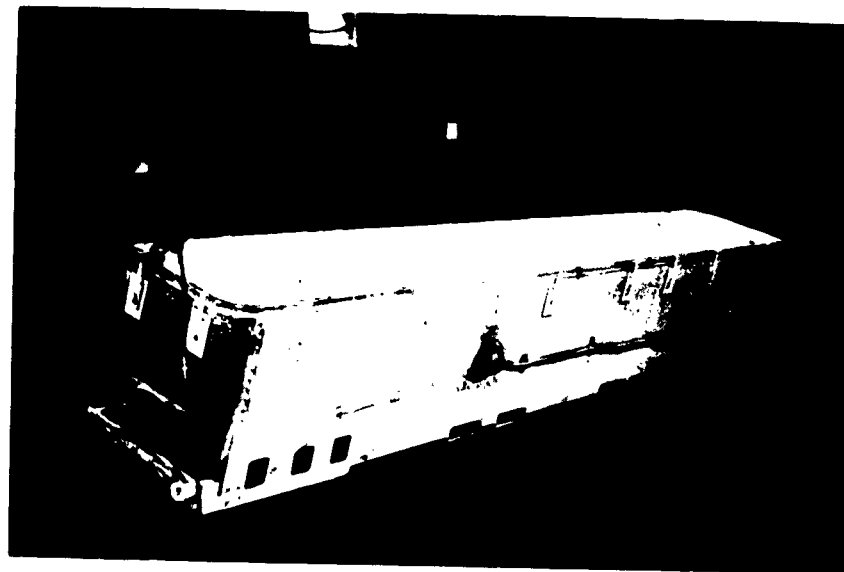


Fig. 9 - Rotational end drop test

Roll-Over Test

The roll-over test consisted of tipping the loaded container slowly sideways until it fell by its own weight to one of its sides. This was repeated with the container rolling from its side to its top to its opposite side and back to its base. Crystal accelerometers were mounted on the missile inside the container and shock traces were permanently recorded by a recording oscilloscope.

Vibration Tests

The test specification required that the container be subjected to vertical forcing vibrations over the range of 2 to 300 cps. The magnitude of vibration input was 1 g or 1-inch total displacement. Input accelerations to the container and accelerations transmitted to the missile were recorded at each frequency step to determine resonant frequencies. It was further required that the container be subjected to continuous vibration for 1 hour at each resonant frequency. Vibration input was supplied by hydraulically actuated platforms at each end of the container (Fig. 10). The vibration tests disclosed a design deficiency. The container shock isolation system was designed to provide a soft cushion for the missile which resulted in a system resonance of 8 to 10 cps. Vibration

amplification at this frequency was in excess of that permitted by the test specification. Amplification in this resonant area was so severe that the "rubber" sandwich shear mounts overheated and fractured in periods as short as five minutes. The condition was corrected by adding frictional damping devices at each handling attachment guide position. These frictional dampers reduced the amplification factor to below the specified maximum.

Box-Car Impact Test

Loaded containers were stacked 3 high and installed with inflatable dunnage bags* into a standard 40-foot boxcar. The contents of the containers were instrumented to record shocks in the direction of the boxcar travel. The loaded boxcar was then caused to impact against two stationary boxcars at a velocity of 12 mph. The impact was repeated with the loaded boxcar striking from the opposite direction. The shocks experienced by the containers and their contents

*Recent boxcar impact tests conducted under BuWeps direction have indicated that the inflatable dunnage bags are not required for shipment of the MK 199, Mod 0 containers.

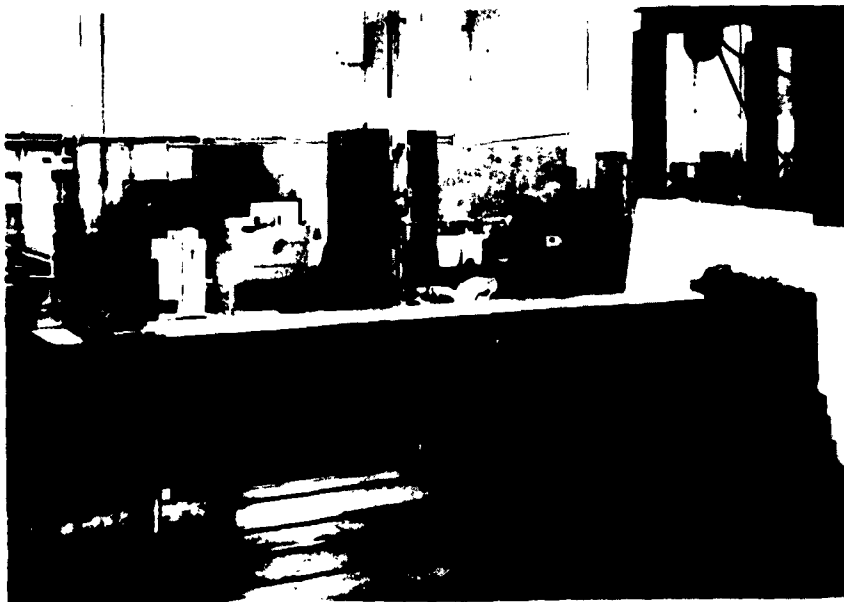


Fig. 10 - Vibration test

were considerably below the maximum of 10 g. The highest recorded acceleration was 4.5 g. Damage was limited to some slight bending of fastening latches when the containers shifted during the 12 mph impact.

The evaluation tests were concluded with a shipping test in which a boxcar was loaded at Pomona, California with 15 containers and sent to Yorktown, Virginia. An inspection at Yorktown revealed no damage to containers or contents.

CONCLUSION

The Terrier container fulfills all of the requirements of the missile logistic system.

It will protect its contents from rain, snow, sand and salt spray; it will withstand accidental drops up to 18 inches and provide protection against all transportation environments, at temperature extremes from -65°F to +160°F. The container is but 10 inches wider and 10 inches higher than the cross-section outline of the missile and it weighs only half as much as the missile.

All of these characteristics testify to the results of the application of engineering principles to container design. There is, however, more to be accomplished. In addition to satisfying the demands of the missile system, there is the ever growing necessity for simplification and for standardization of containers and handling equipment and for the development of materials and processes to lower container costs.

* * *

SHOCK RESPONSE OF A NONLINEAR MISSILE SUSPENSION SYSTEM

E. Y. W. Tsui and P. Stern
Lockheed Missiles & Space Division
Sunnyvale, California

This paper presents solutions for the dynamic response of a missile package with linear and nonlinear isolators subjected to shock inputs. Analytical and analog methods are introduced to solve the differential equations of motion, with effects of damping considered in these methods. The paper also includes the findings from an investigation of the relative maximum response of a system for edgewise rotational drops. These findings were developed from a parametric study for the dynamic behavior as a function of the location of isolators. Results are plotted in dimensionless form, using responses obtained by the energy method as reference. Finally, the effects of spring nonlinearity, damping, and the location of isolators on the design of suspension systems are discussed.

INTRODUCTION

The design of a container and suspension system capable of protecting a missile or its components against various shock and vibration environments is a major problem confronting missile packaging engineers. The designer requires a knowledge of the maximum displacement and forces on a suspended component when a packaged system is subjected to dynamic loading. From this information, he may develop a container configuration which would package the missile so as to prevent contacting the container walls and hold the resultant forces within the component's allowable design load. In this paper, the shock inputs which are usually assumed to be critical are considered in the absence of design conditions for the vibration environments. The main purpose of the paper is to present results of a study of dynamic behavior of a suspension system using rubber sandwich isolators [1].

The load-deflection characteristics of the sandwich isolators are quite nonlinear (Fig. 1), particularly when deflections become large [2]. Since the available studies [3, 4, 5, 6] indicate that the dynamic response of nonlinear systems with multiple degrees of freedom has not been fully investigated, the present work includes an examination of the effect of the

nonlinear isolators on the maximum response of the system. Results are compared with those obtained by use of the linear theory.

It has been a common practice [7] to obtain the maximum displacement and forces of the suspended component by the energy method, assuming the equivalent springs are located at a distance from the c.g. equal to the radius of gyration of the system. However, there are cases in which this condition cannot be satisfied. How this would affect the behavior of the system, especially when dampers are present, is also considered in this paper.

NOTATION

y, x, θ vertical translational, horizontal translational, and rotational displacement of the center of gravity of the system (point G) at any time t

a_j offset of isolator j from c.g.
(in.)

c_j coefficient of viscous damper
 j (lb/sec/in.)

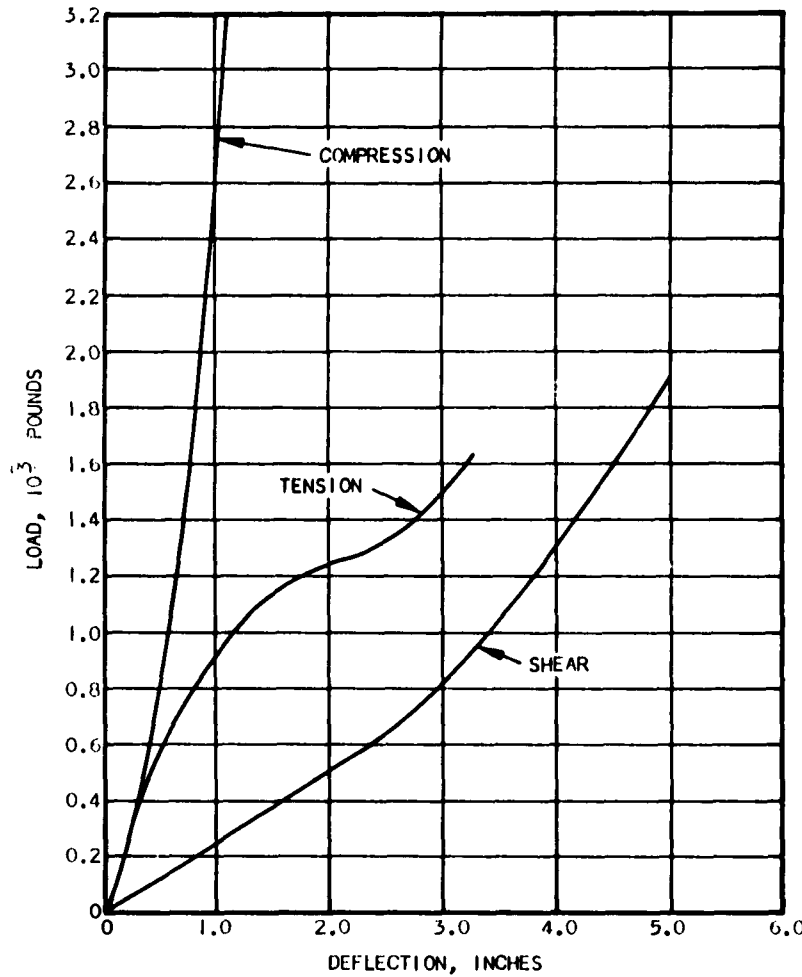


Fig. 1 - Load-deflection curves for JB-5425
"Lord" shear mount

g	gravity constant (in./sec ²)	y_o, x_o, θ_o	vertical, horizontal, and angular displacement at equilibrium
H	height of drop at corner (in.)		
h	height of drop of c.g. (in.)	ρ	radius of gyration of sprung mass about c.g.
K_j	dynamic modulus of isolators j in lb/in.	t	time (sec)
$\dot{y}, \dot{x}, \dot{\theta}$	$dy/dt, dx/dt, d\theta/dt$ vertical, horizontal, and angular velocity at any time after impact	I	mass moment of inertia about c.g. of sprung mass (in./lb-sec ²)
$\dot{y}_o, \dot{x}_o, \dot{\theta}_o$	vertical, horizontal, and angular velocity at the instant of impact ($t = 0$)	I_0	mass moment of inertia about point 0 ($= I + m \times \overline{OG}^2$)
		w	weight of sprung mass (lb)

W_1, W_2, W_3	energy (in./lb)
m	sprung mass (lb/sec ² /in.)
\overline{OG}	distance from point 0 to point G
\overline{OE}	horizontal projection of \overline{OG} (Fig. 3)
η	fraction of critical damping
ϵ	OG/ρ
Q_j	force in mount j (lb)
A, B, C, D, E, F, G, H, J, L, M, λ , a , γ , N, ψ , ω	parameters defined in the text.

GENERAL CONSIDERATIONS

The geometry and sign convention for the system we are considering are shown in Fig. 2. It is assumed that the system is symmetric in the y-x plane — a valid assumption for a large percentage of missile components. A rectangular coordinate system is used, having its origin the center of gravity of the suspended body, in which the springs are in a state of zero stress.

The basic assumptions are as follows:

- The packaged unit and the container are rigid bodies.
- The container does not rebound after impact. Thus, the packaged unit is assumed to have only initial velocity boundary conditions.
- The system has one-fold symmetry and is defined by three degrees of freedom.

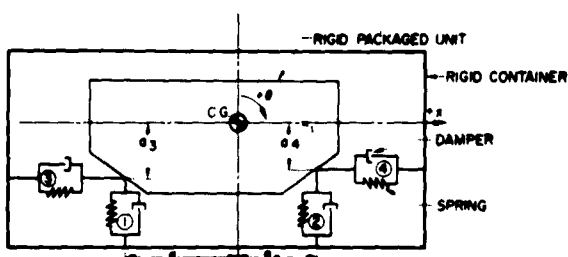


Fig. 2 - Geometry and sign convention

The determination of spring rates of the isolators (Fig. 2) is important. The schematic representation of springs may be misleading, for it is advantageous to combine many springs to yield what is called an equivalent spring for both linear and nonlinear springs. Viscous dampers are implied whenever damping terms are involved which are characterized by force proportional to velocity. For example, the force F due to a damper in the x-direction is given by $F = CX$

where

$$C = \text{damping constant } \left(\frac{\text{lb-sec}}{\text{in.}} \right)$$

$$X = \frac{dx}{dt} = \text{velocity in x-direction } \left(\frac{\text{in.}}{\text{sec}} \right)$$

MATHEMATICAL FORMULATION

Differential Equations of Motion

It can be shown that the equations of motion for the nonlinear system being considered (Fig. 2), with assumptions as noted, can be written as

$$\begin{aligned} \ddot{y} + B\dot{y} + C\dot{\theta} + \frac{1}{m}F_1(y_1) + \frac{1}{m}F_2(y_2) &= g \\ \ddot{x} + F\dot{x} + G\dot{\theta} + \frac{1}{m}F_3(x_3) + \frac{1}{m}F_4(x_4) &= 0 \\ \rho^2\ddot{\theta} + L\dot{\theta} + C\dot{y} + G\dot{x} - \frac{1}{m}F_1(y_1) - \frac{1}{m}F_2(y_2) \\ - \frac{1}{m}F_3(x_3) - \frac{1}{m}F_4(x_4) &= 0 \end{aligned} \quad (1)$$

and for the equivalent linear system as

$$\begin{aligned} \ddot{y} + B\dot{y} + C\ddot{\theta} + Dy + E\theta &= g \\ \ddot{x} + F\dot{x} + G\dot{\theta} + Hx + J\theta &= 0 \\ \rho^2\ddot{\theta} + L\dot{\theta} + Cy + Gx + M\theta + Ey + Jx &= 0 \end{aligned} \quad (1a)$$

where

$$\begin{aligned} B &= \frac{1}{m} \sum_{j=1}^2 C_j & E &= \frac{1}{m} \sum_{j=1}^2 K_j a_j \\ C &= \frac{1}{m} \sum_{j=1}^2 C_j a_j & F &= \frac{1}{m} \sum_{j=3}^4 C_j \\ D &= \frac{1}{m} \sum_{j=1}^2 K_j & G &= \frac{-1}{m} \sum_{j=3}^4 C_j a_j \end{aligned}$$

$$H = \frac{1}{m} \sum_{j=3}^4 K_j$$

$$L = \frac{1}{m} \sum_{j=1}^4 C_j a_j^2$$

$$J = \frac{-1}{m} \sum_{j=3}^4 K_j a_j$$

$$M = \frac{1}{m} \sum_{j=1}^4 K_j a_j^2$$

$F_j(y_j)$ = Force in mount j due to vertical displacement y_j

$F_j(x_j)$ = Force in mount j due to horizontal displacement x_j .

Initial Conditions

The geometry for an edgewise rotational drop is shown in Fig. 3. One edge is raised to a height H and the container is then permitted to fall freely. It is assumed that the vertical springs are in equilibrium until impact. The initial circular velocity is then determined by the following equation:

$$\ddot{\theta}_o = \sqrt{\frac{2gh}{\rho^2(1 + \epsilon^2)}}. \quad 2)$$

The velocities in the vertical and horizontal direction are

$$\dot{y}_o = \bar{G}\dot{\theta}_o \text{ and } \dot{x}_o = \bar{G}E\dot{\theta}_o. \quad (3)$$

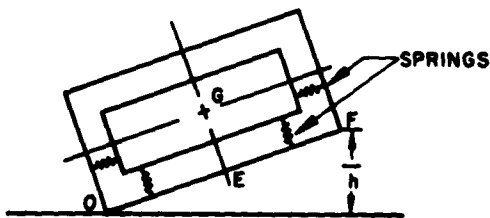


Fig. 3 - Edgewise drop of container

METHODS OF SOLUTION

Analytic-Energy Method

When the three degrees of freedom are all uncoupled and undamped, an energy approach may be used to obtain the maximum deflections in each degree of freedom.

Linear System

If the springs are linear, the equations of the motion previously derived are valid, with the coupling terms omitted. Thus

$$\ddot{x} + Hx = 0$$

$$\ddot{y} + Dy = g$$

$$\rho^2 \ddot{\theta} + M\theta = 0. \quad (4)$$

Using the expressions

$$\ddot{x} = \dot{x} \frac{dx}{d\theta}, \quad \ddot{y} = \dot{y} \frac{dy}{d\theta}, \quad \ddot{\theta} = \dot{\theta} \frac{d\dot{\theta}}{d\theta} \quad (5)$$

and integrating, we obtain the following energy equations for maximum displacements:

$$x_{max} = \frac{\dot{x}_o}{\sqrt{H}}, \quad y_{max} = \frac{\dot{y}_o}{\sqrt{D}} + y_o, \quad \theta_{max} = \frac{\dot{\theta}_o}{\sqrt{M}} \quad (6)$$

From the above expressions, assuming knowledge of the initial velocities, we can calculate the magnitude of x_{max} , y_{max} , and θ_{max} . However, these maxima generally do not occur simultaneously; therefore, use of a direct combination of these coordinates to obtain the maximum deflection at any point P of the missile will result in a calculated deflection which is larger than the actual deflection, unless the degrees of freedom being combined have the same frequency. In the case of y and θ , for example, the two frequencies would be equal if $M/\rho^2 = D$. If this condition were satisfied, then the maximum deflection at any point of the missile could be obtained by direct combination of y_{max} and θ_{max} through the following equation:

$$(y_P)_{max} = y_{max} + a_x \theta_{max} \quad (7)$$

where a_x is the horizontal distance from the c.g. of the missile to point P.

When the two frequencies are not equal, there is no way to predict by energy methods what the maximum deflection at a given point will be, since the energy method gives no information about the time history of the displacement. However, even when the frequencies are not equal, using the given formula as if the frequencies were equal will give a result which usually is not too much in error and is always on the conservative side; that is, it is always higher than the actual deflection.

Nonlinear System

When the mounts have nonlinear spring characteristics, the problem of the general response of a missile package becomes considerably more complicated. There seems to be no acceptable approach to an analytical solution of the general problem, and in all but the simplest cases, solution on the analog computer appears to be one recourse.*

Among those few problems which can be handled by analytical means is the case of the rotational drop when the vertical mounts are located at a distance from the c.g. equal to the radius of gyration of the sprung mass about its own c.g. (i.e., $a_1 = a_2 = \rho$), and the horizontal mounts are located such that $a_3 = a_4 = 0$. Let the force-deflection characteristics of the four mounts be given by the functions $F_1(y_1)$, $F_2(y_2)$, $F_3(x_3)$, and $F_4(x_4)$. Thus, $F_1(y_1)$ is the force in mount No. 1 due to the vertical displacement y_1 . For this problem, the displacements y_1 , y_2 , x_3 , x_4 are given by

$$\begin{aligned} y_1 &= y + \rho\theta, \quad y_2 = y - \rho\theta \\ x_3 &= x_4 = x. \end{aligned} \quad (8)$$

With the above information, the equations of motion (1) can be written as

$$\begin{aligned} m\ddot{y} + F_1(y_1) + F_2(y_2) &= mg \\ \rho m\ddot{\theta} + F_1(y_1) + F_2(y_2) &= 0 \\ m\ddot{x} + F_3(x_3) + F_4(x_4) &= 0. \end{aligned} \quad (9)$$

Adding the first two of Eq. (9) yields

$$m\ddot{y}_2 + 2F_2(y_2) = mg. \quad (10)$$

Subtracting the first from the second Eq. (9) yields

$$m\ddot{y}_1 = 2F_1(y_1) = mg. \quad (11)$$

Then the new equations are

$$\begin{aligned} m\ddot{y}_2 + 2F_2(y_2) &= mg \\ m\ddot{y}_1 + 2F_1(y_1) &= mg \\ m\ddot{x} + F_3(x) + F_4(x) &= 0. \end{aligned} \quad (12)$$

*Solutions can also be obtained by a finite difference approximation as demonstrated in Ref. 8.

Substituting the expression

$$\dot{x} = \dot{x} \frac{dx}{dy}, \quad \dot{y} = \dot{y} \frac{dy}{dx} \quad (13)$$

in the new equation of motion yields

$$\begin{aligned} m\ddot{y}_2 \frac{dy}{dx} + 2F_2(y_2) \frac{dy}{dx} &= mg \frac{dy}{dx} \\ m\ddot{y}_1 \frac{dy}{dx} + 2F_1(y_1) \frac{dy}{dx} &= mg \frac{dy}{dx} \\ m\ddot{x} dx + F_3(x) dx + F_4(x) dx &= 0. \end{aligned} \quad (14)$$

Integration between proper limits and rearranging gives

$$\begin{aligned} \frac{1}{2} m(\dot{y}_2)_0^2 &= \left(2 \int_0^{y_{2\max}} F_2 dy_2 - mg y_{2\max} \right) \\ &- \left(2 \int_0^{y_{20}} F_2 dy_2 - mg y_{2\text{static}} \right) = W_2(y_2) \\ \frac{1}{2} m(\dot{y}_1)_0^2 &= \left(2 \int_0^{y_{1\max}} F_1 dy_1 - mg y_{1\max} \right) \\ &- \left(2 \int_0^{y_{20}} F_1 dy_1 - mg y_{1\text{static}} \right) = W_1(y_1) \end{aligned}$$

$$\frac{1}{2} m(\dot{x})_0^2 = \int_0^{x_{\max}} F_3 dx + \int_0^{x_{\max}} F_4 dx = W_3(x). \quad (15)$$

The integral on the side represents the area under the force-displacement curves from the static displacement up to maximum displacement. A plot of $W_1(y_1)$, $W_2(y_2)$, $W_3(x)$ versus displacement yields curves as shown in Fig. 4. To use this plot, assume that the initial values of $(\dot{y}_2)_0$, $(\dot{y}_1)_0$, $(x)_0$ are known. Then values of $\frac{1}{2} m(\dot{y}_2)_0^2$, $\frac{1}{2} m(\dot{y}_1)_0^2$, $\frac{1}{2} m(\dot{x})_0^2$ are computed. Enter the ordinate with these initial values and read the maximum displacements as noted in Fig. 4.

Analog Method — Basic Elements

The analog computer, or electronic differential analyzer, is a valuable tool in solving the dynamical problem under consideration [9, 10], for it is possible to solve the equations of motion for both linear and nonlinear springs with and without damping.

If the damping coefficient were considered nonlinear, this could also be handled.

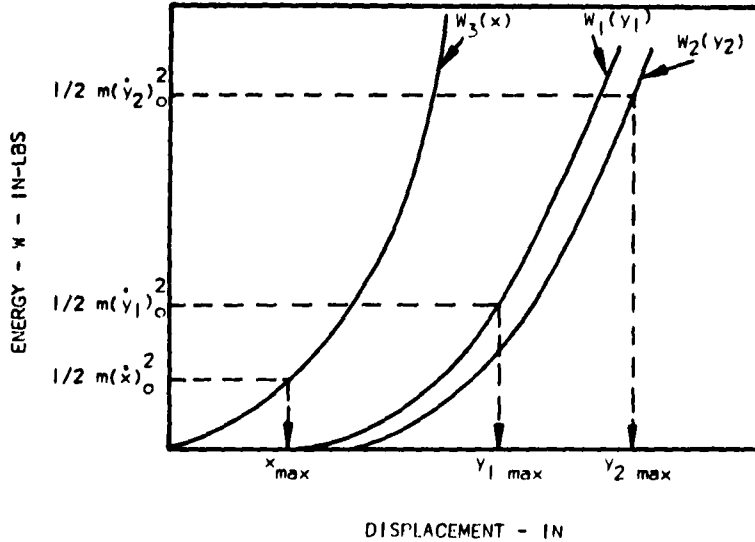


Fig. 4 - Energy displacement curves for isolators

An interesting feature in using an analog computer is that the maximum response of the system can be obtained from inspection of the output curves. This maximum response becomes quite difficult to compute in the analytical procedure, especially when there are coupled modes with damping. The analog, then, is a practical and powerful method to obtain the response of a nonlinear suspension system with coupled modes and damping.

The basic component of the computer is the dc operational amplifier, around which elements can be constructed to perform mathematical operations such as addition, multiplication, differentiation, integration, and function generation. When these elements are properly connected they will represent the equations of motion. Table 1 shows various basic elements of a computer and their operation.

To solve the differential equations of motion (Eq. (1)) on this device, it is necessary that the voltages in the machine vary with time, in a manner prescribed by these equations. Thus, the machine uses voltage as the dependent variable and time as the independent variable. Since the computing elements operate in real time (machine time), it is necessary to convert the problem time (t) to machine time (τ). Then, two types of scales are necessary to convert the physical problem to the machine problem: one scale between

the dependent variables x , y , θ , and voltage, the other scale between the independent variable t and τ . These can be written as

$$\begin{aligned} x &= \frac{1}{\alpha_x} X; \quad y = \frac{1}{\alpha_y} Y; \quad \theta = \frac{1}{\alpha_\theta} \theta \\ t &= \frac{1}{\alpha_t} \tau \end{aligned} \quad (16)$$

The selection of the scale factors is such that the machine variables X , Y , θ will vary between plus and minus certain limiting voltages. The time-scale factor is governed by the computing elements such as the integrators and function generators.

Linear System

When the springs are assumed to be linear, the differential equations of motion, when transformed to machine equations, become

$$\begin{aligned} \ddot{Y} &= \frac{\alpha_y}{\alpha_t^2} g - \frac{1}{\alpha_t} EY - \frac{\alpha_y}{\alpha_0 \alpha_t} C\theta - \frac{1}{\alpha_t} DY - \frac{\alpha_y}{\alpha_0 \alpha_t} E \\ \ddot{X} &= -\frac{1}{\alpha_t} FX - \frac{1}{\alpha_t} HX - \frac{\alpha_x}{\alpha_0 \alpha_t} G\dot{\theta} - \frac{\alpha_y}{\alpha_0 \alpha_t} JU \\ \ddot{\theta} &= -\frac{1}{\alpha_t \rho^2} L\theta - \frac{\alpha_H}{\alpha_y \alpha_t \rho^2} CY - \frac{\alpha_H}{\alpha_x \alpha_t \rho^2} GX \\ &\quad - \frac{1}{\alpha_t \rho^2} MH - \frac{\alpha_H}{\alpha_y \alpha_t \rho^2} EY - \frac{\alpha_H}{\alpha_x \alpha_t \rho^2} X \end{aligned} \quad (17)$$

TABLE 1
Analogue Computer
Basic Elements

Operation	Block Diagram Symbols	Machine Equations
Multiplication by a constant by use of a potentiometer		$x_0 = \alpha x_1$ $0 \leq \alpha \leq 1$
Summation		$x_0 = -R_o \left[\frac{x_1}{R_1} + \frac{x_2}{R_2} + \frac{x_3}{R_3} \right]$ Note sign change due to amplifier
Integration		$x_0 = -\frac{1}{RC} \int_0^t x_1 dt + K$ K = initial value of x_0
Function Generation (Electronic)		$x_0 = F(x_1)$

The initial conditions become

$$\begin{aligned} y_0 &= \alpha_y y_0 & x_0 &= \alpha_x x_0 & \theta_0 &= \alpha_\theta \theta_0 \\ \dot{y}_0 &= \frac{\alpha_y}{\alpha_t} y_0 & \dot{x}_0 &= \frac{\alpha_x}{\alpha_t} x_0 & \dot{\theta}_0 &= \frac{\alpha_\theta}{\alpha_t} \theta_0 \end{aligned} \quad (18)$$

The following outputs are obtainable

Deflections

$$x, y, \theta$$

$$y_1 = y - a_1 \theta$$

$$y_2 = y + a_2 \theta$$

$$x_3 = x - a_3 \theta$$

$$x_4 = x + a_4 \theta$$

Forces

$$Q_1 = K_1 y_1 + C_1 y_1$$

$$Q_2 = K_2 y_2 + C_2 y_2$$

$$Q_3 = K_3 x_3 + C_3 x_3$$

$$Q_4 = K_4 x_4 + C_4 x_4$$

Nonlinear System

When the mounts are nonlinear the equations of motion are written as

$$\begin{aligned} \ddot{y} + B\dot{y} + C\dot{\theta} + \frac{1}{m} F_1(y_1) + \frac{1}{m} F_2(y_2) &= g \\ \ddot{x} + F\dot{x} + G\dot{\theta} + \frac{1}{m} F_3(x_3) + \frac{1}{m} F_4(x_4) &= 0 \\ \ddot{\theta} + \frac{L}{\rho^2} \dot{\theta} + \frac{C}{\rho^2} y + \frac{G}{\rho^2} x - \frac{a_1}{m\rho^2} F_1(y_1) - \frac{a_2}{m\rho^2} F_2(y_2) \\ - \frac{a_3}{m\rho^2} F_3(x_3) - \frac{a_4}{m\rho^2} F_4(x_4) &= 0 \end{aligned} \quad (20)$$

(19) where

- $F_1(y_1)$ = load in spring No. 1 due to y_1
 deflection
 $F_2(y_2)$ = load in spring No. 2 due to y_2
 deflection
 $F_3(x_3)$ = load in spring No. 3 due to x_3
 deflection
 $F_4(x_4)$ = load in spring No. 4 due to x_4
 deflection.

The functions of F_1 , F_2 , F_3 , F_4 are given in curve form to be approximated in the function generators. Figure 5 shows the block diagram for the system under consideration.

EXAMPLES — ENERGY METHOD

Numerical examples are presented to show the method of obtaining the solutions of the equations of motion. A packaged system having certain constant parameters is considered. The responses of the system to changes in mount location and the damping coefficients for linear and nonlinear springs are required. These responses are then plotted for comparison. In the following examples, only the edgewise rotational-drop case is considered. However, it can be easily extended to include other cases such as flat drop and longitudinal impact.

Assume the following constant parameters:

$$\begin{aligned}
 W &= 1100 \text{ lb} & \overline{OG} &= 47.4 \text{ in.} \\
 I &= 920 \frac{\text{in. lb}}{\text{sec}^2} & \overline{OE} &= 40.75 \text{ in.} \\
 \rho &= 18 \text{ in.} & \overline{GE} &= 24.25 \text{ in.} \\
 m &= 2.84 \frac{\text{lb/sec}^2}{\text{in.}} & K_1 = K_2 &= 250 \text{ lb/in.} \\
 & & K_3 = K_4 &= 420 \text{ lb/in.}
 \end{aligned}$$

Parameters to be varied are:

Mount Location:

$$\begin{aligned}
 a_1, a_2 &= 9 \text{ in. through } 27 \text{ in.} \\
 a_3, a_4 &= 0 \text{ in. through } 8 \text{ in.}
 \end{aligned}$$

Damping Coefficients — For

$$\begin{aligned}
 \eta &= 0, 0.20 \\
 C_1 = C_2 &= 0, 7.52 \\
 C_3 = C_4 &= 0, 9.75
 \end{aligned}$$

The initial conditions as computed from Eqs. (2) and (3), using the above constants, are

$$\dot{y}_o = 22.2 \sqrt{\frac{h}{2}}, \quad \dot{x}_o = 13.3 \sqrt{\frac{h}{2}}, \quad \dot{\theta}_o = 0.544 \sqrt{\frac{h}{2}}.$$

Two cases are considered, each with the mounts in the same location, i.e., $a_1 = a_2 = \rho = 18$ inches, $a_3 = a_4 = 0$. Case (a) presents the solution for linear mounts and Case (b) gives the solution for nonlinear mounts without damping ($\eta = 0$).

Linear Mounts — Case (a)

The maximum response of x , y , θ for this case is given by

$$\begin{aligned}
 y_{\max} &= \frac{\dot{y}_o}{\sqrt{D}} + y_o = 1.67 \sqrt{\frac{h}{2}} + 2.2 \\
 x_{\max} &= \frac{\dot{x}_o}{\sqrt{H}} = 0.774 \sqrt{\frac{h}{2}} \\
 \theta_{\max} &= \frac{\dot{\theta}_o}{\sqrt{M}} = 0.041 \sqrt{\frac{h}{2}}. \tag{21}
 \end{aligned}$$

In this particular case, the maximum response of mount No. 2 is quickly established since the frequency of y and θ are equal; then $y_{2\max}$ becomes

$$y_{2\max} = 2.41 \sqrt{\frac{h}{2}} + 2.2.$$

Nonlinear Mounts — Case (b)

Since the mounts are considered nonlinear, the method given in Nonlinear System is used. The load-displacement curves for the mounts are shown in Figs. 6 and 7. The equations to be solved are

$$\begin{aligned}
 \frac{1}{2} m \left(\dot{y}_2 \right)_o^2 &= w_2(y_2) \\
 \frac{1}{2} m \left(\dot{x}_2 \right)_o^2 &= w_1(x_1) \\
 \frac{1}{2} m \left(\dot{\theta}_2 \right)_o^2 &= w_3(x).
 \end{aligned}$$

Fig. 5 - Block diagram for the nonlinear system

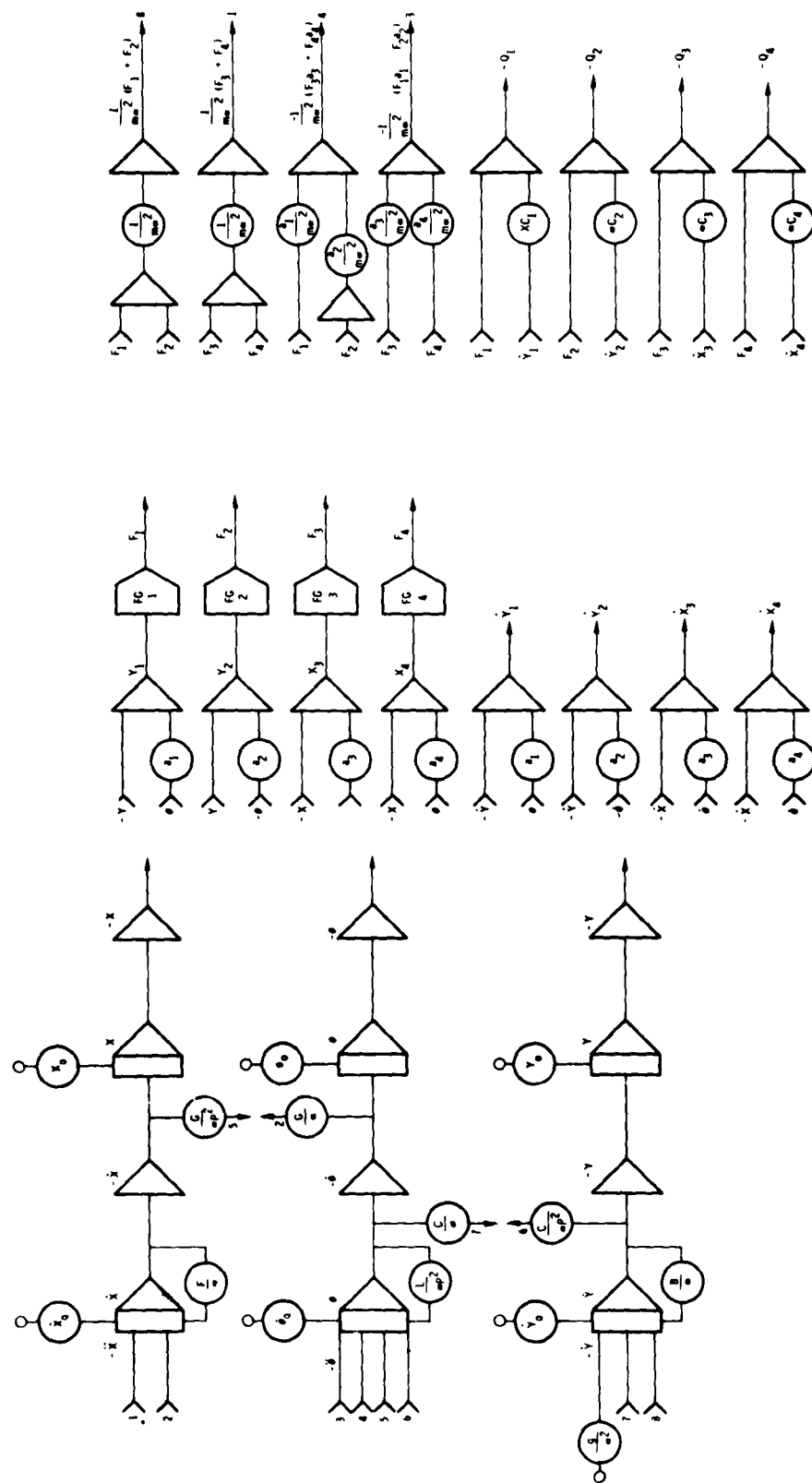
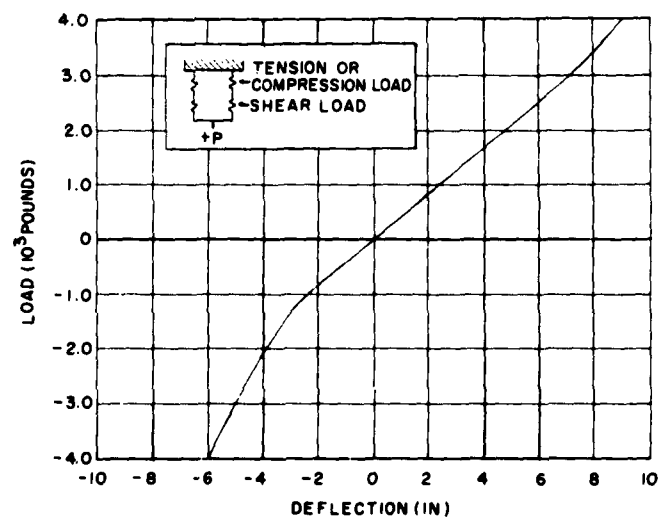


Fig. 6 - Load-deflection curves for mounts 1 and 2



The curves for $w_1(y_1)$, $w_2(y_2)$, $w_3(x)$ were obtained by a numerical integration of the load-displacement curves. These are presented in Fig. 8. Using the expressions for initial conditions, the above equations can be written as

$$1,460 \left(\frac{h}{2} \right) = w_2(y_2)$$

$$219 \left(\frac{h}{2} \right) = w_1(y_1)$$

$$250 \frac{h}{2} = w_3(x)$$

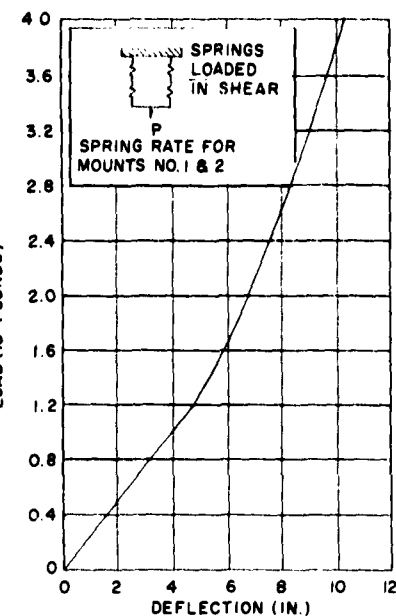


Fig. 7 - Load-deflection curve for mount 3

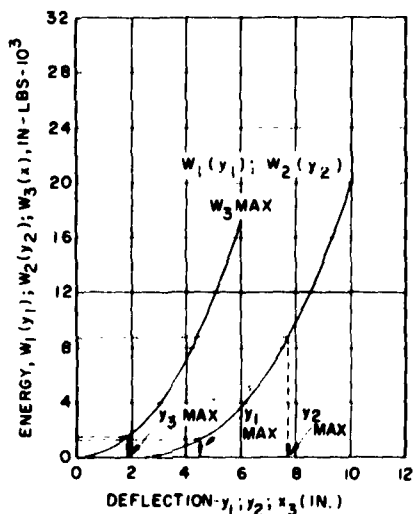


Fig. 8 - Displacement curves for isolators 1, 2, and 3

if $\bar{h} = 12$ inches, then

$$8,740 = W_2 y_2$$

$$1,310 = W_1 y_1$$

$$1,500 = W_3 x$$

Entering the curves of Fig. 8, one obtains for the maximum displacements

$$y_{2\max} = 7.7 \text{ in.}$$

$$y_{1\max} = 4.5 \text{ in.}$$

$$x_{3\max} = 1.9 \text{ in.}$$

Analog Solutions

The example problem, Case (b), in which the springs were considered nonlinear was run on the analog computer. A setup similar to that shown in Fig. 5 was used. Mount locations chosen were $a_1 = a_2 = 9, 18, 27$ inches; $a_3 = a_4 = 0, 8$ inches. Two variations in damping of 0 and 20 percent and three drop heights of 4, 12, and 18 inches were run. Output curves were obtained for

$$x, y, \theta, \dot{x}, \dot{y}, \dot{\theta}, y_1, y_2, x_3, Q_1, Q_2, Q_3$$

The results for the maximum response of y_2, Q_2, X_3 and Q_3 are given in the summary of results.

As an example of the analog output, a specific case is presented in Fig. 9.

SUMMARY OF RESULTS AND CONCLUSIONS

Results of this study are summarized in Figs. 10 through 15. The maximum deflections and forces for springs No. 2 and 3 for the linear case, where $a_3 = a_4 = 0$ and $a_1 = a_2 = 18$ inches are shown in Figs. 10 and 11 as functions of the drop of height \bar{h} . Figures 12 through 15 show the effect of mount location and damping on the magnitudes of these deflections and forces. The curves designated as nonlinear are taken from analog solutions. Analytical solutions based on the assumption of linear springs are shown for comparison where such results were available. All curves are nondimensionalized by

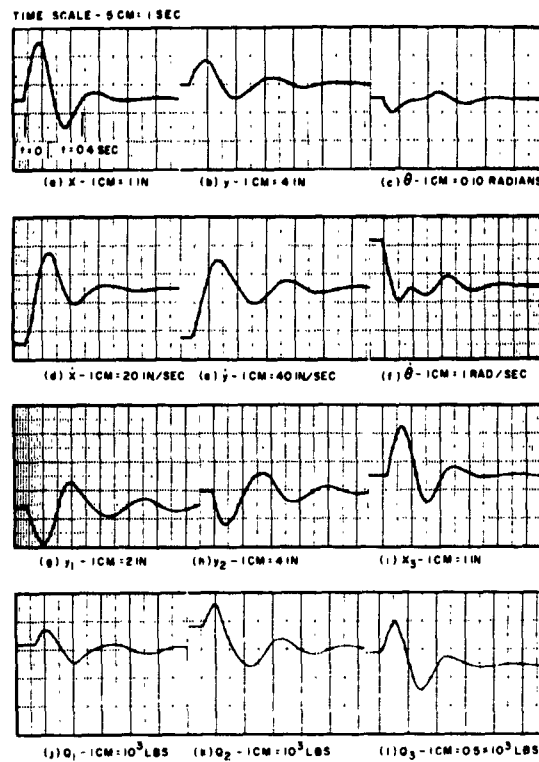


Fig. 9 - Response curves for $\bar{h} = 18$ inches; $a_1 = a_2 = 27$ inches; $a_3 = a_4 = 8$ inches; $\eta = 20$ percent

dividing the actual response by the corresponding values shown in Figs. 10 and 11 for a drop height $\bar{h} = 12$ inches.

It may be observed from Figs. 13 and 15 that the nonlinear springs produce lower maximum deflections but higher maximum forces than the linear springs. For example, when the drop height $(\bar{h}) = 12$ inches, the reduction of deflection as well as the force increase in the nonlinear springs is about 10 to 15 percent of that for linear springs. This fact is true for both undamped and damped cases up to 20-percent critical.

The results of this study show that the maximum deflections and forces are lessened by the inclusion of damping in the system. It should be noted, however, that it would be erroneous to assume that this trend continues beyond a certain point with increased damping. The maximum deflection would continue to decrease for a time with increased damping, but

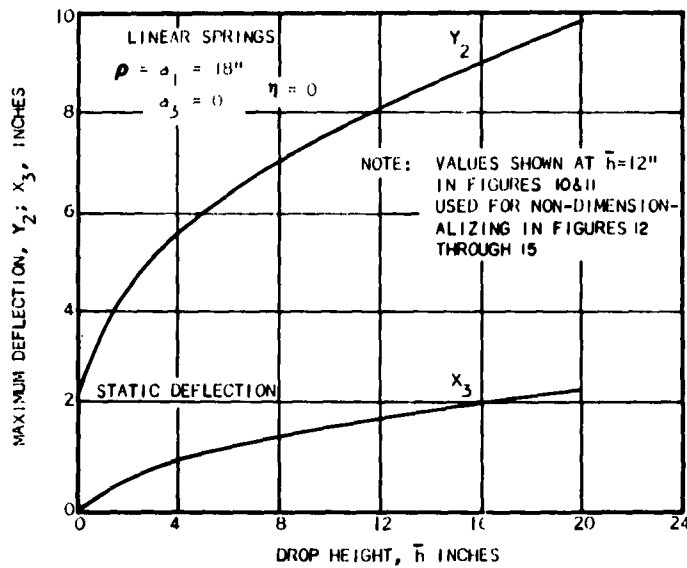


Fig. 10 - Maximum deflection of springs 2 and 3 versus drop height for linear springs as computed by energy method

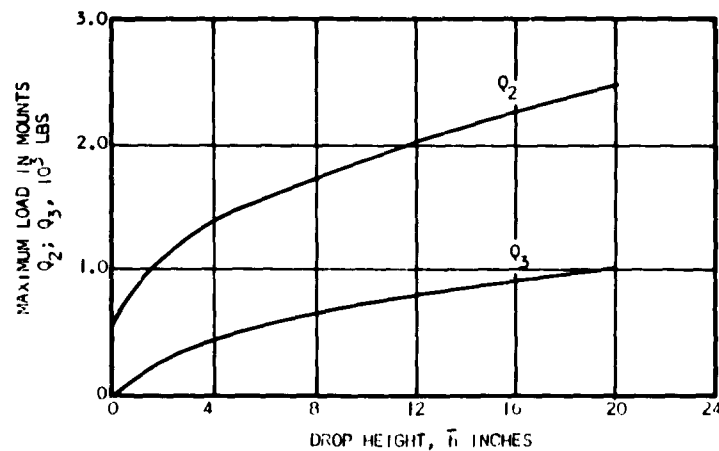


Fig. 11 - Maximum load in springs 2 and 3 versus drop height

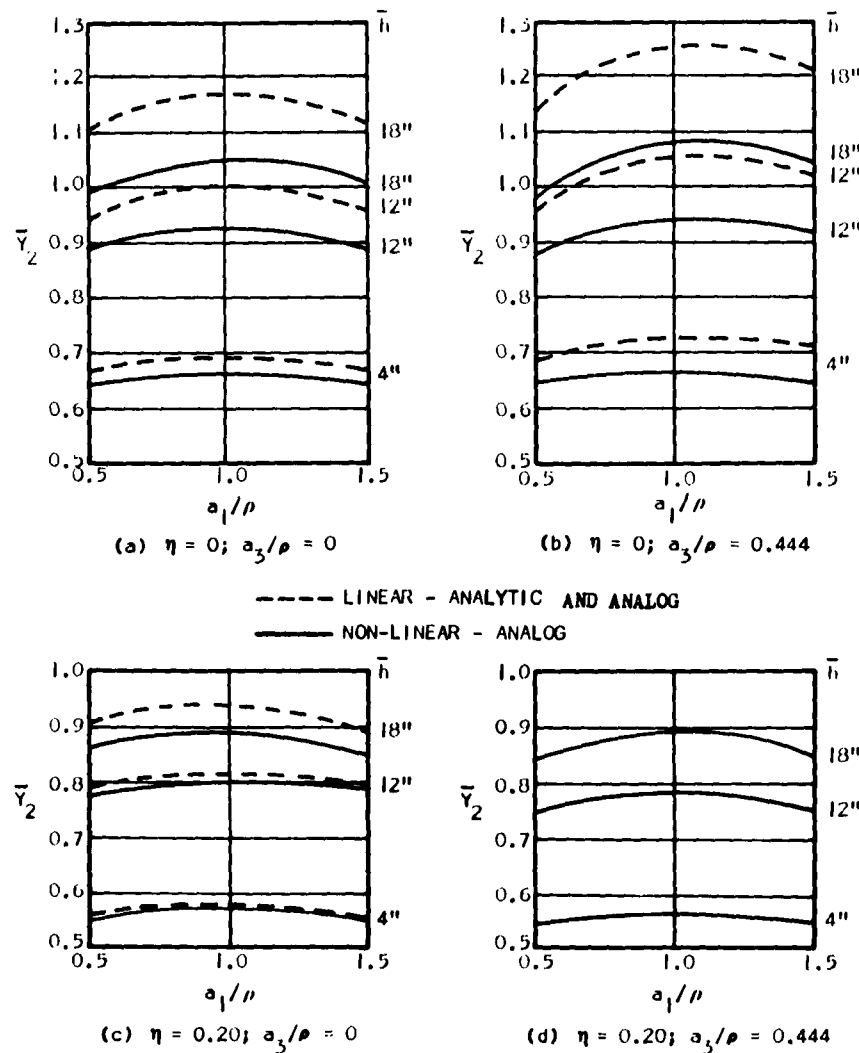


Fig. 12 - Effect of mount location and damping on relative magnitude of $y_{2 \max}$, $\bar{Y}_2 = y_2/8.1$ (Ref. Fig. 10)

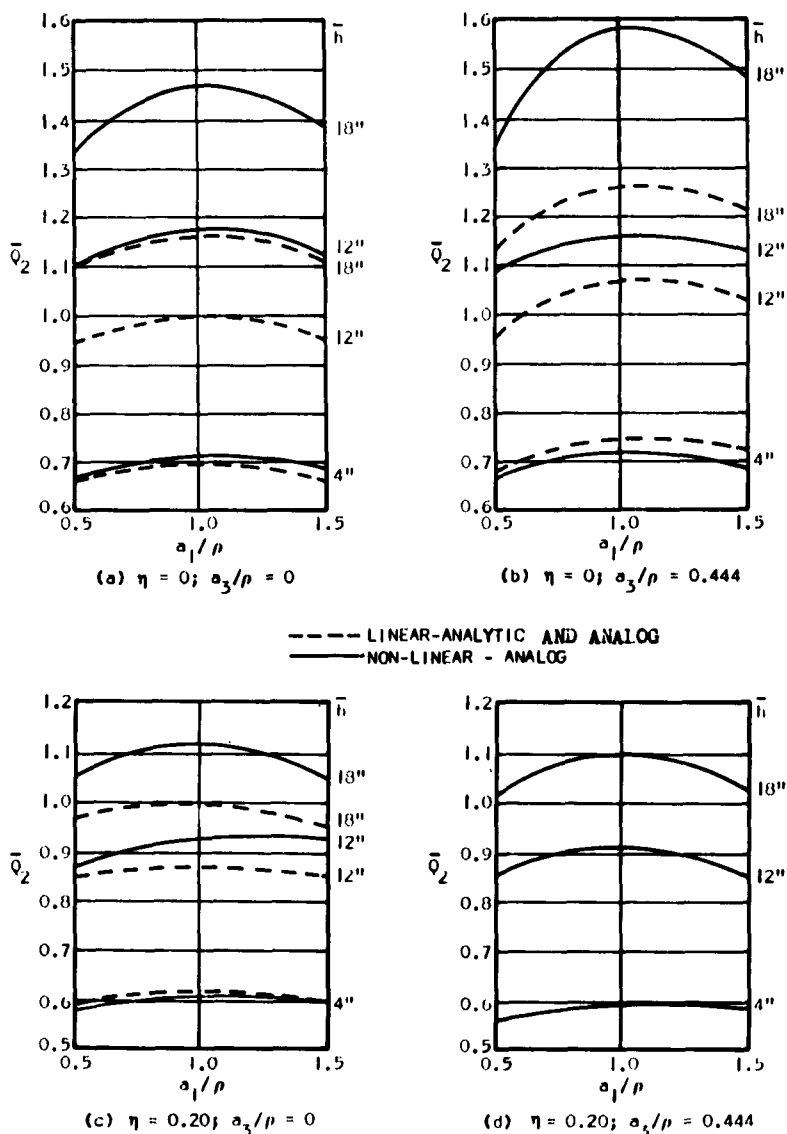


Fig. 13 - Effect of mount location and damping on relative magnitude Q_2 . $Q_2 = Q_2/202 \times 10^3$ (Ref. Fig. 11)

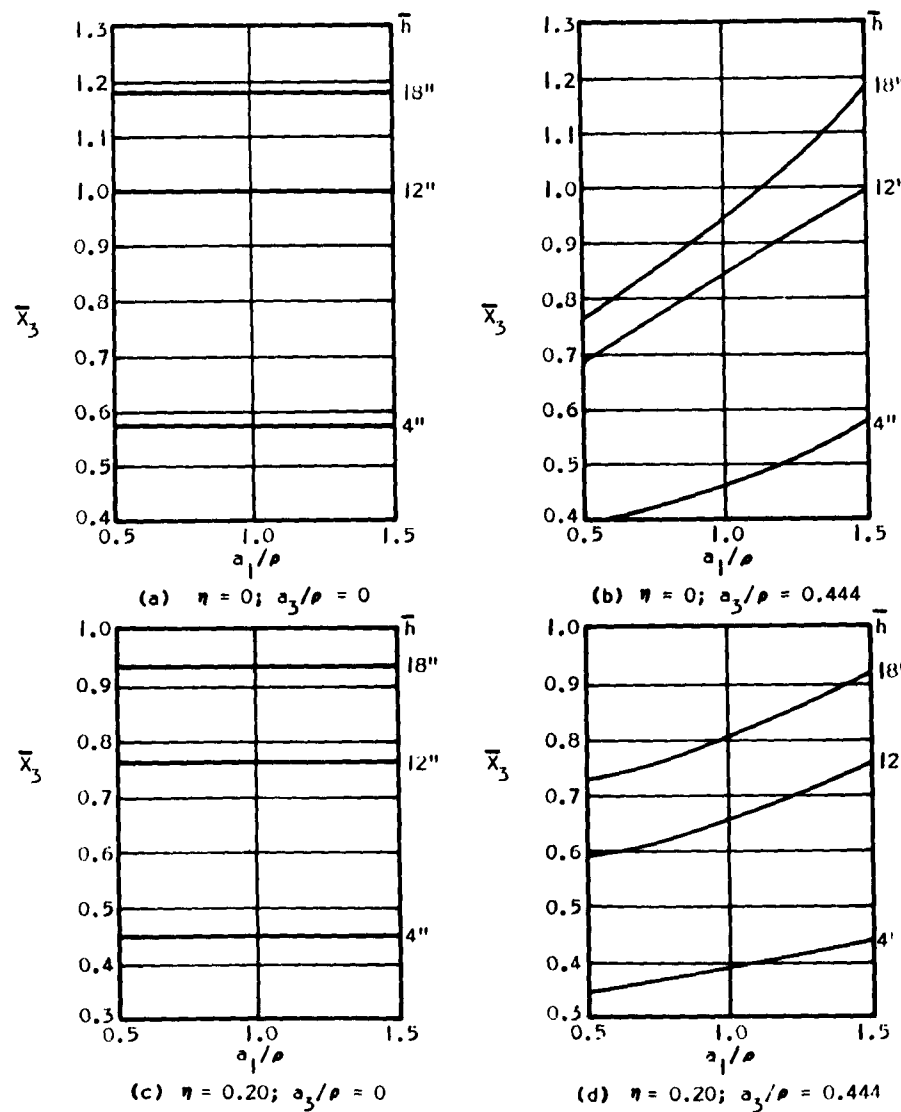


Fig. 14 - Effect of mount location and damping on relative magnitude of X_3 , $\bar{X}_3 = X_3/1.90$ (Ref. Fig. 10)

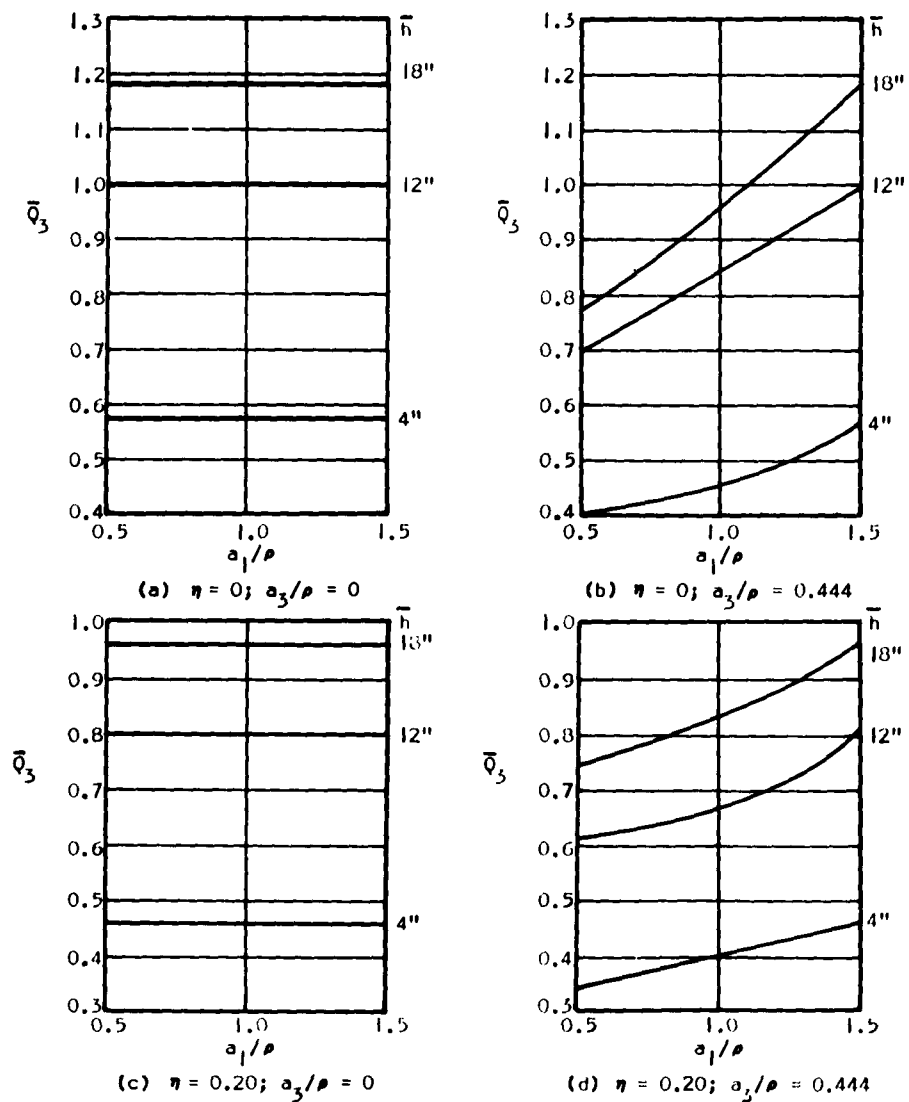


Fig. 15 - Effect of mount and damping on relative magnitude of
 Q_3 , $\bar{Q}_3 = Q_3/0.80 \times 10^3$ (Ref. Fig. 11)

there would be some magnitude of damping, peculiar to the particular problem being investigated, beyond which the magnitude of the maximum force would increase with increased damping. For this study, however, the point of reversal is not reached by a 20-percent damping magnitude, the highest value considered. It is observed that maximum forces and displacements at the mounts occurred in the first-quarter cycle for most of the cases considered.

The last effect to be noted is that of varying the mount locations. In every case the maximum force and deflection for spring No. 2 occurs when $a_1/\rho = 1.0$. Either increasing or decreasing the ratio a_1/ρ , within the range from $a_1/2\rho$ to $3a_1/2\rho$, tends to decrease these maxima. These changes are in the order of 0 ± 10 percent of the value of a_1/ρ for $\bar{h} = 12$

inches. In the case of spring No. 3, the results are not so consistent. It is noted that when $a_3/\rho = 0$, there is practically no effect on the behavior of this spring due to varying a_1/ρ . However, when $a_3/\rho = 0.444$, both displacements and force x_3 and Q_3 seem to be directly proportional to the distance a_1 or a_2 . In particular, when $a_1/\rho = 1.5$, the values of displacements and forces are almost equal to those when $a_3/\rho = 0$.

Consequently, it can be concluded that using the energy method and linear springs as a basis to predict the response of a system having nonlinear isolators and damping is only applicable when there is a small amount of spring nonlinearity and damping. Otherwise, the nonlinear theory should be used, especially for the cases where the locations of mounts are arbitrary.

REFERENCES

- [1] J. J. Goodill, "Flexible Suspension Systems for Equipment in Transit," Lord Mfg. Co., Erie, Pa., 1955
- [2] J. C. Hanson, "Evaluation of Silicone Rubber Shock Mounts for Rocket Power Plant Shipping Container," Rock Island Arsenal Laboratory, 1958
- [3] R. D. Mindlin, "Dynamics of Package Cushioning," Bell System Tech. J., Vol. 24, Nos. 3 - 4, 1945
- [4] C. E. Crede, Vibration and Shock Isolation, New York: Wiley, 1951
- [5] J. J. Stoker, Non-Linear Vibrations, New York: Interscience Publishers, Inc., 1957
- [6] A. L. Lang, Jr., J. W. Lincoln, "Combat Shock Protection of Missiles Aboard Ship," Bulletin No. 27, Shock, Vibration and Associated Environments p. 27, June 1959 (Bulletin Confidential, Article Unclassified)
- [7] Office of the Assistant Secretary of Defense, Research and Development, "Fundamentals of Guided Missile Packaging," RD 219/3, Washington, D. C., July 1955
- [8] T. R. Beal, "Finite Difference Analysis of the Shock Response of a Packaged Missile with Non-Linear Suspension Mounts," Lockheed Missiles and Space Division, LMSD-703088, Sunnyvale, California, September 1960
- [9] D. W. Hagelbarger, C. E. Howe, R. M. Howe, "Investigation of the Utility of an Electronic Analog Computer in Engineering Problems," Dept. Of Aeronautical Engineering, Univ. of Michigan, Ann Arbor, Michigan
- [10] G. A. Kron, T. M. Korn, Electronic Analog Computers, New York: McGraw-Hill, 1956
- [11] T. V. Karman, M. A. Biot, Mathematical Methods in Engineering, New York: McGraw-Hill, 1940

* * *

LIGHTWEIGHT SHOCK ISOLATION SYSTEM FOR A MOBILE NUCLEAR POWER PLANT

J. W. Blakley
Research and Development Division
Aerojet-General Nucleonics
San Ramon, California

Design and testing of a shock and vibration isolation system for a mobile power plant is described. Vertical isolation is achieved by special shock mounts, horizontal shock isolation by nylon tiedown ropes. Railroad impact tests and component tests in various environments are described. A method of imposing aircraft emergency landing loads is presented.

INTRODUCTION

This paper describes the design of a shock isolation system for a mobile nuclear power plant, the ML-1. This plant, designed and built by Aerojet-General Corporation, consists of a compact gas-cooled reactor and an advanced closed-cycle turbogenerating system. The ML-1 is designed to operate for 10,000 hours without refueling and to deliver its rated output of 330 kw(e) at ambient temperatures ranging from -65°F to 100°F.

For fast, expedient transport and field assembly, the ML-1 is of modular construction. The primary modules, or skids, are the reactor and the power conversion packages, each of which weighs 30,000 pounds. The ML-1 plant is transportable on Army vehicles, military aircraft, ships, standard railroad flatcars and sleds. The reactor skid, loaded on an Army semitrailer, is shown in Fig. 1.

The mobility of the plant, weight and space limitations, and the wide variation of shock spectra, presented a difficult task for shock isolation design. The major requirement of the isolation system was to provide lightweight shock protection for the ML-1 plant during loading, transport and operation, throughout the environmental temperature range.

Because of the requirement to drastically reduce input shocks, no conventional standard tiedown system could be used. Nor could

available commercial mounts meet the requirements of lightweight, mobility, and total loading capacity. Therefore, it was necessary to design special mounts and tiedowns. The design used the shock dissipation properties of nylon and of silicone elastomer material.

DESCRIPTION

The major horizontal shock protection for the plant is provided by the nylon rope tiedown system; the vertical protection by silicone shock isolators.

The tiedown rope chosen was a 1-1/8-inch diameter three strand filament nylon having a breaking strength of 30,000 pounds.

The specially designed shock mounts (Fig. 2) consist of three basic parts bonded together in the mold: (1) top core, (2) elastomer, and (3) a cylindrical retaining ring.

The shock mount uses a combination of shear and compressive loads to isolate the input shock. The elastomer material, GE-SE565U, belongs to the methyl-phenol-vinyl polymer class; conforming to MIL-R-5847C, Class 1. This particular material was selected because it can be molded in large sections and has favorable low-temperature properties.

The elastomer is molded in the form of a cylindrical annulus with a tapered core. The larger diameter in the lower section of the

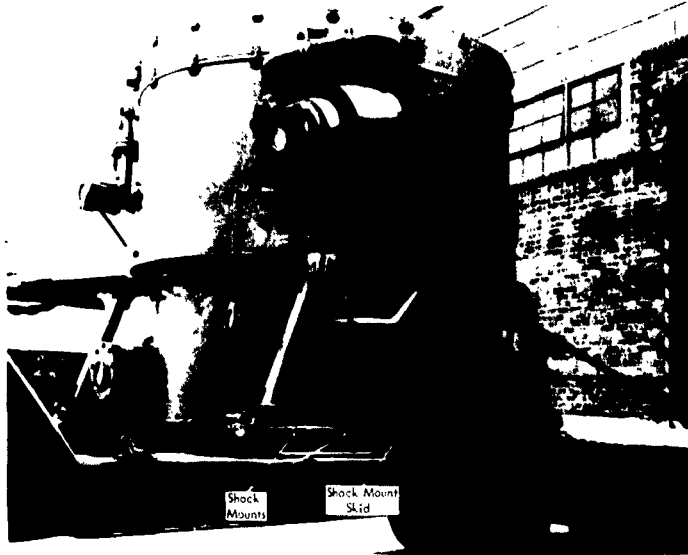


Fig. 1 - MIL-1 reactor, location of shock mounts
and shock mount skid

tapered core allows clearance for vertical deflection. Initially, a compressive load transmitted from the top core assembly, places the elastomer in shear. At higher compressive loads, the elastomer loading changes from shear to compression as the void is filled and as the outer core of rubber flows over the container flange. Lateral loads are supported by the large bearing area of the core which places the elastomer in compression against the container. In normal operating ranges, the predominant mechanism for isolating vertical shocks is shear loading of the elastomer. Shear loading provides better shock isolation than does compressive loading in these ranges. A flange on the top of the container rim provides an added overload feature by using the increased contact area created by elastomer plastic flow between the container flange and the top core.

COMPONENT TESTS

Nylon

Static and dynamic tests were conducted on the nylon rope to determine the performance characteristics under widely varying environmental conditions. Dynamic test data were obtained from a specially designed fixture. Rope elongations were measured with scratch gages and electronic transducers. The elongation

was recorded by high-speed camera, and strain gages were placed in series with the rope to measure the load as a function of time. The output of all transducers was recorded on a 14-channel oscilloscope.

The tests were conducted at rope temperatures which varied from -65° to +150°F. Required rope temperatures were achieved with a special shroud surrounding the rope. The static load-deflection curve at various temperatures is shown in Fig. 3. All tests were based on a "worked" rope which had been subjected to five cycles of loading to 40 percent breaking strength.

The first series of impacts tested the dynamic response of the nylon rope. The dynamic response due to an impact, compared to the static load deflection and dynamic amplification at various rope temperatures is shown in Fig. 4. The term dynamic amplification, as used here, is defined as the apparent increase in stiffness of the shock isolator as opposed to the static response when a shock is applied at a high-strain rate.

Silicone Elastomer

Because limited performance data were available on the elastomer material selected for the shock mounts, an initial screening

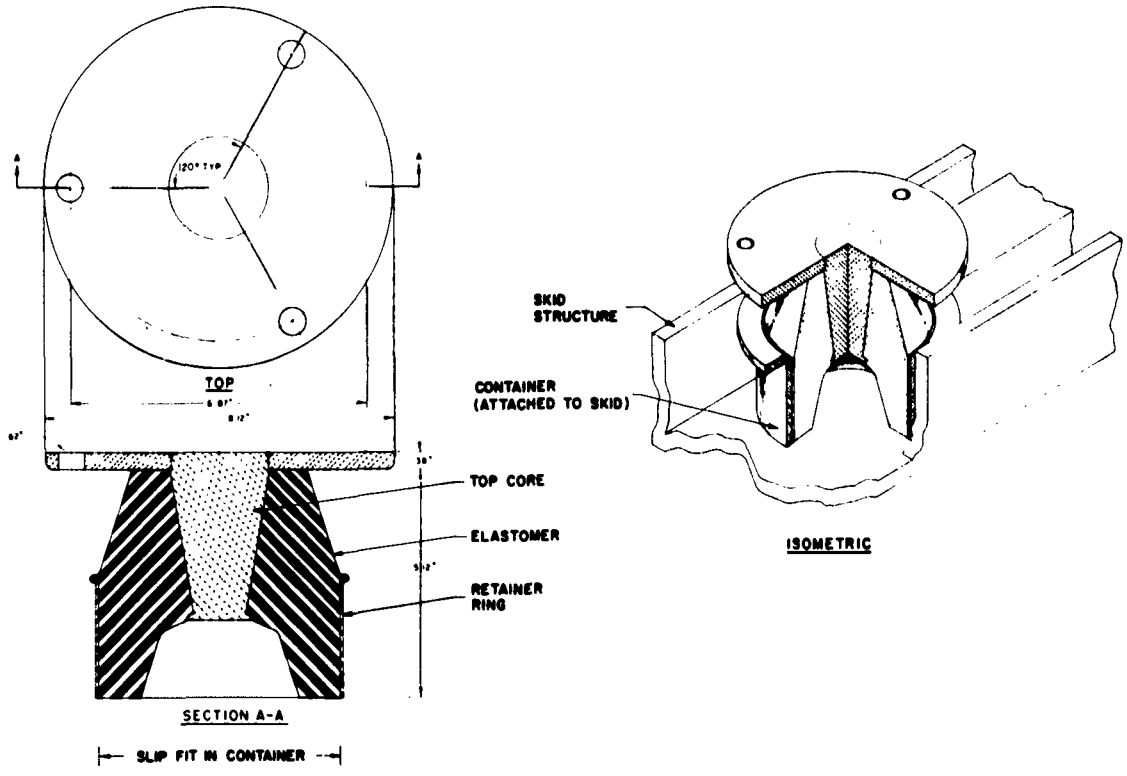


Fig. 2 - Shock mounts for ML-1 mobile nuclear power plant

program was undertaken. The 60-durometer specimen appeared to have the best properties for the shock mount application and it was selected for use. The experimental static load-deflection curves are shown in Figure 5. The mount was operating in shear at low deflections giving good shock isolation and high-frequency damping throughout the linear range. When high-compression loads were encountered (during ramping phases of the loading operations), the primary shock isolation mechanism changed from shear to compression; thus, the shock mounts provided high resistance to concentrated loads.

Tests to determine the dynamic properties of the shock mounts in the performance range of -65° to $+150^{\circ}\text{F}$ were conducted on the equipment used to test the nylon rope after some modifications were made to accommodate the shock mounts.

Figure 6 shows that approximately 70 percent of the input energy was absorbed in the first impact of the falling weight dropped from 6 feet onto the shock mount and 90 percent of the total input energy was absorbed on the second bounce.

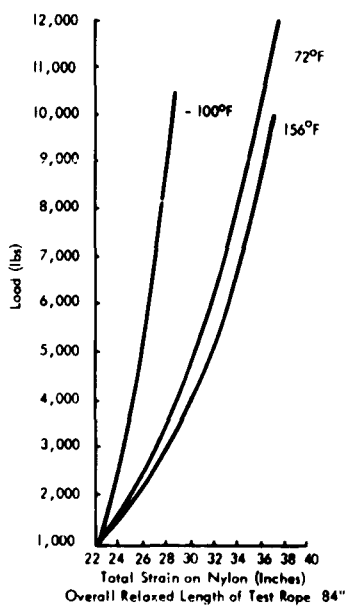


Fig. 3 - Static load-deflection curves for 1-1/8-inch nylon rope at various temperatures

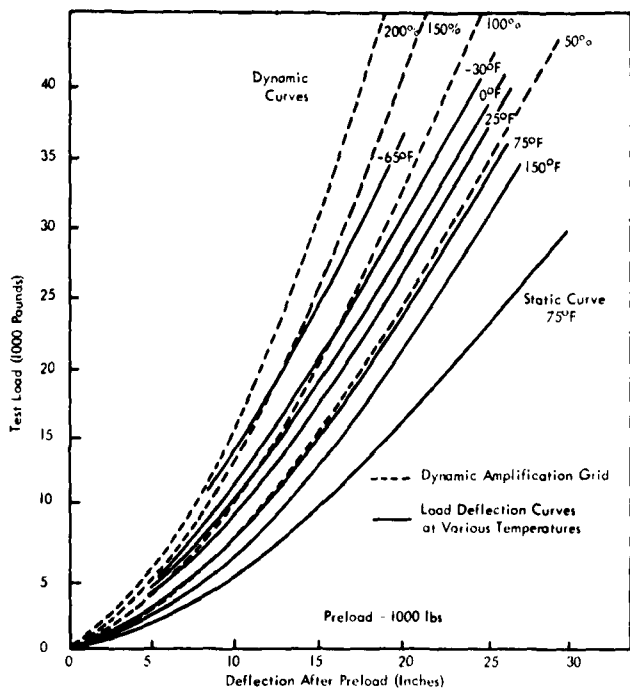


Fig. 4 - Dynamic response curves of 1-1/8-inch nylon rope at various temperatures. Shock applied by impacting with a 332-pound weight

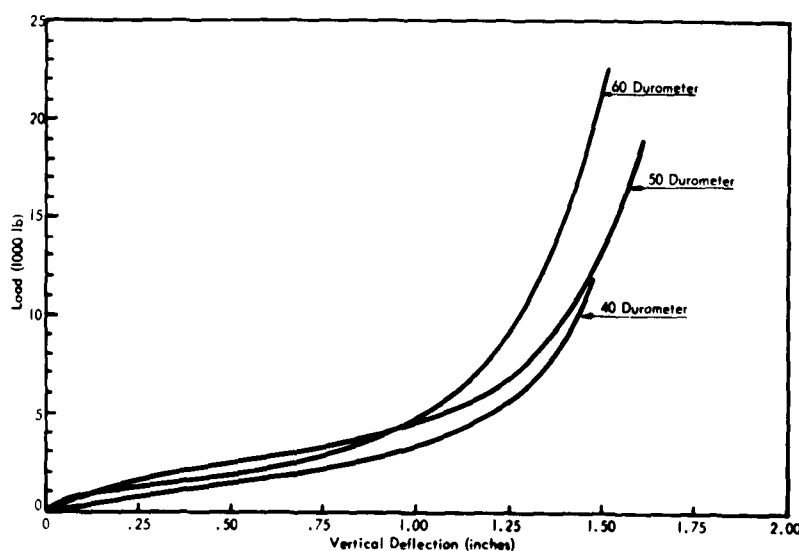


Fig. 5 - Experimental static load versus deflection curves for 40, 50, and 60 durometer silicone rubber

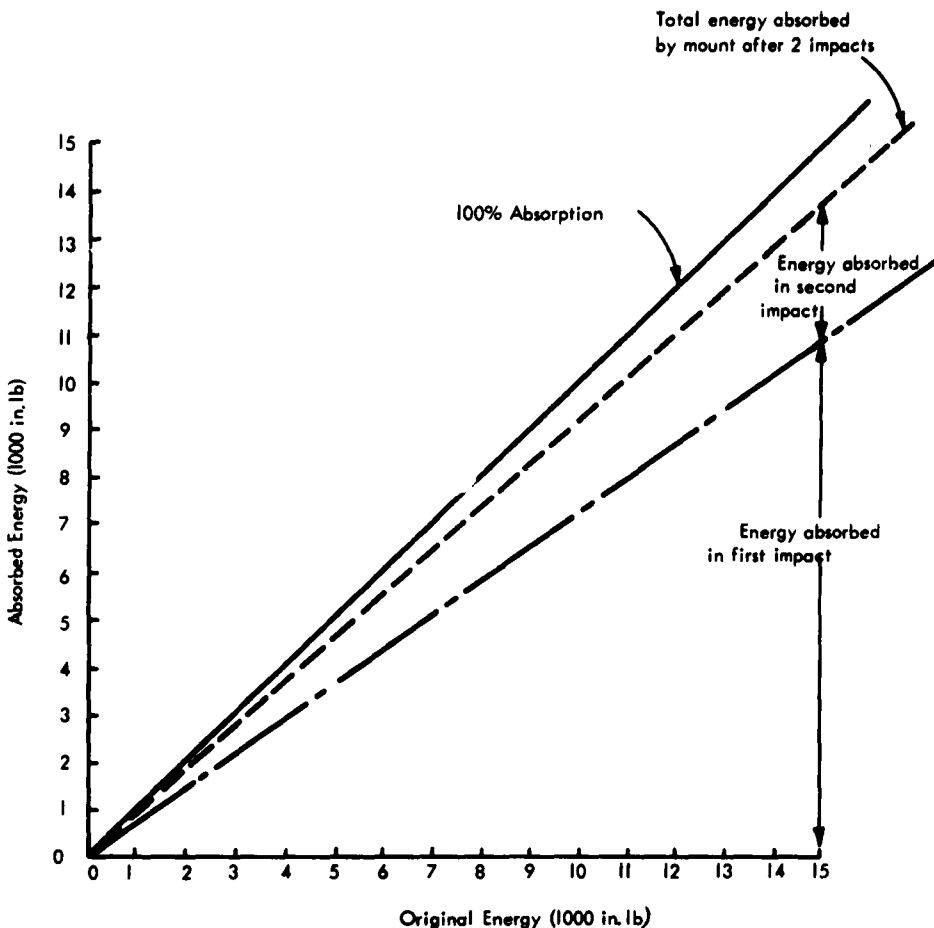


Fig. 6 - Shock mount dynamic properties - energy absorption for successive impacts by free-falling weight in test machine

The natural frequency of the shock mounts was determined by the following expression given by Crede [1].

$$f_{(n)} = 3.13 \sqrt{\frac{k}{W}}$$

where k = stiffness of isolator (lb/in)
(spring constant)
 W = weight supported by isolator, (lb)
(2140 lb/per isolator)

A plot of the natural frequencies of the mount during drop tests and an estimated

corresponding operating curve of the ML-1 plant is shown in Fig. 7.

FIELD TESTING

A full scale mockup of the ML-1 reactor was constructed to comprehensively test the proposed loading and tiedown techniques and to demonstrate that the plant satisfied the transportability requirements specified by the customer. The field testing was performed for two purposes. The first was to determine the shock isolation properties under severe railroad switching and humping operation. The second was to simulate an aircraft emergency landing and establish the effectiveness of the tiedown during such a landing.

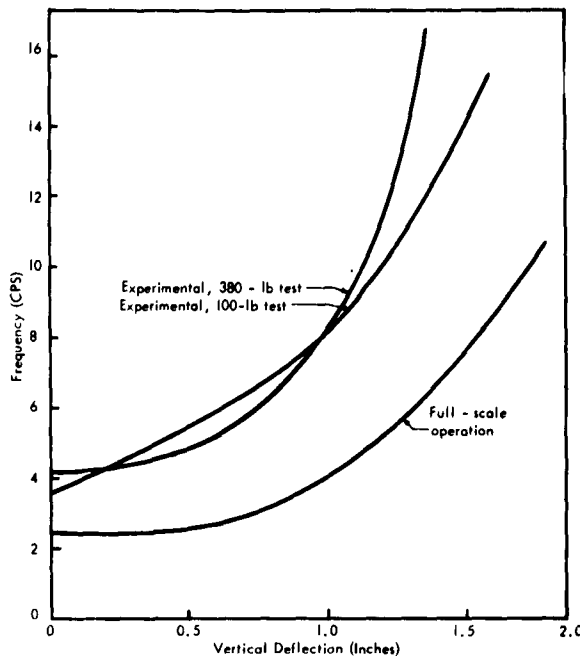


Fig. 7 - National frequencies of the 60-durometer silicone rubber shock mount from drop tests and an estimated operating curve with the ML-1 plant

Switching and Humping

A complete set of electronic and mechanical devices was installed on a test flatcar and on the ML-1 mockup. Accelerometers measured the horizontal, vertical and transverse acceleration of both the package and test car. A dynamometer measured the tension in a typical nylon rope. Dynamometer readings were recorded by a high-speed camera (approximately 400 frames per second). Scratch gages measured the displacement of the package along the bed of the flatcar and the vertical motion of the package relative to the flatcar. Horizontal and vertical motions were also recorded on the optical recording oscilloscope. The velocity of the impacting car at the moment of impact was determined by a series of microswitches mounted alongside the track and activated by a bracket on the impacting car. Two mechanical impact meters were provided by the Southern Pacific Railroad Company to correlate the impact on the test car and on the package with the impact measured by the electronic equipment.

The first tests were designed to determine the effects of switching and humping on the ML-1 during transportation. The 60,000-pound ML-1 mockup was tied down on a standard railroad flatcar using nylon rope. Fifty runs were made at impacting velocities varying from 4 to over 14 miles per hour. The mass of the impacting

cars varied from 59,000 pounds to 169,000 pounds. Typical tiedown arrangements used during these tests are shown in Fig. 8.

The horizontal shock reduction achieved at various impacting velocities is shown in Fig. 9. In no case throughout the testing did the measured impact on the package exceed 2-1/2 g, although the measured value of the test car acceleration exceeded 15 g in several runs. The vertical acceleration of the test car reached a peak value of 11-1/2 g, which was reduced to less than 1 g on the test package by the shock mounts. In only one run did the vertical acceleration of the package reach a value as high as 1.4 g. A graphic comparison of the vertical acceleration of the test car and of the package as a function of the velocity of the impacting cars is shown in Fig. 10. The graph indicates that at higher impacting velocities (10 miles per hour and over) the vertical shock reduction has about the same magnitude as the horizontal shock reduction, i.e., about ten to one.

The acceleration of the test car as a function of the velocity of the impacting car is shown in Fig. 11. One curve represents data taken from runs in which a sand-filled car was used for impacting and the other curve shows the results of a single impacting refrigerator car. These data will have application to similar switching and humping operations.

**SHOCK TEST INSTRUMENTATION
ML-1 REACTOR & POWER CONVERSION
PACKAGE, COUPLED**

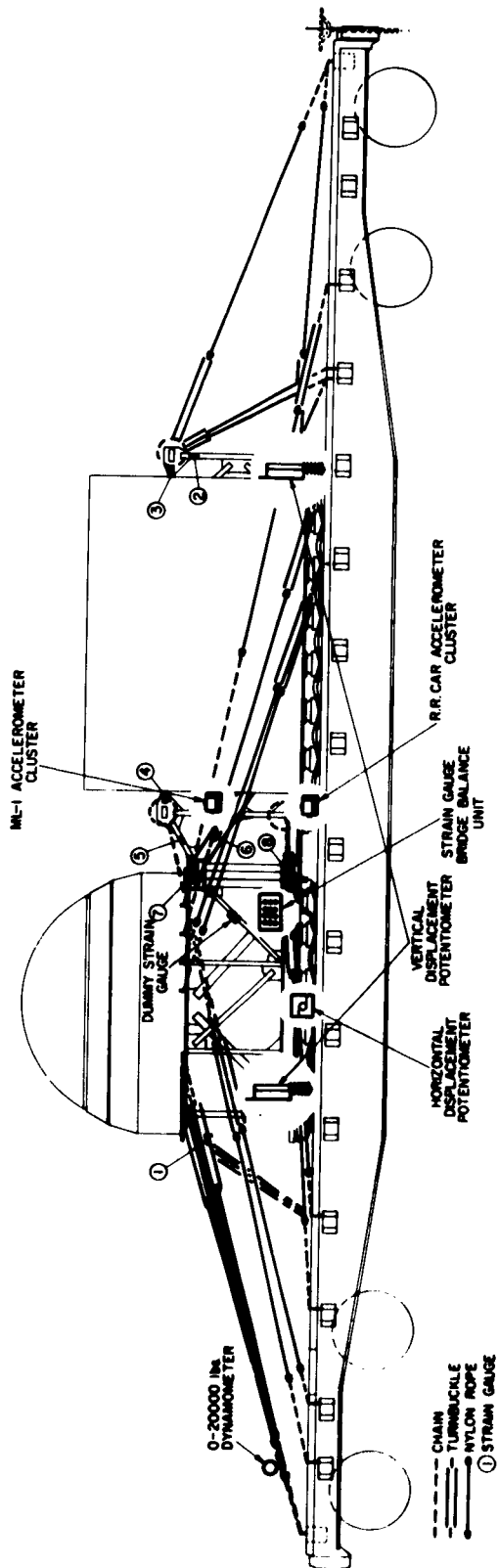
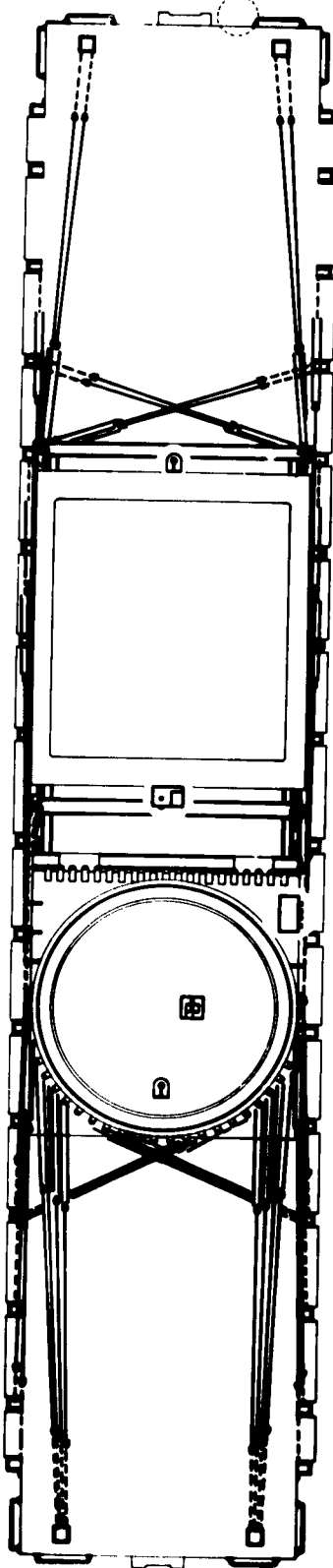


Fig. 8 - ML-1 reactor and power conversion package - tiedown and instrumentation for shock tests

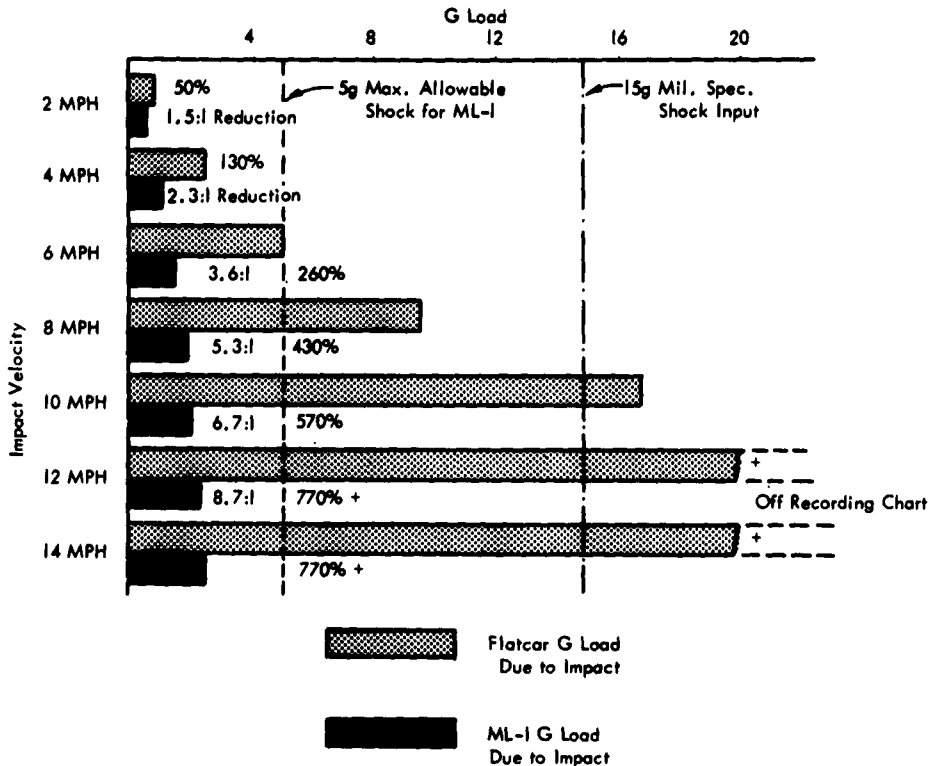


Fig. 9 - Horizontal shock reduction achieved by ML-1 shock isolation system at various impacting velocities

Another curve of interest to the test engineer is shown in Fig. 12. A correlation of the Southern Pacific impact meter data was made with the measured impact velocities obtained from the oscillograph charts. The impact meter underestimated the velocity of impact in nearly every case. This was especially true where the test car was impacted with a relatively small mass, such as an empty refrigerator car.

Only when the large masses were impacted did the impact meter data approximately correspond to the measured values. The meter data, however, corroborated the ratio of shock isolation between the test car and ML-1 package. All impact meter readings recorded on the ML-1 package fell within the safe (normal handling) range of the meter regardless of the impacting mass and velocity.

Figure 13 is a reproduction of an oscillograph chart, run at a speed of 50 inches per second. Ten-millisecond timing marks at the top of the chart were inscribed by a pulse generator. Each division on the chart represents

0.5 g for all accelerations. A peak of 16 g for the test car longitudinal acceleration was obtained 87 milliseconds after impact. The double peak was caused by the interaction of railroad draft gears. Note that the ML-1 longitudinal acceleration reached a peak of only 1-1/2 g, 214 milliseconds after impact. The relative longitudinal displacement was 5.8 inches. The test car vertical acceleration had a peak of 6 g which was reduced by the shock mounts to 1.25 g. Vertical shock mounting eliminated all of the high-frequency vibrations.

SIMULATED EMERGENCY LANDING LOADS

A second series of runs were made for the purpose of simulating as nearly as possible the conditions encountered in an aircraft emergency landing as outlined in the military air transportability specification [2]. This specification defines a pulse of 8 g in the forward direction applied along the horizontal axis for a minimum of 100 milliseconds.

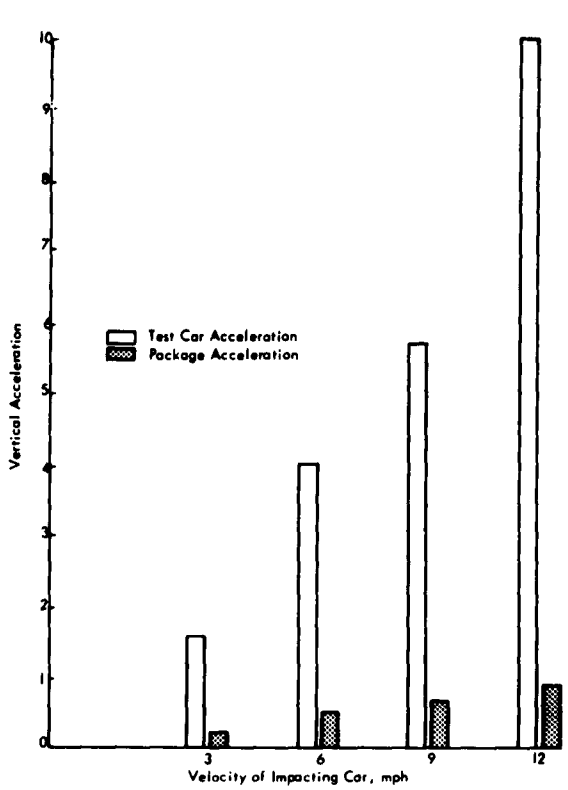


Fig. 10 - Comparison of the maximum vertical accelerations measured on the test car and on the ML-1 package

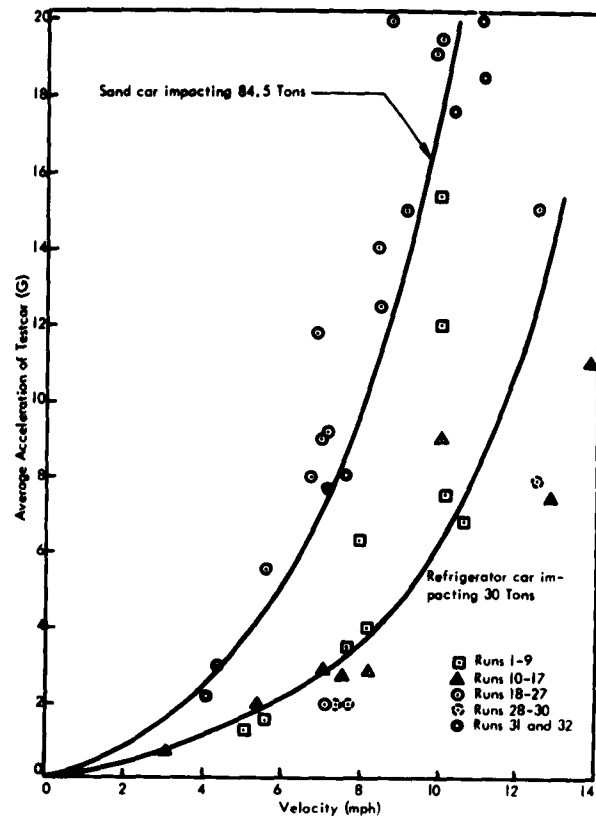


Fig. 11 - Average acceleration of the test car as a function of the velocity and mass of the impacting car

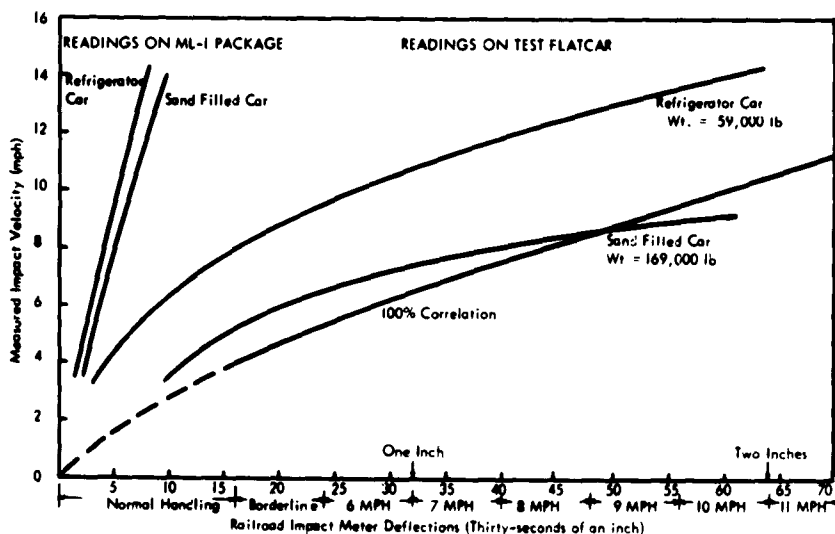


Fig. 12 - Correlation of Southern Pacific impact meter readings with measured impacting velocities

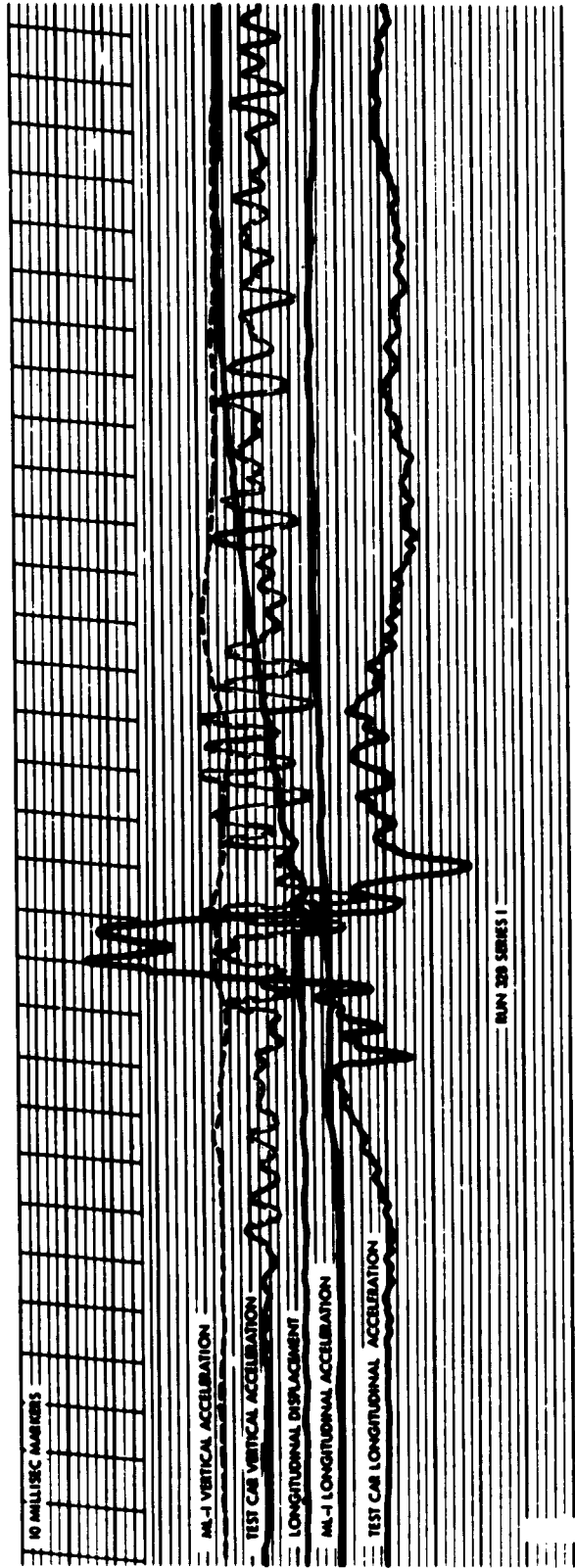
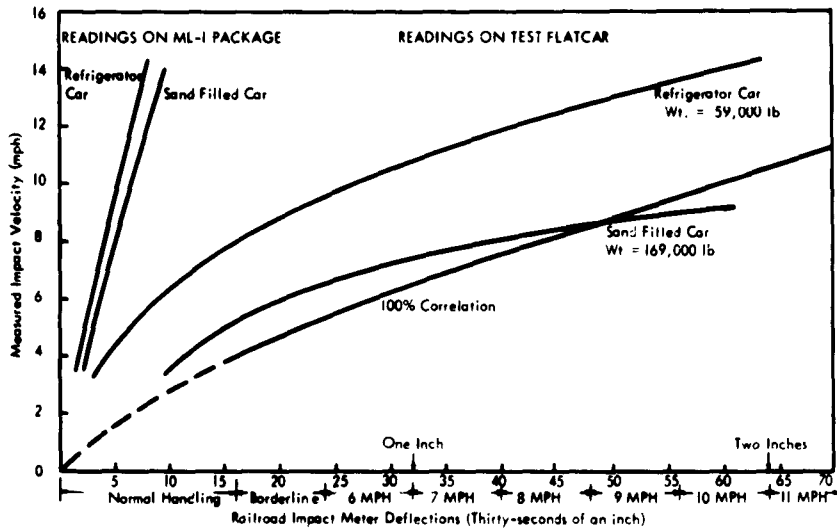
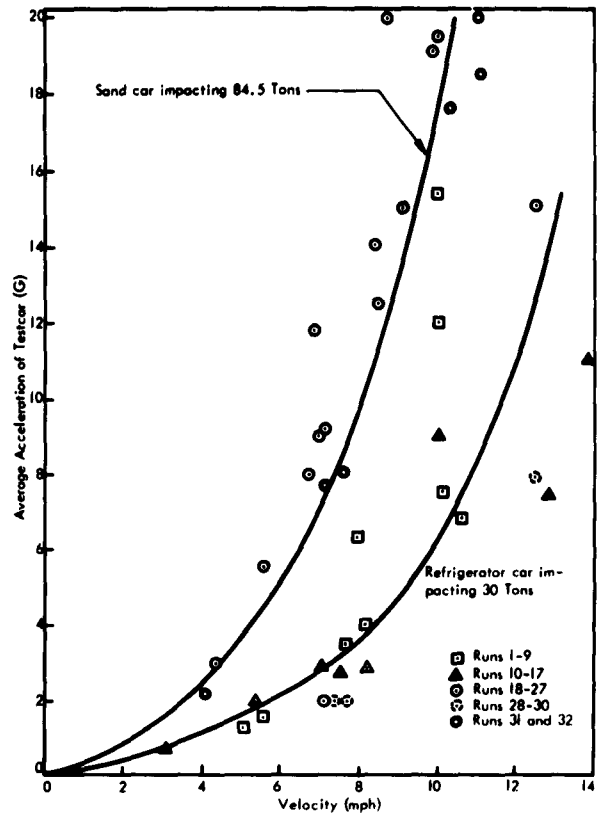
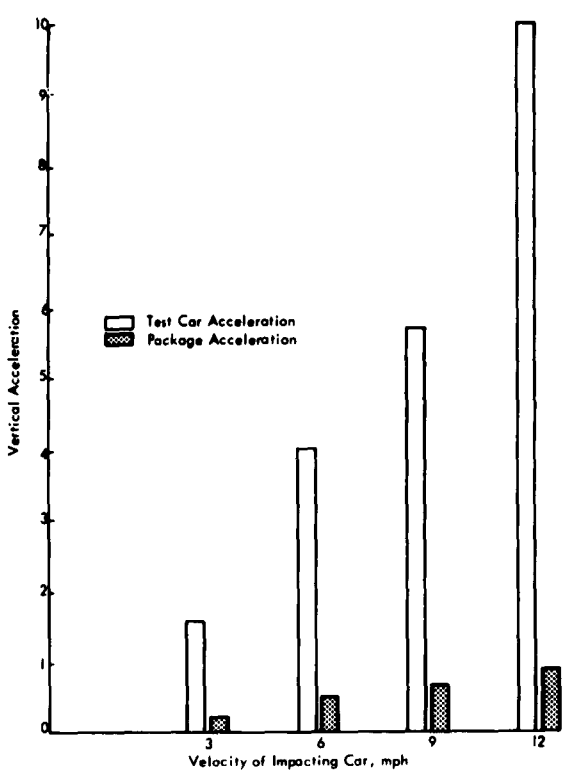


Fig. 13 - Oscillograph chart of data from switching and humping tests



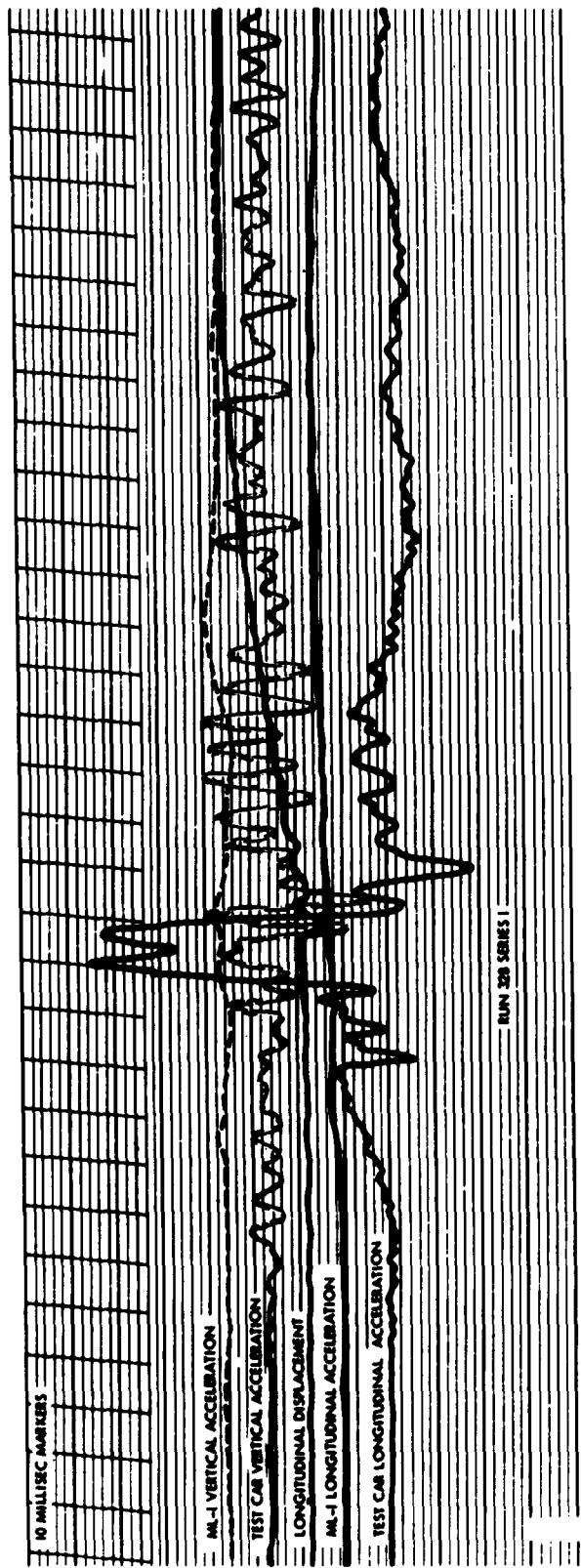


Fig. 13 - Oscillograph chart of data from switching and humping tests



Fig. 14 - Test setup for simulated aircraft emergency landing tests

To simulate the mass of the C130 aircraft, a refrigerator car was coupled to the flatcar. Aircraft tiedown configuration was duplicated on the flatcar and greased shoring was used throughout the test to duplicate normal aircraft loading techniques (Fig. 14).

Wooden blocks were placed between the railroad car couplings to lengthen the pulse duration. These blocks fulfilled their purpose in making the impact pulses long; however, they added an uncontrollable factor which made data correlation difficult. The wood did not compress in exactly the same way in any two runs and undoubtedly caused the flatcar draft gear to give more variable results than those obtained during the switching and humping tests. Data from the simulated landing test series are more widely scattered than those from the switching test.

To determine whether or not the specifications of the test were met, an equivalent time was calculated for each horizontal pulse. This equivalent time was defined by measuring the area under the trace on the oscillograph chart from the moment the pulse originated to the

point where the "faired in" curve crossed the horizontal axis. The pulse duration for an equivalent versine curve (i. e., a curve with an area equal to the area of the actual pulse) was calculated, using the peak of the "faired in" pulse as amplitude of the versine curve. In one run this peak was 8 g and the equivalent time was 100 milliseconds. Pulses of 11.3 g for shorter time durations (85 milliseconds) were also recorded. The maximum horizontal acceleration of the package throughout the tests was 2.4 g.

CONCLUSIONS

The testing program demonstrated that the specially designed shock isolation system using nylon rope and elastomer mounts will protect fragile cargo subjected to heavy shock loads. The system is effective over a wide range of temperatures.

The design should have application in the transport of various types of heavy, but fragile, cargo such as missiles, solid rocket engines, and mobile electronic field calibration systems.

REFERENCES

- [1] C. F. Crede, "Vibration and Shock Isolation," John Wiley & Sons, Inc., New York, 1951.
- [2] MIL-A-8421A (USAF), "General Specification for Air Transportability Requirements," 6 November 1958.

SHOCK AND VIBRATION OF APCHE TRAILER

S. A. Lever
Radio Corporation of America
Van Nuys, California

Effects of damping provided by shock absorbers of a vehicle suspension system were studied to determine their influence on the response of the vehicle body to bumps in the road. The study was undertaken to evaluate the feasibility of rigidly mounting electronic equipment to the vehicle body and using the vehicle suspension system as the basic shock mounting for the equipment. Results of the analysis are presented in the form of curves of body response versus road velocity for various bump heights. Results of road tests of the vehicle and a discussion of the test results as compared to analytical results are presented.

INTRODUCTION

A basic decision must be made concerning electronic equipment which is mounted for operation in a highway vehicle. The equipment items must be protected against accelerations caused by motion over irregularities in the road. The protection can be provided by shock mounting the items inside the vehicle body. On the other hand, the equipment can be rigidly mounted to the vehicle structure and the basic shock mounting provided by the vehicle suspension system. The latter design philosophy was followed in the design of the Automatic Programmed Checkout Equipment (APCHE) semi-trailer. Some of the considerations which led to the decision are the subject of this paper.

Once the decision has been made that rigid mounting of electronic components to the vehicle structure is advantageous, the desired characteristics of the vehicle suspension system and the reaction of the structure to irregularities in the road must be determined. In determining the desired characteristics of the vehicle suspension system, the most difficult problem occurs in specifying the damping ratio, as determined by the shock absorbers. Analyses were performed, using the damped single-degree-of-freedom spring-mass system as an analytical tool, to estimate the acceleration and amplitude response of the body. Practices in the trade were investigated to

determine values of damping ratio and natural frequency which are readily obtainable in practice. A value of damping ratio was then assumed for the analysis. Inputs to the vehicle wheels were based on specified road shapes and irregularities. For the shock conditions of the analysis and for normal road velocities, damping was generally found to be harmful on the upstroke and beneficial on the downstroke.

The most severe vibration input was found to occur in travel over the Belgian-block road. A transverse section was assumed for the Belgian-block road, and the acceleration of the trailer body was plotted versus road velocity. The most severe acceleration response of 1.2 g was found to occur at the maximum specified road velocity of 20 mph.

Results of the shock analysis were plotted in the form of curves of spring compression and trailer body acceleration versus velocity for various bump heights. The results indicated that on the upstroke of the shock absorber the damped system generally transmits more acceleration to the body than an undamped system. Also, the amplitude of spring compression is nearly equal to the bump height for an undamped system and is only slightly less for the damped system. On the downstroke, damping was found to be beneficial in that it reduces both acceleration and amplitude response. Under the most severe shock conditions

specified, a 4-inch-high bump at 20 mph, and for the parameters assumed for the numerical analysis, the maximum acceleration response was calculated to be 1.8 g for an undamped system and 3.4 g for the damped system.

DESIGN REQUIREMENTS

The APCHE semitrailer was designed to transport and house electronic equipment and personnel required for checkout of the ATLAS Missile at the launching site. The semitrailer must traverse paved highways at speeds up to 60 mph, graded gravel roads at speeds up to 25 mph, and the Belgian-block road of the Aberdeen Proving Ground at 20 mph. The relatively severe requirement was imposed by RCA that the trailer be capable of traversing a 4-inch-high bump (similar to a 4- by 8-inch railroad tie) at 20 mph without damage. The purpose of this requirement was to simulate the worst type of obstruction likely to be encountered on a paved highway.

From manufacturers of trailer suspension systems, information was obtained on characteristics of suspension springs, damping properties of the shock absorber systems and the degree of damping which is practicable. An overall natural frequency of the suspension system of 1 to 2 cps is obtainable and has been used in semitrailer suspension systems. A damping ratio of 0.25 is a practical maximum. The almost universal practice is to apply less damping on the compression stroke than on the rebound. A common proportion is three to four times as much damping on rebound as on compression. In spite of the general acceptance of this practice, however, no analytical basis for the practice was found to be available in the literature.

Several considerations influence the choice of a spring constant or natural frequency of the suspension system. As soft a spring as possible is desirable in this portion of the system for several reasons. From a dynamic standpoint the mounting system for electronic components can be considered to comprise the chassis, which are mounted on the cabinets, which in turn are mounted on the trailer body. Finally the trailer body is mounted on the suspension system. The suspension system is thus that part of the dynamic system which transmits irregularities in the road to the rest of the system as shock and vibration inputs.

Using as low a natural frequency as practicable for the suspension system makes it possible to use the design philosophy of constructing

components which are mounted on other components with progressively more rigidity. The shock load transmitted by the suspension system increases with the natural frequency. For this reason also it is desirable to have a low-natural frequency of the suspension system. A disadvantage of the low-natural frequency of the suspension system is that larger motions are then possible, and excessive sway of the trailer body may result. This condition may be alleviated by devices such as an antisway bar and, under some conditions, by an air suspension system.

The analysis of shock response of a spring-mass system with damping to a shock input is somewhat complex. Although analyses of response to various shock inputs are discussed in the literature for undamped systems, meager information was found on the shock response of damped systems. An analysis was performed on the response of a damped and an undamped single-degree-of-freedom system to a ramp type input. The limitations of such an analysis in describing the actual motion of the vehicle are many and the intention is not to minimize the importance of these limitations. Nevertheless, the single-degree-of-freedom system whose damping ratio can be varied is an extremely useful analytical tool, and by its use useful information not otherwise readily available can be obtained. The single-degree-of-freedom case was judged to be useful and amenable for exploratory analyses. Cases with more degrees of freedom were reserved for solution with analog computers after some of the parameters of the system become more clearly defined. The case in which the wheels leave the ground also falls into the class of those with more than one degree of freedom and is reserved for solution with analog computers.

MODEL OF SYSTEM

A diagram of the overall vibrating system which was considered is shown in Fig. 1, only the vertical translatory motion of the trailer is considered. Rolling and pitching motions were not considered. The forward point of attachment of the semitrailer to the tractor, referred to in the trade as the fifth wheel, is not a rigid type of attachment. The front suspension system for the APCHE semitrailer is a torsion bar type with shock absorbers to provide damping.

The cabinets in which electronic chassis and parts are mounted were assumed to be rigidly mounted to the interior trailer structure. Preliminary stress analyses of the cabinet structure indicated that the natural frequency

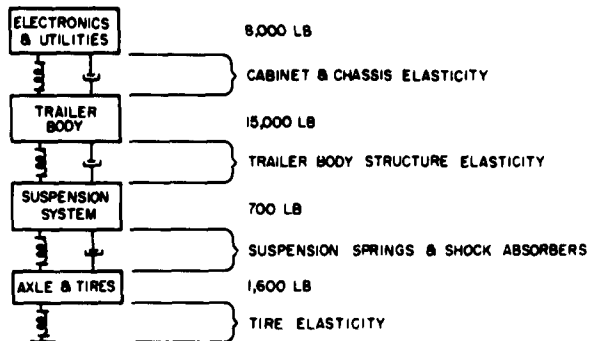


Fig. 1 - Diagram of system, step 1

of a fully loaded cabinet was at least three times that of the trailer body. The assumption of rigid mounting of chassis and cabinets to the trailer structure was therefore judged to introduce a relatively small error.

From data presented in Ref. 1 the tires were assumed to have a spring constant which would result in a natural frequency of 10 to 17 cps. Since this was at least five times the natural frequency of the spring suspension system, the spring constant of the tires was neglected.

The assumptions was made that the tires do not leave the road. The vertical motion of the tires then corresponds to that of the road, and the weight of the axle and tires can be neglected. The model of the system was then as shown in Fig. 2.

Some discussion is in order concerning the assumption that the wheels do not leave the ground. In automobile suspension design, control of the motion of the unsprung mass is considered one of the most serious problems in suspension system design. In an automobile,

however, the unsprung mass comprises perhaps one-third of the total mass of the vehicle. In the vehicle presently under consideration the unsprung mass comprises about one-twelfth of the total vehicle weight. This particular problem was therefore considered to be much less serious.

Since the natural frequency of the trailer body, considered as a vibrating beam, is many times that of the suspension system, the springs in Fig. 2 which represent the elasticity of the trailer body might well have been neglected. A rigid coupling between the trailer body and the suspension system would then have been assumed. The decision was made, however, to investigate the response of the combined system to a vibration input.

NOTATION

Symbols

<i>a</i>	= rise time, sec
<i>A</i>	= maximum input amplitude, in.
<i>b</i>	= ratio of forcing frequency to undamped natural frequency
<i>d</i>	= distance, in.
<i>e</i>	= voltage, volts
<i>f</i>	= frequency, cps
<i>f_n</i>	= natural frequency, cps
<i>k</i>	= spring constant, lb/in.
<i>m</i>	= mass, lb sec ² /in.
<i>n</i>	= an integer
<i>r</i>	= damping constant, lb sec/in.
<i>r_c</i>	= damping constant required for critical damping, lb sec/in.
<i>R</i>	= tire radius, in.
<i>s</i>	= Laplace operator
<i>t</i>	= time, sec
<i>t_m</i>	= time at which maximum or minimum occurs, sec
<i>T</i>	= transmissibility
<i>u</i>	= symbol indicating unit step function
<i>v</i>	= velocity, in./sec
<i>x</i>	= displacement, in.
<i>X</i>	= Laplace transform of <i>x</i>
<i>y</i>	= normalized spring compression

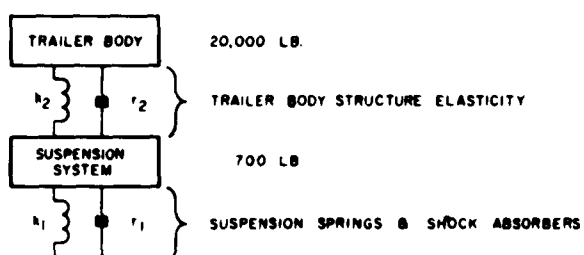


Fig. 2 - Diagram of system, step 2

- α = decrement factor, radians/sec
 β = angular damped natural frequency of vibration, radians/sec
 ζ = damping ratio
 ω = angular frequency of input vibration, radians/sec
 ω_n = angular undamped natural frequency of vibration, radians/sec.

Subscripts

- m = maximum or minimum
 n = natural
 o = applied.

VIBRATION ANALYSIS

The determination of the response of the system of Fig. 2 to a vibration input was considered. Specifically, the problem considered was that of determining the variation with frequency of the transmissibility of the trailer body spring-mass system in conjunction with the spring and damper which comprise the trailer suspension system.

Transmissibility Under Vibration Input

The trailer body structure was idealized as a beam on hinged supports with a total uniformly distributed weight, fully loaded, of 20,000 pounds, including the weight of cabinets, chassis, electronic components, and the utility system. The maximum specified deflection was 0.05 inch. The Rayleigh method was used to find a factor by which the distributed weight might be multiplied to determine an equivalent concentrated weight which would have the same effect on vibration as the distributed weight.* The factor was determined to be 0.493. Using beam deflection formulas and the relationships

$$\omega_n = \sqrt{\frac{k}{m}} \quad (1)$$

and

$$\omega = 2\pi f \quad (2)$$

the natural frequency of the body structure was determined. A list of numerical values is given in Table 1.

*Reference 2, Page 459

The damping constant of the trailer was estimated by assuming that the transmissibility at resonance of the trailer body alone would be 20. The damping ratio was then found from Fig. 3. Then using the relationships

$$r_c^2 = 4km \quad (3)$$

$$\zeta = \frac{r}{r_c} \quad (4)$$

the damping constant of the beam was found. The trailer body could then be represented as a damped single-degree-of-freedom spring-mass system.

The characteristics of the spring (or pneumatic) suspension system were then considered. The assumption was made that if the suspension system were required to support a 20,000-pound load of infinite stiffness, its natural frequency would be 1.5 cps. Then by using Eqs. (1) to (4) and determining the damping ratio from Fig. 3, the calculated values shown in Table 1 were found.

In combining the damped spring-mass systems comprising the trailer body and the suspension system, the mass of the suspension system was neglected since its weight was assumed to be only 5 percent of that of the trailer body. The model of the vibration system considered was thus reduced from that shown in Fig. 2 to that shown in Fig. 4.

In the analog of Fig. 4, voltage is analogous to velocity. Therefore

$$T = \frac{e_2}{e_o} = \frac{x_2}{x_o} = \frac{\dot{x}_2}{\dot{x}_o} = \frac{\ddot{x}_2}{\ddot{x}_o} \quad (5)$$

Impedance analogs for mechanical terms are indicated in Fig. 4. The term ω represents the applied or forcing frequency. Analysis of the circuit and use of Eq. (5) produced Eq. (6).

$$T = \frac{1}{j\omega m_2 \left(\frac{1}{j\omega m_2} + \frac{j\omega}{k_1 + j\omega r_1} + \frac{j\omega}{k_2 + j\omega r_2} \right)} \quad (6)$$

A plot of the absolute (or vector) value of T versus ω is shown in Fig. 5. Figure 5 indicates that the maximum transmissibility of the system, assuming a sinewave input, is 1.8 at a natural frequency of 2.0 cps.

TABLE 1
Numerical Values

Trailer Body		
Assumed Values		
Weight	= 20,000 lb	$\omega_n = 99.0$ radians/sec
Maximum deflection	= 0.05 in.	$f_n = 15.75$ cps
T_m	= 20	$k_2 = 2.50 \times 10^5$ lb/in.
Length of beam	= 360 in.	$r_{c_2} = 5050$ lb sec/in.
		$r_2 = 126.4$ lb sec/in.
		$\zeta = 0.025$
		$m_2 = 25.5$ lb sec ² /in.
Suspension System		
Weight supported	= 20,000 lb	$k_1 = 4600$ lb/in.
f_n	= 1.5 cps	$r_{c_1} = 977$ lb sec/in.
ζ	= 0.25	$r_1 = 244$ lb sec/in.
Combined System		
		$r_3 = 235$ lb sec/in.
		$k_3 = 4450$ lb/in.
		$\zeta = 0.35$
		$\alpha = 4.66$ radians/sec
		$\beta = 12.5$ radians/sec
		$\omega_n = 13.3$ radians/sec

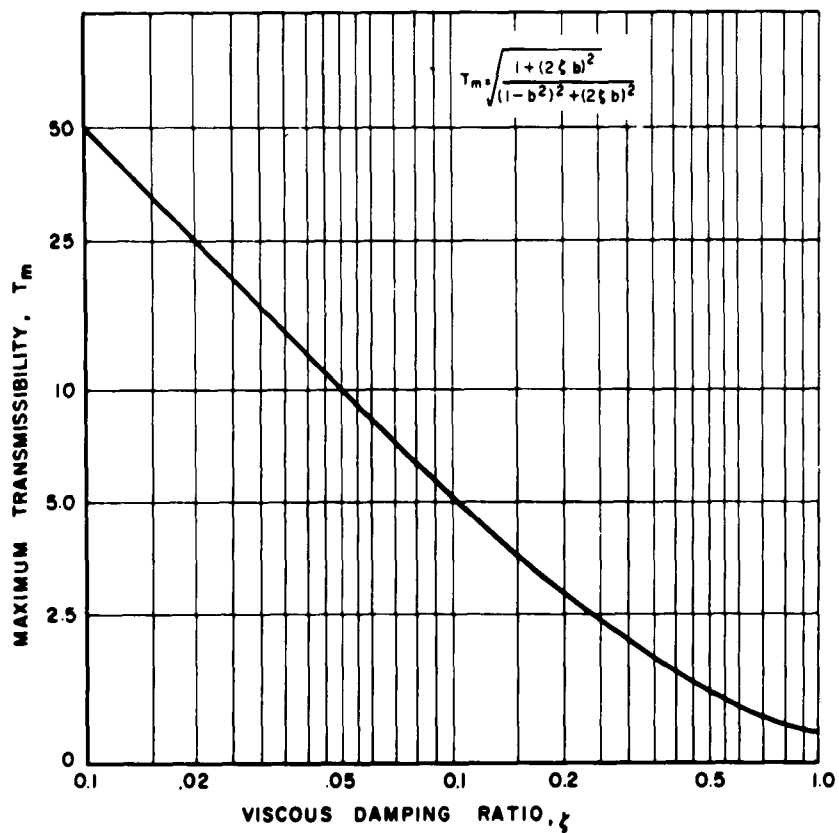


Fig. 3 Transmissibility at resonance versus damping ratio for a damped single-degree-of-freedom system

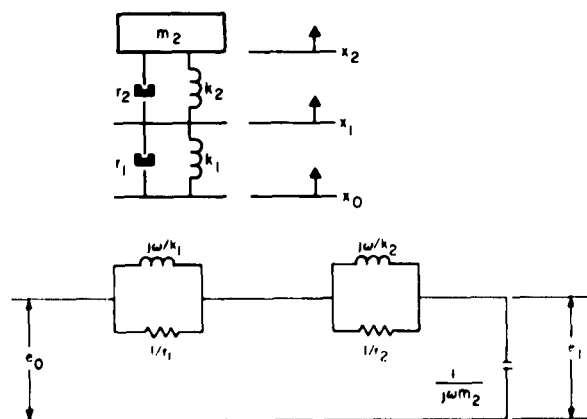


Fig. 4 - Diagram and electrical analog of system, step 3

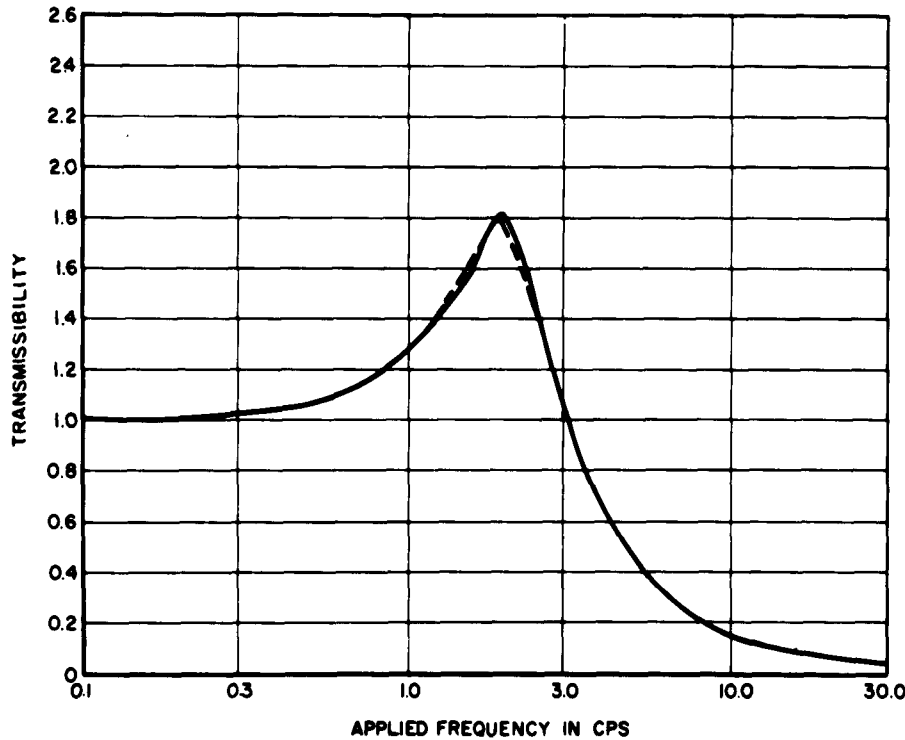


Fig. 5 - Transmissibility of combined suspension system and trailer body versus input frequency

Single-Degree-of-Freedom System

Consideration was next given to the possibility of approximating the model shown in Fig. 4 by the model shown in Fig. 6.

This involves replacing two parallel branches in series with one parallel branch. Expressed mathematically,

$$\frac{j\omega}{k_3 + j\omega r_3} = \frac{j\omega}{k_1 + j\omega r_1} + \frac{j\omega}{k_2 + j\omega r_2} . \quad (7)$$

Equation (7) was solved for k_3 and r_3 by equating real and imaginary parts.

$$r_3 = \frac{(k_1 + k_2)(r_1 k_2 + r_2 k_1) - (r_1 + r_2)(k_1 k_2 - \omega^2 r_1 r_2)}{(k_1 + k_2)^2 + \omega^2(r_1 + r_2)^2} . \quad (9)$$

It was found that for the numerical values used in the analysis and for input frequencies below about 20 cps k_3 could be closely approximated by the equation

$$k_3 = \frac{k_1 k_2}{k_1 + k_2} \quad (10)$$

and that r_3 could be closely approximated by the equation

$$k_3 = \frac{(k_1 k_2 - \omega^2 r_1 r_2)(k_1 + k_2) + \omega^2(r_1 k_2 + r_2 k_1)(r_1 + r_2)}{(k_1 + k_2)^2 + \omega^2(r_1 + r_2)^2} \quad (8)$$

$$r_3 = \frac{r_1 k_2^2}{(k_1 + k_2)^2} . \quad (11)$$

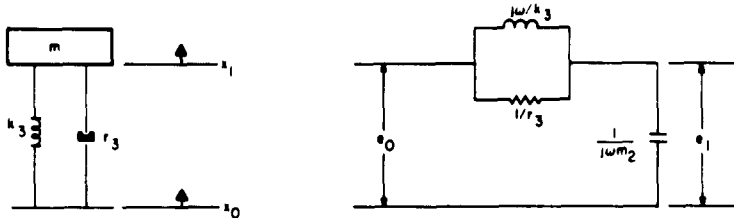


Fig. 6 - Diagram and electrical analog of system, step 4

Equation (11) is interesting in that it indicates that at low input frequencies the value of the composite damping constant r_3 is not greatly influenced by the value of the damping constant assumed for the trailer body structure. An approximation was made by obtaining k_3 from Eq. (10) and r_3 from Eq. (9) or (11). A plot of the response of the system of Fig. 6 using these values was then made and is shown as the dotted line of Fig. 5. It can be seen that the simplified single-degree-of-freedom system is a good approximation to the combined system. The numerical values shown with subscript 3 in Table 1 were therefore used in the shock analysis. The mass m of Fig. 6 was assumed to represent the trailer body, and the spring and damper to represent the suspension system springs and shock absorbers.

Vibration Input and Response

The most severe vibration input encountered by the trailer occurs as the result of travel over the Belgian-block road. From information supplied in Refs. [1] and [3], the longitudinal section of the Belgian-block road was assumed to be as shown in Fig. 7. From this figure the input displacement of the trailer wheels is

$$x_0 = A \cos \omega t \quad (12)$$

where $A = 1$ inch. Also

$$\omega = \frac{\pi v}{36} \quad (13)$$

The input could then be determined in terms of road velocity. Using Fig. 3 to find transmissibility Fig. 8 was obtained. Figure 8 shows the input acceleration and the response acceleration of the trailer body as a function of trailer velocity on the Belgian-block road.

SHOCK ANALYSIS

To perform the shock analysis, the transfer function for the system was first derived. The input function was expressed in terms of amplitude in order to be able to relate the input to the conditions of the road. The input was assumed to be of the ramp type and to rise linearly with time during the ramp, until a certain rise time, τ , had elapsed at which the input amplitude reached a magnitude A . After the ramp, the input amplitude was assumed to remain constant at the amplitude A for an infinite time. Rise times were calculated in terms of vehicle speed for various bump heights. The input function could then be completely defined. The purpose of allowing the amplitude to remain constant for an infinite time after the ramp was to be sure that the response had time to reach its maximum.

The equation of motion of the system under the shock input was solved. The solution was expressed in terms of compression of the spring and acceleration of the trailer body, for the time periods during and after the ramp. In each case, the maximum acceleration or displacement during the time period under consideration was desired. The time at which the maximum occurs was solved by setting the derivative with respect to time equal to zero. Since the response, in general, has the form of a sinewave or damped sinewave this procedure gives the time at which the maximum of the absolute value occurs. By addition of multiples of 180° to the solution for the angle at which the absolute maximums occur, successive relative absolute maximums can be found.

When the procedure of setting the derivative equal to zero is followed, the times at which relative absolute maximums occur are found, but attention must also be given to the physical situation in that the mathematical

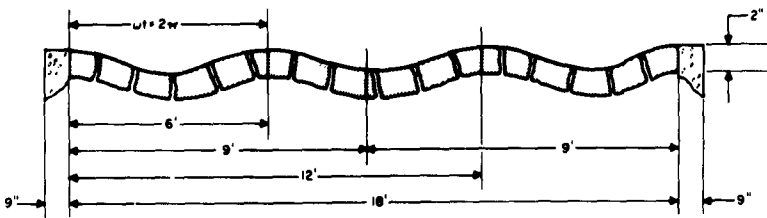


Fig. 7 - Assumed longitudinal cross section of Belgian-block road

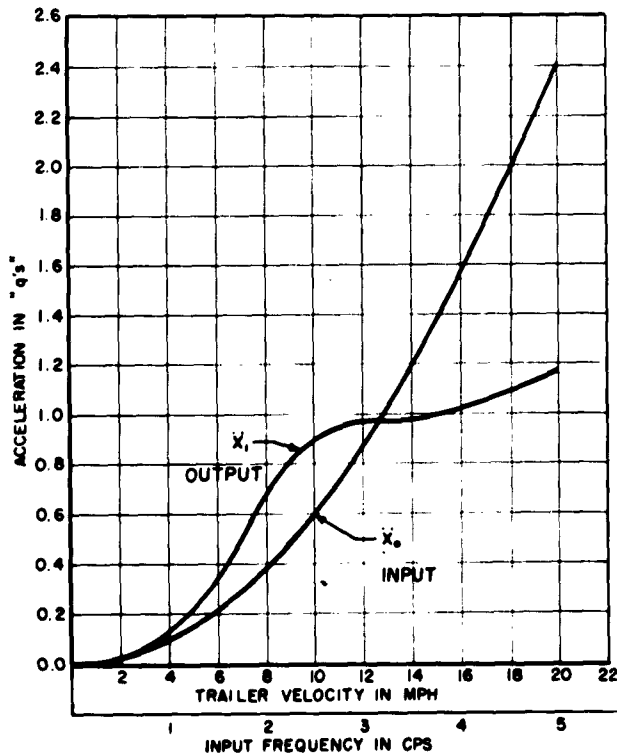


Fig. 8 - Input and response acceleration versus velocity on Belgian-block road

solution is sometimes physically impossible. In some cases, the maximum absolute response occurs at the end of the ramp (when $t = n$). In general the maximum absolute response on the compression part of the stroke was found for the period during the ramp, and the maximum absolute response on the rebound part of the stroke for the period after the ramp.

Transfer Function

In this section, the transfer function of the single-degree-of-freedom system shown in

Fig. 6 is derived. In later sections the shock input function and the response of the system are treated.

The differential equation of motion of the system of Fig. 6 is

$$m\ddot{x}_1 + r(\dot{x}_1 - \dot{x}_0) + k(x_1 - x_0) = 0 \quad (14)$$

In the shock analysis, the subscript 3 from Fig. 6 was dropped, and all values of r and k were assumed to be those shown with

subscript 3 in Table 1. Taking the Laplace transform, where capital letters represent transformed variables, the transfer function of the system may be found to be

$$\frac{x_1}{x_0} = \frac{2\alpha s + \omega_n^2}{(s + \alpha)^2 + \beta^2} \quad (15)$$

where

$$\alpha = \zeta \omega_n \quad (16)$$

and

$$\beta = \omega_n \sqrt{1 - \zeta^2}. \quad (17)$$

The terms α and β have physical significance in that β is the actual natural frequency of the vibrating system (sometimes called the damped natural frequency), and α (sometimes called the decrement factor) defines the exponential rate of decay of the transient response.

Shock Input

The input function for purposes of the shock analysis, was assumed to have the form shown in Fig. 9. This pulse may be expressed in terms of unit step functions as

$$x_0 = \frac{A}{n} [tu(t) - (t - n)u(t - n)] \quad (18)$$

where the unit step functions are defined as in Eqs. (19) and (20)

$$\begin{aligned} u(t) &= 1 \text{ when } t > 0 \\ u(t) &= 0 \text{ when } t < 0 \end{aligned} \quad (19)$$

and

$$\begin{aligned} u(t - n) &= 1 \text{ when } t > n \\ u(t - n) &= 0 \text{ when } t < n. \end{aligned} \quad (20)$$

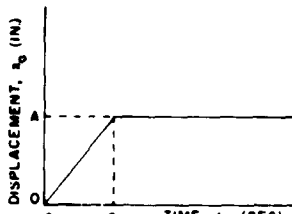


Fig. 9 - Shock input pulse shape

Taking the Laplace transformation of Eq. (18),

$$X_0 = \frac{A}{n} \frac{1 - e^{-ns}}{s^2} \quad (21)$$

Equation (21) is combined with Eq. (15) in later sections to find the transform of the output.

The relationships among rise time, vehicle velocity, and bump height were investigated. Figure 10 shows a vehicle tire ascending the type of bump assumed for the analysis. Assuming that the tire is solid and of radius R , in ascending the bump the center of the axle will move from the point 1 to the point 2 along an arc of radius R with its center of rotation at the point 3. The time n which is required to ascend the bump of height A is the time required to traverse the horizontal distance d . To make this picture compatible with the input pulse shape represented by Fig. 9 it remains only to approximate the arc 1-2 by a straight line and to calculate the time n as a function of the horizontal velocity v .

Using the triangle 1-3-4 to solve for the distance d , the rise time can be expressed in terms of velocity, bump height, and tire radius:

$$n = \frac{\sqrt{A(2R - A)}}{v}. \quad (22)$$

The tire radius R was taken as 20 inches. By the use of Eq. (22) the rise time n , as a function of velocity and bump height, was calculated.

If the wheel descends into a pothole of depth A with sheer sides, the motion is in the opposite direction from that considered here. The complete solution for this condition would require the consideration of a two-degree-of-freedom case which, as stated previously, is outside the scope of the present analysis. Preliminary calculations indicated, however, that the response for the case of descending from a given height is less severe than for the case of ascending.

SHOCK RESPONSE

Combining Eqs. (15) and (21), and solving for x_1 ,

$$X_1 = \frac{A}{n} \frac{2\alpha s + \omega_n^2}{s^2 [(s + \alpha)^2 + \beta^2]} (1 - e^{-ns}). \quad (23)$$

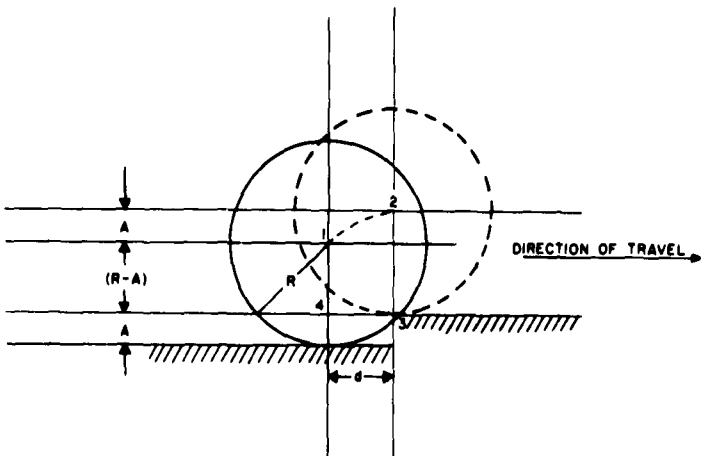


Fig. 10 - Vehicle tire ascending bump

Taking the inverse transform, the normalized response is

$$\frac{x_1}{A} \approx \frac{1}{a} \left\{ t - \frac{1}{\beta} e^{-at} \sin \beta t + u(t-a) \left[(t-a) - \frac{1}{\beta} e^{-a(t-a)} \sin \beta(t-a) \right] \right\}. \quad (24)$$

The solution was divided into two time periods: (1) the response during the ramp and (2) the response after the ramp. Each time period was considered separately.

Response During the Ramp

Considering the time period during the ramp (when $t < a$), the normalized response is

$$\frac{x_1}{A} = \frac{1}{a} \left(t - \frac{1}{\beta} e^{-at} \sin \beta t \right). \quad (25)$$

It is convenient at this time also to present the first, second, and third derivatives:

$$\frac{\dot{x}_1}{A} = \frac{1}{a} \left[1 + e^{-at} \left(\frac{\alpha}{\beta} \sin \beta t + \cos \beta t \right) \right] \quad (26)$$

$$\frac{\ddot{x}_1}{A} = \frac{e^{-at}}{a} \left[\frac{\beta^2 - \alpha^2}{\beta} \sin \beta t + 2\alpha \cos \beta t \right] \quad (27)$$

$$\begin{aligned} \frac{\ddot{x}_1}{A} = & \frac{e^{-at}}{a} \left[\frac{\alpha}{\beta} (\alpha^2 - 3\beta^2) \sin \beta t + \right. \\ & \left. + (\beta^2 - 3\alpha^2) \cos \beta t \right]. \end{aligned} \quad (28)$$

Response After the Ramp

Considering the time period after the ramp (when $t > a$), the normalized response is

$$\begin{aligned} \frac{x_1}{A} = & \frac{1}{a} \left[a - \frac{1}{\beta} e^{-at} \sin \beta t + \right. \\ & \left. + \frac{1}{\beta} e^{-a(t-a)} \sin \beta(t-a) \right]. \end{aligned} \quad (29)$$

The first, second, and third derivatives are

$$\begin{aligned} \frac{\dot{x}_1}{A} = & \frac{1}{a} \left\{ e^{-at} \left[\frac{\alpha}{\beta} \sin \beta t - \cos \beta t \right] - e^{-a(t-a)} \right. \\ & \left. \left[\frac{\alpha}{\beta} \sin \beta(t-a) - \cos \beta(t-a) \right] \right\} \end{aligned} \quad (30)$$

$$\begin{aligned} \frac{\ddot{x}_1}{A} = & \frac{1}{a} \left\{ e^{-at} \left[\frac{\beta^2 - \alpha^2}{\beta} \sin \beta t + 2\alpha \cos \beta t \right] - e^{-a(t-a)} \right. \\ & \left. \left[\frac{\beta^2 - \alpha^2}{\beta} \sin \beta(t-a) + 2\alpha \cos \beta(t-a) \right] \right\} \end{aligned} \quad (31)$$

$$\frac{\ddot{x}}{A} = \frac{1}{n} \left\{ e^{-at} \left[\frac{a}{\beta} (a^2 - 3\beta^2) \sin \beta t + (\beta^2 - 3a^2) \cos \beta t \right] \right.$$

$$- e^{-a(t-a)} \left[\frac{a}{\beta} (a^2 - 3\beta^2) \sin \beta(t-a) \right] \quad (32)$$

$$+ (\beta^2 - 3a^2) \cos \beta(t-a) \right\}$$

SPRING DISPLACEMENT UNDER SHOCK INPUT

The suspension system spring compression is the difference between the displacement of the body x_1 and the displacement of the axle x_0 . For convenience a normalized spring compression y was defined as

$$y = \frac{x_1 - x_0}{A}. \quad (33)$$

With reference to the static equilibrium position of the spring, a positive value of y indicates that the wheels and the body are farther apart; a negative value indicates that they are closer together. A study of this term was then required to gain an indication of whether the suspension springs will bottom under certain road conditions.

Displacement During The Ramp

During the ramp, or in the time interval when $t < a$,

$$x_0 = \frac{At}{a}. \quad (34)$$

Combining Eqs. (25), (33), and (34),

$$y = \frac{-1}{a\beta} e^{-at} \sin \beta t \quad (35)$$

and

$$\dot{y} = \frac{-1}{a\beta} e^{-at} (a \cos \beta t - \beta \sin \beta t). \quad (36)$$

In the case under consideration, the maximum response with respect to time as the rise time varies was desired. To maximize y , the first derivative with respect to time was set equal to

zero. Setting \dot{y} from Eq. (36) equal to zero, the times at which y is a relative maximum are

$$t_m = \frac{1}{\beta} \tan^{-1} \frac{\beta}{a} + \frac{1}{\beta} n\pi. \quad (37)$$

If the smallest value of t_m from Eq. (37) is used in Eq. (35), the maximum response of the system is determined. Then using Eq. (22) to find the rise time a , a plot of maximum spring displacement versus vehicle speed for various bump heights can be obtained. This curve is shown in Fig. 11.

Caution must be exercised in using the result of Eq. (37). When the smallest value of t_m as determined by Eq. (37) is greater than a , the solution has no physical meaning. In such a case, it may be shown that the maximum value of y occurs when $t = a$. This procedure was followed in obtaining Fig. 11.

Displacement During The Ramp With Zero Damping

If the system has zero damping, then $\zeta = 0$, $a = 0$, and $\beta = \omega_n$. From Eq. (35), the response is

$$y = \frac{-1}{a\omega_n} \sin \omega_n t. \quad (38)$$

The maximum absolute value of this expression occurs when the angle is $\pi/2$ radians. Again, caution must be used to be sure that $t_m < a$. If setting the angle equal to $\pi/2$ radians produces a solution in which $t_m > a$, it is evident that the maximum of y occurs when $t = a$. The case of zero damping is included in Fig. 11.

Displacement After The Ramp

After the ramp, or in the time interval when $t > a$,

$$x_0 = A. \quad (39)$$

Combining Eqs. (29), (33), and (39),

$$y = \frac{e^{-at}}{a\beta} [-\sin \beta t + e^{a(t-a)} \sin \beta(t-a)] \quad (40)$$

and

$$\dot{y} = \frac{e^{-at}}{a\beta} \{ a \sin \beta t - \beta \cos \beta t + e^{a(t-a)} [\beta \cos \beta(t-a) - a \sin \beta(t-a)] \}. \quad (41)$$

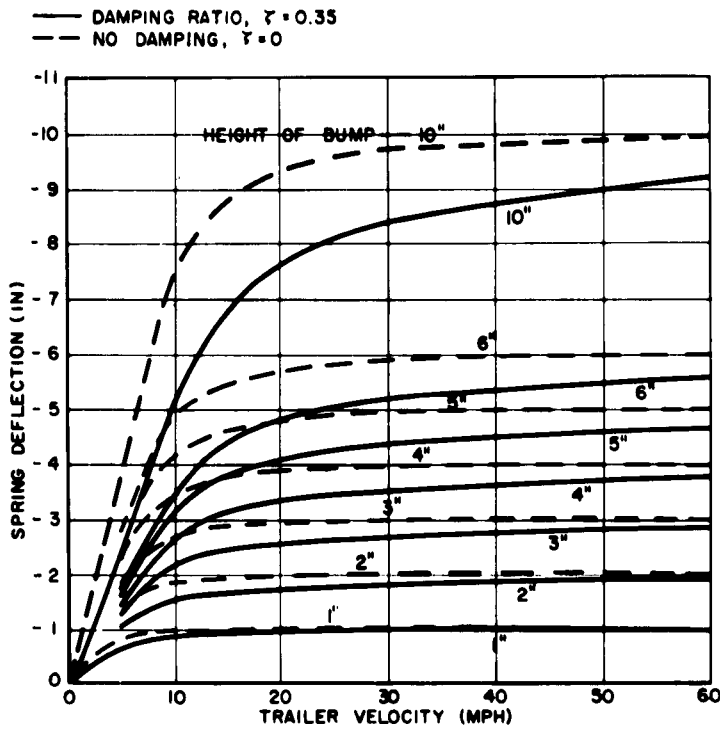


Fig. 11 - Maximum spring deflection during ramp versus trailer velocity

The first derivative \dot{y} was set equal to zero to find the times at which y is a relative maximum. These times were found to be

$$t_m = \frac{1}{\beta} \tan^{-1} \frac{\beta - e^{a\alpha} (\beta \cos \beta a + a \sin \beta a)}{a + e^{a\alpha} (\beta \sin \beta a - a \cos \beta a)} + \frac{1}{\beta} n \pi. \quad (42)$$

If the result of Eq. (42) is used in Eq. (40), the maximum response of the system is determined. Using Eq. (22) to find the rise time a , a plot of spring displacement after the ramp versus vehicle speed for various bump heights was obtained. This curve is shown as Fig. 12.

Caution must be exercised in interpreting the result of Eq. (42). When the smallest value of t_m as determined by Eq. (42) is less than a , this solution has no physical meaning. In such a case the maximum absolute value of y may occur at the next subsequent value of t_m , or it may occur when $t = a$. Numerical analysis may be used to determine which value is greater. The objective of the analysis was to find the maximum absolute value of the response on the downstroke. Analysis of the results indicated that in general this could be found by using the smallest value of t_m which is greater than a .

This procedure was followed in obtaining the results plotted in Fig. 12.

Displacement After The Ramp With Zero Damping

When $\zeta = 0$ from Eq. (42)

$$t_m = \frac{1}{\omega_n} \tan^{-1} \frac{1 - \cos \omega_n a}{\sin \omega_n a} + \frac{1}{\omega_n} n \pi \quad (43)$$

The expression for y reduces to

$$y = \frac{1}{\omega_n a} [\sin \omega_n t + \sin \omega_n (t - a)]. \quad (44)$$

Equation (43) may be combined with Eq. (44) to find the maximum value of y after the ramp with zero damping. Again caution must be exercised to be sure that $t_m > a$, or else a procedure analogous to that described in the previous section must be followed. When the

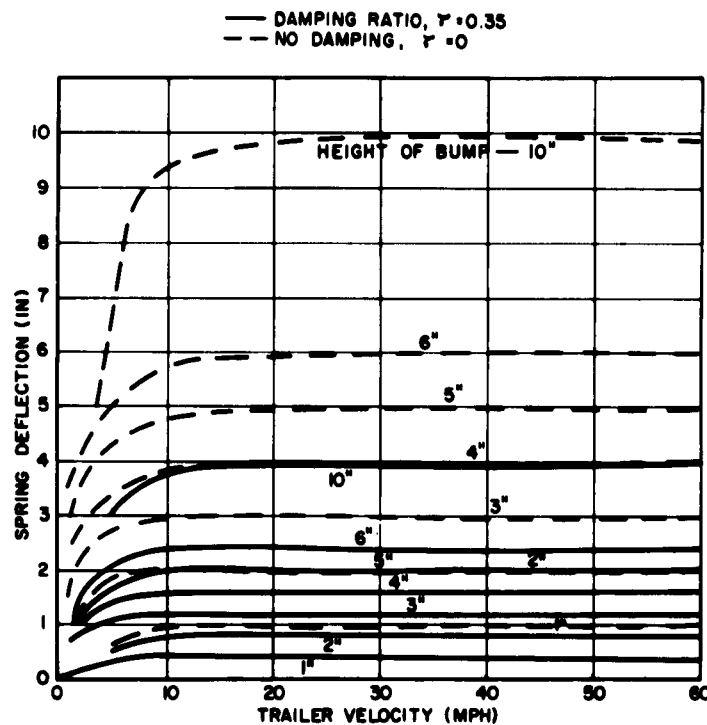


Fig. 12 - Maximum spring deflection after the ramp versus trailer velocity

conditions are met such that Eq. (43) can be used in Eq. (44) to find the maximum, then

$$y_m = \pm \frac{2}{\omega_n a} \sin \frac{\omega_n a}{2}. \quad (45)$$

The case of zero damping is also shown in Fig. 12.

Aside from relative simplicity of Eq. (45), it is interesting to note the plus-or-minus sign in the equation. This sign properly indicates that when damping is absent, the response is as great in the positive as in the negative direction. Also, the response is not attenuated with time. As a practical matter, however, even without shock absorbers, some damping will be present, and the amplitude will damp out eventually.

ACCELERATION OF THE BODY UNDER SHOCK INPUT

The acceleration of the trailer body as the result of a shock input is given by Eqs. (27) and (31). As before it was convenient to consider separately the times before and after the ramp.

Acceleration During The Ramp

During the interval when the trailer is ascending the ramp the acceleration experienced by the body is given by Eq. (27). The maximum acceleration with respect to time as the rise time varies was desired. To find this time, the third derivative as expressed by Eq. (28) was set equal to zero. The time at which the acceleration x_1 reaches a relative maximum was determined to be

$$t_m = \frac{1}{\beta} \tan^{-1} \frac{\beta(3\alpha^2 - \beta^2)}{\alpha(\alpha^2 - 3\beta^2)} + \frac{1}{\beta} n\pi. \quad (46)$$

To calculate maximum values of x_1 , the result of Eq. (46) was used in Eq. (27) to obtain the maximum acceleration during the ramp. If the smallest value of the time t_m from Eq. (46) is greater than a , it can be shown that the maximum acceleration occurs at $t = a$. A plot of maximum acceleration versus vehicle speed for various bump heights is given in Fig. 13.

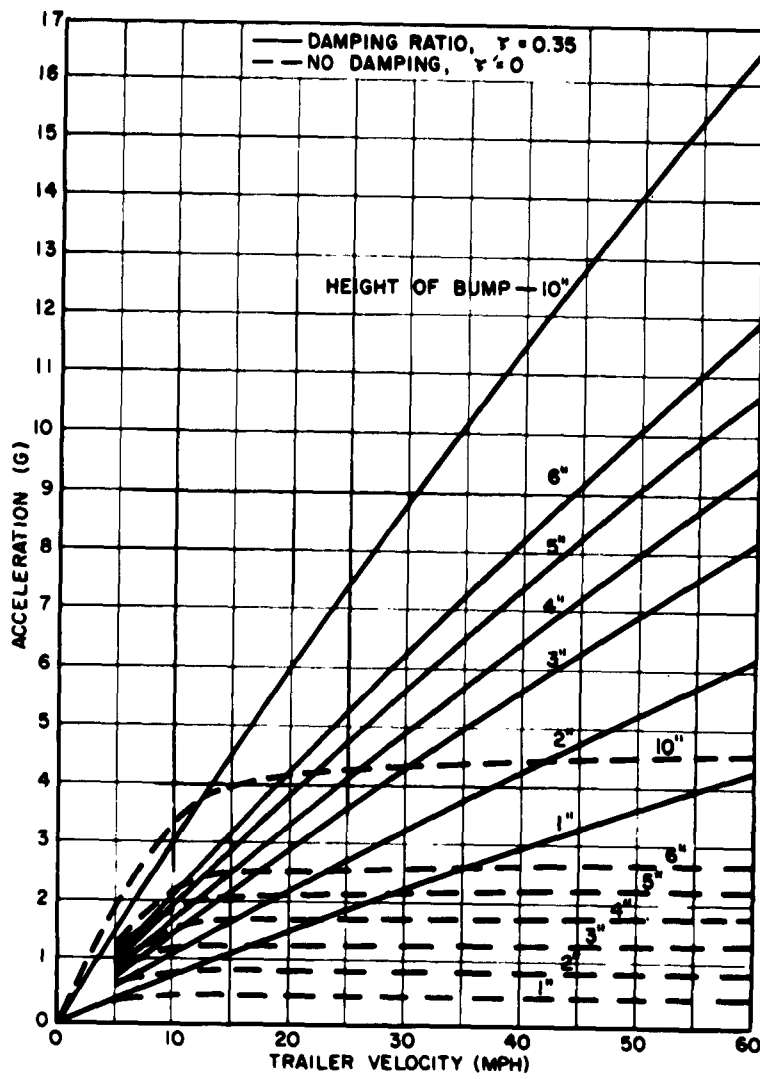


Fig. 13 - Maximum response acceleration during ramp versus trailer velocity

Acceleration During The Ramp With Zero Damping

The acceleration with zero damping may be found from Eq. (27) to be

$$\frac{\ddot{x}_t}{A} = \frac{\omega_n^2}{a} \sin \omega_n t. \quad (47)$$

The maximum acceleration occurs when the angle becomes $\pi/2$. If the time when this occurs proves to be greater than a , it is evident

that the maximum acceleration occurs when $t = a$. The case of zero damping is also shown in Fig. 13.

Acceleration After The Ramp

After the ramp, the acceleration of the body can be determined from Eq. (31). The time when the absolute value of the acceleration is a maximum can be obtained by setting the third derivative, from Eq. (32), equal to zero. The result is

$$t_m = \frac{1}{\beta} \tan^{-1} \frac{\frac{a}{\beta} (3\beta^2 + \alpha^2) e^{\alpha a} \sin \beta a - (3\alpha^2 + \beta^2) e^{\alpha a} \cos \beta a + 3\alpha^2 + \beta^2}{\frac{a}{\alpha} (3\beta^2 + \alpha^2) e^{\alpha a} \cos \beta a + (3\alpha^2 + \beta^2) e^{\alpha a} \sin \beta a + \frac{a}{\beta} (3\beta^2 + \alpha^2)} \quad (48)$$

The result of solving for t_m in Eq. (48) can be used in Eq. (31) to find the maximum acceleration, provided that $t_m > a$. If, from Eq. (67) the resulting $t_m < a$, a procedure analogous to that described previously must be followed. A plot of maximum acceleration versus vehicle speed for various bump heights is given in Fig. 14.

Acceleration After The Ramp With Zero Damping

When zero damping is assumed to be present, Eq. (31) reduces to

$$\frac{\ddot{x}_1}{A} = \frac{\omega_n}{a} [\sin \omega_n t - \sin \omega_n (t - a)]. \quad (49)$$

Solving for the times at which the acceleration is a relative maximum in the same manner as before,

$$t_m = \frac{1}{\omega_n} \tan^{-1} \frac{1 - \cos \omega_n a}{\sin \omega_n a} + \frac{1}{\omega_n} n\pi. \quad (50)$$

The result of Eq. (50) was used in Eq. (40) to determine the maximum acceleration after the ramp. If the result of Eq. (50) is a value of $t_m < a$, a procedure analogous to that described previously must be followed. The case of zero damping is also plotted in Fig. 14.

DISCUSSION OF ANALYTICAL RESULTS

One of the problems under consideration was the amount of damping required on the up-stroke as opposed to the downstroke. Separation of the solution into two time periods, during the ramp and after the ramp, provided a convenient means of studying the problem. In general, the maximum response during the ramp represented the maximum response on the compression part of the stroke; the maximum response after the ramp represented the maximum response on the rebound part of the stroke.

The spring deflection during the time the wheel is ascending the ramp approaches the height of the bump as vehicle speed increases (Fig. 11). At all speeds the spring deflection

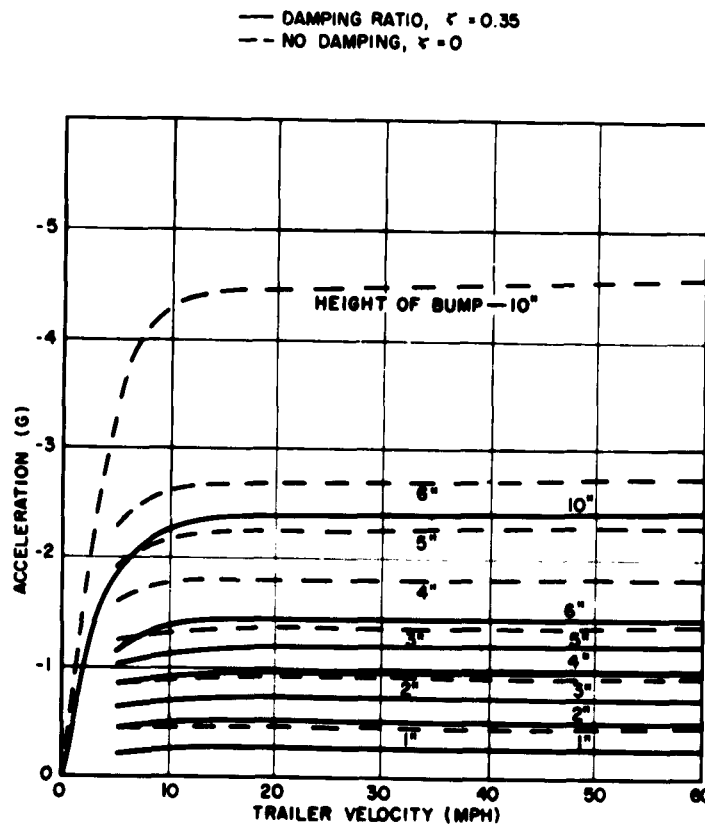


Fig. 14 - Maximum response acceleration after the ramp versus trailer velocity

for the damped system was less than that for the undamped system. The difference, however, was small. For a 4-inch-high bump and a vehicle speed of 20 mph, the spring deflection for the damped system was 3.3 inches and for the undamped system 3.9 inches. For most design problems, this difference would not be considered sufficient to warrant providing damping on the upstroke to limit deflection. The acceleration of the trailer body during the ramp, for the 4-inch bump at 20 mph, is 1.8 g for the undamped system and 3.4 g for the damped system (Fig. 13). This difference may be significant depending on the fragility of the components mounted inside the trailers. Figure 13 indicates that at speeds greater than 10 mph and bump heights less than 6 inches, the trailer body acceleration is less for the system without damping than for the damped system.

In general, the analysis indicated the analytical basis for the practice in the trade of supplying less damping on the upstroke of a shock absorber than on the downstroke. Less acceleration is applied to the vehicle, and a better "ride" results. In cases such as racing cars where the ride is less important and the handling, or deflection, characteristics of the vehicle are all important, the practice in the trade is to supply equal amounts of damping on the up and downstrokes. The analytical basis for this practice was also shown.

After the ramp, both the amplitude and acceleration response are less severe than for the period during the ramp. Since, with no damping, the motion of the trailer body theoretically continues without attenuation, both the amplitude and acceleration response are the

same in both the positive and negative directions. The damped maximum amplitude response after the ramp is such that the body and wheels are farther apart. This is in contrast to the period during the ramp when the body and wheels are closer together. The damped maximum acceleration response after the ramp, reached its maximum absolute value in the negative direction. In the case of both acceleration and amplitude, damping was found to be beneficial in that it attenuated the response after the ramp, or on the downstroke.

In the case of vibration, the maximum amplitude response occurs at the resonant frequency. Since the amplitude of the input on the Belgian-block road was assumed to be 1 inch, and the maximum transmissibility is 1.8, the maximum response amplitude is 1.8 inches. The maximum acceleration of the body was found to be 1.2 g. The maximum acceleration occurred at the maximum specified velocity of 20 mph and an input frequency of 4.9 cps. The maximum acceleration response did not occur at the resonant frequency of the suspension system since with a constant-amplitude input, the input acceleration increases with the square of the input frequency or vehicle velocity. Then since the acceleration increases faster than the transmissibility decreases, the maximum response acceleration occurs at the maximum velocity.

ROAD TESTS

A view of the APCHE trailer undergoing road tests is shown in Fig. 15. Views of the front and rear suspension systems are shown in Figs. 16 and 17. The trailer body, frame,



Fig. 15 - APCHE trailer and instrumentation vehicle

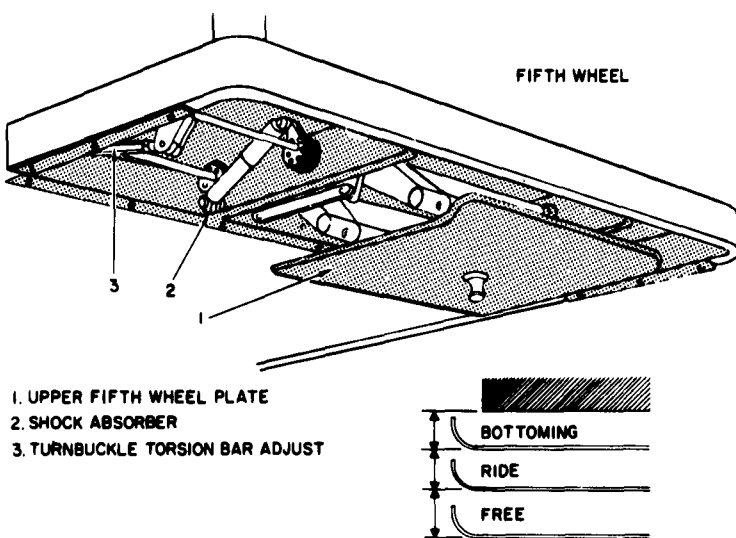


Fig. 16 - Front suspension system (fifth wheel)

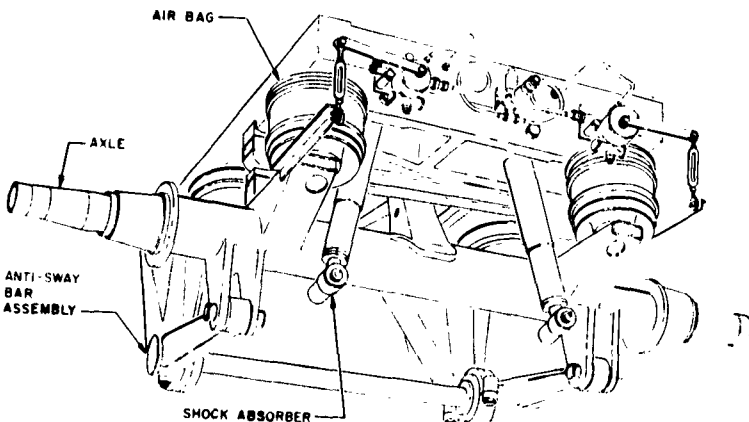


Fig. 17 - Rear suspension system

air conditioning, and suspension systems were assembled by the Gerstenslager Co., of Wooster, Ohio. Road tests were conducted by the National Malleable and Steel Castings Company; the test reports on the entire series of road tests were submitted in Ref. 4. Table 2 is an abstract of the test results which are applicable to this study.

Road tests were conducted by towing the trailer with a military M-52 tractor over a pre-assigned course at scheduled speeds. Fifteen accelerometers were located in the trailer as shown in Fig. 18. Accelerometer calibration

procedures are detailed in Ref.[4.] Equipment to record accelerometer readings was installed in a separate truck and electrical connections were made to the trailer by means of a 12-channel cable as illustrated in Fig. 15.

For the maximum acceleration test, 12 timbers measuring 4 by 4 inches and of sufficient length to cover adequately the wheel span of the test vehicle were firmly anchored to level ground. The timbers were placed parallel and spaced as shown in Fig. 19. Two test runs were made at 20 mph in the direction of travel shown in the figure. The trailer traversed the timber

TABLE 2
Summary of Road Test Results

Accelerometer Location	Maximum Acceleration - Up (g)					Maximum Acceleration - Down (g)				
	1	4	6	7	11	1	4	6	7	11
Maximum Acceleration Test	18.8	1.53	2.40	7.30	6.65	15.3	2.30	1.80	4.80	6.65
Belgian-Block Road	3.57	0.73	9.64	0.99	1.67	3.40	0.44	0.40	0.88	1.61
Paved Highway	2.64	0.22	0.64	0.24	0.83	2.13	0.22	0.25	0.32	0.91
Gravel Road	3.48	0.38	0.28	0.63	1.57	3.20	0.37	0.25	0.40	2.53

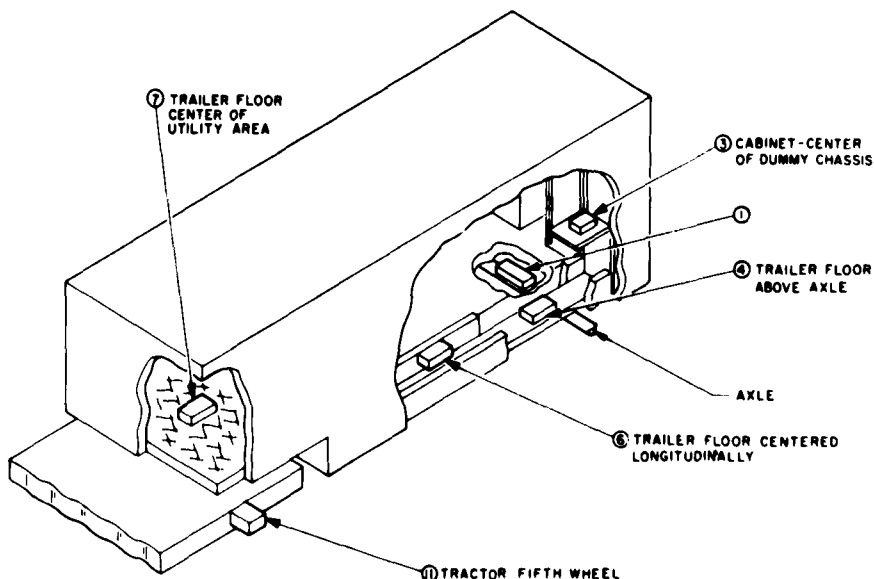


Fig. 18 - Accelerometer locations

course in such a manner that a shock was transmitted to the trailer by each timber through each pair of wheels in turn.

Road distances and velocities during the road tests followed the schedule listed below:

- Belgian-block, 1.1 miles, 20 mph
- Paved highway, 2.1 miles, 55 mph
- Gravel road, 2.6 miles, 25 mph.

Results of the tests are shown in Table 2.

The results of the analysis were intended for use as a guide to the design specifications. For example, the trailer frame and body were designed as a semimonocoque structure with a maximum deflection of 0.05 inch, as assumed in Table 1. Damping ratios, as governed by the shock absorbers for the suspension systems, were specified as a minimum of 0.25 on the downstroke and approximately one-fourth of this value on the

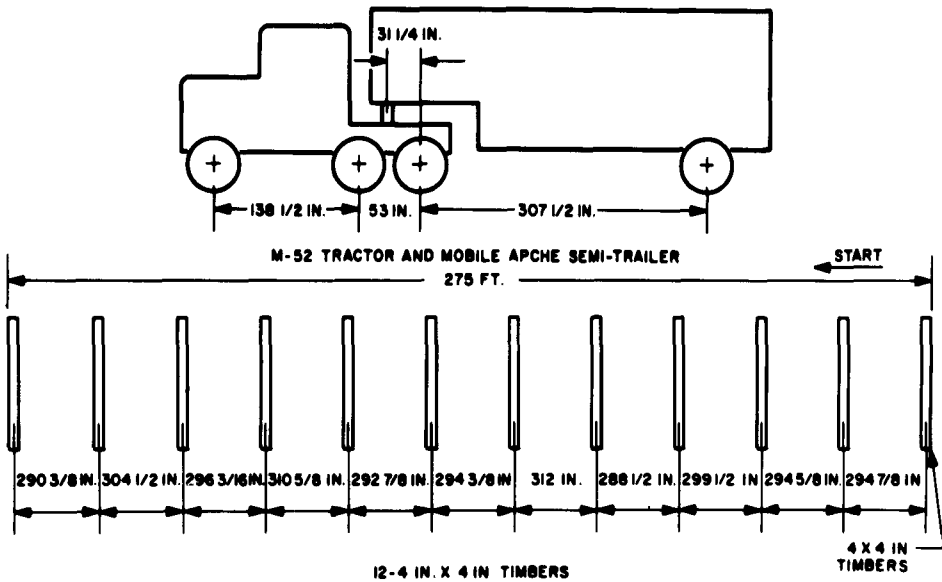


Fig. 19 - Maximum acceleration test course

upstroke. Spring deflections for the suspension systems were also specified on the basis of the analytical results.

Because of the relative simplicity of the analytical model, compared to the physical system, and the relatively large number of assumptions made in arriving at the analytical model, only order-of-magnitude agreement was expected between the analytical results and the test results. Nevertheless, a relatively good agreement was obtained.

At accelerometer location 4, on the trailer frame over the axle, the test value for acceleration in the up direction during the 4-inch bump test was 1.53 g; at location 6, near the center of the trailer body, the test value was 2.40 g (Table 2). From Fig. 14, the analytical results show an acceleration during the ramp of 1.8 g without damping and 3.4 g with damping for the upstroke. Since some damping was present on the upstroke during the tests, test values between 1.8 g and 3.4 g but closer to 1.8 g showed excellent agreement between analytical and test results.

Comparison of analytical and test results for the down direction of acceleration is much more difficult because of the directional nature of damping during the tests. The numerical results and examination of the equations showed that damping is beneficial on the downstroke. The numerical analytical results which assumed damping to be present on the downstroke assumed that it had also been present on the upstroke. The test results (Table 2) showed

2.30 g down at location 4 and 1.80 g down at location 6. The numerical analysis (Fig. 14) showed 1.0 g with damping and 1.8 g without damping. Test results between these two figures would have been expected. Because of the relatively greater difficulty in comparing test and analytical results in the down direction, however, the agreement was still considered to be good.

At location 7, on the trailer floor of the utility area above the fifth wheel, the agreement between analytical and test results is nonexistent. In fact, the reaction exceeded the input. The disparity may be attributed to many factors, but it was judged to be due largely to an unfortunate choice of location for the accelerometer—in the center of a large unsupported flat plate. Earlier but unofficial test results with the accelerometer mounted more rigidly had shown acceleration values comparable to those at locations 4 and 6. Interaction between the trailer and the towing tractor during the 4-inch bump tests is also a likely cause of the disparity.

For the Belgian-block road test, results of the vibration analysis (Fig. 8) and the test results (Table 2), indicate good agreement in spite of the directionality of damping. The trailer body acceleration from Fig. 8 at 20 mph is 1.17 g. The test results show a body acceleration which varied from 0.64 g to 0.99 g. For the remainder of the ride tests, satisfactory attenuation of input accelerations was indicated.

REFERENCES

- [1] D. A. Firmage, "Transportation Shock and Vibration Studies, Final Report." Engineering and Industries Experiment Station, University of Florida. Project No. 8 91-06-002, Engineer Research and Development Laboratories, Fort Belvoir, Virginia, March 1956.
- [2] J. P. Den Hartog, Mechanical Vibrations, 3rd edition. McGraw-Hill, New York 1947.
- [3] "Standard Load Vibration Test on the Munson Test Area." Automotive Division, Development and Proof Services, Aberdeen Proving Ground, Maryland. February 1958.
- [4] "Report of Test for the Gerstenslager Company on the Ride Qualities of the WS-107A-1 Semitrailer." Report No. 2060, Technical Center, National Malleable and Steel Castings Company, Cleveland, Ohio. 20 January 1960.

* * *

MISSILE TRANSPORTER VIBRATION ANALYSIS

R. R. Simun and R. S. Peterson
Douglas Aircraft Company
Santa Monica, California

This paper presents a simple and reliable technique of dynamic analysis of a typical missile transporter designed for mobility type conditions. The method of analysis is based on a transporter ground vibration test (gvt) integrated into a dynamic mathematical model mechanized on an analog computer. The model is then tested by inputting road contours such as those of the Aberdeen "Munson" test course. These theoretical data are then compared with the field test results to demonstrate the level of confidence that can be expected from this technique of analysis.

INTRODUCTION

A transporter is subject to dynamic loads and vibration environments. The design of the vehicle must consider the effects of these conditions. A mathematical model and its equations of motion of a typical 4-wheeled transporter present a simple and reliable method to determine the vibration and dynamic loads the transporter and its transported package will experience while under mobility conditions. The system degrees of freedom are shown schematically in Fig. 1. As indicated, 7-rigid body degrees of freedom are considered. The equations (Table 1) are of the form $M\ddot{q} + C\dot{q} + Kq = f(t)$ and are formulated by standard procedures.* These equations are coded for the analog computer and solved simultaneously for any specific input function. This method permits easy changes in the equations parameters to determine optimum design values.

The transporter with its load was subjected to a ground vibration test from 0 to 20 cps. The resonant frequencies and mode shapes were determined and compared with a similar simulated vibration test of the mathematical model. The first 4 longitudinal rigid body modes were considered significant. The body bending modes were considered to be sufficiently high as not to introduce any appreciable amount of

*The terms of equations are not necessarily consistent with Fig. 1.

error if their effects were omitted from the equations of motion.

The critical parameters in this analysis are the theoretical springs K_x and K_y , Fig. 1, placed on the model to represent the bending of the chassis. These spring rates were unknown prior to the analysis of the 4th mode. They were previously calculated from static loading of the vehicle, however the calculated value was approximately 25 percent lower than the spring rate determined from the vibration test.

The transporter nonlinearities were mechanized on the analog computer. Only two nonlinear parameters were considered important, these were the tee-slot free play and the damping characteristics of the undercarriage shock absorbers. The analog computer easily accepted these nonlinear characteristics.

MATHEMATICAL MODEL

The mathematical model (Fig. 1) and its equations of motion are intended to represent the actual transporter and package as accurately as possible without introducing a large number of degrees of freedom. This model is a 2-dimensional system which considers vertical, fore and aft and pitching motion. The roll and yaw motions are considered to be small and to have no detrimental effect on the system.

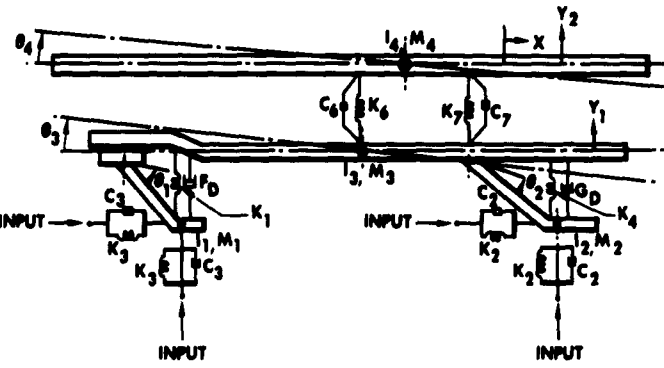


Fig. 1 - Mathematical model of transporter

Table 1

No.	Equations of Motion	
1	$M_{21} \ddot{Y}_{21}$	$= K_6 (Y_{22} + \mu \theta_4 - Y_{21} - r \theta_3) - M_{21} g + K_7 (Y_{22} - V \theta_4 - Y_{21} + s \theta_3)$ $+ C_6 (\ddot{Y}_{22} + \mu \dot{\theta}_4 - \dot{Y}_{21} - r \dot{\theta}_3) + C_7 (\ddot{Y}_{22} - V \dot{\theta}_4 - \dot{Y}_{21} + s \dot{\theta}_3)$
2	$M_{22} \ddot{Y}_{22}$	$= -K_7 (Y_{22} - V \theta_4 - Y_{21} + s \theta_3) - K_6 (Y_{22} + \mu \theta_4 - Y_{21} - r \theta_3) + F_{1y}$ $+ F_{2y} + F_{3y} + F_{4y} + F_{5y} + F_{6y} - M_{22}g - C_6 (\ddot{Y}_{22} + \mu \dot{\theta}_4 - \dot{Y}_{21} - r \dot{\theta}_3)$ $- C_7 (\ddot{Y}_{22} - V \dot{\theta}_4 - \dot{Y}_{21} + s \dot{\theta}_3)$
3	$I_1 \ddot{\theta}_1$	$= (h_1 - d_1) F_{7y} + R_1 F_{7x} - (h_1 - b_1) F_{2y} - (h_1 - a_1) F_D - M_1 g (h_1 - d_1)$
4	$I_2 \ddot{\theta}_2$	$= (d_2 - g_2) F_{8y} + R_2 F_{8x} - (b_2 - g_2) F_{5y} - (h_2 - g_2) G_D - M_2 g (d_2 - g_2)$
5	$I_3 \ddot{\theta}_3$	$= K_6 r (Y_{22} + \mu \theta_4 - Y_{21} - r \theta_3) - f_1 F_{1x} - K_7 s (Y_{22} - V \theta_4 - Y_{21} + s \theta_3)$ $- f_2 F_{4x} + C_6 (\ddot{Y}_{22} + \mu \dot{\theta}_4 - \dot{Y}_{21} - r \dot{\theta}_3) r - C_7 s (\ddot{Y}_{22} - V \dot{\theta}_4 - \dot{Y}_{21} + s \dot{\theta}_3)$
6	$I_4 \ddot{\theta}_4$	$= -K_6 \mu (Y_{22} + \mu \theta_4 - Y_{21} - r \theta_3) + f_3 F_{1x} + K_7 V (Y_{22} - V \theta_4 - Y_{21} + s \theta_3)$ $+ h_1 F_{1y} + b_1 F_{2y} + a_1 F_{3y} - g_2 F_{4y} - b_2 F_{5y} - h_2 F_{6y}$ $- C_6 r (\ddot{Y}_{22} + \mu \dot{\theta}_4 - \dot{Y}_{21} - r \dot{\theta}_3) + C_7 V (Y_{22} - V \dot{\theta}_4 - \dot{Y}_{21} + s \dot{\theta}_3)$
7	$(M_{21} + M_{22}) \ddot{X}$	$= F_{1x} + F_{4x}$

The system is reduced to four separate masses; chassis, missile, front and rear undercarriage. These four masses are coupled by spring-damper combinations and are limited to rigid body motion.

In order to keep the system and equations of motion from becoming extremely difficult to solve, all the springs were considered linear except the chassis bending springs (K_6 and K_7) which contain the 3/8-inch dead spot to represent the free play in the tee slot.

EQUATIONS OF MOTION

In the equations of motion there are 7 degrees of freedom plus four positions for input forcing functions. These 7 degrees of freedom are considered sufficient to accurately define the system and to obtain optimum efficiency from the analog computer time. These equations are formulated by standard procedures to represent the rigid body motion of the model. The solutions are recorded simultaneously on the analog computer brush recorder.

SINUSOIDAL TEST COURSE

The vehicle was subjected to a sinusoidal test course, period 6 feet, amplitude 3 inches (Fig. 2). This was considered to be the most critical test course. The vehicle was subjected to other test courses such as the spaced bump and gravel road. The results from these tests were not critical but compared favorably with similar tests of the model. The vehicle was tested on two individual sinusoidal courses and a part of the test results, compared with a test on the model, is shown in Fig. 3.

1 ANALOG SIMULATION STATION 100
2 TEST COURSE, #1 STATION 99
3 TEST COURSE, #2 STATION 99

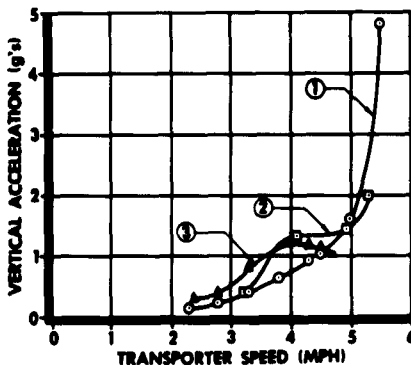


Fig. 3 - Maximum dynamic missile acceleration on the 6-inch washboard course

TRANSPORTER NONLINEARITIES

The forcing function input to the computer is the horizontal and vertical displacement of ground contact points which represents the road conditions. A sinusoidal road, period 6 feet, amplitude 3 inches, was the principle road condition used to determine the vehicles' dynamic reactions (Fig. 2). The model was subjected to this type of road condition prior to an actual road test over the sinusoidal course. It was predicted that excessive loads would be experienced for vehicle speeds in excess of 5 mph.

In the mathematical model the parameters were considered linear with the exception of the theoretical chassis bending springs and the damping rate of the undercarriage shock absorbers. It is shown by the comparison of the model and actual ground vibration test mode shapes that the model is defined sufficiently by using the linear parameters.

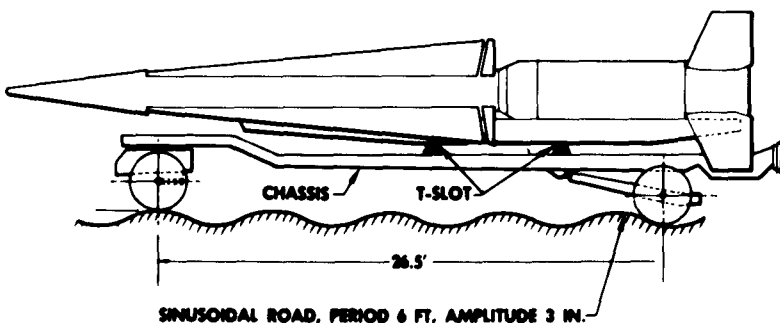


Fig. 2 - Schematic of transporter on the 6-inch washboard course

The chassis bending springs nonlinearity is given by the free play motion of the missile relative to the chassis. This is a 3/8-inch free motion and is visualized as the distance the roller wheel lifts off the tee track before the restraining lip stops this motion. This free motion is sufficient to induce relatively high-shock loads into the system.

The undercarriage shock absorber damping characteristic is defined by the manufacturer's specification which is nearly an inverse square law curve.

FIRST TEST

The transporter with its typical missile load was tested on the sinusoidal washboard course. One pass over the test course was made at a speed of approximately 2.5 mph and showed no adverse effects on the vehicle or its load. A second pass intended at the speed of 4.5 mph was then performed; however, due to the difficulty in maintaining constant speed (no mechanical governor) the vehicle exceeded the speed by 1.2 mphs for a short period of time. Visual observation and a motion picture time study of the vehicle during this test run indicated an out-of-phase pitching mode existed at a frequency of about 5 cps. This mode was not determined previously because it was assumed that the chassis and transported package would remain in-phase. That is, the original equations (prior to the first test) contained only 6 degrees of freedom which did not include the out-of-phase pitch motion. The motion picture time study indicated that the 7th degree should be included and this was later confirmed through the ground vibration test.

GROUND VIBRATION TEST

The vehicle with its load was subjected to a ground vibration test. This test was used to determine the mode shapes and frequencies existing with this system. Four significant rigid body modes were used for comparison with the mathematical model's modes. These four modes were: 1.36 cps undercarriage spring bounce; 1.87 cps body pitch in-phase; 2.34 cps tire spring bounce; and 5.24 cps body pitch out-of-phase. The undercarriage spring bounce and body pitch in-phase modes are not the major cause for excessive loading on any part of the system except perhaps the undercarriage shock absorbers. The shock absorbers are the primary components for

energy release of the system and the input energy could exceed the limitations of these shock absorbers.

The tire spring bounce mode does not appear to cause any excessive loading on the system. The body pitch out-of-phase mode appears to be the most critical frequency of the system. This is due to a very small amount of energy release or structural damping at this frequency plus the extremely high-bending moments along the chassis bed. Displacement modes (Figs. 4, 5, 6 and 7) from the ground vibration test were compared to a simulated vibration test on the analog computer to determine the accuracy of the parameters of the model. It was determined that the parameters were sufficiently accurate except for the theoretical chassis bending springs. These values were found to be about 25 percent higher than previous static calculations. The parameters were modified on the model and the 4th mode shape resulted in the comparison shown in Fig. 7.

VIBRATION TEST RESULTS

Two first body bending modes exist with this system, the chassis bending mode at 7.8 cps and the transported package bending mode at 12.6 cps. These two bending frequencies were considered sufficiently high that no adverse effects would be caused by their omission from the mathematical model. The first 4-rigid body modes were considered sufficient to define the model satisfactorily.

A comparison was made between the ground vibration test and the analog simulated vibration test. The purpose of this comparison was to show to what extent the mathematical model represents the actual configuration. This comparison has also helped to determine the theoretical chassis spring rates since this method is more accurate than other means. The vibration test mode shapes are the solid curves of Figs. 4, 5, 6 and 7. The analog vibration test results are the broken curves. A sinusoid input forcing function simulated as nearly as possible the actual vibration test input.

A comparison of the four modes shows that the comparative accuracy of three of the modes is limited to reading of the test instruments or analog traces. This indicates that the spring and mass distribution of the mathematical model is representative of the actual system and that the actual transporter will

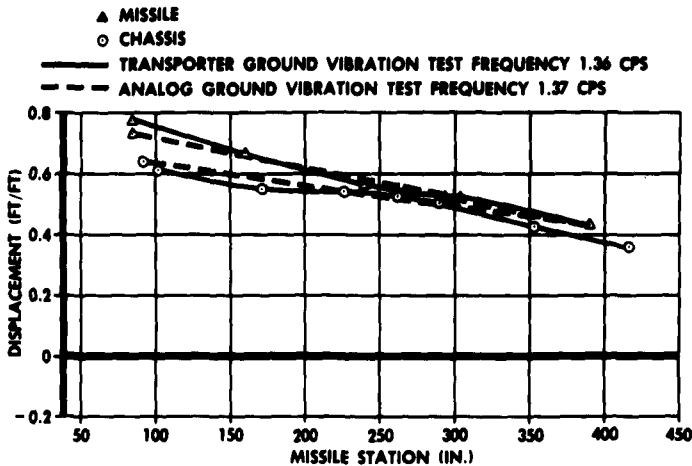


Fig. 4 - Comparison of analog and test results, first mode shape

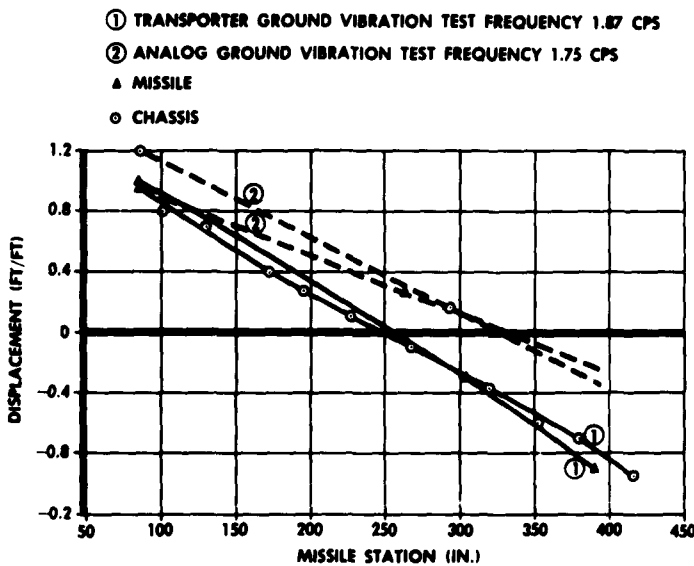


Fig. 5 - Comparison of analog and test results, second mode shape

respond to input to the tires in the same manner as the model. The other mode (1.87 cps) is off slightly; this can be attributed to the criticality of the mode — even a small deviation in the frequency will cause an appreciable change in mode shape. The analog computers error range can easily reflect this condition.

DYNAMIC REACTION

A sample comparison of the mathematical and actual system response to the sinusoidal

washboard road test is shown in Fig. 3. This shows the "g" forces imposed on the missile at Station 100. These forces are presented in the form of a curve of maximum value for each speed over the sine wave. The values plotted are the loads occurring for a time duration greater than 0.05 second. Curve (1) is the analog mathematical model values. Curve (2) is the values obtained from test course #1. Curve (3) is the values obtained from test course #2. The pronounced peaks shown by the two actual tests at the speed of about 4 mph are attributed to the roll motion of the

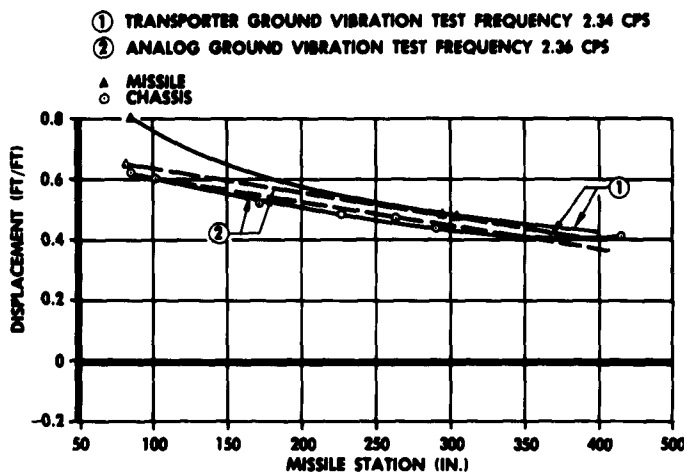


Fig. 6 - Comparison of analog and test results, third mode shape

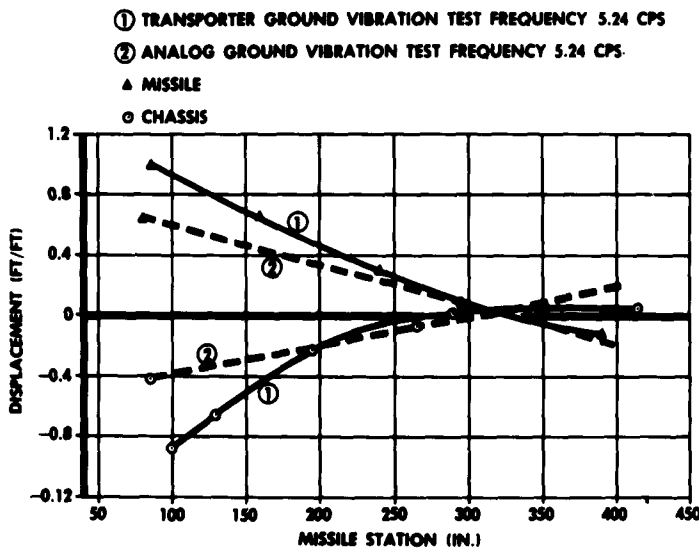


Fig. 7 - Comparison of analog and test results, fourth mode shape

vehicle. Visual observation of the motion of the transporter with respect to roll indicated that an unexpected amount was present during the road test over sine course #1. This rolling motion is due to a nonperpendicular sine wave with respect to the direction of travel.

Displacement, velocity, acceleration or forces can be obtained for any part or position in the system by modifying the equations to give the desired output. One requirement of this study was to determine the acceleration

loads experienced on the missile at Station 100. The "g" loads experienced at this position have been presented to verify further the accuracy of the mathematical model.

CONCLUSIONS

A simple and reliable method to determine the dynamic response of a 4-wheeled transporter is presented. This method uses an analog computer for mechanization and solution. A

7-degree-of-freedom system was formulated to define the actual configuration. These degrees of freedom are limited to rigid body motion since body bending does not appreciably influence the results.

The mathematical representation of the transporter and transported package has proved sufficiently accurate to define the vehicle's response to nearly any desired road condition including nonsymmetrical road beds. This model is readily adaptable to any 4-wheeled vehicle by simply varying the equation's parameters.

It was considered that, for this system the chassis bending could be sufficiently represented by individual springs located at the points of contact between the chassis and the transported package. Analysis of the 4th

mode showed that the cantilever portion of the missile causes extremely high-bending moments along the chassis bed. Therefore the out-of-phase pitch degree of freedom was considered necessary to define the system more accurately. With transporters of well distributed loads this condition will not necessarily occur again.

Comparison of the results from the ground vibration test and the model's simulated vibration test shows a high correlation. This generates considerable confidence in the model's definition of the actual vehicle. Comparison of other theoretical and field test data also, shows a high correlation. This increases the confidence in the mathematical model to the extent that further tests of the actual vehicle become unnecessary and the model will be used to demonstrate the system's response.

* * *

CONTAINER DESIGN FOR NIKE-ZEUS MISSILE

J. R. Erkenbrack
Douglas Aircraft Company, Inc.
Santa Monica, California

This paper describes the approach and methods used for the selection and design of shipping containers for the Nike Zeus Missile. The material covered is directed mainly toward the booster and sustainer rocket motor containers. The design of the suspension system for these containers was achieved by using a continuous layer of cushioning material approximately 3 inches thick to protect a rocket motor section exceeding 10,000 pounds. Results of the qualification tests to substantiate the required shock isolation are also covered. These containers, of complete cushion design, are an optimum package concept for the Nike Zeus Missile, not only for adequate protection but also for minimum cubage and low cost.

DESIGN PHILOSOPHY

Design considerations for both the rocket motor sections and the container were used in the selection of the proper suspension system. These solid propellant motors have a large section modulus over their entire length and are capable of withstanding high-acceleration loads from flight conditions. With this rugged characteristic they also possess a large available surface area for cushioning shock load during handling and shipping. The missile design does not provide heavy structural members needed for individual suspension mounts, therefore a continuous cushion suspension system was selected. This system eliminated the space requirement for mounting systems thereby reducing the overall cube of the containers. Also, the missile will not be subjected to beam loads, and the complexity of the missile and container structure is reduced in cost and weight. Even if the cushion bottoms there is still a barrier between the missile and the container which is less abusive than a hard spot mounting system. The basic container shape for minimum size is a cylindrical shell, only slightly larger than the missile section, with reinforced intermittent frames. The analysis for design of the container to meet the dynamic load conditions will be covered in a later section. In comparing the cost of cushioning with other shock mounts it has been found that the initial

cost of cushioning is usually much lower. In case the cushions are damaged and need to be replaced once or twice, this would still prove less expensive than the individual shock mounts. For example, the cushions for the warhead container were 1/20th the cost of low-temperature shear mounts to provide the same protection for this item.

The logistics of the weapon system also had to be considered in design of the containers. The transportation, supply, and storage of these motor sections must meet the rough handling associated with transportation by air, ship, rail, or truck. Since air transport usually imparts low amplitude - high-frequency vibrations, this mode of shipment does not present a particularly severe condition. Truck and rail transportation, however, impose the higher amplitude - lower frequency range of vibrations which can be damaging since the component begins to gallop, and too great a transmissibility can wreck a suspension system. This area of vibration is an important factor in determining the proper density and natural frequency of cushioning material.

The main concern in cushion container design from the environmental standpoint was the low-temperature extreme of -65°F imposed by contract requirements for qualification. This low temperature is felt to be unrealistic,

especially as regards the vibration spectrum, since only rarely will a container be handled at such extreme temperature conditions. Other factors affecting most container design are reusability, storage life, areas of distribution, humidity, moisture, and corrosive atmosphere. The preservation philosophy adapted for the Nike Zeus container design from a simplicity and cost saving viewpoint was to make the container a free-breathing ventilated type. Since this means the container is not sealed, other protective measures are necessary. The propellant chamber of the motor sections was sealed-off by providing a plug at the nozzle exit. A small desiccant can was designed into this sealing plug to control the humidity and protect the propellant grain. The exterior of the motor section has a moisture resistant finish to protect it from corrosion. The container has drain holes to prevent build-up of excessive condensation.

CUSHIONING CRITERIA STUDIES

Prior to starting the design all known commercially available cushioning materials were reviewed. Several materials were tested, both statically and dynamically, at temperatures of -65°F, room temperature, and +165°F by the Douglas Material and Process Engineering Laboratory. The object of these tests was to evaluate the properties of the various materials under dynamic and static compression in order to select a material of minimum thickness which would satisfy the shock requirements for the container design. Of all the materials tested and reviewed, rubberized molded hair appeared to be most suitable for temperature ranges from -65°F to +165°F. To obtain close control and more consistent results, it was specified that the molded cushion must consist of 100 percent animal hair (75 percent of this must be winter hog hair) with no other filler materials. More extensive tests were conducted including static tests on material densities from 2 lb/cu ft through 15 lb/cu ft. Dynamic tests were also made on densities from 2 lb/cu ft through 9 lb/cu ft.

Stress and energy versus strain curves and cushion factor versus stress curves were plotted from the static test data. This provided the designer with a simple comparison between various curves and a rough correlation between density and energy absorption capacity of the materials; however, for accurate design the use of these curves would require the need of dynamic correction factors. To supplement this static data, dynamic test results and

plotted curves provided a more accurate method for designing to a minimum thickness of cushioning. The dynamic data is more accurate because it takes into account such factors as the pneumatics, the inertia, internal damping, and possibly other factors affected by rapid loading.

The evaluation of all the data obtained by test or from other published material has a varying degree of consistency and can only be used as a guide to obtain an optimum design. Also, the design criteria may be such that it is difficult to apply the test data to meet all the requirements.

APPLICATION OF TEST DATA TO DESIGN OF CONTAINERS

Acceleration limitations were established by a design specification drawing for the Nike Zeus Missile. These limits, 25 g transverse and 50 g axial, were based on the fragility of the rocket motor sections. Knowing the mass and the dimensional size of the motor section, standard dynamic rotational drop calculations can be applied to determine the travel required from instant of impact to stay within these "g" limits (Fig. 1). The derivation of equations used for these calculations can be found in Appendix 8 - IV of Ref. 1. From the geometry of this rotational drop condition which is the maximum shock loading condition for qualification, the linear travel of the c. g. can be determined. The dynamic drop tests were made on the cushioning material at this same distance of travel.

Using the dynamic compression curves for g versus static stress, it is desirable to find a "g" value within the acceleration limits established. It is apparent from Figs. 2, 3, and 4 that, although the variation in "g" for optimum cushioning of a certain density material varies only slightly with temperature, the static stress for these optimum "g" values covers a wide range of stress. Using past experience the designer must evaluate the test data and choose the "g" and stress value of a material to satisfy the design. He must consider the validity of the test data and all the variables such as the material tested, the test apparatus, test procedures, and the instrumentation used. Although material densities of anywhere from 7 lb/cu ft through 10 lb/cu ft would probably provide the proper cushioning, the 9 lb/cu ft material was chosen for this design. Having selected a mean or average static stress from the "g" versus the static stress curve, a

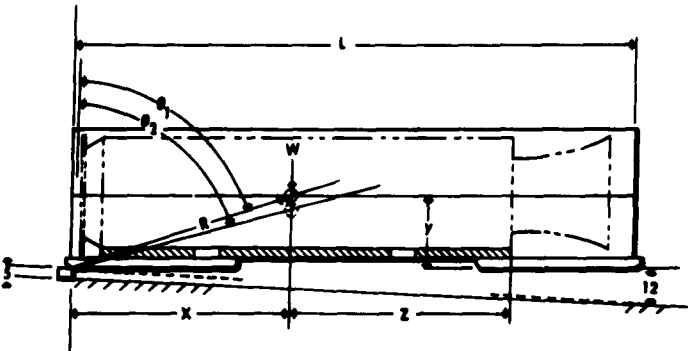


Fig. 1 - Geometry of end drop (for calculations see Appendix)

NASH-HAMMOND
(MOLDED HAIR)
DYNAMIC COMPRESSION
HEIGHT OF DROP 6 INCHES

THICKNESS 2 INCHES
DENSITY 7#/CU FT
TEMPERATURES -65°F, ROOM,
AND 165°F

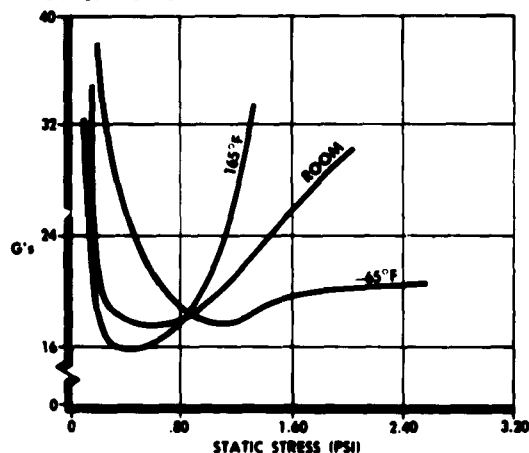


Fig. 2 - G' versus static stress

NASH-HAMMOND (MOLDED HAIR)
DYNAMIC COMPRESSION
HEIGHT OF DROP 6 INCHES
THICKNESS 2 INCHES
DENSITY 8#/CU FT
TEMPERATURES -65°F, ROOM, AND 165°F

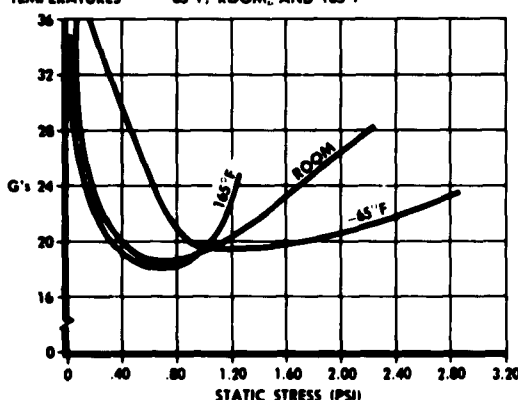


Fig. 3 - G' versus static stress

dynamic strain can be determined from the dynamic strain versus static stress curve. Knowing the distance the cushion must deflect from impact and the dynamic strain from test data the thickness of material is established. In the design of the heavy motor section this determined thickness was approximately 2 inches. An alternate method or approximation of cushion thickness could be obtained by using optimum cushion factor equations. These equations are also subject to several variables which produce only ballpark results. A check using these equations also produced a resulting thickness of approximately 2 inches.

Having determined the thickness of rubberized molded hair the next step is to determine the area of cushioning required. The area can be calculated by using the standard stress equation. The area was determined to be approximately 5,000 square inches. Again, the designer is called upon to determine the effective area of cushioning for the circular shaped motor section. The vertical displacement of the cushion at the bottom center will be maximum and will diminish to zero at the sides. From the volume displaced by the deflection of the cushion the designer can make the assumption that a uniform deflection of the cushion

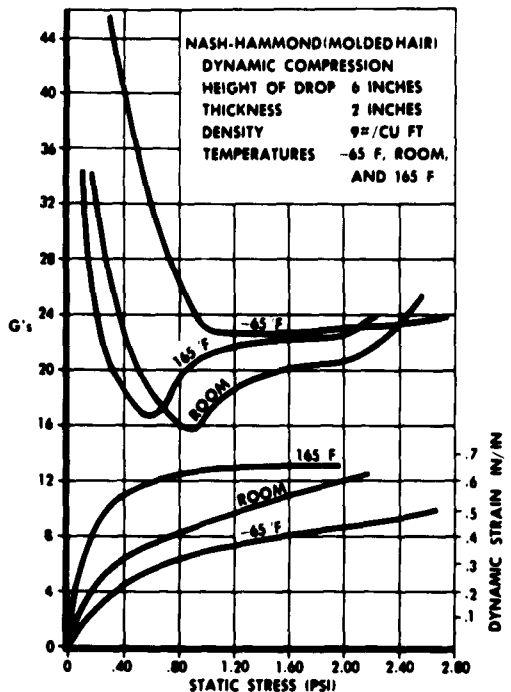


Fig. 4 - Dynamic strain versus static stress

over 90° of the circular surface will be a conservative width of the effective surface area. This width and the length of the propellant section of the motor section give the required area for cushioning protection.

The thickness of cushioning for limiting the axial acceleration was likewise achieved using the pendulum impact geometry and calculations. The results of these figures gave a 2 inch thickness of 15 lb/cu ft density rubberized hair to satisfy the design. It should be noted that the allowable axial acceleration limit is 50 g and the available cushioning area has been greatly reduced.

The analysis of the container shell configuration required several pages of calculations, assumptions, and application of fundamental stress equations which are too involved to include in this paper. It can be stated that the shell was basically analyzed as a structural stressed skin with adequate reinforced stiffening to provide a margin of safety for the design load conditions imposed upon it. The booster container can best be described as two half-shells approximately 18 feet long hinged together with intermittent hinge sections over its length. When the container is closed intermittent latches on the opposite side from the hinges

give the container its overall shell structural efficiency. A thrust structure to resist longitudinal load is built into the shell at the end of the propellant section. The shell aft of this point houses the nozzle portion of the motor section. The interior surface of the shell from the thrust section forward is completely cushioned with rubberized hair. The molded cushions are actually installed in sections and have gaps between each other as well as varying thicknesses. For instance, in the bottom of the container there is a gap of 1/2 inch width along the bottom center line, and the cushion sections on either side are 3 inches thick tapering to a 2-inch thickness over a width of 75°. The tapering thickness was used to compensate for the varying vertical volume displacement of the cushion under load. These cushion sections are bonded to the container shell.

ROUGH HANDLING TEST FOR QUALIFICATION OF CONTAINER

In container design, as in other design, many assumptions are made; and the accuracy of test data used is only as reliable and applicable as the degree of simulation of the actual design condition. Material variations exist from one sample to another, and the shape factor of the material contributes to deviations in actual versus test data. It is evident from the numerous factors which affect the results of container design that testing of the completed article must be used to prove the correctness of assumptions and of pretest data.

Qualification tests were performed to DAC Specification Drawing 7834372 and consisted of the following phases:

Phase 1. Rough handling tests which simulate the shocks the container may receive during handling and shipping.

Phase 2. Vibration tests which subject the container and contents to frequencies and displacements normally found during transportation and also show the durability of the cushioning material.

Phase 3. Stacking and lifting tests which subject the container and contents to conditions found in storing, lifting, and moving, including downward loads of twice the container weight.

A summary of Phase 1 test results is shown in Table 1. It can be noted that the edgewise drop test for the aft end produced the highest "g" loading on the motor section. This value of 23.4 g at the aft end corresponds to

the calculated value of 19.19 g, and is below the allowable 25 g. The accelerations recorded also showed a greater value for low temperature which indicated the effect of temperature on the stiffness of the material. The cornerwise drop tests resulted in much lower accelerations which can be attributed to the added deflection of the container under impact. The pendulum impact test gave the lowest acceleration loading to the motor section, which was expected, since this loading condition is less severe. The longitudinal movement is also resisted by friction between the bottom cushioning and the motor section. This might be considered as shear resistance of the cushioning, especially at the edges; but over a large effective area translation will result, and the frictional resistance will contribute to reducing the "g" loading on the end of the motor section.

TABLE 1
Qualification Test Results-Phase 1

Temperature	Description & Orientation	Maximum g Level
Ambient	Edgewise Forward End	15.9
	Edgewise Aft End	22.8
	Cornerwise Hinge Side	7.4
	Cornerwise Latch Side	11.2
	Pendulum	12.3
+ 160°F	Edgewise Forward End	18.2
	Edgewise Aft End	11.8
	Cornerwise Hinge Side	14.9
	Cornerwise Latch Side	13.9
	Pendulum	3.7
-65°F	Edgewise Forward End	22.8
	Edgewise Aft End	23.4
	Cornerwise Hinge Side	15.2
	Cornerwise Latch Side	15.3
	Pendulum	7.7

Vibration tests were conducted for vertical and lateral translation and rotation, and longitudinal translation at temperatures of -65°F, ambient, and + 160°F. A frequency sweep was made between 2 and 30 cps while recording the accelerations on the missile, maintaining 1/4 "g" on the missile where possible. The container with the missile was then vibrated at 1/2 "g" for 20 minutes at the frequencies of maximum transmissibility. The maximum transmissibility of 3.4 occurs at 23 cps for a lateral rotation at -65°F. Another high transmissibility of 2.9 was recorded at 13 cps for lateral rotation at room temperature. This high transmissibility is probably due to the absence of cushioning material in the latch and hinge areas.

The overall results of the tests substantiated the design approach and methods used. At the conclusion of testing, the container was not severely damaged, nor did the cushioning material show signs of severe deterioration. Any reusable shipping container should be backed-up by an adequate refurbishing facility to replace missing loose items and straighten, repair, and repaint any portion damaged during the shipping cycle.

In summation it should be pointed out that container simplification and economy of design were possible only after a thorough analysis was made of the design, deployment, and fragility of the missile system involved. Evaluation of these factors from a very basic and fundamental standpoint enabled Douglas to develop an adequately protected package at a very nominal cost.

REFERENCE

- [1] E. Klein, Ed., Fundamentals of Guided Missile Packaging, Shock and Vibration Design Factor, RD 219/3, Office of the Asst. Sec. of Defense, Research and Development, July 1955.

APPENDIX

Calculations For End Drop On Motor Section

NOTATION AND NUMERICAL VALUES

w = weight of motor section in lb

M = mass of motor section in lb - sec²/inch

- I_1 = moment of inertia of motor section about its c.g. in inch-lb-sec²
 I_o = moment of inertia of motor section about pivot point "0" in inch-lb-sec²
 g = gravity constant in inches/sec²
 w_o = angular velocity of motor section about pivot point in radians/sec
 ρ = radius of gyration about c.g. of motor section in inches
 R_1 = radius of gyration of motor section about pivot point "0" in inches
 v_1 = vertical instantaneous velocity at c.g. of motor section in inches/sec
 v_2 = vertical instantaneous velocity at end of motor section in inches/sec
 w_1 = vertical translation frequency in radians/sec
 w_2 = rotational circular frequency in radians/sec
 s_1 = vertical instantaneous deflection at c.g. in inches
 s_2 = vertical instantaneous deflection at end of motor section in inches
 R, ρ_1, θ_2 , are radius and angles defined in Fig. 1

From Geometry of Fig. 1:

$$x = 124 \text{ inches}$$

$$y = 27 \text{ inches}$$

$$z = 25 \text{ inches}$$

$$L = 214 \text{ inches}$$

$$h_1 = 12 \text{ inches}$$

$$h_2 = 5 \text{ inches}$$

$$w = 11410 \text{ pounds}$$

$$I_1 = M/2 = 53,000 \text{ lb-in.-sec}^2$$

$$R = \sqrt{x^2 + y^2} = 127 \text{ in.}$$

$$I_o = I_1 + MR^2 = 529,000 \text{ lb-in.-sec}^2$$

$$R_1 = \sqrt{\frac{I_o}{M}} = 134 \text{ in.}$$

$$\theta_1 = 90 - \arctan \frac{y}{x} - \arcsin \frac{h_1 + h_2}{L} = 75.8^\circ$$

$$\theta_2 = 90 - \arctan \frac{y}{x} + \arcsin \frac{h_2}{L} = 79^\circ$$

$$w_o = \sqrt{\frac{2Rg}{R_1}} (\cos \theta_1 - \cos \theta_2) = 0.522 \text{ radians/sec}$$

$$v_1 = R w_o \cos \arctan \frac{y}{x} = 64.76 \text{ in./sec.}$$

CALCULATIONS

Assume restriction of acceleration to 15 g at c.g.

Then

$$w_1 = \frac{15g}{R w_o \cos \arctan \frac{y}{x}} = 90 \text{ radians/sec}$$

$$s_1 = \frac{R w_o}{w_1} \cos \arctan \frac{y}{x} = 0.72 \text{ inches.}$$

Assume additional 5 g at end of motor section

Then

$$w_2 = \frac{5g}{Z w_o} = 148 \text{ radian/sec}$$

$$s_2 = \frac{Z w_o}{w_2} = 0.087 \text{ inches.}$$

Total deflection and total acceleration may now be found

$$\text{Total Deflection} = s_1 + s_2 = 0.807$$

$$\text{Total Acceleration} = 15 \sin w_1 t + 5 \sin w_2 t$$

$$t = \frac{\pi}{2w_1}$$

$$w_1 t = 90^\circ$$

$$w_2 t = 147^\circ$$

$$\text{Total Acceleration} = -15 - 5(0.838) = 19.19 \text{ g.}$$

From Fig. 2 a value of 23 g at 2.2 psi will most closely satisfy all three temperature conditions. This does not fall at the indicated optimum but can be considered within its range for adequate cushioning.

$$\text{Thickness of cushion} = \frac{0.807}{0.45} = 1.8 \text{ inches.}$$

For design a thickness varying from 2 inches to 3 inches was used considering shape factor and load distribution.

DISCUSSION

Mr. Burgess: (United Technology): Did you have any trouble with fungus attack on the animal hair?

Mr. Erkenbrack: As yet we have not had any trouble on this. It could be that in the future

we may be faced with this problem. We are, as most of you know, using these containers to ship missiles to Kwajalein. It is very possible that we will be faced with this problem, as yet we haven't.

* * *

DESIGN CRITERIA FOR UNDERWATER ORDNANCE MISSILE CONTAINERS

Robert J. Sefing
Minneapolis-Honeywell Regulator Co.,
Duarte, Calif.

This paper presents a concept of design requirements in a new field undergoing dynamic expansion, rather than a specific theoretical design criteria in a known field of container development. The paper is an introduction, for the majority, to a field they have heard about, or which they knew existed, but the exact meaning of which, or the design requirement for which, they have not known exactly.

INTRODUCTION

The basic design requirements, known to all in the container field and brought out so forcefully at the 30th Symposium, also pertain to underwater ordnance containers, but they are only a start and not a conclusion. For, along with shock and vibration attenuation, weight, handling requirements, pressurization, size, and so on, which we meet everyday in designing any container, we also run up against supply ship handling, ship to ship transfer, below deck storage, and integration into the firing sequence. This requires designing into the container safe guards against: shock due to depth charge and near miss bomb explosives; ship pitch and roll conditions; high line transfer, with ship in motion; and vibration due to ship propellers and gun fire. Also the container may have to be designed either to sink or to float.

In the old days, all that was required in Underwater Ordnance was to ship a torpedo from the manufacturer to a Navy depot. The design criteria was a shipping container of the "boiler plate" type construction able to withstand railroad vibration and shock and pressurized to 19-20 psi. Arriving at dockside, the torpedo was removed from the container and loaded upon a submarine or ship. The logistic's theory was one of shipping, with protection, and nothing else.

As we moved into the present, and as logistic's became more complex due to system refinement and expansion, packaging was forced

not only to follow but to improve to a point where its state of the art had to exceed that of the weapon system development. In a few short years, the simple theory of shipping a torpedo in a package from one point to another has exploded dynamically until now the package is discussed as an integral part of the weapon system.

THE ASROC CONTAINERS

A prime example of the requirements placed upon a container in a modern Anti-Submarine Weapon System in the underwater ordnance field is the Anti-Submarine Rocket (ASROC) missile container. ASROC is either a rocket thrown depth charge or a torpedo, fired from a ship against submarines. The container is 16 feet long, 3 feet square and weighs 550 pounds, but holds a missile weighing 1000 pounds. This is a vast improvement over the old boiler type container invariably weighing 4 or 5 times the component weight. In the old mode of design, the container had to be strictly a shipping container, but it doesn't stop here now, for the container must now ship containers. Along with the missile, the container was designed to ship other components of the weapon system in their containers (Fig. 1).

The container begins its useful life at an ASW facility. Here the missile is assembled from components shipped in from manufacturers in other containers of the ASROC family of containers. The loaded missile container (Figs. 2,



Fig. 1 - ASROC missile system containers. Reading from left to right; Front row - parachute pack, ISA, fuze power supply, AFS blocks, D/C fin tip extensions; 2nd row - airframe, motor fins, D/C nose cap, fuze, cable assembly, flexible cover; 3rd row - motor, depth charge; back row - ASROC missile

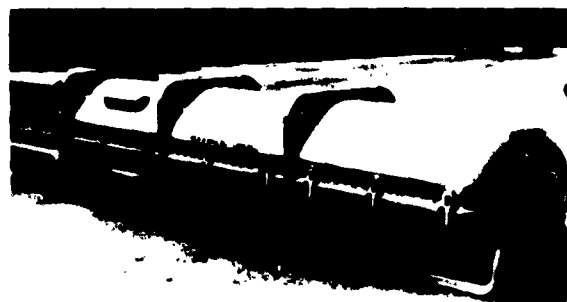


Fig. 2 - The ASROC missile container, Mk 183 Mod 1

3) is now shipped to dockside where it is loaded upon an ammunition ship. Containers are stowed below decks in racks and compartments designed especially for the purpose (Fig. 4). Another principle toppled—for, instead of designing a container to fit a mode of transportation, the mode of transportation is designed to accommodate the container.

The next criteria is to protect the missile during supply ship to firing ship transfer on the high line. The shocks and oscillations experienced during this operation are figured to a design parameter of 7-1/2° pitch, roll and yaw condition; but are greatly magnified by the action of each ship working against the other. This operation may have to be performed during high seas, and with both ships moving at high speed (Fig. 5).

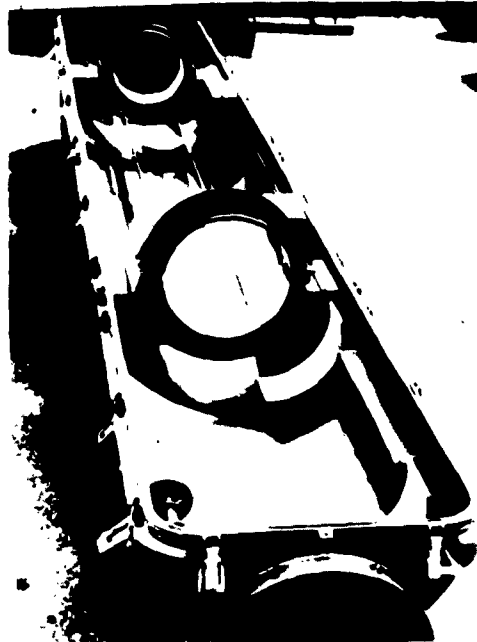


Fig. 3 - Interior of ASROC missile container



Fig. 4 - ASROC motor containers stacked for storage

Upon arrival on the firing ship, the container has to be moved around and over obstacles and protrusions to the loader. This is a pretty good problem in itself, transporting 16-foot long object around decks and through



Fig. 5 - ASROC missile container in a high line transfer to a destroyer

compartments of a ship of the destroyer class. It is accomplished by the use of a specially designed hand lift truck (Fig. 6) which can raise and position the container, move the container at right angles, move it over warped deck plating, and 1-inch risers at a 45° angle, so that no foreign objects contact the container. The hand lift truck incorporates self-locking brakes, its own hydraulic system, and is operated by one man (Fig. 7). Attachment to the container is by friction and no mechanical fasteners are required.

At this point we reach the major design requirement placed on the container. In order to be compatible with the firing system, the container has to be positioned to the loader, hatches opened, cover removed (Fig. 7), retaining straps opened, and missile hooked up for hoist (Fig. 8) in an elapsed space of 30 seconds. In order to accomplish this, special quick-opening latches and retaining straps had to be designed, and the cover had to be removed by hand. This latter requirement demanded that the 16-foot long cover be of light weight, but still possess the structural integrity to absorb impact shocks, vibration, and the stacking upon it of 5 additional containers.



Fig. 6 - Hand lift truck for maneuvering containers



Fig. 7 - Hand lift truck and ASROC missile container with lid being lifted off by hand



Fig. 8 - ASROC missile in container being hooked to loader

This ends the outgoing flow of the containers. The incoming plan is opposite, but is no less demanding on logistic skill.

Additional areas, skipped over lightly, but still demanding pertinent design requirements, are below deck handling in tight, confined gangways, stowage compartments, and hatchways; places where the container has to be swivelled to odd angles to go through 5-foot wide hatches and down many levels into the bowels of the ship, and 1-foot overhead working clearance for hoist operation; the difficult design parameters of having each ship just a little different in regard to gangways, storage compartments, and locations; the problem of preventing the firing of a live missile in a container stowed on the ship's deck in the back lash of the flame from the launcher; and the requirements that the container, with a 1500-pound missile, must be able to float if it accidentally falls overboard or from the high line. It can be seen that the logistics picture assumes challenging proportions for the packaging design engineer.

CONCLUSION

All these design criteria were successfully met in the ASROC missile system, but to perfect the state of the art and to simplify the logistics, additional and sophisticated studies are under development. For instance - "Why individual, exposed latches?" Research and development is in the mill to incorporate internal gang latching - one exposed handle, one pull, and the container is opened. Question, "As long as the container is a major, expensive, and integral part of the program, why not use it as the launcher and fire directly from it?" It would eliminate a major ship installation, save weight, and of course, money. It would also further justify the elaborate packaging necessary for the system. This theory is presently undergoing tests. Thus the passage of time has shown a remarkable progression in container design from a sideline to a position where fully-fledged structural and environmental design studies are inside, the outcome of which plays an essential part in the success of a weapon system.

Section 5

AERIAL DELIVERY OF SUPPLIES AND EQUIPMENT

CUSHIONING FOR AERIAL DELIVERY

J. Neils Thompson and E. A. Ripperger
Structural Mechanics Research Laboratory
The University of Texas
Austin, Texas

This is a tutorial paper concerned with fundamentals and the state of the art in the development of energy-absorbing systems for aerial delivery of supplies and equipment. The desirable properties of a "one-shot" cushion are discussed and the characteristics of a number of cushioning materials and systems are presented. Basic design equations for cushioning with a crushable material such as paper honeycomb are developed and present design criteria are examined.

INTRODUCTION

In June of 1951, a committee on Air Drop of Supplies of the Advisory Board on Quartermaster Research and Development of the National Academy of Sciences - National Research Council, stated that research, "...utilizing present overseas packaging and parachute equipment, but improved methods of cushioning, holds good prospect for increasing the allowable loading per unit area of the parachute."

The requirements of extreme mobility in military field operations demand an increasing use of aerial delivery of supplies and equipment regardless of cost. Techniques used in 1951 were notably expensive and any reduction in unit cost of delivery would result in large savings, which, when simultaneously coupled with increased reliability would bring aerial delivery for large scale operations within the realm of economic feasibility. The combination of energy-absorbing systems and aerial retarders offered considerable promise.

In the fall of 1953, the Structural Mechanics Research Laboratory at The University of Texas began research on energy-absorbing materials and systems for the Quartermaster Corps.

In a report dated February 18, 1955, the University gave indications that certain materials, including paper honeycomb, had good potential as energy dissipators. Following these indications, the Quartermaster Food and Container Institute and the University, using drop-test facilities at the University, initiated drops of equipment cushioned with paper honeycomb. From this research it was proved that paper honeycomb was a good, economical, single-shot-type crushable cushioning material.

STATEMENT OF PROBLEM

At the time of release from an airplane, a packaged assembly has a kinetic energy imparted by the forward motion of the plane, and a potential energy equal to its weight multiplied by the drop height. During descent, wind action may add or subtract energy. Drag effects will

subtract energy. The remaining total energy at contact with the ground must be dissipated during the impact at a rate sufficiently slow to prevent damage to the packaged items.

While there are certain tactical advantages to be gained from free-fall delivery of supplies, with no retardation except that provided by the aerodynamic resistance to the falling body, the greatest economy and capacity for delivery of large quantities of material can probably be achieved with an economical balance in combining the use of cushioning with the use of parachutes or other types of retarders.

There are many potential sources of ground-impact energy absorption, including that provided by soft earth, or water; that provided by the structural framework of the packaging system and of the items packaged; and that offered by the cushioning system provided.

Many varieties of cushioning and energy absorption systems are in use today, but almost universally they are concerned with, and must be designed for, continued operation under multiple repetitions of vibratory or impact loads. In contrast, the air-drop problem is concerned with absorption of energy during a single impact. Recovery of deformation after

loading is not required. Thus, the field of investigation has been opened to systems which may use materials and devices not applicable to ordinary cushioning problems.

Most of the developments with regard to energy absorption in compressible cushioning pads necessarily have been based on the assumption that dynamic force-displacement characteristics were not significantly different from static behavior. For materials for which this may be a valid assumption, the ultimate problem of designing cushioning is greatly simplified.

In addition to engineering considerations, the ultimate selection of cushioning systems will be based on (a) cost, (b) availability, and (c) ability to function under a wide variety of conditions. These factors have served as a guide in the development of our research programs.

CUSHIONING MATERIALS

Old Quartermaster Felt Shock Pad

In 1951 and until comparatively recently, felt shock pads, (Fig. 1) had been the cushioning



Fig. 1 - Felt shock pad and paper honeycomb

material used for absorbing energy developed by equipment being air-dropped. Figure 2 shows a typical stress-strain curve for a felt pad and for a paper honeycomb. It is readily apparent from examining these two curves that such materials as paper honeycomb are superior to felt pads in the dissipation of energy.

Ideal Characteristics

The ideal cushioning material from the standpoint of energy dissipation is one which crushes inelastically to a very small volume at a constant stress. Obviously, the cushion would be destroyed and could not be reused. Hence cushioning for aerial delivery is a "one-shot" affair. Clearly the stress-strain energy characteristics of a material will be a most important factor in determining the suitability of the material for this "one-shot" type of service. A number of different characteristic quantities have been suggested and used during the past few years to indicate the relative efficiencies of materials. These quantities have been given descriptive names such as efficiency factor, cushion factor, resilience, energy per crushed volume, etc. The property or characteristic of the material which each of these terms seeks to describe or to convey is indicated by the stress-strain diagram for the material. Since large deformations are involved and materials seldom crush uniformly, stress-strain diagrams may be dependent, to some extent, on the test-specimen configuration, as

well as on the material property. After due allowance is made for this, the fact still remains that the stress-strain diagram is the primary source of information regarding the material.

It should also be noted that in aerial-delivery service, it is the dynamic loading of the cushioning that is most significant. Consequently, stress-strain curves should also be obtained dynamically. From the paper-honeycomb curve in Fig. 2, one may determine the average crushing stress of the material, the total energy absorbed and the strain at which "bottoming" begins and the elastic energy absorbed. "Bottoming" at high strains is a characteristic which all cellular materials exhibit. It represents the strain at which virtually all of the original cellular structure has been destroyed and as a consequence of this destruction, the material begins to act like a much denser medium, and stress-strain characteristics begin to change drastically. The strain at which bottoming begins is also the strain at which the cushion begins to absorb an appreciable amount of elastic energy. Bottoming is obviously something to be avoided. A study of dynamic stress-strain curves for different materials indicate that the strain at which bottoming begins is quite often the strain at which stress becomes equal to the initial peak stress. This strain is a reasonable optimum or design strain.

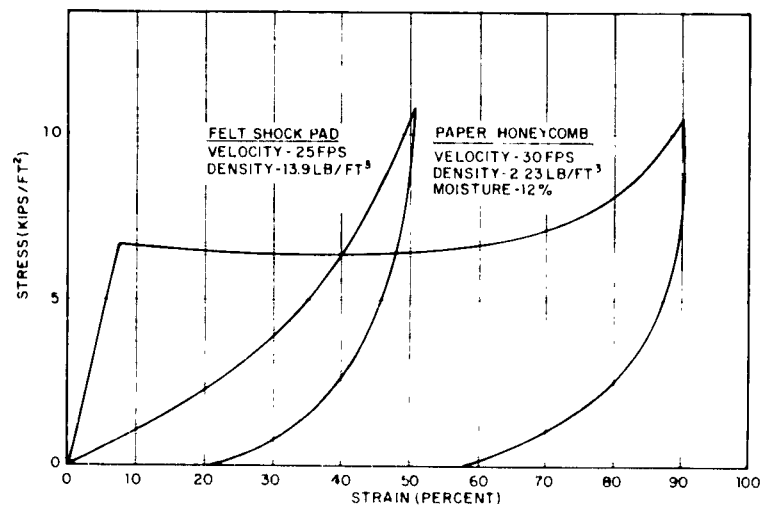


Fig. 2 - Stress versus strain for honeycomb and felt shock pad

Efficiency

There are two commonly used efficiency expressions for comparing cushioning materials, both of which are based on energy absorbed. The first of these, suggested by Gretz [1], is determined only by the shape of the stress-strain curve. It is the ratio of energy absorbed to a given strain to the product of the maximum stress and the given strain. Thus

$$E_{ff} = \frac{E_n}{S_m \epsilon_1} \times 100\%.$$

By this definition, a material with a rectangular stress-strain curve is always 100-percent efficient regardless of the strain ϵ_1 .

The second efficiency expression denoted as thickness efficiency, E_z , is based on the assumption that an ideal material that crushes at constant stress S_m to zero final thickness has an efficiency of 100 percent.

Thus

$$E_z = \frac{E_n}{S_m \times 1.0} \times 100\%.$$

Maximum thickness efficiency occurs usually at a strain just beyond that which produces

a stress equal to the initial peak stress. Cushions should be designed so the maximum strain is near the optimum strain.

Paper Honeycomb

The energy-absorbing characteristics of many different materials ranging from popcorn to steel cylinders have been determined. Of all materials studied to date, paper honeycomb appears to be the most economical from the standpoint of cost per foot pound of energy absorbed. It also has a stress-strain curve which approaches the ideal form. This material has been studied quite extensively at The University of Texas under contracts with Quartermaster Research and Engineering Command. In these studies, dynamic stress-strain curves were obtained by dropping a rigid mass on a suitable sample of honeycomb and recording the impact force as a function of the deformation of the cushion.

Stress-strain curves with different sample thicknesses—A typical set of stress-strain curves obtained with different cushion thicknesses is shown in Fig. 3. Since the mass and impact velocity were the same for each drop, the maximum strain varied with the thickness of the cushion. Actual stress-strain records are not as smooth as the curves shown here. Oscillations

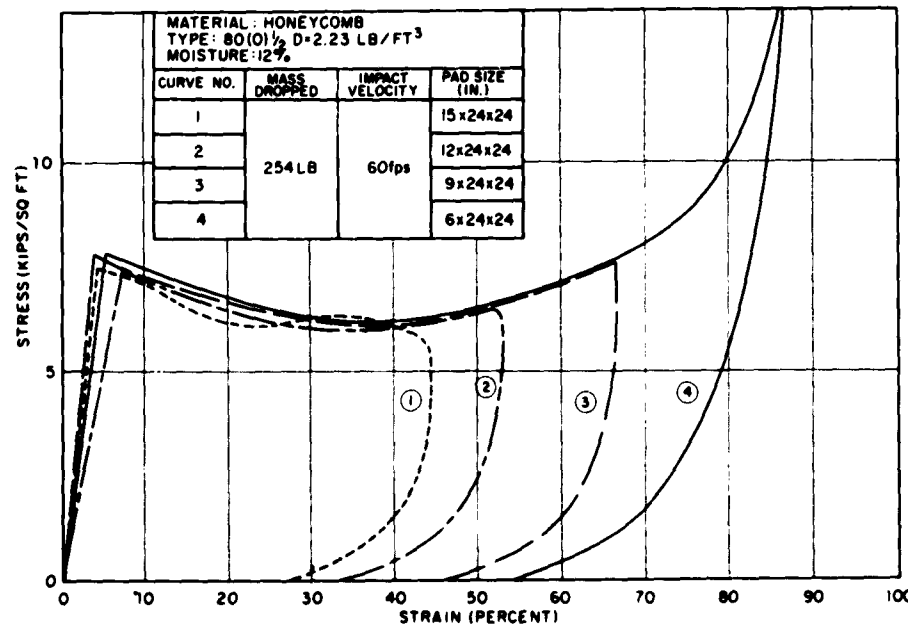


Fig. 3 - Stress versus strain for honeycomb with maximum strain varied

which appear on the original data are believed to be more characteristic of the measuring system than the material, consequently they are smoothed out when records are prepared for study.

Effect of density—Both the initial peak stress and the energy absorbed by paper honeycomb is largely a function of the overall density of the material as shown in Figs. 4 and 5. In these figures, the solid curve represents the best fit for experimental data which are based on the faced density of the material. The dashed curve indicates how much the data would be shifted by basing the density on the core only.

Effect of moisture content—The possibility that paper honeycomb may change its physical characteristics appreciably as its moisture content varies has been considered one of the major shortcomings of this material. Studies at The University of Texas [2] have shown, however, that although there is definitely a reduction in average crushing stress and energy absorbed as moisture content increases, the reduction does not become significant until the moisture content reaches approximately 20 percent and even at 24-percent moisture content, the deterioration in significant properties

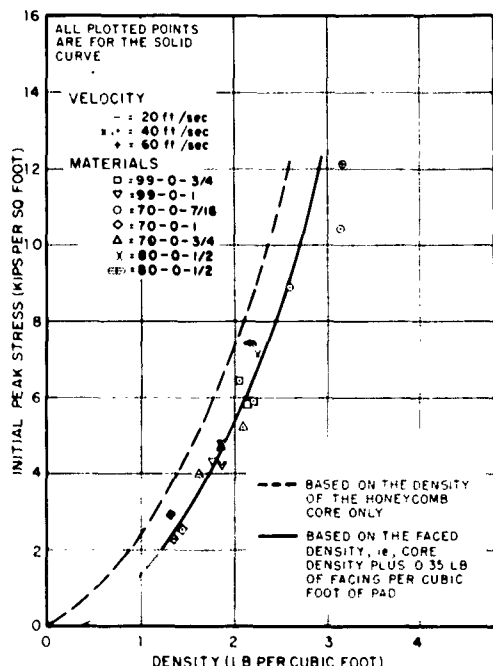


Fig. 4 - Peak stress versus density

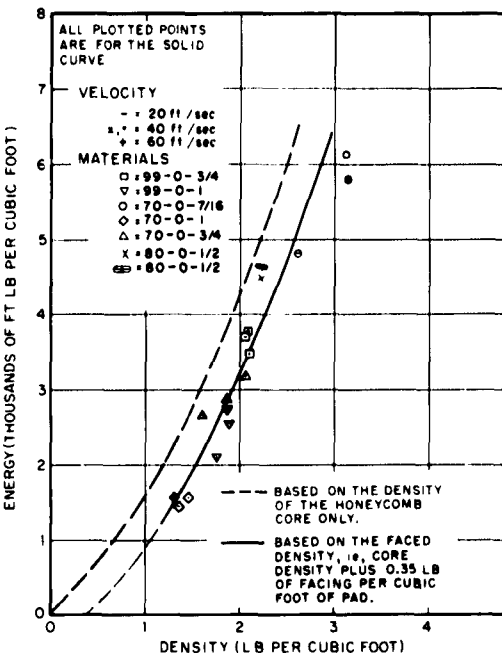


Fig. 5 - Energy absorption at 70-percent strain versus density

is not catastrophic. The effect of moisture content on stress-strain curves are shown in Fig. 6. It should be noted, in connection with these results, that according to tests performed by the Forest Products Laboratory [3], paper honeycomb must be exposed to an atmosphere of 80F and 90-percent relative humidity for 14 days to reach a moisture content of 20 percent. It will attain a moisture content of 17 percent when exposed to such environment for 2 days. These figures were determined from tests which were conducted with very small 4 x 4 x 3-inch samples. Large samples would, in general, take longer to reach an equilibrium condition. In this same connection, a study of the effects of weathering at The University of Texas showed that samples exposed for 30 days to the weather, including 4.5 inches of rain, and dried before testing by 3 days exposure to the sun, were not appreciably affected insofar as crushing strength and energy absorption were concerned. It appears that if reasonable precautions are taken to protect honeycomb from exposure to extreme conditions, moisture is no major problem. Indeed, in some respects, cushioning properties may be improved by a moderate amount of moisture.

Effects of impact velocity or rate of strain—Studies [2, 4] have shown that although there is

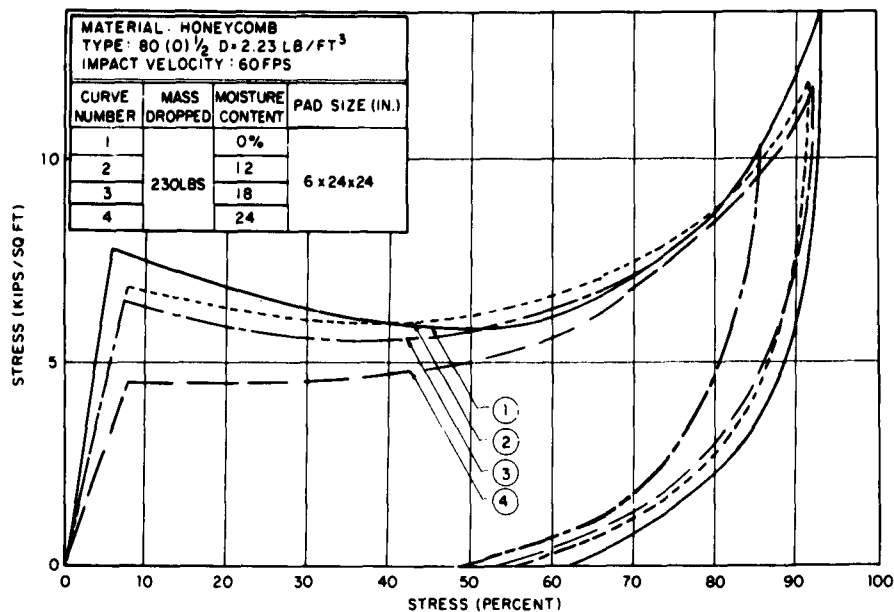


Fig. 6 - Stress versus strain for honeycomb with varied moisture and 60 fps velocity

an appreciable difference between static and dynamic stress-strain curves, there is no significant difference in stress-strain curves over the range of 30 fps to 90 fps impact velocities. This lack of effect is illustrated by the curves shown in Fig. 7. The cushion thicknesses and the mass were varied with impact velocity to produce approximately the same maximum strain for each drop. As a consequence, the maximum strain and the shapes of the curves at strains beyond 70 percent vary somewhat.

Effects of cushion area—The results discussed above were all obtained with 2 x 2-foot pads. It is not always possible in cushioning applications to use pads of this size. As a consequence, the variations in stress-strain characteristics which changes in pad size may produce are a matter of some concern. Studies have shown that as the perimeter-to-area ratio of a pad is increased, the average crushing stress and energy absorption decrease somewhat. Cushion designers should use pads with large areas as much as possible; and if small area pads must be used, the crushing characteristics of the small pads should be determined.

Foamed Plastic

Rigid foamed plastics such as the polyurethanes have some very desirable

characteristics as cushioning material. They are good energy dissipaters, they crush at essentially a constant stress, they are relatively unaffected by moisture conditions, are non-flammable, and unlike paper honeycomb, they have isotropic strength characteristics. Unfortunately, at the present time, these materials are expensive and do not compete with paper honeycomb on a price-per-unit-of-energy-absorbed basis.

Some dynamic stress-strain curves for a foamed polyurethane designated as 108C are shown in Fig. 8. These curves are quite similar to those obtained for paper honeycomb, but the plastic does not produce a peak starting stress as large as that found for paper honeycomb, and bottoming begins at about 50-percent strain as compared to 80 percent for paper honeycomb. One feature of the characteristics of a foamed plastic such as 108C, represented in Fig. 8, which is not apparent in the stress-strain curves, is the brittleness of the material. The samples used to obtain the stress strain curves literally exploded when struck by the falling mass. Pieces of plastic which were either uncrushed or only slightly crushed fly in all directions after the impact. From this, it would appear that confining the plastic would increase its efficiency as an energy dissipater. Tests of specimens confined in burlap or in cardboard cartons produced no

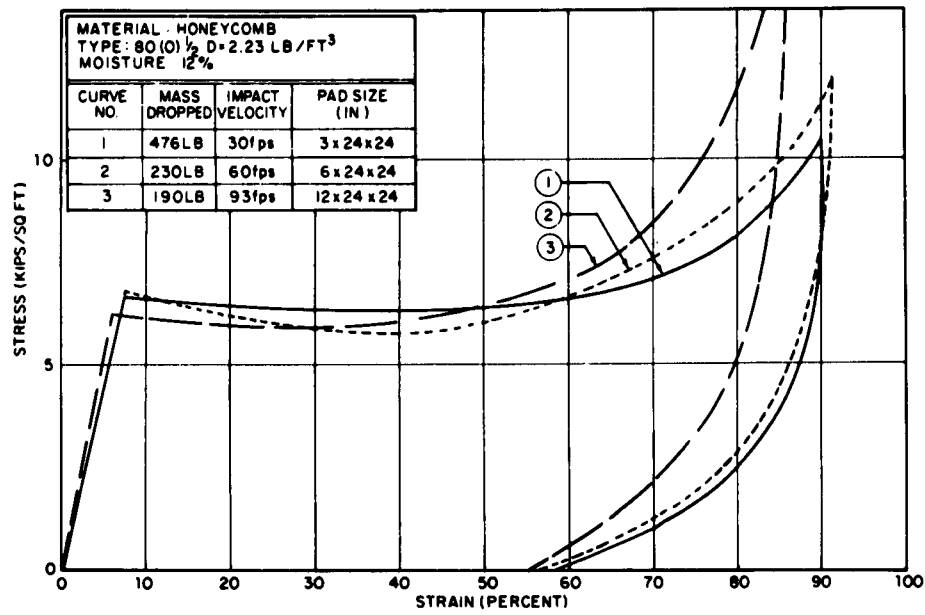


Fig. 7 - Stress versus strain for honeycomb with 12-percent moisture and velocity varied

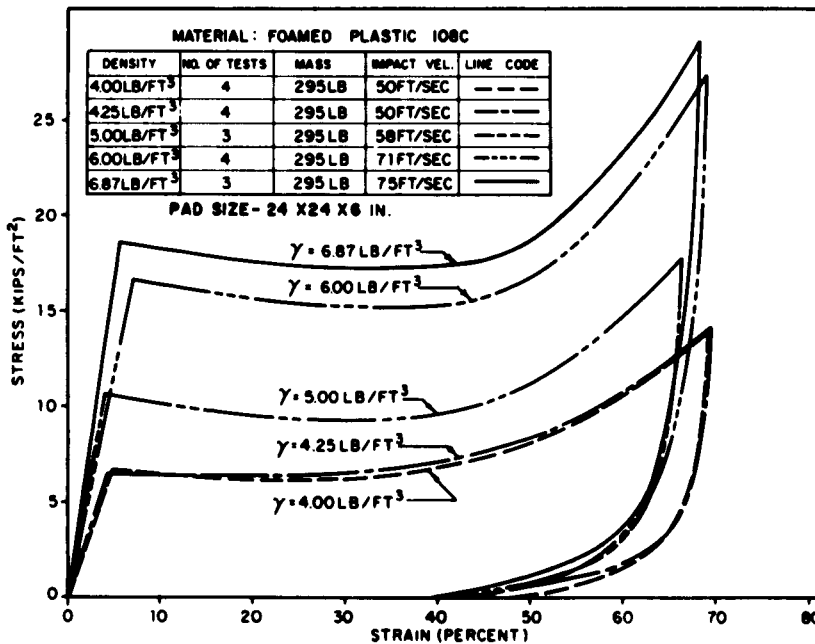


Fig. 8 - Effect of density on the stress-strain curve for foamed plastic 108C

really significant increases in energy dissipation [5], however.

Foamed plastics have a special interest for the military service because of the possibility of producing them in the field from the basic materials. Lockfoam [6], for example, can be produced in the field without need of any special equipment. At the present time, however, there seems to be appreciable variation from one batch to another in the properties of the finished product when it is produced by unskilled operators in the field.

Metal Cylinders

It has been found that when thin-walled metal cylinders are subjected to an axial impact, the walls of the cylinders buckle, and the cylinder crushes at a reasonably constant force. Some typical force-strain curves are shown in Fig. 9. Two of the curves shown were obtained from cylinders filled with water which was forced out through holes drilled in the sides of the containers [7]. These results are of special interest because of the possibilities they offer for improvisation of cushioning systems in the field. Empty beer cans, oil cans, coffee cans, or any type of empty can crushes very much the same as the seamless steel tube shown in Fig. 9. Also, it should be noted that an empty can provides a convenient device for dissipating the energy associated with a point impact load, applications in which it is frequently inconvenient to use paper honeycomb or foamed plastic.

Metallic Honeycombs

Several metallic honeycombs, such as aluminum, mild steel, and stainless steel are available. These materials have characteristics which are quite similar to those of paper honeycomb. A stress-strain curve for aluminum honeycomb is shown in Fig. 10. Note that the average crushing strength is about 15,000 psf as compared to about 7000 psf for a paper honeycomb of about the same density, and 6000 psf for foamed plastic 108C of about the same density. The metal honeycombs, aluminum in particular, have a number of characteristics that make them desirable as cushioning materials. Unfortunately, the cost of these honeycombs is so high as to make them economically unfeasible except possibly for a few very special applications.

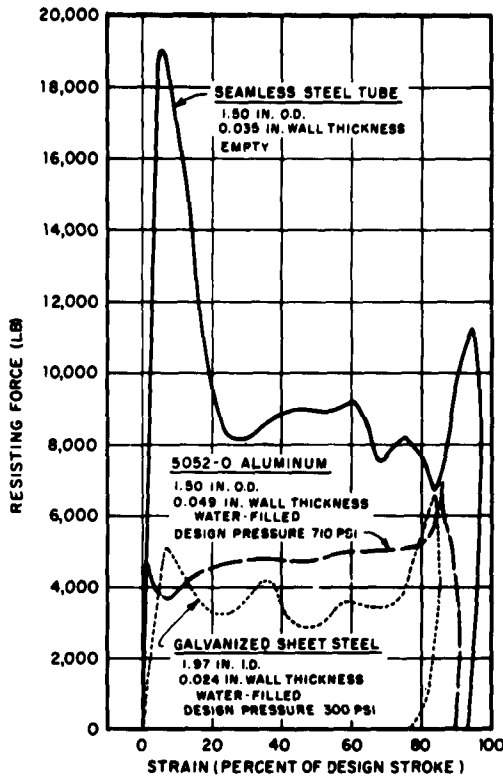


Fig. 9 - Force-strain curves for dynamic tests of steel, aluminum and galvanized sheet steel tubes

Other Materials

Many other materials are produced and sold for cushioning use. Stress-strain curves have been obtained for a number of these materials [7], as well as for a number of materials which are readily available but which are not sold as cushioning material [8]. These curves show that most of these materials are unsuitable for aerial-delivery-type cushioning. Those which are suitable are too expensive for general usage. Some may be usable for certain special application.

Airbags

A number of agencies in this country and the United Kingdom have investigated the use of airbags to absorb energy. The Structural Mechanics Research Laboratory made a limited investigation of the characteristics of British airbags and Goodyear airbags [9].

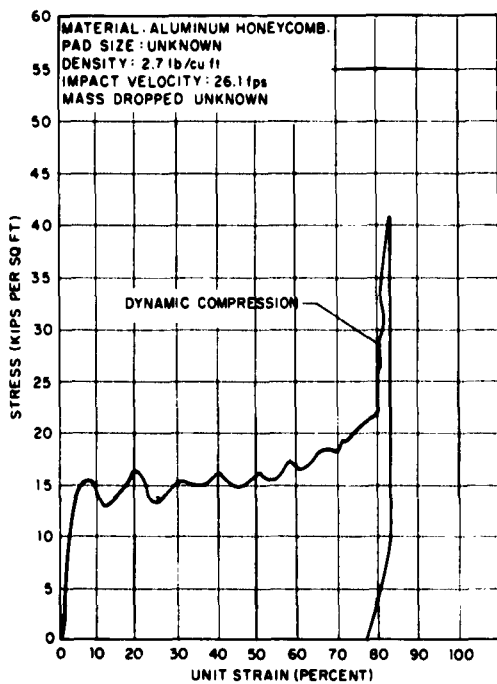


Fig. 10 - Dynamic stress-strain curve for aluminum honeycomb

The UK cylindrical bags were rubberized fabric envelopes 37 inches in diameter, each bag having four orifices 3-1/4 inches in diameter. These orifices were positively sealed with a latex rubber membrane which was normally ruptured by internal pressure as the bag was compressed.* At the bottom of the bag, a 12-inch-diameter filling sleeve, or orifice, was closed on impact as the sleeve collapsed against a mesh net.

The Goodyear bags were cylindrical, of heavy rubberized fabric, and were 35-1/2 inches in diameter. The outlet orifice was 4-1/2 inches in diameter, and included 4 gum rubber gussets which permitted expansion of the orifice as the pressure increased. This orifice was closed by a 6-inch-diameter plug made up of a stiff rubber ring and a rubberized fabric diaphragm. As the pressure built up in the bag, the stiff ring was forced out through the stretched orifice. The filling ports consisted of five 2-1/2-inch-diameter holes covered by a single one-way flap valve inside the bag. The extended bag was 4 feet, 3 inches long.

*The original membranes were replaced after rupture to permit additional tests on each bag.

Figure 11 shows a drop being made on a Goodyear airbag. Figures 12 and 13 show the force and pressure versus displacement curves for the Goodyear airbag and the UK cylindrical airbag.

The conclusions derived from these brief investigations were in part as follows:

- When used under conditions permitting vertical displacement only, the Goodyear airbags are capable of dissipating up to 18,000 foot pounds of energy at an impact velocity of 35 ft/sec in completely arresting a 960-pound mass without damage to the airbag. The data obtained for the UK bags, while inconclusive, suggests that similar performance may be expected for these units.

- Neither bag gives the ideal pressure-displacement diagram for pneumatic energy-dissipating devices which follows an adiabatic curve to a maximum pressure then maintains this pressure to the end of the impact. Both the Goodyear and UK airbags must then be considered inefficient on the basis of their force-displacement diagrams.

- For the range of impact velocities under consideration, i.e., 20 f/s to 35 f/s, the



Fig. 11 - Goodyear Bag - ready for drop at 64-foot drop site

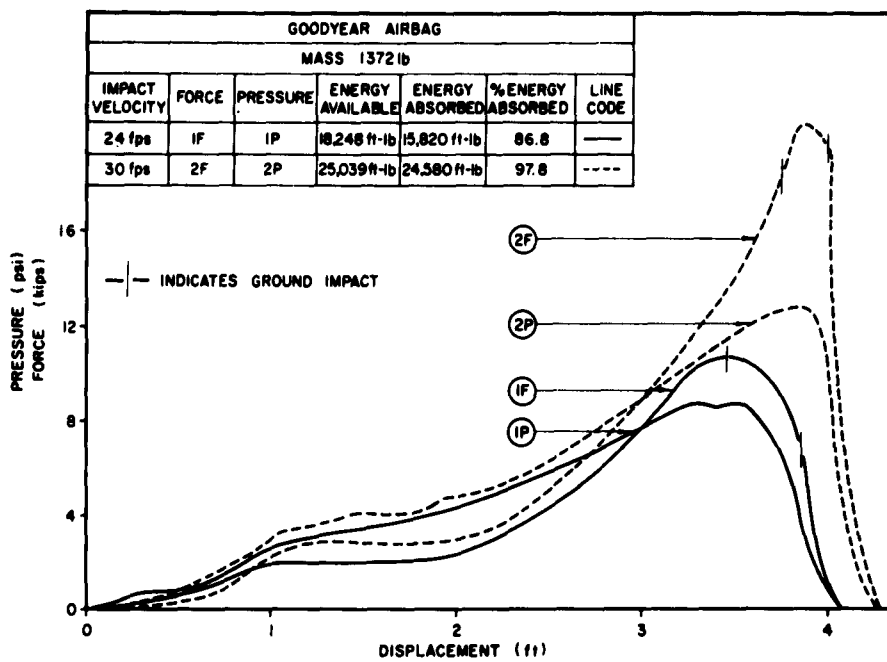


Fig. 12 - Force and pressure versus displacement
Goodyear airbags

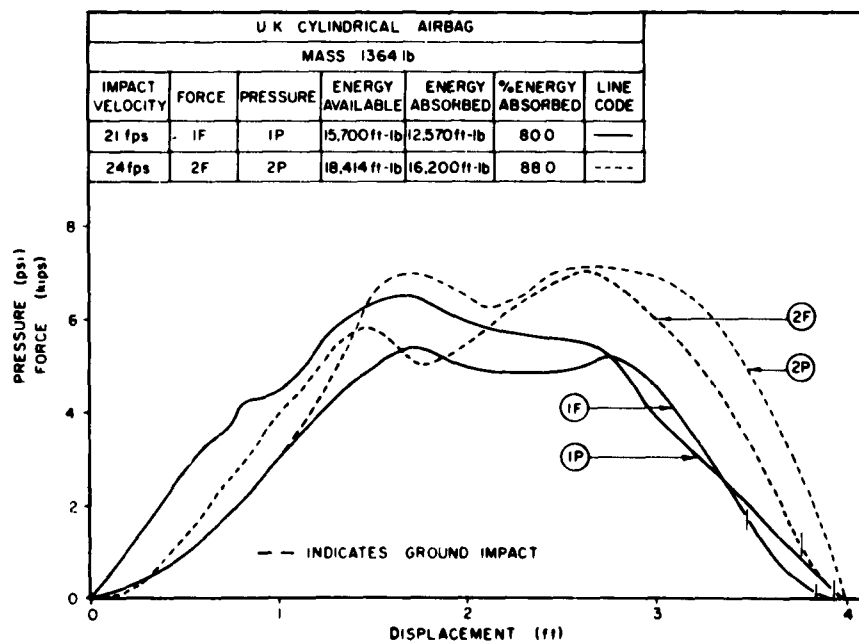


Fig. 13 - Force and pressure versus displacement
U.K. cylindrical airbags

allowable loads per bag are of the order of 1000 to 1300 pounds, the higher loads applicable at the lower velocities. The Goodyear and UK bags are of approximately equal capacity.

4. Raising the blowout pressure for the Goodyear airbag should result in a higher load-carrying capacity for this unit.

5. Prepressurization of both types of bags would give an increased effective stroke by reducing that part of the stroke now lost in expanding the bags laterally, and closing the intake ports. Alternately, a shorter and more stable bag could carry the present allowable loads if provided with a pressurization device.

DESIGN OF A CUSHIONING SYSTEM

Basic Principles and Equations

At the present time, it is customary to assume that the most significant design criterion is the maximum acceleration applied to the dropped item. Other factors such as rise time of the applied acceleration pulse, duration of the acceleration pulse, and the natural period or periods of the cushioned item are also known to be significant. The effects of these things will be discussed in more detail later. However, satisfactory design criteria which take these factors into consideration have not yet been developed. As a consequence of this, and also the fact that designs based on peak acceleration have been quite successful in drops under laboratory conditions, the method to be presented is based on the maximum g , or peak acceleration concept.

Development of the design equations, which are quite simple, begins with Newton's second law

$$F = Ma$$

or

$$F = WG$$

where $G = a/g$, the instantaneous acceleration, a , of the item in g 's and the other terms have the usual significance. Consider now a mass impacting a cushion as shown in Fig. 14. In this example, the force acting on the mass during the impact is the vector sum of the resistance of the cushion and the weight of the mass.

Thus

$$\sigma A + W = WG$$

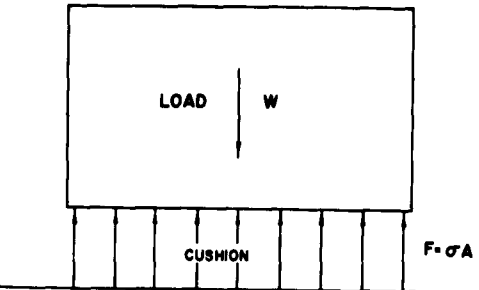


Fig. 14 - Mass impacting cushion

where σ is the instantaneous crushing stress in the cushion

A is the effective area of the cushion

$$\text{thus } \sigma = \frac{W(G + 1)}{A} \quad (\text{A})$$

Now suppose that an item is to be dropped and the average acceleration is to be limited to some value, say G' . It will be assumed that the cushioning material crushes at a constant stress σ' . This leaves only the area and thickness of the cushion to be determined. The area A' is determined by the crushing strength of the cushioning material and the design acceleration. Thus, from Eq. (A)

$$A' = \frac{W(G' + 1)}{\sigma'} \quad (\text{B})$$

Note that for a given value of σ' , the greater the area of the cushion, the greater the G loading will be. This contradicts the popular notion that if a little cushioning is good, a lot should be even better. Obviously, an excess of cushion area could cause considerable damage and thus defeat the whole purpose of the cushioning. The thickness of the cushion is determined by the energy to be dissipated. This energy is given by

$$E_i = \frac{1}{2} \frac{W}{g} v^2 + Wd\epsilon \quad (\text{C})$$

where v is the impact velocity and d is the thickness of the cushion and ϵ is the design strain. The energy dissipated by the cushion is given

$$E_d = A'\sigma' \epsilon d = W(G' + 1) \epsilon d. \quad (\text{D})$$

Equating the energy to be dissipated to the dissipation the cushion

$$W(G' + 1)\epsilon d = \frac{1}{2} \frac{W}{g} v^2 + Wd\epsilon. \quad (E)$$

From which the relationship

$$G'\epsilon d = \frac{1}{2} \frac{v^2}{g}$$

hence

$$d = \frac{1}{2} \frac{v^2}{\epsilon g G'}. \quad (F)$$

Equations (B) and (F) give all the basic information needed to design a simple cushion once the crushing strength of the cushioning material, the impact velocity, and the allowable G load are specified. There are additional factors, however, which must be considered. For example, if the item to be cushioned is a complicated device such as a vehicle, the cushioning area must be properly distributed so as to insure uniform crushing and protection of all parts of the vehicle. Parts of the vehicle will absorb some of the impact energy. If the system is properly designed, this will all be elastic strain energy. This plus the possibility of interference between parts demands that this energy be limited. Effective limitation can be provided by proper placing of cushioning materials or by blocking between components. Heavy components of the vehicle should be cushioned so that energy is taken directly from these components into the cushion rather than having it flow indirectly to the cushion through mounting brackets, frames, supports, etc. A good arrangement of the cushioning will insure that the heavy components and the surrounding members move as a single unit. It is virtually impossible to specify design procedures for all details to which these considerations apply. In that sense, designing a cushioning system is still a mixture of art and science.

FRAGILITY OF ITEMS TO BE AIR DROPPED

In order to proceed rationally with the design of a cushioning system, something must be known of the ability of the cushioned item to withstand shock loads. The possibility of damage occurring depends on the characteristics of the impact and of the item. These factors are, to a large extent, ignored in the design procedure outlined above. As pointed out, however, in the previous discussion, it is necessary to resort to this oversimplification for the sake

of expediency. No simple, and at the same time reliable, method for characterizing the damage-producing capability of an acceleration pulse in terms of the characteristics of the cushioned item has been developed. The shock spectrum which has been used for characterizing earthquake shocks and blast waves does not appear to be satisfactory for the aerial-delivery problem. Studies which have been conducted to date have uncovered no correlation [10, 11] between the damage produced by a given acceleration pulse applied to a simple system and the shock spectrum of the pulse. It has been observed in the course of several hundred drops of military vehicles at The University of Texas [12, 13, 14, 15] that the damage most commonly produced in these vehicles is a permanent deformation of some part; the frame of the vehicle may be bent, or a bracket is bent. All parts that possess some degree of ductility are much more likely to bend and undergo permanent deformation than they are to fail completely at the strain rates involved.

These observations have led to a series of studies of the permanent deformation produced in simple structures by various types of impact loading reported in another paper in this Section* and Ref. 10. Consequently, only a few general remarks will be made here. If a simple single-degree-of-freedom system with a yielding spring is considered, it seems obvious that there is some peak acceleration level below which no matter what the form or duration of the applied pulse, no permanent deformation will be produced in the system. It seems equally obvious that if an acceleration in excess of the limiting value referred to above is applied to the system, the longer the system is subjected to this acceleration, the greater the permanent deformation is likely to be, particularly if the force required to produce the acceleration exceeds the yield stress of the spring. Conversely if the time during which the system is subjected to the acceleration in excess of the limiting value is made shorter and shorter, it might be expected that the permanent deformation will decrease until it vanishes altogether. One might also expect the longer the period of the system, the greater the permanent deformation will be. Consequently, a complete design criterion probably should contain all these factors, and indeed the paper presented later shows a definite theoretically computed relationship and some experimental confirmation.

Theoretical studies, not yet complete or complex multi-degree-of-freedom systems are showing that these systems under the type of

*Page 302.

loading experienced in aerial delivery work, behave largely as though they had only one degree of freedom, with a frequency equal to the fundamental frequency of the system.

Other studies have shown that internal damping in a simple system has a considerable influence on the permanent deformation produced in the system by a given acceleration pulse [11]. These results indicate that if a cushioning system is designed for a complex item without consideration of the internal damping of the item, an optimum design will not be achieved, but a very substantial margin of safety may be built into the system.

Until some method for completely characterizing a shock, or impulsive loading in terms of the natural characteristics of the impacted item is developed, it appears that each supply item or vehicle which is to be air-dropped will have to have a specific cushioning system designed for it. This will involve some cutting and trying and a brief laboratory testing program. It should be possible, however, to reduce this testing to a bare minimum; one drop perhaps to verify the design, and then one more to provide verification of any changes suggested by the results of the first drop. It should be borne in mind that the design procedure, as well as all the discussion so far, is based as stated previously on an assumption of no lateral component of velocity at impact. This is a condition which will probably be the exception rather than the rule under actual conditions. In some of the earlier studies of aerial delivery problems, the lateral component of velocity was considered. More recently, however, this problem has received little attention. It appears that further research in this area should be instigated.

DESIGN CONSIDERATIONS FOR ITEMS TO BE DROPPED

Experience has shown that in many instances, relatively minor changes in the design

of items to be dropped, and this is particularly true of vehicles, can produce significant increases in the fragility rating or ruggedness of the item. For example: frames of vehicles should be strong enough and stiff enough to allow transfer of considerable load from one member to another since it is generally not possible to support all frame members with cushioning material. Also, lower frame members should be flat-bottomed and as wide as possible, and spaced at reasonably close intervals to make placement of cushioning material and load spreaders simpler. No parts of the vehicle should protrude below the lower frame members. The airline shown in Fig. 15, passing underneath the frame instead of above or through the frame is an example of simple design detail which causes considerable trouble when an actual cushioning system is being designed. It would also be helpful to the cushion designer if manufacturers would provide with each vehicle, or other items to be dropped, detailed weight distribution charts with the center of gravity located in the plan view. Painted markers on the vehicle locating the center of gravity should also be required.



Fig. 15 - Airline beneath frame member on the water tank trailer, XM107E2

REFERENCES

- [1] John L. Gretz, "Engineering a Cushioned Package," Flow Magazine, Vol. 7 April 1952, (also Modern Packaging, Vol. 25, 1952, pp 125-133).
- [2] James W. Turnbow, et. al., Cushioning for Air Drop, Part III, Characteristics of Paper Honeycomb under Dynamic Loading, Austin, Texas, Structural Mechanics Research Laboratory, The University of Texas, 1956.
- [3] J. P. Hopf, Equilibrium Moisture Content of Paper Honeycomb and its Effect on Energy Absorption, Forest Products Laboratory, Project No. 7-87-03-004B, Report No. 1, December 1955.

- [4] Charles H. Karnes, et. al., High-Velocity Impact Cushioning, Part V, Energy-Absorption Characteristics of Paper Honeycomb, Austin, Structural Mechanics Research Laboratory, The University of Texas, 1959.
- [5] Richard Shield and Clarke Covington, High-Velocity Impact Cushioning, Part VI, 108C and 100C Foamed Plastics, Austin, Structural Mechanics Research Laboratory, The University of Texas, 1960.
- [6] Ahmin, Ali, Cushioning for Air Drop, Part VIII, Dynamic Stress-Strain Characteristics of Various Materials, Austin, Structural Mechanics Research Laboratory, The University of Texas, 1957.
- [7] C. W. Morgan and W. L. Moore, Cushioning for Air Drop, Part V, Theoretical and Experimental Investigations of Fluid-Filled Metal Cylinders for Use as Energy Absorbers on Impact, Austin, Structural Mechanics Research Laboratory, The University of Texas, 1956.
- [8] Hudson Matlock, et. al., High-Velocity Impact Cushioning, Part II, Energy-Absorbing Materials and Systems, Austin, Structural Mechanics Research Laboratory, The University of Texas, 1957.
- [9] J. W. Turnbow and William Ogletree, Energy-Dissipating Characteristics of Air Bags, Austin, Structural Mechanics Research Laboratory, The University of Texas, 1959.
- [10] Wallace Fowler, An Analytical Study of an Undamped Nonlinear Single-Degree-of-Freedom System Subjected to Impulsive Loading, Austin, Structural Mechanics Research Laboratory, The University of Texas, 1961.
- [11] Michael D. Reifel, The Effects of Acceleration Pulse Parameters on the Permanent Deformation of a Damped Single-Degree-of-Freedom System, Austin, Structural Mechanics Research Laboratory, The University of Texas, 1961.
- [12] Clarke Covington, et. al., Fragility Studies, Part I, Utility Truck, 1/4-Ton, Austin, Structural Mechanics Research Laboratory, The University of Texas, 1960.
- [13] Clarke Covington and Richard Shield, Fragility Studies, Part II, Cargo Truck, M37, 3/4-Ton, Austin, Structural Mechanics Research Laboratory, The University of Texas, 1960.
- [14] Richard Shield and Clarke Covington, Fragility Studies, Part IV, Cargo Trailer, M101, 3/4-Ton, Austin, Structural Mechanics Research Laboratory, The University of Texas, 1960.
- [15] Richard Shield and Clarke Covington, Fragility Studies, Part V, Water Tank Trailer, XM107E2, 1-1/2-Ton, Austin, Structural Mechanics Research Laboratory, The University of Texas, 1960.

DISCUSSION

Mr. Munson (General Dynamics): I think Fig. 13 on the United Kingdom airbag trial drops shows an energy absorption of 80 percent on one drop and 88 percent on the next drop. If there is complete deflation of these bags, I don't see on the curve where the remaining energy went?

Prof. Thompson: Obviously we could not give you adequate coverage of this without spending a lot of time, and I think we probably should defer the discussion for the experts from the United Kingdom who will be on later. I am sure they will talk about airbags. Rip, would you like to give him an answer on this?

Dr. Ripperger: If I understood the question correctly you were asking where the energy went that wasn't absorbed. It went into rebound of the item. The rebound came from the thing hitting the ground; it wasn't the rebound provided by the compression of the air in the airbags itself.

Prof. Thompson: I might add to this, that at higher velocity these bounce like rubber balls and there was a good bit of rebound energy.

R. E. Jones (Marshall SFC): I would like to ask if anyone has done any work with exceedingly high friction energy absorbers which are reusable and which is exactly what you have on an

automobile? Of course the configuration here doesn't apply.

Prof. Thompson: Not on energy absorbers such as you would use on an automobile, but we have worked with friction devices. Devices that were really a combination of friction and crushing of wood such as the squeezing of a wood member in a vise of some type, and this has shown some promise. But in general we have not worked with devices such as you describe. I know of no other work.

Mr. Opalinski (Woodland Container Co.): I was curious why you used 12-percent moisture content on your foam. Equilibrium moisture content will probably bring it up to around 15 percent in most parts of the country. Up north here it will probably be 12 percent, but down south you probably are going to get higher than that aren't you?

Prof. Thompson: Not too much higher. I'd say between 12 and 15.

Mr. Opalinski: Was 12 percent chosen for any particular reason?

Prof. Thompson: No, we just pulled that out of the air 'or analysis purposes.

E. Schell (Aeronautical Systems Div. WPAFB): Mr. Thompson, I am wondering about the initial peak effect on these energy absorbers. We have been working with them ourselves and we find that we get a considerable initial peak, particularly in aluminum honeycomb. This initial peaking occurs in practically all energy absorbers. We were wondering if you would care to discuss this initial peaking?

Prof. Thompson: We have been concerned about it too. We have spent a lot of time studying this initial peak, trying to analyze why it occurs and if we are really getting the correct response. Of course we know that this is an important peak as regards the effects on the structure. Yet on the other hand, in from 2 to 3 hundred drops of vehicles we have not experienced any problems. We have probably been operating at levels considerably below where they would cause us trouble. But I'm sure these peaks would be more serious in the case of metal honeycombs and in the case of paper honeycombs you amplify it. This is a problem! We are concerned with it as you will see later on in our second paper.

* * *

DESIGN OF CUSHIONING SYSTEMS FOR AIR DROP

M. P. Gionfriddo
Quartermaster Research & Engineering Center
Natick, Massachusetts

This paper presents complementary analytical and empirical techniques for the design of energy dissipater configurations for air dropped items.

INTRODUCTION

The techniques described in this paper apply to the use of single-shot, sheet-type energy dissipater materials that are used for the control of accelerations during an air drop impact. An air drop impact is different from most transportation impacts in that the item being dropped is impacted on a selected surface and the energy absorbed is from three to ten times greater than that in a typical transportation shock. This increased energy usually results in a requirement for a greater deflection of the energy absorber than is normally considered for transportation packaging.

The energy dissipater materials that fall within the scope of the paper are assumed to have mechanical properties similar to those exhibited by the paper honeycomb (Fig. 1) now in use by the Army. Specifically these

mechanical properties are: (a) An essentially rectangular stress-strain curve over a wide range of strain. (b) Low-rebound energy. (c) Mechanical properties which are constant over a wide range of environments.

Figure 2 shows typical stress-strain curves for standard Army paper honeycomb for two maximum strains. It is apparent that the curve with a maximum strain of approximately 70 percent does have an essentially rectangular stress-strain curve while the curve with a maximum strain of approximately 85 percent departs from being essentially rectangular and rises rapidly in the region of 75 to 85 percent strain. This phenomenon which occurs as the paper packs together at the conclusion of its crushing is called "bottoming". Energy dissipater configurations are usually designed so that the honeycomb is strained from 60 to 70 percent. The amount of rebound energy stored

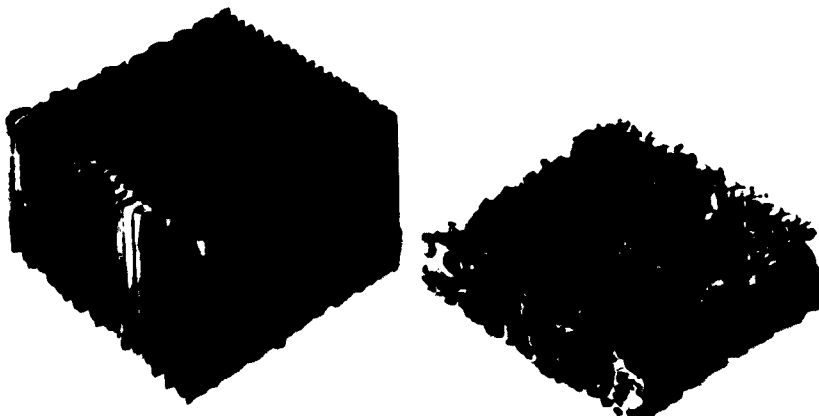


Fig. 1 - Typical paper honeycomb - expanded and crushed

in the paper honeycomb is indicated by the area under the unloading curve as shown in Fig. 3 and is equal to about 8 percent of the energy absorbed for strains up to 70 percent. Above 70-percent strain, the percentage of rebound energy rises rapidly.

ANALYSIS

The standard analytical technique for the use of energy dissipators within the scope of this paper is based on the assumptions that the body being accelerated is rigid and that there are only two forces to consider; one, the weight of the body and two, a constant force exerted

by the paper honeycomb. With these assumptions, the use of Newton's second law results in the following equation:

$$A = \frac{W(G + 1)}{S_a} \quad (1)$$

where

A = Area of paper honeycomb - square feet
 W = Weight of item - pounds
 G = a/g

where

a = acceleration of item - ft/sec²
 g = acceleration of gravity - ft/sec²
 S_a = Average crushing stress of energy dissipater lb/sq ft.

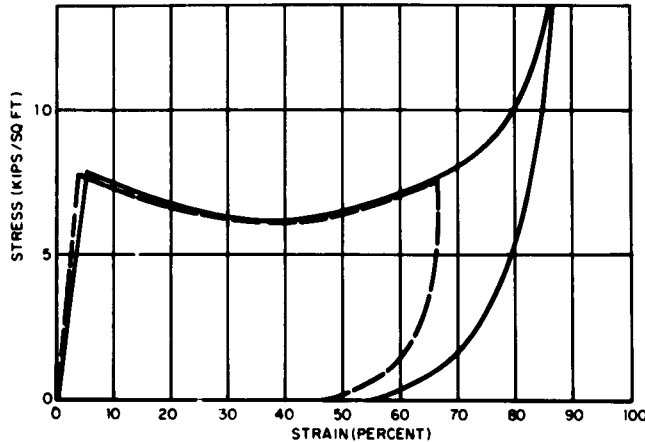


Fig. 2 - Stress versus strain for 80-0-1/2 paper honeycomb

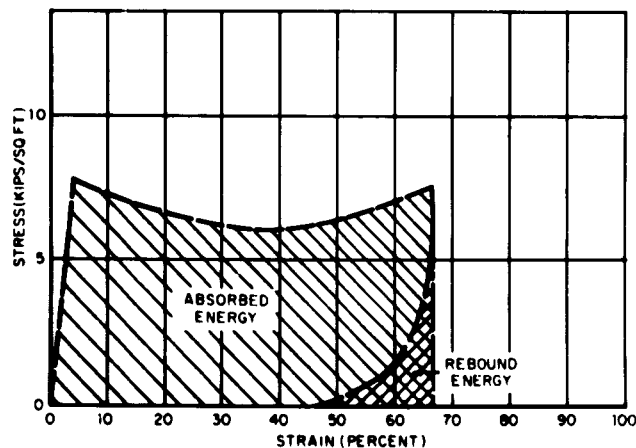


Fig. 3 - Rebound energy of 80-0-1/2 paper honeycomb

Obviously, this equation is used to determine the area of energy dissipater necessary to decelerate a given item a given amount. Further, this equation shows that the dissipater area is the factor that is most significant in controlling the deceleration of an item. As long as the dissipater crushes, but does not bottom; impact velocity, drop height, or dissipater thickness have no effect on the deceleration of the item. Normally, impact terrain has little effect on the deceleration of the item and, usually, this effect can be neglected. There then remains the need to determine what thickness of energy dissipater of area A is required to insure that the item is decelerated to zero vertical velocity without bottoming the energy dissipater.

The deceleration distance of the item can be obtained by equating the work done by the energy dissipater to the change in kinetic and potential energy during crushing. This yields the following equations:

$$S_A s = \frac{1}{2} \cdot \frac{w}{g} V^2 + W_s$$

solving for s :

$$s = \frac{V^2}{2gG} \quad (2)$$

where

s = Deceleration distance - feet

V = Impact velocity - feet per second.

The thickness of energy dissipater required to provide this distance without bottoming is calculated from the following equation:

$$t = \frac{s}{E} \quad (3)$$

where

t = dissipater thickness - feet

E = Maximum strain - expressed as a fraction.

Combining Eqs. (2) and (3) results in the following equation:

$$t = \frac{V^2}{2gGE} \quad (4)$$

The area equation, Eq. (1), and the thickness equation, Eq. (4), form the basis for the design of energy dissipater configurations.

These equations are most easily applied in the design of energy dissipater configurations for items which can be considered homogeneous and are uniformly supported by the energy dissipater. Such Army items as rations, ammunition, and liquids in drums, rigged in the usual manner for air delivery (see Figs. 4, 5), fall within this category and the configurations as designed are quite successful.

The main difficulty in the application of these equations arises in determining the value of G that an item can withstand. In the air delivery field, the symbol G when it is used to

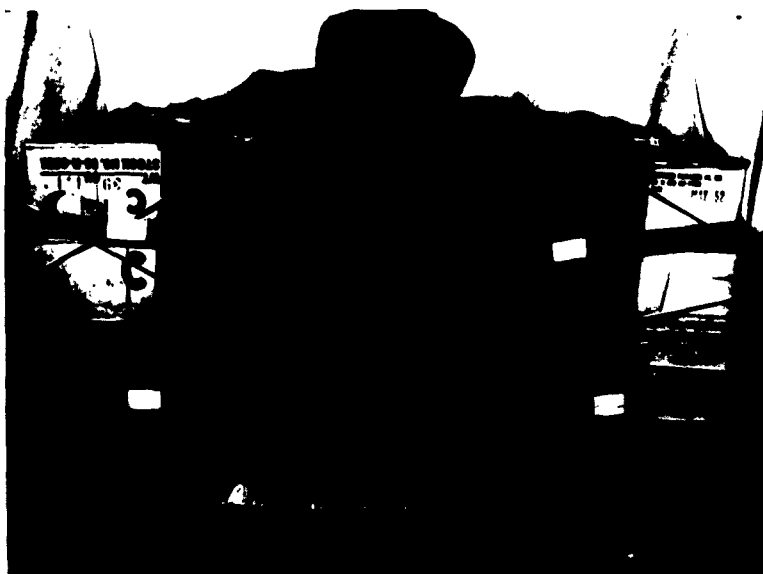


Fig. 4 - C-rations rigged for air delivery using paper honeycomb as energy dissipater

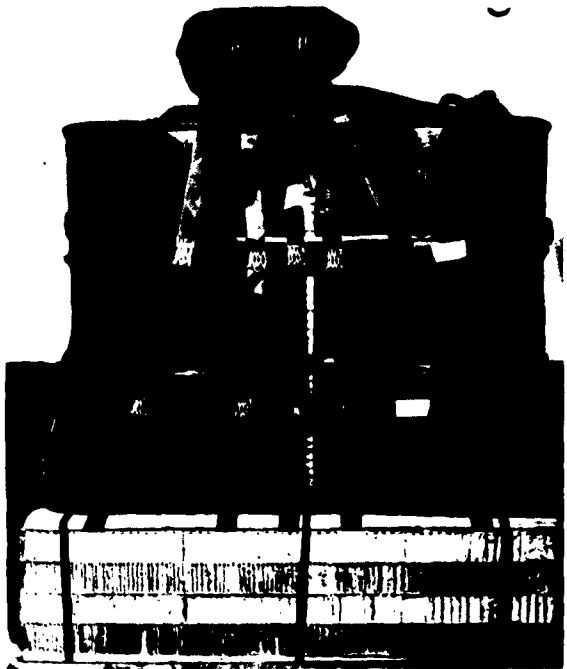


Fig. 5 - Fifty-five-gallon drums rigged for air delivery using paper honeycomb as the energy dissipater

describe the inherent strength of an item has been identified by a variety of names such as shock rating, fragility factor, or damage susceptibility factor. All of these terms imply that the ability of an item to withstand an impact can be described by a single number. As will be shown later, this concept oversimplifies the problem but it does present a convenient tool for considering air delivery impacts.

The Army's main use for energy dissipaters in air delivery is for the protection of large, complex, built-up structural items such as trucks, howitzers and tank-like vehicles. The energy dissipater configurations for such structures are characterized by a number of small stacks of energy dissipater positioned at various locations beneath the item and between the item and a platform. An energy dissipater configuration for a typical Army vehicle is shown in Fig. 6. A sketch of the same configuration with the vehicle removed is shown in Fig. 7. Configurations of this type make it unrealistic to specify a single value of G which describes vehicle strength. In the case of the homogeneous item that is uniformly supported, deceleration at too high a value of G would most likely result in a simple compressive failure of

the item. However, for vehicles, the energy dissipater stacks can be positioned at an infinite combination of locations beneath the item. Since each configuration will introduce the applied forces in a different manner, structural failures of various types can occur at many locations. Thus the item can have a number of different values for the factor, G , describing its inherent strength depending on the dissipater configuration. Presently, there are no suitable analytical techniques for determining a value of G even for the rather simple items such as rations, ammunition, and liquids. Since G is shown here to be a rather nebulous number, or numbers, a purely analytical application of the area and thickness equations is not possible. At this point, testing techniques must be used to supplement the analysis in order to arrive at a usable energy dissipater configuration.

In the past, consideration has been given to a variety of testing machines that could be used to determine some significant parameters of the items or to subject the items to a duplication of the impact environment. Because of the inadequacies of the analytical work conducted to date, measurement of item parameters such as static strength, natural frequencies, etc., is not useful since these values cannot be correlated to any impact damage criterion. Thus, it appears that duplication of the impact environment is now probably the best way to determine a value of G . It has been found that in light of the range of item weights and impact velocities of interest to the Army, the cheapest, most reliable, and most imitative method of duplicating an air delivery impact without actually air delivering the item is to free-fall the item from a height calculated to produce the desired impact velocity and to use paper honeycomb in its energy dissipater configuration to produce the applied forces on the item.

ENERGY DISSIPATER CONFIGURATIONS FOR RIGID BODIES

For items that can be considered rigid bodies, the energy dissipater configuration can be obtained through either of the following procedures depending upon whether the item is rigged one unit high such as the 55-gallon drums in Fig. 5 or stacked in layers such as the boxes of rations shown in Fig. 4.

For Single-Layer Items

1. Choose a low value of G

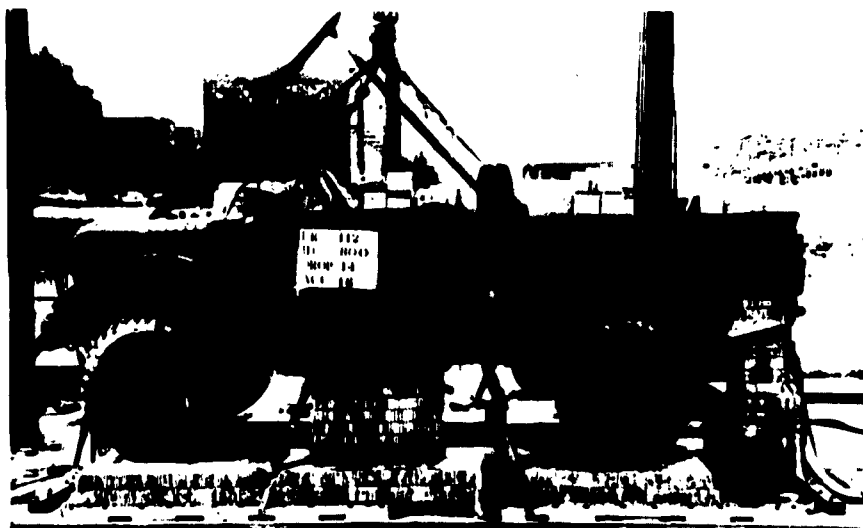


Fig. 6 - Typical energy dissipater configuration
for standard army vehicle

2. Calculate the required area and thickness of paper honeycomb based on chosen value of G.

3. If the calculated area is much smaller than the base area of the item, a suitable load spreader should be used to preclude bending of the item. In air delivery practice, if an item is undamaged when subjected to the accelerations produced by having the area of the honeycomb equal or just slightly larger than the item's base area, no further increase in honeycomb area and thus G level is tested as long as the thickness of honeycomb required at that G level is not unreasonable. For instance, in Fig. 5, the area of honeycomb shown is not necessarily producing the maximum deceleration that the drums can withstand. However, at the G level that the honeycomb is producing, the thickness of honeycomb required is quite reasonable and forms a stable energy dissipater configuration. A further increase in honeycomb area would serve only to reduce the required thickness of dissipater at the expense of a larger, heavier load spreader to insure crushing of the entire area and would result in a less efficient utilization of the aircraft floor space.

4. Rig the item and drop from the necessary height to produce desired impact velocity.

5. If the item is undamaged, choose a higher value of G and repeat the testing procedure until damage occurs.

6. If damage occurs after a number of drop tests, it would be well to test again at the damaging G level with a new item to negate any effects due to the repeated impacts.

For Multilayered Items

The testing procedure is modified to duplicate the forces acting on the item in the bottom layer which is the most severely loaded item. This can be accomplished by simply placing ballast on the test item equal to the weight supported by the item and conducting the remainder of the test as described for the single-layer items.

ENERGY DISSIPATER CONFIGURATIONS FOR FLEXIBLE BODIES

For items that are considered to be single flexible bodies, that is, bodies that are not continuously supported by the energy dissipater and thus are allowed to bend, the determination of the energy dissipater configuration becomes somewhat complicated. The practical objective in determining dissipater configurations is to arrive at the minimum number of dissipater stacks necessary to decelerate the item with no bending failure and preferably with a minimum of elastic bending. With this in mind the following procedure is used:

1. Choose an arbitrary low value of G (between 7 and 10 G's is reasonable for typical Army Vehicles and equipment).

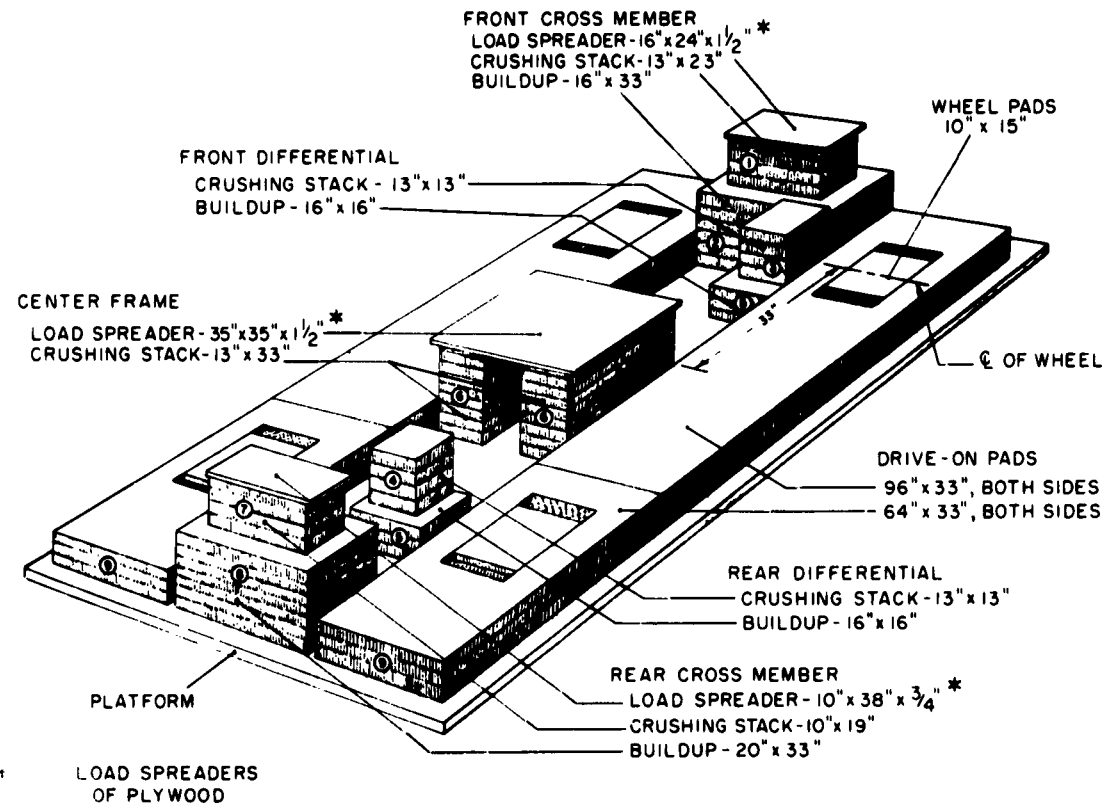


Fig. 7 - View, with vehicle removed, of typical energy dissipater configuration

2. Based on this value of G and the total weight of the item, calculate the total area of paper honeycomb required.

3. Arbitrarily select a number of locations on the item where the individual small dissipater stacks are to be positioned. (Intuition and experience show that the locations should be near or at large dense components of the item such as near or at the engine, transmission, or differential housings of a vehicle.) Also stacks can be placed beneath the main structural members of the item.

4. From a knowledge of the weight distribution of the item, calculate the weight supported by each energy dissipater stack. Often the exact weight distribution is not known and is not available. In this case estimates of the weights of the major components of the item and the assumption that all other weight is uniformly distributed will suffice for the first trial.

5. Calculate the area required for each stack that will produce the same acceleration at each point (most logically the original value of G chosen).

The reason for calculating the total area initially when it isn't used in the calculations is to provide the designer with a feel for the amount of energy dissipater that will have to be distributed among a number of stacks. This feel will allow the designer to better estimate the number of stacks he can use without having intolerably large or small stack areas.

6. Calculate the energy dissipater thickness required.

7. Rig the item and subject it to the impact.

8. Inspect the item and the energy dissipater after impact. This inspection can provide much information. Bottoming of a stack

indicates that the weight supported by the stack at this point was underestimated and the resulting acceleration which was quite low required a longer crushing stroke. Incomplete crushing of a stack indicates that the weight supported by the stack was overestimated and the resulting acceleration was quite high or the impact energy was absorbed wholly or partially by the structure of the item. Care must be taken at this point to understand that the height of the stacks is only an indication of the maximum strain to which the energy dissipater was subjected. As can be seen in Fig. 2, paper honeycomb which is dynamically strained to 70 percent returns to approximately 50-percent strain after impact. Permanent deformation of the item indicates that the accelerations at the various stacks were different enough so that the relative motion between portions of the item was great enough to exceed the elastic limit of the structure or if the acceleration of the item was uniform, that the deformation of the structure due to the inertia loads was too great. In the first case, appropriate changes in the stack areas to insure an approximately uniform acceleration at each stack are necessary. In the second case, either the overall G level must be reduced or additional stacks must be inserted at appropriate locations to insure elastic deformations only.

In the initial determination of the locations of the dissipater stacks, a helpful aid in precluding bending failure of the main structural members of an item is to conduct a static load analysis of the item structure based on the dynamic forces exerted on it during the impact. The applied loads will be the weights of the item's major components and the distributed weights each times ($G + 1$). The reactions will be the average forces exerted by the energy dissipater stacks while crushing. The bending moments and the bending stresses throughout the item structure are then calculated. Although the numerical values of the moments and stresses so calculated will not be too meaningful, the occurrence of a relatively large bending stress at one point will indicate that that point will probably be the first location of a failure in the structural members. To carry the analysis one step further, if the first solution does indicate a point or points on the structure where the bending stresses are relatively high, the locations of the reaction forces (the energy dissipater stacks) should be changed until the bending stress peaks and valleys have been smoothed out as much as practical.

This method is useful because it has been found through extensive drop testing of Army

equipment that structural failure often seems to occur because of an excessive aperiodic displacement of the structure, thus somewhat analogous to a static loading structural failure. Of course, because most of these tests were close duplications of standard operational conditions, many parameters which could influence the type of structural failure were held approximately constant. For instance, since paper honeycomb-type energy dissipaters were always used, the shape of the input acceleration pulse did not change markedly during the tests; most of the instrumented tests were conducted at impact velocities between 20 and 30 feet per second; and the duration of the impact pulse was usually between 20 and 100 milliseconds. Thus, all of the Army's experience has been in a regime as partially defined above and may not be indicative of results of impacts outside this regime.

9. If item is undamaged, choose progressively higher values of G and repeat the tests, shifting, changing, or adding energy dissipater stacks as necessary until a suitable configuration is established. If the item is damaged, modify the stacks as necessary and repeat at the same G level until successful.

ENERGY DISSIPATER CONFIGURATIONS FOR MULTIPLE FLEXIBLE BODIES

An item is considered to be composed of multiple flexible bodies when it consists of identifiable parts that are connected, but are able to move with respect to each other an amount that is much greater than the amount that these parts deform in themselves during impact. Therefore, in essence, the determination of whether an item is a single flexible body or is composed of multiple flexible bodies depends on the amount of coupling between the parts of an item. An item consisting of tightly coupled parts is considered to be a single flexible body; an item consisting of loosely coupled parts is considered to be composed of multiple flexible bodies. Thus a vehicle with its wheel-axle combinations, which in themselves are flexible, that are loosely coupled through the suspension system to a flexible frame is considered to be composed of multiple flexible bodies.

In this case, the procedure for the design of the energy dissipater configuration is essentially the same as for the single flexible body case. An additional consideration, however, is that each of the flexible bodies can have a different inherent strength and thus each could be accelerated at a different G level. This

permits some alternate methods of designing energy dissipater configurations which, in certain cases, can simplify the configurations.

If, for some reason, it is desired to decelerate all of the bodies at the same G level, the method described for a single flexible body is used for each body. Calculation of the weight supported by each stack must take into account the load transfer through the coupling devices which, in the scope of this paper, usually are springs and dampers. Then, if the calculation or estimate of the weight distribution was accurate, each of the flexible bodies would be decelerated at approximately the same G level and there would be very little relative motion between the flexible bodies.

Alternate designs are based on the non-uniform acceleration of the flexible bodies. Two possibilities arise here. Either the relative motion of the various bodies under different accelerations is small and thus the coupling devices (springs) are not bottomed, i. e., the bodies remain loosely coupled; or the relative motion is large and the springs bottom. Either possibility can be predicted and controlled by choice of the proper dissipater areas and thus the accelerations of each body. Dissipater designs which are based on nonuniform accelerations of the bodies usually require less thickness of energy dissipater than those based on uniform accelerations. This occurs because in the case of the uniformly accelerated bodies, each body must be accelerated at the amount that can be sustained by the weakest body. In the case of nonuniform accelerations, each body is accelerated according to its own inherent strength. Therefore, an item composed of multiple flexible bodies decelerated nonuniformly can be decelerated at a higher average or overall G level than when it is decelerated uniformly. Of course, the higher average G level case requires less dissipater thickness.

Specific steps for the design of energy dissipater configurations for an item composed of multiple flexible bodies which are not uniformly accelerated are as follows:

1. Choose an arbitrary low value of G for each flexible body (in many cases a low value of G for one body may be a very high value of G for another).
2. Based on the chosen values of G and the total weight of each body, calculate the total area of honeycomb required for each body.
3. Arbitrarily select a number of locations on each body where the individual

dissipater stacks are to be positioned. (In some cases, one or many of the bodies could be uniformly supported by the energy dissipater stacks.)

4. Calculate the weight supported by each energy dissipater stack.
5. Calculate the area of dissipater required for each stack.
6. Calculate the energy dissipater thickness required. This step can become quite complicated because of the different design accelerations of the bodies and the changing acceleration of each body as the load on the body exerted by the coupling devices varies. In this case, it is often simpler to consider the absorption of the kinetic and potential energy of the item by the paper honeycomb. Basically, the solution would consist of equating the energy absorbed by the paper honeycomb under each of the bodies (which is simply the honeycomb crushing force times the deceleration stroke) to the total energy change of the item. For any given item, some analysis, ingenuity, and knowledge of the characteristics of the coupling devices is required to determine the relative motion of the bodies and the proportion of the total energy that honeycomb under each body absorbs.
7. Inspect the item and the energy dissipater after impact using the criteria described for single flexible bodies.
8. If the item is damaged, modify the stacks as necessary, and repeat the tests at the same G level until successful. If the item is undamaged, choose progressively higher values of G and repeat the tests, modifying the stacks as necessary until a suitable configuration is established.

INSTRUMENTATION

In describing the detailed steps to be taken to determine an energy dissipater configuration, it will be noted that the term "inspect the item after impact" was used consistently and no mention was made of any data measurement. It has been found during numerous drop tests of Army vehicles that, except for special cases, the use of extensive instrumentation is not too helpful. An example of a special case is where a small item or a small component of a large item has had extensive shock testing in the laboratory, the maximum shock accelerations that can be applied to it are well known, and it is desired to insure

that these accelerations are not exceeded during impact. (The question then arises whether the dynamic forces were applied to the item in the laboratory in the same manner as they are applied in the cushioned drop test.) Another case is where the data is required to substantiate or help construct impact damage theory. Consider the points discussed below.

The mechanical properties of the energy dissipater are well defined. As long as the honeycomb crushes, the dynamic input forces to the item are known by calculation. Accelerometers placed on the dissipater stacks would merely substantiate the values of the mechanical properties of the dissipater.

An accelerometer mounted at a location on the structure of an item will certainly read the acceleration of the structure at that point. However, to the structural designer, the fact that point A on the structure was subject to "X" g's is meaningless. He will not know whether the structure is overstrength or understrength. He does not know what mass is associated with that acceleration so he will not even be able to calculate a force. The designer will want to know, however, if the structure failed or not.

The use of strain gages seems desirable. However the chances of a strain gage rosette being located at a point of maximum stress are debatable. A prodigious amount of gages could be mounted so that even though a gage was not located at a maximum stress point, the stress at the critical point could be extrapolated from plots of the readings at other points. There is still the problem of what stress the structure can withstand under the dynamic conditions encountered. The designer still cannot determine whether his structure is overstrength or understrength unless he knows whether the structure failed or not.

The measurement of vibrational frequencies has not provided any usable data either. Although much work has been carried out in the past years to determine theories that predict vibrational damage from shock pulses, the results of impact tests of many Army vehicles and equipment conducted at a number of test facilities have indicated no failure of any component due to vibration. All failures were discovered either through visual inspection of the item after impact or through deficiencies in the operation of the item after impact. As stated previously, most failures appeared to be caused by excessive aperiodic deflection of the damaged item. The other failures were caused by mutual collision of adjacent bodies

none of which were necessarily deflecting excessively.

Information that is quite useful is that obtained from high-speed motion pictures in the range of 1000 to 4000 frames per second. The relative motion between parts of the item during the impact may be observed and correlated with the conclusions obtained from the observation of the crushed dissipater stacks after impact. Sometimes, the nature of the failure of a component can be ascertained. Also, the maximum dynamic strain of each energy dissipater stack can be measured and compared with calculated values or with other stacks.

Until theories are developed that will allow the designer to determine from the data presented him (other than that the structure failed) whether the structure is overstrength, understrength, or satisfactory, the designer has no basis for determining whether or not he should redesign the structure. Also without adequate theories the data gathered from a successful test conducted at "X" g's cannot be used to determine if a test conducted at "X plus delta" g's will cause structural failure.

It is well known that there are a number of researchers studying this problem, and it appears to be only a matter of time before the sought after theories will be available.

REBOUND ENERGY

An important property of any energy dissipater is its plasticity, that is, its lack of resiliency. The resiliency of a practical energy dissipater must be low enough to preclude damage to an item occurring from secondary impacts of the protected surface and to prevent overturning which would result in impacts of unprotected surfaces. Quantitatively, resilience is defined as the ratio in percent of the rebound energy to absorbed energy. Figure 8 shows the resilience of standard Army paper honeycomb plotted versus maximum strain. For maximum strains from 40 to 70 percent, the resilience is constant at 8 percent. Above 70-percent maximum strain, the resilience rises rapidly and is double at approximately 85-percent maximum strain. Since most paper honeycomb configurations are designed to be strained to 70 percent or less, it will be assumed for the remainder of this discussion that resilience is a constant. A constant resilience implies that the amount of rebound energy provided by the paper honeycomb is determined by the amount of energy that the

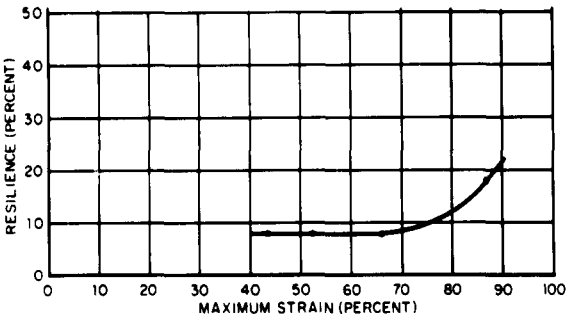


Fig. 8 - Resilience versus maximum strain for 80-0-1/2 paper honeycomb

item has at impact. Thus, if a given item protected by an energy dissipater impacts at a certain velocity, the rebound energy due to the energy dissipater will be a fixed amount regardless of the thickness or distribution of the energy dissipater. The effect of the rebound energy can be determined by equating the rebound energy to the change in potential energy of the item as it bounces upward.

Thus:

$$0.08 \left(\frac{1}{2} mV^2 + W_s \right) = Wh$$

where

h = height of rebound - feet

$$h = \frac{0.08V^2}{2G} \left(1 + \frac{1}{G} \right).$$

This equation shows that rebound height is primarily a function of impact velocity and is independent of item weight.

In the range of G 's that are encountered in typical air delivery operations, the calculated height of rebound due to the energy dissipater does not present much of a problem at impact velocities of 20 to 30 feet per second. However at impact velocities of 80 feet per second and up, which are encountered in special cases of air delivery operations, the calculated rebound heights are quite large, on the order of 10 feet, and would certainly present problems. Fortunately, some unpublished data from University of Texas tests show that the actual rebound height is never as high as calculated and that as the impact velocity increases, the ratio of actual rebound height to calculated rebound height decreases. In the range of impact velocities from 20 to 30 feet per second, the actual and

calculated rebound heights were not too different. However, at 80 feet per second, the actual height of rebound was as low as half of the calculated heights. The difference in heights can probably be attributed to the random use of the rebound energy such as rotating the item or imparting some horizontal motion to the item.

A second source of rebound energy is the item itself. It is quite obvious that while the energy dissipater is crushing, all parts of the structure being decelerated are deforming also. If the energy dissipater configuration has been designed satisfactorily, none of the parts will yield or fail. Thus all of the structural deformations will be elastic deformations, and therefore, efficient sources of rebound energy. No analytical methods are available to quantitatively determine the amount of energy absorbed elastically by the item and returned as rebound energy. A limited amount of data obtained from tests conducted at the University of Texas show that as the energy dissipater G level increases the item absorbs more and more of the impact energy and the energy dissipater less and less. A point is eventually reached where the force required to crush the very large area of energy dissipater is so great that the item deforms sufficiently, either elastically or plastically, to absorb all of the impact energy without crushing the paper honeycomb. Since the derivation of the thickness equation (Eq. (4)) is based on the assumption that the item being decelerated absorbs none of the impact energy, it can be seen that solution of this equation yields the maximum required thickness of energy dissipater. In practice, absorption of some of the impact energy through means other than the energy dissipater such as item flexibility, impact surface flexibility, etc., will cause less than the maximum required thickness of energy dissipater to be necessary. Figure 9 shows a typical decrease in the amount of actual crushing of an energy dissipater configuration compared to the calculated amount as the design G 's are increased.

PRACTICAL CONSIDERATIONS

The preceding discussions of the design of energy dissipater configurations have stressed heavily the need for drop tests closely duplicating air delivery impacts. In preparing for and conducting these drop tests, there are a number of practical considerations that should be taken into account for maximum effectiveness of the configuration. Some of these considerations derived through first-hand experience in conducting drop tests and which may be no more than rules of thumb will be described.

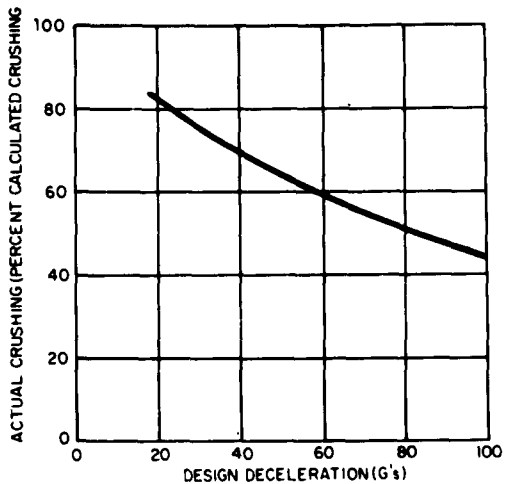


Fig. 9 - Typical variation in crushing of 80-0-1/2 paper honeycomb with design deceleration G's

An important consideration while initially determining the area and thickness of the energy dissipater stacks is the aspect ratio of the stacks. The aspect ratio of an energy dissipater stack is defined as the ratio of the thickness of the stack to the length of the shortest side. This ratio is an indication of the stability of the stack, that is, the ability of the stack to resist toppling when transverse motions are imparted to the stack to resist column failure under compressive loads. No experimental data on the effect of aspect ratio on stack stability is available; however, experience has shown that little difficulty is encountered when the aspect ratio is not much higher than a value of one. Of course, some variance from this value will be necessary in special situations. In many instances, dodges must be used to circumvent the equation mathematics which sometimes dictate the use of high-aspect ratio stacks. The most effective dodge is to use a paper honeycomb of lower average crushing stress which would allow a larger area (thus longer sides) of the dissipater without increasing the force level. At present, the Army is using only one type of paper honeycomb for obvious reasons of logistics and thus this method is not available to it. Another dodge is, if possible, to combine adjacent stacks to form one stack of a larger area. Other methods which are limited in number only by the ingenuity of the designer consist of changing the planform of the stack. The objective is to increase the length of the sides of the stack while retaining the same total area. This can be accomplished

by using more complex shapes for the stacks such as hollow squares and rectangles, or gluing a number of small spaced unstable stacks to load spreaders top and bottom to form a stable sandwich construction.

Another consideration to be taken into account is the use of build-up stacks. In the situation where the required thickness has been determined either analytically or experimentally and it is found that this thickness is less than the distance between the particular portion of the structure that it is to support and the platform, built-up stacks are used to fill the void. Their use can be seen in Fig. 7. When build-up stacks are used, they are usually of larger area than the stacks to be crushed and are of stable proportions. Thus their use helps reduce the problem of too high an aspect ratio.

The final consideration to be discussed is the use of load spreaders. Often, that part of a structure that is in contact with an energy dissipater stack has a smaller area than the area of the stack. This presents the problem that although the stack area has been carefully chosen to provide a given force level, the structure will crush only a portion of the dissipater area and the desired force and acceleration will not be achieved. The solution to this problem has been to insert a load spreader with an area equal to the stack area between the structure and the stack. The load spreaders are generally made of sheets of plywood of sufficient thickness to preclude failure in bending upon impact. Presently the thickness is determined by trial and error during the conduct of the impact tests to determine dissipater area and thickness. It is possible to analytically determine the required thickness of the load spreader by the use of standard static stress analysis methods. The solution would require the analysis of a flat plate uniformly supported on its bottom surface with its top surface loaded according to the nature of the contact surface of the structure. This static analysis of the dynamic loading will probably be conservative and will result in a load spreader thickness greater than physically necessary. It does, however, provide a good beginning for a small number of trial and error tests to determine the minimum load spreader thickness.

In special cases, load spreaders can be built up using beams and sheets to match complex contours of the structures. Even in these cases, wooden load spreaders are preferred for a number of reasons. One, wooden load spreaders used in this one time application are

expendable; two, they are easily fabricated even into complex shapes; three, they are easily glued to the paper honeycomb to form a good secure stack; and four, they locally deform easily and preclude stress concentrations due to irregularities of the structure.

SUMMARY

In summary, there are two basic analytical tools for the design of energy dissipater configurations for air delivery. These tools are the equations for the calculation of the required area and maximum thickness of the energy dissipater. The area equation is used to calculate the area required to produce a given G level. The thickness equation is used to calculate the maximum required thickness necessary for the energy dissipater to decelerate the item to zero velocity without the dissipater bottoming. The actual thickness crushed is usually less than calculated because some of the impact energy destined to be absorbed by the paper honeycomb is absorbed elsewhere. The application of the equations in practical problems is hindered by the lack of analytical techniques to determine the inherent strength of an item and therefore a means for choosing a value of G for insertion in the equations. Drop testing, wherein the impact velocity and energy dissipater configuration are duplicated, must be used in conjunction with the equations to achieve successful configurations. The actual procedure for the drop testing is varied depending on the complexity of the structure of the item. Instructions are included in the text for the drop testing of an item that may be considered to be:

- a single rigid body

- a single flexible body

- multiple flexible bodies.

The use of instrumentation in these tests is limited because the data obtained is not too helpful. There are no analyses for the data to be compared with, nor are there any analytical methods which would use the data to predict results under different test conditions. The tests are primarily a succession of go-no go tests until either a suitable energy dissipater configuration has been achieved or the item fails.

A consideration of the rebound energy that is available during the impact from a number of sources other than the paper honeycomb indicates that the actual thickness of honeycomb crushed is always less than calculated from the thickness equation and, therefore, allows a reduction in the necessary thickness of energy dissipater. The greater the G's exerted by the energy dissipater, the more energy is absorbed by the item, and the less the thickness of energy dissipater crushed.

Finally there are a number of practical considerations that must be used in performing the drop tests.

The aspect ratio of the dissipater stacks should not be much greater than a value of one for stack stability; build-up stacks are used to increase the stability of the stacks while filling the voids between item and platform; and load spreaders, usually fabricated from plywood, are used to insure that the entire area of the energy dissipater stacks is crushed.

BIBLIOGRAPHY

1. Charles H. Karnes, James W. Turnbow, E. A. Ripperger, and J. Neils Thompson, High-Velocity Impact Cushioning, Part V, Energy-Absorption Characteristics of Paper Honeycomb, Structural Mechanics Research Laboratory, The University of Texas, Austin, May 25, 1959.
2. Clarke Covington and Richard Shield, Fragility Studies, Part II, Cargo Truck, M37, 3/4-Ton, Structural Mechanics Research Laboratory, The University of Texas, Austin, April 12, 1960.
3. Richard Shield and Clarke Covington, Fragility Studies, Part V, Water Tank Trailer, XM107E2, 1-1/2-Ton, Structural Mechanics Research Laboratory, The University of Texas, Austin, May 25, 1960.
4. Fundamental Techniques for the Use of Paper Honeycomb and Foamed Plastics as an Energy Dissipator During Impact, Aerial Delivery Systems Office, Quartermaster Research & Engineering Command, Natick, Massachusetts, November 1958.
5. Maurice P. Gionfriddo, Notes on the Design of Energy Dissipater Configurations for Shock Attenuation, Air Delivery Equipment Division, Quartermaster Research and Engineering Command, Natick, Massachusetts, July 1961.

Mechanics Research Laboratory, The University of Texas, Austin, September 1960.

Fundamental Techniques for the Use of Paper Honeycomb and Foamed Plastics as an Energy Dissipator During Impact, Aerial Delivery Systems Office, Quartermaster Research & Engineering Command, Natick, Massachusetts, November 1958.

Notes on the Design of Energy Dissipater Configurations for Shock Attenuation, Air Delivery Equipment Division, Quartermaster Research and Engineering Command, Natick, Massachusetts, July 1961.

DISCUSSION

Mr. Opalinski (Woodland Container Co.): When you place your vehicle on the platten in preparation for an impact, how do you avoid having a force introduced into the wheels? Do you actually pyramid the vehicle up high enough to get the wheels off the bottom platten?

Mr. Gionfriddo: In the cases of the vehicles where there is honeycomb under the wheels, the wheels do take some of these impact forces and depending on the situation you can calculate an area of dissipater under the wheels so that they are decelerated at the same rate as the vehicle. Then the wheels and the vehicle move as a unit. Only if the vehicle is strong enough, can you permit the wheels and suspension to deform and deflect, thus imposing forces on the vehicle.

Mr. Opalinski: Whose honeycomb have you been using? Have you been using any specific manufacturer?

Mr. Gionfriddo: We buy it from one manufacturer now because it seems the others are not too interested in it and this is the Union Bag-Camp Paper Corp.

Mr. Welton (Northrop): Perhaps your slide wasn't clear. It seemed that for the truck you had a large cushion of honeycomb and then your little stacks. There wasn't any spreader for the large cushion.

Mr. Gionfriddo: I agree with you the slide probably wasn't clear. You may have noticed on those large cushions, there were four places that seemed to be cut out or crushed. These were the portions that we expected the wheels to crush. The other part of the honeycomb does not crush and is not included in the area calculation. It's only there to provide what we call a "drive-on" configuration. We lay a couple of 2x6's or 2x8's on the back end of the honeycomb. We can then drive the truck up this ramp and across the paper honeycomb layers until the wheels are positioned over the small areas that they are destined to crush.

So it's to give us ability to rig the vehicle without using fork lifts or cranes to lift the vehicle onto the paper honeycomb.

Mr. Olmstead (Hughes, Tucson): I am wondering, is this honeycomb material effected by high or low temperatures?

Mr. Gionfriddo: Prof. Thompson can probably tell you better than I. In general no. People at

the University of Texas have conducted tests at high and low temperature and found no large effects due to the temperature.

Mr. Gleck (Firestone): Do I gather correctly that displacements of the order of several feet are generally necessary to achieve decelerations which are within an acceptable range for most of the things you have studied? In other words, something of the order of a foot or a foot and a half I would guess, based on what you say, would not be sufficient displacement. I am thinking of the beer cans that were mentioned earlier.

Mr. Gionfriddo: With our vehicles, 6 to 9 or maybe even 12 inches is about the thicknesses that we do use. Those seem to be adequate. If you look at the thickness equation at about a 20 g input, whatever that means, and a 30 foot per second impact velocity, the thickness comes out to be about 12 inches. Because the vehicle itself absorbs some of the energy at impact, we find we don't always have to use the calculated thickness. We can get away with less.

Voice: Would a reusable device which has such capabilities be of interest to the military?

Mr. Gionfriddo: If it was cheap enough. But this brings in problems of how many times you reuse it and then you can cut the initial cost down by that factor, then it gets beyond my comprehension.

Mr. G. Spalding (Sperry Gyroscope): On the subject of reusables, we at Sperry have done some work with rubber honeycomb which has been very successful. Using the same general type of approach that you have here, we obtained the same type force-deflection curves with rubber. This has been tried, I believe, on some helicopter drop tests, not full-scale drops of the type you're talking about here.

Mr. Gionfriddo: That's very interesting. I would like to comment on a question to Prof. Thompson's paper. A gentleman back here asked about the peak stresses that occur on the stress-strain curves. Mr. Venetos, who is in the audience, from QM Food & Container Institute, Chicago, ran some tests some years ago on aluminum honeycomb in which he found need to get rid of that initial peak stress. What he did was to make a sawtooth pattern on the top of the honeycomb, he actually cut wedges out of the top of the honeycomb, so that the area

that was first in contact, that first gets crushed, is much less than the total area available. This serves to reduce the impact force. We haven't used this technique ourselves, but it is intriguing. Another trick Prof. Ripperger points out is to precrush the honeycomb. You can do this statically ahead of time by compressing it, maybe 10 percent of its original thickness. This also reduces the peak.

Mr. E. Schell (Aeronautical Systems Div., WPAFB): These methods are both very successful, but our experience has been that they can increase the thickness of the energy absorber

in configuration by a great deal. In order to use precrushing and get this initial peak down, the precrush has to approach the thickness of uncrushed material remaining.

Mr. Gionfriddo: I don't think that has been our experience. When you sawtooth the material, of course, the peak stress usually occurs somewhere between 5 and 10 percent strain. We usually just sawtooth the first 10 percent. This does mean an increase in height because you've removed material and some energy is not being absorbed.

* * *

PROBLEMS OF EFFICIENCY, DEFINITION AND MEASUREMENT OF SHOCK ASSOCIATED WITH PARACHUTED LOADS

G. W. H. Stevens
Royal Aircraft Establishment
Farnborough, England

The United Kingdom approach to the problems of aerial delivery is described, including the measurement and definition of shock levels, the methods of investigating shock sensitivity, the establishment of design requirements for shock absorbers and design techniques.

INTRODUCTION

The extraction of heavy loads from aircraft by parachute and landing them on a combined system of parachutes and shock absorbers has become an acceptable military technique. It is practised with limited scope and the stage has been reached when it is opportune to review the limits to which this type of operation can be extended and the efficiency with which it can be conducted. The answers to these problems will not be exact but a compromise. Whilst it is essential to deliver equipment efficiently and reliably in a serviceable condition by air drop it should be done with a reasonable economy of weight and cost and at the same time the design must be such that the preparation for the drop and the release for action can be carried out expeditiously as befits a military operation.

After making a summary statement of the present practice in the United Kingdom and the scientific and engineering problems that are revealed this paper discusses efficiency in relation to the present practice in order to suggest the lines along which research and development should proceed. The discussion is extended to the definition of the physical characteristic of shock, to the modes of behaviour of a shock absorber and to the physical quantities that are measured.

THE PRESENT PRACTICE IN AIR DROPPING

In the Royal Air Force supply dropping falls technically into two classes; small

equipment which can be bundled into packages up to one ton and larger equipment which is carried on a load bearing or stressed platform. Although the equipment is designed to withstand some mechanical shock it cannot necessarily withstand the forces of impact with the ground associated with the parachute descent. Thus additional shock absorption is used particularly with the platforms.

In the United Kingdom there is no heavy load in service where the extraction or suspension loads are taken through the equipment and all the current service loads are carried on a stressed platform. Whilst this stressed platform is primarily designed to transfer the weight of the load to the platform slings it is also essential for providing a stressed base for the main shock absorber and for providing full restraint factors in the aircraft up to the actual moment of release. Two sizes of platform have been designed; one known as the medium platform, for loads up to 12,000 pounds and the other, still under development, a larger platform for engineering equipment.

These stressed platforms are at present equipped with airbag shock absorbers and it is in connection with the development of this type of shock absorber that the Royal Aircraft Establishment has contributed.

SHOCK ABSORBING UNITS

There are three types of shock absorbing units in use. Airbags are used under the stressed

platform, shock struts are used between vehicles and the platform and honeycomb paper is used on smaller bundles. The latter material is further being considered for loads under development.

Airbags

The airbag is attractive as a shock absorbing unit because it can be stowed folded in a small space. In the present system 6 or 8 bags, according to the load, are carried in two long compartments under the platform 16 feet by 2 feet 5 inches wide by 4-1/2 inches deep (Fig. 1). The underside of the compartments is formed by 2 doors which are held locked closed whilst the load is in the aircraft and during extraction. As the load leaves the aircraft a timing unit is started which determines the time delay after load release before the latch of the doors is unlocked and this time should be just longer than that required to bring the load to its terminal velocity. The doors are spring-hinged to open against the residual air pressure and swing back to a position slightly above the horizontal to act as skidboards on landing. The bags fall down under their weight and are inflated through a tunnel valve to the small pressure of the residual air velocity.

The bags are made of rubberized cotton ply and are strengthened by grommets of steel wire. The original bags were barrel-shaped as it was claimed that this shape favoured the oblique impact but since this shape was expensive to make the present bags are cylindrical (Fig. 2). The valve at the base of the bag is nonreturn tunnel valve and at the top of the bag there is a bursting patch. On impact with the ground the tunnel valve closes and the pressure in the bag rises. The bursting patch fails under the pressure and allows the air to escape at the rate permitted by the orifice size.

There are a number of features of behaviour of these bags which will be discussed later.

Shock Struts

When a vehicle is mounted on a platform some protection of the vehicle suspension is required and this is achieved with a simple shock strut (Fig. 3). This consists of an oversize mandrel which is forced into a circular tube. The mandrel threads into a long collar over a wooden post which can be sawn approximately to length. The thread length

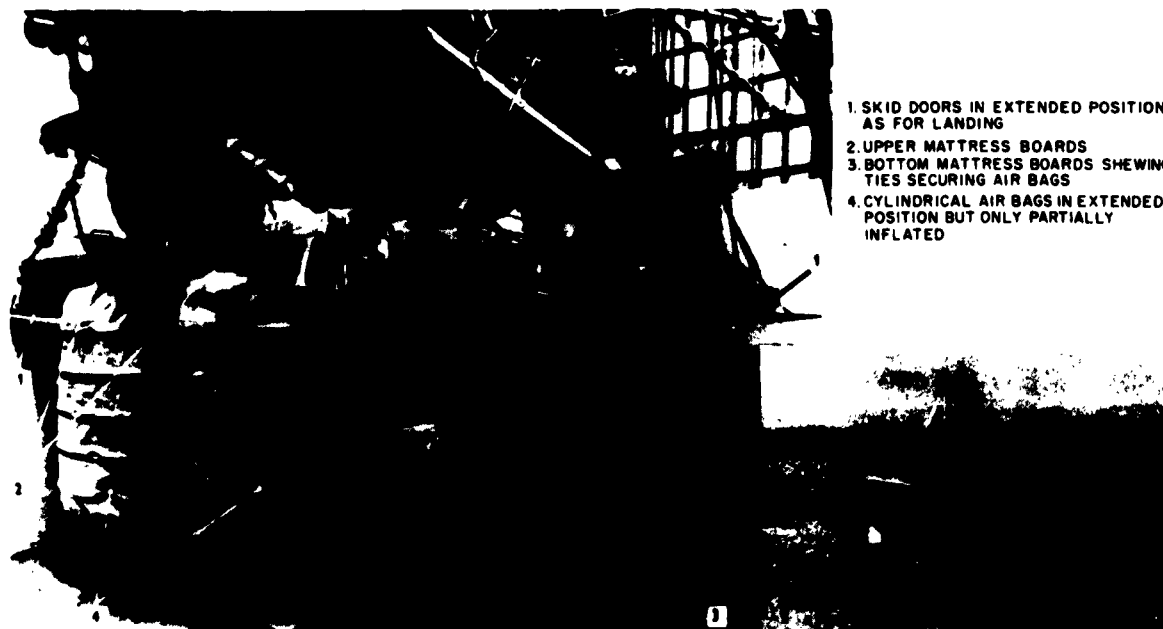


Fig. 1 - Illustration of rigged platform with airbags distended.
Small insert shows general view of platform and store just after touchdown with air bags partially compressed.

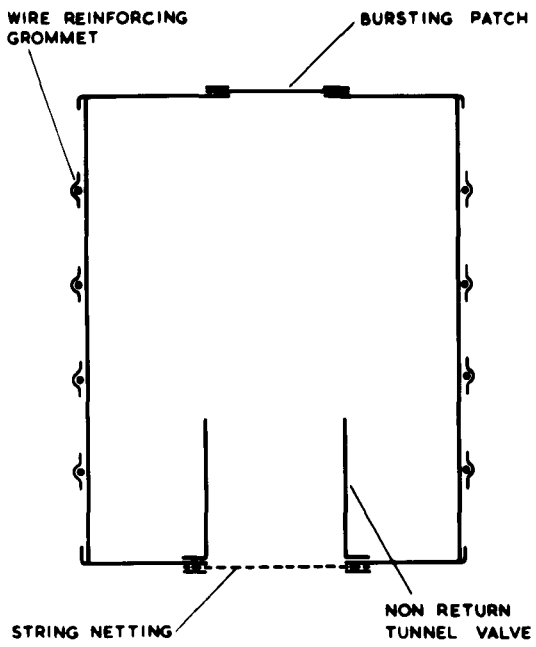


Fig. 2 - Schematic diagram of airbag

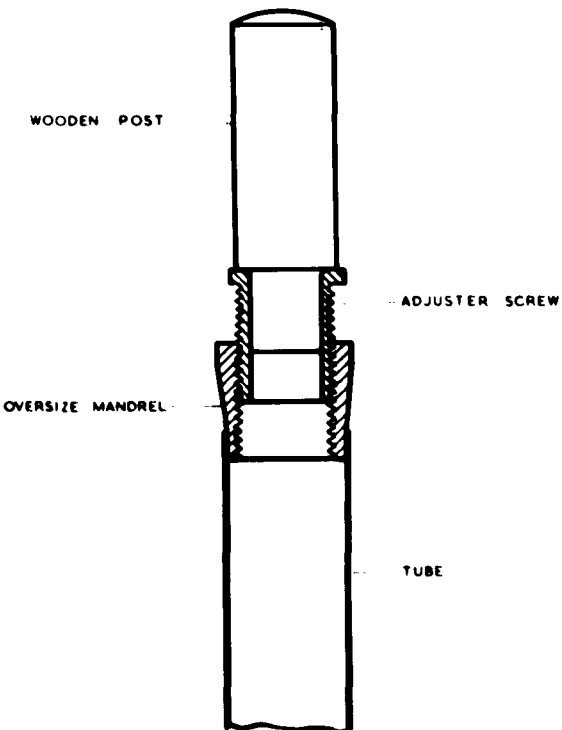


Fig. 3 - Schematic diagram of shock strut

of the collar is made sufficiently long to provide adjustment to secure the shock strut firmly between the vehicle and the platform. Shock struts are situated at the various positions as indicated in Fig. 4.

Honeycomb

Honeycomb in the form of paper, resinated or plain, or sheet metal is not greatly used in service although its application is being considered in connection with systems under development. The main use is under bundle and small supplies dropping platforms. It is used in much the same way as in the U.S.A.

SOME GENERAL OBSERVATIONS FROM PRESENT PRACTICE

In the present practice it is apparent that the shock absorber has been developed as an ancillary part of the equipment and the system was not examined initially as a whole.

Some theoretical assessments of efficiency in heavy dropping have been done in both the U.S.A. and in the U.K. which, by making certain assumptions relating weights of parachutes and shock absorbers to the forces which can be applied, have shown that there is an optimum velocity of descent for a given gross load for which the total additional weight of parachutes and shock absorber is a minimum. This occurs at a higher rate of descent as the gross load is increased.

Gross and Net Weight

The weight of some typical loads is analyzed in Table 1 and it is seen that the useful load is only about two thirds of the total weight dropped. The platform with its lashings constitutes about 25 percent of the gross load and the actual airbags only about 2.5 percent. The platform has been counted as part of the shock absorber system although it is essential in supporting the load on the parachutes. It is a significant constant term in the additional weight. In the analysis of Table 1, the shock absorbing system comes out heavier but if the platform is counted as a separate constant term then the parachutes outweigh the shock absorbers. The heavy test load does not require a stressed platform but the heavy fixings required have brought the weight of the shock absorber to about three quarters of the parachute weight.

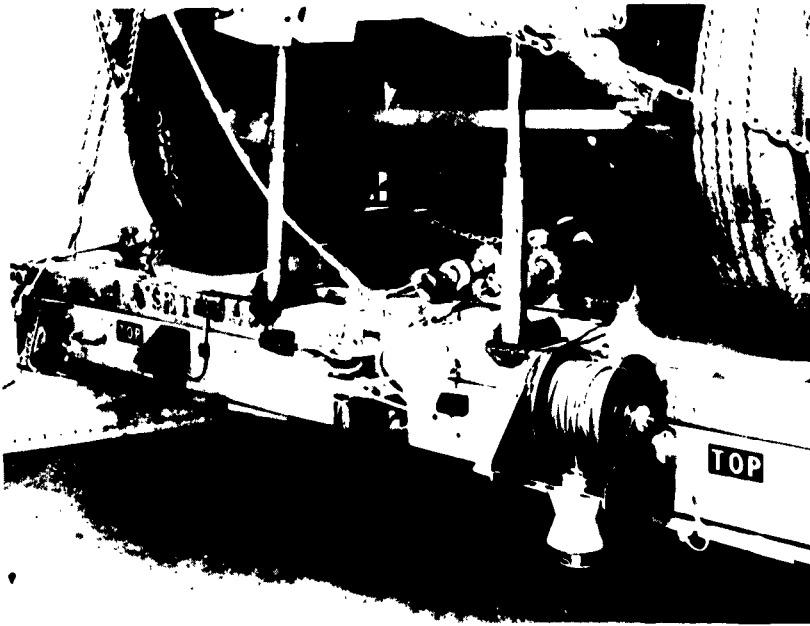


Fig. 4 - Illustration of use of shock struts

The present platform is an expensive piece of equipment if in fact it is expendable. However, it is argued that the large platforms are recoverable from where they are used to drop civil engineering and airfield construction equipment as soon as aircraft can land or road transport can operate.

Vehicle Suspension

A transport or a fighting vehicle is normally designed with a shock absorbing suspension and antivibration mountings for its power components appropriate to its normal use. The suspension may not be suitable for the decelerations of the air drop and thus the vehicle shock absorber, which is part of the wheel and axle suspension, has to be paralleled by some additional device such as a shock strut. The behaviour of a vehicle suspension during a landing is well illustrated in Fig. 5.

Drift in Landing

A feature of Fig. 5 is a large cross drift on landing and this draws attention to an

uncontrolled feature of parachute drops in the form of a random and substantial drift. The drift of a parachuted load in the wind is an overriding feature in air dropping and the direction of approach to the ground is often more than 45° from the vertical. This uncertainty of direction of approach is a severe handicap to the design and prevents a consistent high efficiency of performance being achieved.

The mean accelerations on the load when it is extracted from the aircraft and the parachutes are opened are substantially lower than during the landing. At present, any pair of slings have a factor of six and no protection is given to the shock struts during this stage. There is no evidence that they have actuated during descent for, if they had, they would probably fall out in the air.

DESIGN REQUIREMENTS FOR AN AIR DROP SHOCK ABSORBER

The shock in an air drop is primarily one of sudden impact but it rarely causes a simple compression of the shock absorbing structure. Because of drift airbags will be compressed

TABLE 1
Weight Analysis of Parachute Systems

Description of Load	Rover 1/4 Ton Truck & Trailer	Morris One Ton Truck (Unladen)	Morris One Ton Truck (Laden)	Heavy Test Load
Net Payload	5,280 lb	6,730 lb	8,970 lb	24,440 lb
Parachute System	Eight Type 42	Three Type 66	Four Type 66	Eight Type 66 +
Parachutes	700 lb	800 lb	1,065 lb	2,130 lb
Ancillary Mechanisms	60 lb	45 lb	60 lb	120 lb
Flying Wires	195 lb	60 lb	80 lb	740 lb
Slings	70 lb	70 lb	70 lb	180 lb
Sub-Total	1,025 lb	975 lb	1,275 lb	3,170 lb
Shock Absorber System				
Platform	1,460 lb	1,460 lb	1,460 lb	
Lashings & Fixings	100 lb	100 lb	100 lb	1,950 lb
Airbags with Mattress Boards	190 lb	290 lb	290 lb	535 lb
Sub-Total	1,750 lb	1,850 lb	1,850 lb	2,485 lb
Total Gross 1	8,055 lb	9,555 lb	12,095 lb	30,095 lb
Weight Efficiency	65.5%	67.5%	74%	81.2%

obliquely and quasi-solid materials like plastic foam or honeycomb will be subjected to both shear and compression. A shock strut will be subjected to both bending and compression, unless it is effectively freely pivoted, as the vehicle becomes slack on its lashings.

It must be remembered that for a given descent velocity it is not possible to specify independently the desired peak acceleration and the permissible stroke of the shock absorber. The equation $V^2 = 2as$ gives the relationship between velocity of descent, shock absorber stroke and mean acceleration. However, the equipment being landed will be sensitive to peak acceleration rather than the mean acceleration, and as a practical shock absorber will not have an efficiency of 100 percent and

will therefore produce accelerations in excess of the mean value, for a given shock absorber stroke higher accelerations than given by the above equation will be realized.

It has been suggested that, for overall efficiency, one should aim to have the same order of acceleration during parachute deployment and opening as during landing. This would present new design problems because the slings would be much heavier and the shock struts would require to be protected against operation during the first shock unless a design capable of operating a second time could be used. This is a field for more precise assessment which has not been attempted so far. Development is, however, tending towards slightly higher accelerations in the extraction stage.

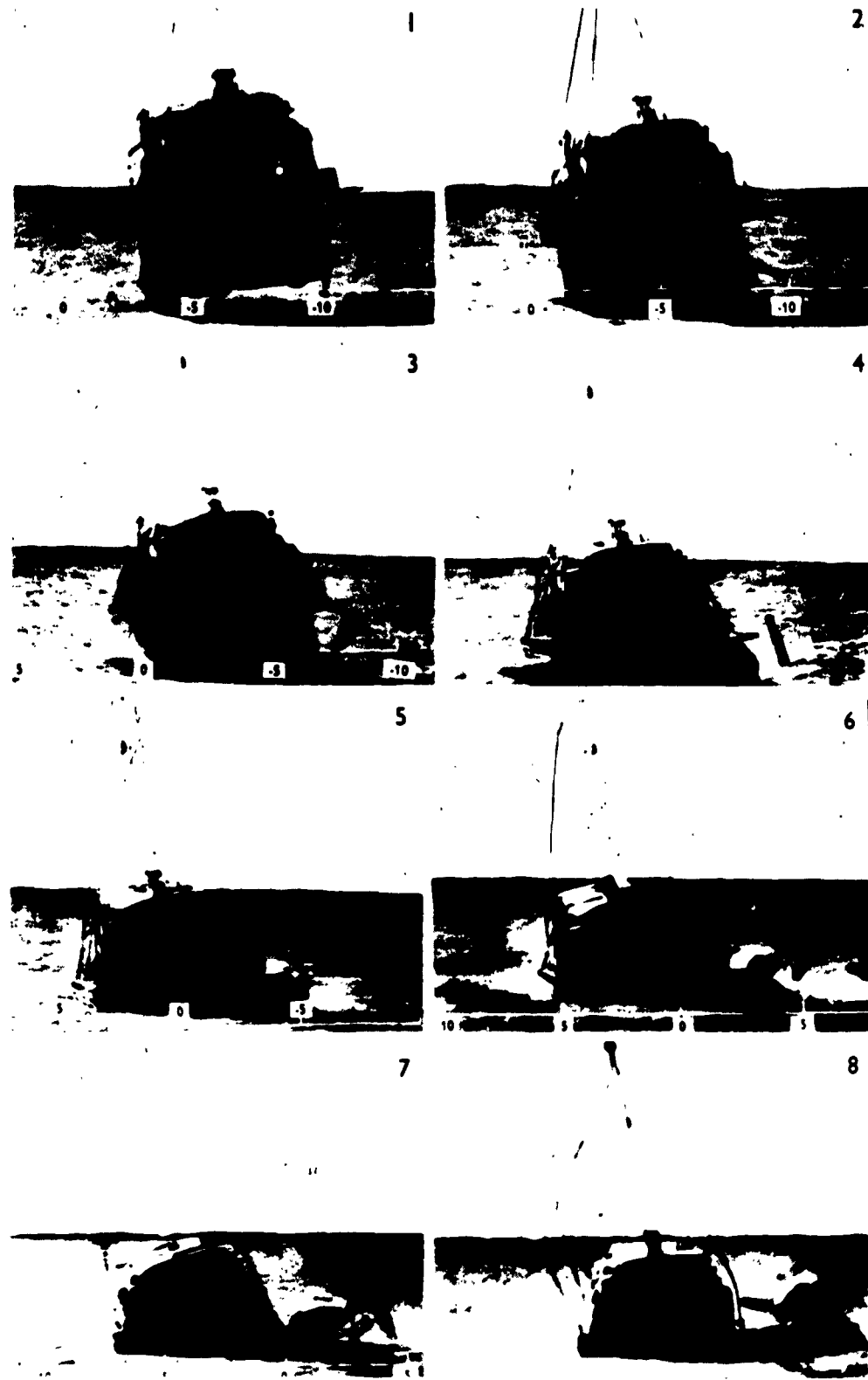


Fig. 5 - Sequences of an oblique landing

A shock absorber for an air drop can be a "once-only" device destroyed in the process of inhibiting the shock but, it must not be resilient and cause a bounce. Although at present the object is to produce a shock absorber which is wholly dissipative some, such as the foam plastic and, under certain conditions the airbag, are somewhat springy. In the present state of the art, the resultant lateral and pitching stability cannot be controlled and the consequences may be disastrous. There is a technique of air drop, however, under development in which a controlled bounce would be an advantage.

The shock strut is a very good nonresilient dissipative shock absorber. With careful design a high initial peak acceleration can be avoided. This device then has almost ideal characteristics because it exerts a constant force. However, there is an initial high rate of change of acceleration and therefore the proportion of the kinetic energy of descent which goes into the equipment as strain energy is large.

In view of the different characteristics of performance of airbags and shock struts it is unsound design to mix them on the same load.

THE DEFINITION OF SHOCK IN AN AIR DROP

In order to understand the mechanism in shock absorption or shock prevention for an air drop it is necessary to define what is understood by shock and impact. Moreover, it is necessary to introduce the ideas of primary and secondary shock and primary and secondary impact.

In this work shock is defined as any transitory force-strain disturbance to which a mechanical system is subjected. This is probably the generally understood meaning. Impact is a particular form of disturbance to a system which is initiated as a finite change in particle velocity. Impact leads to compression strain and is complementary to a snatch which leads to extension strain.

The propagation of strain from the impact takes place at a high speed but the time taken for the strain disturbance to pass through the system is not always negligible in comparison with the total transient time. In short transients it is necessary to consider the effects of strain propagation.

In a practical shock absorber the definition of the types of impact are of first importance. Primary impact is the contact between the main shock absorber and the ground and the

primary shock which the main structure and the component equipment receives is the stress-strain disturbance directly propagated by this primary impact. Owing to the imperfections of the shock absorbing device the equipment can receive further impacts before it comes to rest. The most serious subsequent impact is that which can occur when the equipment does not approach the ground normally, or when it tilts during the compression of the main shock absorber, with the result that a secondary impact of significant magnitude is made on a side or a corner of the equipment. The stress-strain propagation from this impact is superimposed on high stresses resulting from the main action of the shock absorber and thus an impact velocity which would not cause damage in a free drop, can in these circumstances seriously damage the equipment.

Secondary shock arises on a component of equipment as a result of the mechanical interaction of the numerous components which make the complete item. To illustrate, most pieces of equipment are made up of a complicated distribution of stiffness and inertia and parts can be recognized as locally resonant systems. If the equipment is properly designed most components will be stressed much to the same degree in relation to their ultimate strength and, when stressed to the limit, the equipment has no one mode of failure. In yielding to the stress the behaviour of one component will be influenced by the others. Thus two components whose natural frequencies are nearly the same are excited by the primary impact. They vibrate and, due to the mechanical coupling between them, transfer substantial energy from one to the other. The capacities of the two components for energy may be very different and the one unit is broken by secondary shock from the other of greater energy content.

MEASUREMENT OF SHOCK LEVEL

Because of the complex mechanical equivalence of equipment in terms of resonant, dissipative or yielding units it is difficult to define the detail quantity to measure to represent the magnitude of a shock. The experimental technique and procedure for air drop cushioning should basically follow the principle used in the investigation of packaging and the points made in this paper by Mr. Schuler and in particular the work of Mr. Orba at Messrs Wilmot Mansour & Co. Ltd., Southampton, England broadly apply.

Assessments of the shock level have been made in terms of the peak acceleration in an

acceleration time curve. These can be indefinite because when measurements are made at more than one point on a piece of equipment significant differences are observed. The difference can be exaggerated by the characteristic response of measuring devices, particularly peak accelerometers.

Most acceleration records show a high frequency content with large amplitude of acceleration. In our laboratory testing we have recorded accelerations of over 100 g in circumstances where such magnitudes would not be expected. However, when the structure of a test load is studied its local resonances are apparent and these large accelerations are associated with the internal energy. Although it is possible to record large vibratory accelerations due to poor instruments or instrument attachment, some are a real part of the shock. Thus it is useless to do a test on a live load, that is the actual load which is to be parachuted, to measure the basic characteristics of the shock absorber.

We are only just entering upon the problems of assessing shock absorbers operating at higher acceleration levels and we have appreciated the need to have test loads with a high level of internal damping. It is desirable to use wood, plastics and similar imperfectly elastic material in the construction wherever possible.

In testing airbags in the vertical drop we have recently experienced difficulties with the vibration of the test load and the guides as we have increased the loading but much of the investigation was done on small bags and we have only experienced maximum accelerations less than 20 g. The test rig is illustrated in Fig. 6 and the recording equipment is very elementary. It consists of a board carrying a strip of paper which is attached to the dropped load and passes a vibrating pencil held on the fixed frame pressing lightly against the board. This produces a wavy line from which a time-distance record is obtained. Accelerations are obtained by the following method. The distance between each period of the trace is measured and converted to a velocity. The square of this velocity is plotted against distance travelled for each position read. A curve is drawn through the points and the tangent to this curve is acceleration (Fig. 7).

In assessing shock struts and honeycomb paper, measurements have so far been restricted to boundary performance relating kinetic energy dissipated to the distance the shock absorber is compressed. (Figs. 8 and 9)

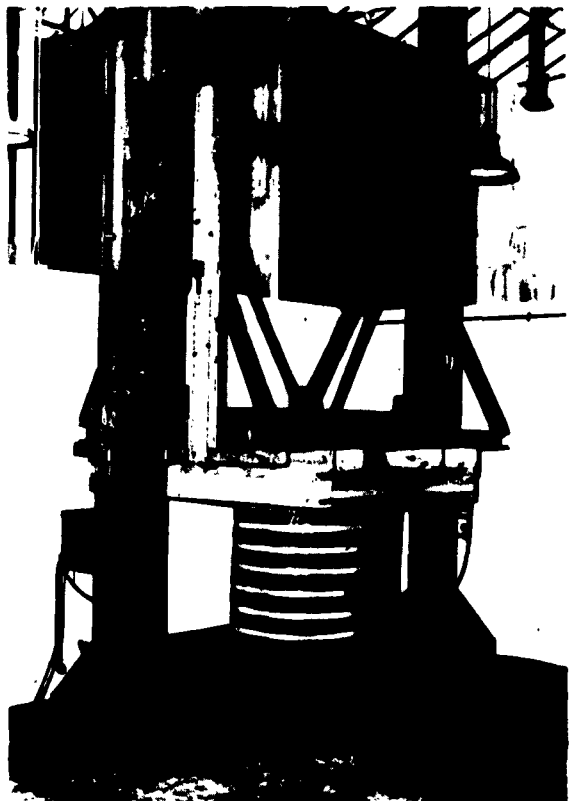


Fig. 6 - Rig for testing airbags

Studies with acceleration and pressure transducers have only recently been attempted and we are not in a position to report.

DEFINITION OF EFFICIENCY

In our early work at the Royal Aircraft Establishment peak acceleration was used as the measure of the effectiveness of a shock absorber. However, peak acceleration does not completely specify an inefficient shock absorber because certain boundary requirements of efficiency may not be satisfied. There are three things that can happen with a practical device

- (a) The load can be tilted
- (b) The final velocity of impact can be substantial
- (c) The load can bounce.

All these effects are known to occur with airbags.

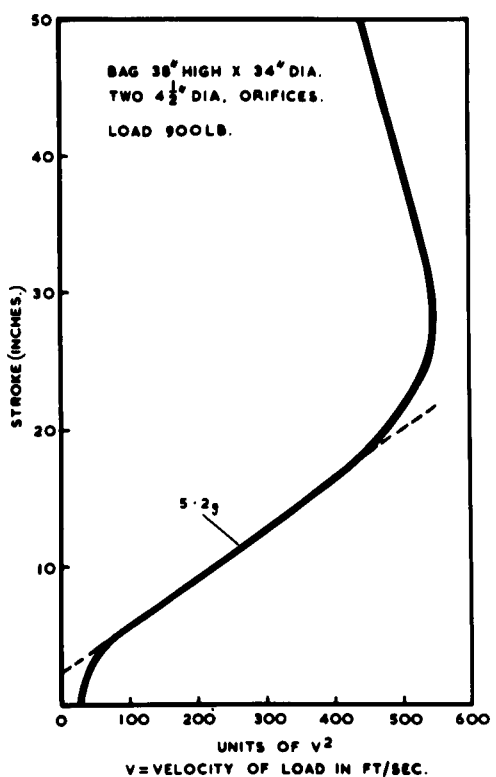


Fig. 7 - Typical test on cylindrical airbag

In our earlier work on airbags an attempt was made to define the efficiency as the ratio of the peak acceleration to the average acceleration as defined by the relation $v^2 = 2as$ where v is the initial impact velocity and s is the stroke. Whilst this did serve as a useful start in comparing airbags it did not help very much when the terminal conditions were not satisfied and arbitrary conditions of terminal stroke and bounce had to be imposed. It was possible to have a bag whose acceleration did not exceed the mean but which could not be 100-percent efficient because it still allowed the load to strike at a finite velocity.

Efficiency is also defined in terms of energy. In packaging work Mr. Orba records efficiency as the ratio of energy absorbed by the cushion up to a given stress level to the energy absorbed in compressing an ideal cushion to the same degree, working at the same constant stress level. This definition is very similar to the one made in terms of acceleration but it is not certain that the internal energy in the stressed equipment can be ignored.

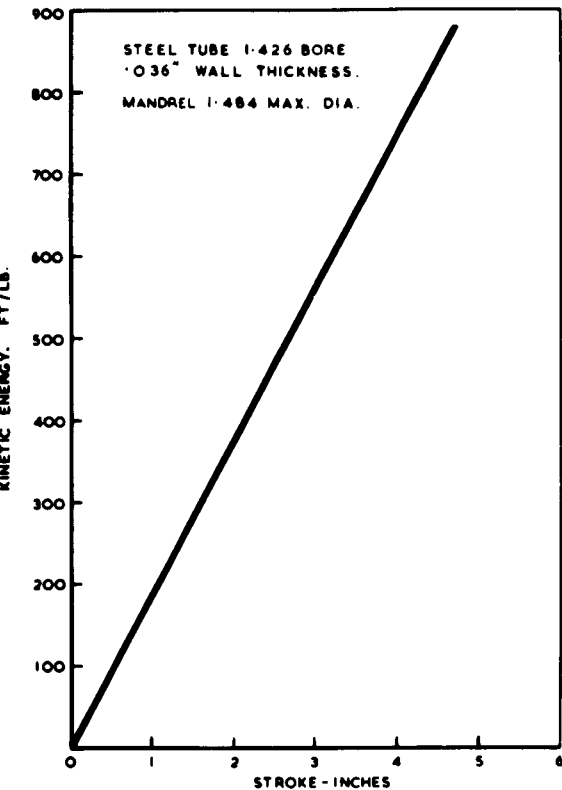


Fig. 8 - Dynamic performance of a shock strut

Efficiency measurements should take account of the partition and dissipation of energy during a decelerated landing and little is known about this at the moment.

SPECIFIC STEPS TO IMPROVE EFFICIENCY

Whilst the efficiency can be changed by using different materials there are specific principles that should be followed throughout. Firstly a technique of air drop which has little randomness of performance should be aimed at. This is one reason why interest has been taken in a skid-on technique at low level at a forward speed rather larger than any likely wind speed. There are, however, ways of making the standard drop more consistent. One is to try to work with a shorter stroke of shock absorber and higher accelerations; the other is to try to align the load with the wind drift. We have shortened our airbags but have not made any serious approach to the alignment problems although schemes have been put forward over the years.

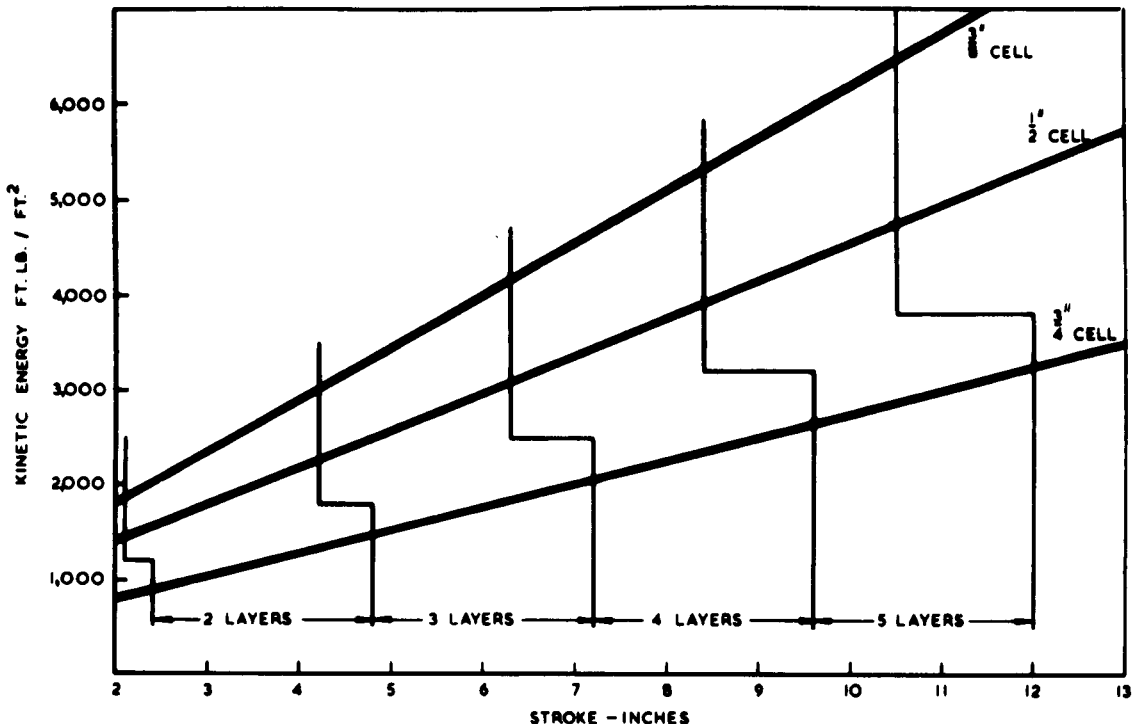


Fig. 9 - Dynamic tests on layers of dufaylite paper

The second step to improve the efficiency is to match the movements of the various stages and components in the system better than is done at present. To do this it is necessary to express the dropping system as a simpler mechanical system which will be illustrated by the case of a vehicle on a stressed platform.

THE SIMPLIFIED MECHANICAL SYSTEM

The stressed platform type of air drop system can be expressed as a 3-mass unit of which the first is the stressed platform. The second is the vehicle less a particular component which will constitute the third. For the third unit there are many components from which to choose and the engine is probably a good example since its mounting for normal operation is designed to prevent the transmission of engine vibration. The shock absorbing devices are represented by spring damping systems as illustrated in Fig. 10.

Although a so-called simplified system it is still complicated to analyse mathematically

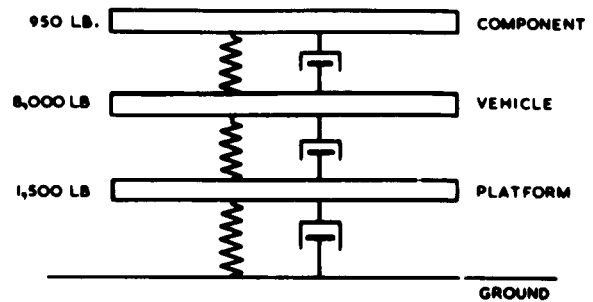


Fig. 10 - Parachute system - simplified mechanical equivalent for analysis

and, in fact, can only usefully be done numerically. However, to anyone who has to analyse the system it is well to note first the boundary conditions which cannot be varied. All the masses are substantially fixed and in the second and third stages on the vehicle the maximum displacement is fixed. Stiffnesses and dissipative forces can be adjusted. The

dissipative forces should be as high as can conveniently be made and the stiffness should be adjusted to the available travel.

The three masses are, of course, yielding structures for which a maximum permissible stress level has to be determined from suitable tests. The stress level in the weakest component of the vehicle should be taken as the starting point and within this stress level and within the permissible strokes the other stages should be designed.

THE PRESENT STATE OF STRESS MATCHING

Little is known about the present state of stress matching but it is not thought to be good for many vehicular loads. Accepted packaging practice is not being followed. On electronic equipment it is usual to short out an antivibration mounting with solid stops before packaging, but this is not done with the vibration mounting of an engine of a vehicle. The low stiffness of an antivibration mounting can allow the engine to strike the limit stop with a substantial velocity. That this secondary impact and shock has not caused more failures is due to the gentle way in which the loads have so far been treated.

The importance of this point is illustrated by the disparity of the order of peak accelerations reported in packaging work on radar components and on air dropped equipment. In the former work general experience shows that accelerations ranging from 25 g to 75 g can be experienced without a failure of the structure. It has been stated that equipment which failed to withstand 25 g invariably revealed a design weakness. 50 g was the more usual limit for well-designed equipment and 75 g for robust equipment. These accelerations are of a different order from those experienced in parachuting equipment where the mean accelerations on the equipment are in the range from 10 to 20 g. Where serious damage in parachuting has been observed it can usually be attributed to secondary impact and shock. If these mean accelerations are increased it will be necessary to stiffen up the mountings. The solution in this case can be a shock strut on the principle of the leather eyelet. This is operationally preferable to a solid stop as it would become free by the action of the shock and the engine could be started and run normally.

The shock strut is, of course, mainly a dissipative element and it is significant that so much energy can be absorbed without having to

stiffen the mountings with springs. To mix airbags and shock struts in a system is somewhat inconsistent because all conditions of performance cannot be satisfied with an airbag which neither bounces nor has a residual strike velocity. A residual strike means that there is a secondary impact on a highly decelerated stressed object and a bounce means that units which were protected by shock struts are now unprotected against a secondary impact.

It should be recorded that honeycomb and plastic foams have a high volumetric air content and behave dynamically partly as airbags and can bounce.

A design study of a complete shock strut system which can be made to be efficient over a wide variation of direction of action is worth while and if a successful design can be produced such a system is worth making and testing.

PROPOSALS FOR EXPERIMENTAL STUDY

Experimental study appears to be required along 3 distinct lines. The first is to determine the stress level to which the equipment can be safely subjected. The second is the characteristics, and the scale of action, of the energy dissipating or shock absorbing devices and the third is how and where to deploy the latter devices on the equipment. The determination of the stress level is part of the fragility problem.

In order to understand what is happening better it is important to attack the problem on at least 2 different lines so that some comparison can be made. It is suggested that this principle could be followed in studying the stress levels by a drop technique and by a frequency survey. However these are quite recent thoughts on experimentation and have not been tried as yet.

Frequency surveys for resonances, and in particular for lightly damped ones, is already an accepted practice. In these surveys it is particularly desirable to look for frequencies which are close together and to locate their sources. It is further necessary to look for the evidence of mechanical coupling. If the energy capacity of one unit is much larger than that of the other this can be serious for the smaller one can be damaged by secondary shock from the excited larger unit. Troubles of this kind can sometimes be cured by quite small adjustments in weight and stiffness of the component units.

Whilst it is agreed that instrumented retardations of equipment are of limited value some value may be obtained from an instrumented release. When a heavy body is released and allowed to fall it has been subjected to, what is called in Fourier analysis, a unit disturbance and the response should be the unit function. The measuring devices would require to be more sensitive than in an investigation of impact but there can be almost complete freedom from extraneous disturbance during the short time of free drop.

The free drop would be instrumented with strain gauges and perhaps accelerometers for cross checking but it is necessary to have the instruments in the correct positions. These are best selected after making a frequency survey which should give a good lead to the profitable positions.

One feature about this approach is that, although the amplitude of response in local strains will be small and difficult to detect, those detected will be in the regions where attention should be focused. On the basis of limiting accelerations which equipment withstands strains about 4 percent of the ultimate are expected.

One criticism of this experiment is that it is necessary to make some assumptions about the proportionality of strain with load in order to apply the results. It is unlikely to be proportional but the deviation is likely to be an increase of stiffness with load. If this is so the strain amplitude for the unit disturbance may

be 5 percent or more. Another criticism is that in the motion of the structure, in particular the platform, there is a marked difference between holding the load from slings at the side and applying a pressure uniformly to the under surface.

CONCLUSIONS

To obtain greater efficiency of air drop systems it appears from the points made in this paper that it is necessary to prepare the equipment suitably. This raises an important logistic question because it is uneconomical to have special equipment. However, it should be acceptable to have a standard of preparation, which can be applied to equipment at an earlier stage before it arrives at an air despatch unit where loads are finally rigged to a platform.

There is further research to be undertaken. It appears necessary besides looking at the requirements for shock absorption in critical areas e.g., under the stressed platform, between the platform and the equipment and within the equipment itself, to look at the matching in an integrated system.

It is important to design a good primary shock absorber which does not tilt the main load to cause a secondary impact and which does not cause the load to bounce uncontrollably. The state of the art at present is such that success is more likely to be achieved quickly with heavily damped devices such as shock struts.

* * *

THE RESPONSE OF YIELDING STRUCTURES TO SHOCK LOADING

E. A. Ripperger and W. T. Fowler
Structural Mechanics Research Laboratory
The University of Texas
Austin, Texas

A theoretical and experimental study of the response of a tip-loaded, mild, steel cantilever beam to acceleration pulses applied at the root is described. The relationship between permanent deformation of the beam, and the characteristic features of the acceleration pulse is described. It is found that within certain prescribed limits, the peak acceleration, the pulse duration, and the natural period of the beam are all equally effective in producing permanent deformation. Pulse shape is also shown to be a significant factor.

INTRODUCTION

It has been observed during the course of many drops of vehicles under controlled laboratory conditions that the damage to these vehicles produced by impact consisted almost always of a permanent deformation of some part or parts of the vehicle [1, 2, 3]. Only rarely did a part actually break. When breakage did occur there was a strong probability that it was produced by fatigue rather than the first impulsive load, since the vehicles were dropped many times. These observations suggest that those characteristics of an impulsive load and of a vehicle which tend to produce permanent deflections should be determined if the design of cushioning systems is to be placed on a completely rational basis.

Since a vehicle is, in general, much too complex a structure for direct analysis of its dynamic response, analytical and experimental studies intended to shed a little light on the probable response of vehicles to various types of input acceleration pulses are usually made on simple single-degree-of-freedom systems. The study reported here follows that pattern. As a first step, linear elastic systems were studied analytically [4, 5]. It was hoped that some useful correlation might be found between the parameters associated with the maximum deflection of a linear system, and those which produce maximum permanent deformation of a nonlinear system. These studies were followed

by an experimental program in which simple systems with yielding springs were subjected to impulsive loading, after which the permanent deformation was measured [6]. Although it proved to be very difficult to control some of the interesting parameters, the results obtained were sufficient to show that little or no correlation existed between experimental and analytical results. As a consequence, studies of linear elastic systems were discontinued. Since that time attention has been concentrated on simple systems with nonlinear yielding springs.

The response of such systems has also been the subject of a number of previous investigations in other laboratories. Mentel [7] has reported the results of a study of the response of a mild steel cantilever beam subjected to a transverse acceleration at the root. Good agreement was found between theoretical and experimental results, but no attention was given to the relationship between acceleration pulse parameters and total deformation.

A considerable amount of excellent work has also been done by Barton and his associates [8, 9, 10] on the response of nonlinear systems. Their work was stimulated by an interest in exploiting nonlinear devices as shock isolators. Some of their results suggest that a correlation should exist between elastic response and the permanent deformation produced in a yielding system.

In the present investigation the following specific questions are considered.

1. What are the significant pulse parameters insofar as the permanent deformation of the system is concerned?
2. How do computed deformations compare with experimental results?

FORMULATION OF THE PROBLEM

Assumptions

Consider a system consisting of a cantilever beam clamped at one end with a concentrated mass at its tip (Fig. 1).

Assume the following:

1. The mass of the beam is negligible in comparison to the tip mass. Thus the beam and mass can be regarded as a single-degree-of-freedom system.
2. The relative displacement, z , is small with respect to the length, l , of the beam, and consequently, rotational effects are negligible.
3. Strain rate effects are negligible, i.e., the material has a unique stress-strain relation.
4. An external acceleration, $\ddot{x} = a(t)$, is applied to the clamped end of the beam.
5. The force-deflection curve is the static load-deflection curve for a mild steel cantilever beam, and is approximated for purposes of computation by three straight lines as shown in Fig. 2.

6. When unloading occurs, the force-deflection curve is a straight line parallel to the first section of the loading curve (Fig. 2).

The Equation of Motion

As the clamped end undergoes an acceleration, $a(t)$, differential movement takes place between the clamped end and the tip. This sets up a restoring force, $F(z)$, where z is the relative displacement between the tip and the root of the beam. This function is defined by the straight-line approximation of the static load-deformation curve as shown in Fig. 2.

From Fig. 1, it is seen that $z = y - x$, and hence $\dot{y} = \dot{z} + \dot{x}$.

By definition, $\ddot{x} = a(t)$.

Thus

$$\ddot{y} = \ddot{z} + a(t). \quad (1)$$

Since the only unbalanced force on the mass is the restoring force due to the bending of the beam, $m\ddot{y} = F(z)$. Substituting for y from Eq. (1), and solving for \ddot{z} , this equation becomes

$$\ddot{z} = \frac{F(z)}{m} - a(t). \quad (2)$$

This is the differential equation of motion for the system. Although this equation is relatively simple, it involves all of the characterizing parameters of the pulse and of the beam.

A dimensional analysis will help determine the most effective procedure for studying the effects of these parameters.

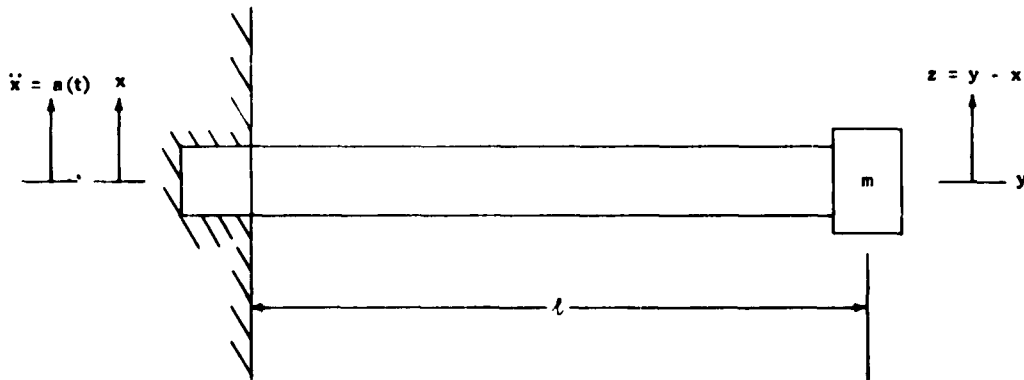


Fig. 1 - Cantilever beam with a tip mass

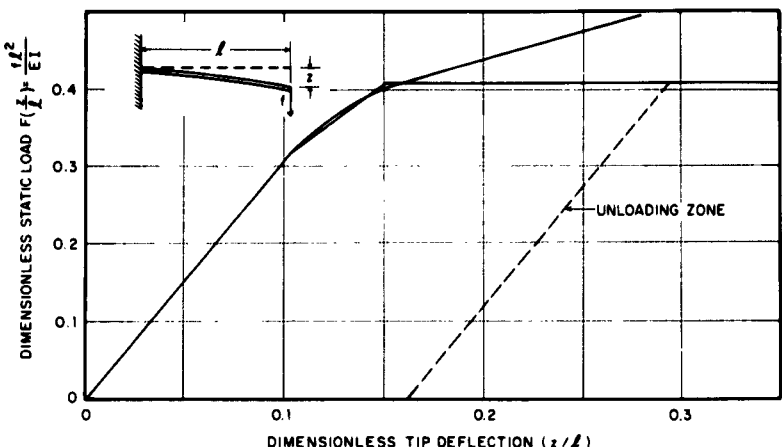


Fig. 2 - Dimensionless static load $F(z/l)^2 / EI$ versus dimensionless tip deflection z/l for a mild steel cantilever and corresponding straight line approximation

Dimensional Analysis

The first step in making a dimensional analysis is the listing of the parameters which are believed to be significant (Table 1).

TABLE 1
Significant Parameters

Quantity	Definition	Units
Acceleration Pulse Parameters		
A	Maximum Pulse Amplitude	L/T^2
T_d	Pulse Duration	T
t_r	Rise Time (used with triangular pulses)	T
ΔV	Area under the $a(t)$ vs t curve	L/T
Material Properties		
δ_y	Displacement at which elastic limit is reached	L
ℓ	Length of beam	L
τ	Natural period of beam based on an elastic system	T
F_y	Force at elastic limit	F
Interrelated Parameter		
S	Permanent Deformation	L

It will be noted that a number of parameters which could conceivably enter the problem have been omitted from this list. The most conspicuous among those parameters omitted is m , the tip mass. Note that the analysis included ℓ , τ , F_y , and δ_y , and the mass m is defined by these factors. To include m would be redundant. The others omitted are believed to be insignificant. If this is not the case, the functional relationship obtained is not complete. This may, in turn, lead to an erroneous interpretation of results. Comparisons of experimental results with predicted functional relationship among the variables should provide an indication of the completeness of the analysis.

In the tabulation there are 9 quantities expressed by three fundamental units (F, L, and T). According to the Buckingham Pi Theorem [11], six linearly independent dimensionless groups can be formed using these 9 quantities. These groups can be selected somewhat arbitrarily, subject only to the requirement that they be linearly independent and that each quantity must appear at least once in the 7 groups. The groups selected for this analysis are as follows:

δ/δ_y This is the nondimensional permanent deflection of the tip of the cantilever.

t_r/T_d This group represents the nondimensional rise time of the pulse.

AT_d^2/ℓ This group represents the nondimensional displacement of the root of the cantilever in a time equivalent to the natural period of the system.

$\Delta V/AT_d$ This group is a pulse shape factor, It is the ratio of the actual area under the pulse and the area of a rectangular pulse with the same peak value and duration.

T_d/τ This group represents the nondimensional pulse duration.

δ_y/ℓ This group represents the nondimensional yield deflection.

A functional relationship between the deflection and the other parameters may now be written as follows:

$$\delta/\delta_y = G \left(\frac{AT_d^2}{\ell} \cdot \frac{t_r}{T_d} \cdot \frac{\Delta V}{AT_d} \cdot \frac{T_d}{\tau} \cdot \frac{\delta_y}{\ell} \right). \quad (3)$$

Rise Time

In this study, the material and beam properties δ_y , F_y , and ℓ will not be varied, hence the dimensionless group δ_y/ℓ will be constant. For the rise time study only, it is convenient to use a dimensionless grouping not present in those originally chosen. This grouping, t_r/τ , forms a linearly dependent set with t_r/T_d and T_d/τ . Any two members of the set are suitable for inclusion as dimensionless variables, but some redundancy would result from including all three groups. Choosing t_r/τ and T_d/τ to be included for the rise time study, Eq. (3) can be written as

$$\delta/\delta_y = H \left(\frac{AT_d^2}{\ell} \cdot \frac{t_r}{\tau} \cdot \frac{\Delta V}{AT_d} \cdot \frac{T_d}{\tau} \right). \quad (4)$$

It is now apparent that if the effect of pulse rise time is to be determined, all other parameters can be held constant and Eq. (4) becomes

$$\delta/\delta_y = J \left(\frac{t_r}{\tau} \right). \quad (5)$$

Here, it must be noted that to study rise time, an acceleration pulse must be used in which rise time is uniquely defined.

Pulse Amplitude

To study the effect of pulse amplitude, first assume a given pulse shape. Also, as above in the rise time study, keep the beam properties constant. Thus the dimensionless groupings t_r/T_d , δ_y/ℓ , and $\Delta V/AT_d$ will remain constant. The ratio $\Delta V/AT_d$ will remain constant despite changes in A because, for a specified pulse shape, $\Delta V/AT_d = k AT_d/AT_d = k$ where k is a constant, $k \leq 1$. Thus, for studying pulse amplitude of a given pulse shape, Eq. (3) may be written as

$$\delta/\delta_y = k \left(\frac{AT_d^2}{\ell} \right) \quad (6)$$

Natural Period of the System

It is seen from Eq. (3) that only the term T_d/τ contains the natural period τ . If the effect of changing τ is to be studied, this parameter must be varied. However, if all other parameters in Eq. (3) are to be kept constant, then T_d/τ must be varied by varying only τ . Otherwise the effect obtained will be that of varying AT_d^2/ℓ and T_d/τ together instead of T_d/τ alone.

Pulse Duration

For a given pulse shape, Eq. (3) can be written

$$\delta/\delta_y = P \left(\frac{AT_d^2}{\ell} \cdot \frac{T_d}{\tau} \right) \quad (7)$$

since, as explained above, $\Delta V/AT_d$ will be constant and, likewise, t_r/T_d is constant. This function is the equation of one of a family of surfaces. A hypothetical example of one of these surfaces is shown in Fig. 3. Due to the discontinuous nature of the force-deflection function shown in Fig. 2, this surface is also discontinuous in the sense that there is some minimum value of A which will produce permanent deformation. For values of A less than this minimum, T_d can be increased indefinitely and no permanent deformation will result. The surface shown has been drawn for values of A greater than the minimum.

An increase in T_d , with A and τ remaining constant, results in a considerable increase in the permanent deflection if the surface shown is qualitatively correct. If instead of holding A

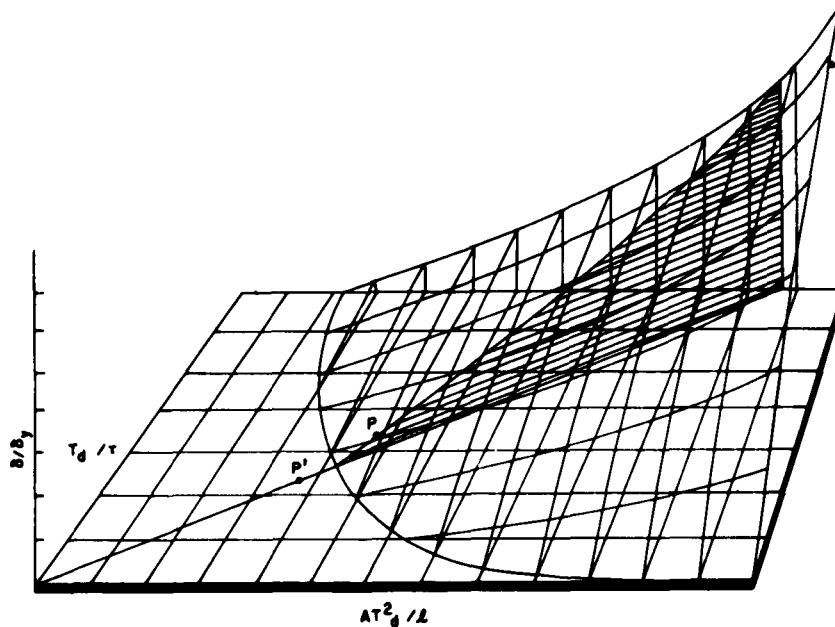


Fig. 3 - Hypothetical relationship between permanent deformation and the significant parameters for a given pulse shape

constant, the product AT_d is held constant while T_d varies, the projection on the base plane of the resulting curve for δ/δ_y is a straight line, as shown by the shaded area in Fig. 3. Thus it may be seen that for the set of parameters represented by point P on the diagram, an increase in A and the resultant decrease in T_d required to keep AT_d constant moves the deflection to a point P' on the diagram. If the surface is qualitatively correct, further increases in A will not produce any significant changes in δ/δ_y .

SCOPE OF THE INVESTIGATION

With the functional relationships of Eqs. (4), (6), and (7) as guides, the program of investigation was designed to show how the dimensionless permanent deformation of a tip loaded cantilever beam of mild steel representing a single-degree-of-freedom system varies with pulse shape, rise time, and pulse duration.

Beam parameters were kept constant during the investigation as they are implicit in the definition of the $F(z)$ function, and do not appear explicitly in the equation of motion. The length, l , used in the study was taken to be 1.1 feet, the reference peak acceleration

$A_c = 80$ g, and the basic pulse duration $T_d = 60$ milliseconds. These values were chosen to correspond with those of a previous experimental study [6] of the nonlinear system in order that a comparison could be made.

Displacement-time and velocity-time curves were obtained for 27 sets of input conditions. Sixteen different forms of the function $a(t)$ were used. These forms are shown in Fig. 3, and the pulse parameters are given in Table 2. Pulses 1 through 10 were used to investigate the effect of rise time with all other parameters held constant. Pulses 11 through 16 were included to show the effect of changes in pulse shape. Pulse number 16 is an approximation of the pulse which a system cushioned with paper honeycomb would receive.

In addition to the variations indicated above, pulses 1, 6, and 15 were used in a study of the effect of variations in the dimensionless parameter AT_d^2/l . For pulses 1 and 15, A only was varied, for pulse 6, A, T_d , and τ were varied.

The actual values of the AT_d^2/l parameter used in the calculations will be shown later in the discussion of results. (See Table 5)

TABLE 2
Pulse Shape Parameters for Pulses of Fig. 3

TRIANGULAR PULSES (Numbers 1 - 10)															
		$A/A_c = 1.00$		$T_d/\tau = 1.288$											
Pulse Number		1	2	3	4	5	6	7	8	9	10				
Dimensionless Rise Time t_r/τ		0.000	0.107	0.250	0.344	0.429	0.644	0.805	0.966	1.127	1.288				
PULSES MADE UP OF RECTANGULAR ELEMENTS (Numbers 11 - 15)															
		$A/A_c = 1.00$ (except Number 14) $T_d/\tau = 1.288$													
Pulse Number		Other Pulse Shape Parameters													
11		$t_1/\tau = 0.429$								$A_1/A_c = 0.250$					
12		$t_1/\tau = 0.483$		$t_2/\tau = 0.805$				$A_1/A_c = 0.333$							
13		$t_1/\tau = 0.161$		$t_2/\tau = 1.127$				$A_1/A_c = 0.333$							
14		$A/A_c = 0.500$													
15		None													
PULSE SHAPE 16 (PAPER HONEYCOMB PULSE)															
$A/A_c = 1.00$		$t_1/\tau = 0.043$		$t_3/\tau = 0.751$				$A_1/A_c = 0.500$							
$T_d/\tau = 1.288$		$t_2/\tau = 0.537$		$t_4/\tau = 0.966$											

METHOD OF ATTACK

The solution of Eq. (2) in closed form is complicated by the nonlinearity of the $F(z)$ function, and the many variations made in the $a(t)$ function. Therefore, a numerical integration method of solution was set up which employed an IBM 650 digital computer for the calculations.

The second-order differential equation of motion was reduced to two simultaneous first-order differential equations and these were then solved numerically using the Runge-Kutta procedure [12, 13].

The advantages of this method are as follows:

No knowledge of conditions at previous times is required. Only data at a single point

on the time scale are needed to calculate conditions at the next point. This contrasts to Milne's method and the Adams-Moulton method [13] which both require data at several preceding points for calculations of conditions at the next point, and thus require use of an auxiliary method for getting started.

The Runge-Kutta method is numerically stable. This is not the case with Milne's method [13].

The time range of computation is small. The greatest number of consecutive time increments taken in any one loading was 240. Although the accumulated random error (round off, truncation, etc.) builds up more rapidly in the Runge-Kutta method than in the Adams-Moulton method or the Milne method, the limited time range keeps these errors negligible.

DISCUSSION OF RESULTS

Displacement and Velocity Versus Time

Graphs showing computed displacement and velocity versus time for the beam subjected to each of the 16 acceleration pulses of Fig. 4 have been prepared. A representative sample of these graphs for the triangular pulses is shown in Fig. 5. Each point on the displacement-time curves where the restoring force of the beam goes to zero, i.e., the equilibrium point for the beam after a deformation, is indicated by an arrow. The vertical distance from the horizontal axis to the point on the curve indicated by the arrow is the permanent deformation.

Effect of Rise Time

Rise time is defined here as the time required for the acceleration, starting from zero, to increase monotonically to its maximum value.

The values of the ratio, t_r/T_d , of the pulse rise time to the pulse duration for pulses 1 through 10 of Fig. 4 are given in Table 3.

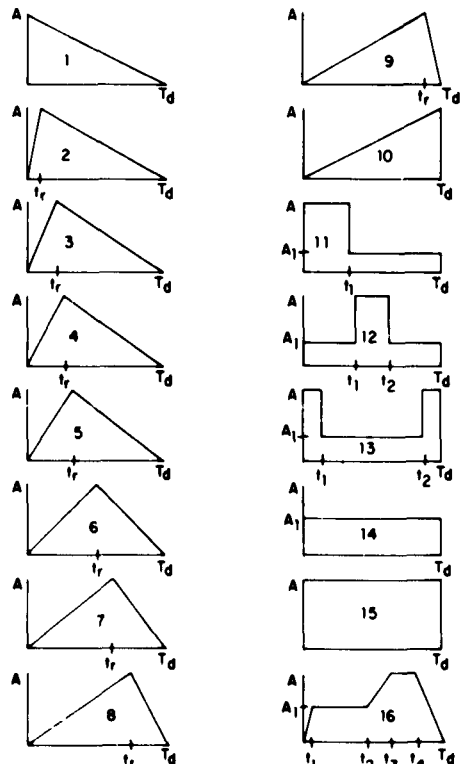


Fig. 4 - Acceleration pulse shapes used in pulse shape and rise time investigations

TABLE 3
Values of t_r/T_d for Pulses 1 through 10
of Fig. 4

Pulse No.	t_r/T_d	Pulse No.	t_r/T_d
1	0.000	6	0.500
2	0.083	7	0.625
3	0.194	8	0.750
4	0.267	9	0.875
5	0.333	10	1.000

The permanent deformation produced by these pulses, is determined as indicated above, and shown in Fig. 6 in dimensionless form as a function of t_r/T_d . Maximum deformation is produced by a pulse with a rise time just slightly less than one fourth of the natural period of the beam; the natural period in this case being based on the elastic portion of the force-deflection diagram. This ratio of one-fourth corresponds to the resonant condition for the elastic case.

Effect of Pulse Shape

To study the effect of pulse shape all 16 of the pulses shown in Fig. 4 were used. The first 14 of these pulses have the same area under the acceleration-time curve and all of the pulses except number 14 have common values for A and T_d . Pulses 15 and 16 have larger areas under their acceleration-time curves than the first 14 pulses, while pulse 14 differs from the others in that it has a maximum value of acceleration equal to one-half that of the other pulses. A typical response curve is shown in Fig. 7. The permanent deformations produced by these pulses are shown in Table 4.

Note that pulse 16, although having a greater area under the acceleration-time curve (i.e., a greater velocity change and thus a greater average acceleration during (T_d) than pulses 1 through 10 produces a smaller permanent deformation than the first 7 of these pulses. Also note that pulses 11, 12, and 13 while having the same values for A , T_d , ΔV , and average acceleration during T_d , produce noticeably different values for δ/δ_y . This, along with the results of the rise-time investigation, seems to suggest that some sort of phase relationship between the pulse duration and the natural period of the system is an important criterion in determining permanent deformation.

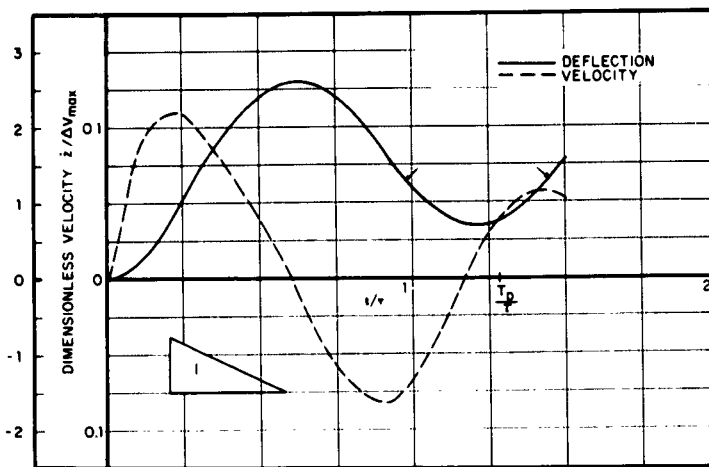


Fig. 5 - Dimensionless deflection $z/\Delta V_{\max}$ and dimensionless velocity $z/\Delta V_{\max}$ versus dimensionless time t/τ for pulse shape 1

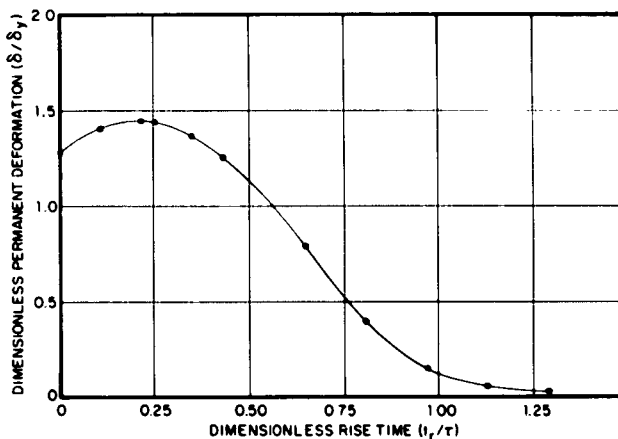


Fig. 6 - Dimensionless permanent deformation δ/δ_y versus dimensionless rise time t_r/τ for triangular pulses

If complex pulses such as pulses 11, 12, 13, and 16 of Fig. 3 are to be analyzed in detail, parameters such as A_1 , t_1 , t_2 (defined in Table 2 and Fig. 4) should be included in the dimensional analysis. It is beyond the scope of this paper to attempt such an analysis, and in the case of a general irregular pulse, a complete analysis of this type is impossible.

Effects of A , T_d , and t

The parameters A , T_d , and t were investigated in a group as the dimensionless

parameter AT_d^2/t . This was suggested by the dimensional analysis (see discussion concerning Eqs. (6) and (7)). Pulse shapes 1, 6, and 15 of Fig. 4 were chosen for study. The manner in which the AT_d^2/t parameter was varied and the resulting permanent deformations are shown in Table 5.

From the data of Table 5, plots of δ/δ_y versus AT_d^2/t were obtained for each of the 3 pulse shapes investigated. These curves are shown in Fig. 8. The difference between the 2 curves for the triangular pulses can be attributed to the difference in the pulse shapes

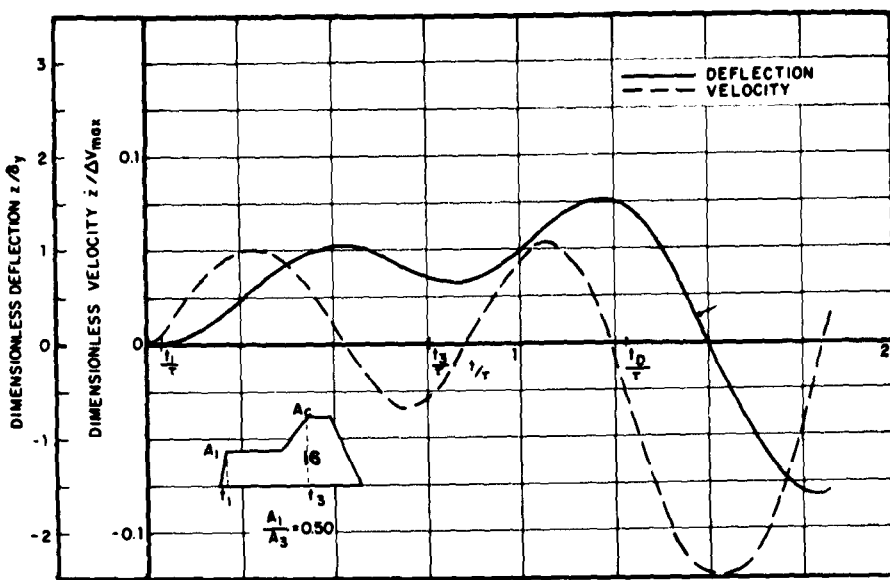


Fig. 7 - Dimensionless deflection z/δ_y and dimensionless velocity $z/\Delta V_{max}$ versus dimensionless time t/τ for pulse shape 16

TABLE 4
Permanent Deformation Obtained from 16 Acceleration-Time Relationships

Pulse No.	Dimensionless Permanent Deformation δ/δ_y	Pulse No.	Dimensionless Permanent Deformation δ/δ_y
1	1.268	9	0.054
2	1.400	10	0.031
3	1.414	11	1.985
4	1.365	12	0.281
5	1.245	13	0.221
6	0.788	14	0.081
7	0.398	15	6.889
8	0.133	16	0.223

represented since there were no other variables. The rectangular pulse has the same A and T_d as the triangular pulses, hence the velocity change for this pulse is twice that of the other pulses. From the similarity of these curves, it is seen that the effect of the AT_d^2/t parameter on a system has certain characteristics regardless of pulse shape.

Curves of the type shown in Fig. 8 appear to have almost universal application. This is not true, however. A definite limitation

exists, since as has been previously suggested, there is, presumably, a range of acceleration amplitudes which would produce no permanent deformation no matter how long the pulse might be. On the other hand, it is conceivable that a pulse could have a very large amplitude but have such a short duration as to be incapable of producing damage. Consequently, use of curves of the type in question should be restricted to those pulses with an amplitude which will produce permanent deformation if the duration of the pulse is made sufficiently long.

TABLE 5
Values at AT_d^2/t and Resulting Permanent Deformations for
Pulse Shapes 1, 6, and 15

$t = 1.1$ feet		$\delta_y = 0.117$ feet
Pulse Shape No.	AT_d^2/t	δ/δ_y
1	0.5505	0.1014
1	0.6880	0.4056
1	0.8256	1.0006
1	0.9633	1.8957
1	1.1007	3.1814
1	1.2383	4.9091
6	0.5620	0.0513
6	0.6322	0.0867
6	0.6859	0.1470
6	0.7376	0.3280
6	0.8430	0.7863
6	1.0537	2.5528
6	1.1239	3.4274
6	1.2644	5.6136
15	0.5620	0.5103
15	0.6743	1.4449
15	0.8430	6.8895
15	1.2646	24.4043

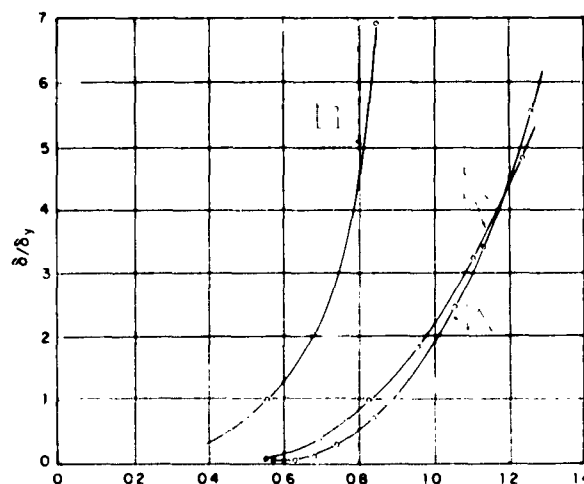


Fig. 8 - Dimensionless permanent deformation
versus AT_d^2/t for pulses 1, 6, and 15

The results shown in Fig. 8 indicate that inside the restrictions set forth above, the effects of the parameters A , T_d , and t are interdependent and cannot be separated. In previous cushioning work, the maximum acceleration parameter A has been considered the most important of these parameters, and methods of investigation were planned accordingly. Accelerations were increased, but the nature of the cushioning problem required that T_d be decreased. Even though the acceleration was increased by a factor of 4 or more, no damage was observed. This was puzzling at the time, but the explanation now seems obvious. If the analysis presented here had been available at the time these cushioning studies were conducted, no doubt different methods of attack would have been used, and a better understanding of the test results would have been obtained.

Acceleration Shock Spectra

No correlation between shock spectra for the various pulse shapes and the permanent deformation produced could be established. Although some correlation could be seen when the triangular pulses alone were examined, all semblance of correlation was lost when the spectra from the pulses made of rectangular elements were included in the comparisons. The correlation obtained in the case of the triangular pulses was much more poorly defined than that of the rise-time relation of Fig. 6.

The shock spectra were based on a linear system with characteristics similar to those represented by the first straight-line portion of the load-deflection curve of Fig. 2.

EXPERIMENTAL STUDIES

Technique and Equipment

For the experimental program, small, tip-loaded, cantilever beams were clamped on the platform of a Hyge accelerator and subjected to the desired type of acceleration pulse. Acceleration was monitored with a Statham accelerometer clamped to the platform, and an oscilloscope equipped with a Polaroid camera. The permanent deflection of the beam was measured with respect to the platform using a vernier height gage.

The beams were all made of hot rolled mild steel, and were $1/4 \times 1$ inch in cross section. Lengths and tip weights were varied to produce the desired natural period. To obtain true cantilever action, the beams were prepared in the form of simple beam with weights at each end. This beam was then clamped at the middle to a heavy block which was attached to the Hyge platform. Details of the assembly are shown in Fig. 9. Since 2 beams were, in effect, included in each shot, 2 permanent deformations were measured and the deformation reported for the shot is the average of these two. Despite the symmetry and the fact that both beams were subjected to the same acceleration, the permanent deflections at the 2 ends were rarely the same. The discrepancies varied from less than 1 percent to as much as 10 percent expressed in terms of the average of the 2 deflections. Reading errors might account for as much as 1 percent of the discrepancy, but no more. This means that most of the discrepancy must be due to setup errors, i.e., lack of symmetry, or to variations in the material behavior. The latter is believed in this case to be the principal cause of variations.

Scope of the Experimental Program

The experimental program completed to date has been limited in scope due to the time-consuming nature of each test. Two series of measurements have been made.

In the first series, the beams were subjected to the best approximation of a rectangular acceleration pulse available from the Hyge. The peak amplitudes of these pulses were varied from 28.4 g to 50.7 g. Durations ranged from 32.1 to 24.5 milliseconds. All the beams were identical, with a length of 1.1 feet and a natural period of 46.5 milliseconds.

In the second series, the applied acceleration pulse was approximately a half sine wave with an amplitude of 14.2 g and a duration of 57 milliseconds. The acceleration pulse parameters were held constant in this series while the natural period of the system was varied. The variation was produced by changing the tip weights on the beam.

Representative Polaroid records of the 2 pulse forms are shown in Fig. 10. The negative acceleration which follows the main pulse is produced by the braking of the platform. As far as could be determined, this small negative acceleration had no effect on the permanent deformation.

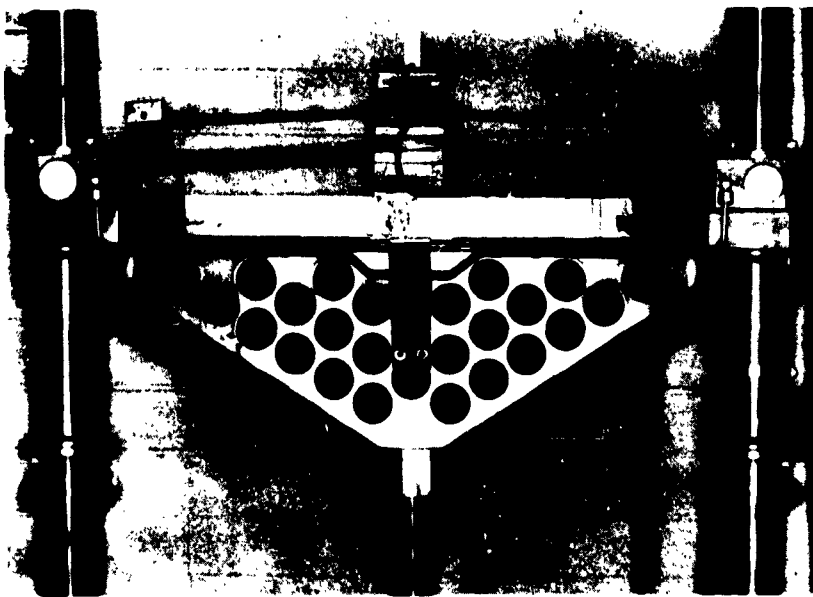


Fig. 9 - Twin cantilevers mounted on a Hyge accelerator. Note the permanent deformation of both beams from a shot just completed

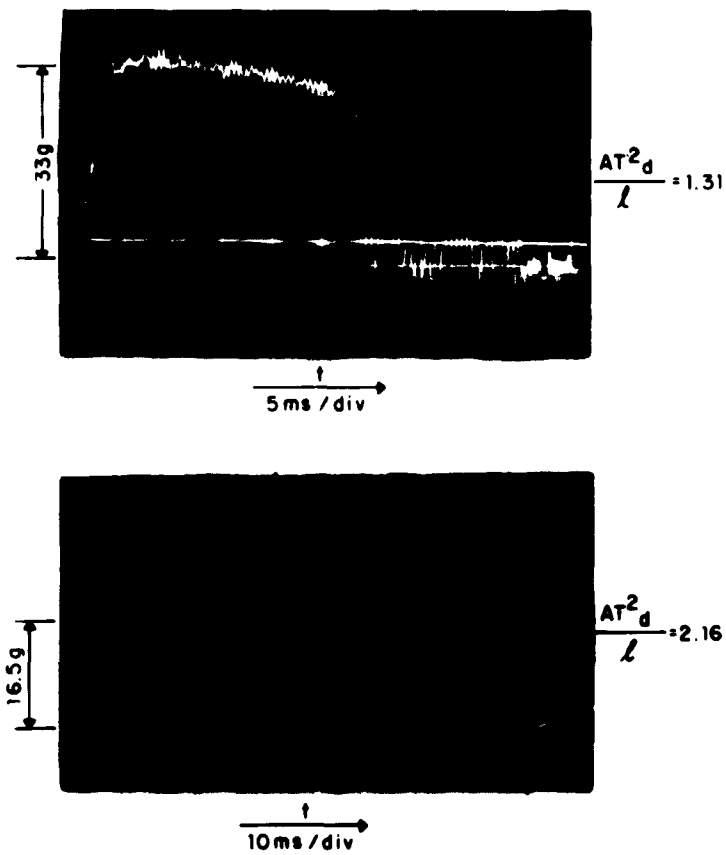


Fig. 10 - Typical acceleration pulses applied at the root of the cantilever

Experimental Results

It will be noted that in both series of tests, the nondimensional group AT_d^2/ℓ is the controlled variable. For the first series, all the terms in the functional relationship given by Eq. (3) with the exception of AT_d^2/ℓ were held essentially constant. Therefore, the data from this series should be comparable to the computed results shown in Fig. 8 and particularly to the results computed for the rectangular pulse. However the range of parameters available from the experimental equipment was outside the range of the previously computed results. Consequently, the experimental results for the rectangular pulse are shown separately in Fig. 11. The general shape of the curve is the same as that seen in Fig. 8 for the computed results. It will be noted however, that the permanent deformations observed experimentally are appreciably higher than the computed deformations would appear to be for corresponding values of AT_d^2/ℓ . The explanation for this is not apparent but it is believed to be associated with the rise-time effect previously discussed. For the computed results, the rise time was infinitely short, whereas for the experimental results, the pulse was actually trapezoidal with a rise time of approximately 5 milliseconds. The natural period of the system subjected to the acceleration was 45 milliseconds. It is conceivable that the surface pictured in Fig. 3 bulges out toward the T_d/τ axis as the ratio t_r/τ approaches 1/4. If this were the case, it could account for the discrepancy between experimental

and computed results. Further work, both experimental and computational, is necessary to establish the surface better and thus resolve this point.

The results of the second series of measurements in which the half-sine wave acceleration pulse was used and the natural period of the beam varied, are shown in Fig. 12. These results represent a cross section through the hypothetical surface, parallel to the $\delta/\delta_y - T_d/\tau$ plane. From purely physical considerations, the deflection would not be expected to increase indefinitely with increasing T_d/τ , but would probably reach a constant value. Consequently, the results presented do not cover a wide enough range of T_d/τ values to give a true picture of the variation of the deflection with variations in this parameter.

CONCLUSIONS AND SUMMARY

It is not intended that the results presented be applied directly to vehicles or other complex structures. However, it is apparent that if the behavior of a complex structure can be approximated by a combination of simple structures, then the pulse shape, rise time, and AT_d^2/ℓ parameters are all quite significant in the relationship between the applied acceleration and the resultant permanent deformation. Some of the specific effects of the various parameters are:

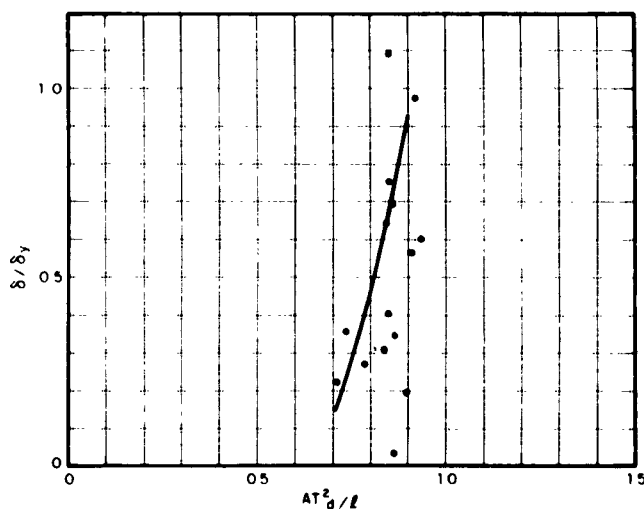


Fig. 11 - Measured permanent deformations produced by a rectangular pulse

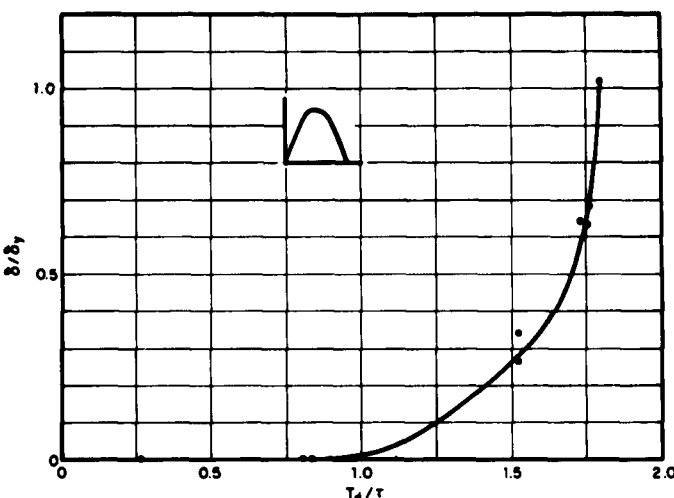


Fig. 12 - Measured permanent deformations produced by a half sine wave pulse

1. If the parameters A , T_d , ΔV , and t are specified, and if it is possible to define a rise time for the pulse shapes being considered, then,

(a) Where t_r/τ has a value near $1/4$, a maximum in permanent deformation may be expected.

(b) As t_r/τ becomes large with respect to $1/4$, permanent deformation will decrease.

2. The shape of the acceleration-time pulse, in general, has a marked effect on permanent deformation. Changing the pulse shape from that of pulse 3 to that of pulse 10 decreases the permanent deformation by a factor of $1.414/$

0.034 or 45.6 . The two pulses differ only in pulse shape and rise time.

3. The effects of A , T_d , and t cannot be separated. For a given general pulse shape and a given beam (i.e., τ and t constant), the deformation increases as either A or T_d increase if a certain minimum acceleration amplitude is exceeded.

4. Experimental results are not conclusive, but they seem to agree generally with the theoretical conclusions. Further experimental investigation is needed.

5. The two parameters AT_d^2/t and T_d/τ seem to be the most significant in determining the deformation a given pulse will produce in a given system.

REFERENCES

- [1] Clarke Covington and Richard Shield, "Fragility Studies, Part III, Cargo Trailer, M100, 1/4-Ton, 2-Wheel," Austin, Texas, Structural Mechanics Research Laboratory, The University of Texas.
- [2] Richard Shield and Clarke Covington, "Fragility Studies, Part IV, Cargo Trailer, M101, 3/4-Ton," Austin, Texas, Structural Mechanics Research Laboratory, The University of Texas, March 7, 1960.
- [3] Clarke Covington, et. al., "Fragility Studies, Utility Truck, 1/4-Ton," Austin, Texas, Structural Mechanics Research Laboratory, The University of Texas, March 7, 1960.
- [4] Robert R. Luke, "The Impact Response of a Single-Degree-of-Freedom System

- With Viscous Damping," Austin, Texas, Structural Mechanics Research Laboratory, The University of Texas, 1960.
- [5] Albert P. Richter, "The Response of a Two-Degree-of-Freedom Undamped System Subjected to Impulsive Loading," Austin, Texas, Structural Mechanics Research Laboratory, The University of Texas, 1960.
- [6] James D. Huckabay, "A Study of the Plastic Deformation of a Single-Degree-of-Freedom System Subjected to Impulsive Loading," Austin, Texas, Structural Mechanics Research Laboratory, The University of Texas, 1960.
- [7] T. J. Mentel, "Impact Deformation of a Cantilever Beam," Journal of Applied Mechanics, Vol. 25, No. 4, December 1958.
- [8] M. V. Barton and R. J. Savage, "Semiannual Report on Shock Characteristics of Nonlinear Systems," Los Angeles, California, Space
- [9] R. J. Savage and M. V. Barton, "Final Report on Shock Characteristics of Nonlinear Systems," Los Angeles, California, Space Technology Laboratories, 31 December 1960.
- [10] Y. C. Fung and M. V. Barton, "Shock Response of a Nonlinear System," Los Angeles, California, Space Technology Laboratories, no date.
- [11] Glenn Murphy, "Similitude in Engineering," New York, The Ronald Press Company, 1950.
- [12] K. S. Kunz, Numerical Analysis, McGraw-Hill, pp. 167, 187-188, 1957.
- [13] F. B. Hildebrand, "Introduction to Numerical Analysis," McGraw-Hill, Chapter 6, 1956.

DISCUSSION

S. Schuler (Royal Radar Establishment, England): I would like to congratulate Dr. Ripperger on his extremely interesting presentation. I am mindful of the difficulties with mechanical machines for producing pulses for analyses such as he has described. We have had a little experience on electronically derived pulses, being generated through an

electrodynamic generator, and applied to structures. I would like to ask him whether he has any experience at deriving his shock patterns in this way.

Dr. Ripperger: I have heard of this procedure but I have not had any experience with it. I am interested and would like to know more about it.

* * *

AERIAL DELIVERY OF A HEAVY UNIT LOAD BY PARACHUTE EXTRACTION

2nd Lt. D. C. Turk, USAF
Hq 6511th Test Group (Parachute)
El Centro, Calif.

This paper describes the system for extracting a 35,000-pound test load from a C-130B aircraft using a dual side rail extraction system. Included are details of the parachute load systems and of the instrumentation used to obtain data on aircraft behavior during extraction and on action of the test load on deployment of parachutes.

INTRODUCTION

Aerial delivery by parachute extraction methods is not a new concept. Progress has been slow but sure as more and more has been learned about the factors influencing the extraction process. The progress in this field has been reflected in the ever-increasing requirements imposed upon aerial delivery systems and in the design of those systems which will fulfill the requirements.

It is the purpose of this paper to present the engineering results of the testing of an advanced version of an aerial delivery system. To this end, one test will be discussed in some detail. The test under consideration was made on 16 January 1961 by the 6511th Test Group (Parachute), El Centro, California. The extraction was initiated at 150 knots IAS from an altitude of 5000 feet. The drop aircraft was a C-130B with modified ramp support arm brackets. The gross extracted load was 35,010 pounds. (A special waiver for single unit extractions above 25,000 pounds was obtained for this test.)

The extraction process was initiated by the pilot who electrically activated the pendulum ejection system. The drag force of the deployed extraction parachutes then accomplished the following:

- Activated the mechanical load release which disengaged the restraining latch mechanisms from the fixed pin platform, thus freeing the load for extraction.

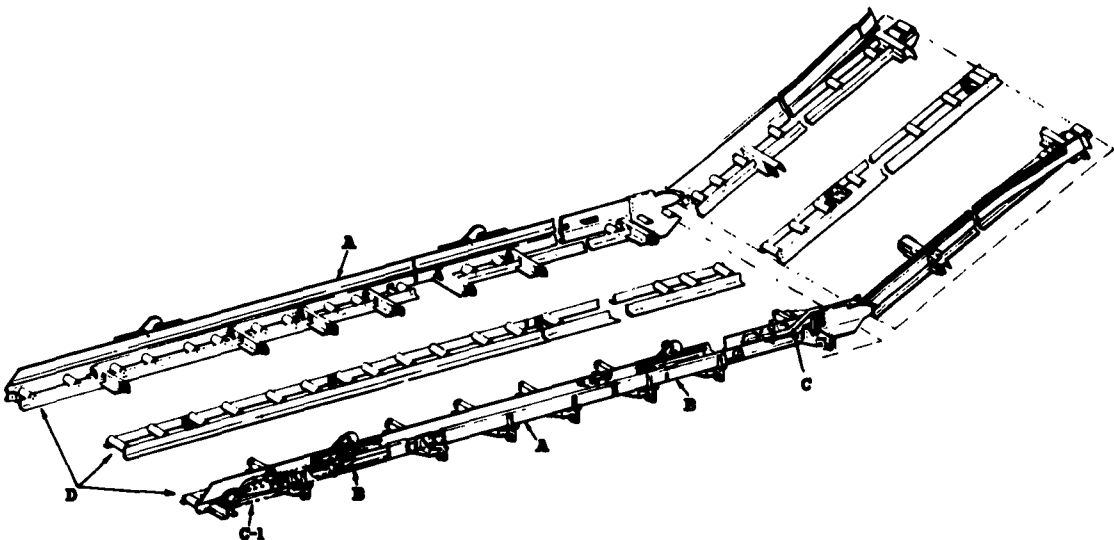
- Withdrew the load from the aircraft.
- Deployed the recovery parachute system.

The major test objectives were first, the functional evaluation of rail modifications for fixed pin 108-inch wide platform usage. Second, the functional evaluation of the fixed pin 108-inch "Comex" combat expendable platform. Third, the evaluation of the controllability of the C-130B during heavy drop aerial delivery. And, fourth, the gathering of force data on extraction and recovery parachutes and on platform suspension risers.

AERIAL UNLOADING KIT AND TEST LOAD

The Aerial Unloading Kit, Model AF/A32H-1 (nonstandard) is an improved version of a similar kit which is presently in service use. It was developed by Brooks and Perkins, Inc. The major components of the kit, as shown in Fig. 1, are:

- The frame assembly rails, A, for lateral and vertical restraint during flight.
- The latching mechanisms, B, for fore and aft restraint of the load. These mechanisms are basically hooks which fit over fixed pins on the platform to be extracted.
- The automatic load release C. This is activated by a lanyard which is connected to the extraction line. As the extraction line pays



A FRAME ASSEMBLY RAILS
 B LATCHING MECHANISMS
 C AUTOMATIC LOAD RELEASE
 C-1 EMERGENCY LOAD RELEASE
 D ROLLER CONVEYOR SYSTEM

Fig. 1 - Aerial unloading kit

out, a cable contained in the frame assembly rails is pulled which activates the cams that release the latching mechanisms. In case of failure of the automatic release system, there is an emergency release, C-1, which is hand-operated. This emergency release is located forward and left of the load. It operates the same cam as the automatic load release, through an independent cable system.

- The roller conveyor systems, D, on which the platform rides. There are three tracks of conveyors in this system, allowing unit loads up to 35,000 pounds to be loaded and extracted.

The "Comex" combat expendable platform was also developed by Brooks and Perkins, Inc. This item consists of modular panel sections, side rails with fixed pins and accessory fittings. The panel sections are 108 inches wide and 48 inches long and are of sandwich construction with thin aluminum skins bonded to a foamed-plastic core and a frame made up of extruded aluminum channels. The platform used in this test consisted of 6 panels for a total of 24 feet.

A weight test platform was used as the test load. The platform was ballasted with iron plate to obtain the desired weight. The weight test platform was restrained to the "Comex" platform with cargo tie-down devices, type MB-1.

Twelve layers of paper honeycomb were used between the "Comex" platform and the weight test platform for impact energy dissipation and center of gravity requirements. The c.g. was located 45 inches above the top of the "Comex" platform. The configuration of the test load is depicted in Fig. 2.

Two turns of 3000-pound tubular tape (MIL W-5625) were used between the "Comex" platform and tie-down rings on the aircraft floor. This break restraint was used to obtain sufficient platform resistance to allow partial inflation of the extraction parachutes prior to movement of the platform. This results in a more decisive platform movement and a slightly higher peak extraction force.

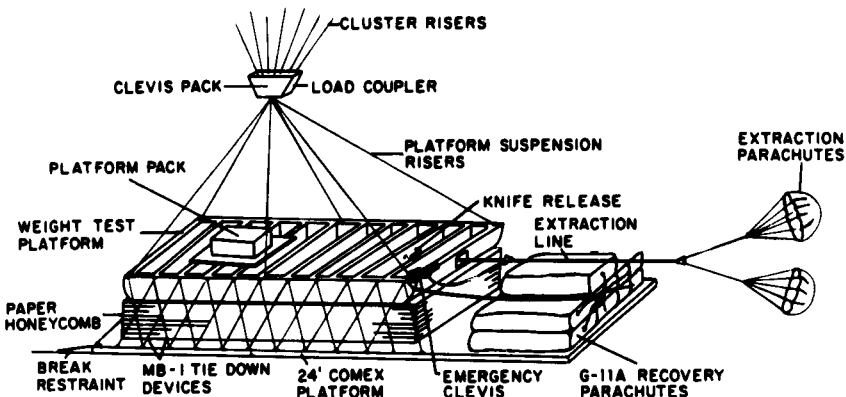


Fig. 2 - General view of system

EXTRACTION

A cluster of two 28-foot ring-slot parachutes was used for extraction; the connection between the load and parachutes being made by a 60-foot, 12-ply, Type X nylon extraction line.

The maximum theoretical force for this combination of parachutes at a constant 150 knots IAS is 55,200 pounds. Experience has shown, however, that the probable actual maximum for the combination as used would be 41,000 pounds, the difference being attributed to two factors.

First, the decrease in actual deployment velocity due to platform movement prior to full inflation. And second, clustering loss which occurs because the axes of the parachutes are not parallel to the relative air stream. The angle they assume with respect to the relative air stream is determined by the length of the cluster risers which attach the individual parachutes to the common extraction line and the diameter of the parachutes.

Thus we could expect a ratio of maximum extraction force to gross extracted weight of $41,000/35,000 = 1.17$. Past test results indicate that this was a reasonable ratio to use from a flight safety standpoint.

As was previously mentioned, the extraction force was also used to deploy the recovery parachutes. This meant that provisions had to be made for removal of the extraction force from the weight test platform and its transfer to the recovery system. The removal of the extraction riser was

accomplished by a spring-loaded knife system (Fig. 3), the compression on the knife springs being approximately 600 pounds. The knife was actuated from the right static line cable by a standard 15-foot static line. This method insured that the extraction force would remain on the platform until the instant the platform started to clear the C-130B ramp. The force could then be transferred to the recovery parachutes.

A safety problem arose when the possibility of a jammed load was considered. This would necessitate the removal of the extraction force without the transfer of this force to the recovery system as would happen in the normal sequence. Therefore, the following provisions had to be made; first the knife release had to be designed so that it could operate off the static line or off an emergency hand pull release; and second the connecting device between the extraction force and the recovery system had to be a mechanical one, designed so that the actual connection was made only after the platform had moved far enough to insure its safe exit from the aircraft. This device was termed the emergency clevis (Fig. 4). It was operated from a lanyard tied to an aircraft ceiling support member as the platform moved out of the aircraft. The lanyard was long enough to allow a platform movement of 8 feet before the emergency clevis was activated.

RECOVERY SYSTEM

The recovery system consisted of seven 100-foot diameter G-11A's with 40-foot, 2-second reefing. Six-ply, Type X nylon parachute cluster risers, 120 feet long, were used between the load coupler and the parachutes.

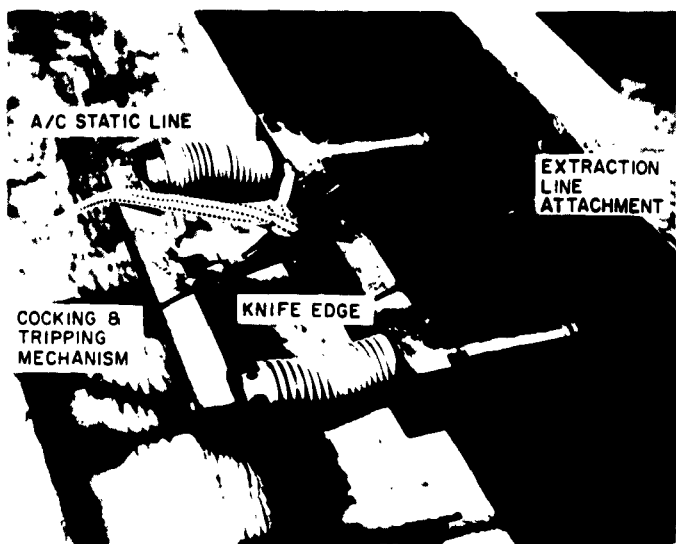


Fig. 3 - Knife release

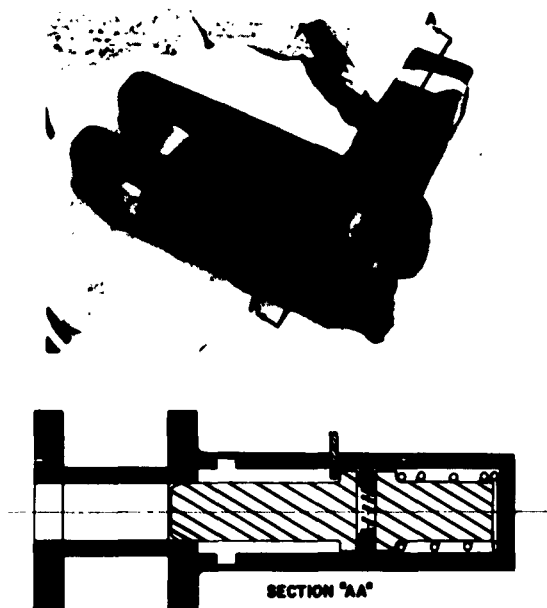


Fig. 4 - Emergency clevis

The load coupler was designed to serve two purposes. It had to provide for a confluence point between the parachute cluster risers and the platform suspension risers;

and it had to provide a housing for a telemetry package. The 6-platform suspension risers were constructed of 6-plys of Type X nylon webbing.

The ejection of the extraction parachutes was initiated by the pilot who electrically released the extraction parachutes which were suspended from the aircraft ceiling. The parachutes then behaved as a pendulum, traveling in an arc prescribed by the pendulum arm which was a length of cord attached to the aircraft ceiling. The parachutes traveled in this arc until they possessed enough momentum to clear the clip connecting the pendulum arm to the ceiling. This allowed the parachutes to be thrust from the aircraft at a 45-degree angle to the longitudinal axis of the aircraft. The parachutes then were deployed by the combination of snatch force and air blast.

TEST OBJECTIVES AND INSTRUMENTATION

The test objectives required that the following information be obtained from the test:

- Visual evaluation of the functional performance of the aerial unloading kit and the "Comex" platform.

- Acceleration of the nose section, the aft section and the approximate center of gravity of the aircraft.
- Pitch and rate of pitch of the longitudinal axis of the aircraft.
- Forces sustained by the ramp support arms during extraction.
- Forces sustained by the platform suspension risers.
- The extraction force.
- Velocity of extraction.
- Recovery parachute forces.
- Rate of descent at impact.

There were three major sources of information — instrumentation, cinetheodolite coverage, and photographic coverage.

The instrumentation used is shown in Table 1. There were two means of transmission of the data from the sensing instruments to the recording instruments. One method used was telemetry, the other was direct recording on board the aircraft whenever possible. There were 18 channels of telemetry and 11 channels of direct recording used. The sensing devices and their locations also are described in the table.

Three telemetry transmitting packages were used. One package was installed in the C-130B and designated the ON-BOARD PACK. One package was installed in the load coupler and designated the CLEVIS PACK. The remaining package was installed on top of the weight-test platform and designated the PLATFORM PACK.

There were 2 telemetry receiving stations. The master station, a Bendix TGRS-1, and a mobile telemetry van. All recordings were made on Ampex 500 tape recorders.

Five cinetheodolite cameras were used at a rate of 5 frames per second. The cameras covered the aircraft until the load was clear of the ramp. The coverage was then switched to the platform system. The principal data sought from this coverage were (1) Pitch, change of altitude and change of velocity data on the aircraft during the extraction process, and (2) Trajectory, velocity and rate of descent for the platform system.

Photographic coverage was used as back-up for time and events analysis and as a permanent record of the tests. Details are as follows: — Two 16mm cameras inside the test aircraft, one mounted in the flight compartment to photograph the pilot's instrument panel during the test and 1 hand-held in the cargo compartment to photograph the extraction of the load; one 16mm movie camera located in a T-28 chase aircraft to photograph the extraction of the load; one 16mm movie camera and one 70mm "sequence still" camera located on the drop zone to photograph all events possible; an additional 70mm sequence still and a 16mm movie camera located in a hovering helicopter to photograph the extraction and recovery sequences.

RESULTS

Figure 5 presents the recovery system forces starting at platform clearance of the aircraft ramp and ending at the steady state force condition. The damage to the parachutes is classified as none, light and medium. Medium damage is defined as that which is economically repairable. The term economically repairable takes into consideration such factors as age of the parachute, extent and location of damage on canopy and previous canopy damage. Light damage is defined as damage that permits the reuse of the parachute without repair.

It is to be noted that there is a random overloading of some parachutes while others sustain only a small portion of the load prior to the steady state force condition. This is believed to be due to the clustering effect previously discussed, i.e., the angle at which some parachutes are presented to the relative air stream. The amount of this overload is variable, depending upon the size of the parachutes, the length of the cluster risers, the number of parachutes in the cluster and the reefing system used. To this date, there is insufficient information available for a detailed study of this clustering phenomenon.

Figure 6 shows the force histories of the platform suspension risers. There was a loss of information on one of these risers due to a broken telemetry lead.

During the extraction process, the pilot applied forward elevator control to correct for the changes in attitude. Power and flap settings remained constant. This technique did not entirely prevent pitch-up but it did produce substantially different results from previous techniques that had been employed.

TABLE 1
Instrumentation

Desired Measurement	Sensing Device	Location of Instrument	Method of Transmittal
Force of recovery chutes	Baldwin - Lima - Hamilton, SR-4 strain gages	Cluster risers	Telemetered from CLEVIS PACK
Force on platform suspension risers	Baldwin - Lima - Hamilton, SR-4 strain gages	Platform suspension	Telemetered from PLATFORM PACK
Extraction para-chute force	Baldwin - Lima - Hamilton, SR-4 strain gages	60 foot ext. line	Telemetered from PLATFORM PACK
Ramp support arm forces	Baldwin - Lima - Hamilton, SR-4 strain gages	Left and right C-130 ramp support arms	ON-BOARD PACK; On-Board direct recording
Extraction time	Micro switches	Aft end of ramp	ON-BOARD PACK; On-Board direct recording
Velocity of extraction (relative to C-130)	Magnetic drum, locally designed and manufactured	Between the "Comex" platform and C-130 cargo deck	ON-BOARD PACK; On-Board direct recording
Aircraft pitch	Gyro	Forward of load and to the right of centerline of aircraft	On-Board direct recording
Aircraft rate of pitch	Gyro	Forward of load and to the right of centerline of aircraft	On-Board direct recording
Vertical acceleration of aircraft nose	10 g inertial accelerometer	Midway between pilot's rudder pedals and inclined to measure vertical acceleration	On-Board direct recording
Acceleration of aft section of aircraft	10 g inertial accelerometer	On aft centerline on furthest accessible aft support member in the vertical direction	On-Board direct recording
Acceleration of aircraft c.g.	3 axes inertial accelerometer: 3 g vertical 2 g lateral 2 g longitudinal	Slightly right of aircraft centerline at Station 530	On-Board direct recording

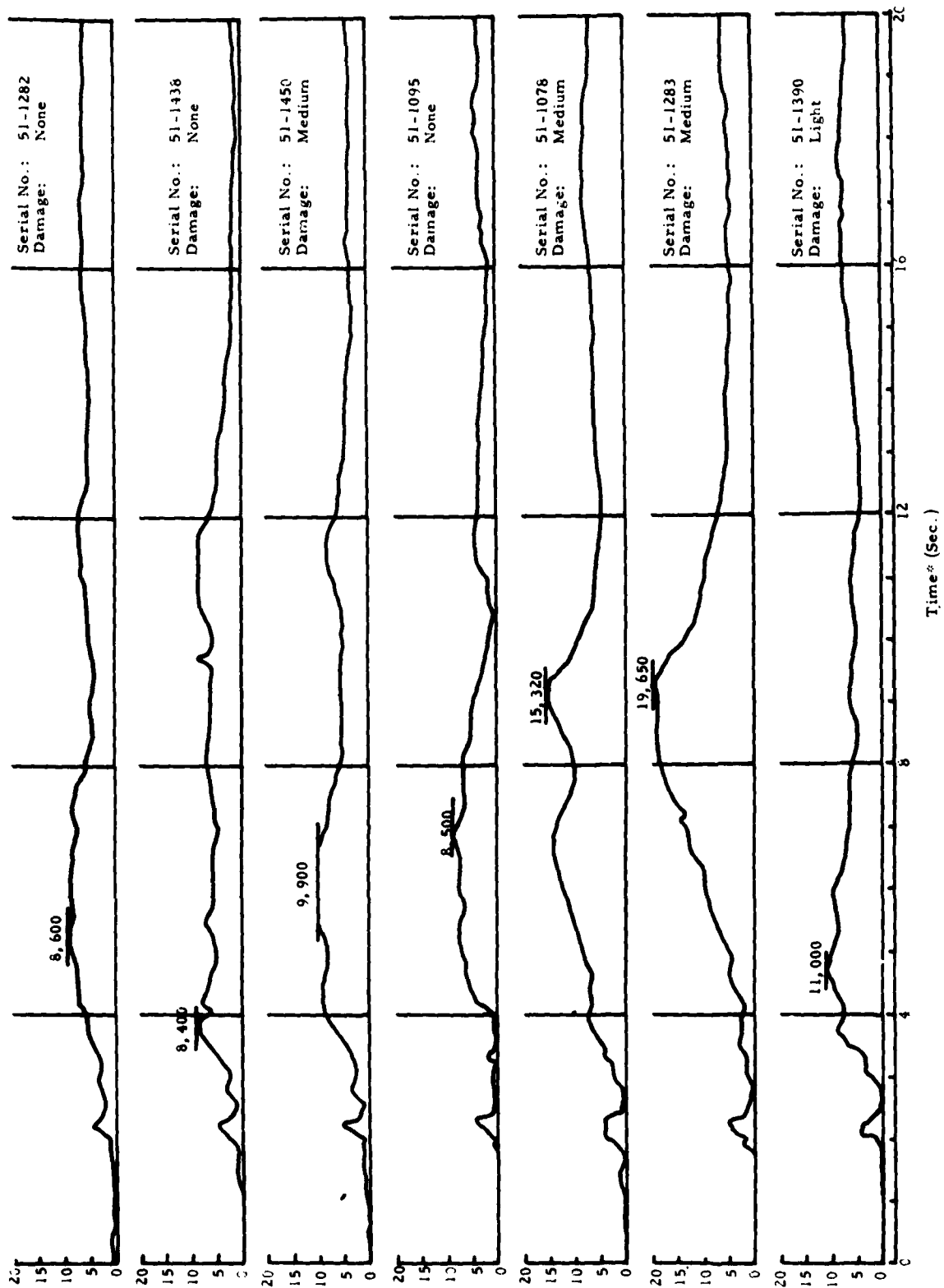


Fig. 5 - Force versus time histories of F-11A recovery parachutes.
(*Platform clearance of aircraft ramp used as zero reference.)

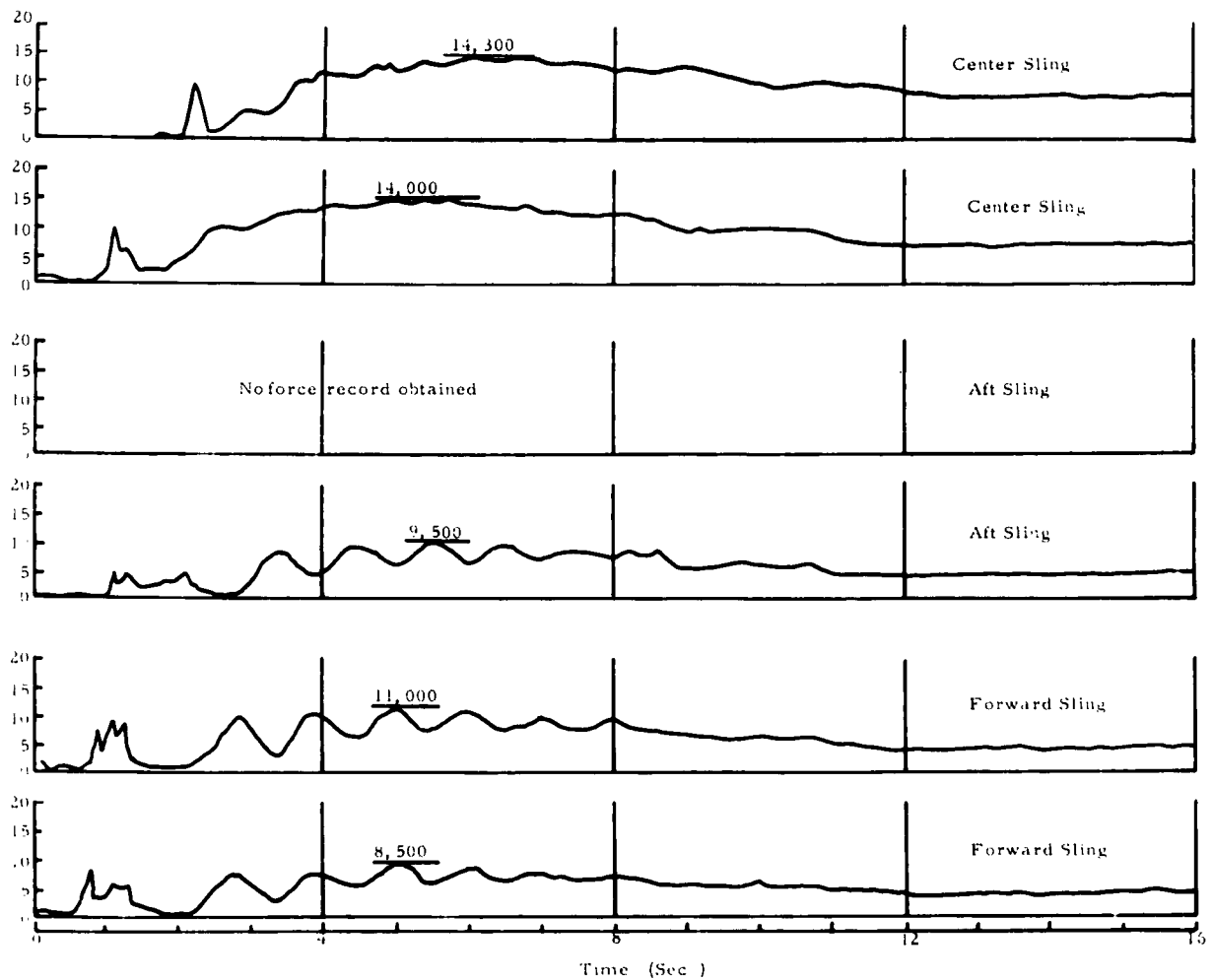


Fig. 6 - Force versus time histories of platform suspension slings.
(*Platform clearance of aircraft ramp used as zero reference.)

The following information was obtained:

Gross weight on take-off: 122,944 pounds
Initial pitch attitude: 1.75 degrees
Maximum pitch attitude: 4.75 degrees
Minimum pitch attitude: 0.50 degrees
Maximum change of pitch: 4.25 degrees
Maximum rate of change of pitch: 10.5 degrees per second
Change in IAS: 0 knots
Change in altitude: 20 feet

Ramp support arm forces -

Total: 33,000 pounds
Left: 15,100 pounds
Right: 18,200 pounds

The extraction force and the velocity of extraction are shown in Fig. 7

The aircraft accelerations in "g's" were as follows:

Nose section	0.80 ± 0.05	(vertical)
Tail section	2.40 ± 0.15	(vertical)
Center of gravity	1.25 ± 0.08	(vertical)
	0	(longitudinal)
	0.19 ± 0.05	(lateral)

For purposes of comparing flying techniques, the maximum change of pitch on a similar drop of 40,000 pounds, with the pilot applying no corrections, was 18.5 degrees, and the rate of change of pitch was 19.5 degrees per second.

The installation of the kit in the aircraft uncovered some minor discrepancies, principally in the compatibility of the kit with the C-130B. The plexiglass landing gear inspection windows prohibited installation and lock-down of 4 sections of the conveyors. (These windows were removed for the tests.) Some litter stanchions would not seat due to the

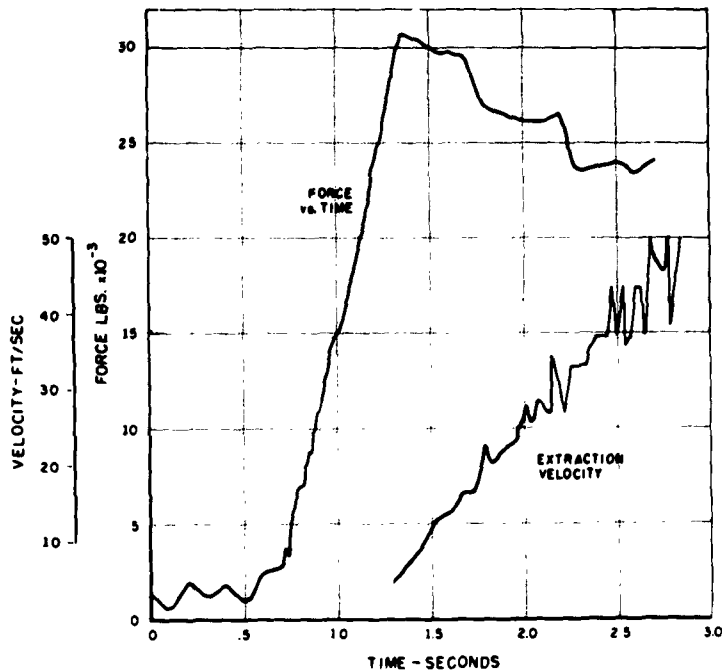


Fig. 7 - Extraction force and extraction velocity

proximity of rollers. The cocking handle of the extraction parachute cable release was located in an exposed position where it could be damaged and could cause tripping of personnel.

The kit functioned satisfactorily except for contact between some of the roller conveyor cross members and the "Comex" platform. This contact was due to the deflection of the fairly flexible "Comex" platform. This deflection can be minimized by proper loading and rigging, but it cannot be eliminated since the nature of the combat expendable platform prohibits more rigid construction. The problem can be solved by tapering the roller conveyor cross members. This would in no way affect the strength or effectiveness of the kit.

It was not practical to consider the flexibility of the "Comex" platform as undesirable; therefore, the performance of the platform was entirely satisfactory. There was damage on impact due to the platform landing broadside to the prevailing surface wind of 10 knots. This resulted in the loss of the left side rail and 5 of the 6 panels. However, the load remained upright and there was no other damage.

Impact rate of descent was 28.6 feet per second, corrected to the ICAO Standard Atmosphere.

CONCLUSIONS

Based upon the results of this test, the following conclusions were drawn:

1. The 24-foot, 6 panel "Comex" platform is suitable for extraction and air drop up to 35,000 pounds.
2. The Aerial Unloading Kit, Model AF/A32H-1, although generally functionally suitable for usage with the 108-inch "Comex" platform, should not be accepted for operational use until the necessary modifications are made to correct the discrepancies previously discussed.
3. Although no aircraft stability or control problems were encountered and no evidence of structural damage to the aircraft was apparent, adequate instrumentation of the aircraft was not available during this test to determine if design limitations of the aircraft are exceeded when dropping a unit load of 35,000 pounds.

* * *

THE TELEMETERING CLEVIS

Captain W. Gourlay, Jr., USAF
6511th Test Group (Parachute)
El Centro, Calif.

An unusual application using proven techniques; a telemetering package uniquely constructed to afford accurate transmission of measured data from relatively remote locations in a recovery parachute system.

INTRODUCTION

Recently the 6511th Test Group (Parachute) established a world's record by extracting a load of over 20 tons from an aircraft. In that program the purpose had been to determine the ultimate extraction capability of the C-130 aircraft and to develop an efficient extraction system. Recovery of the load was only a secondary consideration. Now it was desired by the Army to determine the capability of the C-130 in the aerial delivery and recovery of 35,000-pound loads.

The primary item of instrumentation used on previous heavy cargo delivery programs has been the parachute tensiometer (Fig. 1). Two types of these devices were employed; the mechanical type and the photo type. In the mechanical type, tension applied to both ends of the device caused forces, transmitted through an annular disc spring, to scribe on a rotating drum of aluminum foil. In the photo type the force was transmitted hydraulically to cause rotation of a mirror and the mirror caused the image of an illuminated slit to be recorded on a moving strip of photographic



Fig. 1 - Tensiometers - left mechanical, and right photo types

film. Each device carried its own independent timing device and both types were actuated by an arming lanyard just before force application.

For the new test some 13 tensiometers were required for adequate instrumentation. Six were required for the 6 load lines between the platform and the clevis; 6 more were needed between the clevis and the recovery chutes; and one was required between the load and the extraction chutes. In addition, it was desired that all records have a common time base. It seemed possible that some scheme might be devised for an adequate time base but it was then found that only 7 high-load-range tensiometers were available. Some other means of gathering data had to be devised.

THE TELEMETERING CLEVIS

It was decided to turn to a system of variable resistance strain gage transducers, subcarrier oscillators, an FM transmitter and a telemetry ground receiving station with a light beam oscillograph. The telemetry would provide a common time base and allow the recording of information from extraction to impact. However, a number of problems presented themselves. The only available subcarrier oscillators required an ac input signal and experience had shown that distributed capacitance, even in low-loss cables, might attenuate these signals sufficiently to drive them below the noise level. Moreover, the long leads extending from the platform, on which the telemetry package would be mounted, would be subjected to tremendous wind blast effects. Whipping of the leads might generate noise in the cables. Tying the leads to the risers might give trouble as the webbing stretched with the parachute load and abrasive effects between the nylon webbing and the lead insulation also had to be considered. The problem of the whipping leads was solved by routing them through sleeves sewn to the risers. The leads were folded within the sleeves to permit the risers to stretch without loading the leads. To lessen abrasive effects tough teflon coated leads were used.

The length of the leads remained a problem. It was then decided to use 2 separate telemetering packages and thus reduce the length of the leads to a few feet each. One package would be on the platform and the only, and obvious, place to locate the second was at the clevis. There was no room in the clevis and externally it was too small to attach telemetry chassis even if this had been desirable. It was not desirable since anything attached to the outside

might interfere with recovery system deployment and lead to loss of the whole platform.

Therefore, a new clevis was designed and built to house oscillators, batteries, power supply, transmitter, pins, bolts, bushing and risers (Fig. 2). It was intentionally overdesigned using heat-treated 4130 steel to protect the interior as well as to serve as a supporting connection between the parachutes and the load. Standard telemetry practices were used and a quarter wave antenna was routed through one of the sleeves. The completed clevis and telemetry package weighed 130 pounds--a monster --but it worked!

The clevis package was the significant factor in the successful accomplishment of the program. A total of 28 channels of information, per-drop, were recorded during the project. Both the clevis package and the platform used telemetry. The C-130 utilized a direct-recording system. Parameters measured were:

- (a) Riser Forces
- (b) Extraction Force
- (c) Rate of Extraction
- (d) C-130 Pitch Angle
- (e) C-130 Rate of Pitch
- (f) Acceleration of Platform
- (g) Accelerations of C-130
- (h) Events
- (i) Timing.

RATE OF EXTRACTION REEL

A rate of extraction reel (Fig. 3), designed and manufactured at El Centro, was used to measure the rate of extraction in this test. Basically it consisted of a ball-bearing mounted, cylindrical, aluminum drum, upon which a spiral groove was machined. The depth of the groove was equivalent to the outside diameter of the wire which would be wound around it and attached to the platform load. From the leading edge of the load to the trailing edge of the ramp, the measured distance was 43 feet. The groove was machined to hold 43 feet of wire $\pm 1/4$ inch. This was felt to be within the tolerance of the original measured distance of 43 feet and served only as a guide to the length

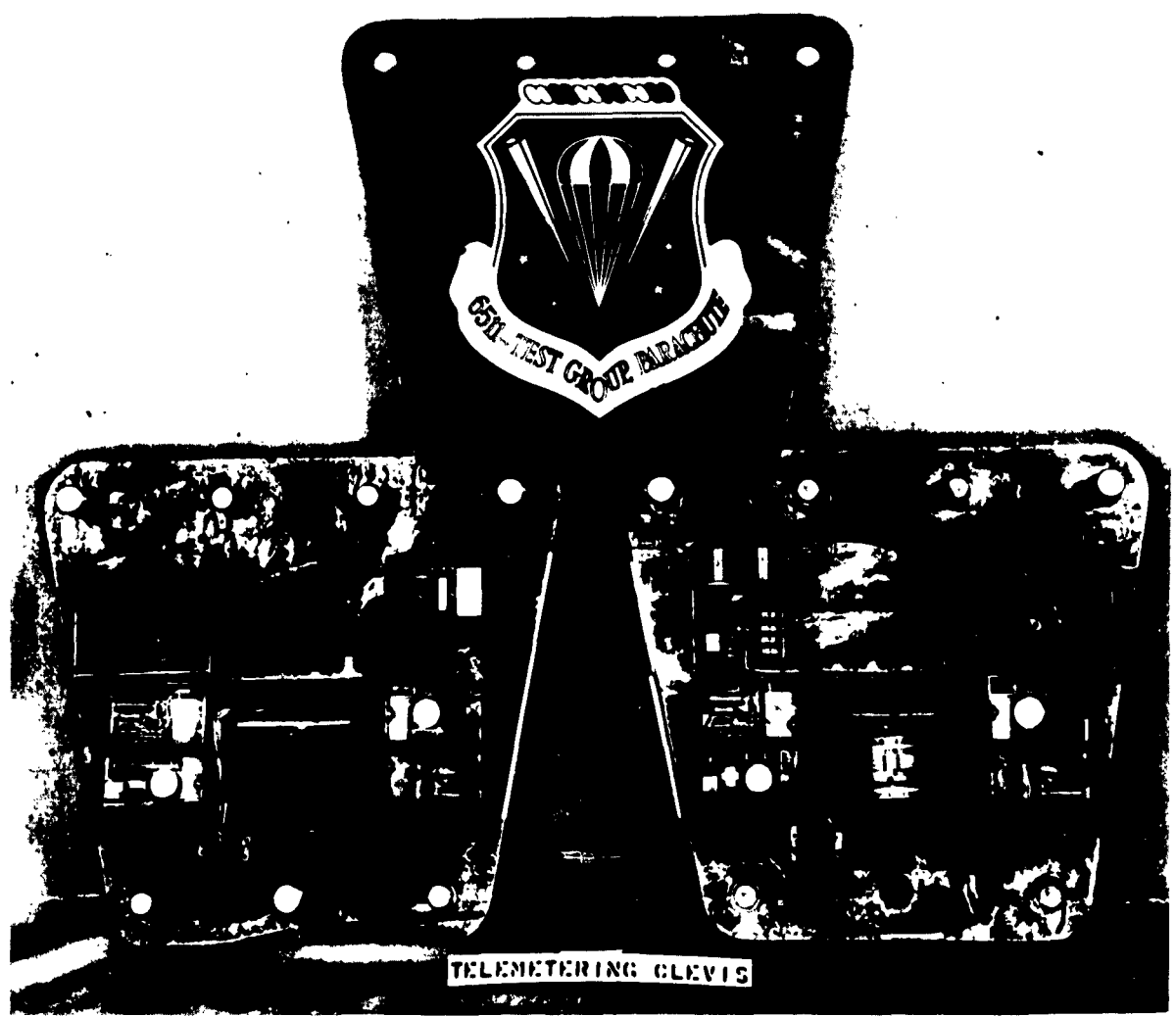


Fig. 2 - Internal view of telemetering clevis

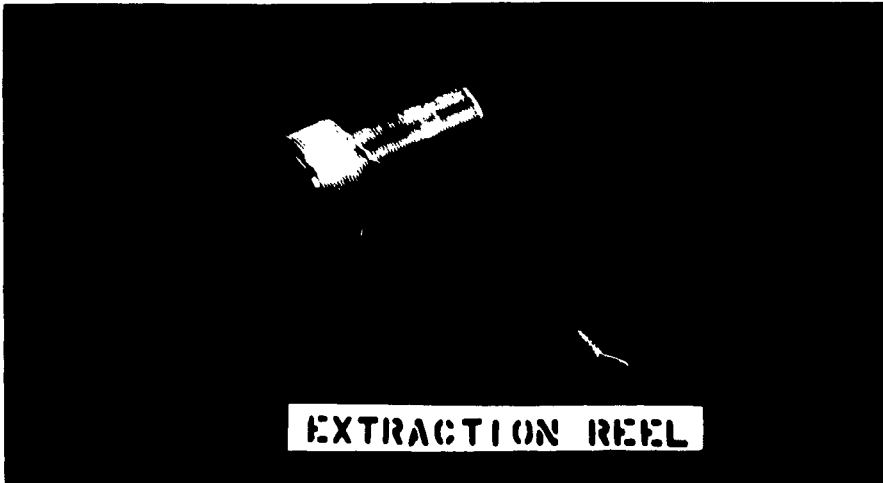


Fig. 3 - The rate of extraction measuring reel

that would be required. Two permanent magnets were mounted on one face of the drum. These were diametrically opposed and spaced 6 inches apart around the circumference. A magnetic pickup coil was mounted on the supporting bracket in such a position as to allow the magnets to pass beneath the pickup. As the drum rotated, the signal impressed upon the pickup was fed into a voltage controlled subcarrier oscillator to be telemetered and also recorded directly on an oscillograph. Spurious signals were received. The suspected sources were needless magnetic mounting

screws on the opposite end plate of the drum and excessive holes on both end plates. The entire system was modified to use only one magnet and in such a way that the end plates were screwed on the drum, like the lid of a jar, rather than mounted with screws. This new construction eliminated the spurious signals and provided accurate extraction data. This extraction and recovery test, which was conducted in support of the U.S. Army, the most successful heavy cargo drop ever conducted by the USAF, was accomplished at El Centro, California, by the 6511th Test Group (Parachute).

A SIMPLE, EFFICIENT, ONE SHOT ENERGY ABSORBER*

C. K. Kroell
General Motors Research Laboratory
Warren, Michigan

INTRODUCTION

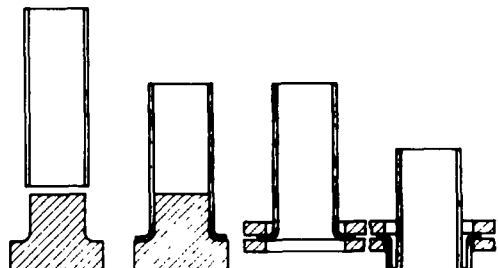
The frequency in engineering practice of requirements for a single shot expendable energy absorber provides a stimulus to search for additional and improved devices to serve this function. Such devices are in general employed either to adequately dissipate the excess energy of a single deliberate mechanical process or to function normally as a rigid structural member while possessing inherent energy absorption capacity as a protective measure against accidents or overloads.

This paper describes an energy absorber of the above type which has been developed at the General Motors Research Laboratories. The device is inherently simple and is characterized by a rectangular force-displacement relationship and high specific energy absorption capacity. Both a qualitative discussion of the mechanics of the plastic deformation process involved and a graphical summary of the experimental performance data which have been collected to date, are presented.

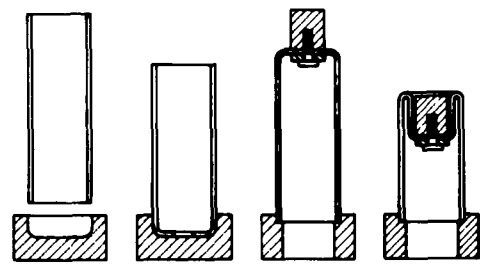
DISCUSSION

Basically, the energy absorption process involved is that of simply turning a thin walled ductile metal tube inside out. The units, or capsules, are preformed by flaring one end of a length of tubing, clamping around the flare periphery and applying an axial load to the opposite end. At a sufficiently high force level, yielding within the flare radius occurs and results in a progressive transformation into a fully developed circular roll radius. The flaring can be either of internal or external character, and the entire forming sequence for both types is illustrated in Fig. 1. Figure 2 exhibits the

*This paper was not presented at the Symposium.



Forming Sequence For Type A Capsules



Forming Sequence For Type B Capsules

Fig. 1 - Forming sequence for Type A and B capsules

basic geometry and characteristic dimensions of an externally flared or type A capsule to which virtually all of the experimental data which have been collected apply.

Once the roll radius is fully developed, subsequent deformation consists of a uniform rolling action in which the tube is literally turned inside out. An interesting characteristic of this action is that the lower extremity, or roll radius domain, of the capsule displaces axially only one-half the input stroke (i.e., the maximum available stroke is twice the original capsule length), as can be seen in Fig. 3. Also, an efficient energy absorption process is involved since every elemental volume of the tubular shell

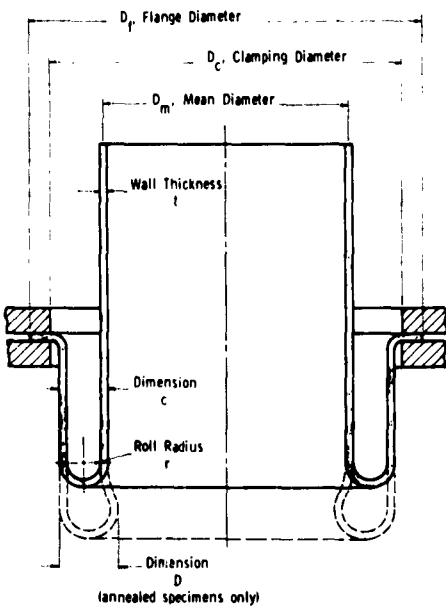


Fig. 2 - Characteristic dimensions of Type A capsule

deformation process involved precludes an analytical treatment, and performance data are therefore by necessity of experimental origin.

3003 ALUMINUM

Most of the work has been carried out with 3003 aluminum at P_{cr} levels in the range 600-4000 pounds. The data accumulated to date are summarized in Figs. 4 through 11*.

Figure 4 is a typical static force-displacement diagram covering both the preform and subsequent collapse stages. The behavior of a preformed unit initially unloaded is indicated in broken line. The constant force characteristic of the process is clearly indicated.

Figure 5 exhibits plots of static critical rolling load P_{cr} versus wall thickness for a constant mean diameter and for both the annealed and half-hard conditions. The nonlinear characteristics of the plots are not surprising when it is considered that the wall thickness acts somewhat in the form of a beam depth factor

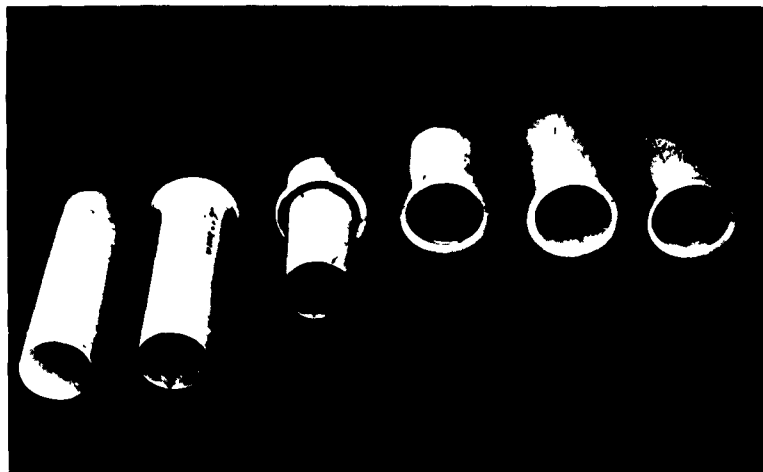


Fig. 3 - Photograph illustrating sequence from original tubular blank through preforming and the various stages of collapse

which progresses around the roll radius is subjected to 3 discrete plastic deformations: (1) flexure into the arc of the roll radius, (2) a simultaneous circumferential extension and (3) a reversed flexure back into a straight segment. The action occurs under a constant axial force, or critical rolling load, P_{cr} , which is a function of tube diameter, wall thickness and material properties. The complexity of the plastic

within the roll radius domain, where the plastic flexural action occurs.

Figure 6 is a plot illustrating the variation of P_{cr} and the characteristic dimension C

*Capsule specifications as to dimensions and heat treatment are provided on the individual figure sheets

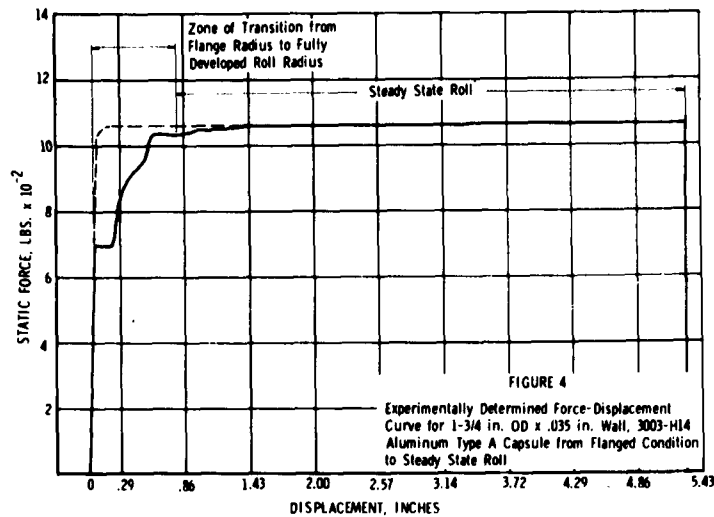


Fig. 4 - Experimentally determined force-displacement curve for 1-3/4-inch OD x 0.035-inch wall, 3003-H14 aluminum Type A capsule from flanged condition to steady state roll

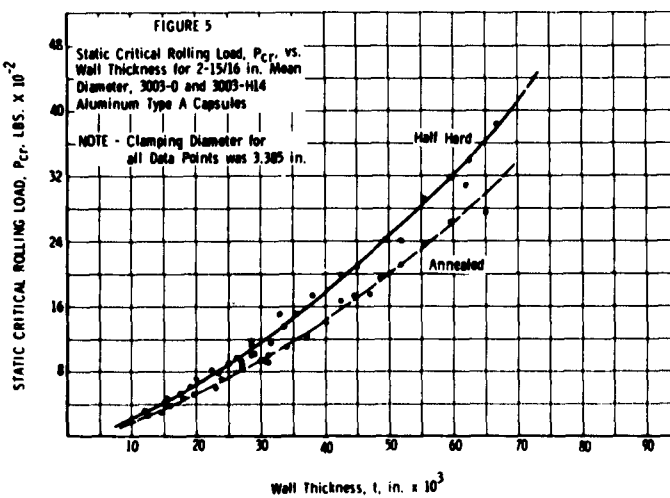


Fig. 5 - Static critical rolling load, P_{cr} , versus wall thickness for 2-15/16-inch mean diameter, 3003-0 and 3003-H14 aluminum Type A capsules

with mean diameter for a constant wall thickness. Both quantities are observed to increase with the mean diameter. Because of the great sensitivity of P_{cr} to small variations of t , and because t is not exactly identical for every data point comprising the curve, the accuracy of this plot is limited, but the general trend should be established.

Figure 7 illustrates the variation of dimension C with wall thickness at constant mean

diameter for both the annealed and half-hard conditions. Dimension D, which is characteristic of the annealed specimens only, is also shown as a function of wall thickness. The relationship appears to be essentially linear in both cases.

Figure 8 exhibits another dimensional variation with wall thickness at constant mean diameter — that of the ratio of roll radius to

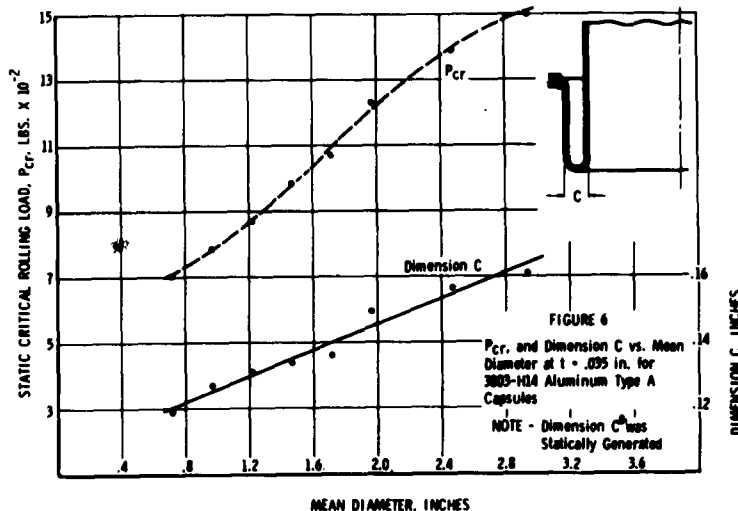


Fig. 6 - P_{cr} . and dimension C versus mean diameter at $t = 0.035$ inch for 3003-H14 aluminum Type A capsules

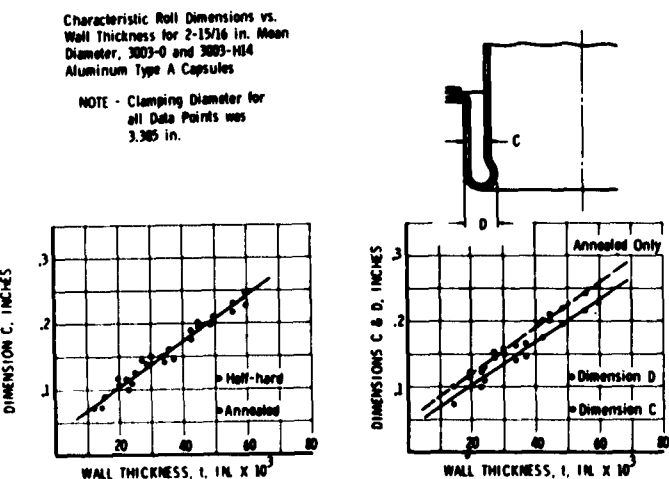


Fig. 7 - Characteristic roll dimensions versus wall thickness for 2-15/16-inch mean diameter, 3003-0 and 3003-H14 aluminum Type A capsules

wall thickness, r/t . It is observed that this ratio decreases nonlinearly with an increase in wall thickness and appears to approach a value of 1 at the higher thickness levels. It is obvious that there exists an upper limit of the wall thickness for any mean diameter beyond which the

rolling process will break down, but these values have not been experimentally determined.

Figure 8 illustrates the manner in which the specific energy absorption capacity (in units of ft lb/lb) varies (1) with wall thickness for a

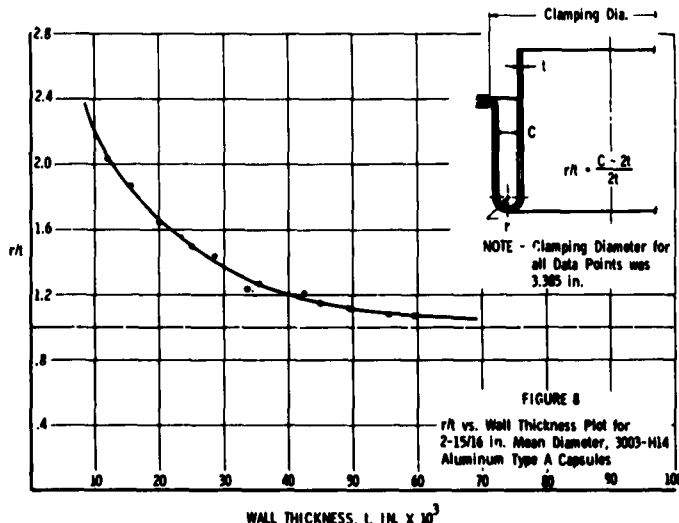


Fig. 8 - r/t versus wall thickness plot for 2-15/16-inch mean diameter, 3003-H14 aluminum Type A capsules

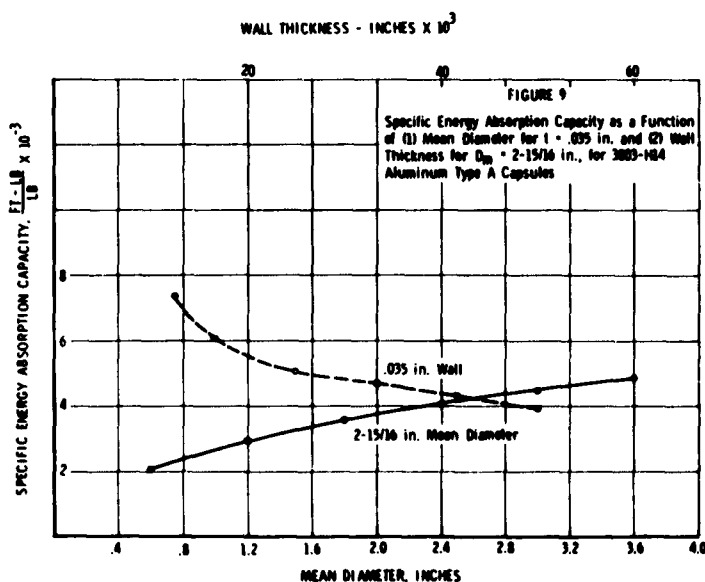


Fig. 9 - Specific energy absorption capacity as a function of (1) mean diameter for $t = 0.035$ inch and (2) wall thickness for $D_m = 2-15/16$ inch, for 3003-H14 aluminum Type A capsules

constant mean diameter and (2) with mean diameter for a constant wall thickness. The points for these curves were computed from the P_{cr} values taken from the plots of Figs. 5 and 6. It is seen that the units become more efficient on a weight basis as the ratio of wall thickness to mean diameter is increased.

The values given are practical values, i.e., the energy absorption capacity of a specimen of length 1 stroked through a distance 1. Actually, since it is possible to achieve a stroke length of 21, the theoretical specific energy absorption capacity for the process would be double the curve values. However, since in practice it is necessary to provide a member to transmit the load into the specimen, the weight of this member (regarded as an extension of the specimen) must be taken into consideration.

The rolling action has been observed to occur at a load considerably less than that required to collapse the original tubular blank under direct compression. It would appear that there exists a theoretical maximum energy absorbing capacity which may be associated with an unrestrained thin walled cylindrical shell loaded along its longitudinal axis and stroked through a given distance, regardless of the mode of deformation involved. This value is determined by the collapse load in direct compression, although it is not achieved in this process because of the load fluctuations

which occur subsequent to incipient buckling. If, however, by some means it is possible to allow the load to build up to just below the direct compression collapse value and then maintain this constant over the entire duration of the stroke, the maximum capacity of the tube as an energy absorber would be realized. As an effort in this direction, attempts were made to supplement the capsule rolling process with various auxiliary load generating processes, such as gouging or scraping material from the surface.

Figure 10 is a plot of P_{cr} as a function of the depth of penetration of variously shaped discrete drag elements for a particular capsule specification, the normal P_{cr} of which is 3800 pounds. The drag elements in this case were (1) a 100° conical point, (2) a 0.20 inch diameter hemispherical point and (3) a conventional set screw "dog point." It is seen that 6 dog points advanced into the capsule wall 0.027 inch effected an increase in rolling load to 5840 pounds, or slightly more than one and one-half times the normal value.

Better results have been obtained with a continuous, closely spaced assemblage of drag elements distributed uniformly around the exterior surface of the capsule. This has been achieved by knurling (both diamond and straight patterns) the inside diameter of a split ring and then tightening this around the outside diameter of the specimen just above the clamped flange.

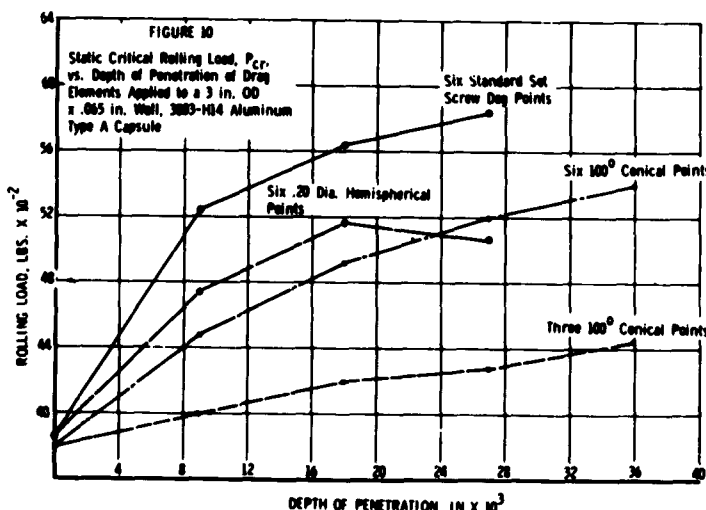


Fig. 10 - Static critical rolling load, P_{cr} , versus depth of penetration of drag elements applied to a 3-inch OD x 0.065-inch wall, 3003-H14 aluminum Type A capsule

Figure 11 illustrates the manner in which the rolling load was observed to vary as the knurled split ring was clamped more tightly around the surface. An increase in the rolling load to 9000 pounds, or 2.37 times the normal value, was achieved in this manner.

It has been established that changes in capsule stiffness locally can be effected by various techniques such as by reducing the wall thickness over a given capsule length or by cutting longitudinal slits into the wall. However, no pertinent quantitative data are currently available. The observation has also been made that there is an increase in the critical rolling load under dynamic loading conditions. Even within the impact velocity range of 10-30 ft/sec. indications of a significant increase with velocity have been observed. Increases of the order of 15 percent of the static value have been estimated for the upper end of this range, but further closely controlled experiments are considered necessary to verify these values and to firmly establish the true relationship between rolling load and impact velocity.

OTHER MATERIALS

All of the foregoing has applied to 3003 aluminum in either the annealed or half-hard conditions. Very limited work has been conducted with other materials with various results.

6061-T6 Aluminum

All attempts to roll 6061-T6 aluminum, regardless of dimensions, have been unsuccessful. However, wall thicknesses less than 0.035 inch have not been tried and may conceivably include a range wherein the rolling process could be established.

Mild Steel

Mild steel has performed very well as a capsule material within the range of variables investigated. Table 1 shows most of the data collected on steel to date. Since the range of parameters was large for a relatively few data points the plotting of informative characteristic curves was precluded.

APPLICATIONS

A study of the potential application of these energy absorption capsules to the design of force attenuating collapsible steering wheels has been made. They have also been considered for use in lunar and planetary soft landings of spacecraft, for cushioning air drop cargo and as one-shot overload protectors for railway rolling stock. Other potential applications are as follows: as a safety device for elevators; as buffer elements for nuclear reactor control rods and as yieldable seat anchors for installation in airliners.

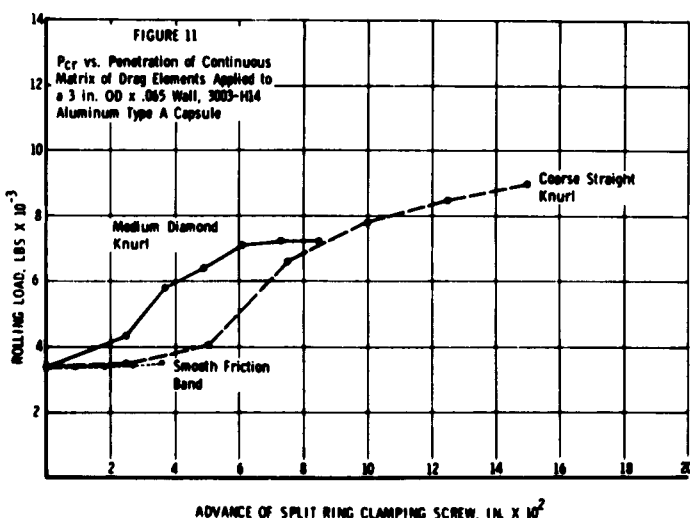


Fig. 11 - P_{cr} versus penetration of continuous matrix of drag elements applied to a 3-inch OD x 0.065 wall, 3003-H14 aluminum Type A capsule

TABLE 1
Data on Mild Steel Capsules

Capsule Size (Type A) (in.)	Heat Treatment	Construction	P _{cr} (lb)	Remarks
1-7/16 ID x 0.017	N ¹	Spot Welded	900	Rolled well although seam tore
1-7/16 ID x 0.030	N ¹	Spot Welded	2160	Rolled well although seam tore
1-7/16 ID x 0.030	FA ²	Spot Welded	2150	Rolled well although seam tore
1-7/16 ID x 0.030	FA ²	Arc Welded	2100	No tearing
2-15/16 ID x 0.017	FA ²	Spot Welded	1140	No tearing
2-15/16 ID x 0.017	N	Spot Welded	1230	No tearing
2-15/16 ID x 0.030	N	Spot Welded	2900	No tearing
2-15/16 ID x 0.030	N	Arc Welded	2800	Seam tore
2-1/2 OD x 0.067	N	Seamless	11500	No tearing
2-1/2 OD x 0.067	FA	Seamless	11400	No tearing
3-1/2 OD x 0.066 ³	N	Seamless	14500	No tearing

¹No heat treatment

²Fully annealed

³Type B capsule

* * *

Section 6 PANEL SESSION I

ENGINEERING APPROACH TO THE PROTECTION OF A FRAGILE ITEM

Moderator - F. J. Lindner, U. S. Army Engineer Research and Development Laboratories, Fort Belvoir, Virginia

Panelists - Paul Franklin, North American Aviation
Gordon Mustin, Reed Research, Inc.
S. C. Schuler, Royal Radar Est., Malvern, England
Robert Leonardi, Picatinny Arsenal

FOREWORD

Package designers are frequently faced with the problem of how to protect a sensitive item during shipment. Approaches to this problem may vary in their degree of technical sophistication, but, in some way, the designer must always have information concerning:

1. The fragility characteristics of the item.
2. The environment to which the package will be subjected.
3. Characteristics of cushioning materials that may be used in design.

Discussions during this session touched upon some aspects of each of these areas. These discussions have been summarized and rearranged, insofar as possible, under four appropriate subject headings. All comments were edited for clarity and a few comments were not included, either because they were not recorded or because they repeated a point brought out earlier in the discussion.

In an informal session of this type the discussion is likely to be centered around the subject brought up by the first questioner. In this case it happened to be the railroads which

bore the brunt of the attack and therefore are treated in the first subject area. By mere chance, then, the problems of other transportation media were not discussed even though they may have been equally in need of treatment. The reader will discover, however, that the position of the railroads was well defended by its representatives.

The second area treated is on the subject of fragility, a rather nebulous term to indicate the degree of susceptibility of an item to damage by shock or vibration. It is interesting to note the British approach to this problem and the reaction of some American engineers to it. The one point that all participants agreed upon was that in testing to determine fragility one should attempt to simulate the complete service pulse and not just some peak value of acceleration.

The third subject area is really a "catch-all" for comments dealing with design philosophy, testing, reliability and topics of this sort.

There was very little discussion on the last subject, but it is considered important enough to separate from the others. The problem of statistically defining the handling environment of packages could indeed form the basis for a session all its own.

RAIL SHIPMENTS

Mr. Rice of Goodyear Aircraft commented: "Harper Welton and I have been working with an AIA Committee whose aim is to get some idea of what these environments are going to be. For a long time I have had to make up my own rules concerning what to do about humping loads. For this reason I sent out a questionnaire to most of the aircraft companies asking, among other things, how they handled this problem. It seems that they are in the same boat. Some of them responded, "Well, we use the applicable specification." MIL-E-5272, for example, designs for 10-pound items and they apply this to 10,000-pound objects. As far as I'm concerned, the question of what humping loads to use for big fragile items is a serious one. There is some agreement on 8 miles per hour which may not be bad, but we really must know what these loads are or our items are going to arrive in pieces. Several of ours have done just that. So, I would like to have humping loads discussed here. Do you use g or velocity change? If you use velocity change, what do you use, how fast do you stop it, and so on?"

Mr. Mustin (Panelist) responded: "The only valid data in which I personally have any confidence is the study run by the Pullman Company many years ago on the statistical distribution of humping impact speeds. There were some 555 events in the yards around Chicago. The range covered from about 2 mph to 14 mph. Now if it is assumed that we must have 95-percent confidence that our velocity change is going to duplicate the railcar impact, we would be dropping our containers about 65 inches.

"This raises a real question concerning the validity of the tests used to simulate coupling loads. They don't simulate! Why don't they? Simply because we are banging our containers into a barrier as rigid as we can make it, whereas in a railcar there are at least two degrees of freedom if not three or more, and the coupler itself acts as a spring. Also, there is the dynamic deformation of the car itself. Mindlin's classic paper* has an approach which a person can easily follow and prove to himself that he can bang a container into a wall at 8 ft/sec and be very happy with it, yet in a coupling situation at the same velocity the load will go through the end wall of the container. Fortunately for my major client, the Bureau of Naval Weapons, the humping, inclined impact and pendulum impact tests simulate quite well one situation they are concerned with: the slamming of a load against the side of a ship.

*Mindlin, R. D., "Dynamics of Package Cushioning," Bell System Technical Journal, 1945.

"Mr. Rice's question really was, "What impact velocity should we use in the laboratory?" Although there is no easy answer to this question, there is reasonable confidence in using an average of about an 8-mph impact. However, the test is not a go-no go test. One should analyze the type of car he is going to use, do a two-degree-of-freedom system analysis and allow extra travel room if he needs it."

Mr. Haber of Lord Manufacturing Company mentioned that Sandia Corporation had also done extensive work on this subject. He mentioned that in 1953 they gave a paper in Los Angeles.*

Mr. Mustin agreed, but said that he didn't recall seeing a decent statistical distribution on the thing. He confessed that it may have been his omission, but stated that he did preface his remarks by saying that one can draw a statistical distribution curve of the Pullman Company data and the sample is adequate.

Mr. Welton of the Northrop Corporation raised the question as to what can be done to assure 100-percent shipment reliability of an extremely expensive and important item when humping is involved.

Mr. Mustin suggested, "Sixteen miles per hour and prayer."

Mr. Leonardi (Panelist) asked "What is the natural frequency of the suspension system of this large item?"

Mr. Welton said that it was very low.

Mr. Leonardi then commented as follows: "There you have a real problem. In railroad humping you have to watch out for the response level more than the velocity of impact or rate of velocity change. If you have a very low natural frequency, say 6 to 10 cps, the big danger in humping is in exciting the mass on its suspension system at its own natural frequency. Normal railroad impacts range in response time anywhere from 20 to 80 ms. If your system natural frequency is in this range, you might be better off to rigidize it or soften it to avoid this area. The real problem in softening it, however, is that you just don't have enough room to do so. One approach that was used on Nike guidance systems was to use something on the order of a Lord dissipator which controlled the response enough so it could be shipped."

Mr. Rice continued: "We make the Nike Zeus antennas and they are very soft. Their

*Shock and Vibration Bulletin No. 21, Nov. 1953, ASTIA No. AD 55364 (Confidential).

natural frequency is 4 to 5 cps and you can't change it. They are huge things and we ship them in the biggest possible piece you can put on a flatcar, which is usually overwidth, overlength, and overheight. We clear tunnels by inches. These antennas have to reach the west coast absolutely undamaged, since a boat picks them up there to carry them to an island. We have found that the Southern Pacific special car solves the problem. The Lord Tylastics are helpful too. However, if you do a dynamic analysis on these things, they are devils because the impulse time comes right in at the natural frequency."

Mr. Mustin observed that comments have been concerned about specialized containers and packaging problems. He further remarked:

"I think it appropriate to remember that in the simulation of railcar coupling, we have to go into the laboratory with an idea of the kind of damage we are going to get. If you have a container which is in some way rigidly mounted to the car structure, then a two-degree-of-freedom analysis is reasonably feasible. However, overtravel or overshock is not the cause of all forms of damage found on the railroads. The vast majority of goods are shipped in corrugated fibreboard containers more or less tightly packed in the car. There are some very interesting ASME papers covering this area and it is quite clear that the first shock often doesn't do any damage at all. It compresses the whole load and this compression is resisted by friction forces and the flat crush strength of the fibreboard. The first shock does produce about 18 inches of slack in the opposite end of the car and if the car starts with a jerk or is coupled in the opposite direction, the load tumbles. This, I believe, is the prime cause of damage to canned goods, for example. On the other hand, this original shift can cause compression-type failures in certain brittle loads. We can't use nice mathematical relations on this, but if we try to simulate the humping shock, we should try to simulate the kind of damage we expect to get."

After considerable discussion on other subjects, Mr. Guins of C&O Railroad defended the position of the railroads. He said: "I hesitated to stand up and say anything because I have only a white badge and I'm here under sufferance. Even though I'm the cause of most of your troubles I find I'm probably the lowest man on the totem pole because nobody even asked me what I produce. Instead, they go to the aircraft companies to find out about it. I felt, however, that I ought to put some of you people at rest a little bit.

"We do actually operate railroads. We do deliver things to destinations without damage,

occasionally. You talk about things like Zeus that really don't mean anything to me, but I do understand that they have a few electronic tubes in them, and so on. We do ship a tremendous number of radios and television sets all over the country and, whether they're fragile or not, they seem to get there.

"I was annoyed when the first questioner said he had sent a questionnaire to the aircraft companies and didn't get any answers. He didn't send a questionnaire to the railroads that do move the stuff. Since reading the article by Mindlin, we have made a tremendous effort in the last 10 years to find out what the environment is. We did get some data and we published it. Nobody reads it.

"We also spend a lot of effort on railcars to reduce the environment to a level that will not damage things. We were given the compliment that if you howl loud enough you'll get a car with a hydrocushion. Actually we have quite a few thousand cars like that. If we are consulted about fragile equipment we will give a lot of advice and provide the equipment that will move the stuff where it needs to be. When the items are off-sized and very expensive, we even go so far as to provide special trains which move at low speeds to eliminate a lot of the frequencies which might be involved at higher speeds. We will move it on short trains to eliminate a lot of impacts and we don't switch the equipment.

"There is considerable data on humping speeds. Someone mentioned the statistics of the Pullman Company. It does give a distribution of impact speeds, but it really doesn't mean a whole lot unless you also get some idea of what happens during the impact. Every car has a draft gear. I admit that the draft gear might not be as adequate as you would like, but we try to improve it. This draft gear produces an impulse somewhat different from the impulse produced by dropping something on the floor at the same impact velocity. If we ever dropped railroad cars like you do packages, we wouldn't have any railcars left.

"We do produce damage, but it is a reasonably small percentage. When the draft gear goes solid, roughly at 4 mph for a fully loaded 50- or 70-ton car, a force of about 500,000 pounds is produced on the car which is somewhat over 2 g on the lading. At 10 mph impact the force on the coupler might go to 1,500,000 pounds which is still only about 10 or 15 g. We don't produce anything like 30 or 50 g in our operation because our cars couldn't possibly take it. We are not really as guilty as we were painted in the beginning.

"This is really a problem of three groups of people. The transportation people have to define the environment and try to improve it so that the hazards are reduced. The manufacturers have to develop the fragility factors or decide the levels to which the items must be protected. For one-time expensive items like the Saturn, special arrangements must be made to move it, for example, by barge. On the other hand, when items are produced in quantity, I doubt that they couldn't afford to spoil a few to get them there. The third group has to design the cushion and has to know both sides of the story before an effective job can be done."

Mr. Mustin said he was sorry that Mr. Gunins had misinterpreted him, that he didn't quote any g factors. Since he hadn't seen any of Mr. Guins' papers, he asked where they were published. Mr. Guins responded, "In the Shock and Vibration Bulletins."*

Mr. Mustin cited some additional references† and said, "The burden of my remark was that in the velocity change that is produced during coupling, starting, or stopping, overtravel may occur for a shock-mounted item in a container even though input to the container via the car floor may be less than 10 g."

Mr. Eustace of the Martin Company directed a question either to the panel or a representative of the railroad. "We have up until now mentioned impact speed as the main criteria, but this was just questioned by Mr. Guins. I would like to add a comment in the form of a question. What is the likelihood, in statistical terms or otherwise, of the classical case developing for which we often test, i.e., a car being humped at x miles per hour

into a 150,000-pound loaded railroad car with the draft gear closed and the brakes set with half a million pounds of loading behind it? Or, in fact, do we usually have loose draft gears and nonset brakes, etc.? Is there any consensus of opinion as to what constitutes a practical worst condition in this respect?"

Mr. Lindner, the moderator, cited recommended AAR test procedures and some references in Shock and Vibration Bulletins † where impact speeds are given.

Mr. Eustace pursued the matter further. "This does not require getting at this classical worst condition for a practical test. Assume one can test under any condition he wishes. Where one must hump and the procedure is at the option of the test engineer, which way should he do it? Does he produce the worst conditions and design for them, 16 miles per hour, closed draft gear, locked brakes, and so on, to get the absolute 10-sigma probability of assurance?"

Mr. Williams of AAR commented: "I'll refer to that impact test procedure that Mr. Lindner described. We've used it for many materials, including explosives, on open top and closed cars for many years. The test simply involves 3 impacts in one direction at 4, 6, and 8 mph; turn the test load around and impact it once more at 8 mph. You refer to the classical example and ask what the expectation would be. You can expect almost anything, obviously, but we have found through many years that this test is practical."

A gentleman who did not give his name offered the following comment: "Three years ago we conducted some tests at Redstone on one of our pieces of equipment. In fact, we hit the car so many times and at so many speeds that we finally tore the car up. We cracked the coupler and ripped out the rivets. We were testing an antenna mounted on a trailer. At high speeds we were getting 70 g on the bed of the car, but on the bed of the trailer, due to shock mounting, we were getting around 10 g. On the antenna we got 7 g."

He went on to say that if AAR publications on how to load, block and brace a car are followed, very little difficulty would arise with respect to rail damage. He recommended that AAR should inspect loads to see that their procedures are followed. He applauded the new "damage-free" freight cars.

* Theory Behind the Damage to Lading Due to Vibration, "Shock and Vibration Bulletin No. 15, March 1950, ASTIA No. ATI 93010 and "Reduction of Available Vibration Data Gathered on Railway Boxcars for Engineers and Designers," Shock and Vibration Bulletin No. 16, Oct. 1950, ASTIA No. ATI 111265.

† Roehm, J. M., "Dynamic Testing of Freight Cars," ASME Paper 52-SA-41, Jan. 1952; Peterson, W. H., "Cushioning Requirements for Adequate Lading Protection" ASME Paper 59-A-312, Dec. 1959; Newcomer, G. H., "Study of Vibration Frequencies Under Impact Conditions," Dec. 1959; Abbott, R. E. and Lanning, H. K., "Increased Cushioning Capacity, A Requirement of Tomorrow's Freight Car," ASME Paper 59-A224, Dec. 1959; Bickle, T. T., a paper on the Santa Fe special car (title not known), ASME Paper 59-A-221, Dec. 1959.

‡ Shock and Vibration Bulletins No. 15, 16, and 21, as referenced earlier.

Mr. Rice wanted to assure the railroads that he was not persecuting them. He said, "As a matter of fact, it's amazing how inexpensive it is to get a private train of your own. We had one that went up and down the west coast consisting of an engine, a flatcar with a rotating bearing, and a caboose. They sent really high calibre people, a supervisor of the railroad, who watched the train from the time it left until it got there. They made sure it never was humped, that it never reached critical speeds, that the bearing was still rotating, etc. We got good cooperation and it only cost a couple of thousand dollars. When I sent a questionnaire to the aircraft companies I just wanted to know what they were shipping to, not that they were right. They hadn't asked the railroads either."

Mr. Eustace restated his earlier question, this time directing it to Mr. Guins. "We agree that the criteria of 4, 6, and 8 mph in one direction and 8 mph in the other are probably realistic. I would still like some sort of an answer as to the condition of the static load or the impact anvil cars. Do we need twice the weight of the car, half a million pounds, or two-million pounds with the draft gear closed? What is the general practice? How does the industry feel on this particular issue?"

Mr. Guins responded, "As usual, I'm only going to stick my neck out a mile. In impact testing you put an item in your test car, then hit the test car with a loaded car and let them roll. The question is, what would happen if you had it backed up, a condition that frequently occurs in a railroad yard when making up a train. You have to remember that behind the car you have two draft gears. Their period is on the order of 0.01 second. By the time a peak is reached, the cars begin to move and the other two draft gears come into action. Our experience indicates that the number of backup cars is not really too important except in the case of a very light load, because the main parameter that produces the resistance is the inertia of the car itself."

Mr. Butler of the Lord Manufacturing Company cited some experience gained during hump tests conducted for the purpose of protecting automobiles during shipment. They were impacting an 85-foot, low-deck car into a standing buffer car loaded with approximately 50-85 thousand pounds of scrap steel at 2, 4, 6, 8, and 10 mph. The brakes on the buffer car were set. Even at 10 mph they found it impossible to get more than 10 g into the deck of the impacting car. On impacting into two cars loaded with scrap they obtained about 10-12 g at 8 mph.

However, probably because of the long length of the car, the vertical components started to climb. They found that, in order to get a fairly realistic figure that could be duplicated, they had to impact into three cars loaded with scrap with the brakes set at 10 mph. This produced 15 g horizontal and 6 g vertical. The vertical component was a function of the structure of the car. On the other hand, they found that, with the brakes off and slack in the system, they had to impact at about 14 mph to get the same g input.

Mr. Leonardi said that their experience tended to confirm Mr. Butler's findings. Impact tests on flat cars of 1945-47 vintage produced vertical components at the midpoint of the car as high as 20 g, but of short duration. At 8 mph longitudinal pulses were of the order of 60 ms while vertical components were 10-15 ms.

Mr. Eustace directed a question to the panel member from England. "Some of us have had a controversy, somewhat in jest, as to whether a problem of railroad humping exists with the European class of cars with their different type of construction. Do they hump? On shipping our equipment around the world in military usage should we anticipate railroad humping in foreign countries and, if so, what might it be?"

Mr. Schuler, Royal Radar Establishment, Malvern, England answered, "I've been advised to answer, no. I really don't understand what is meant by the term 'humping.' I believe it's a colloquial American term. Perhaps you are referring to 'shunting.'"

"I really can't help you very much because, quite honestly, this hasn't come my way. We do have an inclined plane test for certain very heavy items, of the order of 1000 pounds and upwards. I can't tell you what this test amounts to, but it appears to be extraordinarily difficult to meet. As a consequence a — over here I think you use the expression — waiver is usually sought for and given.

"We, of course, are a very small country, thus the bulk of our equipment, including missile equipment and electronics, is moved by truck. We don't have the heroic programs that you have here. Our production items in this type of hardware are relatively small ground-to-air missiles for which the accent is on lightweight and high mobility.

"I'm sorry I can't help you very much, but I can get you the details of this test which is so eagerly bypassed from time to time."

Mr. Guins felt he could give an answer to Mr. Eustace. He said, "To my great shame I have to say that our friends in Europe are much easier on equipment than we are. They start out with equipment at least half the size of ours while their protection devices are about twice as good as ours. They run short trains, therefore their humping speeds are lower. If you pass our requirements, you won't have any problem at all in Europe."

Mr. Butler directed a question to Mr. Leonardi and Mr. Guins as follows: "We have found on test runs that we have made that the position of a test car in the train made a fabulous amount of difference to the amount of damage that was produced. The indications are that the ideal spot to be located in a multi-car train is six cars behind the engine. For example, on a 30-car train it was determined that anywhere from the sixth to the twentieth car was reasonably good. I'm not talking about humping or building up a train, but strictly about impacts received due to take-up of slack or extending slack in the system as various grades are traversed and the train changes speed. Of course, as the train speed increases and the length of the train increases, the corresponding slack taken out of or put into the system is varying. For example, on one test with 130 cars we found that the 90th or 100th car was constantly taking from 12 to 15 g on the entire trip.

"The question that comes up is, how good is the recording equipment? The data is no better than the equipment used. I think in this area we could stand to improve. Do you have any comments or experience in that respect?"

Mr. Leonardi commented, "I did get some data on this once from the Sandia Corporation and AAR. They have done some work along these lines which is pretty much based upon the concept of a marching column. The fellow 4 or 5 back from the leader can maintain a pretty steady pace, but the guy in the rear is running like the devil to catch up. Most data that I've seen seems to bear this out."

"With respect to humping, the military might do well to stipulate the use of idler cars in the makeup of a train when highly fragile items are involved. The figures now indicate loaded idler cars, perhaps two in front and two in the rear of the makeup car. This pretty well bears out what the gentleman from AAR said, in that not too much benefit is derived from draft gears beyond the two additional loaded cars."

Mr. Guins offered these comments with respect to the environments during train

operation. "There is a lot of misconception about the 'whip' on a train. One talks about a man in the caboose flying all over the place during the train starting, etc. It is true that the worst place in a train is about 3/4 length; it is here that damage is more or less expected. We do occasionally break a train in two when we have a 'run-in' and 'pull-out,' but I can't conceive how 12 g is produced because the maximum force the coupler will take is about 500,000 pounds. Beyond that it busts."

"I was very much interested in that problem about 10 years ago because I felt that we might be overstating the seriousness of switching speeds and that the train operation might be responsible for a lot of damage. We spent three months riding in a train with test equipment. We located ourselves at 1/4, 1/2, and 3/4 length, on short trains and long trains, going at slow speed and high speed, through Michigan where there are lots of little hills. We found that if you have a car with an operating draft gear you never exceed 1 g. We also tried it with an inactive draft gear, 2-3/4-inch slack instead of the gear, and found the forces to be very high. Under this condition we burst the bolts on the first run."

"Under normal conditions, even though a man may find himself on the floor when he was standing a second ago, an empty pail on the floor won't move, primarily because of the higher center of gravity of a man. Therefore, after three months, I concluded that the running of the train really wasn't responsible for too much damage. The main problem is still switching."

Mr. Olson of the American Association of Railroads submitted the following comments with respect to what had been said earlier. "Regarding the magnitude of acceleration on a long train, if we convert this to force at the end of a 100-car train probably the maximum force produced in buff or pull (tension or compression) as far as the coupler goes is 400,000 pounds. This could be just a fraction of the force under impact conditions."

"Mr. Guins was talking about certain g values and these correspond with what you would get by computation using Newton's second law of motion, $F = ma$. Some guided missile handbooks, government manuals, and publications of aircraft companies have quoted values anywhere from 30 to 50 g. One prime contractor was talking about 80 g vertical and 60-70 g horizontal. Why do we have these differences in values? The answer lies in the instrumentation used and its frequency response."

Mr. Olson went on to emphasize that peak acceleration readings without associated

frequencies or time durations are rather meaningless. He stressed the difference between measurements made with a ride recorder of low-natural frequency and those made with an unbonded strain gage accelerometer having a frequency response to 500 cps. A lack of understanding of the meaning of data has been a problem for many years.

He said, "When people come to us and ask what the worst condition or maximum g level that they can expect is, we have to ask what their equipment will stand. Is 0.001 second important? If not, why worry about 40 g and 0.001 second? Maybe they should worry about 3 g and 0.02 second. It is important, therefore, to consider the time factor along with acceleration."

With regard to the kind of shock pulse to use in evaluating a package, Mr. Olson recommended a triangular pulse or a half-sine pulse, but felt that a square wave was too severe.

Finally, he recommended that in dealing with the railroad, one should tell them all one can about the equipment involved.

FRAGILITY

Mr. Schenck of Rossford Ordnance Depot opened the discussion on fragility as follows: "The last few days we have heard a lot of excellent papers and discussion on how to determine the characteristics of various cushioning materials. However, along this same line we are going to have to know how to determine the fragility of an item we want to package before we can use this information. Are there any answers on that? The only thing I have heard is by Mr. Schuler from England. He said that they are using a lead base mass for determining fragility. Are we doing anything in this country? We are always at a loss because industry doesn't want to run destructive tests on their equipment."

Mr. Franklin (Panelist) offered these comments. "I think there have been a lot of people who have attempted to determine fragilities without considering the eventual packaging. For this reason we tend to find input pulses of very short rise time and duration which we are fairly certain will not be the case when the item is packaged. I'm not sure that a great deal has been done with respect to determining fragilities when the item is packaged for shipment."

"Classic analytical methods are available, but these are laborious and all sorts of simplifying assumptions have to be made, thus these

methods are usually not too much use. The situation is improving in that people who have computers available to them can sometimes use analytical methods to determine fragility for packaging purposes.

"The test to failure is probably the best method and we can simulate the pulse that we would get in a packaging application very simply by using package cushioning material to put the pulse in. However, as was pointed out, most manufacturers are particularly unwilling to let equipment be tested to destruction because it involves not just one piece but several in order to get a statistical distribution.

"There are proposals in the mill for programs to determine fragility for packaging purposes. My division of our company has made one to the Navy which we hope will be well received. I understand that Armour Research is doing a fragility study right now, but I don't know the details of it. However, at this point there is not a great deal of information available.

"To be quite frank, the crude methods that we have used have proved to be fairly successful, at least to the extent that our damage percentage has been very low. Of course, we may be overpackaging to a tremendous degree, but the way we do this is to check with persons who have a great deal of experience in handling the kind of equipment we need to ship. Those concerned with bench maintenance, and so on, usually have a pretty good idea what a piece of equipment will stand. We started this method several years ago simply by asking the field service people what they thought an item could stand in the way of a drop. Because they were familiar with materials like cellulose wadding, they were often able to tell us that an item would break if it were pushed off a workbench onto two thicknesses of cellulose wadding, for example. Knowing something about the characteristics of the material we were successful to some degree in relating this back in terms of maximum allowable acceleration. Granted that peak acceleration is not a complete definition of fragility, we did find ourselves to be fairly safe since the natural frequency of the items we were packaging was considerably higher than the natural frequency of the cushioning system we were using.

"Even though we have been fairly successful in using this method for determining fragility, most of us know that we are going to be too far on the conservative side and it's costing us too much to package and ship these items. Further, if everyone were doing it this way they would

each get a different idea of the fragility of the items concerned and would package to a different fragility level, thereby producing different packages even for the same item. So, we feel that a definite degree of standardization is necessary in the methods of obtaining fragility. As yet, I don't believe this has been done."

Mr. Schuler said, "I would like briefly to enlarge on what we do in the UK. It may possibly interest the questioner because, perhaps, I didn't make it very clear in my paper.*

"You may recall the slide showing a drop tester using a pneumatic ram. We have had this design for almost ten years. The approach that we take in regard to military electronic equipment is that fragility assessment tests should take place in the development phase of the hardware itself. Therefore, in our joint service environmental testing specification, the one that serves most equipment projects with respect to environments, is what was called ten years ago, a packaging information test. This test calls for the contractors to do a series of investigations using the machine I just mentioned. They are quite free, of course, to alter the deceleration arrangements, but there is a specification for the machine. No matter what they are developing, however, they are required to do a series of fragility assessments on this machine. Of course there are difficulties when one gets beyond a certain size and weight. The machine will cope with electronic packages in the order of 100 pounds and 3 feet³. This is by and large in the area where cushioning and low fragility figures, say 20 to 50 g, are particularly significant.

"We feel that this is a thing which is a part of equipment design and that these studies should be done in order that the person responsible for subsequent packaging design will have this data. As to what shape pulse, these are primarily half-sine pulses since the bulk of our cushioning media does have this type of characteristic. However, with the trend toward higher efficiency systems we ought to be looking for something which puts in a square pulse. I postulate the idea of using a lead block decelerator."

Mr. Humbert of Dow Chemical mentioned that, as a materials supplier, people come to him and ask, "Will your materials protect our items down to 5 g?" He wondered whether 5 g was a realistic value or whether, perhaps, they should more realistically say 25 or 30.

*"Recent British Developments in Package Cushioning, Dynamic Testing, and Instrumentation," page 87.

Mr. Mustin suggested that with rare exceptions you can't make anything that weak.

Mr. Franklin said that a lot of people are prone to quote design specification criteria for packaging purposes. This is the minimum level for acceptance of the item and doesn't tell anything about the maximum allowable acceptance levels. This is of concern to packaging people because if the minimum levels are adhered to overpackaging is the result. This is the basis for the entire problem of establishing realistic fragility levels.

Mr. Leslie of the Boeing Company remarked, "It seems to me that we are using shock as a fragility level where vibration can also be one. You see g's both places. A shock impulse may be on the order of 60-100 g for a short time duration and not hurt the item, yet 5 or 10 g vibration over a wide-frequency span can tear the thing to pieces."

Mr. Lindner agreed that there is a difference between the two and suggested that failures under vibration were fatigue failures whereas shock failure may be of the fracture type. He cited an example from his experience to indicate that misunderstanding in this area sometimes produced complaints about overtesting from designers.

Mr. Henny of the Boeing Company asked, "Wouldn't it be more realistic to define fragility in terms of g and frequency in all the harmonics rather than just in terms of g?"

Mr. Mustin allowed that it was reasonable but not practical.

Mr. Grabowski of Armstrong Cork offered the following: "Packaging engineers of the world, unite. You have nothing to lose but low g."

"As I sit back here, it seems to me that we are kind of skirting the issue. We have some of the best brains in package engineering in this room, as I understand it, and it must be that there is a general feeling of discouragement on some of these fragilities that are quoted so often. I frequently come across packaging engineers who say that the stress analyst or the designer is plain crazy. You have the group here that's supposed to represent the very forefront of the packaging industry. Why don't you get together and put across some of the views that all of you have concerning this abominable problem of low g? I would like some opinions from some of the people who have been working in the field much longer than I have as to what fragilities they feel

should be assigned to 90 or 95 percent of the 'delicate' items shipped in the country today."

Mr. Leslie of Boeing said that it was his experience that if an item gets by the vibration test it will, 90 out of 100 times, survive 50 to 60 g shock with a variation of around 6-15 ms time duration on the pulse. A lot of the time if the vibration spec is sufficient and if the designer is required to make his item meet the specification the item will have a pretty high-fragility level. He pointed out that this was the case at Boeing where the requirement is 0.4-inch double amplitude from 5-16 cps and 5 g from 16-2000 cps. Most of these packages, he said, will take 70-80 g at 6 ms.

Mr. Schuler stated, "I can't offer anything really novel in answer to Mr. Grabowski. Surely the point is, however, that the designers responsible for the actual item to be packaged should not consider their work done if they are going to divorce the final stage of the process. I mean, if you are going to spend a lot of time and energy developing a new piece of apparatus, then you must take into your design considerations the fact that it has to get to the end user in a reliable state. Therefore, to my mind, the environmental studies such as have been outlined must be included. I do agree absolutely with the last speaker from Boeing that, if you do really exhaustive and comprehensive vibration analyses of your structure to get rid of damaging resonances, etc., then you end up with an item very easy to package because you have improved it as you went along. However, this should not inhibit you from doing the last thing, some simple fragility assessments. This will just prove your work. I think this is the responsibility of the designer, since it's far too late in the story to give some fictitious figures to the package designer and expect him to go from there."

Mr. Mustin added, "I presume all of us cut our teeth at one time or another on Ray Mindlin's paper in 1945. If you will recall, he said that you have to know to what level to protect the thing or all the rest is, and I misquote him deliberately, 'hogwash.' Now let's face the issue squarely. Packaging engineers are pretty low men on the totem pole in their companies. As a contract designer who has a living to earn by pleasing the customer, I'm pretty low man with respect to arguing with the customer too far."

"I think the challenge is clear-cut for our government colleagues. If they are going to have the kind of progress they want, they must write it in the requirements. I think it's pretty shameful, as a matter of fact, that our British

colleagues have been doing this for ten years. It's perfectly possible to do it in the United States. Let's go spec writers!"

Mr. Borkenhagen commented, "Very seldom will I agree with Gordon Mustin, but I do work for Uncle. Although I have little to do with influencing spec writers, I definitely think our English friend is way ahead of us. We get the part after industry has developed it for us under contract. I'm going to do all I can to have our spec people put in a requirement that the fragility factor be determined. I hope it won't cost too much more."

Mr. Welton pointed out that, in the case of fragile items, the way a packaging engineer supports the item in the package has a lot to do with how fragile the item is.

Mr. Rice spoke up in defense of the designer. "I'm not a packaging engineer by trade. I'm a dynamicist. It is one horrible job to predict the fragility of a complex structure. First, you have to compute all the normal modes, then the damping, then the half-period of the impulses. This looks wonderful on paper but, as you know, it doesn't mean very much. So, if you are concerned with a very big, complex item like a console, you really can't blame the designer too much if he tells you it has a low g value. He has probably gone to the dynamics people and they have given him the best answer they can, this is probably the worst condition they can think of, cut in half."

Mr. Smith of Douglas Aircraft asked that Mr. Schuler let go of a few trade secrets on the subject of obtaining fragilities since the British have been doing this for 10 years. He pointed out that the thing that seems to scare everyone is that fragility curves are associated with many frequencies. He asked Mr. Schuler, "Just exactly how many parts are you willing to break in order to get what you consider a useable fragility curve?"

Mr. Schuler responded, "When I talk about our experience it is in relation to the machine that we use for small assemblies. The reason why this is important is that the items that end up with a package weight of 50-60 pounds are likely to get the most brutal treatment. They are manageable sizes to contend with for fragility assessment using our machine."

"Owing to all the assumptions that have to be made, I don't believe that fragility assessment can be a very exact science, but it is an integral part of design. It is intimately related

to all the other environmental tests and I know that vast efforts are deployed in assessing the vibration characteristics and performance of an item. When you have terribly expensive items such as large missile assemblies, nobody is going to give you a half dozen of these to use for fragility assessments. However, under the over-all management concept, these items are broken down into different areas from which you can choose the vulnerable ones. For example, you can get to work on the guidance and control unit which may be quite a small manageable box.

"All I'm making a plea for is that this is a problem to be faced. Your engineers who get green fingered by doing vibration studies on equipment can also acquire a knowledge about shock. Even if your junior engineers, quite lowly folk, do some fragility assessments on inexpensive hardware, you can learn a mighty lot about how to put things together that won't break at low g shock impulses. This isn't an overwhelmingly frightening problem. A lot more can be done without enormous budgets to get a feel for what you can do, particularly in electronic engineering design. You can make significant improvements with quite small changes.

"I think Mr. Smith was concerned with what sort of faith we can have in these measurements, or how many sigma have we taken it to. I'm sorry, but I can't say that we really can put this on a statistical basis except, perhaps, on certain things like klystrons, magnetrons, or cathode ray tubes. In these cases it's not too impossible under the development contract to call for 50 items for this particular task. The contractor is used to setting aside funds for heat runs, cooling trials, vibration, etc. Why not do a bit on fragility assessment as well?"

Mr. Jones of Nopco Chemical Company offered these remarks which, he said, in effect elaborate on Mr. Franklin's remarks. "We talk rather vaguely about the various frequencies that may make up a certain shock pulse. It seems to me that the way to avoid this is to test items on cushions, thereby producing substantially the same pulse that the item will see in a package. All those close to packaging and cushioning are aware of optimum stresses, cushion factors or g versus dead loads. I think the secret would be to pick a drop tester, select the suitable drop height, determine the dead load and make a series of drops on progressively thinner and stiffer cushions until you obtain a failure. The change in stiffness with the decrease in thickness is to assure that you are always at the optimum range of stiffness for the cushion or close to the minimum on a cushion factor-stress curve (a deflection of 40 to 60 percent which is what you expect in a properly designed pack).

"There are lots of good cushioning materials available to do this. Two examples are fiberglass and urethane foam, both of which can be stabilized after preworking. I think this is a simple, straightforward system that bypasses a lot of problems that arise when you do it other ways.

"In summary, for an item where the height is fixed, there would be about 5 drops to make. Starting with your thicker cushion, perhaps you would test at 20 g, then 30 g, 50 g, and 100 g or some logarithmic scheme that is similar. It seems like you should end up with something very useful which will then tie into the cushioning data that we get."

Mr. Schuler responded, "I'm really not a cushioning expert in spite of what the Chairman said. My knowledge in this area is rather sketchy, but there is one thing to be said about ignorance, and that is that it usually causes a lot of interesting arguments.

"In answer to our friend, we did in fact adopt the approach of using cushioning materials. Of course, the immediate snag that occurs to you is that in fragility assessment you are doing a lot of drops and, while cushioning materials are often very good in packs where they don't receive too many drops, they do quickly fatigue and change their characteristics. The other thing is that they are not always the easiest things when frequent changes of thickness are required.

"I don't want to keep flogging my pneumatic ram machine, but it's just too simple for words. You just put a little more air in the ram and you have a 9-inch sweep covering g values from 5 to 90; you can reset the ram at will. Similarly, with the lead-block decelerator, all that is required is to unscrew a spike, put in another spike and you are all ready to go on your next program of work."

Mr. Williams of the 6511th Test Group (Parachute) intervened with a plug for the little black box. "Back in Chicago,* we had a little Donner analog computer on which we could set up, on a single amplifier, a single-degree-of-freedom system and vary damping and frequency simply by turning a few knobs. By playing through a tape of a transportation impact, or the like, it wasn't too difficult to say that at a certain point damage would occur and

*Mr. Williams was formerly with the QM Food and Container Institute, Chicago, Illinois.

this would establish the fragility level. My approach was to look for the weakest structure in the item that could be simulated on the analog and check its response to shock. By doing this, perhaps I would only have to break up 10 items to get a fragility factor instead of 100."

Mr. Jones agreed with Mr. Schuler that if one simulates the pulse that occurs in the actual package he will get the right answer no matter what method he uses. He felt that it could be done with cushions.

Mr. Schuler agreed and pointed out that the important thing was to get the job done. Use a machine if it is available; if not, use cushioning materials.

Mr. Jones restated his plea that anyone making fragility studies familiarize themselves with the cushioning data to be sure they simulate the pulse involved.

Mr. Grabowski gave assurance that he wasn't taking issue with Mr. Schuler, but as an example of Mr. Jones' approach, "A gyroscope manufacturer was getting a good deal of breakage even with his cushioned pack and came to us for help. He estimated a 30-inch drop height and a fragility of 15 g. We decided to use Bob Jones' approach, however, and designed packages for 35, 50, and 100 g protection. Instrumented tests proved the package designs and live items were then placed in them. It was found that the item could withstand 100 g in this particular package. After thousands of shipments in the 100-g pack there has been no breakage. I recommend this procedure whenever you can get live instruments to evaluate."

Mr. Kerstner of Autonetics suggested that a lot of information on fragility could be obtained by using obsolete items that are basically the same as the new item being made. These obsolete items are frequently easier to get than the new ones.

Mr. Schuler agreed that this was a good approach and pointed out that in England they have a contract underway in which older equipment is to be used. He continued, "In addition to endeavoring to get this fed into all new items, we feel there is a need for a comprehensive report, particularly in the electronics sphere, where designers are provided with illustrations and guidelines as to how they can improve the overall strength factor of equipment. We are using for this study a lot of readily available obsolete equipment. We can be criticized on the grounds that these do not represent techniques

of construction currently in use, but a lot of it is much the same and we hope to learn quite a lot."

DESIGN AND EVALUATION

Mr. White of Western Electric Company commented: "We are in the Zeus business and electronics in general. I'm a packaging engineer and in the ten years I've been in packaging we have become more and more concerned about failures in equipment after it is installed and in operation. Even though the package arrived safely, how much of the cause of this later failure can be traced back to the package, handling in the plant or the like? Using your best design practices you come up with a package that meets all your drop requirements. Perhaps a fellow in the shop does something he shouldn't. A lot of times this is blamed on the packing when it's not at fault. How far should you go in finding out?"

Mr. Mustin said that in his experience the package gets blamed for everything. He continued, "I don't think there is any general answer to your question. You have enough trouble from the reliability boys on premature failure. I do think that, when you have premature failure, you must examine all possible causes and one of them is the package."

"The military specifications are pretty conservative. I believe the experience of Hughes, Tucson with the Falcon is instructive but subject to correction as I state it. I vaguely recall numbers like 20,000 of these things being shipped all over the country and never a damage. The shipping history included such things as trucks rolling down the sides of mountains. They ran rough road tests in the desert near Tucson and the most damage they did was to the poor driver who was trying to make some speed over the rough road. The conclusion is that they really had overpackaged, but they met the specifications."

Mr. Welton queried, "If you can assume that you have assigned a reasonable fragility level and you have a military specification that you are designing your container to, should you use a safety factor in your cushion design?"

Mr. Schuler responded, "I wanted to ask the penultimate questioner whether in his design he had any safety factor. I think it is important to assign a safety factor in your fragility assessment because it is related to the type of cushioning used and its characteristics."

"Someone asked earlier what you do about 5 g. It is surprising how the operation requirements in another area of the specification would sometimes get handed down the line. Suppose an airplane must in fact withstand proved stresses of 5 or 8 g. Eventually someone says, 'Oh well, my piece of apparatus is going in this plane so I've got to design it so that it never sees more than 5 or 8 g.' Alas, what people are not understanding is that 5 or 8 g of continuously applied acceleration such as on a centrifuge is quite different from a short shock pulse even of several hundred g.

"We find on evaluation of many of our simple electronic structures that it is easy to calculate the stresses and achieve these very low figures, but, in fact, the structure would be so fragile that it wouldn't be a sensible structure at all. Doing these simple exercises does not involve a lot of sophisticated equipment. A lead-block decelerator, for example, costs only a few hundred pounds sterling, and with it you can make marked improvements in your design without going to a lot of engineering complexity.

"People seem to imagine that values like 25 or 50 g impose some impossible requirement on their design. This is not so in our experience. Time and time again we have been able to demonstrate that by the simple rearrangement of components, slight changes in bracket configuration, or other quite small engineering detail which presents no serious headache to anyone, we can make a 12-g item withstand 50 or 60 g. The problem is that people won't do these simple exercises. They just get frightened off by these figures."

Mr. Mustin commented, "Mr. Welton's question was assuming that you have a 'reasonable' fragility factor. There's the rub. Now, if you accept as a definition of 'reasonable' one that is experimentally determined such as advocated by Mr. Schuler in which there is already a factor of safety, then you have certain other built-in factors of safety working for you. First, you are not going to use the cushion at the minimum thickness indicated by your analysis, but are going to round it out on the fat side to make something that the shop can hold tolerances on. Further, all of our analyses assume that the container is a rigid body and most also assume that the item is a rigid body. These are elements of conservatism working on your side. If I had a reasonable g factor, my factor of safety would be predicated on the inherent variability of the cushioning material and nothing else."

Mr. Rice commented with respect to overpackaging. He said, in effect, that we must

distinguish between a one-of-a-kind prototype and a black box. We shouldn't hesitate to overpackage in cases where an item costs 20 or 30 million dollars or if the project would be stopped if it didn't get there.

Mr. Leonardi offered the following remarks: "Regarding the reliability area, you have two basic philosophies; one concerning economics and the other concerning catastrophic failure. The safety and reliability people are concerned with the probability of having a hazard which will cause a malfunction and also the probability of having a hazard which will be catastrophic. They want to know numbers like 1 in 10^6 or 1 in 2×10^6 , etc. As far as I'm concerned, these numbers are impossible to attain because transportation hazards are too problematical. Even if they follow a gaussian distribution, I have never seen enough data to indicate whether it's skewed to one side or the other. So in these cases we overpackage and hope like heck it gets there.

"With respect to fragility, it would be ideal to have a level and a response time. Along this line there have been several documents on components like diodes, resistors, etc., attempting to indicate maximum allowable vibration response levels and shock levels under which they would still function. This becomes more complex as other variables, such as temperature, are introduced. At most, these documents are only guides.

"We find that we can generally package electronic gear which is in a carrying case to 25 or 30 g and not have too much trouble. In the vibration spectrum we don't appear to get too much damage up to 40 or 50 cps. In go-no go checks we start into frequencies above 40 or 50 cps and get damage because we are exciting the natural frequencies of small rigid masses contained in the structure. Because in a given test we may not be able to determine what we're measuring the response of, I feel it is difficult, if not impossible, to get a natural response level and a composite g factor for a complex piece of equipment."

Mr. White stated that they had recently revised their thinking about fragility because of figures received in design manuals about electronic spare parts they ship. They've started using mail bags and completely eliminating cushioning on many smaller electronic components and they seem to be arriving all right. He wanted to know if anyone else had any feelings about mail-bag shipments of electronic components.

Mr. Schuler felt that some of his work tends to confirm the point raised by Mr. White. His findings indicated that many components are extremely robust items and that, by and large, most of the failures noted were in the fixtures or mountings and not the components themselves.

Mr. Schell of ASD cited some experience to indicate that handling in the post office is very severe.

Mr. Mustin tended to confirm this by saying, "I think it useful to discriminate between the types of shipment involved. When I was at Container Laboratories, the most severe test cycle we had was for parcel-post and third-class mail handlings. However, Army Ordnance experience shows that when you load your own mail bags and take them directly to the post office you'll not get the same kind of damage."

Mr. White told of a case in his company where considerable money was saved by lowering the design criteria on a console. This was accomplished simply by deciding that the drawers in the console were to be removed during shipment. He also stated, in answer to some earlier remarks, that the Packaging Engineer at Western is rated rather high.

Mr. Henny raised a question about the drop test requirements in MIL-C-7936. He wanted to know why different drop heights were spelled out for level A and level B packaging for the same weight package.

Mr. Junker of the Bureau of Naval Weapons agreed that the drop height requirements should be the same. He pointed out that in his section they use MIL-W-21927 which does specify the same drop height regardless of level. He added that the height specified would be a function of the reliability desired.

ENVIRONMENTAL RECORDERS

Mr. Schuler asked about current practice in the USA regarding the use of shock recorders on actual packs, particularly in the missile fields. He wasn't referring to recorders to evaluate anything, but merely as an insurance to indicate whether or not a certain critical level had been exceeded. He also wanted to know about current practice with respect to the use of humidity indicators.

Mr. Rice cited his experience with shock recorders. "We had the Lockheed Instrument people develop a shock recorder that we use

with the Subroc missile. The recorder is really just a limit switch and doesn't measure the pulse length. We asked a number of companies around the country what they would charge to develop a recorder to measure pulse length. It was quite expensive and we had to give it up. It's quite easy to get these limit switch affairs, however, that will record the number of times a certain g level is exceeded. This record is being kept for the Subroc missile as it's transported around the country."

Mr. Schuler asked whether it was a general policy for the military to specify the use of these recorders.

Mr. Rice could not say, but stated that NOL did require it for the Subroc.

Mr. Junker remarked that, at the request of the Marine Corps, shock indicators are used on shipments of the Terrier missile. He then pointed out the importance of establishing realistic criteria in the beginning of a program. On the Terrier a level of 10 g was established as the maximum shock it should receive in the longitudinal direction. Recently a shipment of boosters arrived with all the 10-g shock indicators tripped. As a result, even though the boosters may function properly, expensive check-out procedures are required before anyone will use them. This cost resulted directly from uncertain fragility requirements.

Editor's Note:

It appears that the answer to Mr. Schuler's question is that there is no general policy in the U.S. military calling for the use of shock indicators, but that certain programs have employed them to learn whether the item had exceeded a certain shock level during shipment. There are several studies underway, both with respect to peak reading indicators and more elaborate shock recorders to define the environment statistically. Further information on these efforts may be obtained from Code 4021, U.S. Naval Research Laboratory, Washington 25, D.C.

Response to Mr. Schuler's question regarding humidity indicators was rather indefinite, but in general the opinion was that the red and blue spot indicators were predominately used in dehumidified containers.

COMMENTS BY THE MODERATOR,
F. J. LINDNER (Submitted
subsequent to the Symposium)

As the discussion in this session indicates, scientific methods are gradually replacing "cut and try" techniques in package design. Although this is encouraging there are still problem areas which need more precise definition.

Traditionally, the initial design of cushioned packs has been an entirely empirical process, a matter of incorporating in the pack a quantity of cushioning material usually chosen, as to type, quantity, and arrangement, on the basis of the designer's experience of the handling and shipping hazards expected. A shipping history of this pack has then been accumulated showing the amount of damage experienced and adjustments are made in the design until an acceptable percentage of items shipped arrive in good condition.

This elementary approach to a problem of great economic significance often works quite well. Its success depends entirely on the proper use of accumulated experience. However, the process of accumulating this experience is time consuming and, until a satisfactory package design is achieved, many items are lost. Also, in many cases, the final result is costly over-packaging. In this rapidly changing age of missiles and space systems we cannot afford such an approach. We must deal in more precise engineering terms, our design parameters must be carefully defined, and acceptance must be based upon the measured results of controlled laboratory tests. The three basic areas in which design parameters must be defined are listed in the Foreword to this session.

One of the more important problems facing us is the measurement and definition of the shipping and handling environment. It was brought out during the session that there have been a number of efforts in this direction and that some data are available, but in many cases the usefulness of this data suffers from numerous limitations. It is not always clear at what point measurements were made or how the data were analyzed. Not enough attention is given to defining whether the environment was shock, vibration (random or periodic), or a mixture of all of these. Further, many measurements are made for a specific purpose and the results are either lost to posterity or are not useful for general application. An earnest effort toward the

coordination of all programs of this kind, the funneling of data to a central point for dissemination, and a standardization of data presentation are sorely needed.

The problem of determining characteristics of cushioning materials has received considerable attention in the past few years. Investigators are now evaluating the dynamic properties of these materials instead of conducting the traditional static tests. This is an important advance since studies have shown dramatically the difference between the two.

Methods of designing package cushions are quite well-known and straightforward. They consist basically of the use of a peak "g" for the fragility level and of an expected height-of-drop to define the environment. What is often overlooked is the vibration response of the system. There are differences of opinion as to the importance of this omission. Some feel that since cushioning systems are, by nature, soft, troublesome high-frequency vibration is effectively isolated. The writer feels that, in some cases at least, the system vibration response may be very important. Mount manufacturers give, in addition to a load rating, the resonant frequency for a given load for any specific mount. When requested, they will also provide transmissibility curves for their mounts. Why can't something similar be done for cushioning materials?

With respect to establishing the fragility characteristics of an item, the reader will have already noted the British approach and will have read the discussion on American efforts, or perhaps lack of effort, along these lines. The British method, as well as American methods that simulate the shock pulse which the packaged item will encounter in service, have a lot of merit, but they are destructive tests. It is clear that items are not always available for destructive tests.

It is suggested that a resonance survey of the item in question, conducted on a vibration exciter with a low-g input, will provide a lot of useful information on a nondestructive basis. A survey of this kind, perhaps in several orientations, will reveal the critical frequencies thus enabling the designer to select a cushion that will not produce a damaging pulse.

Finally, in integrating all the parameters relating to the environment, the materials, and the item to be packaged, the definitions must be such that existing design formulae can be successfully applied.